GEOLOGICAL SURVEY OF CANADA OPEN FILE 3247

Geological Survey of Canada

SHORT COURSE MANUAL

BOREHOLE GEOPHYSICS IN MINERAL EXPLORATION

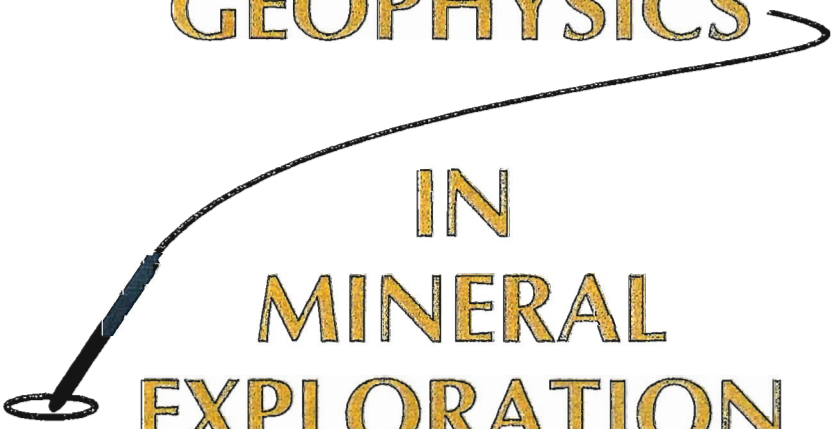

P.G. Killeen
C.J. Mwenifumbo
B.E. Elliott
K.A. Pflug
L.D.Schock
G.R. Bernius

Borehole Geophysics Section
Applied Geochemistry and Geophysics
Mineral Resources Division
Geological Survey of Canada
January, 1996

GSC SHORT COURSE
on
BOREHOLE GEOPHYSICS IN MINERAL EXPLORATION

January 24 & 25 1996

presented by
the
Borehole Geophysics Section, Mineral Resources Division
Geological Survey of Canada, Ottawa

PREFACE

This volume, GSC Open File 3247, is a modified version of the material prepared for a short course held in Ottawa after the 1996 GSC Minerals Colloquium. The Open File was prepared in response to numerous requests for copies of the course material by people unable to attend the course. The changes relate to improvements in the bibliography, revision of the tables and redrafting of the tool diagrams and standard spectra in the Appendix (now called Part C), substitution of two of the reprints to avoid copyright difficulties, and to expand the subjects covered (borehole orientation surveys). The original three separate tables of contents have been improved and combined into one table near the front of the text. To coincide with this new table of contents, the entire text has been numbered from front to back, while the original page numbers on the reprinted material have been preserved for reference.

Acknowledgements

We wish to acknowledge those involved in putting this short-course together, in particular Vince Gerrie, Bill Hyatt, Jacques Parker, Yves Blanchard, Sue Davis, Cindy Aoki and Mary Ann Blondin. We are grateful to the Canadian Institute of Mining and Metallurgy, the Society of Professional Well Log Analysts (the parent of the Minerals and Geotechnical Logging Society), and to the Geological Survey of Canada for permission to reproduce published material for this short course manual.

TABLE OF CONTENTS

SYNOPSIS

The short course manual is divided into three parts:

PART A: An outline of the principles of the various logging techniques, some description of the hardware and borehole probes used to make the measurements, and some information relating to the interpretation of the logs. **This draws heavily on the GSC logging equipment for "typical" examples,** but of course other variations exist in available logging systems. The oral presentations by the course instructors will elaborate on this.

PART B: A compilation of selected reprints of our papers on borehole geophysics to provide additional details on the principles/physics of the different logging methods, example applications and case histories, and a hard copy reference for the course participants.

PART C: Primarily a reference section, it contains a bibliography of Borehole Geophysics Section publications, a list of recommended further reading material (text books), tables of drill rod, bit, casing and hole sizes, standard gamma ray spectra from calibration and density tool sources, measured and theoretical spectra for natural uranium and thorium, diagrams of typical logging tool dimensions and configuration details, and other information useful to the borehole geophysicist.

The Authors

INTRODUCTORY REMARKS ON THE ROLE OF BOREHOLE GEOPHYSICS IN MINERAL EXPLORATION

Borehole geophysics is simply geophysics in a nontraditional environment. In mineral exploration, tradition dictates that airborne and surface geophysical measurements be made prior to drilling the target. In the past, borehole geophysical measurements which were feasible were not used to any great extent to obtain additional information because it was cheaper to drill more holes. However, since drilling is now such an expensive part of exploration, it is important that maximum advantage be taken of the methods offered by geophysics to evaluate apparently barren ground (i.e. a "dry" hole) and to increase the probability of striking significant mineralization during subsequent drilling.

The primary objectives of drilling a hole are to obtain information about the geological environment and to detect the presence and measure the quantity of economic minerals which will (hopefully) be intersected by the borehole. The information obtained from the borehole has until recent years been entirely based on the drill core taken from the hole. However the core is often missing for critical sections of the hole because of difficult drilling conditions, while in inhomogeneous rock the true ore distribution cannot be deduced because the core is not representative.

Thus the borehole itself becomes a valuable pathway for geophysical logging instead of a worthless hole left after retrieving the drill core. The borehole geophysical measurements can be used to detect the presence of nearby mineralization missed by the borehole, to evaluate zones where the core was lost, or to evaluate large-volume bulk samples of the ore mineralization in the walls of the borehole. Some techniques such as those based on nuclear methods, can even be used inside steel drill pipe or casing. Electrical, electromagnetic and seismic methods can be used in a hole-to-hole configuration to study the rocks between adjacent boreholes. Surface-to-hole, and hole-to-surface measurements can be used to increase the radius of investigation around the borehole.

The Borehole Geophysics Section at the Geological Survey of Canada has examined the application of these methods to mineral exploration in various mining areas across Canada. Borehole geophysical measurements have included IP, resistivity, self potential, magnetic susceptibility, conductivity, natural gamma (K, U and Th), spectral gamma-gamma (density, heavy element assay), temperature, temperature gradient and acoustic velocity. These have been used for delineating mineralized zones, mapping alteration zones associated with mineralization, hole-to-hole lithologic correlation, assaying of mineralization, detecting groundwater flow patterns within the holes, and determining in-situ physical properties for use in the interpretation of ground and airborne geophysical data. Examples will be described showing interpretations of these logs from various mining areas in Canada, which include gold, lead, copper, zinc, and uranium deposits.

SHORT COURSE OUTLINE

COURSE DESCRIPTION: The course is designed to provide an introduction to borehole geophysical logging, commencing with an overview and brief description of the available methods which have potential for application in mineral exploration. Detailed explanations will be given for those methods which are being applied today, either routinely, or experimentally in various exploration environments (excluding pulse EM). Physical principles of the methods, the instrumentation, calibration, data acquisition procedures, correction factors, possible sources of error, and methods of data presentation with examples, will be described.

Methods to be covered in some detail:

Gamma-ray spectral (Total Count, K, U, Th)
Spectral gamma-gamma (density, heavy element content)
Electrical (IP, R, SP)
Magnetic Susceptibility and 3-component Magnetometer
Conductivity
Temperature (and temperature gradient)
Acoustic (velocity, full waveform)
Orientation (surveying dip and azimuth of a hole)

Case Histories:

To illustrate the application of these borehole geophysical techniques, examples from several mining areas (base metal, gold, kimberlite) across Canada will be examined. The use of multiparameter logs will be discussed to illustrate how ambiguities can be reduced as the available information increases.

Hardware Demonstrations:

The borehole probes in the above list will be shown, some of them disassembled, to illustrate their construction, size, complexity etc. and to provide participants with an appreciation for the hardware involved in borehole geophysics. Depending on availability of time and equipment, a portable, and truck-mounted logging system will be on view.

Software Demonstrations:

The GSC-developed software **LogView** will be reviewed with a hands-on demonstration. This Windows-based data-presentation software was developed to provide publication quality output of borehole geophysical logs. In April 1995, **LogView** was released as GSC Open File 3055, and is now available at a cost of $75.00.

Course Instructors:

The course will be given by members of the Borehole Geophysics Section, Mineral Resources Division. These include Patrick G. Killeen, C. Jonathan Mwenifumbo, Barbara E. Elliott, Karen A. Pflug, Gordon R. Bernius and Laurel D. Schock, all of whom have been involved for a number of years in various aspects of borehole geophysical research at the GSC, and have published numerous papers on the subject.

PART A PRINCIPLES, PROBES AND INTERPRETATION: AN OUTLINE

A1. THE GSC BOREHOLE GEOPHYSICAL LOGGING SYSTEM

Applications of geophysical logging encompass both mining exploration and geotechnical problems. These include: delineating ore zones, identifying and mapping alteration associated with ore, mapping lithology and hole-to-hole stratigraphic correlation. Also possible is in situ assaying of ore, and in situ determination of physical rock properties for calculating geotechnical (rock strength) parameters. Groundwater flow patterns in joints and fractures intersected by the holes can be detected as well.

The primary components of the GSC R&D logging system are:

1. the borehole probe containing the geophysical sensor;
2. the logging cable and winch for sending the signal to the surface instruments, and for sending power down to the probe;
3. a depth counter attached to a wellhead pulley for keeping track of the location of the probe in the hole;
4. an analog-to-digital converter (ADC) to convert the signal to digital form for recording;
5. a computer, keyboard and CRT monitor to acquire data and display information;
6. a 9-track magnetic tape recorder;
7. a multi-pen chart recorder to provide a hard copy in the field.

In addition to the truck mounted system, the GSC operates an IFG Corporation portable logging system for use in inaccessible areas. This system has the basic components as above, except data are recorded on the hard disk of the computer and displayed on the monitor, and hard copies are not produced at the field site.

Most modern 'slim-hole' probes (tools), 38 to 50 mm in diameter, are designed to run in BQ or larger holes. The logging speed is usually about 6 m/minute. The probes can be run in air- and/or water-filled holes depending on the sensor. Data sampling rate ranges from 1 to 5 samples per second, providing a measurement every 2 to 10 cm along the hole.

The two GSC logging systems have seven logging probes with different sensors that in total can measure over twenty parameters. The characteristics of the logging probes and their measuring principles are briefly described below.

A2. GAMMA-RAY SPECTRAL LOGGING

A2.1 Geological Interpretation of Gamma-Ray Spectral Logs

Gamma-ray measurements detect variations in the natural radioactivity originating from changes in concentrations of the trace elements uranium (U) and thorium (Th) as well as changes in concentration of the major rock forming element potassium (K). Since the concentrations of these naturally occurring radioelements vary between different rock types, natural gamma-ray logging provides an important tool for lithologic mapping and stratigraphic correlation. Gamma-ray logs are important for detecting alteration zones, and for providing information on rock types. For example, in sedimentary rocks, sandstones can be easily distinguished from shales due to the low potassium content of the sandstones compared to the shales.

In sedimentary rocks, potassium is in general the principal source of natural gamma radiation, primarily originating from clay minerals such as illite and montmorillonite. In igneous and metamorphic geologic environments, the three sources of natural radiation may contribute equally to the total gamma radiation detected by the gamma probe. Often in base metal and gold exploration areas, the principal source of the natural gamma radiation is potassium because alteration, characterized by the development of sericite (sericitization), is prevalent in some of the lithologic units and results in an increase in the element potassium in these units. The presence of feldspar porphyry sills, which contain increased concentrations of K-feldspar minerals, would also show higher than normal radioactivity on the gamma-ray logs. During metamorphism and hydrothermal alteration processes, uranium and thorium may be preferentially concentrated in certain lithologic units.

For details on natural gamma ray logging in volcanic rocks, see Mwenifumbo and Killeen, 1987.

A2.2 Principle of Gamma-Ray Spectral Logging

A gamma-ray probe's sensor is usually a sodium iodide or cesium iodide scintillation detector. Unlike a total count gamma-ray probe, the spectral gamma-ray probe measures the energy of each gamma ray detected. K, U and Th emit gamma rays with characteristic energies so estimates of the concentrations of the three radioelements can be made.

Potassium decays into two stable isotopes (argon and calcium) which are no longer radioactive, and emits gamma rays with energies of 1.46 MeV. Uranium and thorium, however, decay into daughter-products which are unstable (i.e. radioactive). The decay of uranium forms a series of about a dozen radioactive elements in nature which finally decay to a stable isotope of lead. The decay of thorium forms a similar series of radioelements. As each radioelement in the series decays, it is accompanied by emissions of alpha or beta particles or gamma rays. The gamma rays have specific energies associated with the decaying radionuclide. The most prominent of the gamma rays in the uranium

series originate from decay of ^{214}Bi (bismuth), and in the thorium series from decay of ^{208}Tl (thallium).

Because there should be an equilibrium relationship between the daughter product and parent, it is possible to compute the quantity (concentration) of parent uranium (^{238}U) and thorium (^{232}Th) in the decay series by counting gamma rays from the daughter products ^{214}Bi and ^{208}Tl respectively, if the probe has been properly calibrated (Killeen, 1982).

While the probe is moving along the hole, the gamma rays are sorted into an energy spectrum and the number of gamma rays in three pre-selected energy windows centred over ^{40}K, ^{214}Bi and ^{208}Tl peaks in the spectrum are computed each second, as is the total gamma-ray count. These four numbers represent gamma rays originating from potassium, uranium, thorium and Total Count (TC) detected during that one second of counting time.

These data are recorded along with the depth and are displayed on the chart recorder to produce gamma-ray spectral logs. The raw gamma-ray spectral logs (Total Count log, K log, U log and Th log) provide more information than a non-spectral (gross count) log, and it is possible to convert them to quantitative logs of K, U and Th concentrations. This requires that the probe be calibrated in model boreholes with known concentrations of K, U and Th such as the models constructed by the GSC at Bells Corners near Ottawa (Killeen, 1986).

Because gamma rays can be detected through steel, logging can be done inside drill rod or casing with a slight decrease in sensitivity.

A2.3 The Gamma-Ray Spectral Logging Equipment

The GSC R&D logging system utilizes gamma-ray spectral data acquisition equipment similar to that found in modern airborne gamma-ray spectrometers. Full 256-channel gamma-ray spectra over an energy range of approximately 0.07 to 3.0 MeV are recorded from a scintillation detector in the probe. The storage medium is 9-track magnetic tape. Scintillation detectors of different materials, and of different sizes are used by the GSC. These include:

Name	Composition	Density (g/cm^3)
Cesium Iodide	CsI (Na)	4
Sodium Iodide	NaI (Tl)	3.67
Bismuth Germanate (BGO)	$Bi_4 Ge_3 O_{12}$	7.0

Probe housings of outside diameter 1.25" (32 mm), 1.5" (38 mm) or 2" (50 mm), contain detectors of sizes ¾" x 3", 1" x 3", and 1.25" x 5", respectively, for use in AQ, BQ, and NQ holes, respectively. The probe (and detector) selection is determined by the hole diameter. The largest diameter probe that will safely fit in the borehole will maximize the count rate and provide better counting statistics. For smaller probes, the higher density (higher efficiency) materials are chosen. (These are also higher cost). If the count rate is too low due to the extremely low concentrations of K, U and Th, as is often the case in limestones for example, it is not possible to produce K, U and Th logs. In that case only the Total Count log, which is the count rate of all gamma rays above a preselected threshold energy (usually 100 KeV or 400 KeV), is produced. A number of factors determine the logging speeds and sample times during the acquisition of gamma-ray data. The critical factors are the anticipated levels of radioactivity and the size of detector in the probe. Gamma-ray spectral logging is usually done at 3 m/minute but can be done as fast as 6 m/minute or as slow as 0.5 m/minute for more detailed information. The volume sampled is about 0.5 cubic metres of rock surrounding the detector, at each measurement (i.e. 10 to 30 cm radius depending on the rock density).

A3. DENSITY/SPECTRAL GAMMA-GAMMA (SGG) LOGGING

A3.1 Geological Interpretation of Density and SGG Logs

The density/SGG logging tool measures rock density and SGG ratio. The SGG ratio (defined below) is related to the effective atomic number of the rock, which depends on the chemical composition of the rock. The SGG ratio log is particularly useful for detecting base metals; these elements have high atomic numbers compared to major rock-forming minerals, and they can occur in high enough concentrations to increase the effective atomic number of the rock significantly . The SGG ratio log may also be useful for lithologic mapping in areas where the iron content differs significantly among different rock types.

The density of rock is affected by porosity, water content and composition. Most of the density variations within igneous and metamorphic rocks are due to variations in mineralogical composition. Rocks with higher percentages of mafic minerals (Fe, Mg silicates) have higher densities than those with higher percentages of felsic minerals (Ca, Na, K, Al silicates). The presence of minerals containing heavy elements such as base metals increases the overall density of the host rock. In sedimentary rocks, density variations may be a result of differing degrees of compaction (induration) rather than changes in elemental composition.

In ore tonnage and reserve computations, one of the factors used is the specific gravity and hence a knowledge of in-situ densities of the rocks may provide valuable information. The density log is also useful for locating fractures since open fractures intersected by the borehole often appear as low density zones on the density log (Wilson et al, 1989).

A3.2 The Density/SGG Logging Equipment

The density and SGG ratio (or heavy element indicator) logs are derived from the spectral gamma-gamma probe (Killeen and Mwenifumbo, 1988). The density/SGG tool is essentially a spectral gamma-ray logging tool with the addition of a weak (10 millicurie = 370 MBq) gamma-ray source (e.g. ^{60}Co) on the nose of the probe. The tool has a 23 mm by 76 mm (0.9" x 3") cesium iodide detector which measures gamma rays from the source that are backscattered by the rock around the borehole.

Complete backscattered gamma-ray spectra are recorded in 1024 channels over an energy range of approximately 0.03 to 1.0 MeV. Density information is determined from the count rate in an energy window above 200 keV while information about the elemental composition or heavy element content is derived from the ratio of the count rates in two energy windows (spectral gamma-gamma ratio, SGG): one at high energy (above 200 keV) and one at low energy (below 200 keV). When the density of the rock increases, the count rate in both windows will decrease due to the change in compton-scattered gamma rays reaching the detector. However, if there is an increase in the content of high-Z (atomic number) elements in the rock, the associated increase in photoelectric absorption (which is roughly proportional to Z^5) will cause a significant decrease in count rate in the low energy window with a small change in the high energy window. Since the low energy window is affected by both density and Z while the high energy window is mainly affected by density, the ratio of counts in the high energy window to the counts in the low energy window can be used to obtain information on changes in Z. This ratio increases when the probe passes through zones containing high-Z materials. Thus the log can be considered as a heavy element indicator, and can be calibrated in some conditions to produce an assay tool for quantitative determination of the heavy element concentration in situ along the borehole, without resorting to chemical assaying of the core (Killeen and Mwenifumbo, 1988).

The SGG sample volume is smaller than for natural gamma ray logging since the gamma rays must travel out from the probe, into the rock and back to the detector. A 10 to 15 cm radius around the probe is "seen". Data are acquired at a logging speed of 6.0 m/minute, with a sample time of 1 second giving a measurement every 10 cm.

A4. INDUCED POLARIZATION/RESISTIVITY/SELF POTENTIAL LOGGING

The Induced Polarization (IP) tool consists of an assembly of electrodes, usually including a current electrode and two potential (measurement) electrodes. A square wave current with an 'off' time between positive and negative parts of the waveform is transmitted (waveforms may be from 1 second to 8 seconds duration). Potential measurements made at selected times in the waveform can be related to the IP effect (chargeability of the rocks), the resistivity (R) of the rocks, and to self-potentials (SP) generated in the rocks. The transmitter is a constant current source located at the surface. A detailed explanation of the IP probe will be given below.

A4.1 Geological interpretation of IP/R/SP Logs

A4.1.1 Induced Polarization

In time domain IP measurements, the ratio of the secondary voltage measured during the current off-time to the primary voltage measured during the current on-time is related to the electrical polarizability of the rock and is called chargeability. A high chargeability response is an indication of the presence of metallic sulphides and oxides or cation-rich clays such as illite and montmorillonite (Mwenifumbo, 1989). One of the major alteration processes within a number of base metal and gold mining camps is pyritization and this is a target for most IP logging in gold exploration.

A4.1.2 Resistivity

The electrical resistivity of rocks depends on several factors including the presence of conductive minerals such as base metal sulphides or oxides and graphite in the rock. Most rocks without these minerals are usually poor conductors and their resistivities are governed primarily by their porosity, degree of fracturing, salinity of the pore water, the degree of saturation of the pore spaces, and to a lesser extent by the intrinsic minerals that constitute the rock. Some alteration processes such as silicification and carbonatization tend to reduce the porosity and hence increase the resistivity of the rock. In igneous and metamorphic rocks, the resistivity log is useful mainly in mapping conductive minerals and fracture zones. In sedimentary rocks, the resistivity log is frequently used in lithologic mapping because changes in lithology are often associated with changes in porosity.

A4.1.3 Self Potential or Spontaneous Polarization

SP anomalies are mainly an indication of the presence of graphite and/or high concentrations of base metal sulphides including pyrite. Large self potentials observed within and around sulphide and graphite bodies are mainly caused by electrochemical processes (Sato and Mooney, 1960, Hovdan and Bolviken, 1984). Low resistivity anomalies correlating with SP and IP anomalies are, therefore, good indications of the presence of conductive minerals. SP anomalies can be also generated by fluid flow in porous media (electrokinetic or streaming potentials - Bogoslovsky and Ogil'vy, 1970, 1972) and heat flow (thermal electric coupling - Corwin and Hoover, 1979).

A4.2 The IP Logging Probe Description

The transmitter on surface is a constant current source capable of supplying up to 250 mA. There are 4 selectable pulse times for the current waveforms: 0.25s, 0.5s, 1s and 2s (i.e. full waveforms of 1 second to 8 seconds duration). The long pulse times would be used when logging at very low speeds in order to avoid errors that could be introduced by smearing measurements over large depth intervals. The volume of rock sampled is related to the electrode spacings. The full waveform is recorded (digitized at 4ms intervals) on 9-track

magnetic tape. Logging speed ranges from 1 to 6 m/minute according to the chosen pulse length (waveform duration). The sample interval is dependant on the logging speed and waveform period. Typically, a 1 second period with a logging speed of 6 m/minute results in sampling every 10 cm along the borehole. This tool must be run in uncased, water-filled holes.

A4.2.1 Induced Polarization

The standard IP parameter is the chargeability determined during the middle of the 'off' time of the decaying waveform. The apparent chargeabilities can be measured with 3 types of electrode arrays: 40-cm normal array, lateral array (pole-dipole array) and the 10-cm Dakhnov micronormal array. The downhole current and potential electrodes are gold-plated brass cylinders, 40 mm in diameter (Mwenifumbo, 1990).

A4.2.2 Resistivity

The resistivity measurements are derived from the waveforms received during the constant current 'on' time of the square waveform, after the initial IP charging effects are over. Resistivity measurements are made with the same arrays as are used in the IP measurements. Single point resistance measurements can also be made using a single downhole current/potential electrode (Pb) and a return/reference electrode on the surface.

A4.2.3 Self Potential or Spontaneous Polarization

The self potential is determined during the late 'off' time of the IP decay waveform. SP measurements are carried out either in the gradient mode with the same arrays as are used in the IP measurements, or in the potential mode with a single Pb or $Cu/CuSo_4$ electrode downhole and a reference electrode on the surface. SP can be measured simultaneously with the IP/Resistivity measurements or in a separate logging run with current off. The latter is the preferred approach.

A5. MAGNETIC SUSCEPTIBILITY LOGGING

A5.1 Geological Interpretation of Magnetic Susceptibility Logs

The magnetic susceptibility (MS) of a volume of rock is a function of the amount of magnetic minerals, (mainly magnetite and pyrrhotite), contained within the rock. MS measurements can provide a rapid estimate of the ferromagnetism of the rock. These measurements can be interpreted to reflect lithological changes, degree of homogeneity and the presence of alteration zones in the rock mass. During the process of hydrothermal alteration, primary magnetic minerals (e.g. magnetite) may be altered (or oxidized) to weakly- or non-magnetic minerals (e.g. hematite). Anomalously low susceptibilities within an otherwise homogeneous high susceptibility (ferromagnetic) rock unit may be an indication of altered zones.

Basic flows and diabase dikes containing higher concentrations of magnetic minerals can be easily outlined with magnetic susceptibility measurements when they occur within a sedimentary sequence that normally contains little or no magnetic minerals.

A5.2 The Magnetic Susceptibility (MS) Logging Probe Description

A5.2.1 MS Measurement with the Geoinstruments TH-3C Probe

The magnetic susceptibility tool is a Geoinstruments model TH-3C probe which uses a signal processing unit developed at the GSC (Bristow and Bernius, 1984; Bristow, 1985). The probe contains a coil, 42 mm in diameter by 0.5 m in length, in an electrical bridge circuit energized at a frequency of 1400 Hz. When the probe passes through magnetically susceptible material, the coil inductance changes causing the bridge to become unbalanced. The bridge is balanced automatically by changing the energizing frequency. This change in frequency is proportional to magnetic susceptibility. Since the measurements are made inductively (i.e., with EM coils not contact electrodes), the tool can be used inside plastic casing and in dry holes. Susceptibilities in the range of 0 to 2.0 SI can be measured with this tool. The volume of investigation or `sample volume' is roughly a sphere of 30 cm radius, surrounding the sensing coil in the probe. Logging is normally carried out at 6 m/minute and a measurement is taken every second or each 10 cm along the hole.

A5.2.2 MS Measurement with the BRGM 'ROMULUS' probe

The Romulus probe is a low-frequency (4 KHz), two-coil electromagnetic induction probe. It consists of coaxial transmitting and receiving coils spaced 85 cm apart. It compensates for the primary field and measures in-phase and quadrature components of the secondary field. These two quantities are approximately proportional to magnetic susceptibility and electrical conductivity of the rock around the borehole.

For the magnetic susceptibility (in-phase) measurement, the sensitivity is 3.14×10^{-3} μSI/volt and the measuring range is 10^{-5} to 3.5×10^{-2} μSI.

A5.3 The Conductivity Logging Probe Description

A5.3.1 Conductivity Measurement with the Geoinstruments TH-3C probe

The Maxwell-bridge circuit which is used in the TH-3 probe also allows conductivity of material close to the coil to be measured simultaneously with susceptibility. This is accomplished by resolving the change in complex impedance seen by the bridge into its inductive and resistive vector components. (Resistive material around the coil causes the coil to behave as a transformer with the resistive material acting as a combined and distributed "secondary winding" and "load"). Resistivity measurements using this technique are limited to a range of 10^{-1} ohm-m to 10^{3} ohm-m (conductivity = 10 mho/m to 10^{-3} mho/m). In practice only a few sedimentary formations would normally have resistivities low enough to fall within this range, while in igneous rocks only graphitic

conductors or mineralized zones such as massive sulphides would be included (Bristow and Bernius, 1984).

A5.3.2. Conductivity measurement with the BRGM 'ROMULUS' probe

As mentioned above in the section on magnetic susceptibility, the secondary field at the receiver coil is measured and the out of phase component is proportional to electrical conductivity (quadrature). The sensitivity is 0.46 mho/m/volt and the measuring range is 10^{-3} to 5.5 mho/m.

A6. TEMPERATURE/TEMPERATURE GRADIENT LOGGING

A6.1 Geological Interpretation of Temperature Logs

Temperature measurements are used to detect changes in thermal conductivity of the rocks along the borehole or to detect water flow through cracks or fractures. Fractures or shear zones may provide pathways for groundwater to flow if hydrologic gradients exist within the rock mass. Groundwater movements produce characteristic anomalies and their detection may provide information on the location of the fractured rock mass and hence aid in the structural interpretation of the area. The temperature gradient log amplifies small changes in the temperature log, making them easier to detect.

Large concentrations of metallic sulphides and oxides may perturb the isothermal regime locally since metallic minerals have very high thermal conductivities. This perturbation may be delineated with the high sensitivity temperature logging system. This, however, would be observed only in a thermally 'quiet' environment. In areas where there are numerous fracture zones with ground water movements, thermal anomalies due to ground water movements are much larger than those that would be caused by the presence of metallic minerals.

For more details on temperature logging, consult the following references: Bristow and Conaway, 1984 and Mwenifumbo, 1993.

A6.2 The Temperature Logging Probe Description

The ultra-high sensitivity temperature probe designed at the GSC has a 10 cm long and 7 mm diameter tip of thermistor beads with sensitivity of 0.0001 degrees Celsius. Changes in temperature of the fluid in the borehole are measured and sent as a digital signal to the surface. The signal is then converted into true temperature after correcting for the effect of the thermistor time constants; the temperature gradients are computed from the temperature data. All temperature logging is carried out during a downhole run so the sensor is measuring the temperature of the undisturbed fluid. The usual logging speed is 6 m/minute with data sampled every 1/5 of a second (approximately every 2 cm). This high spatial resolution of data is necessary to determine accurate temperature gradients.

A7. FULL WAVEFORM ACOUSTIC LOGGING

A7.1 Geological Interpretation of Full Waveform Acoustic Logs

In acoustic logging, a transmitter located in the borehole emits a pulse of mechanical energy which is recorded by one or more receivers located in the borehole some distance away from the transmitter (see Figure 7.1). In full waveform acoustic logging, the complete acoustic wave at each receiver is recorded digitally. The character of the acoustic signal that is detected by the receivers is affected by, among other things, the mechanical properties of the rock around the borehole.

Full waveform acoustic logs have many applications, such as:

1) The in-situ determination of compressional and shear wave velocities, which are useful in the interpretation of hole-to-hole seismic tomography and surface seismic data.

2) The compressional and shear velocities can be combined with data from a density logging tool to calculate formation elastic parameters such as Poisson's ratio, Young's modulus, the bulk modulus and the shear modulus, which are important parameters in many geotechnical engineering problems and in mine development.

3) The determination of porosity in porous rocks from the compressional wave velocity (Paillet and Cheng, 1991).

4) The measurement of permeability in porous rocks (Stoneley wave amplitude and velocity).

5) The detection of fractures and the measurement of fracture permeability (Stoneley wave amplitude).

6) Logs of compressional and shear wave velocity can be useful in hole-to-hole lithological correlation.

7) The compressional wave amplitude is used to determine the presence of cement grout behind steel casing and to assess the degree of bonding to the casing and the formation, in 'the cement bond log'.

A7.2 Principle of Full Waveform Acoustic Logging

Figure 7.1 illustrates how borehole acoustic measurements are made using a typical acoustic probe. The probe contains a single transmitter at the base of the probe and two receivers located above the transmitter.

A compressional (P) wave is generated in the borehole fluid by pulsing of the transmitter (Tx). P-waves are characterized by pressure oscillations that are parallel to the direction of propagation. Liquids can only support P-waves, however, solids can support both P-waves and S-waves (shear waves), in which the oscillations are perpendicular to the direction of propagation. The P-wave generated in the borehole radiates away from the transmitter in all directions. At the borehole wall, acoustic energy is reflected back into the borehole and refracted into the rock. Because solids can support both P-waves and S-waves, some of the acoustic energy that is refracted into the rock is converted to S-waves. Some of the energy that strikes the wall at the critical angle for P-waves (determined by the P-wave velocities in the rock and borehole fluid) will propagate as a P-wave along the borehole wall. Likewise, some of the energy that strikes the wall at the critical angle for S-waves (determined by the S-wave velocity in the rock and the P-wave velocity in the fluid) will propagate as an S-wave along the borehole wall. As these P- and S-waves travel along the borehole wall, energy is reradiated back into the borehole at the critical angles as P-waves. The energy that is reradiated back into the borehole is detected at the receivers.

If the compressional wave velocity in the borehole fluid is v_f and in the rock is v_p, and if the probe is centered in the borehole, the travel time from the transmitter (Tx) to the near receiver (Rx_1) is (see Fig. 7.1):

$$t_1 = \frac{a}{v_f} + \frac{b}{v_p} + \frac{a}{v_f}$$

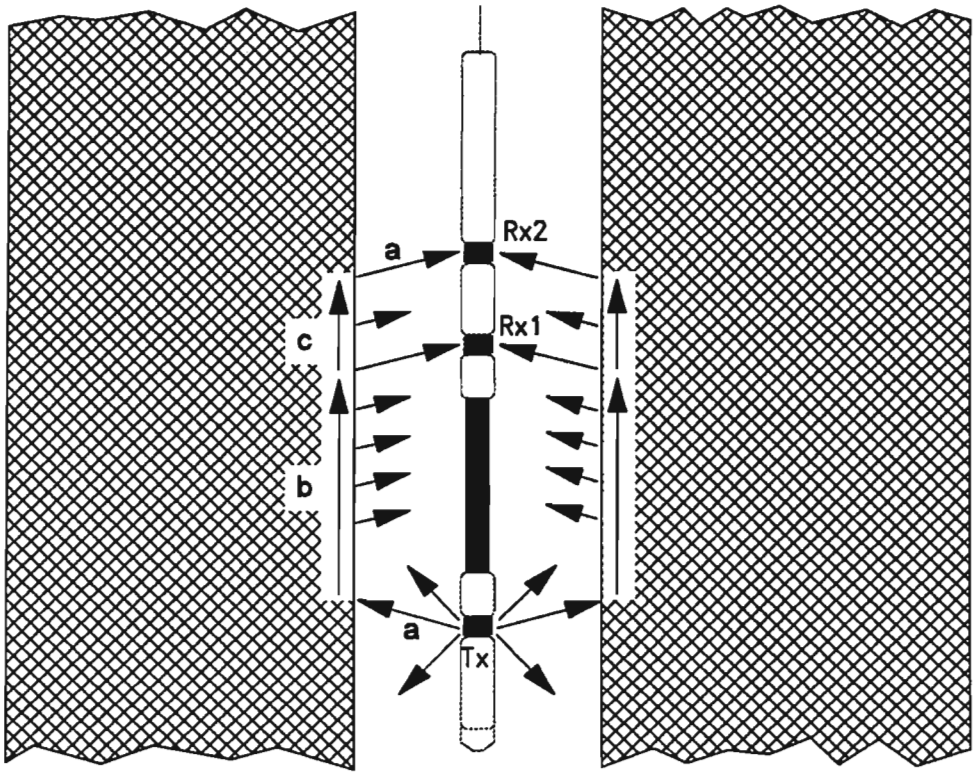

Figure 7.1 Acoustic Velocity Probe

The travel time to the far receiver (Rx_2) will be:

$$t_2 = \frac{a}{v_f} + \frac{b+c}{v_p} + \frac{a}{v_f}$$

The travel time in the rock between the two receivers is, therefore:

$$\Delta t = t_2 - t_1 = \frac{c}{v_p}$$

Thus, acoustic logging probes with two receivers record the travel time between receivers

divided by the receiver separation (the "interval travel time") in units of microseconds/foot.

In full waveform acoustic logging, the complete signal (full waveform) at each receiver is digitized and recorded, in addition to the interval travel time. The waveform signal consists of several different modes of acoustic energy. The P- and S-waves travelling along the borehole wall are known as 'head waves'. Their velocities in the rock are v_p, and v_s ($< v_p$). In addition to the head waves, other modes of acoustic energy are present in the full waveform that arise because acoustic energy that is incident on the borehole wall at angles greater than the critical angle is completely reflected back into the borehole (ie, the borehole acts as a waveguide). These modes are known as guided modes and include the compressional, shear normal, and the Stoneley or tube wave modes. Guided modes travel with velocities less than v_p and they may be prominent in the full waveform. The character of the waveform is determined by the mode content, which depends on such factors as the mechanical properties of the rock around the borehole, the compressional velocity in the borehole fluid, the source frequency and the borehole size. For instance, in "soft formations" in which the S-wave velocity in the rock is less than the P-wave velocity in the fluid, the shear head wave and shear normal modes are absent.

Because v_p is greater than v_s and the velocities of the guided modes, the P-wave through the rock arrives at the receivers first and is known as the "first arrival". The interval travel time that is recorded by acoustic logging systems corresponds to this first arrival. The first arrival is detected at each receiver by determining when the signal crosses a threshold level set by the operator. Two common sources of error in the interval travel time computed this way are caused by cycle skipping and noise. Both errors tend to cause spikes in the interval travel time log.

In cycle skipping, the waveform at the far receiver may be too weak for the first peak to cross the threshold and the acquisition program triggers on a later cycle in the waveform. When this happens, the recorded interval travel time will be too large by the amount of time between the first peak on the far waveform and the peak that actually crosses the threshold.

Noise that is present at the start of the waveform (caused by vibrations in the probe as it bumps along the borehole) may be strong enough at one or both receivers to cross the threshold. The computed interval travel time in this case may be larger or smaller than the real interval travel time, but it also generally appears as a spike on the travel time log. Noise is obvious on the full waveform as a non-flat signal ahead of the full waveform.

Acoustic logging requires water-filled boreholes to make good 'contact' with the surrounding rock. Full waveform acoustic logging is generally done in open (uncased) holes, however it is possible to determine P- and S-wave velocities is cased holes.

The depth of penetration in acoustic logging is about one wavelength, which is a function of source frequency and acoustic velocity. Typical source frequencies cover the range of

about 10 - 30 kHz and compressional wave velocities in hard rocks usually fall in the range of 5 - 8 km/s. The depth of penetration for P-waves for this tool is about 20 cm in hard rocks.

For more details on full waveform acoustic logging, consult the following references: Paillet et al, 1992; Paillet and Cheng, 1991; Astbury and Worthington, 1986a,b; Willis and Toksöz, 1983; Paillet and White, 1982; Cheng and Toksöz, 1981.

A7.3 The Mount Sopris Full Waveform Acoustic Logging Equipment

The full waveform acoustic logging probe used by the GSC (Mount Sopris Instruments Company, Model CLP 4681) is 45 mm in diameter and contains a piezoelectric transducer transmitter, with a center frequency of about 28 kHz, and two piezoelectric transducer receivers. The receivers are separated by a distance of 30 cm and the transmitter-receiver separations are 0.9 m and 1.2 m (3 ft and 4 ft). The transmitter is separated from the receivers by a flexible acoustic isolator to prevent acoustic energy from travelling directly to the receivers through the probe.

The transmitter pulses twice per second and the acoustic signal is digitized alternately by the two receivers for a period of about 1 millisecond at 4 microsecond intervals. The difference in arrival time of the acoustic signal at the two receivers provides a measure of the P-wave velocity in the rock every second. Logging speeds of 3 to 6 m/minute result in a sample depth interval of 5 to 10 cm for this tool.

A8. THE IFG 3-COMPONENT MAGNETIC / ORIENTATION PROBE

A major problem in exploration drilling is knowing exactly where drillholes go since they often deviate from the planned path by significant amounts, both in direction (azimuth) and dip. The GSC has partially supported the development (by IFG Corp. of Brampton, Ontario) of a new borehole orientation probe based on measurements with a 3-component fluxgate magnetometer and solid state tilt meters in the probe. The probe continuously monitors its movement in dip and direction as it moves down the hole at about 6 m/minute sending the data to the up-hole electronics for recording and display on a PC. Because the borehole orientation data are recorded every few centimeters in the hole, noisy parts of the record which may occur due to magnetic anomalies can be easily edited to provide accurate survey results. Most of the older techniques which relied on magnetic measurements were recorded at largely separated points in the hole and anomalous readings were hard to detect and ambiguous to interpret.

The 3-component magnetometer measurements are themselves of interest in mineral exploration for detecting the presence of magnetic bodies at some distance from the hole. The prototype version of the probe being used by the GSC, contains two sets of 3-component magnetometers and the application of borehole magnetic gradiometer measurements are also being investigated.

A9. PART A REFERENCES

Astbury, S. And Worthington, M.H.
1986a: The analysis and interpretation of full waveform sonic data. Part I: dominant phases and shear wave velocity. First Break, 4(4), pp. 7-16.

Astbury, S. And Worthington, M.H.
1986b: The analysis and interpretation of full waveform sonic data. Part II: multiples, mode conversions and reflections. First Break, 4(6), pp. 15-24.

Bogoslovsky, V.A. and Ogil'vy, A.A.
1970: Natural potential anomalies as a quantitative index of the rate of seepage from water reservoirs. Geophysical Prospecting, 18:261-268.

Bogoslovsky, V.A. and Ogil'vy, A.A.
1972: The study of streaming potentials on fissured media models (faults). Geophysical Prospecting, 20:109-117.

Bristow, Q. and Bernius, G.
1984: Field evaluation of a magnetic susceptibility logging tool; in Current Research, Part A, Geological Survey of Canada, Paper 84-1A, pp. 453-462.

Bristow, Q. and Conaway, J.G.
1984: Temperature gradient measurements in boreholes using low noise high resolution digital techniques; in Current Research, Part B, Geological Survey of Canada, Paper 84-1B, pp. 101-108.

Bristow, Q.
1985: A digital processing unit for the GeoInstruments magnetic susceptibility sensors, with analogue and RS-232C outputs; in Current Research, Part B, Geological Survey of Canada, Paper 85-1B, pp. 463-466.

Cheng, C.H. and Toksöz, M.N.
1981: Elastic wave propagation in a fluid-filled borehole and synthetic acoustic logs. Geophysics, 46(7), pp. 1042-1053.

Corwin, R.F. and Hoover, D.B.,
1979: The self-potential method in geothermal exploration. Geophysics, 44:226-245.

Hovdan, H. and Bolviken, B.,
1984: Sulphide self potentials in relation to oxygen content in drill-hole water. Geoexploration, 23:387-394.

Killeen, P.G.
1982: Borehole logging for uranium by measurement of natural gamma radiation - a review; International Journal of Applied Radiation and Isotopes, Vol. 34, No. 1, pp. 231-260.

Killeen, P.G.
1986: A system of deep test holes and calibration facilities for developing and testing new borehole geophysical techniques; in Borehole Geophysics for Mining and Geotechnical Applications, ed. P.G. Killeen, Geological Survey of Canada, Paper-85-27, 1986, pp. 29-46.

Killeen, P.G. and Mwenifumbo, C.J.
1988: Downhole assaying in Canadian mineral deposits with the spectral gamma-gamma method; in Current trends in nuclear borehole logging techniques for elemental analysis, IAEA-ECDOC-464, pp. 23-29

Mwenifumbo, C.J.
1989: Optimization of logging parameters in continuous, time-domain induced polarization measurements. in Proceeding of the Third International Symposium on Borehole Geophysics for Mineral, Geotechnical, and Groundwater Applications, Oct. 2-5, Las Vegas, Nevada, vol. 1, 201-232.

Mwenifumbo, C.J.
1990: Optimization of logging parameters in continuous time domain induced polarization measurements; in Proceedings of the 3rd International Symposium on Borehole Geophysics for Minerals, Geotechnical and Groundwater Applications, 2-5 Oct. 1989, Las Vegas, Nevada, paper N, p. 201-232.

Mwenifumbo, C.J.
1993: Temperature logging in mineral exploration. Journal of Applied Geophysics, 30:297-313.

Mwenifumbo, C.J. and Killeen, P.G.
1987: Natural gamma ray logging in volcanic rocks: the Mudhole and Clementine base metal prospects; in Buchans Geology, Newfoundland, ed. R.V. Kirkham; Geological Survey of Canada, Paper 86-24, pp. 263-272, Report 16, 1987.

Paillet, F.L. and Cheng, C.H.
1991: Acoustic Waves in Boreholes. CRC Press, Boca Raton, Florida, 264 p.

Paillett, F.L., Cheng, C.H. and Pennington, W.D.
1992: Acoustic-waveform logging - advances in theory and application. The Log Analyst, 33(3), pp. 239-257.

Paillet, F.L. and White, J.E.
1982: Acoustic modes of propagation in the borehole and their relationship to rock properties. Geophysics, 47(8), pp. 1215-1228.

Sato, M. and Mooney, H.M.
1960: The electrochemical mechanism of sulphide self potentials. Geophysics, 25:226-249.

Willis, M.E. and Toksöz, M.N.
1983: Automatic P and S velocity determination from full waveform digital acoustic logs. Geophysics, 48(12), pp. 1631-1644.

Wilson, H.C., Michel, F.A., Mwenifumbo, C.J. and Killeen, P.G.
1989: Application of borehole geophysics to groundwater energy resources; in Proceedings of the 3rd International Symposium on Borehole Geophysics for Minerals and Geotechnical Logging, 2-5 Oct., 1989, Las Vegas, Nevada, pp. 317-336.

AN OVERVIEW OF BOREHOLE GEOPHYSICAL RESEARCH AT THE GEOLOGICAL SURVEY OF CANADA

P.G. Killeen[1], L.D. Schock[1], B.E. Elliott[1], A. Cinq-Mars[1], CJ. Mwenifumbo[1], G. Bernius[1], W. Hyatt[1], and S. Birk[1]

P.G. Killeen, L.D. Schock, B.E. Elliott, A. Cinq-Mars, CJ. Mwenifumbo, G. Bernius, W. Hyatt, and S. Birk, An overview of borehole geophysical research at the Geological Survey of Canada; in Proceedings of the 4th International MGLS/KEGS Symposium on Borehole Geophysics for Minerals, Geotechnical and Groundwater Applications; Toronto, 18-22 August 1991

Abstract

Although surface and airborne geophysics are widely accepted in mineral exploration, adoption of borehole geophysics has lagged for two main reasons; 1) the shortage of case histories demonstrating the application of borehole geophysics to mineral exploration, and 2) the lack of suitable slim-hole instrumentation.

At the Geological Survey of Canada (GSC), the Borehole Geophysics Section of the Mineral Resources Division has addressed the first problem by demonstrating the benefits of borehole geophysics for mineral exploration. Calibration facilities have also been developed for quantification of borehole geophysical measurements by government, industry and universities. This has helped to stimulate the development of commercial mineral logging systems and services in Canada.

At the same time, the Instrumentation R&D Section has addressed the second problem by developing new technology required to record a complete data set comprising the geophysical signature of a mineral deposit and its host rock.

This paper briefly outlines the following activities of the Borehole Geophysics Section: calibration, applications and new technology.

A bibliography of selected references which provide more details about these activities is also included.

INTRODUCTION

The activities of the Borehole Geophysics Section can be described under three general topics: calibration, applications and technology (Fig. 1). Highlights of these activities follow.

CALIBRATION

Ideally, borehole geophysical logs should be quantitative measurements of physical parameters, instead of just an indication of the presence of high or low values of these parameters. To provide such quantitative logs, probes must be properly calibrated to determine their response in a known, controlled situation such as a physical model or borehole. Development of quantitative calibration methods must take place in conjunction with developments in technology and methodology as shown in Figure 2. For any given application, the methods will usually provide qualitative results at first, followed by technological adjustments which make calibration possible as well as desirable (e.g. the switch from analog recording to digital recording). The feedback from a quantitative measurement capability results in changes in methodology, or even in the hardware. This feedback process continues between the applications, and the calibration facilities and procedures until an established methodology for quantitative measurements is developed and widely accepted.

[1]Geological Survey of Canada, 601 Booth Street, Ottawa, Ontario, K1A 0E8

BOREHOLE GEOPHYSICS:
Taking Geophysics into the Third Dimension

Providing calibration facilities for industry, government and universities.

Demonstrating exploration, mining and geotechnical applications.

Developing innovative technology for borehole geophysics.

Figure 1

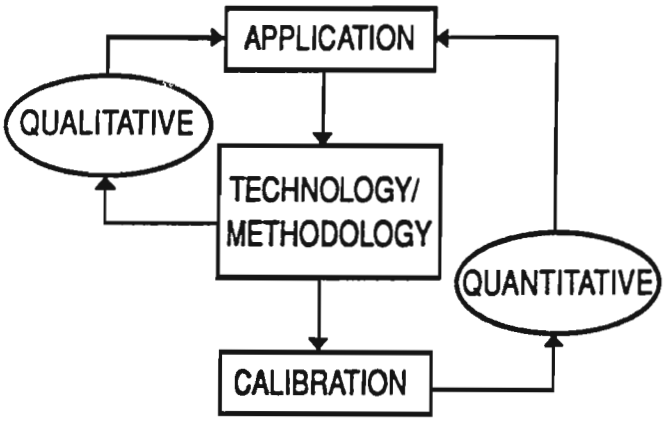

Figure 2

QUANTITATIVE MEASUREMENTS
Developing Calibration Methods

- Uranium Thorium Potassium Assays
- Density
- Magnetic Susceptibility

Figure 3

Figure 3 lists the parameters for which there are currently calibration activities at the GSC in support of quantitative measurements.

An overview of currently available Canadian calibration facilities is given by Schock et al. (in these Proceedings).

On the recommendation of the International Atomic Energy Agency (IAEA), the GSC is also leading an international project to cross reference gamma-ray calibration facilities around the world.

APPLICATIONS

The GSC-developed R&D logging system has demonstrated the application of borehole geophysics to minerals and geotechnical problems from coast to coast in Canada. The map in Figure 4 shows the broad diversity of applications studied by the Borehole Geophysics Section since 1974 and their wide distribution of locations across Canada.

Applications which the Borehole Geophysics Section has targeted for examination encompass both mineral exploration in mining districts across Canada and geotechnical problems, as shown in Figure 5. Applications include: delineating mineralized zones, identifying and mapping alteration associated with mineralization, lithologic interpretation and hole-to-hole stratigraphic correlation, in situ assaying of mineralization, determining in situ physical rock properties for use in the interpretation of ground and airborne geophysical data, detecting groundwater flow patterns within the holes, and groundwater energy research. Work has been done to characterize physical properties of mineral deposits including massive sulphides, and deposits of tin, lead, graphite, gold, coal, iron, and others.

NEW TECHNOLOGY

Figure 6 gives an overview of the logging methods currently in routine use by the Borehole Geophysics section, and Figure 7 details some of the interesting new technology currently being applied to borehole geophysical logging. The Borehole Geophysics Section, working with the Instrumentation R&D Section, attempts to push the leading edge of technology to increase the capability of extracting useful information from borehole geophysical measurements. In doing this, often new commercially developed technology (eg. borehole VLF and 3-component Mag) which is not yet widely used is applied to a variety of geological problems. Some insight into data processing, display and enhancement methods currently in use is given by Elliott (these Proceedings).

The technology and methodology outlined in Figure 7 are generally more advanced versions than those commonly available off the shelf. Some characteristics of some of these "advanced" methods are briefly described below, including both technology and methodology.

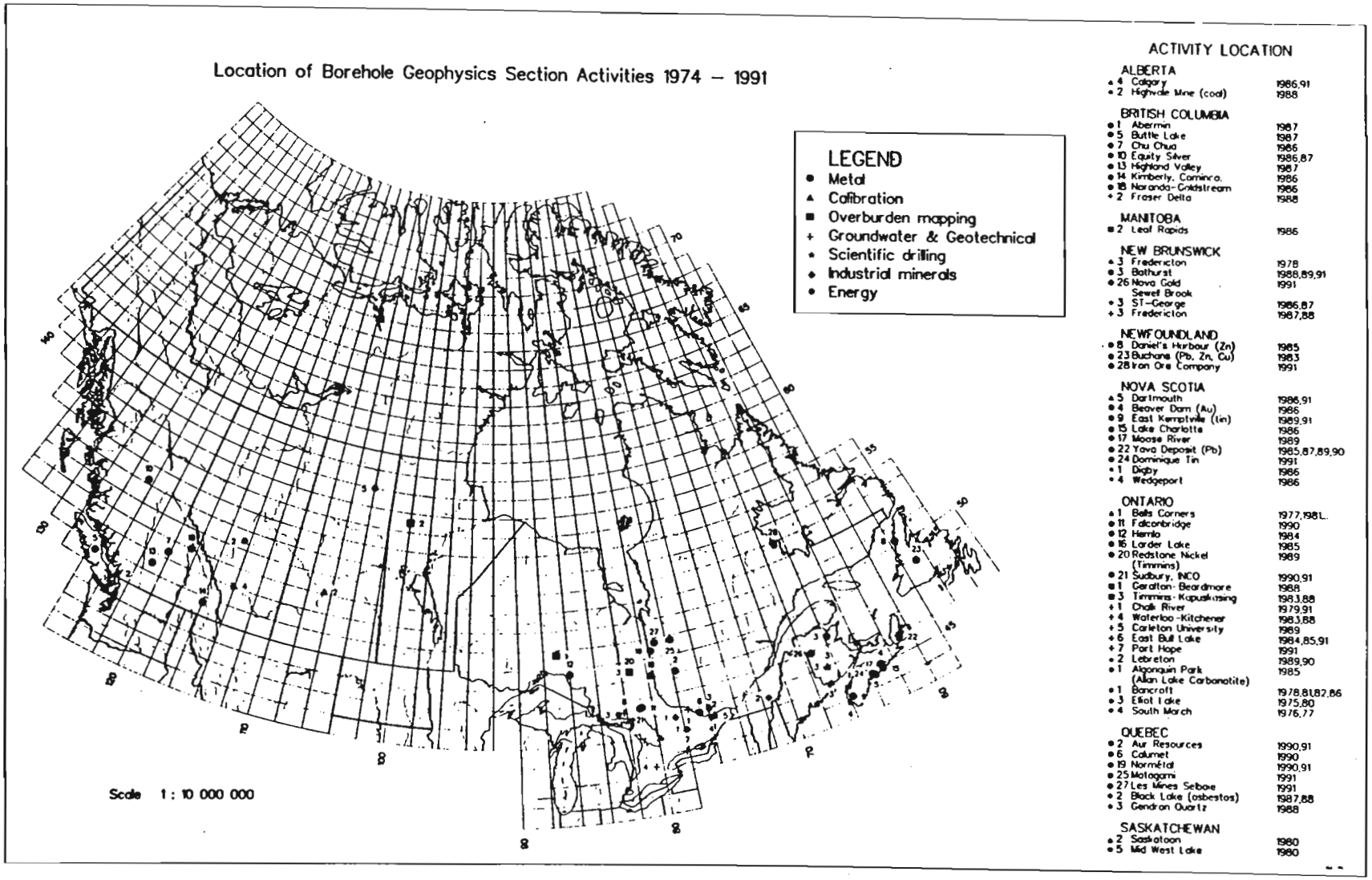
Location of Borehole Geophysics Section Activities 1974 – 1991
LEGEND
Metal
Calibration
Overburden mapping
Groundwater & Geotechnical
Scientific drilling
Industrial minerals
Energy
Scale 1 : 10 000 000
ACTIVITY LOCATION
ALBERTA
4 Calgary 1986,91
2 Highvale Mine (coal) 1988
BRITISH COLUMBIA
1 Abermin 1987
5 Buttle Lake 1987
7 Chu Chua 1986
10 Equity Silver 1986,87
13 Highland Valley 1987
14 Kimberly, Cominco 1986
18 Noranda-Goldstream 1986
2 Fraser Delta 1988
MANITOBA
2 Leaf Rapids 1986
NEW BRUNSWICK
3 Fredericton 1978
3 Bathurst 1988,89,91
26 Nova Gold Sewell Brook 1991
3 ST-George 1986,87
3 Fredericton 1987,88
NEWFOUNDLAND
8 Daniel's Harbour (Zn) 1985
23 Buchans (Pb, Zn, Cu) 1983
28 Iron Ore Company 1991
NOVA SCOTIA
5 Dartmouth 1986,91
4 Beaver Dam (Au) 1986
9 East Kemptville (tin) 1989,91
15 Lake Charlotte 1986
17 Moose River 1989
22 Yava Deposit (Pb) 1985,87,89,90
24 Dominique Tin 1991
1 Digby 1986
4 Wedgeport 1986
ONTARIO
1 Bells Corners 1977,198L.
11 Falconbridge 1990
12 Hemlo 1984
16 Larder Lake 1985
20 Redstone Nickel (Timmins) 1989
21 Sudbury, INCO 1990,91
1 Geraldton-Beardmore 1988
3 Timmins-Kapuskasing 1983,88
1 Chalk River 1979,91
4 Waterloo-Kitchener 1983,88
5 Carleton University 1989
6 East Bull Lake 1984,85,91
7 Port Hope 1991
2 Lebreton 1989,90
1 Algonquin Park (Allan Lake Carbonatite) 1985
1 Bancroft 1978,81,82,86
3 Eliot Lake 1975,80
4 South March 1976,77
QUEBEC
2 Aur Resources 1990,91
6 Calumet 1990
19 Normétal 1990,91
25 Matagami 1991
27 Les Mines Selbaie 1991
2 Black Lake (asbestos) 1987,88
3 Gendron Quartz 1988
SASKATCHEWAN
2 Saskatoon 1980
5 Mid West Lake 1980

Figure 4

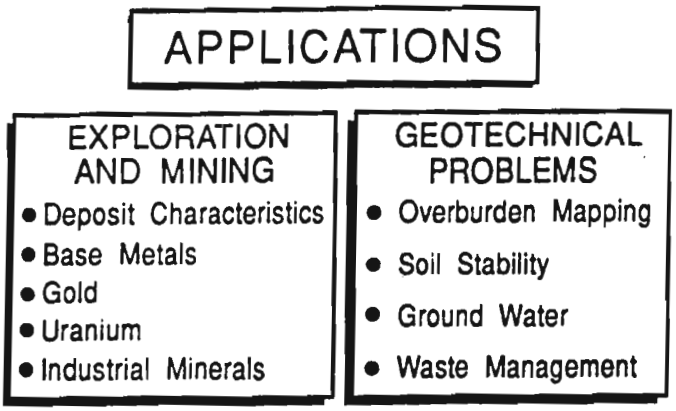

Figure 5

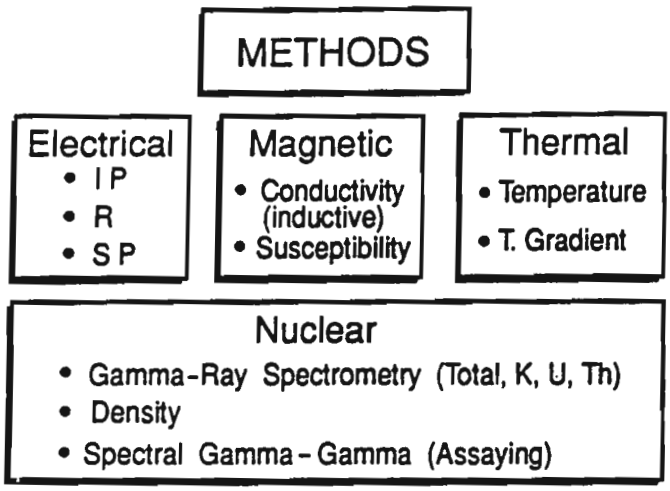

Figure 6

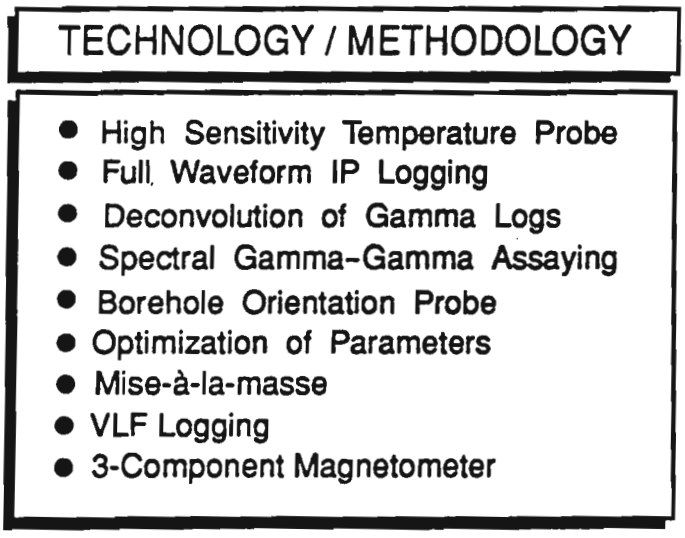

Figure 7

1) The high sensitivity temperature probe can measure to less than one ten-thousandth of a degree Celsius, which is about two orders of magnitude more sensitive than commonly used probes. (See eg. Mwenifumbo these Proceedings.)

2) The IP system measures the full waveform digitized every 4 milliseconds, whereas most systems record a maximum of 8 windows in the decay waveform during the 'off time'.

3) The gamma ray logs are from a spectrometric system with full spectral recording which provides information separately on natural radioactive isotopes of K, U and Th. (See eg. Elliott these Proceedings.)

4) The density logs are also based on a spectrometric system which not only provides density but also is a heavy element indicator which can be calibrated for assaying. (See eg. Killeen and Schock these Proceedings.)

5) The mise-à-la-masse method, long established for use in conductive deposits, is being used for a wide variety of new applications where conductivity contrasts exist.

6) The VLF logs include inphase and quadrature measurements of the E field and the three components of the H field. (See Cinq-Mars and Mwenifumbo these Proceedings.)

7) The magnetometer logs are measurements of the 3 components of the earth's magnetic field and forms part of the measurements of the borehole orientation in combination with solid state tilt sensors.

8) With respect to methodology, optimization of parameters for gamma-ray logging and IP logging have been investigated.

REFERENCES

The following six references are in Proceedings of the 4th International MGLS/KEGS Symposium on Borehole Geophysics for Minerals, Geotechnical and Groundwater Applications; Toronto, 18-22 August 1991, (i.e. in this volume).

Elliott, B.E. (1991) An Overview of Processing, Display and Enhancement Methods used on Borehole Geophysical Logging Data at the Geological Survey of Canada.

Schock, L.D., Killeen, P.G., Elliott, B.E. and Bernius, G.R. (1991) A Review of Canadian Calibration Facilities for Borehole Geophysical Measurements.

Killeen, P.G. and Schock, L.D. (1991) Borehole Assaying with the Spectral Gamma-Gamma Method: Some Parameters Affecting the SGG Ratio.

Mwenifumbo, C.J. (1991) Temperature Logging in Mineral Exploration.

Cinq-Mars, A. and Mwenifumbo, C.J. (1991) Downhole VLF E-Field and H-Field Logging.

Mwenifumbo,. C.J. (1991) Field Evaluation of Electrodes for Drillhole Self Potential Measurements.

BIBLIOGRAPHY

A) Papers Related to Calibration

Killeen, P.G. (1978) Gamma-ray spectrometric calibration facilities - a preliminary report; in Geol. Surv. Can., Paper 78-1A, p. 243-247.

Killeen, P.G. and Conaway, J.G. (1978) New facilities for calibrating gamma-ray spectrometric logging and surface exploration equipment; CIM Bull., Vol. 71, No. 793, p. 84-87.

Bernius, G.R. (1981) Boreholes near Ottawa for the development and testing of borehole logging equipment - a preliminary report; in Current Research, Part C, Geol. Surv. Can., Paper 81-1C.

Killeen, P.G., Bristow, Q. and Mwenifumbo, C.J. (1983) Gamma-ray logging for uranium: status of international efforts to resolve discrepancies in calibration models; in Transactions of the SPWLA (Society of Professional Well Log Analysts) 24th Annual Logging Symposium, Calgary. Paper AA, p. 1-16.

Killeen, P.G., Bernius, G.R., Schock, L. and Mwenifumbo, C.J. (1984) New developments in the GSC borehole geophysics test area and calibration facilities; in Current Research, Part B, Geological Survey of Canada, Paper 84-1B, p. 373-374.

Schock, L.D. and Killeen, P.G. (1985) Establishment of coal logging field calibration facilities: a progress report; in Current Research, Part B, Geol. Surv. Can., Paper 85-1B, p. 459-462.

Killeen, P.G. (1986) A system of deep test holes and calibration facilities for developing and testing new borehole geophysical techniques; in Borehole Geophysics for Mining and Geotechnical Applications, ed. P.G. Killeen, Geol. Surv. Can., Paper 85-27, 1986, p. 29-46.

Killeen, P.G. and Elliott, B.E. (1990) Model boreholes for gamma ray logging: Intercalibration of North American and European Calibration Facilities; in Transactions of the 13th SPWLA European Formation Evaluation Symposium, Budapest, Oct. 22-26, 1990, Paper GG, 14 pages.

B) Papers Related to Applications

Conaway, J.G. and Killeen, P.G. (1978) Quantitative uranium determinations from gamma-ray logs by application of digital time series analysis; Geophysics, Vol. 43, No. 6, p. 1204-1221.

Conaway, J.G. and Killeen, P.G. (1979) Gamma-ray spectral logging for uranium; CIM Bull., Vol. 73, No. 813, p. 115-123.

Killeen, P.G. (1979) Gamma ray spectrometric methods in uranium exploration - application and interpretation; in Geophysics and Geochemistry in the Search for Metallic Ores; Peter J. Hood, editor, Geol. Surv. Can., Economic Geology Report 31, p. 163-229.

Conaway, J.G., Bristow, Q. and Killeen, P.G. (1980) Optimization of gamma-ray logging techniques for uranium; Geophysics, Vol. 45, No. 2, p. 292-311.

Killeen, P.G. (1982) Borehole logging for uranium by measurement of natural gamma radiation - a review; International Journal of Applied Radiation and Isotopes, Vol. 34, No. 1, p. 231-260.

Killeen, P.G. (with Hallenburg, J.K., Furlong, V.L.R. and Duray, J.) (1982) Borehole logging for uranium exploration - a manual; IAEA Technical Report Series No. 212, 279 p.

Mwenifumbo, C.J. (1987) Mise-à-la-masse experiments in the Maclean Extension orebody, Buchans Mine, Newfoundland; in Buchans Geology, Newfoundland: ed. R.V. Kirkham, Geol. Surv. Can., Paper 86-24, p. 251-261.

Mwenifumbo, C.J. (1985) Mise-à-la-masse mapping of gold-bearing alteration zones at the Hoyle Pond gold deposit, Timmins, Ontario; in Current Research, Part A, Geol. Surv. Can., Paper 85-1A, p. 669-679.

Mwenifumbo, C.J. (1986) Drill hole Mise-à-la-masse IP and Potential measurements in a Zn-Pb- Cu sulphide deposit; in Borehole Geophysics for Mining and Geotechnical Applications, ed. P.G. Killeen, Geol. Surv. Can., Paper 85-27, p. 145-158.

Urbancic, T.I. and Mwenifumbo, C.J. (1986) Multiparameter logging techniques applied to gold exploration; in Borehole Geophysics for Mining and Geotechnical Applications, ed. P.G.Killeen, Geol. Surv. Can., Paper 85-27, p. 13-28.

Killeen, P.G. and Mwenifumbo, C.J. (1986) Current developments in nuclear techniques for coal logging in Canada; Proceedings of an Advisory Group Meeting on Gamma, X-Ray and Neutron Techniques for the Coal Industry; International Atomic Energy Agency, Vienna, 4-7

December 1984, p. 67-79.

Killeen, P.G. (with V.L.R. Furlong and D.C. George) (1986) Practical borehole logging procedures for mineral exploration, with emphasis on uranium; IAEA Technical Report Series No. 259, 44p.

Killeen, P.G. (1986) Borehole Geophysics for Mining and Geotechnical Applications, editor, P.G. Killeen, Geol. Surv. Can., Paper 85-27, 400 p.

Mwenifumbo, C.J. and Killeen, P.G. (1987) Natural gamma ray logging in volcanic rocks: the Mudhole and Clementine base metal prospects; in Buchans Geology, Newfoundland: ed. R.V. Kirkham, Geol. Surv. Can., Paper 86-24, p. 263-272.

Mwenifumbo, C.J. (1988) Cross-borehole Mise-à-la-masse mapping of fracture zones at the Bells Corners Borehole Geophysics Test Area, Ottawa, Canada; Proceedings of the 2nd International Symposium on Borehole Geophysics for Minerals, Geotechnical and Groundwater Applications, Oct. 6-8, 1987, Golden, Colorado, p. 151-165.

Mwenifumbo, C.J. (1989) The symmetrical lateral resistivity log in coal seam mapping, Highvale Mine, Alberta; in Current Research, Part D, Geol. Surv. Can., Paper 89-1D, p. 1-8.

Mwenifumbo, C.J., Thorleifson, L.H., Killeen, P.G. and Elliott, B.E. (1989) Preliminary results on the use of borehole geophysics in overburden stratigraphic mapping near Geraldton, northern Ontario; in Current Research, Part C, Geol. Surv. Can., Paper 89-1C, p. 305-311.

Mwenifumbo, C.J., Killeen, P.G. and Graves, M.C. (1990) Borehole geophysical logging at the Lake Charlotte Manganese Prospect, Meguma Group, Nova Scotia; in Mineral Deposit Studies in Nova Scotia, Volume 1, edited by A.L. Sangster, Geol. Surv. Can., Paper 90-8, p. 195-202.

Wilson, H.C., Michel, F.A., Mwenifumbo, C.J. and Killeen, P.G. (1990) Application of borehole geophysics to groundwater energy resources; in Proceedings of the 3rd International Symposium on Borehole Geophysics for Minerals and Geotechnical Logging, 2-5 Oct., 1989, Las Vegas, Nevada, Paper T, p. 317-336.

Killeen, P.G. (1991) Borehole geophysics: Taking geophysics into the third dimension; in GEOS, Vol. 20, No. 2, 1991, p. 1-10.

C) Papers Related to New Technology

Killeen, P.G., Conaway, J.G. and Bristow, Q. (1978) A gamma-ray spectral logging system including digital playback with recommendations for a new generation system; in Geol. Surv. Can., Paper 78-1A, p. 235-241.

Conaway, J.G., Killeen, P.G. and Hyatt, W.G. (1980) A comparison of bismuth germanate, cesium iodide, and sodium iodide scintillation detectors for gamma ray spectral logging in small diameter boreholes; in Current Research, Part B, Geol. Surv. Can., Paper 80-1B, p. 173-177.

Bristow, Q. and Killeen, P.G. (1982) Natural gamma-ray spectral logging using scintillation detectors; Proceedings of the Symposium on Uranium Exploration Methods, Review of the NEA/IAEA R&D Programme, Paris, 1st-4th June 1982, p. 777-792.

Bristow, Q. and Bernius, G.R. (1984) Field evaluation of a magnetic susceptibility logging tool; in Current Research, Part A, Geol. Surv. Can., Paper 84-1A, p. 453-462.

Bristow, Q. and Conaway, J.G. (1984) Temperature gradient measurements in boreholes using low noise high resolution digital techniques; in Current Research, Part B, Geol. Surv. Can., Paper 84-1B, p. 101-108.

Bristow, Q., Conaway, J.G. and Killeen, P.G. (1984) Application of inverse filtering to gamma-ray logs: a case study; Geophysics, Vol. 49, No. 8, p. 1369-1373.

Bristow, Q. (1986) A system for the digital transmission and recording of induced polarization measurements in boreholes; in Borehole Geophysics for Mining and Geotechnical Applications, ed. P.G. Killeen, Geol. Surv. Can., Paper 85-27, p. 127-143.

Bristow, Q. (1988) A multi-frequency slim hole inductive conductivity and magnetic susceptibility probe; in Proceedings of the 2nd International Symposium on Borehole Geophysics for Minerals, Geotechnical and Groundwater Applications, October 6-8, 1987, Golden, Colorado, p. 217-225.

Killeen, P.G. and Mwenifumbo, C.J. (1988) Interpretation of new generation geophysical logs in Canadian mineral exploration; in: 2nd International Symposium on Borehole Geophysics for Minerals, Geotechnical and Groundwater Applications, Oct. 6-8, 1987, Golden, Colorado, p. 167-178.

Killeen, P.G., Schock, L.D. and Elliott, B.E. (1990) A slim hole assaying technique for base metals and heavy elements based on spectral gamma-gamma logging; in Proceedings of the 3rd International Symposium on Borehole Geophysics for Minerals and Geotechnical Logging, 2-5 Oct., 1989, Las Vegas, Nevada, p. 435-454.

Mwenifumbo, C.J. (1990) Optimization of logging

parameters in continuous time domain induced polarization measurements; in Proceedings of the 3rd International Symposium on Borehole Geophysics for Minerals, Geotechnical and Groundwater Applications, Las Vegas, Nevada, Paper N, p. 201-232.

BOREHOLE GEOPHYSICS:

Taking Geophysics into the Third Dimension

by / par Patrick G. Killeen

GÉOPHYSIQUE DES SONDAGES:

Introduction de la géophysique dans la troisième dimension

THE ENERGY OF OUR RESOURCES - THE POWER OF OUR IDEAS

L'ÉNERGIE DE NOS RESSOURCES - NOTRE FORCE CRÉATRICE

Coloured Insert Pages 28 to 39

BOREHOLE GEOPHYSICS: TAKING GEOPHYSICS INTO THE THIRD DIMENSION

by Patrick G. Killeen

In oil and mineral exploration and in geotechnical engineering, scientists drill boreholes to obtain information in the third dimension after surface work has been completed. Unfortunately, adequate information from traditional diamond drill core samples or rotary drill chip samples is often difficult to obtain. Borehole geophysical logs, records of in-hole geophysical measurements plotted as a function of depth in the hole, can augment existing data.

Borehole Geophysics (or Borehole Logging) is the science of interpreting geophysical measurements made with probes lowered into boreholes.

Borehole geophysics is widely accepted in petroleum exploration, but its adoption for mineral exploration has lagged for two main reasons: the shortage of case histories demonstrating the application of borehole geophysics to mineral exploration; and the lack of suitable slim-hole instrumentation.

At the Geological Survey of Canada (GSC), Mineral Resources Division's Borehole Geophysics and Instrumentation R&D sections have attacked these two aspects of the problem. We demonstrate the benefits of borehole geophysics for mineral exploration and help stimulate the development of commercial mineral logging systems and services in Canada.

We are also developing the new technology required for a complete information package comprising the geophysical signature of a mineral deposit and its host rock. This includes developing calibration facilities for quantitative borehole geophysical measurements by government, industry and universities.

The Borehole Geophysics Section examines applications to mineral exploration in mining districts across Canada and to

Figure 1 Main components of the GSC digital borehole logging system.

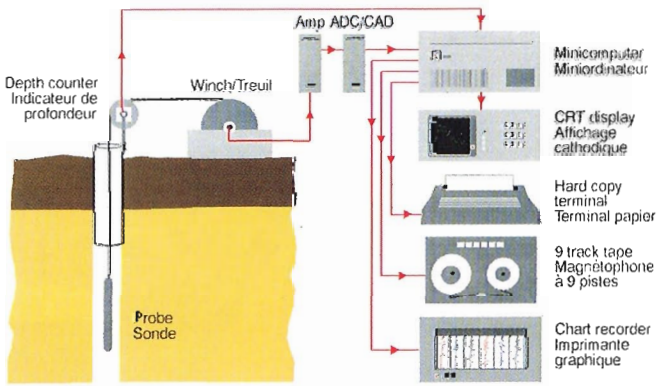

Cover:
Steve Birk lowers a probe into a borehole near the GSC's logging truck.

Couvert:
Steve Birk faisant descendre une sonde dans un forage près du camion de diagraphie de la CGC.

GÉOPHYSIQUE DES SONDAGES : INTRODUCTION DE LA GÉOPHYSIQUE DANS LA TROISIÈME DIMENSION

par Patrick G. Killeen

Dans les domaines de l'exploration pétrolière et minérale et du génie géotechnique, les scientifiques forent des trous de sonde pour obtenir de l'information dans la troisième dimension, une fois que leurs travaux de surface sont achevés. Malheureusement, il est souvent difficile d'obtenir une information suffisante en recourant aux carottes de forage obtenues au moyen de foreuses aux diamants ou à partir des copeaux obtenus à l'aide de foreuses à percussion. La géophysique des sondages (ou diagraphie géophysique), qui enregistre des mesures géophysiques effectuées dans le forage en fonction de la profondeur, permet d'accroître l'information dont disposent les scientifiques.

La géophysique des sondages est la science de l'interprétation des mesures géophysiques effectuées au moyen de sondes que l'on fait descendre dans les forages.

La géophysique des sondages est une science qui est maintenant largement acceptée dans l'exploration pétrolière, mais que l'on tarde à utiliser dans l'exploration minérale pour deux raisons principales; le manque d'histoires de cas démontrant l'application de la diagraphie géophysique à l'exploration minérale et l'absence d'instruments convenables pour effectuer des sondages dans les forages de petite dimension.

Figure 1 Principales composantes du système de diagraphie géophysique numérique de la CGC.

La Section de la géophysique des sondages de la Division des ressources minérales et la Section de recherche et développement en instrumentation de la Commission géologique du Canada (CGC) se sont attaquées à ces deux aspects du problème. Nous démontrons les avantages de la diagraphie géophysique en exploration minérale et aidons à favoriser la mise au point de systèmes et services de diagraphie minérale commerciale au Canada.

Nous développons également la nouvelle technologie nécessaire pour obtenir un ensemble d'informations comprenant la signature géophysique du gisement minéral et des roches qui l'abritent. Cela inclut la mise sur pied d'installations d'étalonnage

geotechnical problems. Applications include delineating mineralized zones, identifying and mapping alteration zones associated with mineralization, lithologic interpretation and hole-to-hole stratigraphic correlation, *in situ* assaying of mineralization, determining *in situ* physical rock properties for use in interpreting ground and airborne geophysical data, and detecting groundwater flow patterns within the holes.

This article describes the fundamentals of borehole geophysics, presents examples of applications, explains some new technological developments and finally describes calibration facilities and test sites developed for quantitative measurements.

Figure 2 Principles of borehole gamma-ray spectral logging.

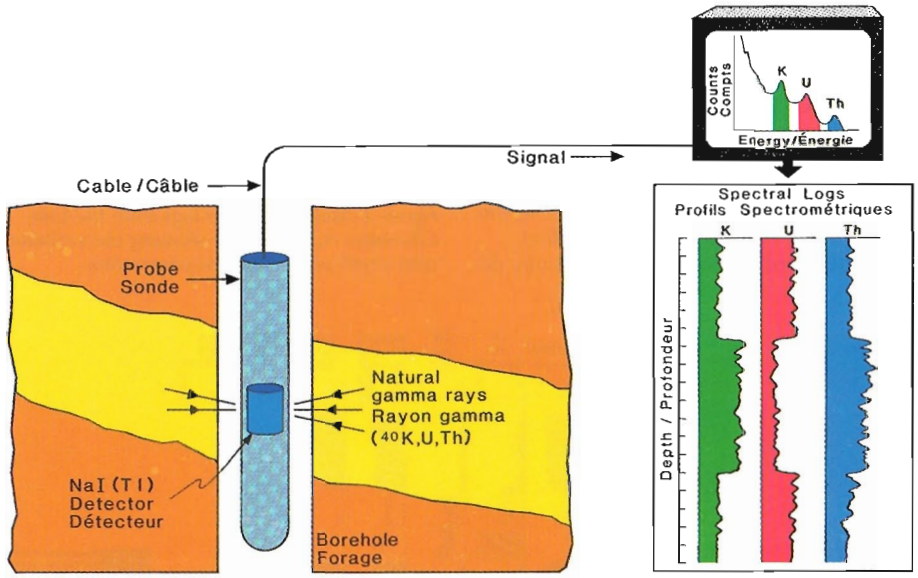

Figure 2 Principes de la diagraphie géophysique spectrale de rayons gamma.

pour les mesures quantitatives de diagraphie géophysique par le gouvernement, l'industrie et les universités.

La Section de la géophysique des sondages examine les applications possibles à l'exploration minérale canadienne ainsi qu'aux problèmes géotechniques. Parmi ces applications, on note la délimitation des zones minéralisées, l'identification et la cartographie des zones d'altération associées à la minéralisation, l'interprétation lithologique, la corrélation stratigraphique d'un forage à un autre, l'échantillonnage in situ de la minéralisation et la détermination in situ des propriétés physiques des roches utilisées dans l'interprétation du sol et les données géophysiques aéroportées, et la détection des modèles de circulation des eaux souterraines au sein des forages.

Cet article décrit les fondements de la géophysique des sondages, donne des exemples de ses applications, explique quelques-uns des nouveaux développements technologiques et décrit les installations d'étalonnage et les sites expérimentaux mis au point pour les mesures quantitatives.

Borehole Geophysical Logging System

The digital logging system (Fig. 1) comprises

- a borehole probe containing a geophysical sensor
- a logging cable and winch which carry the signal to surface instruments and power the probe
- a depth counter attached to a wellhead pulley for tracking the probe's location in the hole
- an analog-to-digital converter (ADC) to digitize the signal for recording
- a computer, with keyboard and display monitor, to enter logging parameters and display information
- a nine-track magnetic tape recorder
- a chart recorder to print out hard copy in the field.

The system, mounted in a four-wheel drive truck, has five logging tools (probes) with sensors that can measure thirteen physical parameters.

Spectral Gamma-Ray (TC, K, U, Th) Logging Tool. Gamma-ray measurements detect variations in the natural radioactivity originating from uranium (U), thorium (Th) and potassium (K) in rocks. The probe's

Système de diagraphie géophysique

Le système de diagraphie numérique (fig. 1) comprend

- une sonde de forage contenant un détecteur géophysique
- un treuil et un câble de diagraphie qui transmet le signal aux instruments de surface et alimente la sonde
- un indicateur de profondeur rattaché à une poulie de tête de puits pour déterminer l'emplacement de la sonde dans le forage
- un convertisseur analogue-digital (CAD) pour numériser le signal pour l'enregistrement
- un ordinateur, avec clavier et moniteur, pour inscrire les paramètres de diagraphie et étaler l'information
- un magnétophone à neuf pistes
- une imprimante graphique.

Le système monté dans un camion à quatre roues motrices, est muni de cinq sondes avec détecteurs qui peuvent mesurer treize paramètres physiques.

Sonde spectrométrique de rayon gamma (CT, K, U, Th). La sonde spectrométrique détecte les radiations gamma naturelles émises par l'uranium (U), le thorium (Th) et le potassium (K) présents dans les roches. Le détecteur de la sonde est un détecteur à scintillation à iodure de sodium. L'enregistrement se produit lorsque l'on descend ou remonte la sonde dans le forage à une vitesse d'environ 3 m/minutes. Contrairement à une sonde de rayons gamma qui n'enregistre que le nombre de rayons gamma détecté, la sonde spectrométrique de rayons gamma enregistre également l'énergie de chaque rayon gamma détecté. Les éléments K, U et Th produisent des rayons gamma ayant des énergies caractéristiques de sorte que les chercheurs peuvent évaluer les concentrations individuelles des trois radioéléments.

L'énergie des rayons gamma sont triées dans la mémoire de l'ordinateur à chaque seconde selon un spectre d'énergie (fig. 2). Quatre fenêtres sont présélectionnées: trois fenêtres sont centrées sur les maximums du spectre, et la quatrième mesure le compte total. Ces quatre chiffres représentent le potassium, l'uranium, le thorium et le compte total (CT) détectés au cours de la période d'une seconde durant laquelle s'effectue le comptage.

Ces données (incluant la profondeur) sont enregistrées sur ruban magnétique et imprimante graphique afin de produire des profils spectrométriques de rayons gamma.

sensor is a sodium iodide scintillation detector and logging occurs while lowering or raising the probe in the hole at about 3m/minute. Unlike an ordinary gamma-ray tool which only counts gamma rays, the spectral gamma-ray tool also measures the energy of each gamma ray detected. K, U and Th produce gamma rays with characteristic energies so researchers can estimate the individual concentrations of the three radioelements.

Gamma-ray energies are sorted into an energy spectrum in the computer memory each second (Fig. 2). The number of gamma rays in three pre-selected energy windows centered over peaks in the spectrum is computed, as is the total gamma-ray count. These four numbers represent potassium, uranium, thorium and Total Count (TC) detected during that one second counting time.

These data (including depth) are recorded on magnetic tapes and on the chart recorder to produce gamma-ray spectral logs. The spectrum in computer memory is then erased to receive the next one-second spectrum. By using two blocks of memory and a flip-flop arrangement, the new spectrum is actually acquired in one block while the previous one is being processed. In this way no data are lost during processing as the probe moves continuously up the borehole. These logs are important for detecting changes in radioelement concentrations which indicate alteration zones, and for providing information on rock types.

The Induced Polarization (IP/R/SP) Logging Tool consists of an assembly of electrodes placed in the borehole, usually including current electrodes and potential (measurement) electrodes. A square wave current with an 'off' time between positive and negative parts of the waveform is transmitted (waveforms may be from 1 second to 8 seconds duration). Potential measurements made at selected times in the waveform can be related to the IP effect (chargeability of the rocks), the resistivity (R) of the rocks, and to self-potentials (SP) generated in the rocks. The transmitter is a constant current source located at the surface.

Temperature (T) Logging Tool. The ultra-high sensitivity temperature probe designed at the GSC has a 10 cm long tip of thermistor beads with sensitivity of 0.0001°C (Fig. 3). Temperature changes of the fluid in the borehole are measured and sent as a digital signal to the surface. The signal is then converted into true temperature after correcting for the effect of thermistor time constants; temperature gradients are computed from temperature data. Temperature logging is carried out during downhole runs so the sensor

Figure 3 GSC-developed, 25mm diameter, high sensitivity temperature probe showing internal circuitry and nose-piece containing thermistor sensors.

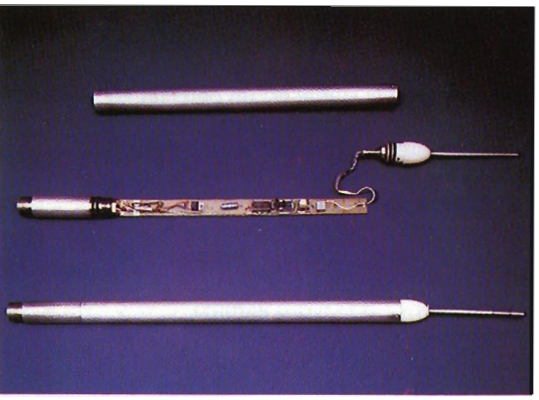

Figure 3 Sonde de température à haute sensibilité de 25 mm de diamètre, mise au point par la CGC; on peut apercevoir le circuit interne et la pointe dotée de thermistors.

Le spectre dans la mémoire de l'ordinateur est ensuite effacé afin de laisser place à un autre enregistrement spectral d'une seconde. En utilisant deux blocs de mémoire et un système d'interchangeabilité, le nouveau spectre est enregistré dans un bloc pendant que s'effectue le traitement du bloc précédent. De cette façon, il n'y a aucune perte de données durant le traitement à mesure que la sonde se déplace de façon continue dans le forage.

Ces diagraphies sont importantes pour détecter les changements dans les concentrations de radioéléments indiquant des zones d'altération, et fournissant de l'information sur le type de roches.

La sonde de polarisation provoquée (PP/R/PS) consiste en un regroupement d'électrodes placées dans le trou de forage, incluant habituellement des électrodes de courant de même que les électrodes de potentiel. Un courant d'onde carrée avec un temps «d'arrêt» entre les parties positive et négative de l'onde est transmis (le cycle de l'onde peut varier 1 à 8 secondes). Des mesures de potentiel effectuées à des intervalles de temps prédéfinis durant le cycle peuvent être reliées à l'effet de chargeabilité (PP : aptitude des roches à emmagasiner une charge électrique), à la résistivité (R) des roches, et à la polarisation spontanée (PS) générés dans les roches. Le transmetteur est une source de courant constant situé à la surface.

Sonde de température (T). La sonde de température à très haute sensibilité fut conçue à la CGC. Sa pointe de 10

Figure 4 Multiparameter logs from the Lake Charlotte, N.S. borehole showing the variation with depth of 11 different parameters.

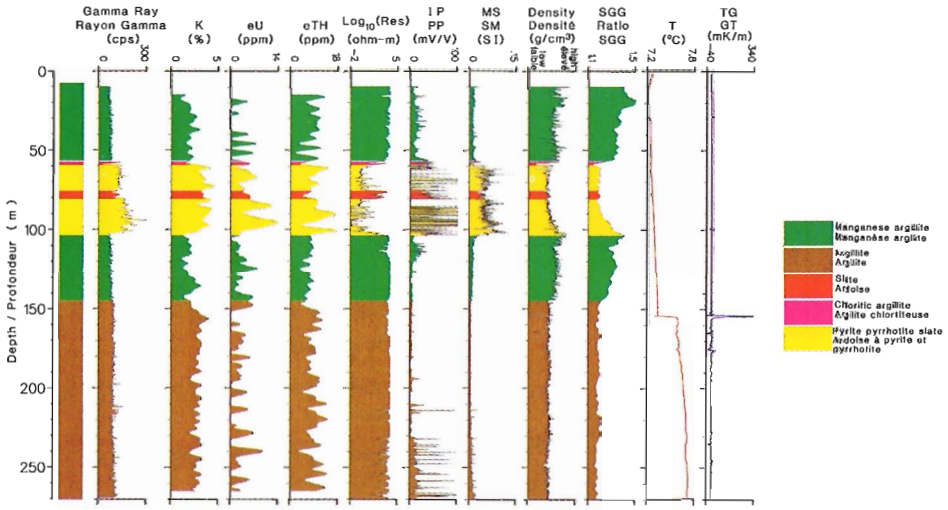

Figure 4 Multiparamètres diagraphiques à Lake Charlotte, N.-É., montrant la variation avec la profondeur de 11 différents paramètres.

centimètres est composée d'une série de thermistors possédant une sensibilité de 0,0001 °C (fig. 3). Les changements de température du fluide dans le forage sont mesurés et transmis sous forme de signal numérique à la surface. Le signal est ensuite converti en température réelle après une correction pour les effets des constantes de temps des thermistors; les gradients de température sont calculés à partir des données de température. L'enregistrement s'effectue durant la descente de la sonde pour que les détecteurs puissent mesurer la température du fluide alors qu'il n'est pas perturbé. Généralement, la vitesse d'enregistrement est de 6 m/min et des données sont échantillonnées chaque 1/5 sec (environ à tous les 2 cm). Cette résolution spatiale élevée est nécessaire si l'on veut déterminer des gradients de température précis. Les gradients de

measures undisturbed fluid. Usual logging speed is 6m/minute with data sampled every 1/5 of a second (approximately every 2 cm). This high spatial resolution is necessary if accurate temperature gradients are to be determined from temperature data. Temperature gradient measurements detect changes in the thermal conductivity of the rocks along the borehole or water flow through fractures.

The Spectral Gamma-Gamma (SGG) Logging Tool is essentially the spectral gamma-ray logging tool with a 10-millicurie (370MBq) gamma-ray source (e.g.60Co) added on the probe's nose. The energy spectrum of the source's backscattered gamma rays is recorded over an energy range of approximately 0.03 to 1.0 MeV. Density information is determined from the count rate from about 0.20 MeV to 0.5 MeV. Information about the rock's elemental composition (assays) can be obtained from the shape of the backscattered spectrum (SGG ratio).

The Magnetic Susceptibility (MS) Logging Tool measures magnetic susceptibility and electrical conductivity. Magnetic susceptibility measurements indicate the presence of magnetite and other magnetic minerals. Since measurements are made inductively, the tool can be used inside plastic casing. Because tool parameters are optimized for magnetic susceptibility measurements, electrical conductivity values are limited to a high conductivity range, (mostly massive sulphides or equivalent conductors). Susceptibility data are acquired continuously and five readings are taken every second. Usually the logging speed is 6 m/minute, providing samples every 2 cm along the hole. Changes in the MS log can be correlated with lithology.

Running all logging tools, **multiparameter logging**, in each hole will maximize information. In a given geological environment, some logs will provide valuable data, while others may measure parameters which show little variation and prove to be relatively uninformative. Experience, as well as knowledge of the physical properties of rocks and minerals are crucial to selecting which geophysical measurements to make.

Multiparameter geophysical measurements made in a borehole at Lake Charlotte, Nova Scotia, detected carbonaceous, pyrrhotite- and pyrite-rich black slates and a manganese-rich argillite (Fig. 4). Slates have a much higher gamma-ray count than argillites. Argillites with manganese mineralization have a higher density and SGG ratio, and a lower potassium content than slates. The pyrrhotite/pyrite-rich slates that overlie the manganiferous argillites

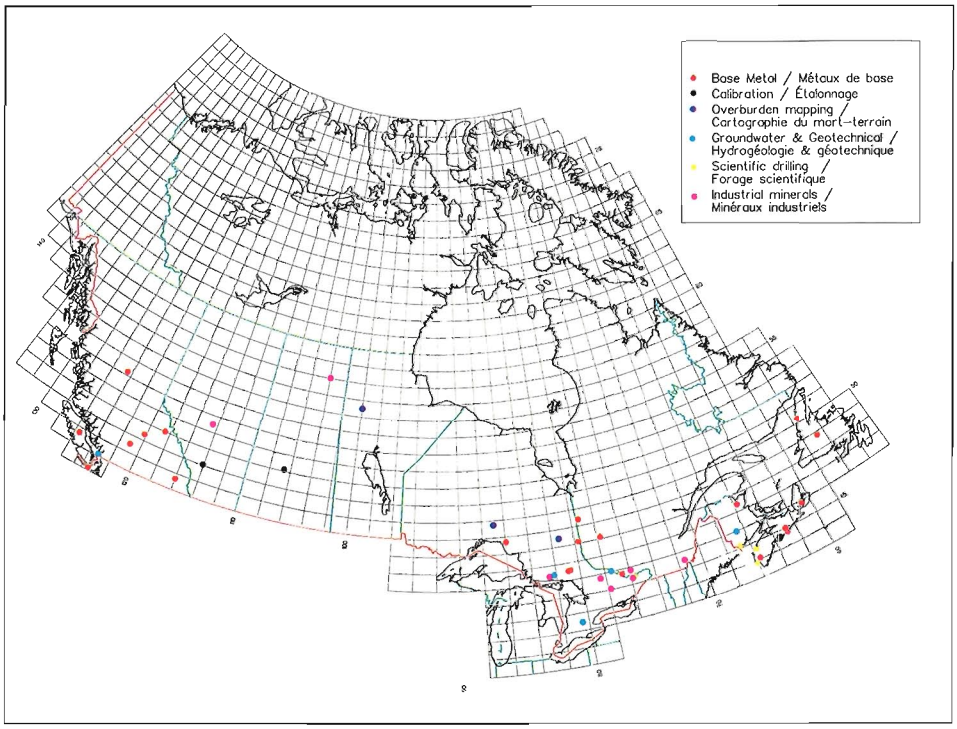

Figure 5 Locations and type of borehole geophysical investigations conducted by the Borehole Geophysics Section.

Figure 5 Localisation des différents types de projets diagraphiques menés par la Section de la géophysique des sondages.

température permettent de détecter les changements dans la conductivité thermique des roches le long du forage, et la circulation d'eau à travers les fractures.

Le sonde spectrale gamma-gamma (SGG) est essentiellement de la sonde de spectrométrie de rayons gamma avec une source de rayons gamma (p. ex., ^{60}Co) de 10 millicuries (370 MBq) ajoutée à l'extrémité de la sonde. Les rayons gamma diffusés sont enregistrés sur une bande énergétique d'environ 0,03 à 1,0 MeV. La densité est déterminée à partir des comptes d'énergie d'environ 0,20 MeV à 0,5 MeV. La composition élémentaire de la roche (étalonnage)peut être obtenue à partir de la forme du spectre des rayons gamma diffusés (ratio SGG).

La sonde de susceptibilité magnétique (SM) mesure la susceptibilité magnétique et la conductivité électrique. Les mesures de susceptibilité magnétique indiquent la présence de magnétite et d'autres minéraux magnétiques. Étant donné que les mesures s'effectuent par induction, la sonde peut être utilisée dans un forage possèdant un tubage de plastique. Comme les paramètres de la sonde sont optimisés pour les mesures de susceptibilité magnétique, les valeurs de conductivité électrique sont limitées à un domaine élevé de conductivité (surtout aux sulfures massifs ou aux conducteurs équivalents). On obtient des données de susceptibilité de façon continue et on prend 5 lectures à chaque seconde. La vitesse habituelle de la sonde est de 6 m/min, ce qui permet d'obtenir des échantillons tous les 2 cm le long du forage. Des changements dans le profil SM peuvent être corrélés à la lithologie.

On arrive à maximiser l'information en utilisant les différentes sondes multiparamètres diagraphiques dans chaque forage. Dans un environnement géologique donné, certaines sondes fourniront des données précieuses, tandis que d'autres mesureront des paramètres qui indiquent très peu de variation et fournissent ainsi relativement peu d'information. L'expérience de même que la connaissance des propriétés physiques des roches et des minéraux sont essentielles lorsque l'on effectue le choix des techniques de diagraphiques que l'on effectuera.

La diagraphie multiparamétrique effectuée dans un forage à Lake Charlotte, Nouvelle-Écosse, a permis de détecter des ardoises carbonatées contenant beaucoup de pyrrhotites et de pyrites et des argilites à manganèse (fig. 4). Les ardoises ont un compte de rayons gamma beaucoup plus élevé que les argilites. Les argilites à manganèse ont une densité et un ratio SGG plus élevés et une teneur en potassium plus basse que les ardoises. Les ardoises riches en pyrrhotite et en pyrite qui recouvrent les argilites à manganèse possèdent une susceptibilité magnétique plus élevée et une résistivité plus basse, de même qu'un effet PP plus fort et une activité naturelle de rayons gamma élevée. Les scientifiques peuvent réussir à cartographier les ardoises

Figure 6 Hole-to-hole lithologic correlation in volcanic rocks using gamma-ray, magnetic susceptibility and density logs.

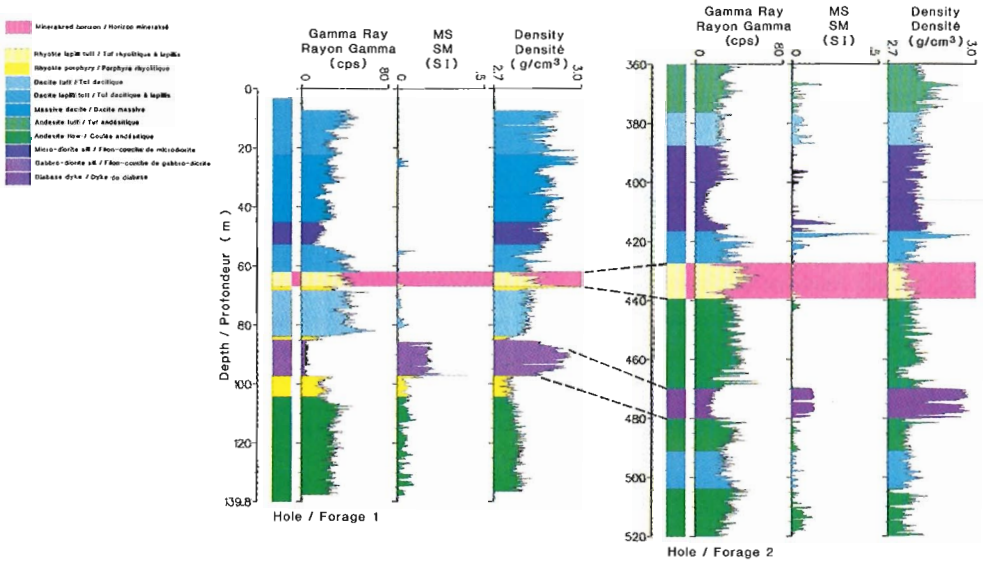

Figure 6 Corrélation lithographique d'un forage à l'autre dans des roches volcaniques en utilisant les diagraphies de rayons gamma, de susceptibilité magnétique et de densité.

noires et les argilites adjacentes en utilisant ces paramètres au cours des levés géophysiques en surface.

Applications

Le système de diagraphie mis au point par la CGC a démontré que l'on pouvait appliquer la diagraphie géophysique aux minéraux et aux problèmes géotechniques partout au Canada (fig. 5). Ces applications comprennent, notamment, des études relatives aux métaux de base, à l'étalonnage, à la cartographie du mort-terrain, aux problèmes reliés aux eaux souterraines et géotechniques, aux forages scientifiques et aux minéraux industriels.

Ceinture de roches vertes. Il est relativement difficile d'effectuer un sondage géologique des carottes de forage pour l'exploration minérale dans la ceinture de roches vertes en raison des différents types de roches qui se ressemblent. Les sondes de diagraphie géophysique mesurent des propriétés physiques invisibles aux géologues et viennent par conséquent compléter les observations effectuées dans les sondages géologiques - et permettent de ce fait d'obtenir une vérification objective. Cette méthode permet également d'établir une corrélation stratigraphique entre les forages, de détecter les altérations potassiques et d'établir une distinction entre

have higher magnetic susceptibility and lower resistivity as well as a stronger IP effect and high natural gamma-ray activity. Scientists may be able to map the black slates and adjacent manganiferous argillites by using these parameters in surface geophysical surveys.

Because information on borehole geophysical measurements related to mineral exploration problems is scarce, the GSC usually runs multiparameter logs in every hole. This provides more information on the response of borehole logging tools in different environments.

Applications

The GSC-developed R&D logging system has demonstrated the application of borehole geophysics to minerals and geotechnical problems from coast to coast (Fig. 5). Applications have included studies related to base metals, calibration, overburden mapping, groundwater and geotechnical problems, scientific drilling and industrial minerals.

Greenstone belts. Geological logging of drill cores for mineral exploration in a greenstone belt is relatively difficult because the different rock types encountered are visually similar.

Figure 7 High sensitivity temperature (T) and temperature gradient (G) logs showing water flow in fractures in two holes.

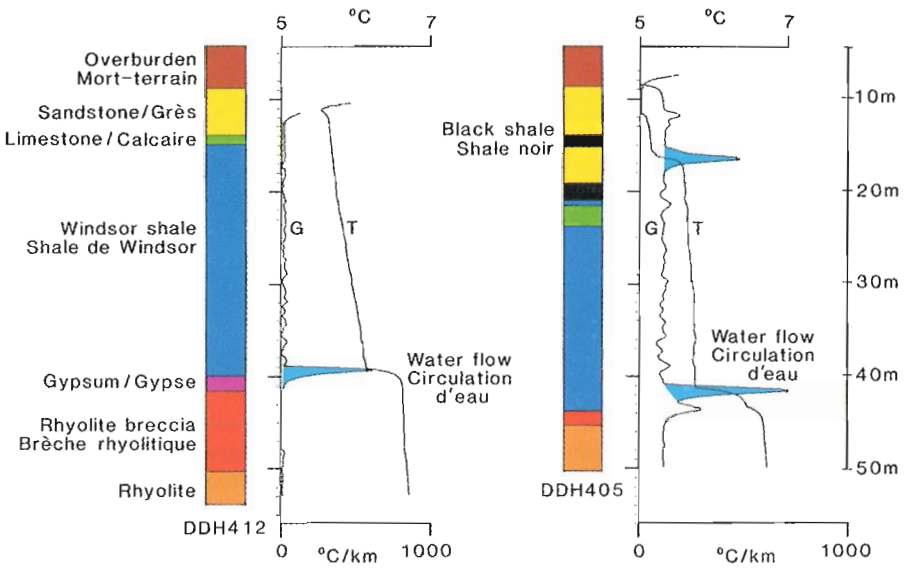

Figure 7 Diagraphie de température à haute sensibilité (T) et de gradient de température (G) montrant la circulation d'eau dans les fractures décelées dans deux forages.

les filons-couches et les coulées volcaniques...

La diagraphie géophysique de deux forages à Normétal, Québec, démontre les possibilités de corrélation de la stratigraphie volcanique (fig. 6). Nous avons cherché à déterminer si les signatures géophysiques des différentes lithologies (coulées de basalte, coulées acides, dykes) sont différentes. Même si les dykes sont fréquents dans cette région, et semblables visuellement aux coulées basiques, on peut facilement les distinguer en utilisant la diagraphie géophysique. Les dykes sont caractérisés par une faible émission de rayons gamma et une susceptibilité magnétique élevée comparativement aux roches volcaniques.

La corrélation entre le dyke à 90 m dans le forage 1 et à 475 m dans le forage 2 devient facilement apparente si l'on se réfère à la signature caractéristique des trois paramètres. La zone minéralisée se situe de 20 à 30 mètres au-dessus du dyke. Tous les dykes que l'on a retracés dans les forages

Figure 8 Gamma-ray log in volcanic rocks near Buchans, Newfoundland.

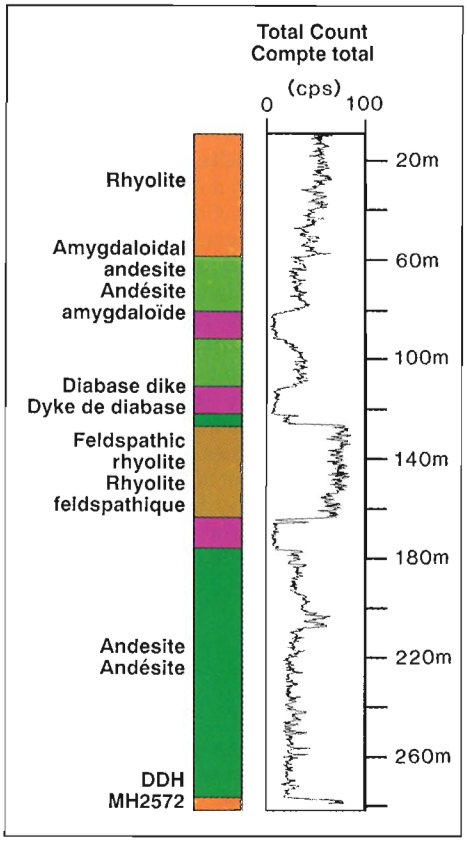

Figure 8 Diagraphie de rayons gamma dans les roches volcaniques près de Buchans, Terre-Neuve.

ont une faible radioactivité et une susceptibilité magnétique élevée mais ils n'ont pas tous la densité élevée des dykes associés à la minéralisation.

On peut retracer beaucoup plus de dykes avec la diagraphie géophysique qu'avec les sondages géologiques. Nous avons également déterminé les zones d'altération potassique de cette région là où la signature naturelle de rayons gamma s'accroît d'une façon significative.

Détection des fractures et circulation d'eau. Les sondages de la température de deux forages du gisement de plomb Yava en Nouvelle-Écosse (fig. 7) indique des changements de température distincts aux endroits où l'eau entre dans le forage à travers les fractures ou les joints présents dans la roche. Ces emplacements sont encore plus évidents dans les diagraphies de gradient de température et se traduisent par des maximums dans le profil (gradients élevés). Par exemple, un maximum localise la zone située juste au-dessus de la brèche rhyolitique dans les deux forages. L'information que l'on obtient est d'un intérêt particulier pour les ingénieurs miniers lors de la conception de mines.

Geophysical logging tools measure physical properties invisible to the geologist and therefore complement observations made in geological logs - in effect an objective verification. Potential uses include correlating stratigraphy between holes, recognizing potassic alteration and distinguishing between sills and flows, and so on.

Geophysical logs of two holes in Quebec's Normetal area show the possibilities for correlating volcanic stratigraphy (Fig. 6). We sought to determine if the geophysical signatures of different lithologies (basalt flows, acidic flows, dikes, etc.) are diagnostic. Although dikes in the section are common and visibly similar to basic volcanic flows, they are easily distinguished using the geophysical logs. The dikes, for example, are characterized by low gamma-ray response and high magnetic susceptibility compared with the volcanics.

The correlation between the dike at 90m in hole 1 and 475m in hole 2 is readily apparent by the characteristic signature of three parameters. The mineralized zone of interest occurs 20 to 30m above this dike. All dikes encountered in the holes show low radioactivity and high magnetic susceptibility but not all have the high density of the dike associated with the mineralization.

Many more dikes can be identified from geophysical logs than from geological logs. We also determined that, in this area, potassic alteration is readily apparent where the natural gamma-ray signature is significantly increased.

Fracture/waterflow detection. The temperature logs in two holes at Nova Scotia's Yava lead deposit (Fig. 7) show

Figure 9 Gamma-ray, density, spectral gamma-gamma ratio and magnetic susceptibility logs through two mineralized zones at the Hemlo gold deposit, Ontario.

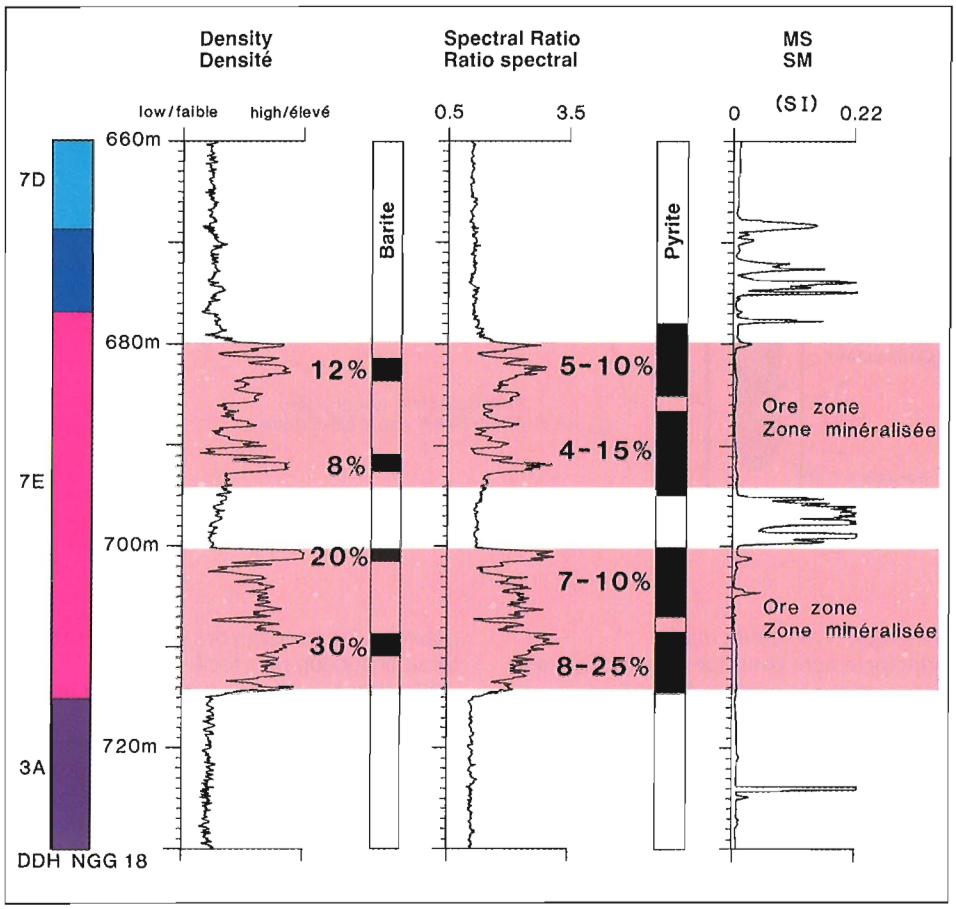

Signature thermique des sulfures. Même s'il est établi que les plus grands changements de température surviennent généralement lorsqu'il y a circulation d'eau, le gradient de température est également proportionnel à la conductivité thermique des roches. Par exemple, la sphalérite possède une conductivité thermique plus élevée que la plupart des roches et des

Figure 9 Diagraphies de rayons gamma, de densité, de ratio spectral gamma-gamma et de susceptibilité magnétique dans deux zones minéralisées du gisement aurifère d'Helmo, Ontario.

distinct temperature changes at locations where water enters the hole through fractures or joints in the rock. These locations are even more evident in the T-gradient logs which show large peaks (high gradients). The zone just above the rhyolite breccia occurs in both holes. This information is of particular interest to mining engineers for designing mines.

Thermal signature of sulphides. Although water flows generally give the largest temperature change, the temperature gradient is also proportional to the rocks' thermal conductivity. Sphalerite, for example, has a higher thermal conductivity than most rocks and minerals. A massive sulphide consisting primarily of sphalerite will therefore have almost the same temperature at the top as at the bottom, instead of the normal increase of temperature with depth. This produces an almost zero gradient value in the T-gradient log. We observed such distortion of the natural isotherms; distortion should be detectable in holes close to a sphalerite body.

Geological interpretation. Geological logging in volcanic and volcanoclastic rocks is difficult. Often the core must be logged a second time for reinterpretation as new information becomes available. Logging drillcore would be much easier and less subjective if a suite of geophysical logs were available to the geologist. The gamma-ray log (Fig. 8) indicates how a single log can aid geological interpretation. Feldspathic rhyolite has the highest gamma-ray count and diabase dikes the lowest. Between these two extremes, in order of increasing gamma count are: andesite, amygdaloidal andesite and rhyolite. Geologists did not note any difference in the zone between 190 and 210m; the gamma-ray log suggests that the zone should be rhyolite.

The Hemlo gold deposits, Ontario. Around Hemlo, gold occurs in a complex sequence of metamorphic rocks. Companies working in the area have attempted to subdivide the sequence of very similar rocks by calling them, for example, 'quartz-mica-schists' or 'siliceous-mica-schists.' Gold is associated with high barite content in strongly pyritized zones. These zones have low magnetic susceptibility values, high densities and high spectral gamma-gamma ratios (Fig. 9). The barite and pyrite cannot be distinguished by the SGG ratio log or the density log, but the distribution of these combined heavy minerals is clearly evident in greater detail in the logs than in the assay estimates.

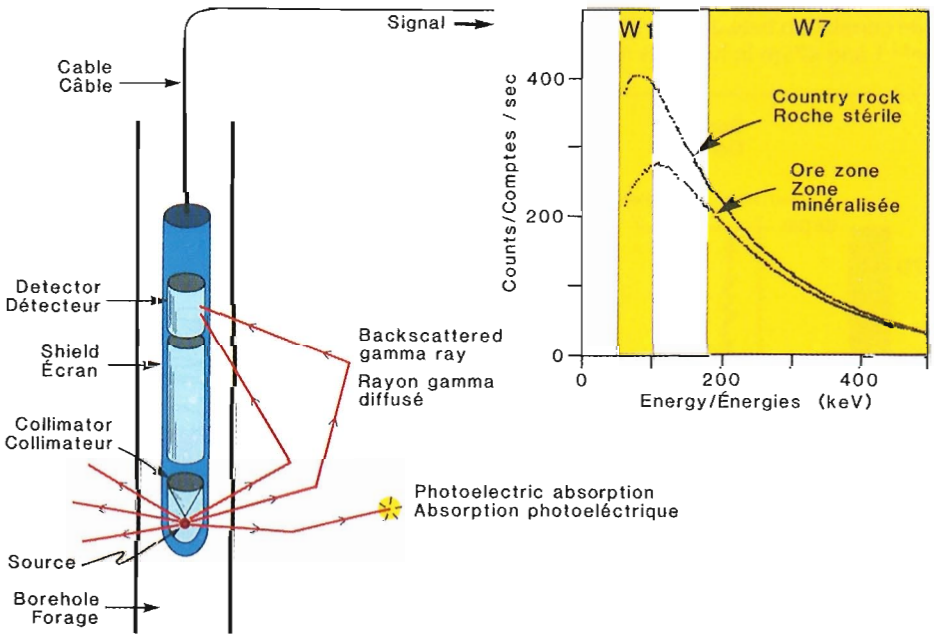

Figure 10 Principle of the spectral gamma-gamma (SGG) method used to develop a borehole assaying system.

Figure 10 Principe de la méthode spectrale gamma-gamma (SGG) utilisée pour mettre au point un système d'étalonnage dans un forage.

Le gisement aurifère d'Hemlo, Ontario. Autour d'Hemlo, l'or se retrouve dans une séquence complexe de roches métamorphiques. Les compagnies qui travaillent dans ce secteur ont tenté de subdiviser les séquences de roche très semblables en les appelant, par exemple, «schistes à quartz et mica» ou «schistes siliceux à mica». L'or est associé avec un contenu élevé de barite dans des zones fortement pyritisées. Ces zones ont des valeurs peu élevées de susceptibilité magnétique, de hautes densités et des ratios spectraux gamma-gamma élevés (fig. 9). La barite et la pyrite ne peuvent être distinguées par la diagraphie du ratio SGG ou la diagraphie de densité, mais la distribution de ces minéraux lourds combinés est clairement plus évidente et de façon plus détaillée dans les diagraphies que dans les estimations d'échantillonnages.

Nouveau développement technologique

Nous avons mis au point une nouvelle sonde diagraphique, la **sonde spectrale gamma-gamma** capable d'effectuer des étalonnages in situ dans un forage, fondés

minéraux. Un sulfure massif principalement constitué de sphalérite sera par conséquent presque à la même température du sommet et à la base du forage, plutôt qu'un accroissement normal de température en fonction de la profondeur. Cela donne une valeur du gradient de presque zéro dans le profil du gradient de température. Nous avons pu observer de telles distorsions des isothermes naturels; cette distorsion devrait être facilement détectée dans les forages situés près d'une masse de minerai de sphalérite.

Interprétation géologique. Il est difficile d'effectuer un sondage géologique dans les roches volcaniques et volcanoclastiques. Il faut parfois vérifier la carotte une seconde fois pour obtenir une réinterprétation à mesure que l'on obtient de l'information nouvelle. Le sondage des carottes de forage serait beaucoup plus facile et moins subjectif si le géologue pouvait avoir accès à toute une série de diagraphies géophysiques. La diagraphie de rayons gamma (fig. 8) indique jusqu'à quel point une simple diagraphie peut aider à effectuer l'interprétation géologique. La rhyolite feldspathique possède le compte le plus élevé de rayons gamma et les dykes de diabase, le moins élevé. Entre ces deux extrêmes, les éléments suivants ont un compte de rayon gamma qui va en s'élevant: l'andésite, l'andésite amygdaloïde et la rhyolite. Les géologues n'ont pu noter aucune différence dans la zone située entre 190 et 210 m; la diagraphie de rayons gamma suggère que cette zone devrait être constituée de rhyolite.

New Technological Developments

We have developed a new logging tool, a **spectral gamma-gamma probe**, capable of making *in situ* assays in a borehole based on the different interactions of gamma rays with barren rocks and mineralized zones. Adding a gamma-ray source to the nose of a spectral gamma-ray probe turns it into a spectral gamma-gamma (SGG) probe (Fig. 10). Gamma rays from the source are scattered in the rock before they reach the detector; the gamma-ray energy spectrum contains information about the rock.

Changes in rock density will cause changes in the count at both high and low ends of the gamma-ray energy spectrum. In general, increased rock density causes a decrease in the number of gamma rays recorded at both ends. However, if heavy elements are present in an ore zone, low energy gamma rays are also decreased by photoelectric absorption.

Thus the log can indicate a heavy element (as demonstrated at the Yava lead deposit), and can be calibrated to produce an assay tool for quantitative determination of the heavy element concentration along the borehole, without resorting to chemical assaying of the core.

Qualitative results have been obtained at a zinc deposit in Newfoundland in which the SGG method clearly showed the zinc-rich zones and provided detailed information on sphalerite distribution within the zones.

The innovative **full-wave recording time domain IP logging system** for acquiring time domain induced polarization (IP) borehole logs has been developed by the GSC's Instrumentation R&D Section. Using a unique method similar in concept to the full energy-spectrum recording of the gamma-ray spectral logging system, the complete measured potential waveform from an IP system is recorded in digital form. Because the entire waveform is recorded on magnetic tape, sections can be selected for subsequent processing of the data if desired, to improve results.

The IP probe (Fig. 11) consists of an electronics section containing a battery pack and a current electrode, and below it on a flexible cable, two additional electrodes between which the potentials are measured. The voltage-to-frequency converter in the probe converts the measured potentials to a digital signal that is sent up the cable. These digital signals are not subject to the electrical noise which interferes with signals on analog systems.

The transmitter on the surface puts out a current in the form of a square wave. The

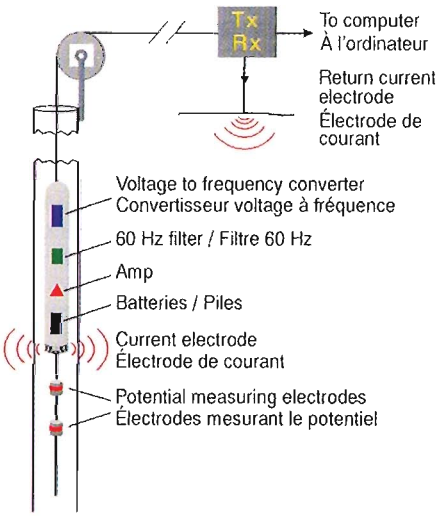

Figure 11 Components of a GSC-developed full-wave recording Induced Polarization (IP) logging system.

Figure 11 Composantes du système d'enregistrement de polarisation provoquée (PP) mis au point par la CGC.

sur les différentes interactions de rayons gamma avec les roches stériles et les zones minéralisées. Nous convertissons la sonde spectrale gamma-gamma (SGG) en ajoutant une source de rayons gamma à l'extrémité de la sonde spectrale de rayons gamma (fig. 10). Les rayons gamma provenant de la source sont dispersés dans la roche avant d'atteindre le détecteur; le spectre d'énergie des rayons gamma contient l'information au sujet de la roche.

Les changements de densité dans la roche entraîneront des changements dans le compte aux niveaux les plus élevés et les plus bas du spectre d'énergie de rayons gamma. En général, une densité accrue de la roche entraîne une diminution du nombre de rayons gamma enregistrés aux deux niveaux extrêmes du spectre. Cependant, s'il y a présence d'éléments lourds dans une zone de minerai, les rayons gamma à basse énergie sont également diminués par absorption photoélectrique.

La diagraphie peut donc indiquer la présence d'un élément lourd (comme il a été démontré au gisement de plomb de Yava), et peut être étalonnée en vue de produire un instrument d'étalonnage pour la détermination quantitative de la concentration de l'élément lourd le long du forage, sans qu'il soit nécessaire de recourir à des échantillonnages chimiques sur la carotte.

On a obtenu des résultats qualitatifs dans un gisement de zinc à Terre-Neuve où la méthode SGG a clairement démontré l'existence de zones riches en zinc et a fourni de l'information détaillée sur la distribution de la sphalérite au sein de ces zones.

Le **système innovateur de diagraphie par enregistrement à ondes entières** de la polarisation provoquée dans le domaine du temps en vue d'obtenir des diagraphies de forage par polarisation provoquée dans le domaine du temps (PP) a été mise au point par la Section de recherche et développement en instrumentation de la CGC. En utilisant une méthode unique et semblable à l'idée de l'enregistrement complet du spectre énergétique sous forme d'onde du système de diagraphie spectrale de rayons gamma, la courbe de potentiel entièrement d'un système PP est enregistrée sous forme numérique. Étant donné que la courbe de potentiel est enregistrée sur ruban magnétique, on peut choisir des intervalles particuliers pour traiter subséquemment certaines données si on le désire, en vue d'améliorer les résultats.

La sonde PP (fig. 11) possède une section électronique contenant un ensemble de batteries et une électrode de courant, et en-dessous, sur un câble souple, deux électrodes supplémentaires entre lesquelles les potentiels sont mesurés. Le convertisseur du voltage en fréquence dans la sonde convertit les potentiels mesurés en un signal numérique qui est transmis vers le haut le long du câble. Ces signaux numériques ne sont pas assujettis au bruit électrique qui crée de l'interférence dans les signaux sur des systèmes analogues.

Le transmetteur à la surface émet un courant sous forme d'onde carrée. Le transmetteur est contrôlé par ordinateur. Celui-ci émet le courant qui est ajusté par étapes numériques à mesure que les potentiels changent, maintient le signal à peu près au même niveau. Ce système est idéal pour l'étude des effets de la courbe par polarisation provoquée. Selon certains chercheurs, la forme de la courbe de la décharge PP est caractéristique des minéraux qui la causent. Le système a permis de détecter une pyritisation associée à des gisements aurifères à Larder Lake, et a établi une distinction entre les argiles polarisables et les autres sédiments.

La nouvelle sonde magnétomètre/orientation à trois composantes. Un des principaux problèmes que l'on rencontre dans les

computer-controlled transmitter, in which the output current is adjusted in digital steps as the measured potentials change, keeps the signal at approximately the same level. This system is ideal for studying the spectral IP effect. Some researchers think that the shape of the IP decay curve is characteristic of the minerals causing it. The system has detected pyritization associated with gold deposits at Larder Lake, and has distinguished polarizable clays from other sediments.

The new 3-component magnetometer/ orientation probe. A major problem in exploration drilling is knowing exactly where drillholes go, since they often deviate significantly from the planned path both in direction (azimuth) and dip. The GSC has helped a private company develop a new borehole orientation probe based on measurements with a three-component fluxgate magnetometer and solid state tilt meters.

The probe (Fig. 12) continuously monitors dip and direction as it moves down the hole at about 6m/minute sending data to the up-hole electronics for recording and display. Because the borehole orientation data are recorded every few centimeters in the hole, noisy parts of the record which may occur due to magnetic anomalies can be easily edited to provide accurate survey results.

The three-component magnetometer measurements are themselves of interest in mineral exploration for detecting magnetic bodies at some distance from the hole. The GSC's prototype version of the probe contains two sets of three-component magnetometers. Researchers are also investigating the application of borehole magnetic gradiometer measurements.

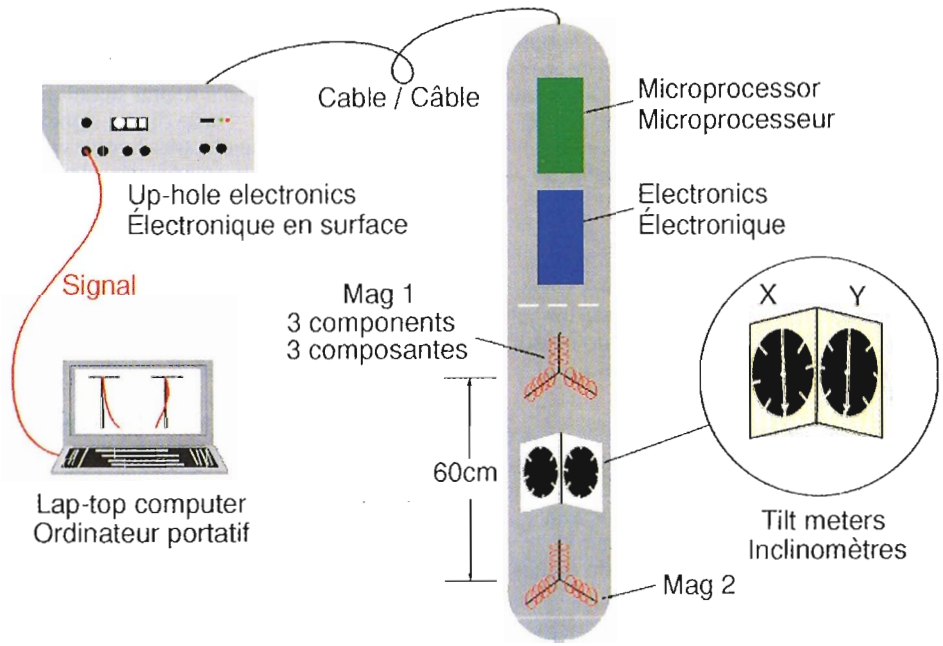

Calibration for Quantitative Measurements

Ideally, borehole geophysical logs should be quantitative measurements of physical parameters, instead of just an indication of the presence of high or low values of the parameter. Quantitative logs are easier to compare from hole to hole, from area to area, and from year to year than qualitative logs. For example, quantitative logs recorded in a hole in Manitoba in 1987 can be accurately compared to similar logs recorded in Nova Scotia in 1990. To provide such quantitative logs, probes must be properly calibrated to determine their response in a known, controlled situation such as a physical model of a borehole.

Initially the GSC constructed **model boreholes** to calibrate spectral gamma-ray probes. The model in Figure 13 is concrete, and the 'ore' zone, located between two barren zones, contains some naturally radioactive materials such as pitchblende uranium ore. Because we know the uranium ore grade in the model, we can derive a calibration factor for converting counts per second to uranium

Figure 12 Three-component magnetometer/orientation probe recently developed by industry with GSC support.

Figure 12 Sonde magnétomètre orientation à trois composantes récemment mise au point par l'industrie avec l'aide de la CGC.

Étalonnage pour des mesures quantitatives

De façon idéale, les diagraphies géophysiques devraient représenter des mesures quantitatives des paramètres physiques, plutôt qu'une simple indication de la présence de valeurs élevées ou basses du paramètre. Les diagraphies quantitatives sont plus faciles à comparer d'un forage à l'autre, d'un secteur à l'autre, et d'une année à l'autre que les diagraphies qualitatives. Par exemple, les diagraphies quantitatives enregistrées dans un forage au Manitoba en 1987 peuvent être comparées avec exactitude à des diagraphies semblables enregistrées en Nouvelle-Écosse en 1990. Afin de fournir de telles diagraphies quantitatives, les sondes doivent être étalonnées de façon appropriée pour que l'on puisse déterminer leur réaction dans une situation connue et contrôlée telle qu'un modèle physique de forage.

Au début, la CGC a construit des modèles de forage pour étalonner les sondes spectrales de rayons gamma. Le modèle qui apparaît à la figure 13 est en béton, et la zone radioactive située entre deux zones

forages d'exploration est de savoir exactement où les trous de forage vont étant donné qu'ils dévient souvent considérablement du chemin prévu à la fois en ce qui concerne la direction (azimuth) et la plongée. La CGC a aidé une société privée à mettre au point une nouvelle sonde d'orientation de forage fondée sur les mesures obtenues au moyen d'un magnétomètre à solénoïde à noyau saturable à trois composantes et des inclinomètres.

La sonde (fig. 12) surveille de façon continue la plongée et la direction à mesure qu'elle descend dans le forage à environ 6 m/min tout en transmettant les données au système électronique en surface pour l'enregistrement et le déploiement. Comme les données sur l'orientation du forage sont enregistrées à chaque parcours de quelques centimètres dans le forage, les parties bruyantes de l'enregistrement qui se produisent en raison des anomalies magnétiques peuvent être supprimées sur le ruban en vue d'obtenir des résultats de levés précis.

De plus, les mesures du magnétomètre à trois composantes revêtent un intérêt particulier pour l'exploration minérale du fait qu'elles peuvent permettre de détecter des gisements de minerai magnétique à une certaine distance du forage. Le prototype de la sonde de la CGC comprend deux magnétomètres à trois composantes. Les chercheurs font également certains travaux sur les applications possibles des mesures de gradients magnétiques dans les forages.

concentrations in parts per million (ppm) or per cent.

Nine model boreholes, constructed in 1977 at Bells Corners west of Ottawa, contain 'ore' zones with different concentrations of potassium, uranium and thorium for calibration of spectral gamma-ray probes. These models have become important standards and are used by government, industry and university groups for calibration.

Figure 13 Principle of gamma-ray probe calibration in a concrete model borehole containing a synthetic uranium ore zone.

Worldwide intercalibration. A true 'standard', such as the calibration models, must be standard with respect to the rest of the world and meet international 'standards.' When the GSC developed its model boreholes, they were only the second such models in the world, the first being in the U.S.A. A third set was being built in Australia. On the recommendation of the International Atomic Energy Agency (IAEA) in Vienna, the GSC conducted an intercalibration exercise in the three countries and important discrepancies were detected among the models (Fig. 14). The assigned 'ore' grades in the Australian models had to be revised upward; grades in the U.S.A. models, downwards.

The important role played by the GSC in this intercalibration work has led to the worldwide gamma-ray model intercalibration project, sponsored by the IAEA, and carried out by the GSC's Borehole Geophysics Section. To date, the GSC's standard has been carried to Australia, Czechoslovakia, Denmark, Greece, Hungary, India, Sweden and the U.S.A. In future, we expect China, Japan and Argentina to join the network of intercalibrated calibration models.

Patrick Killeen is a research scientist in the GSC's Minerals and Continental Geoscience Branch, Borehole Geophysics Section. This article was prepared with the help of researchers in the Borehole Geophysics Section and the Instrumentation R&D Section.

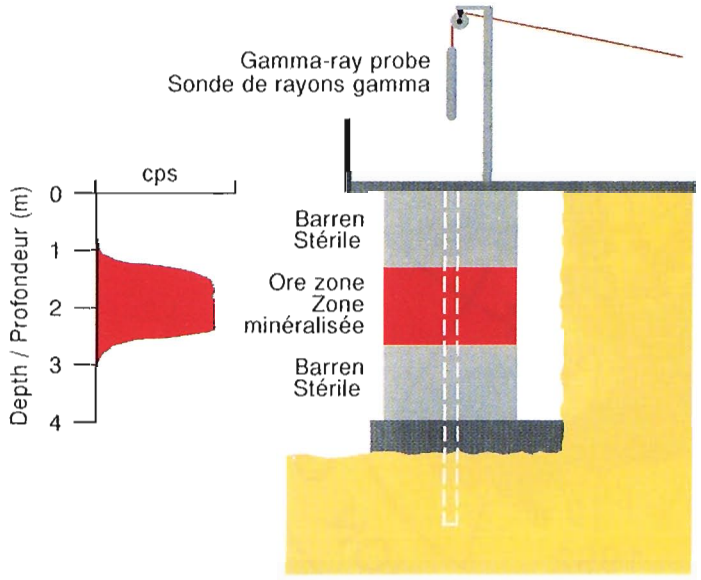

Figure 13 Principe de l'étalonnage d'une sonde de rayons gamma dans un modèle de forage en béton contenant une zone d'uranium synthétique.

Figure 14 Patrick Killeen calibrating a GSC 'standard' gamma-ray probe in Adelaide, Australia as part of an International Intercalibration project to normalize calibration models around the world.

Figure 14 Patrick Killeen étalonnant une sonde de rayons gamma normalisée de la CGC , à Adelaide, Australie, dans le cadre d'un projet d'interétalonnage international visant à normaliser tous les modèles d'étalonnage dans le monde.

stériles. Elle contient des éléments naturellement radioactifs comme du pechblende (uranifère). Comme nous connaissons la teneur en uranium dans le modèle, nous pouvons en tirer un facteur d'étalonnage pour convertir les comptes par seconde à des concentrations d'uranium en parties par million (ppm) ou pourcent.

Neuf modèles de forage construits en 1977 à Bells Corners, à l'ouest d'Ottawa, contiennent des zones radioactives de différentes concentrations de potassium, d'uranium et de thorium pour l'étalonnage des sondes spectrales de rayon gamma. Ces modèles sont devenus des normes importantes et sont utilisés par le gouvernement, l'industrie et les groupes d'universitaires pour l'étalonnage.

Interétalonnage mondial. Un étalonnage véritable, tel que les modèles d'étalonnage, doit être normalisé par rapport au reste du monde et correspondre aux «normes» internationales. Quand la CGC a mis au point ses modèles de forage, il s'agissait du deuxième modèle du genre dans le monde, les premiers ayant été établis aux États-Unis. Un troisième ensemble de modèles a ensuite été mis au point en Australie. Sur recommandation de l'Agence internationale de l'énergie atomique (AIEA) de Vienne, la CGC a mené un exercice d'interétalonnage dans trois pays et d'importantes divergences ont été détectées dans les modèles (fig. 14). Les teneurs des minerais radioactifs choisis dans les modèles australiens ont dû être augmentées; celles des modèles américains ont été diminuées.

Le rôle important qu'a joué la CGC dans ces travaux d'interétalonnage a fait naître un projet mondial d'interétalonnage de modèle de rayons gamma, parrainé par l'AIEA, projet qui sera mis en oeuvre par la Section de la Géophysique des sondages de la CGC. Jusqu'à maintenant, les normes de la CGC ont été adoptées en Australie, en Tchécoslovaquie, au Danemark, en Grèce, en Hongrie, en Inde, en Suède et aux États-Unis. Nous nous attendons à ce que dans un avenir rapproché la Chine, le Japon et l'Argentine se joignent au réseau des modèles d'étalonnage ayant fait l'objet de l'interétalonnage à l'échelle mondiale.

M. Patrick Killeen est chercheur scientifique à la Direction de la géologie du continent et des ressources minérales, Section de la géophysique des sondages. Pour préparer cet article, il a obtenu l'aide de chercheurs de la Section de la géophysique des sondages et de la Section de recherche et développement en instrumentation.


CANADA
1842
1992
GEOLOGICAL SURVEY - COMMISSION GÉOLOGIQUE
ANNIVERSARY
150
ANNIVERSAIRE

A REVIEW OF CANADIAN CALIBRATION FACILITIES FOR BOREHOLE GEOPHYSICAL MEASUREMENTS

L.D. Schock[1], P.G. Killeen[1], B.E. Elliott[1], and G.R. Bernius[1]

L.D. Schock, P.G. Killeen, B.E. Elliott, and G.R. Bernius, A review of Canadian calibration facilities for borehole geophysical measurements; in Proceedings of the 4th International MGLS/KEGS Symposium on Borehole Geophysics for Minerals, Geotechnical and Groundwater Applications; Toronto, 18-22 August 1991

Abstract

The Geological Survey of Canada (GSC) has developed calibration facilities for quantitative borehole geophysical measurements of several parameters. Ideally, borehole geophysical logs should be quantitative measurements of physical parameters, instead of simply an indication of high or low values of the parameter. Quantitative logs make it possible to compare absolute values of log data from one hole to another hole, one area to another area, year to year, and logging system to logging system. To provide such quantitative logs, probes must be calibrated to determine their response in a known, controlled situation such as a physical model of a borehole. As a supplement to the model boreholes and for geophysical measurements which are not amenable to calibration with model boreholes, test holes have been drilled for which detailed geological and geophysical logs are available.

The following GSC calibration facilities are described: nine models at Bells Corners near Ottawa, Ontario, for calibration of gamma-ray spectral logging probes; two models in Fredericton, New Brunswick and four models in Saskatoon, Saskatchewan, for calibration of total count gamma-ray logging probes; the GSC Borehole Geophysics Laboratory in Ottawa and field calibration facilities being established in Dartmouth, Nova Scotia, and Calgary, Alberta, containing multiple interchangeable zones with different physical properties; the Bells Corners geophysical test area with six drilled holes; the test site at Bancroft, Ontario, with four drilled holes; and the Lebreton test hole near GSC headquarters in Ottawa. Worldwide intercalibration will also be discussed.

INTRODUCTION

The Borehole Geophysics Section, Minerals Resources Division of the GSC has been working on research projects ranging from development of new interpretation techniques to design and construction of innovative logging tools (Killeen et al., 1991, these proceedings; Killeen, 1991). The success of these projects depends on measurements in boreholes to evaluate the interpretation techniques and to test the downhole equipment. To advance the application of borehole geophysical methods to mineral exploration and geotechnical problems, the GSC found that for some parameters a system of model boreholes was essential, and that test holes for calibrating and testing borehole geophysical equipment were also needed (Killeen, 1975).

Model boreholes, constructed of concrete mixtures to provide controlled homogeneous zones with documented physical properties, make it possible to calibrate logging tools to produce quantitative logging measurements of the physical properties of rocks. Initially the GSC designed model boreholes (Figure 1) for calibration of gamma-ray spectral logging probes which record measurements of variations in natural radioactivity due to the changes in concentrations of the elements potassium (K), uranium (U) and thorium (Th) in the rocks through which the probe is moving. A typical gamma-ray model consists of an 'ore' zone containing some radioactive materials such as pitchblende uranium ore, located between two barren zones. Figure 1 shows the gamma-ray spectral log recorded as the probe passes through a thorium zone. Since the thorium ore grade in the model is known, a calibration factor

[1]Geological Survey of Canada, 601 Booth Street, Ottawa, Ontario, K1A 0E8

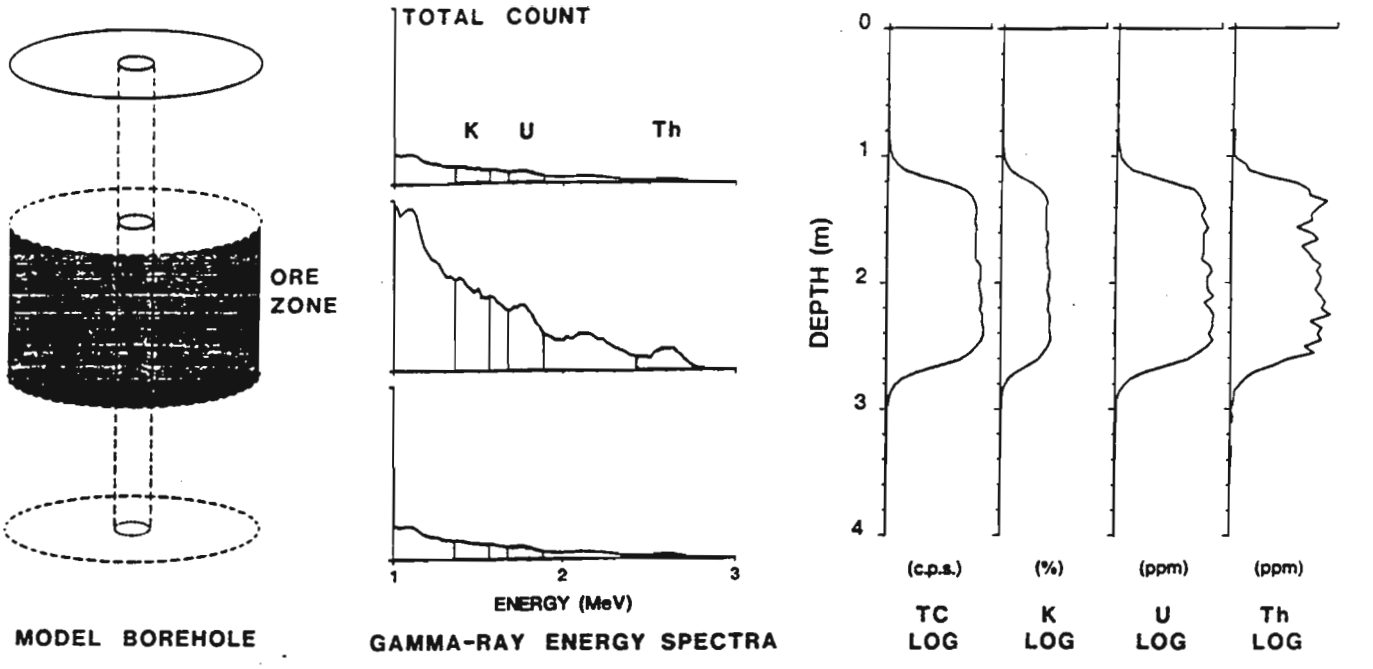

Figure 1 Design of a model borehole for calibration of gamma-ray spectral logging probes which distinguish between the radioelements potassium (K), uranium (U) and thorium (Th). A typical model is made of concrete and the 'ore' zone is located between two barren zones. The gamma-ray spectral log is recorded as the probe passes through the ore zone, in this case thorium. Calibration factors are determined by relating measured count rate (cps) to known ore concentration (ppm).

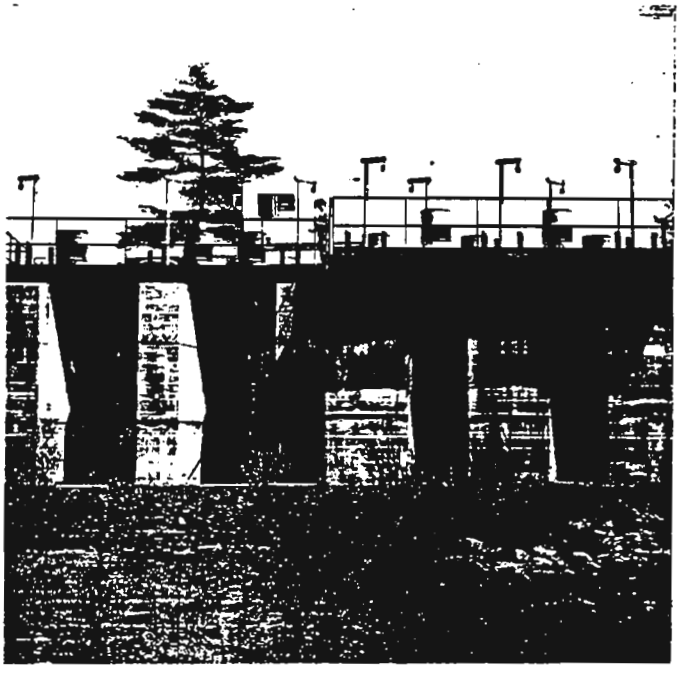

Figure 2 Nine test columns at Bells Corners near Ottawa, Ontario, each containing three different diameter model boreholes for calibrating gamma-ray spectrometric logging equipment.

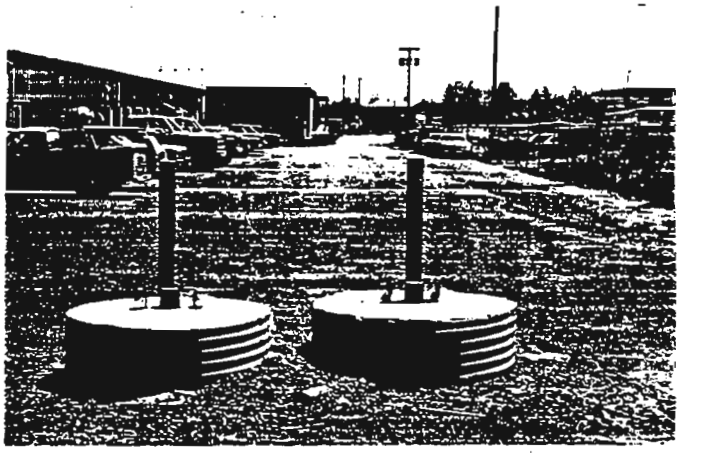

Figure 3 Two model boreholes at Fredericton, New Brunswick.

for converting the count rate from the logging tool to thorium concentration can be derived.

Nine such models, containing different radioelement (K, U, and Th) concentrations, were constructed in 1977 at Bells Corners (Figure 2) on the outskirts of Ottawa, Ontario. Later that same year, two models, with uranium zones only, were built in Fredericton, New Brunswick (Figure 3) and, in 1979, four models, also uranium only, were built in Saskatoon,

Saskatchewan (Figure 4). These were designed for calibration of total count gamma-ray logging probes. All of these models were primarily in support of uranium exploration activities by the mining industry (IAEA, 1982, 1986).

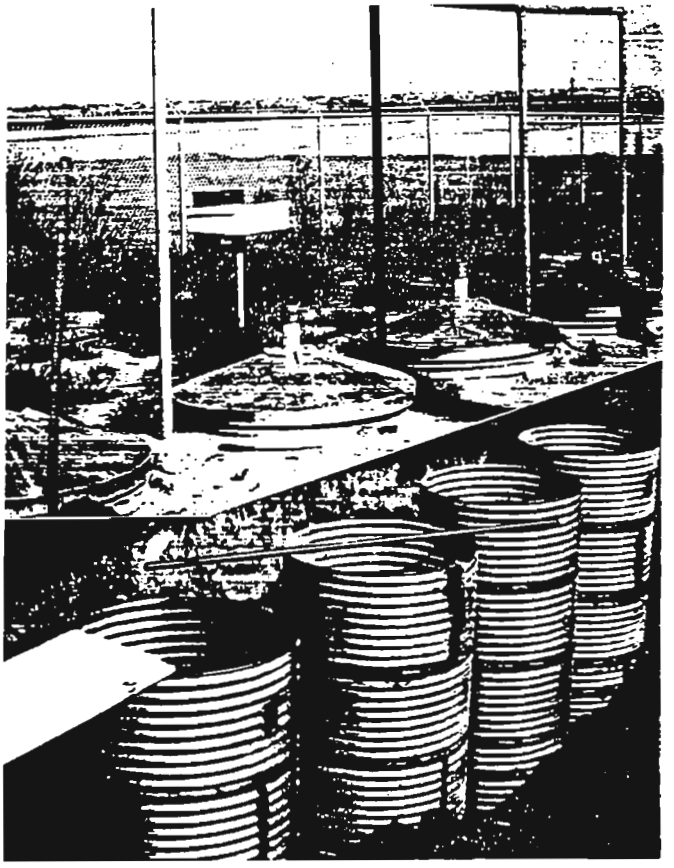

Figure 4 Four model boreholes at Saskatoon, Saskatchewan, showing below-ground construction.

The concept of model boreholes has been extended to include other physical properties such as density, which is a principal log used in the coal mining industry. To increase the flexibility of the models, 'standard' calibration zones (Figure 5) are being constructed in Ottawa in the form of cylindrical blocks with axial drill holes. These 'zones' are tested and certified in the GSC Borehole Geophysics Laboratory (Figure 6), and then shipped to field calibration facilities in Eastern Canada at Dartmouth, Nova Scotia (Figure 7) and in Western Canada at Calgary, Alberta (Figure 8). There they are assembled into multiple-zone model boreholes consisting of a series of zones placed in contact with each other. The Borehole Geophysics Laboratory in Ottawa, the primary facility, uses a horizontal configuration (Figure 9), while zones in the field facilities are stacked in a vertical configuration as shown in Figure 7.

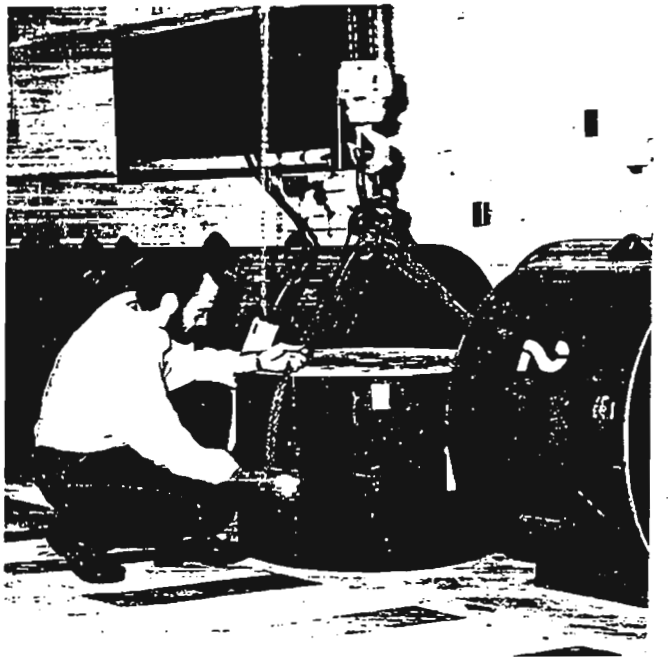

Figure 5 Cylindrical concrete calibration zones, each with specific known physical properties.

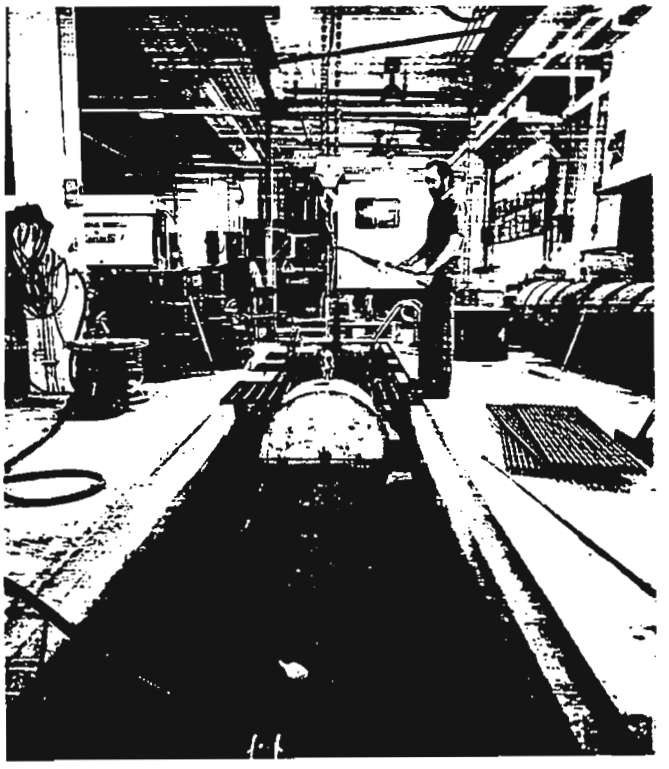

Figure 6 GSC Borehole Geophysics Laboratory at Ottawa, Ontario. The horizontal configuration makes it easy to interchange zones using an overhead crane assembly. In order to simulate most field conditions, it is possible to fill the pit with water to saturate the models.

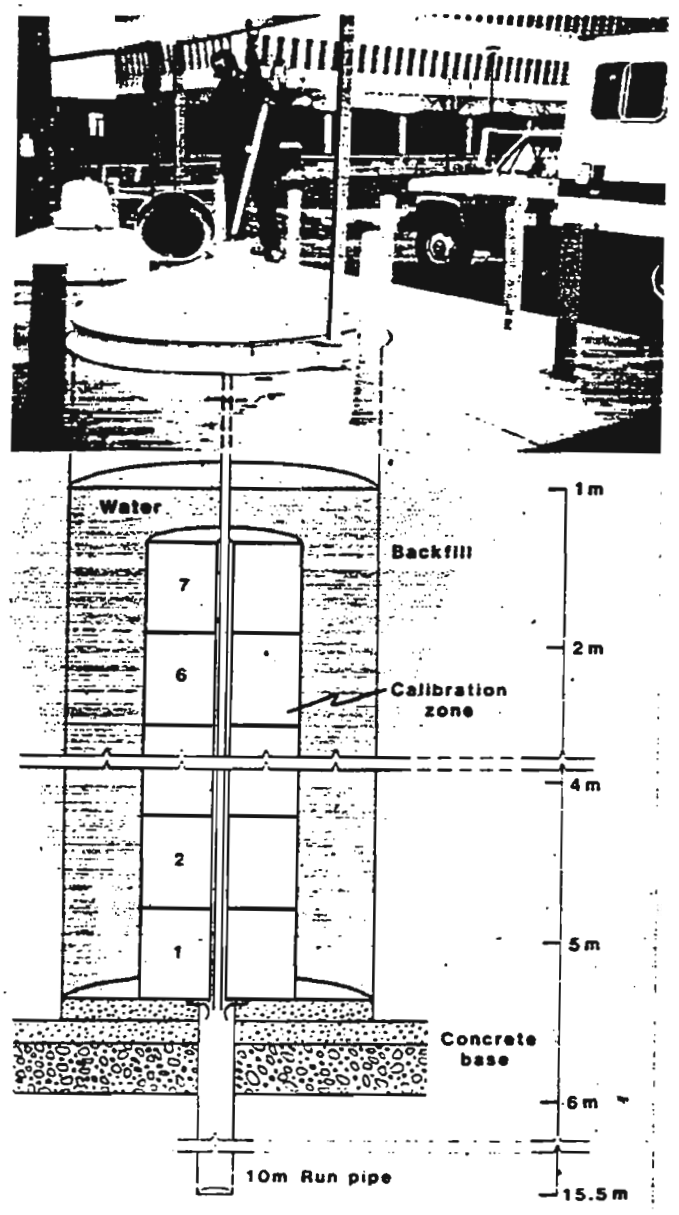

Figure 7 Field calibration facility at Dartmouth, Nova Scotia. The schematic diagram shows the vertical configuration with calibration zones stacked, aligned with the run pipe. An optional drill rod may be suspended from the cover through the borehole to simulate cased hole situations.

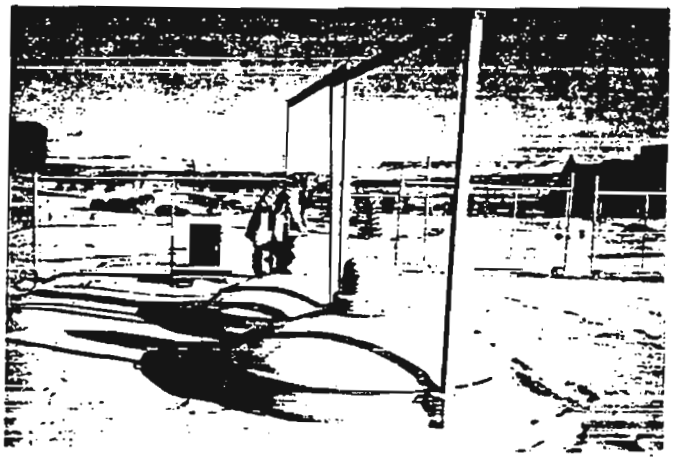

Figure 8 Completed field calibration facility at Calgary, Alberta, showing insulated tanks and covers, and overhead gantry.

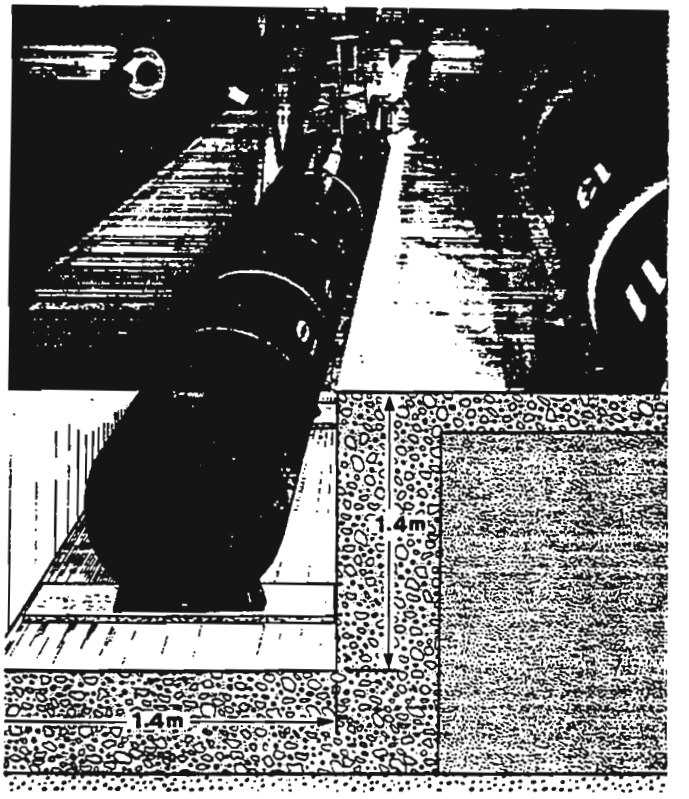

Figure 9 Design of the horizontal configuration of zones.

In addition to model boreholes, test holes have been drilled in Ottawa and in the Precambrian pegmatitic rocks in the Bancroft area, about 125 km west of Ottawa. The Lebreton NQ (76 mm diameter) test hole, located near the Borehole Geophysics Laboratory in Ottawa, drilled to a depth of 442 m, is easily accessible and convenient for testing downhole equipment. It passes through 375 m of sedimentary rock before intersecting basement rock. The Borehole Geophysics Test Area at Bells Corners (Figure 10) consists of six NQ holes drilled in 1981 and 1984. There are four holes of approximately 300 m depth and two of 120 m depth, separated by distances of 10, 20, 30, 70 and 100 m. The location of holes in a triangular pattern is ideal for hole-to-hole seismic, radar and electromagnetic studies. These holes pass through 65 m of sedimentary strata before intersecting basement rock. The Bancroft Test Site has four holes to depths of up to 90 m, two BQ (60 mm diameter) holes drilled in 1979 and two HQ (100 mm diameter) holes drilled in 1981.

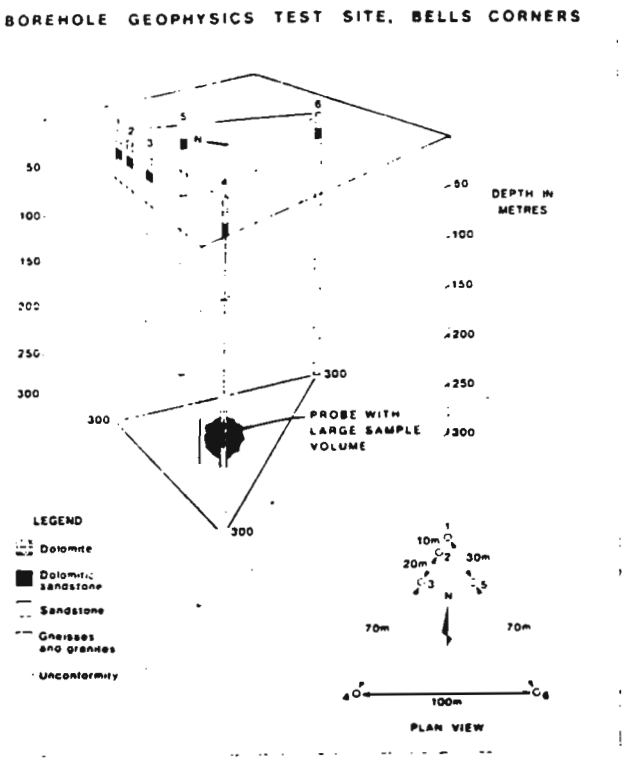

Figure 10 Geology and geometry of the Geophysics Test Area at Bells Corners near Ottawa, Ontario. Relative positions of boreholes, drilled at corners of equilateral triangles, are shown on the inset plan view. Depths of holes are displayed as well as their generalized geological logs. The unconformity at 65 m depth is indicated in the diagram by a dashed line. Logging probes, similar to the one shown in hole BC81-4, are able to determine physical properties of the rock along the hole.

Figure 11 In the GSC Rock Properties Laboratory, measurements (in this case magnetic susceptibility) are made on drill core for correlation with borehole geophysical logs.

Over a period of years, various groups from universities, institutes and private industry have utilized these boreholes in their research and development work, in addition to borehole geophysical measurements conducted by the GSC. Each type of measurement has provided additional information on the physical properties of the rocks in the vicinity of the boreholes, making the test holes more valuable. Detailed geological logs of the drill core, combined with geophysical measurements on selected sections of core conducted in the GSC Rock Properties Laboratory (Figure 11) have been a fundamental part of this work.

Canadian borehole calibration facilities which were described by Killeen (1986) are briefly reviewed here, but the main emphasis is on new developments in the last six years.

GAMMA-RAY SPECTRAL LOGGING CALIBRATION FACILITIES

Model Boreholes at Bells Corners, Ontario

In support of International Atomic Energy Agency (IAEA, 1976) recommendations regarding calibration of radiometric exploration equipment, calibration facilities for borehole gamma-ray spectrometric equipment were constructed in 1977 by the GSC (Killeen,1978; Killeen and Conway, 1978) at Bells Corners about 10 km west of Ottawa, Ontario. The site, located along the wall of an abandoned rock quarry on the property of the Canada Centre for Mineral and Energy Technology (CANMET), consists of nine concrete test columns, as pictured in Figure 2.

Three of the columns contain ore zones of different concentrations of potassium, three of uranium and three of thorium. Each of the columns is 3.9 m in height, with a simulated 1.5 m thick ore zone sandwiched between upper and lower barren zones. The radioelement concentrations were determined by laboratory gamma-ray spectrometric analysis of samples taken from the ore zones during their construction. Re-analysis of samples from the thorium ore zones in 1991, with improved laboratory techniques, produced amended concentration values (see Table 1). The values in Table 1 may differ slightly from previous publications and these are considered to be more accurate.

Each column has three boreholes, of sizes AQ (48 mm diameter), BQ and NQ, intersecting the ore zones. The deck of the working area above the columns supports overhead pulley assemblies, which can be positioned over any one of the three holes in a column, to guide the gamma-ray probe as it is lowered through the hole. The holes may be logged either wet or dry and are available for year-round use. The calibration of logging tools using gamma-ray spectral logs from the models involves the computation of stripping factors and absolute sensitivities as described by Killeen (1979).

Table 1: Radioelement concentrations for gamma-ray model boreholes

Model number	Thickness of ore (m)	Hole size*	K (%)	eU (ppm)	eTh (ppm)
Ottawa, Ontario (Bells Corners)					
BK-1-OT	1.5	A, B, N	0.8		
BK-2-OT	1.5	A, B, N	1.3		
BK-3-OT	1.5	A, B, N	3.3		
BU-4-OT	1.5	A, B, N		16	
BU-5-OT	1.5	A, B, N		108	
BU-6-OT	1.5	A, B, N		998	
BT-7-OT	1.5	A, B, N			11
BT-8-OT	1.5	A, B, N			50
BT-9-OT	1.5	A ,B, N			504
Fredericton, New Brunswick					
BU-1-F	1.5	H		102	
BU-2-F	1.5	H		1162	
Saskatoon, Saskatchewan					
BU-1-S	1.4	N		632	
BU-2-S	1.6	N		2530	
BU-3-S	1.6	N		10170	
BU-4-S	0.21	N		29800	

Note: Additional data regarding concentrations of minor radioelement components and standard deviations of all values may be obtained by contacting the authors.

*Hole size diameters:
A = 48 mm
B = 60 mm
N = 76 mm
H = 100 mm

Model Boreholes at Fredericton, New Brunswick

These model boreholes were designed primarily for calibration of total count or 'gross-count' natural gamma-ray logging tools, for which it is assumed that the radiation from potassium and thorium is negligible. Two model boreholes were constructed in Fredericton on the property of the Department of Natural Resources and Energy of the Province of New Brunswick in 1977. As shown in Figure 3, the models are housed below ground, in corrugated steel cylinders with approximately the upper 50 cm exposed. Each model contains a single borehole of HQ size, which penetrates an ore zone sandwiched between upper and lower barren zones. The 1.5 m thick ore zones have nominal uranium concentrations of 100 ppm for model BU-1-F and 1000 ppm for model BU-2-F (See Table 1 for exact values).

Model Boreholes at Saskatoon, Saskatchewan

These model boreholes were also designed primarily for calibration of total count natural gamma-ray logging tools, and in particular were meant to support the uranium exploration activities in the Athabasca sandstone area of northern Saskatchewan. A set of four model boreholes, similar in configuration to those in Fredericton, was constructed in Saskatoon in collaboration with the Saskatchewan Geological Survey and the Saskatchewan Research Council in 1979. The single hole models of NQ size are shown in Figure 4, a composite photograph showing below-ground construction as well as finished surface appearance. Ore zones have concentrations ranging from about 600 ppm eU to nearly 30,000 ppm eU as shown in Table 1. The last zone, which is only 21 cm thick, represents a high-grade zone with a concentration in the range encountered in actual field work in the Athabasca region.

MULTIPLE-ZONE CALIBRATION FACILITIES

Primary Facility at Ottawa - The GSC Borehole Geophysics Laboratory

A multiple-zone model borehole, designed for calibration of logging probes and for testing and evaluation of calibration zones for use in field facilities, has been constructed in Ottawa in the Borehole Geophysics Laboratory at Lebreton Street (Killeen et al., 1984). The facility consists of a rectangular pit (Figure 9) in which a series of 'ore' zones (concrete cylinders) are placed in contact with each other in a horizontal configuration. As shown in Figure 6, the primary facility has provision for saturating the model borehole zones with water to simulate most field conditions. The pit is watertight to prevent seepage of ground water into the empty pit, or of water from a full pit into the environment, and is free of metallic material to avoid interference during calibration of logging tools which measure electrical or magnetic properties of rocks.

Each cylinder represents a 'zone' as shown in Figure 5 with specific known physical properties for which the logging tool response can be evaluated. The horizontal model borehole produced by the alignment of the axial holes in each zone is used to calibrate logging tools as they are pulled through the successive zones by a system of suspended weights. The horizontal configuration increases the versatility of the model by making it easy to remove and insert different zones, or to shift them for use in any sequence, during testing and evaluation.

Initial construction of the calibration facility included the design of a series of calibration zones made of concrete with different densities covering the range of interest for coal logging (see Table 2). In two of the zones (#4,#5), coal was actually mixed with the concrete. The density zones were constructed in collaboration with the Engineering Department of the University of Ottawa. A prototype zone was first built, and an axial hole was drilled without core recovery. The prototype was followed by eleven working models, which were core drilled to allow more accurate measurements.

Zones were tested for homogeneity, water-saturated and accurately measured for wet density in Ottawa prior to shipment to field locations. To ensure 100% saturation, the GSC acquired a vacuum tank (Figure 12) to evacuate the pore structure of the calibration zone before it is water saturated. Figure 13 shows a zone being placed in the vacuum tank for evacuation and water-saturation. The tank is capable of accepting zones up to 1 metre diameter and thickness.

At present, a set of five density zones (#1,#6,#9,#4,#5) plus the prototype (#13) has been retained for use in the primary facility in Ottawa, while the remaining two sets of three each were shipped to field calibration facilities established in eastern Canada (#2,#10,#7) and western Canada (#3,#11,#8). Dimensions of all zones are 0.9 m diameter and 0.6 m thickness. Zones with their corresponding identification numbers, hole sizes and wet densities, are listed in Table 2.

Table 2: Density zones in primary and field facilities

Zone ID number	Hole size*	Wet density (g/cm^3)
Ottawa, Ontario		
#13 (prototype)	N	2.5
#1	N	2.40
#6	N	1.67
#9	N	1.95
#4 (coal)	N	1.52
#5 (coal)	N	1.77
Dartmouth, Nova Scotia		
#2	N	2.39
#10	N	1.96
#7	N	1.68
Calgary, Alberta		
#3	H	2.40
#11	H	1.96
#8	H	1.63

Note: Additional data regarding standard deviation of values may be obtained from the authors.
*Hole size diameters: N = 76 mm, H = 100 mm.

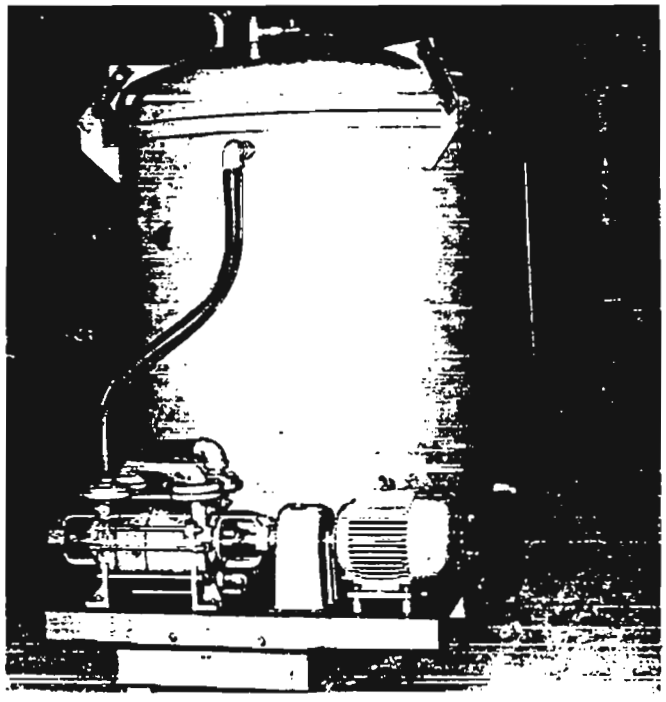

Figure 12 Vacuum tank designed to evacuate air from the pore structure of the calibration zone before it is water saturated.

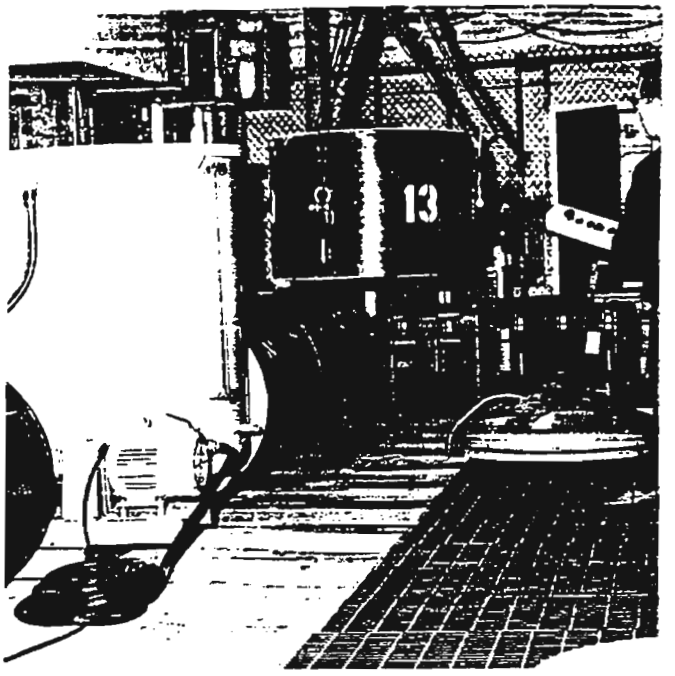

Figure 13 Placing a new calibration zone in the vacuum tank for evacuation and water-saturation. Testing and certification of standard calibration zones are done in the GSC Borehole Geophysics Laboratory at Ottawa, Ontario.

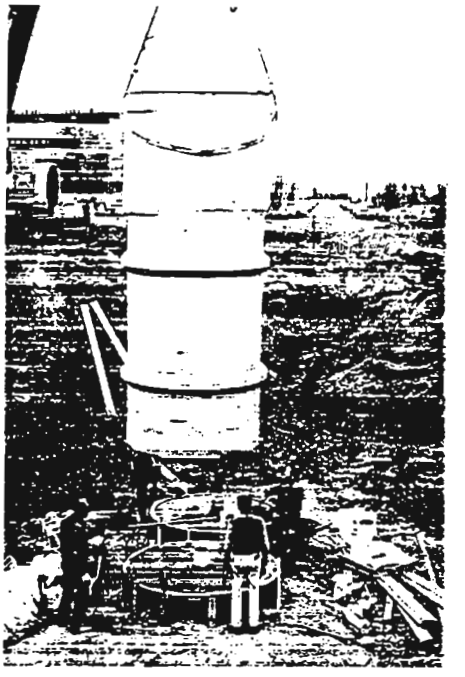

Figure 14 A fiberglass tank is positioned over a run pipe protruding through the concrete base during construction of the field calibration facility at Calgary. Tank and run pipe are attached with a watertight fiberglass bond.

To increase the range of available densities, blocks of rock, each with a drilled BQ hole, have been placed near the model boreholes at Bells Corners. The four rock blocks and their densities are: sandstone (2.49 g/cm^3), granite (2.61 g/cm^3), limestone (2.69 g/cm^3), and basalt (2.85 g/cm^3). Also, the lower barren zone of model BU-4-OT, with a density of 2.33 g/cm^3 and three hole sizes (AQ, BQ, NQ), is available for deriving hole size corrections.

The Ottawa facility will be used to develop standardized calibration zones for other physical properties, such as porosity and magnetic susceptibility, with these being added to the field facilities as they become available in the future.

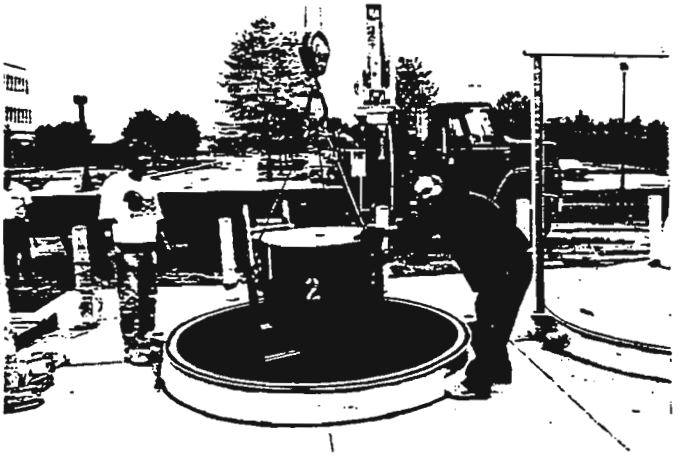

Figure 15 A zone, shipped from Ottawa, is placed into one of the fiberglass tanks of the field facilities, in this case at the Dartmouth site.

Field Calibration Facilities

In Calgary and Dartmouth, zones are stacked vertically and are contained in circular below-ground fiberglass vessels as shown in Figure 7. Similar to the primary facility, the field facilities have provision for filling the fiberglass tanks with water to saturate the model boreholes. They are watertight and free of metallic material, and have electrical and water supplies.

The central hole in each cylindrical zone is aligned such that the stack provides a continuous hole through all the zones, which is aligned with a run pipe protruding below the tank. During the calibration, logging tools would normally be lowered into the model borehole on a cable which runs over a pulley suspended by an overhead gantry assembly. To simulate logging inside a cased hole, a steel drill rod (or pipe) can be temporarily suspended in the model borehole for the calibration measurements.

Field Logging Calibration Facilities at Dartmouth, Nova Scotia

The Eastern Canadian field facility is located in Dartmouth on the property of the Nova Scotia Research Foundation Corporation, which oversees and maintains the facility for their own and public use (Schock and Killeen, 1985). At this site,

two fiberglass tank assemblies (Figure 7) were installed, and into one of these three density calibration zones were placed. Each zone is 0.9 m in diameter and 0.6 m thick with an NQ borehole (Figure 15). Figure 16 shows the guide assembly attached to the upper zone to direct probes into the model borehole. Table 2 lists the three zones from top to bottom, as they are now installed in the stack.

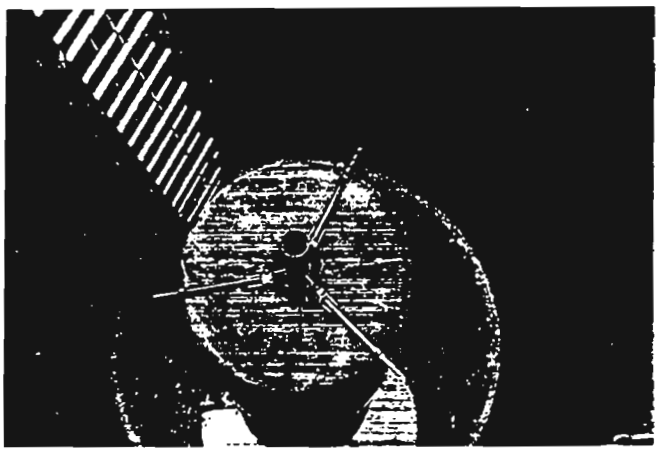

Figure 16 Once zones are positioned in the fiberglass tank, a guide assembly is attached to the upper zone to direct probes into the model borehole. Boreholes in Dartmouth are 76 mm; in Calgary, 100 mm. The run pipe beneath is 200 mm. A reducer allows smooth transition from the run pipe to the zone borehole.

Field Logging Calibration Facilities at Calgary, Alberta

The Western Canadian field facility is located in Calgary at the Institute of Sedimentary and Petroleum Geology, a division of the GSC. Figure 14 shows the site under construction, while Figure 8 shows it completed. Three density calibration zones, 0.9 m in diameter and 0.6 m thick with HQ boreholes, were placed in the Calgary facility in 1991. Table 2 also lists these zones from top to bottom.

TEST HOLES

Bells Corners Test Holes

This site, located near the entrance to the CANMET Complex in Bells Corners and close to the model boreholes, consists of six vertical NQ boreholes. These were drilled in 1981 and 1984, to provide a place for testing various types of borehole probes being used by the GSC, universities and industry. The geological location, which contains a variety of rock types, structural conditions and various degrees of alteration, provides the contrasts needed to test the measuring capabilities of probes available or being developed today.

The top 65 metres of the holes intersect a sequence of nearly horizontal lower Paleozoic sandstones and dolomites lying unconformably on an altered/weathered zone of Precambrian granites and gneisses. The altered zone varies in thickness up to 17 metres. A number of alteration zones near fractures and faults are found within the fresher granites and gneisses. The gneisses are steeply dipping and range in composition from hornblende-biotite-feldspar-quartz to those containing a large amount of carbonate minerals like scapolite and calcite.

The holes are drilled in a triangular pattern, as shown in Figure 10, at intervals of 10, 20, 30, 70 and 100 metres apart. The first four holes, as described by Bernius (1981), were drilled in 1981; BC81-1 was drilled to 300 m and the remaining holes went to 120 m. In 1984, BC81-4 was deepened to 300 m and two additional holes were drilled, BC84-5 to 250 m and BC84-6 to 300 m. The new holes are offset from the previously drilled line of holes to form a 30 m equilateral triangle inside a 100 m equilateral triangle, as shown in Figure 10, to facilitate experimentation with hole-to-hole techniques.

Parameters which have been measured in the test holes include magnetic susceptibility, electrical resistivity and IP, natural gamma, gamma-gamma density, thermal neutron, acoustic velocity, conductivity and temperature. Hole BC81-2 has been logged most frequently by industry and universities, and more geophysical logs are available for it than the other holes. The recovery of core (47.6 mm diameter) was high, allowing detailed petrological and geophysical studies (magnetic susceptibility and density) to be made in the GSC Rock Properties Laboratory. Logs of hole BC81-2 are shown in Elliott (1991, these proceedings).

Bancroft Area Test Holes

In 1979 two BQ test boreholes (BN-79-4,BN-79-5) were drilled near Bancroft to intersect uranium- and thorium-bearing mineralized zones, primarily for testing a gamma-ray spectral logging system. In 1981, two more holes (BN-81-1,BN-81-2) of HQ size were drilled 60 m apart at the same location, primarily to test and evaluate a new X-ray fluorescence probe. The large diameter holes present a unique opportunity to test prototype probes which are often of larger diameter than the final version. The holes are also suitable for hole-to-hole experiments. These test holes are drilled approximately perpendicular to the dip of the rocks at an angle of about 60° from horizontal.[2]

Lebreton Test Hole

Test borehole (LB-1) is located outside the GSC Borehole Geophysics Laboratory in Ottawa. Caliper logging has shown that hole LB-1 does not deviate by much more than 1 cm from

[2]At time of writing the two BQ holes have become blocked and an attempt will be made to reopen them.

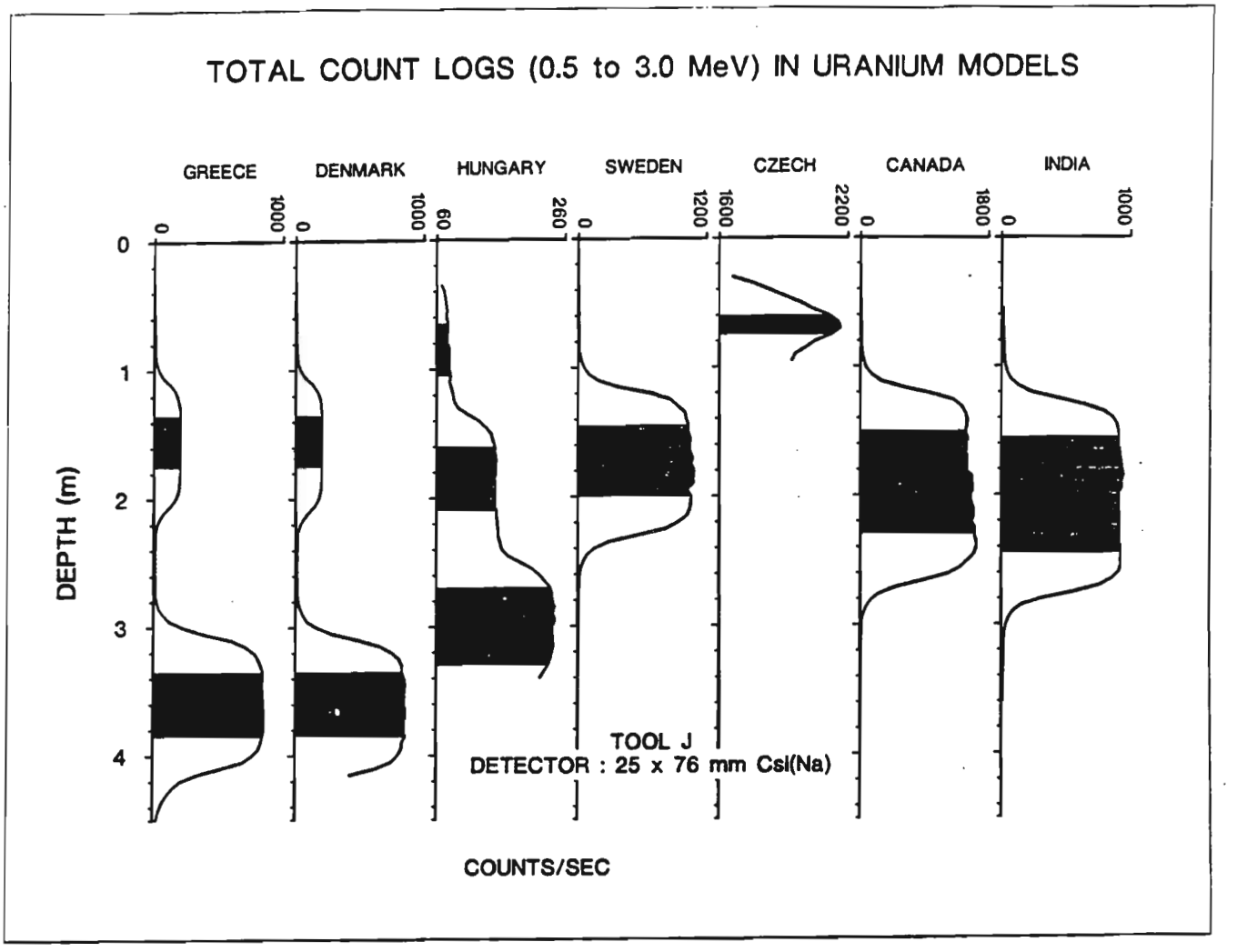

Figure 17 A worldwide gamma-ray intercalibration project, sponsored by the IAEA, is being carried out by the GSC Borehole Geophysics Section following the GSC's initial measurements in Australia and USA. Standard gamma-ray logs in model holes in six additional countries are shown here.

its nominal NQ diameter of 76 mm. The upper 375 m of this 442 m hole is in sedimentary rock. At about 375 there is an unconformity marked by electrical and radiometric anomalies. The upper part of the hole intersects a thick section of limestone and shale before it reaches the same formation in which the Bells Corners holes are collared. For researchers interested in a thicker sedimentary section (about 370 m) than the boreholes at Bells Corners (about 65 m), hole LB-1 should be used. The bottom approximately 75 m of this hole penetrates Precambrian basement rocks. Due to its location, in the midst of buildings and city traffic, this test hole would not be suitable for some high sensitivity seismic or electrical measurements.

WORLDWIDE INTERCALIBRATION

To have international 'standards', calibration models around the world must be consistent. When the GSC developed its gamma-ray spectral model boreholes, they were only the

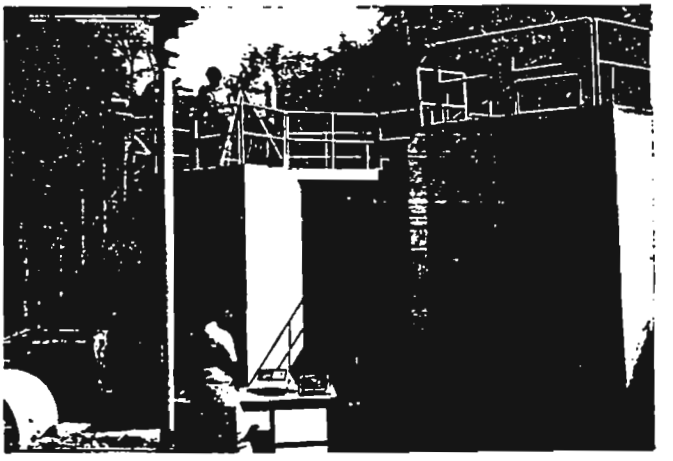

Figure 18 India's calibration models in Hyderabad are similar to the design of the Bells Corners models.

second such models in the world, the first being built in the U.S.A.; the third, in Australia. On the recommendation of the IAEA in Vienna, the GSC conducted an intercalibration exercise in the three countries (Adelaide, Australia; Grand Junction, U.S.A.; and Ottawa, Canada) and important discrepancies were detected among the models. Ultimately, the assigned 'ore' grades in the Australian models were revised upwards; grades in the U.S.A. models, downwards. The results of these measurements have been described by Bristow et al. (1982) and Killeen et al. (1983).

The initial intercalibration work has led to the worldwide gamma-ray model intercalibration project, sponsored by the IAEA, and carried out by the GSC's Borehole Geophysics Section (Killeen and Elliott, 1990). To date, the GSC's set of standard gamma-ray logging probes has been used to compare models in Argentina, Australia, Czechoslovakia, Denmark, Greece, Hungary, India, Sweden, and the U.S.A. Figure 17 shows an example of gamma-ray logs recorded in model holes in six of the countries. It is interesting to note that India's calibration models in Hyderabad (Figure 18) are similar to the design of the Bells Corners models in Canada. In future, it is expected that China, Japan and other countries will add their gamma-ray model boreholes to the network of intercalibrated models.

CONCLUSIONS

Calibration facilities, including models and test holes, have been developed by the GSC for use by private industry, university and government groups involved in using, developing, calibrating or improving the quality of borehole geophysical instrumentation and measurements. Models like these have become important standards and have helped to stimulate the development of commercial mineral logging systems and services in Canada. In the future it is hoped that borehole geophysical test sites can be established at major economic mineral deposits to facilitate development of new logging tools and techniques.

ACKNOWLEDGEMENTS

The authors thank personnel at the New Brunswick Department of Natural Resources and Energy, the Saskatchewan Geological Survey, the Saskatchewan Research Council, the Nova Scotia Research Foundation Corporation, Kerr Addison Mines Limited, the Engineering Department of the University of Ottawa, the Canada Centre for Mineral and Energy Technology, and the Institute of Sedimentary and Petroleum Geology for their contributions to the development and maintenance of these calibration facilities. We are especially grateful to the following GSC employees: S. Birk and W. Hyatt for assistance with work to evaluate, ship and install calibration zones, and log the facilities; S. Davis for drafting; and G. Lemieux and R. Kelly for photography.

REFERENCES

Bernius, G.R. (1981) Boreholes near Ottawa for the development and testing of borehole logging equipment - A preliminary report; Current Research, Part C, Geological Survey of Canada, Paper 81-1C, p.51-53.

Bristow, Q., Killeen, P.G. and Mwenifumbo, C.J. (1982) Comparison of standardized gamma-ray log calibration measurements: Ottawa, Adelaide and Grand Junction; in Symposium on Uranium Exploration Methods, Review of the NEA/IAEA R&D Programme, Paris, June 1-4, p.715-726.

Elliott, B.E. (1991) An overview of processing, display and enhancement methods used on borehole geophysical logging data at the Geological Survey of Canada; in Proceedings of the 4th International MGLS/KEGS Symposium on Borehole Geophysics for Minerals, Geotechnical and Groundwater Applications; Toronto, 18-22 August 1991

IAEA (1976) Radiometric reporting methods and calibration in uranium exploration; International Atomic Energy Agency, Technical Report Series no. 174, 57 p.

IAEA (1982) Borehole logging for uranium exploration - a manual; International Atomic Energy Agency, Technical Report Series no. 212, 279 p.

IAEA (1986) Practical borehole logging procedures for mineral exploration, with emphasis on uranium; International Atomic Energy Agency, Technical Report Series no. 259, 44 p.

Killeen, P.G. (1975) Nuclear techniques for borehole logging in mineral exploration; in Borehole Geophysics Applied to Metallic Mineral Prospecting: A Review, ed. A.V. Dyck, Geological Survey of Canada, Paper 75-31, p.39-52.

Killeen, P.G. (1978) Gamma-ray spectrometric calibration facilities - a preliminary report; Current Research, Part A, Geological Survey of Canada, Paper 78-1A, p.243-247.

Killeen, P.G. (1979) Gamma-ray spectrometric methods in uranium exploration - applications and interpretation; in Geophysics and Geochemistry in the Search for Metallic Ores, ed. P.J. Hood; Geological Survey of Canada, Economic Geology Report 31, p.163-229.

Killeen, P.G. (1986) A system of deep test holes and calibration facilities for developing and testing new borehole geophysical techniques; in Borehole Geophysics for Mining and Geotechnical Applications, ed. P.G. Killeen, Geological Survey of Canada, Paper 85-27, p.29-46.

Killeen, P.G. (1991) Borehole geophysics: taking geophysics into the third dimension; in GEOS, Vol.20, No.2, p.1-10.

Killeen, P.G. and Conway, J.G. (1978) New facilities for calibrating gamma-ray spectrometric logging and surface exploration equipment; Canadian Institute of Mining and Metallurgical Bulletin, 793, p.84-87.

Killeen, P.G. and Elliott, B.E. (1990) Model boreholes for gamma-ray logging: Intercalibration of North American and European calibration facilities; in Transactions of the 13th SPWLA European Formation Evaluation Symposium, Budapest, Hungary, Oct 22-26, paper GG. 14 pages.

Killeen, P.G., Bristow, Q. and Mwenifumbo, C.J. (1983) Gamma-ray logging for uranium: status of international efforts to resolve discrepancies in calibration models; in SPWLA Twenty-fourth Annual Logging Symposium, June 27-30, Paper AA, 15 pp.

Killeen, P.G., Bernius, G.R., Schock, L.D. and Mwenifumbo, C.J. (1984) New developments in the GSC borehole geophysics test area and calibration facilities; Current Research, Part B, Geological Survey of Canada, Paper 84-1B, p.373-374.

Killeen, P.G., Schock, L.D., Elliott, B.E., Cinq-Mars, A., Mwenifumbo, C.J., Bernius, G., Hyatt, W., and Birk, S. (1991) An overview of borehole geophysical research at the Geological Survey of Canada; in Proceedings of the 4th International MGLS/KEGS Symposium on Borehole Geophysics for Minerals, Geotechnical and Groundwater Applications; Toronto, 18-22 August 1991.

Schock, L.D. and Killeen, P.G. (1985) Establishment of coal logging field calibration facilities: a progress report; Current Research, Part B, Geological Survey of Canada, Paper 85-1B, p.459-462.

MINERAL EXPLORATION

Gamma-ray spectral logging for uranium

J.G. CONAWAY and P.G. KILLEEN
Radiation Methods Section
Geological Survey of Canada
Ottawa, Ontario

ABSTRACT

Gamma-ray spectral logging, a useful technique for uranium exploration and evaluation, has generally been underutilized by the Canadian mining industry. Provided that the technique is properly applied, it is capable of yielding reliable quantitative information regarding the distribution of uranium and other radioelements along the borehole under most conditions. In practice, there are numerous factors which potentially can degrade the quality of the log and thus any quantitative interpretation based on it. Fortunately, the appropriate choice of logging equipment and technique can avoid many such problems, and corrections can be applied to the data to compensate for most of the others.

J.G. Conaway

John Conaway received a Bachelor's degree in mechanical engineering in 1970. He received an M.Sc. in geophysics from the University of Western Ontario in 1973, working on geophysical exploration techniques, and a PH.D. in geophysics from UWO in 1976, where he developed a method for continuous logging of borehole temperature gradients with a high degree of precision, On leaving UWO, Dr. Conaway was awarded a Visiting Fellowship with the Radiation Methods Section, Resource Geophysics and Geochemistry Division, of the Geological Survey of Canada. He has subsequently taken up the position of research scientist at that same institution, where he is involved in research and development of borehole logging techniques.

P.G. Killeen

Patrick Killeen received his B.Sc. (Honours) degree in physics from Loyola College (Montreal) in 1963. His M.Sc. (1966) and Ph.D. (1971) degrees in geophysics from the University of Western Ontario concerned field applications of gamma-ray spectrometry and the problem of radioactive disequilibrium respectively. He was closely associated with the developments in gamma-ray spectrometry at the Geological Survey of Canada (GSC), which sponsored field work for his theses. After a year with the GSC, Dr. Killeen was awarded a 1-year fellowship (1972) with the University of Oslo in Norway, investigating radioelement distributions in granitic rocks. In 1973, he returned to the GSC, working as a research scientist with the Radiation Methods Section, of which he is now head. Currently, he is involved in the development of nuclear techniques in borehole logging and, in particular, techniques of calibration and standardization of gamma-ray spectral logging equipment.

Keywords: Exploration, Gamma-ray logging, Total-count logging, Spectral logging, Uranium exploration, Radioactive disequilibrium, Borehole logging.

Introduction

In Canada and around the world, gamma-ray spectral logging is becoming an increasingly important technique for uranium exploration and evaluation. In large part, this is because of the lower cost of percussion drilling compared to diamond core-drilling, and because the gamma-ray log analysis is representative of a much greater volume of rock than a core analysis. Continuing refinement makes the equipment and techniques increasingly reliable and improves the accuracy of the results.

Unfortunately, in some instances the personnel in charge of planning and conducting the logging program, and of interpreting the results, may be lacking in prior logging experience and basic background information on this specialized subject. As a result, gamma-ray logs are commonly misinterpreted, surveys are sometimes so badly run that even an expert would be unable to extract reliable quantitative information from the logs and, in most cases, the technique is not being utilized to its fullest advantage. Although much of the basic information necessary for a good survey can be found in the literature, it is disseminated and difficult to ferret out. In addition, some of the existing gamma-ray logging literature contains misleading, outdated or erroneous information.

This paper is intended to provide a foundation in the basic theory of interpretation of gamma-ray spectral logs, along with some suggestions regarding equipment and techniques. The logger, armed with this information, should be in a better position to plan and conduct a good survey and make a reliable interpretation.

The Gamma-Ray Energy Spectrum

For convenience, the electromagnetic radiation spectrum is subdivided according to the origin, behaviour and frequency of the radiation. The most familiar subgroup is visible light, which is further divided according to colour, which depends on the frequency of the radiation. Gamma rays are a type of electromagnetic radiation having frequencies (and therefore energies) one thousand to one million times greater than visible light. A single gamma-ray is a photon of electromagnetic radiation (like a photon of light) which is emitted during certain types of radioactive decay, that is, while one atom of an element or isotope is changing by nuclear disintegration into another *daughter nuclide* (element or isotope).

In uranium exploration, we are only concerned with the three principal natural radioelements, uranium, thorium and potassium, and their respective decay series, i.e. all of the daughter products from the initial parent radioelement down

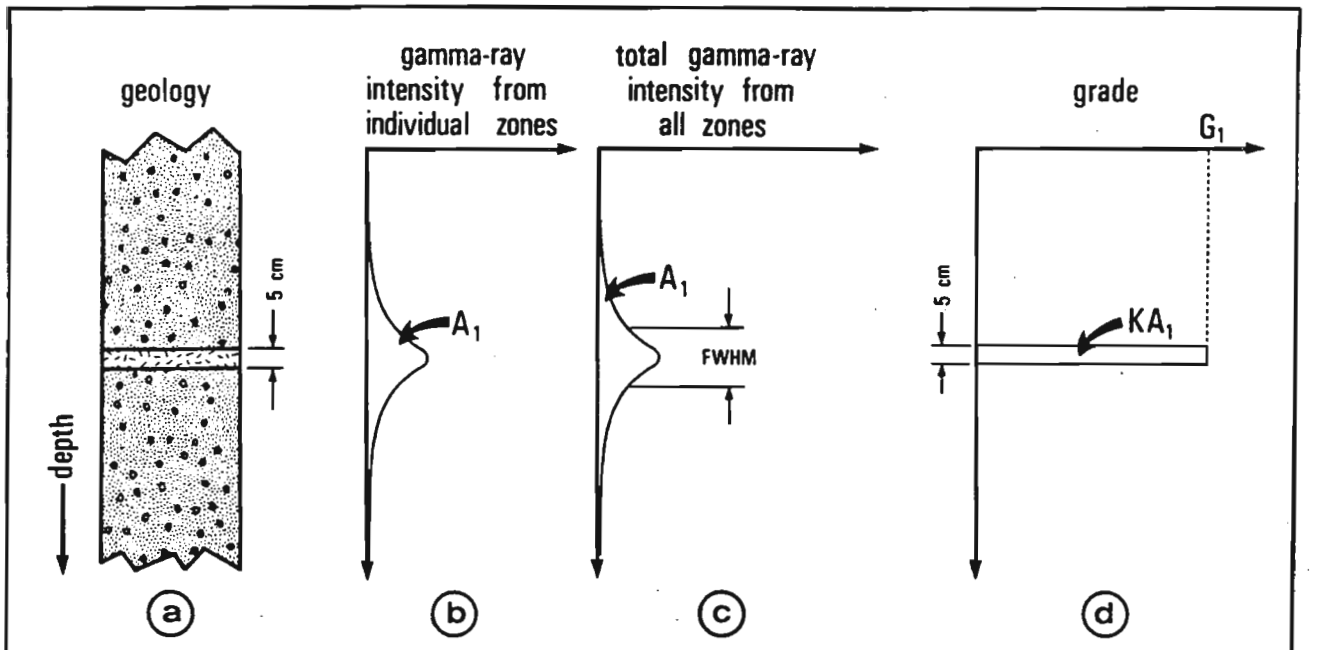

FIGURE 1. (a) Geologic column showing a 5-cm-thick zone of radioactive material embedded in barren rock. (b) Simulated noise-free gamma-ray log past zone shown in (a). (c) Sum of the individual logs shown in (b) (i.e. in this example curves (b) and (c) are identical). (d) Plot of actual grade vs. depth (distribution of radioactive material along the borehole).

to the final stable (non-radioactive) daughter. Specifically, we are interested in uranium, while potassium and especially thorium may provide interference and complicate the interpretation. In logging applications other than for uranium, potassium and thorium may also be of interest.

Traditionally, gamma-ray logging for uranium has been done on a total-count basis. That is, all gamma-rays detected are assumed to be from the uranium decay series, and the interpretation is made on that basis. More recently, especially in Canada, an effort has been made to develop logging equipment which can sort the gamma-rays according to energy and eliminate the contributions of those which are not due to the uranium series. Thus, ideally, the interfering effects of potassium and thorium are eliminated.

Interpretation of the total-count log will be considered first.

Quantitative Uranium Determinations—Total-Count Log

The basic premise behind all standard methods of quantitative interpretation of gamma-ray logs for uranium is simply this: The area beneath the anomaly curve is directly proportional to the quantity of radioactive material along the borehole in that region (Scott *et al.*, 1961). This may be expressed by the simple relationship

$$GT = KA \quad \ldots\ldots\ldots\ldots\ldots\ldots\ldots\ldots\ldots\ldots \quad (1)$$

where G is the average ore grade (%U or other units) over a zone which is T metres thick. In total-count logging, K is the logging system calibration constant which is determined in model boreholes under conditions as nearly like those in the field borehole as possible (see Killeen and Conaway, 1978), and A is the area beneath the anomaly curve (in metres x counts/s or similar units). Grade G is expressed in the units % eU, or equivalent U, because the gamma-radiation is assumed to be entirely from the uranium decay series, although it is not certain that this is the case. The units of K, then, are % eU/(counts/s). The principle expressed by equation (1) is illustrated in Figures 1-3. In Figure 1a, a thin (let us say, arbitrarily, 5 cm) uniform zone of uranium ore of grade G_1 is illustrated diagrammatically. This ore zone produces the gamma-ray anomaly shown in Figure 1b (or 1c). The area under this curve is A_1 (metres x counts/s). Figure 1d shows the uranium concentration (or % eU) plotted against depth. The height of this slim rectangle is equal to the ore grade (G_1) and the width of the rectangle is equal to the thickness of the zone. By equation (1), the area of the rectangle is KA_1.

The important point illustrated by Figure 1 is that by determining the area under the gamma-ray anomaly (from "background to background"), and by knowing the calibration constant of the logging system, it is possible to determine the product of grade times thickness for the ore zone which caused the anomaly. What cannot be determined directly from Figure 1c is the true thickness of the ore zone, and therefore the true ore grade according to the relationship

$$G = \frac{KA}{T} \quad \ldots\ldots\ldots\ldots\ldots\ldots\ldots\ldots\ldots\ldots \quad (2)$$

If, however, the zone thickness can be estimated, then the average grade over that estimated distance can be computed from equation (2). Because it is the product GT which is related to ore tonnage, the problem of determining T precisely is not generally of critical importance, except perhaps in the case of low-grade deposits near the cutoff grade for economic viability.

In Figure 2a are shown four adjacent ore zones, each identical to the one in Figure 1a. Each zone considered individually would cause one of the four anomaly curves shown in Figure 2b, each having an area A_1. Now, the total anomaly is merely the sum of the individual curves (this is called the *principle of superposition*), and is plotted in Figure 2c. Note that, although the ore grade of each of the four zones in Figure 2 is identical to the grade of the single zone in Figure 1, the corresponding total anomaly curves (Figs. 2c and 1c) have different amplitudes. This is an important source of error in gamma-ray log interpretation; the fact is that the height of the anomaly curve is generally not proportional to ore grade, but the total area under the curve is proportional to the total grade-thickness product. Figure 2d once again shown the plot of uranium concentration along the borehole.

In Figure 3a we see 20 adjacent ore zones, each identical to the one shown in Figure 1a. These zones considered individually would give rise to the 20 anomaly curves shown in Figure 3b, each with an area A_1. Once again, the total anomaly due to the complete 1-m-thick ore zone is the sum of the individual anomaly curves, and is plotted in Figure 3c. Notice that the

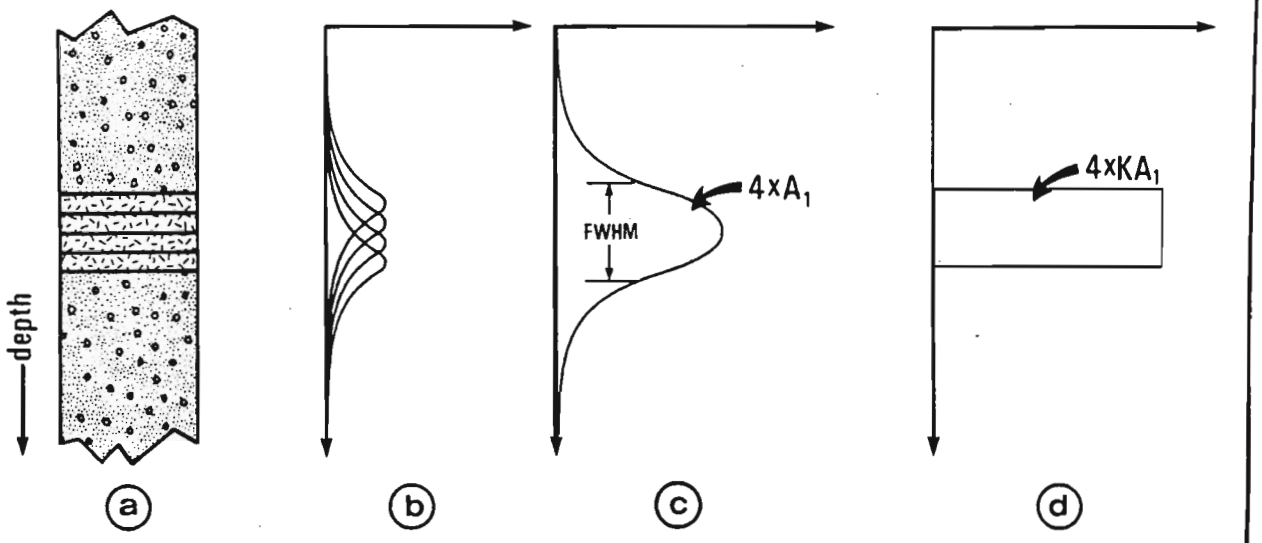

FIGURE 2. (a) Geologic column showing four 5-cm-thick zones of radioactive material (each identical to the zone in Fig. 1a) embedded in barren rock. Each zone considered individually would cause one of the four gamma-ray log anomalies shown in (b); these four anomalies are summed to give the gamma-ray log past the entire 20-cm radioactive zone (c). (d) Plot of actual grade vs depth.

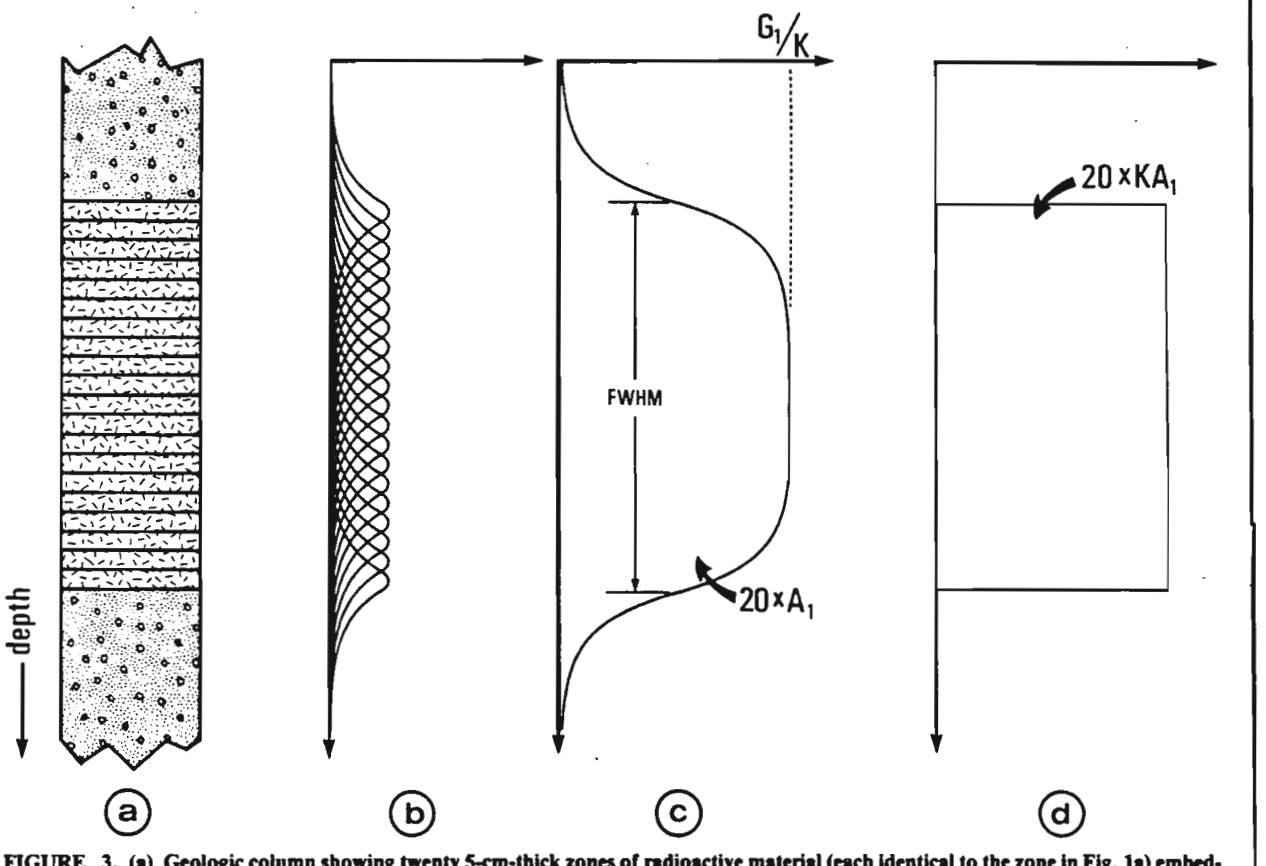

FIGURE 3. (a) Geologic column showing twenty 5-cm-thick zones of radioactive material (each identical to the zone in Fig. 1a) embedded in barren rock. Each zone considered individually would cause one of the twenty gamma-ray log anomalies shown in (b); these twenty anomalies are summed to give the total gamma-ray log past the entire 1-m radioactive zone (c). (d) Plot of actual grade vs depth.

anomaly curve has become flat in the middle. The gamma-ray intensity in the middle of this anomaly is directly proportional to ore grade (in fact, the intensity is G_1/K), and the ore zone is said to be effectively *infinitely thick*. This means that a gamma ray originating in the centre of the ore zone has a negligible change of reaching the barren zone.

As well as having height proportional to the ore grade, the anomaly resulting from an infinitely thick ore zone of *uniform composition* obeys the "full-width half-maximum" (FWHM) rule. That is, the width of the anomaly at half the maximum count rate is equal to the thickness of the ore zone, regardless of detector length or instrument time constant. Thus, for an infinitely thick uniform ore zone, it is a simple matter to determine the true grade and thickness of the zone rather than just

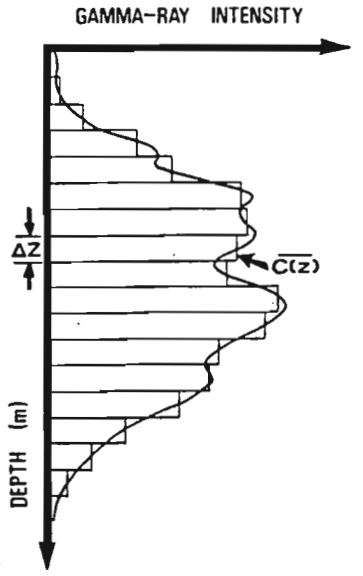

FIGURE 4. Simple procedure for computing the grade-thickness product over an ore zone. The area under the curve is approximated by a number of rectangles of depth extent Δz (distance along the borehole in metres) and intensity C(z) (counts/s). Usually C(z) is taken as the digitized log amplitude at each digitization point. The areas of the individual rectangles are summed to give the total area, A, which, when multiplied by the system calibration factor, K, gives the grade-thickness product GT. When GT has been determined for a given zone based on measurements in a number of boreholes in an area, then tonnage calculations can be made.

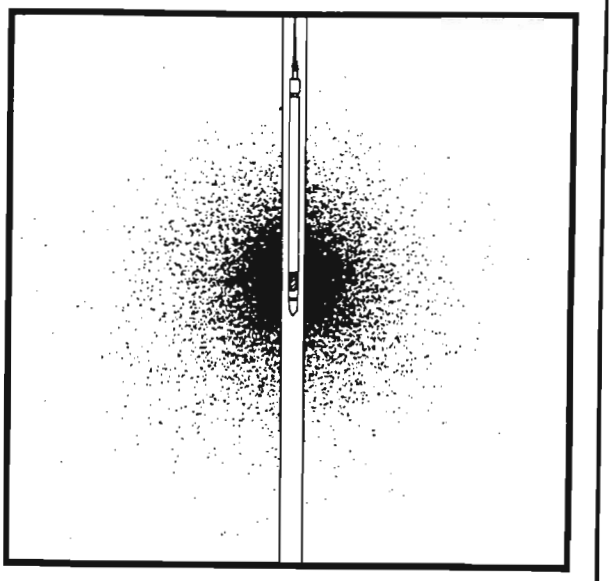

FIGURE 5. Illustration of the sample volume concept as a probability distribution. Although the chance of a given gamma ray being detected falls off rapidly with distance between the emitter and the detector, that chance will nonetheless be finite. Depending on gamma-ray energy, rock density and other parameters, this diagram represents an area roughly 2-3 m on a side.

the product of the two. In the case of Figure 3c, the FWHM is equal to 1 m, the true zone thickness. For Figure 2c, the FWHM is about 25 cm and the true zone thickness is 20 cm, a 25% error. In Figure 1c, the FWHM is about 15 cm and the true thickness is 5 cm, a 200% error. The percentage error in the FWHM method increases as zone thickness decreases. In all cases of radioactive zones which are not infinitely thick, the FWHM rule will give an overestimate of thickness T. When this value of T is used in equation (2), the resulting average G will be an underestimate. Thus, a determination of average grade based on this technique will tend to be a conservation estimate.

For ore zones which are isolated, uniform and less than infinitely thick, graphs have been given by Conaway (1978) which allow the thickness of the zone to be determined (within the limitations of noise, i.e. statistical uncertainty in determining the true radioactive intensity, lateral inhomogeneities in the rock, etc.) based on the FWHM of the anomaly curve. Rules of thumb for determining the thickness of zones less than infinitely thick are generally misleading and should be treated with suspicion.

For the more general (and more common) case of a complex distribution of radioactive material along the borehole, an estimate of the grade-thickness product can be made as shown in Figure 4. More sophisticated computer techniques are available (Conaway and Killeen, 1978a; 1978b; Conaway, 1979a), which are designed to give the true distribution of radioactive material (i.e. true grade and thickness). The extent to which these computer techniques are successful depends on many factors, including detector length, sampling interval along the borehole and relative noise level. The relative noise level is lower (better) for digital recording than for digitized analog strip charts, and is also lower for high count rates than for low count rates. The success of these computer techniques also depends on whether the radioelement distribution varies only with depth along a borehole, or whether there is an inhomogeneous or 'plum-pudding' distribution. Even under the best of conditions, these sophisticated computer techniques serve only to *enhance* the information available in the log. The computer does not *interpret* the log; this is still the task of the trained geophysicist or geologist.

Occasionally in the gamma-ray logging literature, the term *sample volume* or *volume of investigation* is encountered. This is generally defined as the region of rock surrounding the detector from which nearly all (say, 99%) of the gamma-rays arriving at the detector originated. The sample volume is often shown diagrammatically as a solid circle of radius 1 m or less centred on the detector. Visualizing the sample volume this way can be somewhat misleading, as it can be construed as meaning that any small region within the sample volume contributes the same number of gamma rays to the recorded count rate as any other region of the same volume. The actual situation is shown diagrammatically in Figure 5. Here, a cross section along the axis of a borehole through an infinitely thick homogenous zone of radioactive material is plotted showing the borehole, probe and gamma-ray detector. The dots outside of the borehole represent the locations of disintegrating atoms along this section which emitted the gamma rays that subsequently struck the detector and were counted during a given counting period. The probability of a gamma ray from any particular disintegrating atom being counted by the detector decreases rapidly with increasing distance of the atom from the detector. However, at any distance there is always a finite possibility of the gamma ray being detected. Figure 5 helps to explain the shapes of the synthetic gamma-ray logs shown in Figures 1-3. The zone of radioactive material is 'seen' by the detector as the detector approaches the zone, which explains why the anomaly curve begins to rise before the detector reaches the radioactive zone. Furthermore, unless the radioactive zone is infinitely thick, the detector will still be able to 'see' outside of the zone even when the detector is situated in the centre of the zone; thus, only in the case of infinitely thick zones does the gamma-ray intensity become proportional to the radioelement grade. For convenience, it is reasonable to say that the zone is 'effectively infinitely thick' when the gamma-ray intensity reaches 99% of the value which it would attain if the zone were truly infinitely thick (see Conaway, 1978).

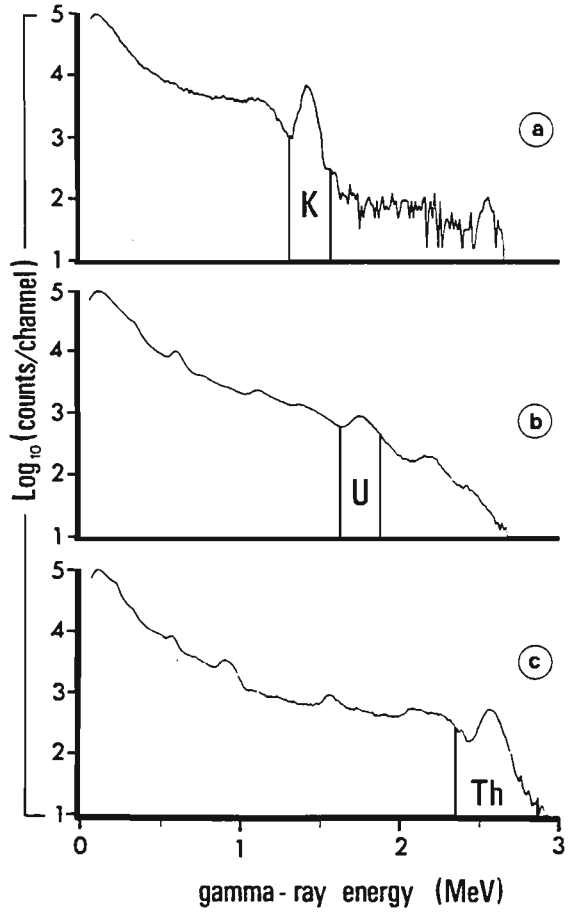

FIGURE 6. Gamma-ray energy spectra obtained in model boreholes using a 32- by 127-mm sodium iodide detector. Figure 6a shows the spectrum from a model borehole containing the radioelement potassium (K), Figure 6b is from a U model and Figure 6c is from a Th model. These spectra were obtained with a 256-channel spectrometer, each channel being about 12 keV wide. The shaded areas are the traditional K, U and Th spectral windows centred at 1.46, 1.76 and 2.62 MeV, respectively. After stripping, all gamma rays having energies between the upper and lower cutoff energies for the Th window are attributed to the thorium decay series, and similarly for uranium and potassium (the spectra shown in Figs. 6a-6c have not been stripped). Generally, the 'contents' of these three windows are stripped and plotted along with the total-count window (i.e. all gamma rays having energies greater than some predetermined minimum such as 0.4 MeV) against depth as the 4-channel spectral log.

Quantitative Uranium Determinations—Spectral Log

Figure 6 shows three gamma-ray energy spectra recorded using the Geological Survey of Canada's nuclear borehole logging R&D truck with a 32 by 127-mm NaI detector inside a 50-mm-diameter stainless steel probe. These spectra were recorded in the GSC's model boreholes for calibration of gamma-ray spectral logging equipment (see Killeen and Conaway, 1978). Figures 6a to 6c represent, respectively, the K (potassium), U and Th spectra. The shaded areas are spectral *windows* which cover important energy peaks from the K, U and Th decay series. In commercially available gamma-ray spectral logging equipment the spectrum is not recorded. Rather, the number of gamma rays having energies falling into each of these three windows detected per unit time is recorded (on magnetic tape, chart recorder or printer) along with total count (all gamma rays with energies greater than, say, O.4 MeV*) and depth.

In general, the measured gamma-ray energy spectrum is smeared rather badly, and what should appear as discrete well-separated energy peaks (each due to a specific disintegration) actually appears as rounded peaks with a great deal of overlap (Fig. 6). The degree of overlap depends on the *energy resolution* of the detector, and on the fact that a given gamma ray may have collided with one or more electrons before arriving at the detector (*Compton scatter*), and thus may have lost part of its energy. Also, the detector may not completely stop the gamma ray, and thus may register only part of its true energy; this factor is determined by the *detector efficiency*. Because of these factors, some gamma radiation from the thorium series, for example, will fall into the uranium window and be counted as uranium-series gamma rays; this is evident from Figure 6. For best results, therefore, a correction known as *spectral stripping* must be made.

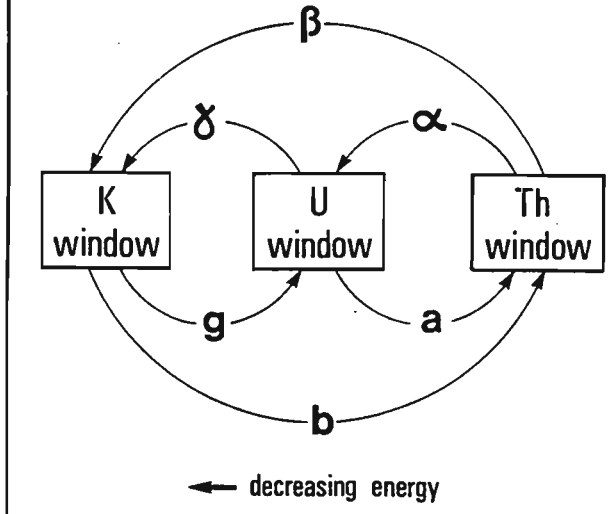

FIGURE 7. The scheme used in naming the six stripping factors. As an example, the stripping factor used to correct for Th gamma rays in the U window is called α, and the stripping factor used to correct for U gamma rays in the Th window is called a.

Figure 7 shows the scheme used in naming the various *stripping factors* or *stripping ratios* (Grasty, 1977). Of the six stripping factors, the most important in borehole logging are α (to remove counts due to thorium-series gamma rays from the uranium window), β (thorium from potassium) and γ (uranium from potassium). The factor "a" will be small for logging equipment, and "b" and "g" will be nearly zero. These stripping factors are equipment-dependent, and must be determined experimentally for each logging system (and each probe); this is most easily accomplished in model boreholes (see Killeen and Conaway, 1978).

The stripping factors are applied to the digitized gamma-ray spectral log as follows:

$$Th_s = \frac{Th(1-g\gamma) + U(b\gamma-a) + K(ag-b)}{D} \quad \ldots\ldots\ldots\ldots \quad (3)$$

$$U_s = \frac{Th(g\beta-\alpha) + U(1-b\beta) + K(b\alpha-g)}{D} \quad \ldots\ldots\ldots\ldots \quad (4)$$

$$K_s = \frac{Th(\alpha\gamma-\beta) + U(a\beta-\gamma) + K(1-a\alpha)}{D} \quad \ldots\ldots\ldots\ldots \quad (5)$$

where Th, U and K are the gamma-ray intensities recorded in the thorium, uranium and potassium windows of the spectral log, respectively, in counts per second. Th_s, U_s and K_s are the

*MeV stands for mega-electron volts, or 1 million electron volts of energy. 1MeV = 1000 keV or kilo-electron volts.

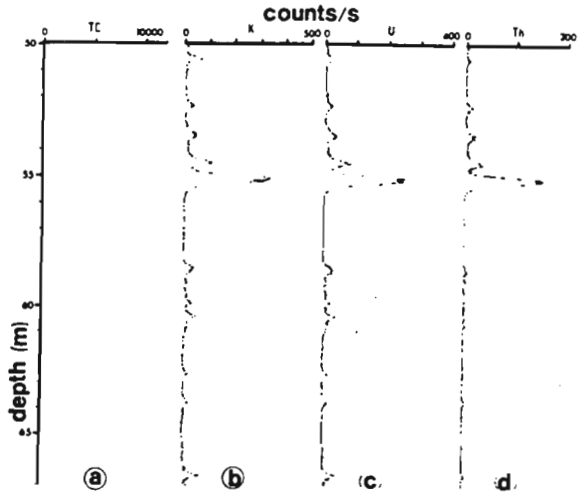

FIGURE 8. Unstripped 4-channel gamma-ray spectral log in a mixed U-Th environment.

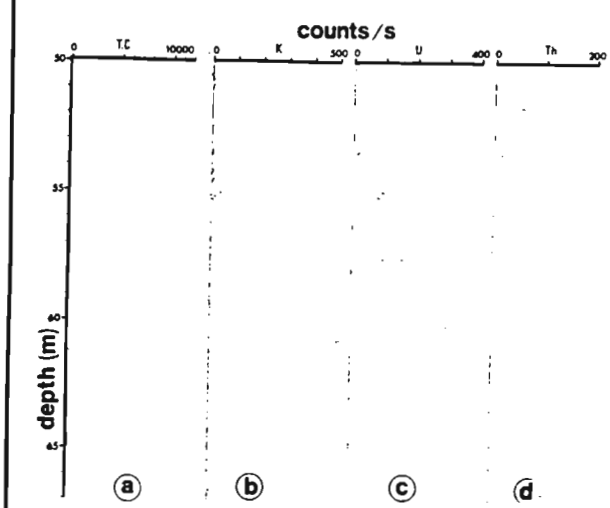

FIGURE 9. The 4-channel gamma-ray spectral log shown in Figure 8 after stripping (and smoothing).

corrected (stripped) gamma-ray intensities in those same windows. The term in the denominator, D, is given by

$$D = 1 - g\gamma - a(\alpha - g\beta) - b(\beta - \alpha\gamma) \quad \ldots\ldots (6)$$

As stated above, the factors b and g are negligibly small for most borehole logging detectors and may generally be eliminated from the above equations, giving

$$Th_s = \frac{Th - aU}{D} \quad \ldots\ldots (7)$$

$$U_s = \frac{U - \alpha Th}{D} \quad \ldots\ldots (8)$$

$$K_s = \frac{Th(\alpha\gamma - \beta) + U(a\beta - \gamma) + K(1 - a\alpha)}{D} \quad \ldots\ldots (9)$$

where D is now given by

$$D = 1 - a\alpha \quad \ldots\ldots (10)$$

The stripped gamma-ray intensities are used to compute the concentrations of potassium, uranium and thorium in a similar fashion to the quantitative interpretation of total-count logs explained earlier (equation 1). In the case of spectral logs, there are calibration factors (like the factor K in equation 1) expressing the sensitivity of the spectral logging system to the thorium (C_{Th}), uranium (C_U) and potassium (C_K) decay series. These spectral calibration factors or "C-factors" have units such as % eU/(counts/s) for C_U, and similar units for C_{Th} and C_K. Equation (1) is modified to give three equations for the three windows of the spectral log:

$$G_{Th}T_{Th} = C_{Th}A_{Th} \quad \ldots\ldots (11)$$

$$G_UT_U = C_UA_U \quad \ldots\ldots (12)$$

$$G_KT_K = C_KA_K \quad \ldots\ldots (13)$$

In equation (11), G_{Th} is the average apparent concentration or grade of thorium in an anomalous zone, based on the area under the anomaly curve (A_{Th}) in the stripped thorium window log; T_{Th} is the thickness of the anomalous zone. The average apparent uranium grade (G_U) or potassium concentration (G_K) can be computed in a similar manner from the stripped uranium and potassium windows of the log using equations (12) and (13). The validity of equations (7-9) depends on the decay series being in radioactive equilibrium, as discussed in the next section.

Figure 8 shows a typical raw (digital) gamma-ray spectral log in a mixed uranium-thorium environment. From the total-count log (8a), it is not apparent which radioelement series is causing the anomalies. From the thorium channel it appears that there is significant thorium in the four distinct radioactive zones between about 52-56 m, but little above or below those zones; however, quantitative information is still lacking. In Figure 9, the log has been stripped (and smoothed slightly to reduce the statistical noise). Now it is clear what radioelements are responsible for the various anomalies, and, using the techniques shown in Figure 4 along with equations (11-13), it is possible to determine the concentration of each of the three radioelements in any anomalous zone. Especially impressive is the virtual elimination by the stripping process of all potassium anomalies in this example. In the case of uranium, it is now clear that about half of the apparent uranium anomaly at 55 metres in the unstripped log was due to thorium gamma rays.

The Problem of Radioactive Disequilibrium

The normal undisturbed condition for a radioelement decay series in nature is called *radioactive equilibrium*. This means that, on the average, for each disintegration of a parent atom, one atom of each of the radioactive daughter products also disintegrates. If element A in the series has a half-life of 10 years and element B in the same series has a half-life of 1 year, then there will be 10 times as much of element A as element B if they are in equilibrium.

All standard natural gamma-ray logging techniques assume that the decay series is in equilibrium, because it is the 1.76-MeV gamma ray emitted by ^{214}Bi (read bismuth-214 where 214 is the atomic weight) which is considered diagnostic of ^{238}U (the most common form of U in nature). The reason for this is that no gamma rays are given off by ^{238}U, and those given off by the daughters between ^{238}U and ^{214}Bi in the decay series are of lower energy and are difficult to resolve without elaborate equipment (including solid-state detectors, which are now in the experimental stage for borehole logging applications). As ^{214}Bi is 9 disintegrations removed from ^{238}U in the decay series, it is obvious that a problem arises when the ^{238}U decay series is not in equilibrium, because the calculated uranium concentration will be in error (i.e. the ^{214}Bi will no longer be diagnostic of the amount of ^{238}U).

If equilibrium is the state toward which the decay series tends to go, what causes disequilibrium? Generally, disequilibrium results when either the ^{238}U or one or more of the

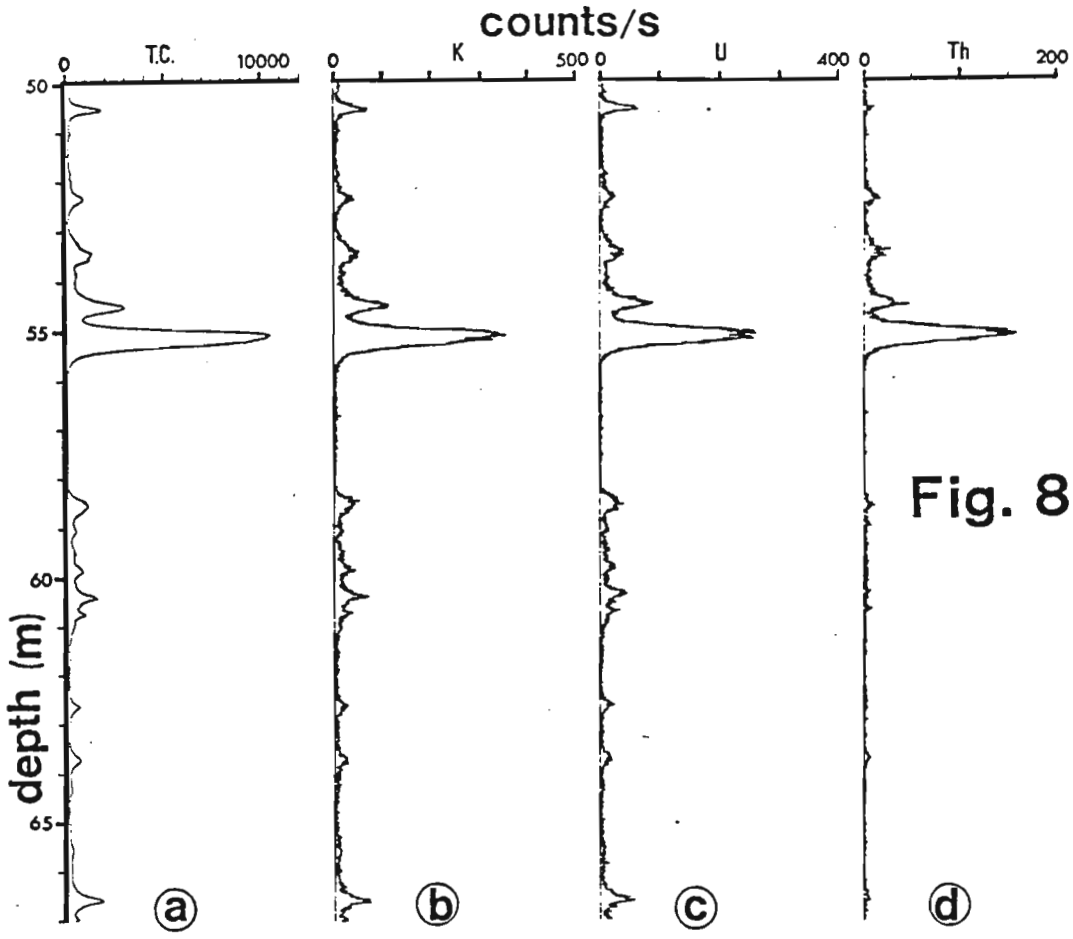
counts/s
T.C.
0
10000
K
0
500
U
0
400
Th
0
200
50
55
60
65
depth (m)
a
b
c
d

Fig. 8

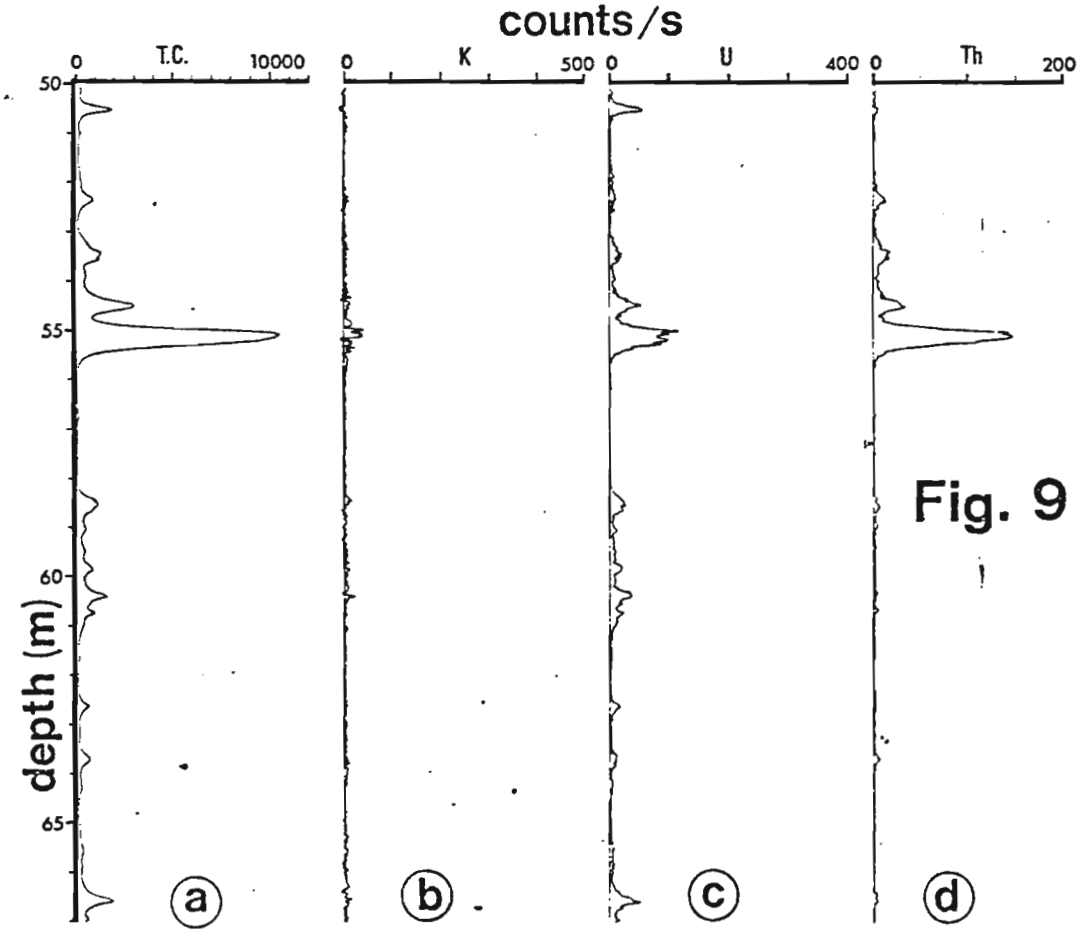
counts/s
T.C.
0
10000
K
0
500
U
0
400
Th
0
200
50
55
60
65
depth (m)
a
b
c
d

Fig. 9

daughter products between ^{238}U and ^{214}Bi migrates away from the rest of the elements in the series. This can occur because each element has different chemical properties. Under certain geologic conditions, ^{238}U itself can be relatively mobile; furthermore, one of the intermediate daughter products (radon) is a gas—albeit with quite a short half-life (3.8 days)—thereby limiting the length of time which is available for it to migrate (see Rosholt, 1959, for more information).

Disequilibrium in a uranium deposit or occurrence does not necessarily rule out gamma-ray logging as an evaluation tool. Satisfactory results may still be obtainable by spot-checking the state of disequilibrium of the deposit by laboratory chemical analyses, and applying appropriate corrections to the gamma-ray logs (Rosholt, 1959; Scott and Dodd, 1960). Gamma-ray logging has been shown to be an effective quantitative evaluation tool in the sandstone-type uranium deposits in the United States, even though these deposits are known to be in radioactive disequilibrium to various degrees.

Gamma-Ray Spectral Logging Equipment

Selecting a suitable logging system can be quite a problem in itself and, of course, no one system is well suited to all applications. Some useful background material may be gleaned from the reports by Killeen (1976), Killeen and Bristow (1976), and Killeen *et al.* (1978). Without going into the matter deeply, several important pointers regarding the equipment can be given here.

Data Recording—An analog recording system will generally be less expensive to purchase than a digital system, and perhaps will be somewhat more reliable under field conditions (although this may be expected to change with future technologcial developments). A digital system eliminates the expense of manual digitization of the data and generally makes the data processing easier, if any but the most basic processing techniques are to be used. The processed results from a digital system will generally be more accurate than those from an analog system (see Conaway *et al.*, 1980). A hybrid recording system wherein the signal is passed through a ratemeter, as in an analog system, and then digitized eliminates the tedious step of manual digitization required by true analog recording. This system shares many of the disadvantages of pure analog recording, however, and should not be confused with the true digital system where the counts are summed for a preselected period (say, 1 second), and then the sum is written on tape along with depth, etc.

The Detector—To evaluate high-grade uranium deposits, the scintillation crystal (detector) must be quite small, perhaps as small as 1 by 1 cm, to avoid swamping the electronics with gamma-ray pulses. A small detector (say, 2.5 by 2.5 cm) is also best for delineating thin zones and resolving complex sequences of zones of different grades. For lower-grade deposits and occurrences, a larger detector, perhaps 2.5 by 7.5 cm, will be needed. For stratigraphic logging in a non-uraniferous environment, still larger detectors may be required in order to detect enough gamma rays to make the results statistically reliable. In the United States, detectors on the order of 5 by 25 cm are commonly used in the standard 11-cm-diameter boreholes there. In Canadian hard-rock areas, where smaller-diameter holes are the rule, large detectors of this type are impractical. In this case, special high-density detector materials (which are still experimental) instead of the standard sodium iodide crystals may provide the answer. For spectral gamma-ray logging, larger detectors will generally give higher-quality spectral information.

The Winch—Hand-cranked winches are often favoured in difficult terrain for their relative reliability and portability, but they also have severe disadvantages. The tedium involved in attempting to crank the winch at a constant low speed for hour after hour is considerable, and tends to lead to operator inattention, resulting in undesirable speed fluctuations. A motor-driven winch is heavier and requires a generator for power, but the convenience of operation and the improved accuracy of the results make the motor drive a highly desirable feature of the winch.

The Depth Counter—Experience indicates that winch-mounted depth counters of the capstan-and-pressure-roller type tend to be inaccurate and unreliable. Such devices should be checked regularly. This may be accomplished by marking off the cable at regular intervals of, say, 50 m (by using a tape measure), and then comparing the cable marks against the depth counter readings as the probe is lowered down the borehole and brought back up again. If significant errors (more than a few cm) are found, the problem is either with the depth counter or due to cable stretch. A well-head pulley depth counter assembly with an optical encoder should give improved accuracy. Calibration as described above can help compensate for the systematic depth errors in any depth measuring system, and allows a cable-stretch correction to be appplied if required.

Spectral Stabilization—As a probe moves along the borehole, ambient temperature changes will affect the properties of the detector and the electronics in the probe. As a result, the spectrum can expand or contract, perhaps to the extent that the energy peaks will move entirely out of the windows set up for them (Fig. 6). Various spectral stabilization techniques are being used to compensate for this shift, but at present all of the techniques used in commercially available equipment have severe limitations. This is just an R&D problem, and hopefully in the near future reliable stabilization will be a reality.

Suggestions Regarding Field Procedure

The best procedure for a spectral logging system without spectral stabilization is to lower the probe into a water-filled section of the borehole (if possible) for some time before bringing it up to calibrate the spectrum (using a ^{137}Cs source, generally). Allow at least 20 minutes for a 3-cm-diameter probe and 30 minutes for a 4-cm-diameter probe to approach the temperature of the water in the borehole. Larger probes require correspondingly longer times to equilibrate. The probe power should be on during this equilibration period. Of course, because the temperature varies with depth along the borehole, the calibration may still shift during the logging.

A constant logging speed is important with both digital and analog systems, otherwise the problem of making a good interpretation becomes difficult or impossible. In tests, we have found that, although it is important to log slowly for accuracy, it is even more important to use a short sampling interval. A sampling interval of about half the detector length or less (down to a practical minimum of 1 or 2 cm) should be used for best results.

Few analog logging systems offer chart speeds which are fast enough to give good results. An analog system that can't produce 5-10 cm of chart recording for each metre of borehole should probably be modified. Of course, this sort of ratio (1:20 or 1:10) may only be required for detailed logging of interesting zones, but it should be available for that purpose for best results (Conaway *et al.*, 1980).

Calibration

Model boreholes have been established near Ottawa for the purpose of calibrating gamma-ray spectral logging equipment. Limited facilities are also available in Fredericton, and further facilities at other locations are envisioned. It is good practice to make use of such facilities before and after each field season (or more often, if convenient) to determine calibration constants and stripping factors. Such tests can also reveal equipment problems which might not be obvious from the field logs. For further information on calibration, see Killeen and Conaway (1978).

Other Problems

In addition to the problems discussed above, many more factors can affect the quality of the gamma-ray log. Some of these

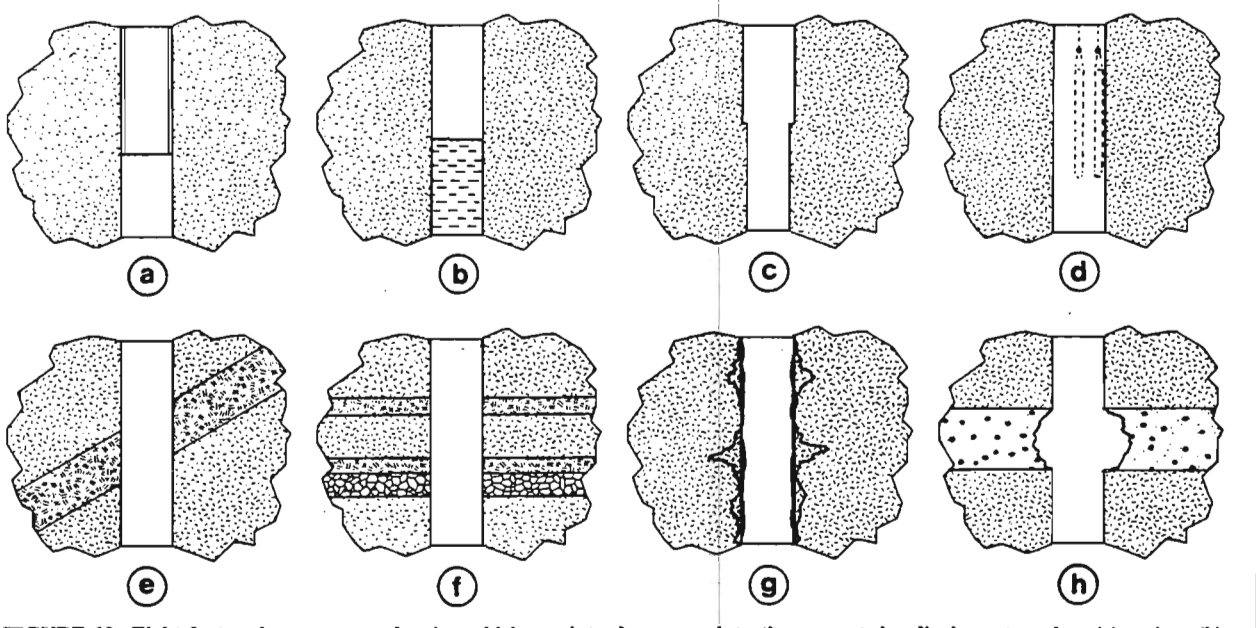

FIGURE 10. Eight factors in gamma-ray logging which can introduce error into the computed radioelement grades: (a) casing, (b) borehole fluid, (c) change in borehole diameter or borehole diameter different from the calibration model, (d) change in probe position (centred or eccentred), (e) dipping radioactive zones, (f) complex distributions, (g) mud or fluid invasion of the borehole walls, (h) caving of the walls.

are mentioned here, with correction methods referenced where available.

Figure 10 illustrates diagramatically eight of these additional problems—casing, borehole fluid and diameter, probe position, dipping beds, complex radioactive zones, and invasion and caving of the borehole walls. The effects of four of these—casing, borehole fluid, borehole diameter and probe position—can be largely eliminated by applying suitable correction factors worked out in model boreholes (Dodd and Eschliman, 1972) or theoretically (Rhodes and Mott, 1966). Of the remaining four factors, dipping beds can be compensated for if the dip is known (Conaway, 1979b), and thin and complex zones can be resolved to a large extent by using a short detector and computer processing techniques (Conaway and Killeen, 1978a; Conaway, 1979a). Invasion of mud, grit, etc. into the borehole walls during drilling, and irregular caving of the borehole walls, are problems which are difficult to correct for in the gamma-ray log, but they should be borne in mind as possible serious sources of error. Of all of these sources of error, potentially the most serious is the dipping bed problem. If the radioactive zone is oriented at any angle other than perpendicular to the borehole (0 degree relative dip), the grade-thickness determination will be too large. Most other sources of error cause the grade-thickness determination to be too low.

A factor which has become important in light of the recent discovery of high-grade deposits in northern Saskatchewan is the problem known as Z-effect (where Z stands for atomic number). The relationship given by equation (1) between gamma-ray intensity and grade-thickness product becomes non-linear as ore grade increases. This is a complex problem, although in general at least partial compensation is possible (see Dodd and Eschliman, 1972). Once again, grade calculations based on equation (2) will tend to err on the conservative side (see Conaway, 1980).

Radioactive decay is a completely random process, therefore any measurement of gamma-radiation intensity is subject to error (*statistical counting noise*). The resulting uncertainty in the true radiation level is proportional to the square root of the number of counts expected in a given sampling period. Therefore, the higher the expected count the lower the percentage uncertainty due to statistical counting noise. Loggers may be tempted to increase the analog time constant or the sampling time of a digital system in an effort to make the log appear smoother. Usually these solutions degrade the quality of the log and limit the effectiveness of any data enhancement techniques which may later be applied (Conaway and Killeen, 1978a).

The smearing effect of the ratemeter time constant of an analog system can generaly be reduced by computer processing. Nevertheless, a short time constant should be used for best quantitative results. Using a long detector also causes loss of spatial resolution in the log, and this effect cannot be completely removed. The use of a shorter detector along with a slower logging speed can give the same statistical reliability as a longer detector, but with improved resolution.

Conclusions

Gamma-ray logging, either total-count or spectral, can be used to good advantage in most (if not all) uranium environments. In practice, the reliability and utility of gamma-ray spectral logging depends largely on the logger's understanding of the technique. Numerous factors affect the quality of a gamma log and the accuracy of the interpretation based on it. In this article, we have touched on many of the most common or most important problems of which the logger should be aware. In addition to this general background, further reading of some of the works referenced herein is recommended. Finally, the staff of the Radiation Methods Section of the Resource Geophysics and Geochemistry Division of the G.S.C. is available to discuss specific problems which may arise regarding instrumentation, calibration, field technique or interpretation.

Acknowledgments

The authors thank A.G. Darnley, K.L. Ford and K.A. Richardson for helpful comments and suggestions. We are grateful to Kerr Addison Mining, Ltd., and their chief geologist, Dale Hendrick, for permission to log their Bancroft area drillholes (Figs. 8 and 9).

REFERENCES

CONAWAY, J.G., 1978: Problems in gamma-ray logging: thin zone correction factors; *Current Research, Part C, Geol. Surv. Can., Paper 78-1C, pp. 19-21.*

CONAWAY, J.G., 1979a: Computer processing of gamma-ray logs: a program for the determination of radioelement concentrations; *Current Research, Part B, Geol. Surv. Can., Paper 79-1B, pp. 27-32.*

1979b: Problems in gamma-ray logging: the effect of dipping beds on the accuracy of ore grade determinations; *Current Research, Part A, Geol. Surv. Can., Paper 79-1A, pp. 41-44.*

CONAWAY, J.G., 1980: Uranium concentrations and the system response function in gamma-ray logging; *Current Research, Part A, Geol. Surv. Can., Paper 80-1A (in press).*

CONAWAY, J.G., BRISTOW, Q., and KILLEEN, P.G., 1980: Optimization of gamma-ray logging techniques for uranium; *Geophysics, V. 45, No. 2 (in press).*

CONAWAY, J.G., and KILLEEN, P.G., 1978a: Quantitative uranium determinations from gamma-ray logs by application of digital time series analysis; *Geophysics, V. 43, pp. 1204-1221.*

1978b: Computer processing of gamma-ray logs: iteration and inverse filtering; *Current Research, Part B, Geol. Surv. Can., Paper 78-1B, pp. 83-88.*

DODD, P.H., and ESCHLIMAN, D.H., 1972: Borehole logging techniques for uranium exploration and evaluation; *Uranium Prospecting Handbook,* S.H.U. Bowie, M. Davis and D. Ostle, eds., *Inst. Min. Metall., London.*

GRASTY, R.L., 1977: A general calibration procedure for airborne gamma-ray spectrometers; *Report of Activities, Part C., Geol. Surv. Can., Paper 77-1C, pp. 61-62.*

KILLEEN, P.G., 1976: Portable gamma-ray spectrometer tests; *Report of Activities, Part A., Geol. Surv. Can., Paper 76-1A, pp. 487-489.*

KILLEEN, P.G., and BRISTOW, Q., 1976: Uranium exploration by borehole gamma-ray spectrometry using off-the-shelf instrumentation; *IAEA Proceedings of the International Symposium on Exploration of Uranium Ore Deposits, Vienna, April 1976, pp. 393-414.*

KILLEEN, P.G., and CONAWAY, J.G., 1978: New facilities for calibrating gamma-ray spectrometric logging and surface exploration equipment; *CIM Bulletin, V. 71, No. 793, p. 84-87.*

KILLEEN, P.G., CONAWAY, J.G., and BRISTOW, Q., 1978: A gamma-ray spectral logging system including digital playback, with recommendations for a new generation system; *G.S.C. Paper 78-1A, Current Research, Part A, pp. 235-241.*

RHODES, D.F., and MOTT, W.E., 1966: Quantitative interpretation of gamma-ray spectral logs; *Geophysics, V. 28, pp. 410-418.*

ROSHOLT, J.N., 1959: Natural radioactive disequilibrium of the uranium series; *U.S.G.S. Bull. 1084-A.*

SCOTT, J.H., and DODD, P.H., 1960: Gamma-only assaying for disequilibrium corrections; *U.S.A.E.C. Report RME-135.*

SCOTT, J.H., DODD, P.H., DROULLARD, R.F., and MUDRA, P.J., 1961: Quantitative interpretation of gamma-ray logs; *Geophysics, V. 26, pp. 182-191.*

(Reprinted from The Canadian Mining and Metallurgical Bulletin, January, 1980)

Printed in Canada

To be published in:Proceedings of the Third International Symposium on Borehole Geophysics for Minerals, Geotechnical, and Ground Water Applications; held in Las Vegas, Nevada, 2-5 Oct. 1989. (Sponsored by the Minerals & Geotechnical Logging Society; - a chapter of the SPWLA.)

A Slim Hole Assaying Technique for Base Metals and Heavy Elements Based on Spectral Gamma-gamma Logging

P.G. Killeen, L.D. Schock and B.E. Elliott
Geological Survey of Canada
601 Booth Street, Ottawa, Canada
K1A 0E8

Abstract

Field logging and laboratory physical model logging have been carried out to investigate the feasibility of using the spectral gamma-gamma method (SGG) for assaying in slim (46 to 76 mm) mineral exploration boreholes commonly drilled in Canada.

The borehole probe consists of a gamma-ray spectral logging tool with a 370 MBq (10 mCi) Cobalt 60 source mounted on the nose with omniazimuthal collimation. This collimation makes it possible to use a low radioactivity source since the gamma-rays travel radially out from the probe in all directions, backscattering to the detector with information. This is in contrast to the sources of 3700 MBq (100 mCi) or greater commonly used in gamma-gamma density logging with highly collimated decentralized probes. In that case only a small percentage of the gamma-rays (the collimated beam) backscatters with useful information about the rock.

Qualitative results have been obtained in a zinc deposit in Newfoundland in which the SGG method was clearly able to resolve the zinc-rich zones providing detailed information on the distribution of sphalerite within the zones. Quantitative results have been obtained in a lead deposit in Nova Scotia where assays of drill core at 10cm intervals were compared to the SGG logs. Correlation between the SGG ratio (the parameter determined from the logs) and the lead assays (range = 0 to 8% Pb) on drill core was excellent (correlation coefficient = 0.87).

Logging was also done in models constructed with crushed lead ore (galena),pyrite and barite. This provided information on the behaviour of the SGG ratio, as the ore material and grade are changed, as well as the effect of hole parameters on the results. It appears that the method is practical for mono-elemental deposits for the range of concentrations considered to be 'ore' grade.

Introduction

The spectral gamma-gamma (SGG) logging technique has been investigated by the Borehole Geophysics Section at the Geological Survey of Canada (GSC) as a possible practical method for in situ assaying of economic mineralization. Initial qualitative evaluations of the method in boreholes at the Yava Lead deposit in Eastern Canada showed promising results. Further work was done to quantify and calibrate the SGG logs to produce in situ lead assays at the same deposit with similar positive results. The method is now being extended with laboratory models constructed of crushed ore materials of different types and grades. Some results of these field and lab studies are presented here.

The Spectral Gamma-Gamma Method

The SGG method is based on the different interactions of gamma-rays with matter. After gamma-rays from a radioactive source have interacted with rock the gamma-ray energy spectrum contains information about the atomic number (Z) of the elements in the rock. The technology for natural spectral gamma-ray logging is already well developed, and can be adapted for SGG logging (Killeen, 1979).

The possibilities for elemental analysis based on the different interactions of gamma- rays with matter, (in this case rocks and minerals) was first described by Czubek (1966). The dominant interaction is Compton scattering in which gamma-rays are reduced in energy by scattering as they collide with electrons in the outer shells of atoms. The second type of interaction is photoelectric absorption in which a gamma-ray loses all its energy in a collision with an electron and ceases to exist. The probability of photoelectric absorption is roughly proportional to the fifth power of the atomic number, Z, of the element with which the gamma-ray interacts, and inversely proportional to about the third power of the gamma-ray energy, E. The probability of Compton scattering is roughly proportional to Z/E. Thus, if a spectral gamma-ray logging tool is used to measure the distribution of energies of gamma-rays from a radioactive source after they have interacted with rock as shown in figure 1, the shape of the spectrum will contain information about the atomic number of the elements in the rock. In particular, as shown in figure 2, the observed count rate at low energies will be greatly reduced if heavy elements (i.e., high Z) are present in the rock. An example application is the iron ore assay method developed by the CSIRO in Melbourne for use in mines of Western Australia (Charbucinski et al., 1977).

The principle of the SGG log can best be understood by referring to the two example spectra shown in figure 2. The positions of a low energy window (W10) and a high energy window

(W3) are indicated in the figure. When there is a change in the density of the rock being measured, the count rates recorded in both windows will increase or decrease due to the associated change in Compton scattered gamma-rays reaching the detector. However, if there is an increase in the content of high Z elements in the rock, the associated increase in photoelectric absorption will cause a significant decrease in count rate in the low energy window W10, but very little change in W3. W10 is affected by both density and Z effect while W3 is only affected by density. Therefore, a ratio of counts in W3 to the counts in W10 can be used to obtain information on changes in Z.

The SGG ratio log is a ratio of counts in a high energy window to counts in a low energy window (here for example W3/W10). This ratio increases when the probe passes through zones containing high Z materials. Experimentation is continuing to determine the optimum energy windows to use for this spectral ratio, as well as to optimize all of the other parameters involved. In particular, the characteristics of the most common Canadian mineral exploration boreholes are taken into consideration (e.g. BQ; 60 mm diameter, water-filled).

The Spectral Gamma-Gamma Probe

At the GSC, a special gamma-ray source holder has been designed to attach to the nose of a spectral gamma-ray logging probe in order to make SGG measurements. In making the measurements it is important to optimize the source-detector spacing and the collimation angle at the source. A series of different collimators designed to focus the gamma-rays radially out into the rock at angles of 90°, 60°, 45° and 30° to the probe, and a series of different spacers to permit variations in source-detector spacing have been fabricated from tungsten (see figure 3). Tungsten provides high gamma-ray attenuation, and permits the use of short source-detector distances if desired. The source holder is omni-azimuthal and is designed for use in the slim holes (e.g., AQ; 46 mm) commonly drilled in Canadian mineral exploration. The source can be of relatively low strength compared to those commonly used in gamma-gamma density probes because the collimators are radially symmetrical focussing gamma-rays at the appropriate angle, outward into the borehole wall in all directions. In addition to the different collimators and source detector spacings, sources with different gamma-ray energies (Cobalt 60, Cesium 137, Iridium 192) have been tested.

Spectral Gamma-Gamma Logs in Mineral Deposits

Yava Sandstone Lead Deposit, Nova Scotia

This deposit located in Nova Scotia consists of galena in sandstones, a relatively simple geology and mineralogy. The lead in galena with its high atomic number (Z=82) causes the spectral

ratio values in the SGG log to increase in proportion to the lead content. This is clearly demonstrated in the logs in figure 4. The lead assays from drill core, plotted in histogram form in the figure show that the SGG log can be considered a semi-quantitative assay log. Note the lead concentration is less than 4%.

These qualitative results showed excellent correlation with the assays of drill core which were available. To calibrate the system and provide quantitative data, detailed assays at 10 cm intervals were obtained on core from new boreholes and additional SGG logs were obtained. Results for hole 404A are shown in figure 5. These data were plotted and correlated as shown in figure 6 to provide calibration data for in situ lead assaying. The correlation between spectral ratios and lead content is excellent (correlation coefficient r = 0.87) . Figure 7 shows the core assays plotted as a log and compared to the computed in situ assay log. Similar results were obtained in other holes.

The periodic table of the elements is shown in figure 8 to illustrate the possibility of extending the method to other 'heavy' elements. In particular iron (atomic number Z=26) is often an important element in the form of pyrite, in massive sulphide deposits. It became the subject of lab experiments to be described later. Field tests in a zinc (Z=30) deposit are described below.

Zinc Deposit, Daniels Harbour, Newfoundland

This deposit consists primarily of sphalerite in limestone, another relatively simple geological setting. Although the atomic number of zinc is only 30, average grades of considerably less than 8% Zn are clearly defined by the high spectral ratio values shown in the SGG log in figure 9. Here the company assays were averaged over core lengths of about 1.5 metres. The SGG log shows that the zinc is concentrated in thin zones, probably less than 0.5 m thick and that the richest zone is at a depth of 23.5 metres. The potential for quantitative assaying with the SGG method is obvious.

The Stratmat Massive Sulphide Deposit, New Brunswick

This poly-metallic deposit contains copper, lead, and zinc. The SGG log and density log shown in figure 10 illustrate the log response to the mineralized zones. The density log appears saturated in the zone between 100 and 120 metres. The SGG log shows a higher spectral ratio in the top half of that zone as it responds to the lead and zinc which is not as abundant in the lower half of the zone where copper dominates.

The question of the possibility to separate or distinguish the elements with the SGG method arises here. Considerable further work is required to answer this question.

Experiments with Laboratory Models

To study the effect on the spectral ratio of different materials, in particular minerals containing heavy elements, an 'ore box' was constructed as shown in figure 11. The SGG probe was placed beneath the box against the bottom as shown in the figure. The ore material was added to the box in layers one centimetre thick. The backscattered spectrum was recorded after each layer was added.

The backscattered gamma-ray spectrum recorded for silica sand in layers 1 cm thick and 15 cm thick, are shown in figure 12. As each successive layer is added, the count rate increased but by smaller and smaller amounts. When there is no further change observed by adding more material to the ore box the thickness is considered to be infinitely thick. Figure 12 shows the location of two typical energy windows in the spectrum which were monitored as the ore thickness increased.

In the experiments ten energy windows were monitored. These included four low energy windows, five high energy windows, and a total count window as shown in figure 13. The results are plotted in graphical form in figure 14 for the case of silica sand. The figure shows that infinity is somewhere between 12 and 15 cm depending on the energy window being considered.

This procedure was followed using different atomic number materials in the ore box including water (H_2O), sand (SiO_2), pyrite (FeS_2), barite ($BaSO_4$) and galena (PbS). As atomic number (and density) of the material increased, the value of 'infinite' thickness became less. This is illustrated in figure 15 which shows the change in count rate in window 7 (defined in figure 13) as 'ore' material thickness increases from one to twenty-three centimetres for the above mentioned materials.

Infinite thickness is plotted against equivalent atomic number Z for these materials, in figure 16. Equivalent atomic number is computed simply on the basis of weighted atomic numbers according to the chemical formula for each material. The graph indicates that 'infinite thickness' ranges from about 17.5 cm for pure water to about 4 cm for pure galena. These data were used to design the cylindrical geometry 'ore box' with the dimensions shown in figure 17. The cylinder has an axial 60 mm ID plastic tube to form the 'borehole'. The outside cylinder of the model is 300 mm diameter which provides 120 mm radial thickness for 'ore' material placed in the model surrounding the borehole. The model was constructed from a waxed cardboard-type form used in concrete construction. The bottom was sealed appropriately to permit water saturation of the ore material, while leaving the borehole dry, and also water-filling of the borehole while leaving the ore dry. The length of the cylinders was sufficient to eliminate end-effects during the

measurements (ie. the cylinder was also considered to be infinitely long).

Variation of Spectral Ratio with Changing Pyrite Concentrations

Preliminary experiments using a 370 MBq (10 mCi) cobalt source were conducted for two cases: dry ore, and wet ore. Figures 18 and 19 show results for the centred and sidewalled probe respectively. In both cases the spectral ratio decreased when the borehole was water-filled, whether the ore was wet or dry. The spectral ratio values ranged from about 4.5 to 7.5 as the pyrite content ranged from about 12% to 50%.

The preliminary conclusions based on a centred probe (figure 18) are:

1. Over the range of pyrite concentrations from 12% to 50% a significant and reasonably linear change in spectral ratio was observed, making a pyrite assaying calibration feasible.

2. Water in the borehole decreases the values of the spectral ratio, by a relatively constant amount making development of a correction factor feasible.

3. Changing the ore from dry to wet (saturated) decreases the value of the spectral ratio making development of a moisture correction factor feasible.

The preliminary conclusions based on a sidewalled probe (figure 19) are:

1. Same as for centred probe.

2. Same as for centred probe.

3. Changing the ore from dry to wet increases the value of the spectral ratio, unlike the case of the centred probe. This unexpected result is the subject of further experiments to confirm or reject this preliminary observation.

Experiments with a cesium source as well as the cobalt source and different ore materials including barite and galena are presently being conducted. Lower and higher concentrations of pyrite and the other ores will also be investigated.

Acknowledgements

The authors wish to thank Bill Hyatt and Steve Birk for their field and lab measurements; Nova Scotia Department of Mines and Energy for logistics support at the Yava project under the Canada-Nova Scotia Mineral Development Agreement, 1984-89 and Noranda Mines and Newfoundland Zinc Mine for permission to publish data. Special thanks are due to Susan Davis for preparation of the figures, and to Jonathan Mwenifumbo for his participation, discussions and constructive criticism.

References

Killeen, P.G. (1979) Gamma-ray spectrometric methods in uranium exploration - application and interpretation; in Geophysics and Geochemistry in the Search for Metallic Ores, (Hood, P.J., Ed.), Geol. Surv. Can., Economic Geology Report 31, 163-229.

Czubek, J.A. (1966) Physical possibilities of gamma-gamma logging; in Radioisotope Instruments in Industry and Geophysics, (Proc. of Warsaw Symp, Oct. 1965) IAEA, Vienna, Vol. 2, 249-275.

Charbucinski, J., Eisler, P.L., Mathew, P.J. and Wylie, A.W. (1977) Use of backscattered gamma radiation for determining grade of iron ores in blast holes and development drill holes, (Proc. Australas. Inst. Min. Metall., No. 262), 29-37.

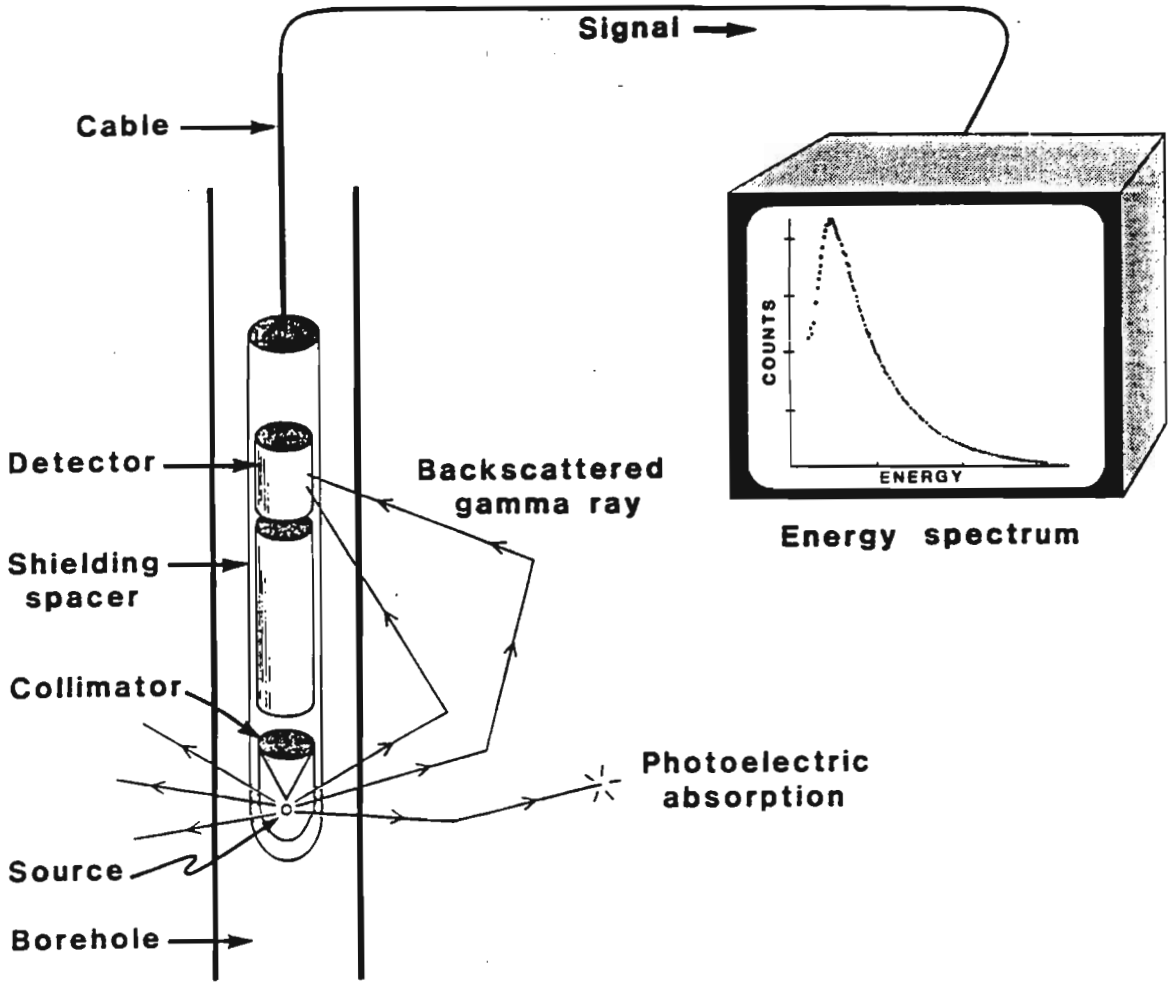

Figure 1: Schematic illustrating the main components in a spectral gamma-gamma (SGG) logging system. The source is separated from the detector by a collimator and a shielding spacer. The energy spectrum of the backscattered gamma-rays is recorded.

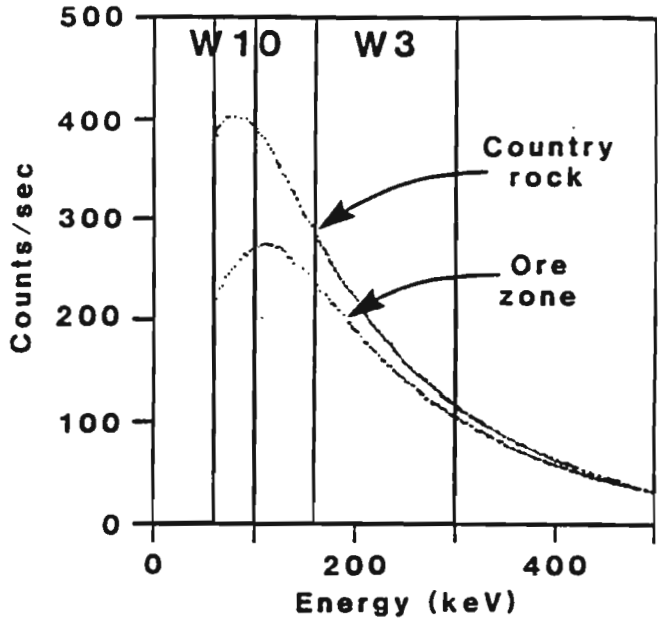

Figure 2: Example of backscattered gamma-ray spectra recorded in country rock and in an ore zone. In the ore zone the large decrease in count rate at low energies (W10=Window 10) compared to the decrease at high energies (W3=Window 3) is easily seen.

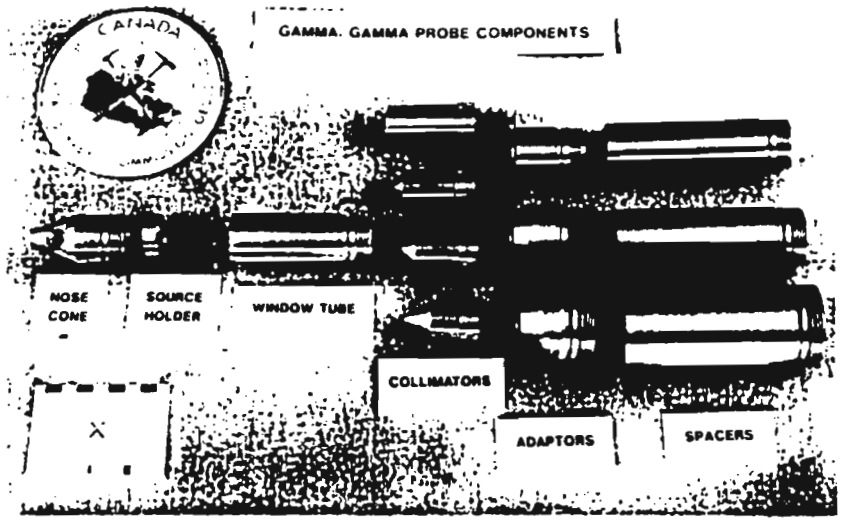

Figure 3: SGG probe components used for experiments with the GSC logging system. The 32 mm diameter source holder with window tube and collimator, is connected by an adaptor to 50 mm, 38 mm or 32 mm diameter shielding spacers for the appropriate diameter logging probes. Any one of the four different collimators shown may be used.

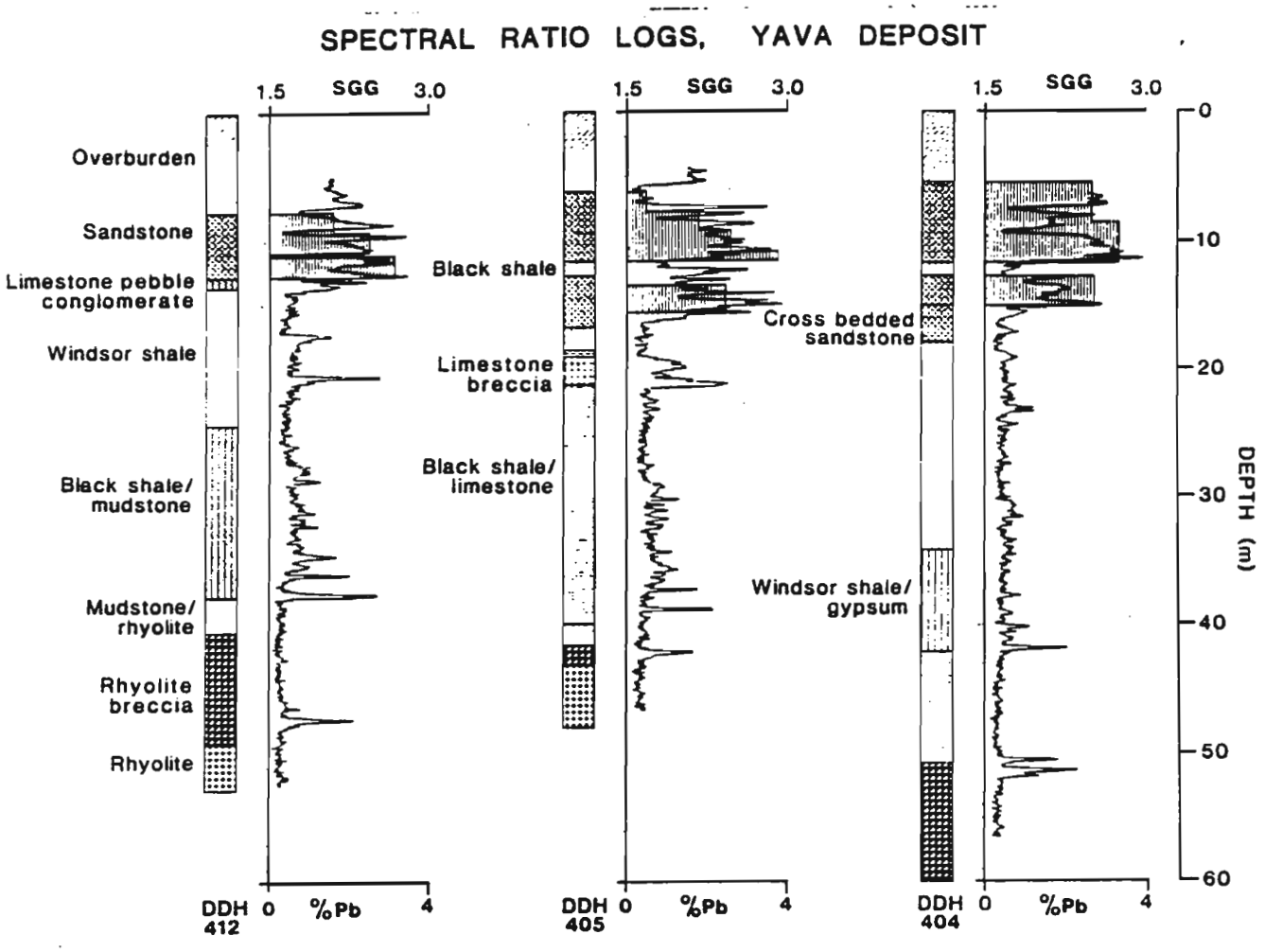

Figure 4: SGG ratio logs obtained in three boreholes in the Yava lead deposit, Nova Scotia. The high ratios correlate with the high lead values from company assays of drill core. Below the main ore zone, narrow high SGG ratio zones indicate thin galena stringers.

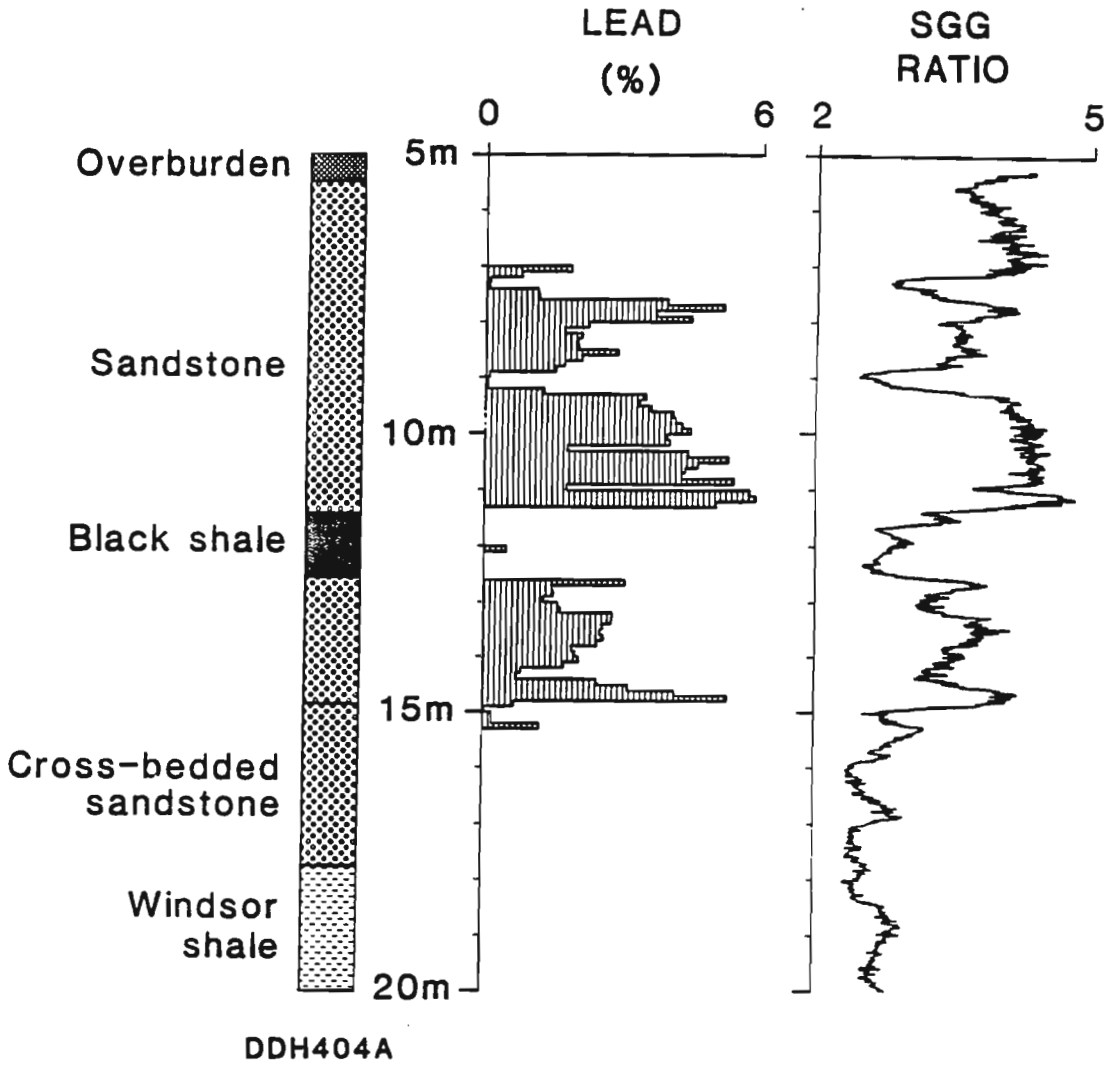

Figure 5: Comparison of detailed lead assays of drill core at 10 cm intervals and the SGG ratio log of the same hole.

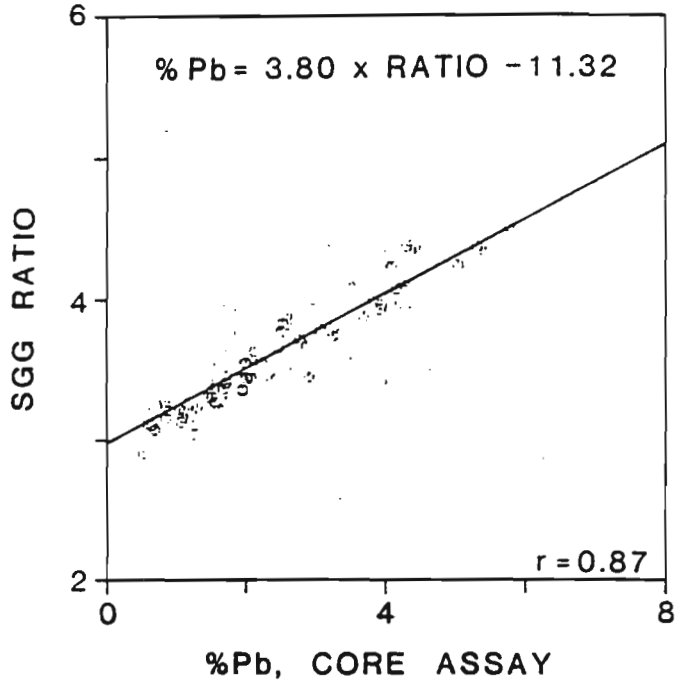

Figure 6: Lead assay calibration graph based on 10 cm core assays and SGG logs as shown in Figure 5.

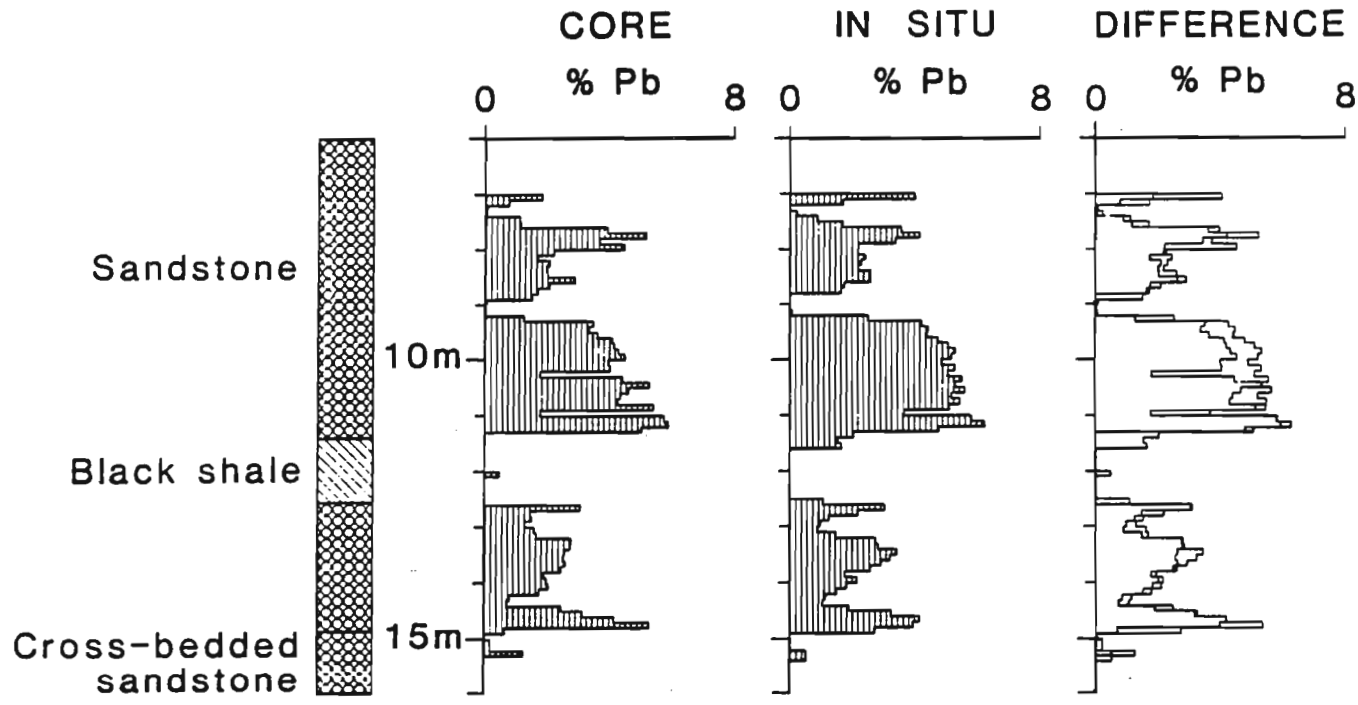

Figure 7: Comparison of laboratory core assay log and in situ computed assay log at 10 cm intervals based on the SGG log using the calibration equation from Figure 6. The absolute difference can be seen in the overlay of the two logs.

1 H																1 H	2 He
3 Li	4 Be											5 B	6 C	7 N	8 O	9 F	10 Ne
11 Na	12 Mg											13 Al	14 Si	15 P	16 S	17 Cl	18 Ar
19 K	20 Ca	21 Sc	22 Ti	23 V	24 Cr	25 Mn	26 Fe	27 Co	28 Ni	29 Cu	30 Zn	31 Ga	32 Ge	33 As	34 Se	35 Br	36 Kr
37 Rb	38 Sr	39 Y	40 Zr	41 Nb	42 Mo	43 Tc	44 Ru	45 Rh	46 Pd	47 Ag	48 Cd	49 In	50 Sn	51 Sb	52 Te	53 I	54 Xe
55 Cs	56 Ba	57 La	72 Hf	73 Ta	74 W	75 Re	76 Os	77 Ir	78 Pt	79 Au	80 Hg	81 Tl	82 Pb	83 Bi	84 Po	85 At	86 Rn
87 Fr	88 Ra	89 Ac															
		90 Th															
		92 U															

Figure 8: Periodic table of the elements showing their atomic numbers. Other 'heavy' elements ranging from iron (Fe=26) and upward are candidates for SGG assaying. Elements involved in this study are shaded.

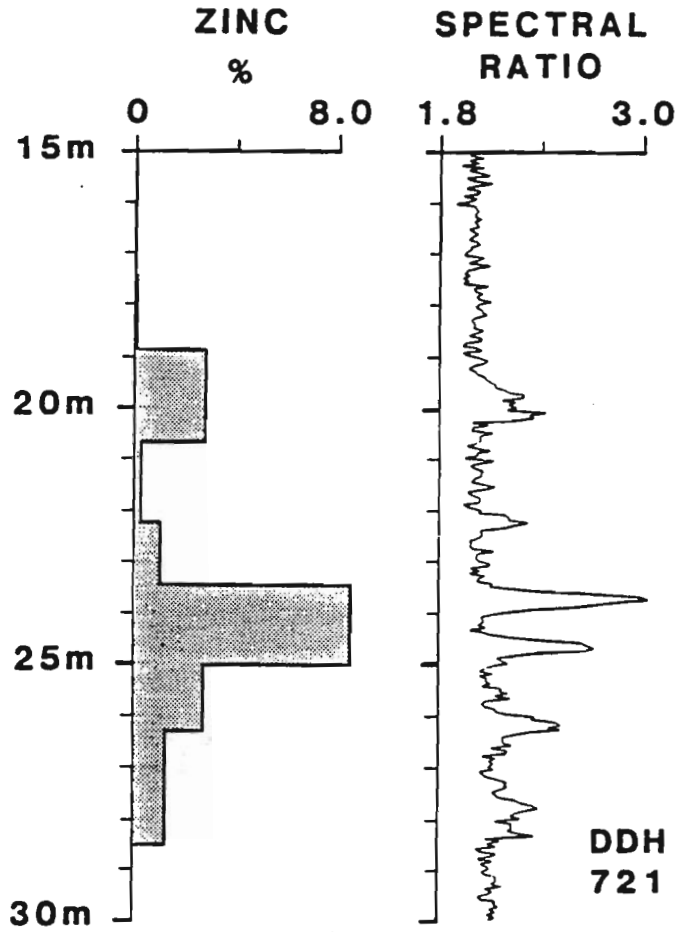

Figure 9: The SGG log in a zinc deposit. The company assays of drill core taken over approximately 1.5 metre lengths show good agreement with the high values of the spectral ratio. The SGG ratio however delineates the position of the mineralized zones in greater detail.

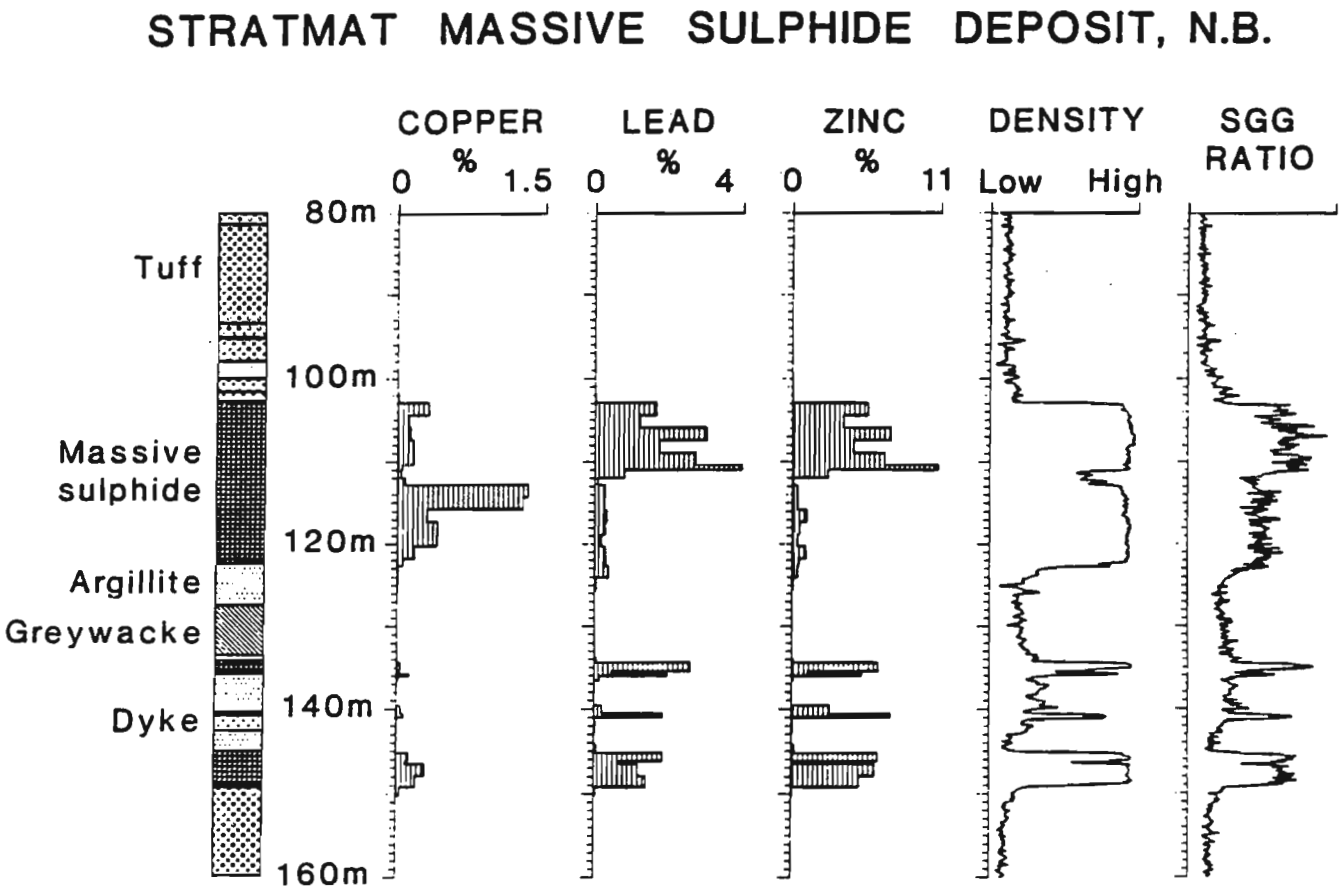

Figure 10: The SGG log in a poly-metallic massive sulphide deposit. Distribution of copper, lead, and zinc as well as the density log is also shown.

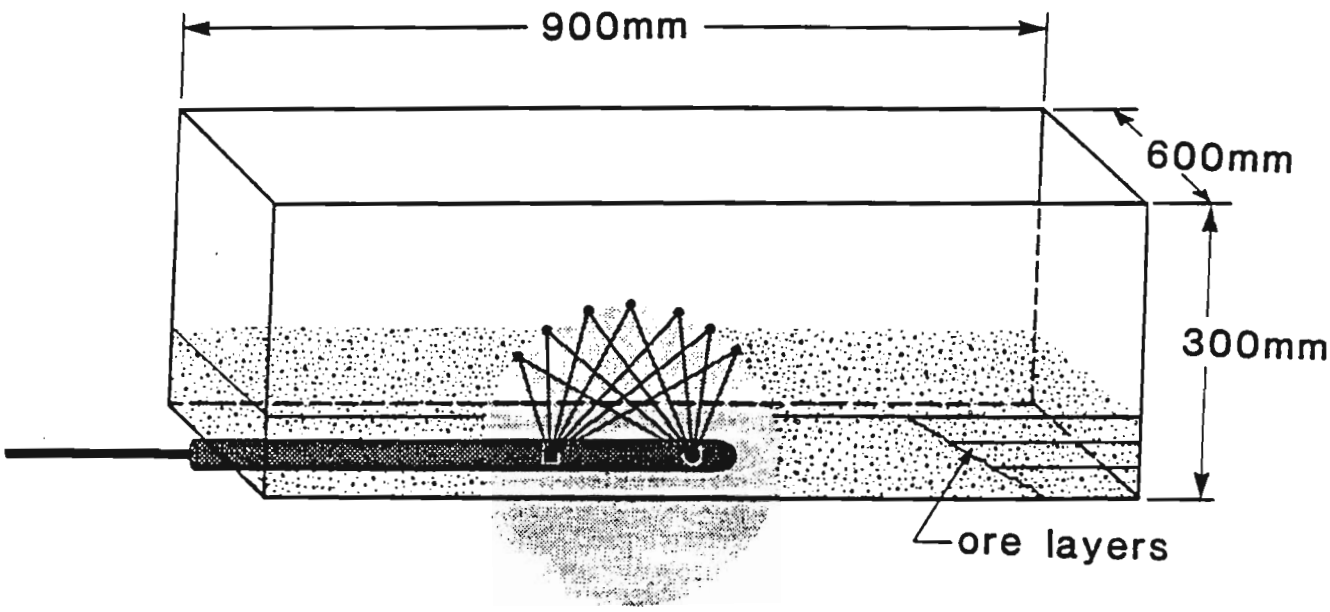

Figure 11: Experimental arrangement to determine 'infinite' thickness for different ore materials. The SGG probe is positioned beneath the box and successive layers of ore material are added to the box.

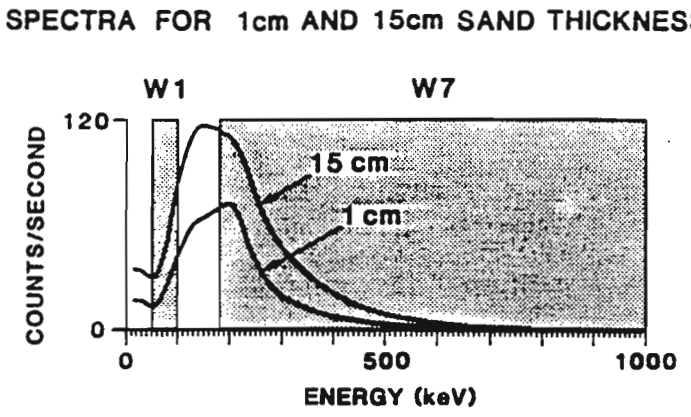

Figure 12: Comparison of backscattered gamma-ray spectra recorded from 1 cm and 15 cm thick layers of sand in the ore box of Figure 11. Two typical useful energy windows, W1 and W7 are shown.

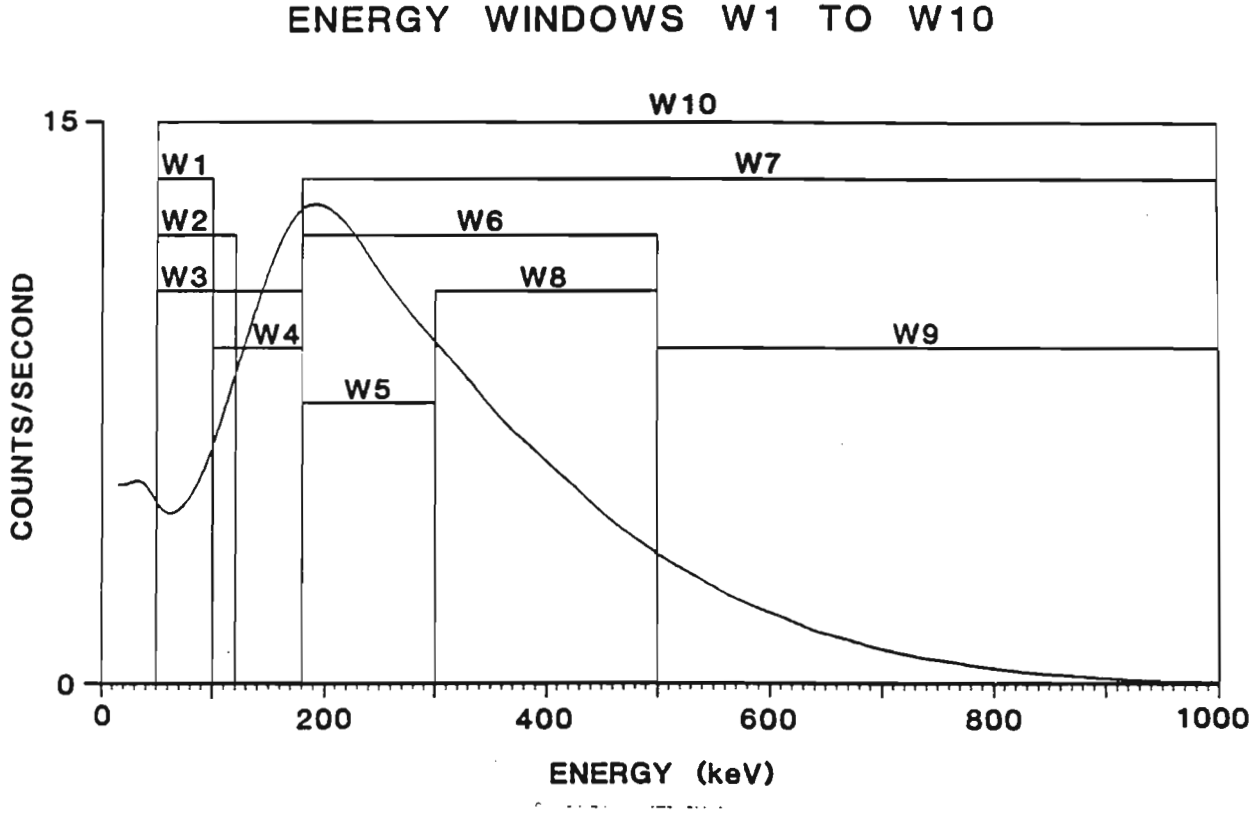

Figure 13: A selection of low energy windows (W1, W2, W3, W4) and high energy windows (W5, W6, W7, W8, W9) used for experimenting with spectral ratios and their relation to ore grade. W10 is a 'total count'window.

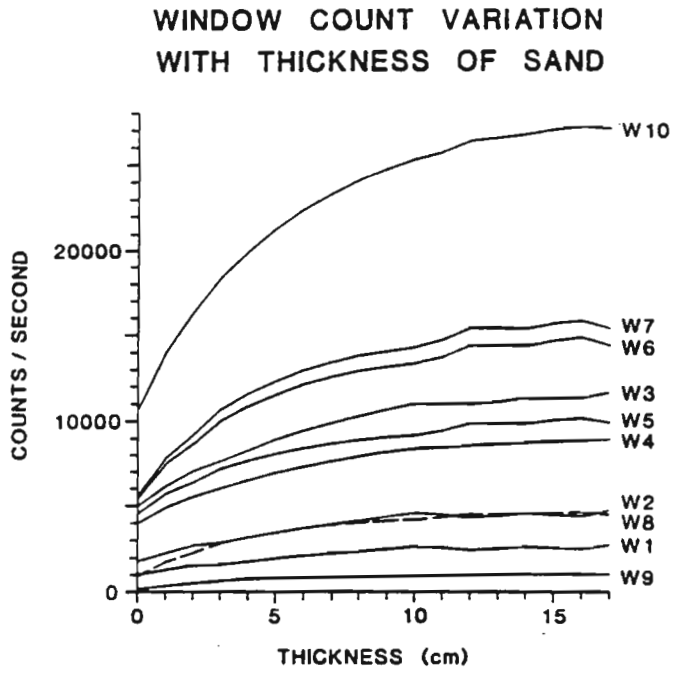

Figure 14: Variation in window count rate for the windows in figure 13, with thickness of silica sand in the ore box shown in figure 11. Infinite thickness is obtained when the curve flattens out.

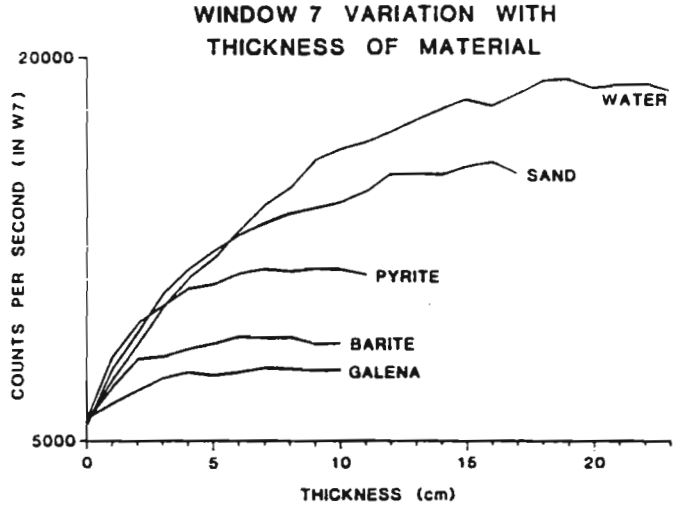

Figure 15: Variation in Window 7 count rate (See Figure 13) with thickness of water, sand, pyrite, barite and galena in the ore box (see Figure 11).

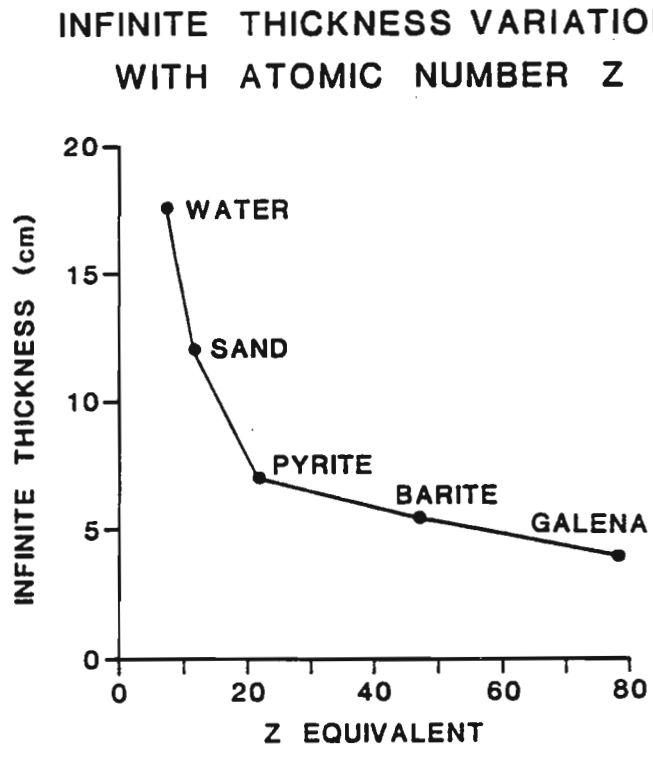

Figure 16: Estimated 'infinite' thickness for materials with different equivalent atomic number based on ore box experiments.

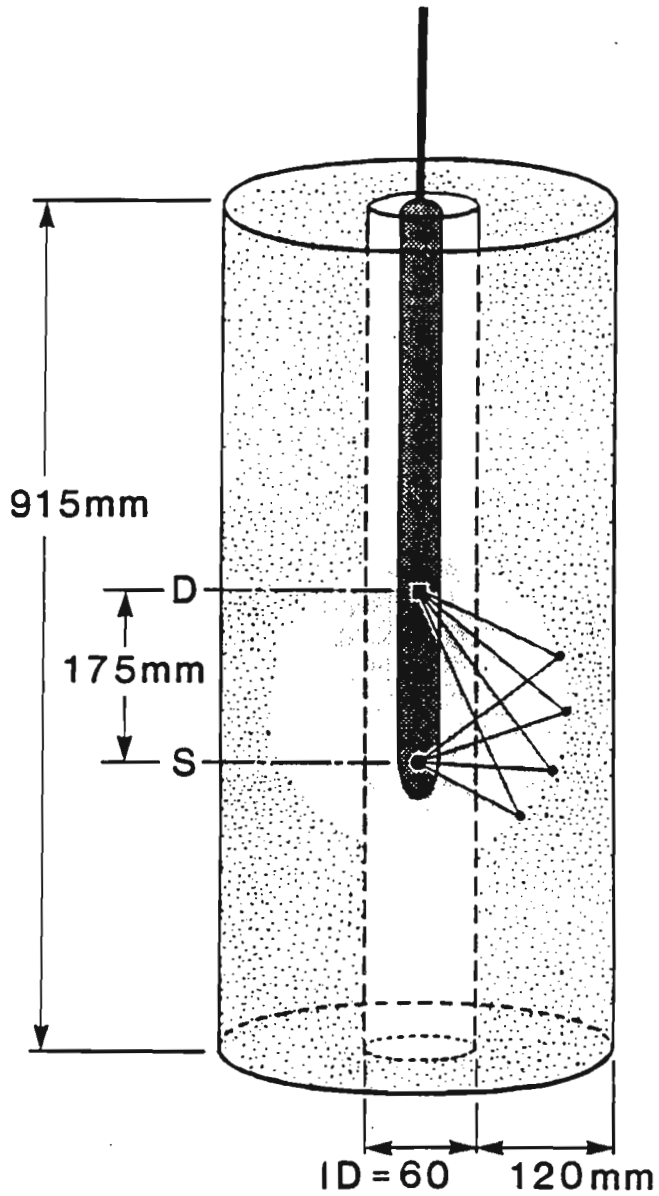

Figure 17: Cylindrical geometry model for deriving quantitative calibration data for the SGG probe in different ore materials.

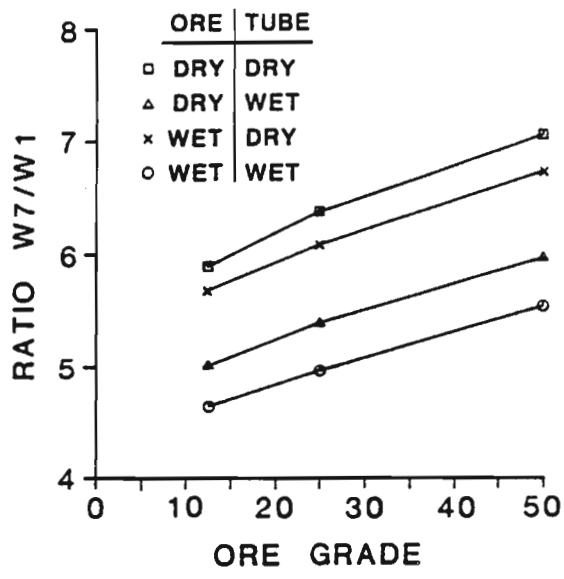

Figure 18: Spectral ratio vs. pyrite ore grade in the cylindrical model. The probe was centered in the hole (tube) and the source used was 370 MBq (10 mCi) cobalt 60. The four lines plotted show the effect of water in the tube, and of adding water to saturate the ore.

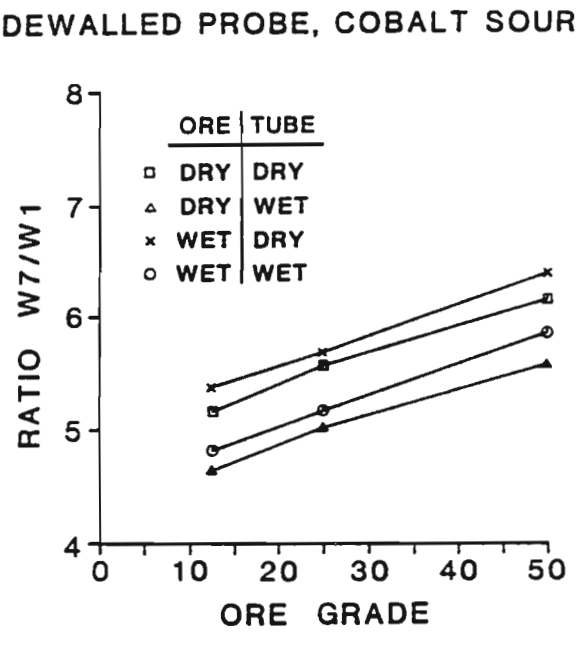

Figure 19: Spectral ratio vs. pyrite ore grade as in Figure 18 but with the probe sidewalled in the hole.

OPTIMIZATION OF LOGGING PARAMETERS IN CONTINUOUS, TIME-DOMAIN INDUCED POLARIZATION MEASUREMENTS

C.J. MWENIFUMBO

Geological Survey of Canada,
601 Booth Street, Ottawa, Ontario, Canada K1A 0E8

ABSTRACT

As part of an on-going borehole geophysics research program at the Geological Survey of Canada (GSC), experiments have been conducted with downhole, continuous, time-domain induced polarization (IP) for the identification and delineation of polarizable sulphides. Fields tests have been conducted to evaluate the different logging parameters that affect IP measurements in a borehole (period of the current waveform, logging speed, sample depth interval, and the integration windows for determining the chargeability parameter). The GSC IP logging system may operate at 4 different periods of the current waveform; 1, 2, 4 and 8 seconds. In continuous IP measurements, it is important to use periods as short as possible to obtain adequate spatial resolution at reasonable logging speeds without sacrificing data quality. Field tests indicate that holes may be logged at speeds greater than 6 m/minute using a 1 second waveform in order to obtain reliable, good quality IP data. An 8 second current waveform would require logging speeds of less than 1 m/minute to obtain the same spatial data resolution with a marginal improvement in the data quality, but there would a substantial increase in logging time and cost.

From: Proceedings of the Third Internetional Symposium on Borehole Geophysics for Minerals, Geotechnical, and Groundwater Applications. October 2-5, 1989. Las Vegas, Nevada
Sponsored by: The Minerals and Geotechnical Logging Society.

Field examples are presented from a number of Canadian base metal sulphide deposits.

INTRODUCTION

Surface induced polarization (IP) measurements have been extensively used in the search for disseminated sulphides for many years. There are, however, a few reports in the literature on IP logging in the mineral logging industry (Bacon, 1965; Dakhnov et al., 1952; Glenn and Nelson, 1979; Ogilvy, 1984; Snyder et al., 1977; Wagg and Seigel, 1963; Webster, 1986; Zablocki, 1966). Most of the logging has been carried out in an incremental mode with the objective of extending the radius of investigation away from the borehole wall using expanding arrays (Ogilvy, 1984; Webster, 1986; Wagg and Seigel, 1963). Continuous borehole IP measurements are rarely made in the mineral logging industry and, to the author's knowledge, the only commercially available continuous IP logging system is the one from the Mount Sopris Instrument Company. The Geological Survey of Canada (GSC) borehole research group has designed and built a time domain IP logging system for continuous measurements down slim holes (Bristow, 1986; Killeen and Mwenifumbo, 1987).

In continuous time-domain IP logging, there are a number of parameters that influence the IP measurements that can be selected by the operator. These include the electrode array geometry, period of the current waveform, logging speed and thus sample depth interval. This paper discusses different combinations of these parameters that are optimum for obtaining reliable, good quality IP data at reasonable cost. Several field examples from a number of Canadian sulphide deposits are presented to illustrate the quality of continuous time domain IP data.

GSC IP LOGGING SYSTEM

Most time-domain IP logging systems currently in use have passive downhole probes fabricated from metal electrodes such as lead or stainless steel (e.g. Mount Sopris, Scintrex systems). There are no active electronics except for occasional amplifiers (Ogilvy, 1984). The signal is transmitted to the surface in an analog fashion. One of the problems in making downhole IP measurements this way is capacitive coupling in the logging cable between the transmitting and receiving cables. Attempts have been made to minimize the coupling by using special shielded cables and fairly low frequency (< 1 Hz) signals. It has also been suggested that having the two current carrying wires of opposite polarity in the borehole would tend to cancel out the coupling (Snyder et al., 1977).

The GSC time domain IP logging system has a downhole receiver and the voltage signal is transmitted digitally as a frequency to the surface (Bristow, 1986). This completely eliminates the serious capacitive coupling problems. Vinegar et al., (1986) described a similar IP logging system for use in the oil and gas industry. The GSC IP logging system was designed for logging in smaller holes that are most frequently drilled in the mining industry. This system records complete waveforms so that one can study the decay curve shape, in addition to chargeability, for further characterization of the IP response. The current waveform consists of a symmetrical sequence of positive "ON/OFF" and negative "ON/OFF" pulses. The period for such a sequence can be set at 1, 2, 4, or 8 seconds. The corresponding voltage waveforms detected at the potential electrodes are digitized at .004 sec intervals. Since the sample rate is fixed, the number of samples per complete waveform are 256, 512, 1024 and 2048 corresponding to 1, 2, 4, and 8 second periods, respectively. Figure 1 shows typical voltage waveforms recorded with these 4 different periods of the current waveform.

Electrode Arrays

Figure 2 shows the electrode arrays that are currently in use with the GSC IP logging system. These are: single point resistance, 40-cm normal, 10-cm micronormal, lateral and symmetrical lateral arrays. The electrode design is modular so that configurations can be easily changed in the system. In the figure, the current electrodes are designated as A and B, and the potential electrodes as M and N. The B current electrode is located at the surface, some distance away from the collar of the hole being logged so that it can be considered to be effectively at infinity. These electrode arrays have been described by Dakhnov et al., (1952). The normal array is an inverted normal (Vinegar et al., 1986), different from the standard Schlumberger normal array. IP data presented in this paper were acquired with either a 40-cm normal or 10-cm micronormal array.

CHARGEABILITY PARAMETER

The standard parameter used to describe the IP characteristics of a rock mass in the time domain is chargeability. The apparent chargeability, Ma, is defined as the ratio of the secondary voltage, Vs, (decay voltage during current off cycles) to the primary voltage, Vp, (voltage at the measuring electrodes when current flows) and is given as

$$M_a(t) = Vs(t) / Vp \qquad (1)$$

The chargeability as presented is a function of time and indicates that it is possible to measure IP values at any time after switching off the current. Because of the low secondary voltages, it is customary to integrate under the decay curve over a specified time interval. The apparent chargeability parameter is then defined as a normalized time integral as follows

$$Ma = \frac{1}{Vp\left|t_2 - t_1\right|} \int_{t_1}^{t_2} Vs(t)\, dt$$

Vp is also integrated over a given time window during the current "ON" time and is given as

$$Vp = \frac{1}{\left|t_2 - t_1\right|} \int_{t_1}^{t_2} V(t)\, dt \qquad (3)$$

The units of chargeability are dimensionless but since it is customary to measure the secondary voltage in millivolts and the primary voltage in Volts, it is generally expressed in mV/V. Chargeability is sometimes expressed in milliseconds when the integral over the given time window on the decay curve is not normalized by the duration of the integration window (t_2 - t_1).

Since arbitrary window limits may be chosen over any desired portion of the decay curve, it is difficult to standardize the IP parameter. Different manufacturers of IP systems (e.g. Scintrex, Huntec and Mount Sopris) use different time windows for their chargeability parameter. Since the amplitude of the apparent chargeability depends on the integration interval, it is difficult to compare values measured with different instruments. Currently there is some active research towards studying the total decay curve shape with the objective of obtaining additional information relating to the nature of the source of the IP response. This, however, is the subject of ongoing research and is not discussed in the present paper. Figure 3 shows the complete IP waveform for an 8 second period (Fig. 3a) and an expanded version of the decay waveforms for both the positive and negative charging currents (Fig. 3b).

For surface IP systems employing an 8 second period, the Vs integrating window from t_1 = 0.45 to t_2 = 1.10 seconds is commonly used. This window is often referred to as the Newmont window in recognition of the Newmont Mining Company that introduced it on their IP systems. Vp is integrated from t'_1 = 0.9 to t'_2 = 1.7 seconds. Both Vp and Vs are averages of the positive and negative "ON/OFF" voltages for these windows.

A number of the IP systems currently employ multiple windows over the decay curve to obtain a more accurate representation of the IP decay waveform. Even though complete waveforms are recorded with the GSC IP system, ten IP windows are routinely determined during the data acquisition and processing. Most of these multiple window IP data are usually presented on the logs. Figure 4 illustrates these integration window limits for an 8 second period and Table 1 summarizes these limits for all the 4 different periods. These windows, adapted from the Scintrex IPR-11 broadband time domain IP receiver, are distributed in a semilogarithmic manner across the decay waveform.

Chargeability window least sensitive to varying periods

Because of the many possible ways of defining the window limits for the chargeability parameter, the question that arose in the present study was, which window limits were to be used for comparing the IP data from the 4 different periods of the current waveform. Arbitrary choices in the window limits are bound to create differences in the amplitudes of the chargeability parameter because of the relative differences in the charge and receive times. Two choices of the chargeability window limits were investigated: 1) a constant window width integrated over the same time interval for all periods, (e.g. a 150 ms wide Vs window determined 100 ms after current interruption). The normalizing voltage, Vp would

also have a constant time interval, integrated over the same time interval, (e.g. a 100 ms wide Vp window determined, ending 40 ms before current interruption), and 2) taking the Newmont IP window for the 8 second period as standard (Fig. 3b), equivalent window limits are determined for the 1, 2, and 4 second period, i.e. t_1 = 0.225T and t_2 = 0.550T seconds, where T is the "ON/OFF" pulse width. The Vp integration was from t'_1 = 0.45T and t'_2 = 0.85T. Figure 5 shows the IP data for the two choices of chargeability window limits for the 4 available periods. The Newmont type window (Fig. 5a) shows fairly similar amplitudes in apparent chargeability values for all the 4 periods. The constant window IP data (Fig. 5b) shows a systematic increase in amplitude from the 1 to 8 second IP data due to differences in charging times. A 0.25 second charge time for the 1 second period does not completely charge the polarizable material, whereas more of the polarizable material is charged up with a longer charge time thus giving higher amplitudes. The Newmont type IP window seems to be the least affected by variations in charging times and was therefore chosen for comparing the 1 to 8 second period IP data.

EFFECTS OF VARYING TRANSMITTING CURRENT INTENSITIES ON IP

The range of formation resistivities in metamorphic and igneous rocks may vary by 3 to 4 orders of magnitude within a single hole and this requires continuous adjustment of current intensities to optimize the signal-to-noise ratio. With the GSC logging system, the current intensities are automatically varied, through uphole software control, based on the received signal strength (Bristow, 1986). The option of using a fixed current (specified from the keyboard) can be selected as an alternative to the automatic adjustment of current intensity during a logging run. The current intensity may be varied from 1 to 256 mA.

Varying the current intensity may affect the value of the chargeability (Bertin and Loeb, 1976). Field tests were carried out in disseminated lead mineralization at a sandstone lead deposit to evaluate the effects of varying the current intensities on the IP value. Figure 6 shows the Newmont type IP data (Fig. 6c) obtained with a varying current intensity (Fig. 6b) and that obtained with fixed current intensities of 2, 4, 8, 16 and 32 mA (Fig. 6d). Current intensities could not be increased beyond 32 mA because of signal saturation within the high resistivity zones. The IP logs obtained at low fixed current intensities (i.e. 2 and 4 mA) are fairly noisy in low resistivity zones because of the low signal-to-noise ratio. The higher fixed current intensities produced IP data that are identical to that obtained with automatic variation in current intensities along the hole during a logging run (Fig. 6e). These data indicate that chargeability is linear in the range of current intensities investigated and one should not be concerned about the effects on IP response of changing current intensity.

EFFECT OF VARYING PERIOD OF THE CURRENT WAVEFORM ON IP RESPONSE

The period of the current waveform was varied from 1 to 8 seconds to investigate the influence of this parameter on the measured IP response. The sample depth interval was maintained at 10 cm by the appropriate variation in the logging speeds. The sample time intervals were 1, 2, 4, and 8 seconds for each respective periods used (i.e. no stacking, with one cycle for each sample point). Table 2 lists the sample depth intervals in cm for varying periods (1 to 8 s) and logging speeds (0.75 to 6 m/minute). Figure 7 shows IP data obtained with the 4 periods in a drill hole that intersected pyrite mineralization. The IP logs are offset for clarity in Figure 7c while the same data are presented without offset in Figure 7d. Every detail of the IP response is reproduced in all four logs, even in the small wavelength anomalies between 45 and 52 metres. It is clear from this comparison that if the hole were

logged for just the detection of polarizable material, there would be no need to log at 0.75 m/minute with an 8 second period; the 1-second IP data logged at 6 m/minute is more than adequate. There are, however, some differences in amplitudes between the 1-, 2-, 4- and 8-second IP data, especially within the broad IP anomaly between 36 and 40 metres (Fig. 7d). These slight differences in amplitude are probably due to differences in the charge and receive times.

The conclusion to be drawn from these observations is that similar IP anomalies in terms of character and amplitude, are obtained from all of the four periods if the Newmont type window is used to represent the IP response of the formation. Thus, there is no need to take measurements with longer time periods that require slower speeds to obtain adequate spatial data resolution.

EFFECTS OF LOGGING SPEED ON IP RESPONSE FOR CONSTANT PERIOD

Figure 8 shows the chargeability data for the standard Newmont type IP window obtained with an 8 second period at different logging speeds. The logging speed was varied from 0.75 to 6 m/minute with the resulting sample intervals of 10 to 80 cm, respectively. Figure 9 shows multiple window IP data for the same logging runs as the data presented in Figure 8 (the early time windows 1 to 5 are noisy due to current switching problems, so only windows 6 to 10 are shown). Multiple window data provide a qualitative assessment of the decay waveforms. The resolution of the IP anomalies progressively decreases with an increase in the length of the sample interval. At an 80 cm sample interval the small wavelength IP anomalies between 45 and 53 metres cannot be resolved. They are averaged into a broader anomaly. The broader IP anomaly between 35 and 40 metres also starts to deteriorate when data is sampled at 80 cm intervals. The multiple window IP data in Figure 9 gives some additional information on the behaviour of the decay waveform at fast logging

speeds and large sample intervals. Normal IP decay waveforms show a progressive decrease in chargeability from the early to late time IP windows. The IP data between 45 and 53 metres indicate distorted decay waveforms at the 80 cm sample interval because of the erratic nature of the earlier time window data.

Figures 10 and 11 show an example from field data, of the problems that may occur when measurements are taken at large sample intervals because of fast logging speeds. The resistivity and IP data shown in Figure 10 were acquired using a 4 second waveform with samples taken at approximately 2.5 cm, logging at approximately 0.3 m/minute. The position of a sample point using an 8 second period and logging at 6 m/minute is also indicated. The current intensity is a constant over the sample distance of 80 cm. The resistivity and polarizability both vary drastically over this distance, causing the primary and secondary voltages to show a corresponding variation as the electrodes pass through. Figure 11 shows the waveform that is recorded across this interval. This type of distortion in the received signal, due to excessive logging speeds, can easily be detected using multiple window IP data or recording complete waveforms.

COMPARISON OF 40-CM NORMAL AND 10-CM MICRONORMAL ARRAY IP DATA

Figure 12 shows multiple window IP logs obtained with the 40-cm normal and 10-cm micronormal electrode arrays. The differences in the response characteristics of the IP data between the two electrode arrays are purely geometric. The 10-cm micronormal array has a better resolution. An interesting feature to note is the double peaked anomaly around 26 metres on the 40-cm normal array IP log. This type of anomaly occurs when the electrode separation is equal to or greater than the thickness of the polarizable zone (Dakhnov, 1959; Vinegar et al., 1986). The 10-cm micronormal array IP log shows a single anomaly.

SOME FIELD EXAMPLES

A few field examples on the application of continuous time domain IP logging to mineral exploration are presented from three different geological environments: a nonconductive, carbonate-hosted zinc deposit, a disseminated sandstone lead deposit, and a massive sulphide deposit.

Carbonate hosted zinc deposit

Figure 13 shows the resistivity, standard-, and multiple-window, continuous time-domain IP data from a zinc deposit in Newfoundland, Canada. The prime ore mineral is sphalerite in a carbonate host rock. Zinc assays from the drill core are also shown in a histogram format with values ranging up to 8 %. The IP data were acquired with a 1 second period at 3 m/minute resulting in a sample depth interval of 10 cm. Although sphalerite is a poor conductor and does not generally give an IP response, the zinc mineralization is easily detected on the IP logs. The IP response within the zinc mineralization may be due to the presence of some other associated polarizable minerals such as pyrite or galena although none of these minerals were noted in the drill core. Microscopic studies are required to resolve this question.

N

Sandstone hosted lead deposit

Figure 14 shows resistivity, current, and multiple window IP logs from a disseminated sandstone lead deposit in Nova Scotia, Canada. These data were obtained with the 10'cm micronormal array using a 1 second period, logging at 3 m/minute and resulting in a sampling interval of 10 cm. The IP data clearly indicate the zones with disseminated galena in the sandstone. In this monomineralic sulphide environment, the IP data may be directly related to the lead content. Although there is a lower resistivity where there is lead mineralization, this log may

not be used as a direct indication of mineralization because of the presence of black shales that are abnormally low in resistivity.

Massive sulphide deposit

Figure 15 shows resistivity, inductive conductivity log and an IP log from a massive sulphide deposit in British Columbia, Canada. This hole intersects phyllite and graphitic phyllite which contains massive sulphide mineralization. IP measurements in highly conductive massive sulphides or graphitic phyllite are unreliable because of very poor signal-to-noise ratio. However, at this deposit, the IP log may be used to distinguish the phyllite containing disseminated sulphides from those that are devoid of sulphide mineralization. Sulphides seen visually in core are indicated on the figure. It is clear from the IP log that a number of zones with disseminated sulphide mineralization (e.g. from 85 - 90 metres) were not noted in the core log. Most of the phyllite/quartz unit between 100 and 130 metres contain disseminated sulphides.

CONCLUSION

Logging parameters that may be varied during continuous, time-domain IP measurements include chargeability window limits, period of the current waveform, logging speed and consequently sample depth interval. The following are some suggestions on the choice of these parameters that provide good quality IP logging data.

1) Chargeability values determined from the Newmont type window do not vary significantly with changes in the period of the current waveform. This window should, therefore, be used to facilitate comparison of IP data acquired using different periods.

2) The 1-second IP data are just as good as the 8-second IP data when sampled at the same depth interval, despite the differences in the charge and decay times. Deep holes should be logged using a 1 second period. This significantly reduces the amount of time spent logging a hole without sacrificing the quality of the data.

3) IP data acquired at logging speeds of up to 6 m/minute using a 1 second period are adequate for most mineral exploration applications. This results in a sample depth interval of 10 cm. Serious distortion of the received signal may occur at this logging speed if an 8 second period is used.

4) The sample depth interval and logging speed are not independent once the period of the current cycle has been chosen. Usually data resolution, i.e. sample depth interval, has to be decided upon first, which then automatically determines the logging speed. A sample interval of 20 cm seemed adequate for resolving narrow IP anomalies observed in the present studies so the logging speeds could be increased to greater than 9 m/minute if the current period were restricted to 1 second

N

Most of the continuous time domain IP logging done in mineral exploration with the GSC logging system uses a 1 second period, logging at 3 m/minute in holes that are less than 100 metres deep (sample interval 5 cm) and at 9 m/minute in holes greater than 400 metres deep (sample interval of 15 cm). If IP data are required for spectral analysis (decay waveform analysis), then 8-second period IP data should be collected, preferably at specific intervals so the records could be stacked.

ACKNOWLEDGMENTS

The author would like to thank colleagues in the Exploration Geophysics Subdivision, especially Q. Bristow and P.G. Killeen, for much helpful discussions and critical reading of the manuscript. W.G. Hyatt assisted in field data acquisition. Some of the field examples were acquired with funding from the Canada-Newfoundland and Canada-Nova Scotia Mineral Development Agreements (1984-89).

REFERENCES

Bacon, L.O., (1965) Induced polarization logging in search for native copper; Geophysics, v.30, p. 246.

Bertin, J. and Loeb, J. (1976) Experimental and theoretical aspects of induced polarization, volume I; presentation and application of the IP method, case studies; in Geoexploration Monographs, series 1, no. 7, published by Gebruder Borntraeger, 250 p.

Bristow, Q.B. (1986) A system for the Digital transmission and recording of Induced Polarization Measurements in Borehole; in Borehole Geophysics for Mining and Geotechnical Applications, ed. P.G. Killeen, Geological Survey of Canada, Paper 85-27, p. 127-143.

Dakhnov, V.N., Latishova, M.G. and Ryapolov, V.A. (1952) Well Logging by Means of Induced Polarization (Electrolytic Logging), Sb. Promislovaya Geofizika, Vnetnoneft; translated by G.V. Keller: The Log Analyst, November - December, 1967, p. 46-82.

Dakhnov, V.N. (1959) Geophysical Well Logging, Moscow petroleum Institute; translated by G.V. Keller (1962), Colorado School of Mines Quarterly, v.57, no.2, 445 p.

N

Glenn, W.E. and Nelson, P.H. (1979) Borehole logging techniques applied to base metal ore deposits; in Geophysics and geochemistry in search for metallic ores; Peter J. Hood, editor, Geological Survey of Canada, Economic geology report 31, p. 273-294.

Killeen, P.G. and Mwenifumbo, C.J. (1987) Interpretation of new generation geophysical logs in Canadian mineral exploration; in Proceedings of the 2nd International Symposium on Borehole Geophysics for Minerals, Geotechnical, and Groundwater Applications, October 6-8, Golden, Colorado, p. 167-178.

Ogilvy, R.D. (1984) Down-hole IP surveys applied to off-hole mineral exploration - some design considerations; Geoexploration, v.22, p.59-73. 1985: Down hole IP/resistivity prospecting in mineral drill-holes - some illustrative filed examples; Geoexploration, v. 23, p. 257-273.

Snyder, D.D., Merkel, R.H. and Williams, J.T. (1977) Complex Formation Resistivity - The Forgotten Half of the Resistivity Log; Transactions, 8th International Well Logging Symposium, Society of Professional Well Log Analysts, June 5-8, p. Z1-Z39.

Vinegar, H.J., Waxman, M.H., Best, M.H. and Reddy, I.K. (1986) Induced Polarization Logging: Borehole Modelling, Tool Design and Field Tests; The Log Analyst, March - April, p. 25-61.

Wagg, D.M. and Seigel, H.O. (1963) Induced polarization in drill holes; Canadian Mining Journal, V. 84, no. 4, p. 54-59.

Webster, B. (1986) Time domain IP borehole logging; in Borehole Geophysics for Mining and Geotechnical Applications, ed. P. G. Killeen, Geological Survey of Canada, Paper 85-27, p. 107-118.

Zablocki, C.J. (1966) Some application of geophysical logging methods in mineral exploration: Transactions, 7th International Well Logging Symposium, Society of Professional Well Log Analysts, May 9-11, p. U1-U13.

N

Table 1: IP window limits and widths

WINDOW	1 sec (CH = 256)			2 sec (CH = 512)			4 sec (CH = 1024)			8 sec (CH = 2048)		
	FROM ms	TO ms	ΔT ms	FROM ms	TO ms	ΔT ms	FROM ms	TO ms	ΔT ms	FROM ms	TO ms	ΔT ms
DELAY	0	8	8	0	8	8	0	16	16	0	31	31
1	8	16	8	8	16	8	16	32	16	31	66	35
2	16	23	7	16	23	7	32	47	15	66	101	35
3	23	31	8	23	31	8	47	62	15	101	136	35
4	31	39	8	31	39	8	62	78	16	136	172	36
5	39	62	23	39	90	51	78	179	101	172	374	202
6	62	86	24	90	140	50	179	281	102	374	577	203
7	86	106	23	140	191	51	281	382	101	577	780	203
8	106	156	47	191	292	102	382	585	203	780	1186	406
9	156	203	47	292	393	101	585	788	203	1186	1591	405
10	203	250	47	393	495	102	788	991	203	1591	1997	406
STD	51	136	85	109	273	164	222	550	328	445	1100	655

STD Standard window equivalent to the Newmont Window i.e. for an 8 second period, the integration is from 445 to 1100 milliseconds.

CH number of channels or data points sampled per complete wave form; sample time interval of 4 milliseconds.

ΔT duration of integration

ms milliseconds

Table 2: Sample depth interval (in cm) for varying combination of periods of current wave form and logging speeds

Logging Speed (m/min) \ Period (s)	1	2	4	8
0.75	1.25	2.5	5.0	10.0
1.50	2.5	5.0	10.0	20.0
3.00	5.0	10.0	20.0	40.0
6.00	10.0	20.0	40.0	80.0

N

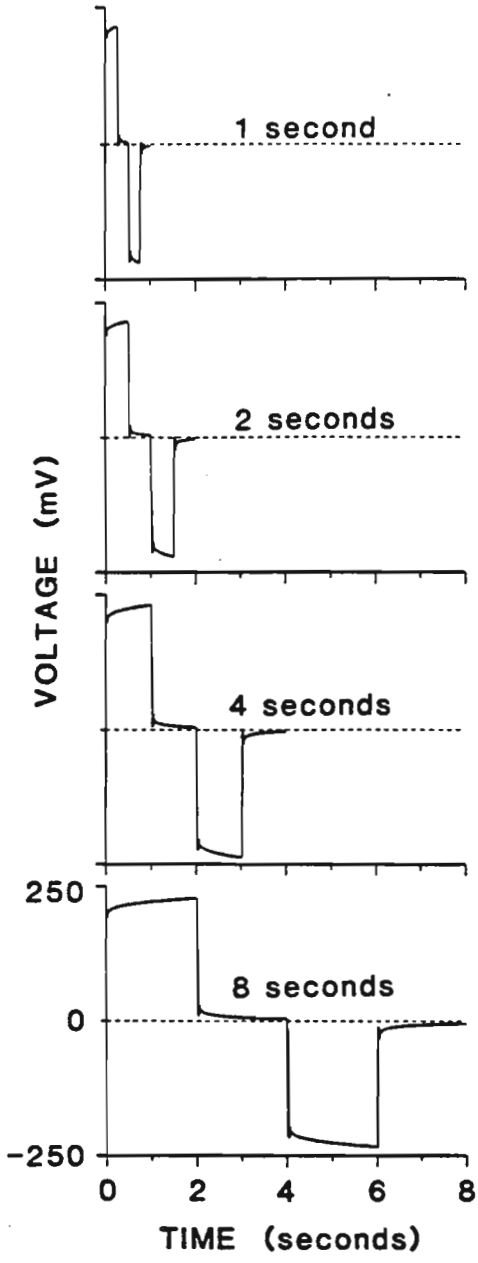

Figure 1: Typical time domain IP wave forms recorded at 4 different periods of the transmitted current signal.

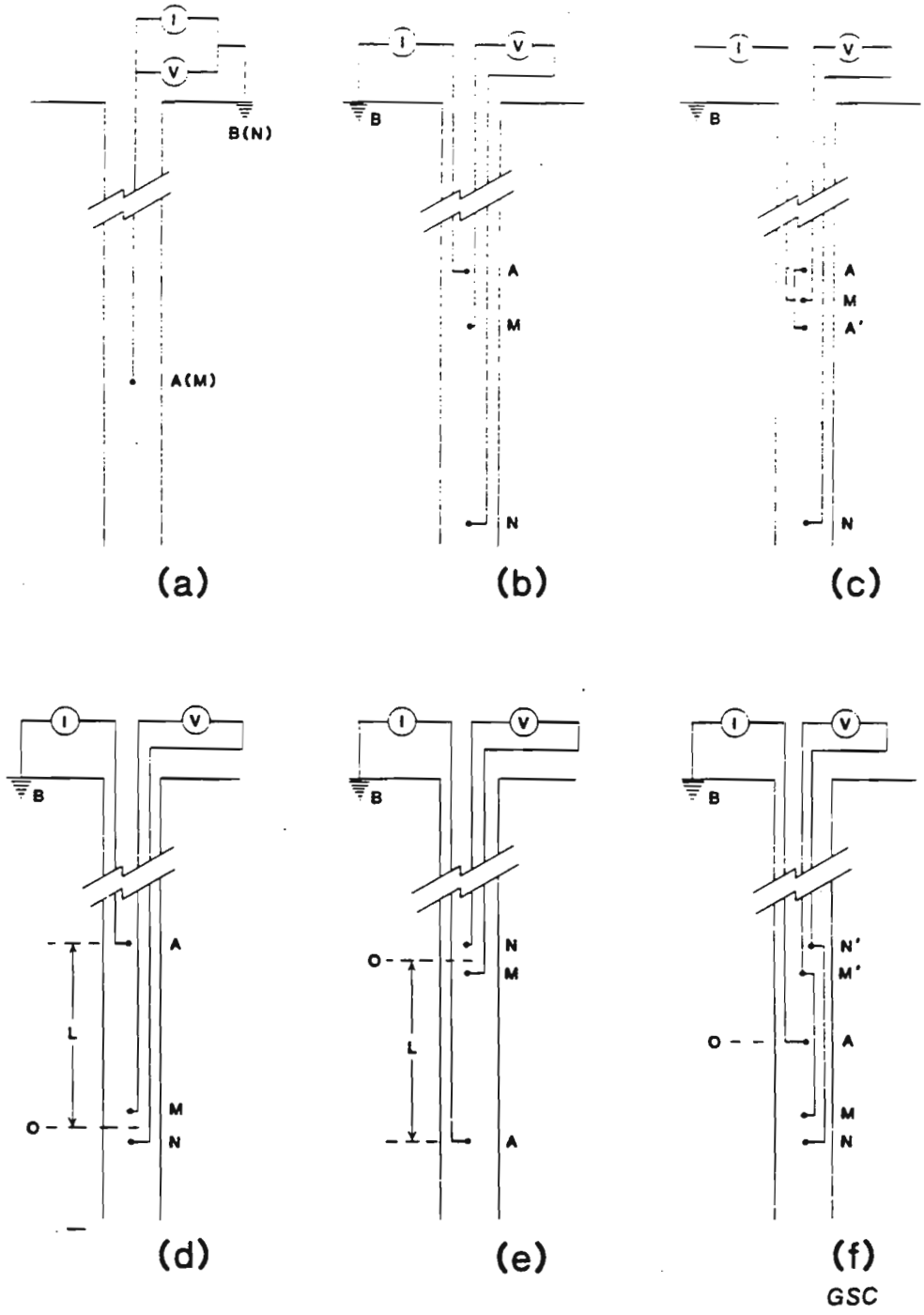

Figure 2: Electrode arrays. Figure 2a, Single point resistance; 2b, Inverted normal, AM=40 cm, MN=2.6 m; 2c, Dakhnov micronormal, AM=A'M=10 cm, A'N=2.6 m; 2d, Lateral, AM=2.6 m, MN=40 cm; 2e, Inverted Lateral and 2f, Symmetrical lateral, AM=AM'=20 cm, MN=M'N'=10 cm.

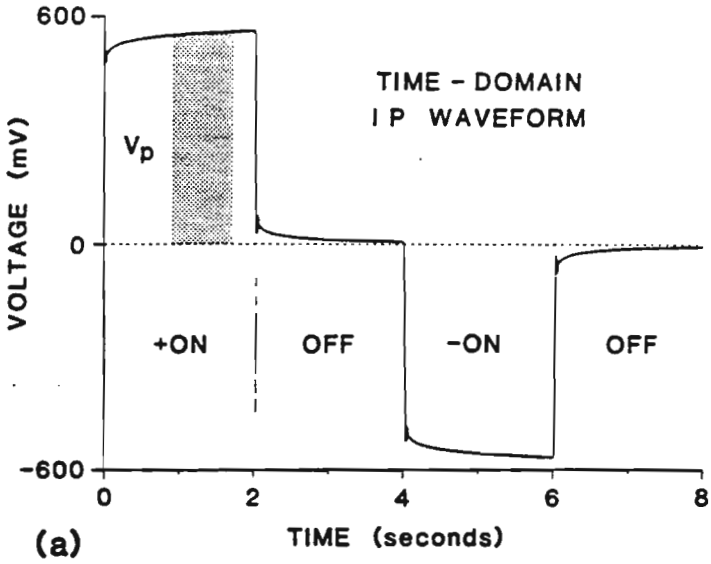

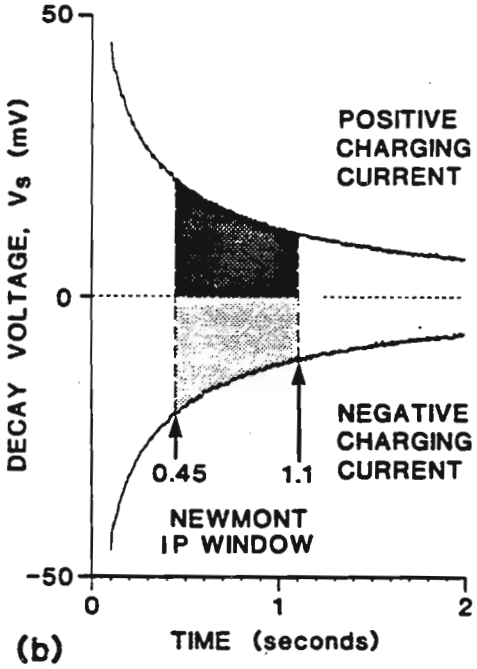

Figure 3: IP wave form for an 8 second period. Figure 3a, complete IP wave form; and Figure 3b, expanded decay wave forms for both the positive and negative charging currents. Vp is the primary voltage measured when the transmitting current is on and the stippled area represents the Vp integration window. The window from $t_1 = 0.45$ to $t_2 = 1.10$ seconds for the 8 second period is commonly referred to as the Newmont IP window.

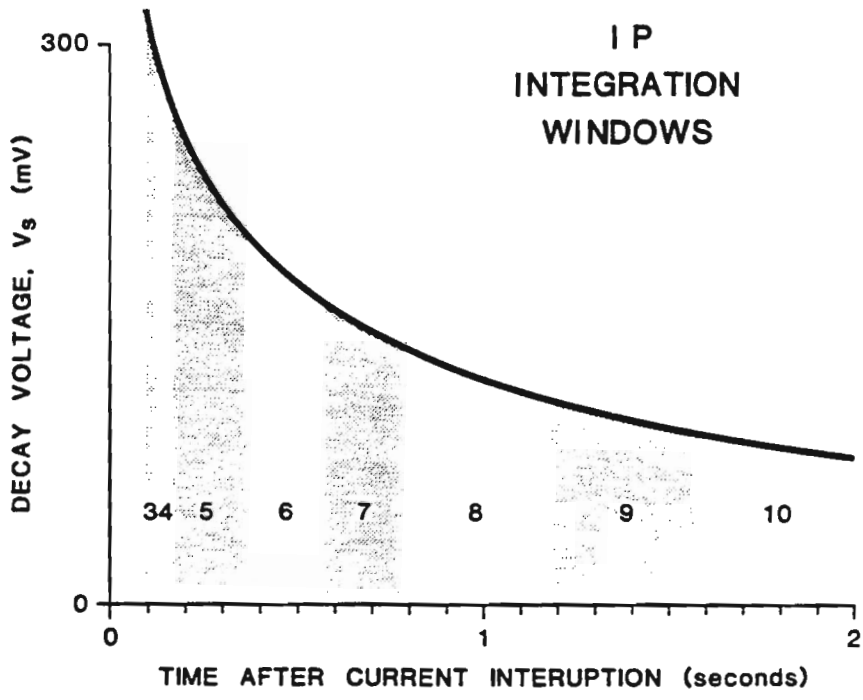

Figure 4: Semi-logarithmically spaced multiple IP windows adapted from the Scintrex IPR-11 broadband time domain receiver.

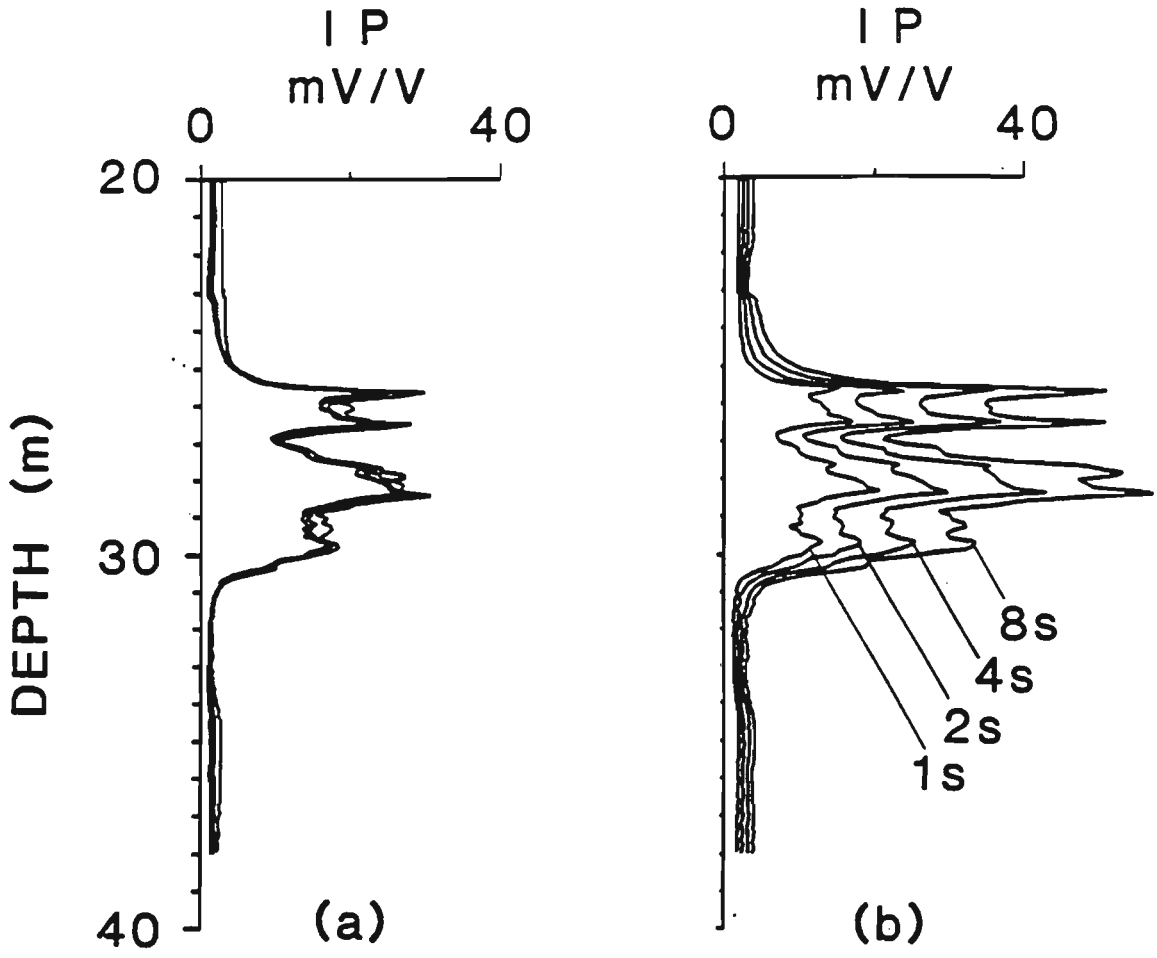

Figure 5: $\overline{IP}$ logs for two types of chargeability window limits for the 1, 2, 4, and 8 second periods. Figure 5a, Newmont type window IP data (Vs integrated from 0.225T to 0.550T seconds, where T is the "ON/OFF" time). The amplitudes of the apparent chargeability values are similar for all the four periods. Figure 5B, Constant time window IP data, 150 ms wide Vs window integrated 100 ms after current interruption for all the four periods. Note the systematic increase in amplitude from the 1 to 8 second IP data due to differences in charging times.

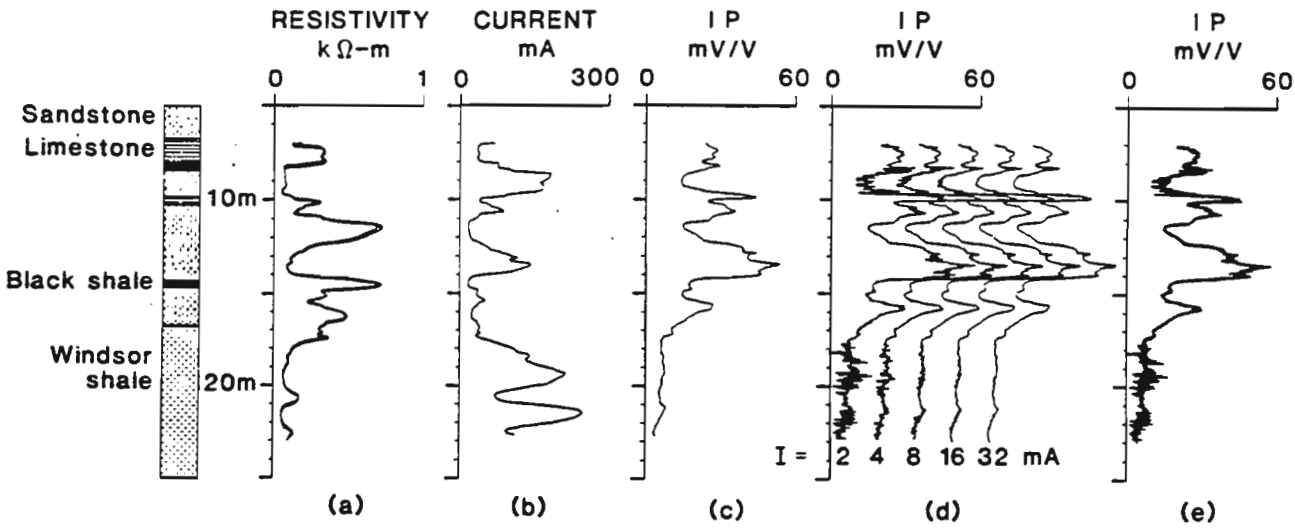

Figure 6: Newmont type IP data showing the effects of varying current intensities. Figure 6a, resistivity log; Figure 6b, current log; Figure 6c, IP log acquired with varying current intensity (current log in Fig. 6c); Figure 6d, IP logs acquired at fixed current intensities of 2, 4, 8, 16 and 32 mA, offset for clarity; Figure 6e, all IP logs (Fig. 6c and D) superimposed without offset. The IP logs are identical except for those obtained at low fixed current intensities which are fairly noisy in low resistivity zones.

N

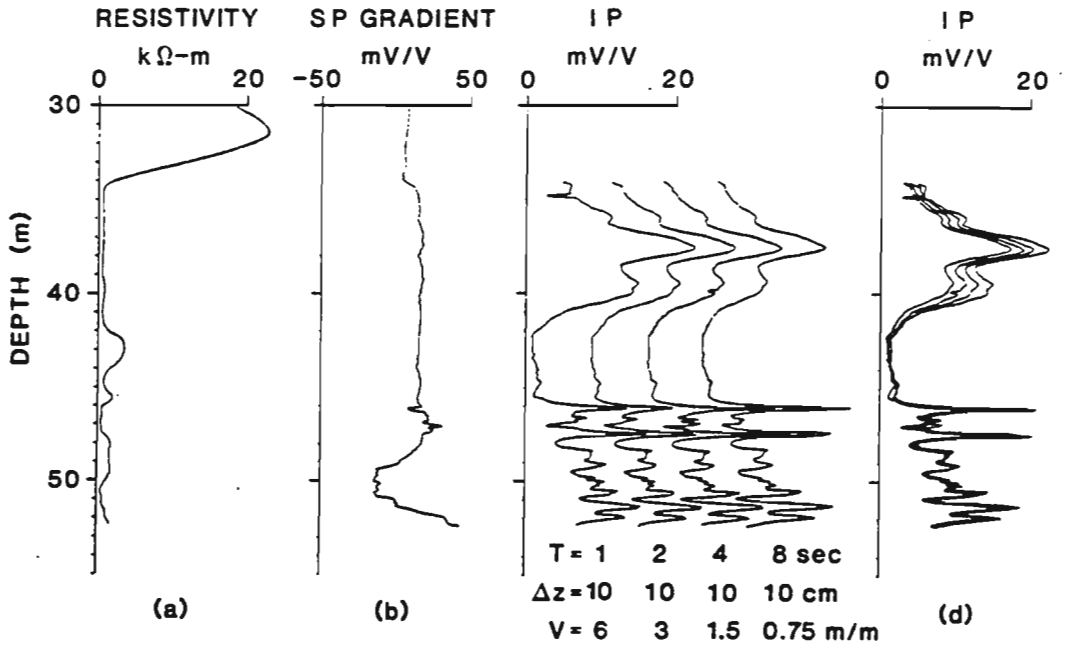

Figure 7: IP logs acquired with 4 different periods, sampled at the same depth interval. The drill hole intersected pyrite mineralization. Figure 7a, resistivity log; 7b, SP gradient log; 7c, the four IP logs offset for clarity; and 7d, the same four IP logs superimposed without offset. Every detail of the IP response is reproduced in all the four logs, even in the small wavelength anomalies between 45 and 52 metres. There are some differences in amplitude responses, especially within the upper broad anomaly.

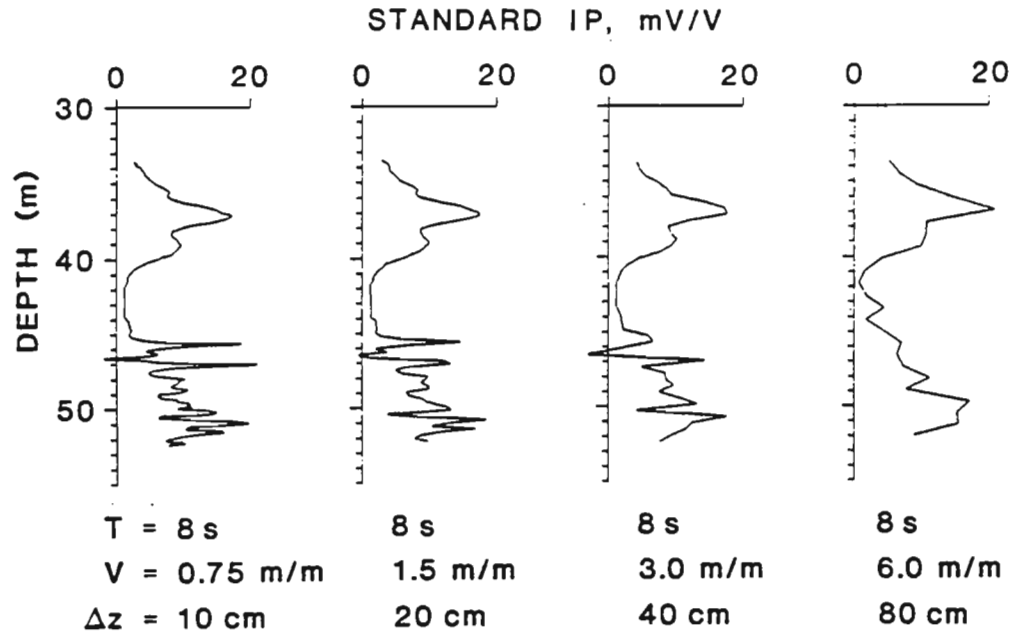

Figure 8: Standard Newmont type IP data obtained with an 8 second period showing the effect of varying logging speeds and hence the sample depth interval. Note the loss of resolution with increasing sample depth interval.

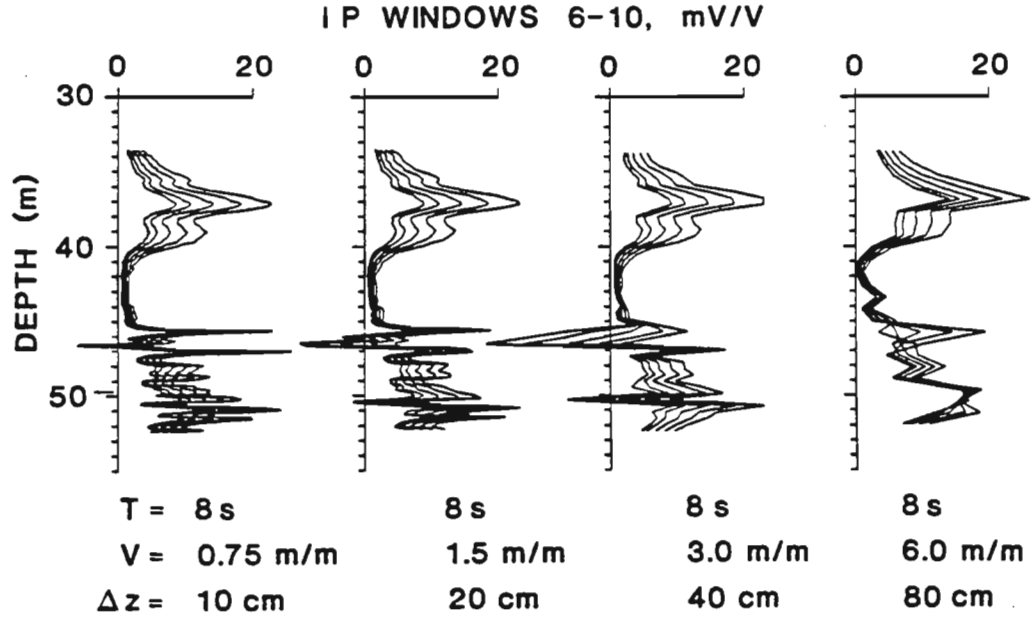

N

Figure 9: Multiple window IP data (windows 6 to 10) for the same logging runs as presented in Figure 8. Note the erratic behaviour of the multiple window data at 80 cm sample depth resulting from the distortion of the wave forms because of excessive logging speed.

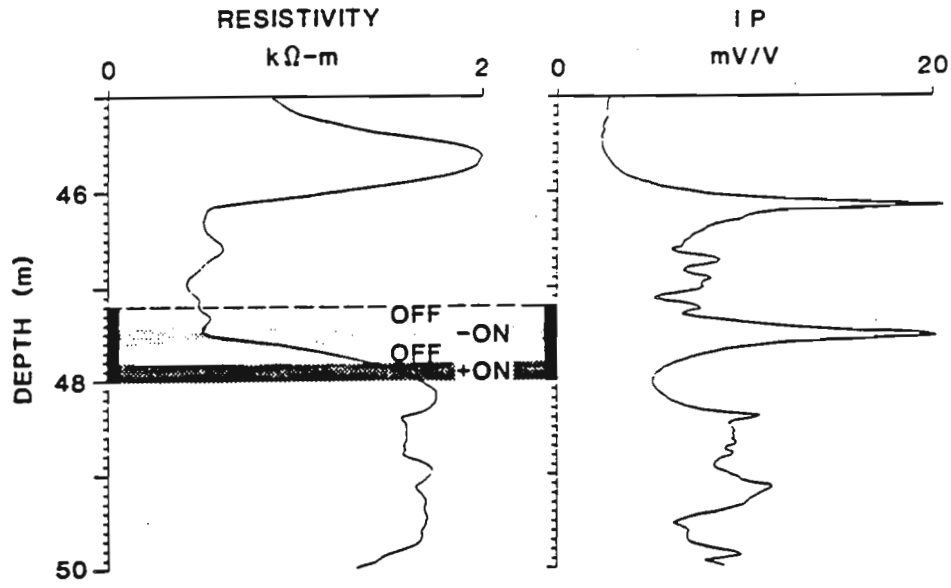

Figure 10: Resistivity and IP data acquired with an 4 second period, sampled at 2.5 cm at a logging speed of approximately 0.3 m/minute. The location of a sample point acquired with an 8-second period at 6 m/minute over a distance of 80 cm is indicated, to illustrate the problems of logging too fast and thereby making the sampling too coarse.

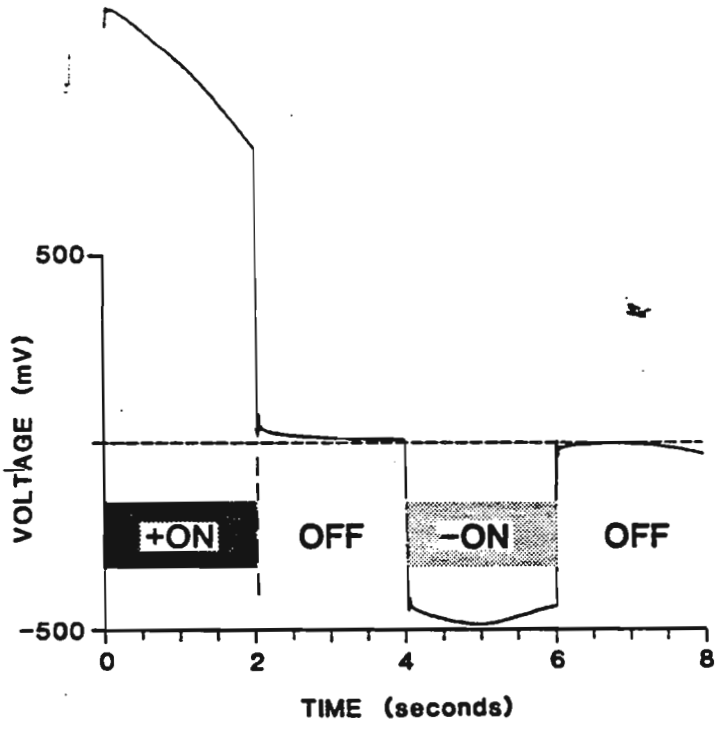

Figure 11: Complete wave form recorded over the interval shown in Figure 10. A constant current is maintained during the sample time. The resistivity and IP values are varying over this distance. High voltages are recorded during the positive "ON" time within the high resistivity zone and these decrease in response to decreasing resistivity. The resistivities are lower during the negative "ON" time and hence produce lower voltages. This results in a severely distorted wave form.

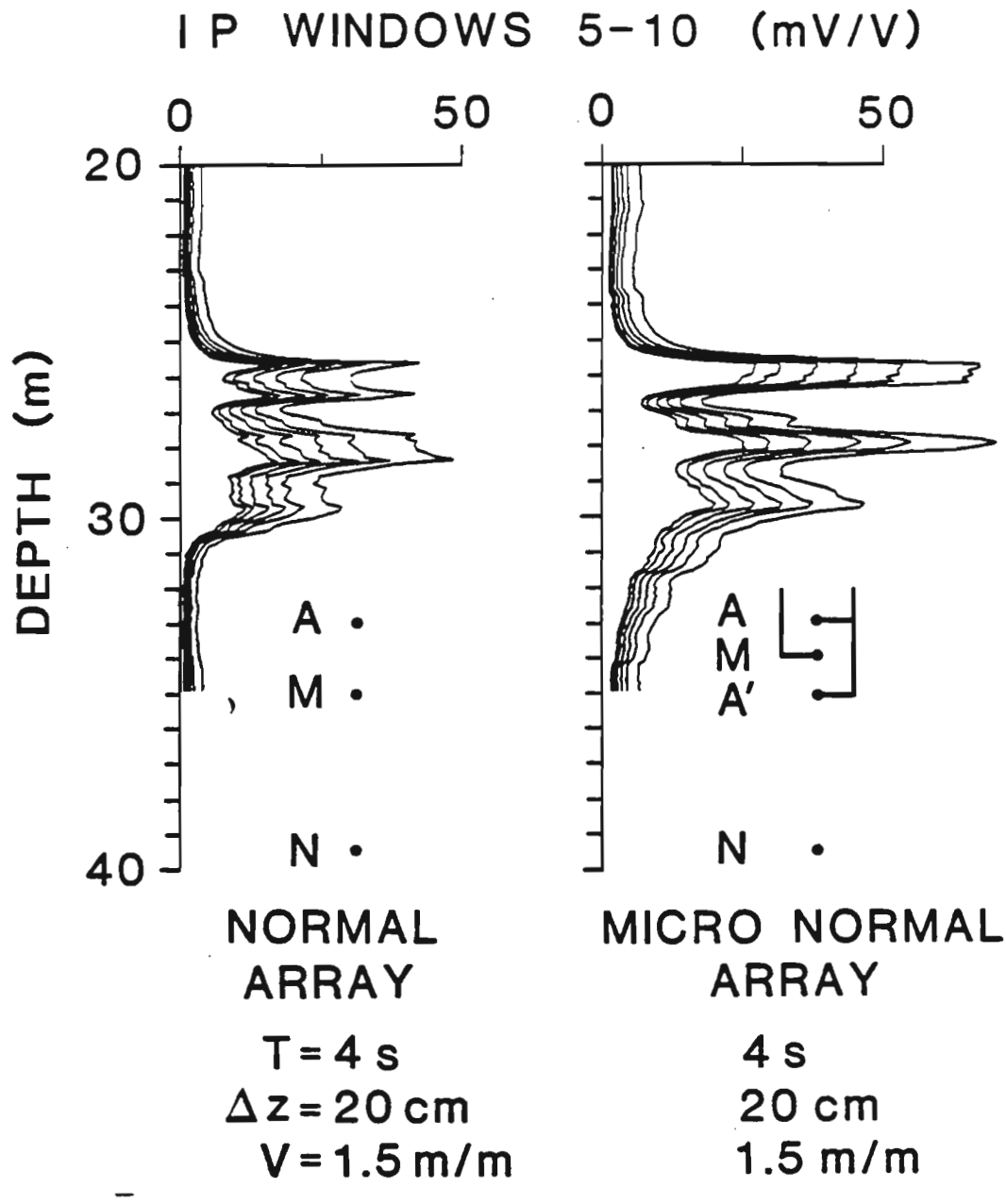

Figure 12: Comparison of the 40-cm normal and 10-cm micronormal array IP data. Better resolution is obtained with the 10-cm micronormal array.

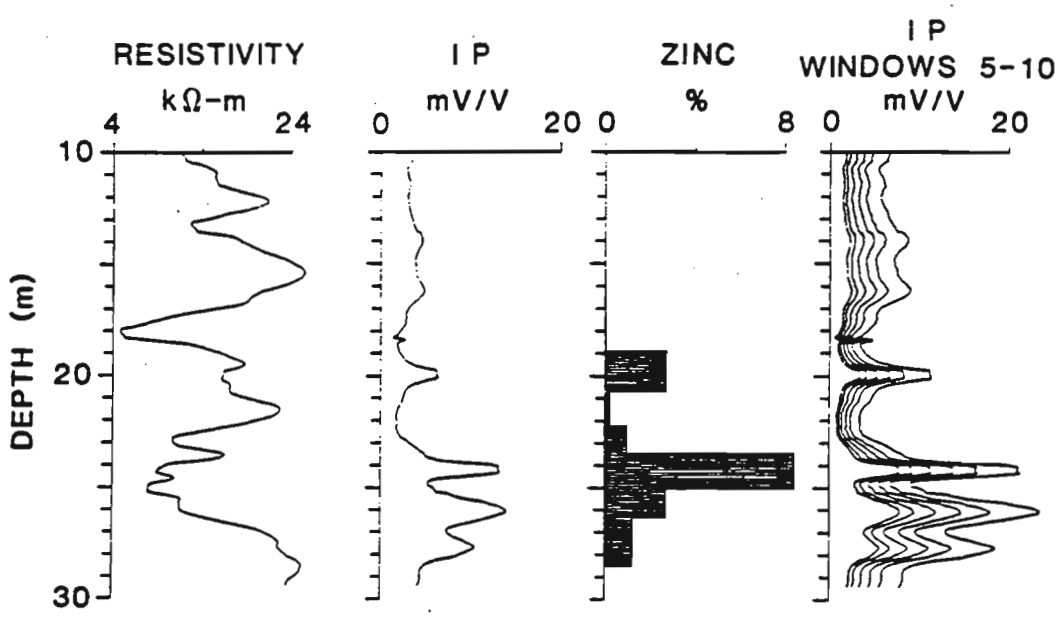

Figure 13: Continuous time domain IP data from a carbonate hosted zinc deposit, Newfoundland, Canada. The data was acquired with a 1 second period at 3 m/minute with a sample depth interval of 10 cm. Zinc mineralization is easily detected on the IP logs, probably because of associated disseminated pyrite or impurities within the sphalerite mineral itself.

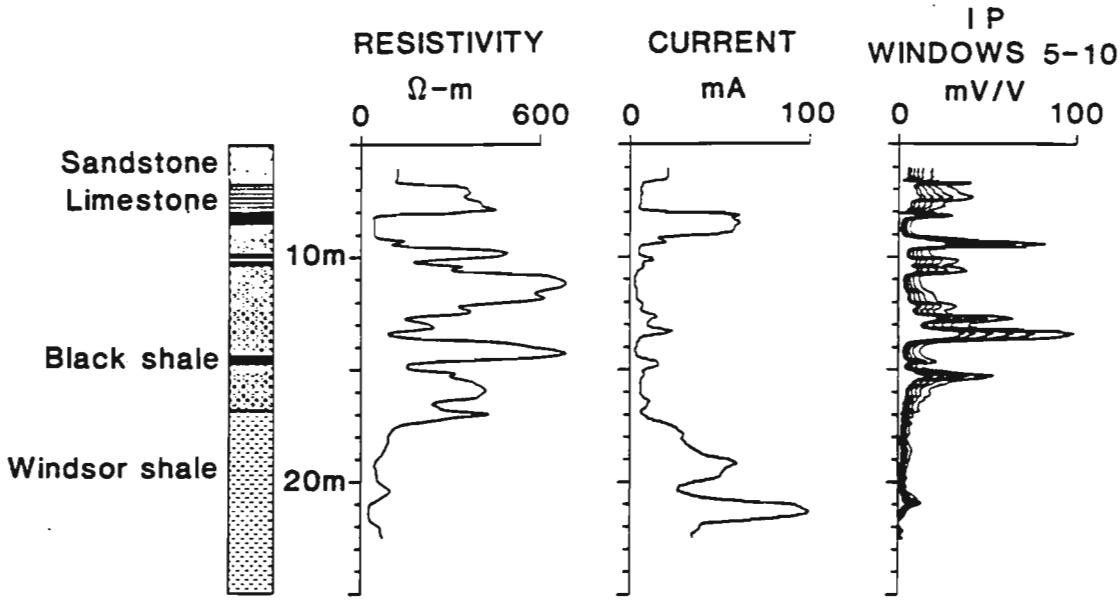

Figure 14: Continuous time domain IP logs from a disseminated sandstone lead deposit, Nova Scotia, Canada. These data were obtained with the 10-cm normal array with a 1 second period, logging at 3 m/minute and a sampling every 10 cm.

N

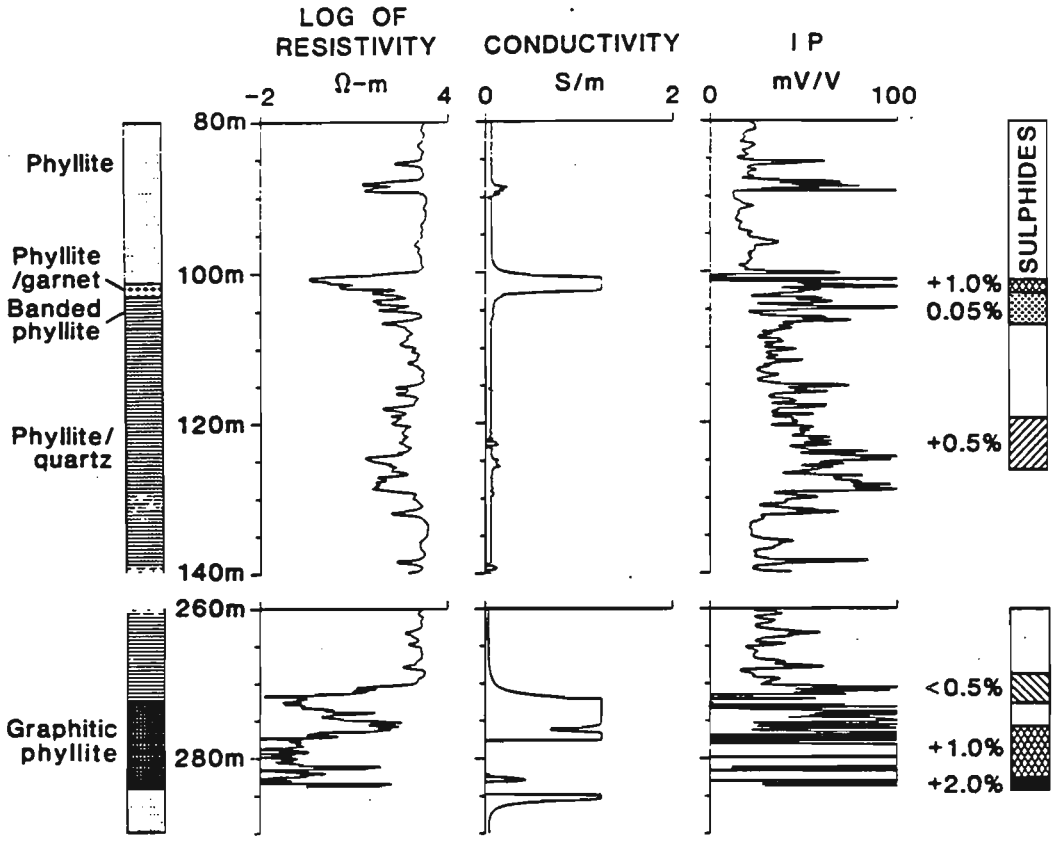

Figure 15: Continuous time domain IP data from a volcanogenic massive sulphide deposit, British Columbia, Canada. Resistivity and inductive conductivity logs are also presented. The hole intersects phyllite and graphitic phyllite with massive sulphide mineralization. IP measurements in highly conductive zones are usually unreliable because of very poor signal to noise ratio, nevertheless this IP log does indicate a number of zones with disseminated sulphides that were missed from visual inspection of the drill core.

The symmetrical lateral resistivity log in coal seam mapping, Highvale mine, Alberta

C.J. Mwenifumbo
Mineral Resources Division

Mwenifumbo, C.J., The symmetrical lateral resistivity log in coal seam mapping, Highvale mine, Alberta; in Current Research, Part D, Geological Survey of Canada, Paper 89-1D, p. 1-8, 1989.

Abstract

Symmetrical lateral array resistivity measurements were carried out at the Highvale coal mine in Alberta to compare their performance with the standard electrical logs; self potential, single point resistance, normal and lateral resistivity logs. The symmetrical lateral logs provide better coal bed thickness and boundary definition with thin beds being clearly resolved. Compared to the conventional lateral array, the symmetrical lateral array gives resistivity logs across resistive coal seams which are symmetrical, clearer and hence easier to interpret. The resistivities are not as severely affected by the finite bed thicknesses of the coal seams. The resistivity variations within the coal seams are clearly resolved, whereas the standard electrical logs tend to produce smoothed logs with less detail. The array is definitely superior to the single point resistance, normal resistivity and the asymmetrical lateral arrays. Bed-boundary resolution of this array is comparable to the high resolution density logs.

Résumé

Des mesures de résistivité en réseau latéral symétrique ont été effectuées à la mine de charbon Highvale en Alberta pour comparer leur qualité avec celle des enregistrements électriques standard, de la polarisation spontanée, de la résistance ponctuelle, des résistivités normale et latérale. Les enregistrements latéraux symétriques permettent une meilleure définition de l'épaisseur et des limites des couches de charbon, notamment des couches minces. Contrairement au réseau latéral classique, le réseau latéral symétrique produit des enregistrements de résistivité en travers des couches de charbon qui sont symétriques, plus nets et plus faciles à interpréter. Les résistivité ne dépendent pas autant de l'épaisseur finie des couches de charbon. Les variations de résistivité dans les couches de charbon sont nettement définies, tandis que les enregistrements électriques standard tendent à produire des enregistrements lissés moins détaillés. Le réseau est définitivement supérieur aux mesures de résistance ponctuelles, aux mesures de la résistivité normale et aux réseaux latéraux asymétriques. La résolution des limites des couches dans ce réseau se compare à celle des enregisrements de densité à haute résolution.

INTRODUCTION

Single and multiple electrode arrays for electrical resistivity logging are frequently used in coal exploration to determine the depth and thickness of coal seams. The most commonly used arrays are the single point resistance, normal and lateral arrays. Bed boundary definition is not as precise as often required with these arrays. The normal array can not resolve beds whose thicknesses are smaller than the electrode spacing. The lateral array was developed in an attempt to improve the bed-boundary resolution for thin beds. The response characteristic of this array is, however, quite complicated and asymmetrical. The results are difficult to interpret. When precise bed boundary resolution and accurate formation resistivity estimates are required, special focused resistivity arrays are currently used. The design of these focused resistivity logging devices is also complicated. We chose to build the symmetrical lateral array because its resistivity response is symmetrical as opposed to the asymmetrical lateral arrays. This electrode configuration is similar to the Schlumberger Limestone Sonde (Schlumberger Document 8, 1958) and was also suggested by Dakhnov (1959). It is essentially a superposition of the lateral and the inverted lateral arrays. It is not an improvement over the special focussed resistivity arrays but provides better bed-boundary resolution than either the asymmetrical lateral or normal arrays. No focussing is used on this configuration. Field results using this array, acquired in summer 1988 at the Highvale open pit mine in Alberta, are presented in this paper and are compared with the standard electrode arrays.

ELECTRODE ARRAYS.

Figures 1a, 1b and 1d show the common electrode configurations used in electrical borehole logging applications to coal exploration. The downhole and surface current electrodes are labelled A and B, respectively and the potential electrodes M and N. The single point resistance array is the simplest of the arrays and consists of one downhole electrode which is used both as a current electrode, A, and potential electrode, M. The return current electrode, B, and the reference potential electrode, N are also the same but fixed at the surface near the drill hole collar. Resistances are measured with this array which reflect changes in the formation resistivities along the drill hole. These measurements have been successfully used for the identification of coal seams and for stratigraphic correlation. Even though the single point resistance measurements are simple and inexpensive to run, apparent resistivities cannot be determined from them and therefore no quantitative interpretations can be made. A 10-cm-long cylindrical lead electrode was used as the downhole current/potential electrode for the data presented in this paper.

The normal array shown in Figure 1b, is the so called inverted normal. The conventional normal array commonly used in the industry has the N electrode above the current electrode A. An 'ideal'' normal array has 2 electrodes, A and M, downhole with the return current electrode and the reference potential electrode placed effectively at infinity on the surface. The normal arrays commonly used are 3-electrode arrays, AMN, with the reference potential electrode, N, placed at a distance large enough for its contribution to the overall measured potentials to be minimal. The different arrays are identified by their various AM separations. The conventional normal arrays currently used in coal, oil and gas industry are the 16-inch short normal and the 64-inch long normal. The normal array frequently used with the GSC logging system is a 40-cm normal array (AM = 40 cm, AN = 260 cm). The normal array resistivity data presented in this paper were acquired with the Dakhnov micronormal array (Dakhnov, 1959). This array is a high-resolution, 10-cm normal array mainly used to improve the resolution of induced polarization measurements. The potential measurement electrode, M, is placed between two closely spaced current electrodes of the same polarity. Figure 1c shows the electrode setup of the Dakhnov micronormal.

Figures 1d, 1e and 1f show the lateral arrays. The conventional lateral array consists of a current electrode, A, and a potential dipole, MN. The common electrode setup for the lateral is shown in Figure 1d with a trailing current electrode. The array is called an inverted lateral if it has a leading current electrode downhole (Figure 1e). The MN spacing for the lateral and inverted lateral used in acquiring the present data was 10 cm with an AM-spacing of 20 cm (AO=L=15 cm, Figure 1e). These dimensions are not the standard arrays used in the coal, oil and gas industry where an 18' 8'' lateral is commonly used (AO = 18' 8''). The resistivity response for the lateral arrays is asymmetrical and complicated to interpret. Figure 1f shows the newly constructed symmetrical lateral array. This array consists of a single current electrode A, and a potential dipole consisting of two measurement electrodes M'M and N'N, spaced at equal distances above and below the current electrode. This array was constructed because of its symmetrical resistivity response, and delineates the boundaries between beds more precisely than the asymmetrical three-electrode lateral array. The apparent resistivities determined from this array provide better approximations of the true formation resistivities.

APPARENT RESISTIVITIES

In a homogeneous medium of resistivity, ϱ, the potential difference, ΔV_{MN} between M and N for a 3-electrode array is

$$\Delta V_{MN} = \frac{\varrho I}{4\pi}\left(\frac{1}{AM} - \frac{1}{AN}\right)$$

Where I is the point source current. The resistivity is therefore computed as follows

$$\varrho = K\,\frac{\Delta V_{MN}}{I}$$

and the geometric factor, K, is given as

$$K = 4\pi\left(\frac{AM.AN}{AN - AM}\right)$$

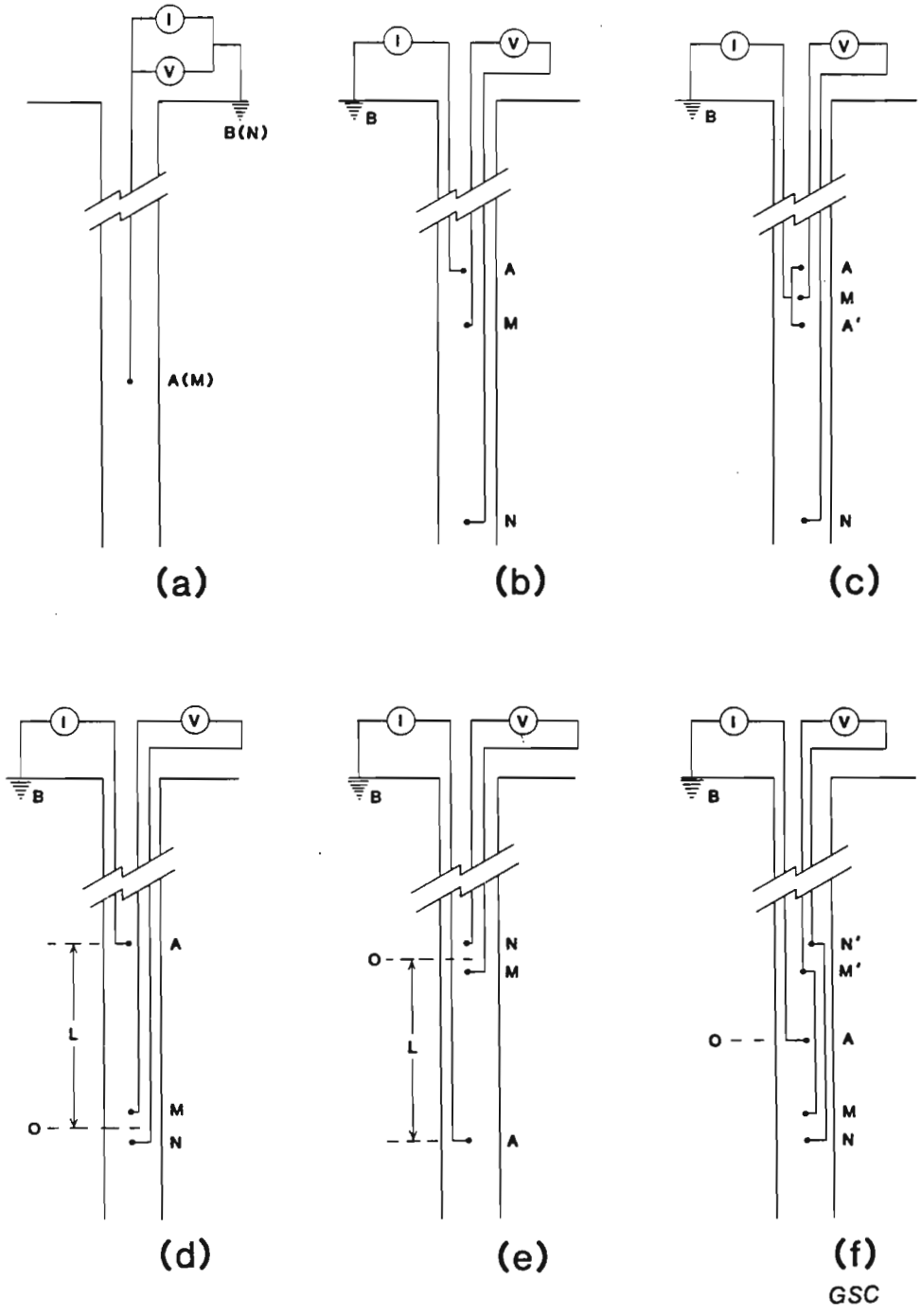

Figure 1. Electrode arrays. 1a Single point resistance, 1b Inverted Normal, 1c Dakhnov micronormal, 1d Lateral, 1e Inverted Lateral and 1f Symmetrical lateral.

Since we are not dealing with a homogeneous medium in the borehole, the measured resistivities are apparent resistivities. The normal, lateral and symmetrical lateral are essentially 3-electrode arrays and the geometric factor for all of them is as given in the equation above. The 10-cm micronormal has AM << AN (AN = 28*AM) and the geometric factor in this case approaches that of an 'ideal '' normal array.

LOGGING EQUIPMENT

The measurements presented in this study were carried out with the GSC R&D, slim-hole, time domain IP/Resistivity logging system. It consists of a minicomputer-based data acquisition system and downhole components which comprise the probe electronics and the electrode arrays. The electrode arrays are designed in a modular fashion so that changes in array type can be made easily. The voltage signal is measured in the probe and the signal is transmitted uphole digitally as a frequency as opposed to analogue signal transmission commonly used by standard industry logging systems. The transmitter used in single hole logging operations is a constant current 40-watt transmitter. The period of the time domain wave form for resistivity measurements is usually set at 1 second (ie. a transmit/receive time of 0.25 seconds) and data are sampled every second. All measurements are made in a continuous mode at logging speeds varying from 6.0 to 1.0 m/minute depending on the sample depth resolution required. The data acquired in this study were recorded at either 1.0 or 3.0 m/minute logging speeds. A full description of the logging system is given by Bristow (1986).

COMPARISON OF ARRAYS

A number of vertical holes were drilled for geotechnical logging studies at the Highvale Coal Mine in Alberta in summer 1988. These holes were 15 cm in diameter and filled with fresh water. Electrical logging with a variety of arrays was carried out in these holes to evaluate their resistivity response characteristics and their performance. The single point resistance, 10-cm micronormal, lateral, inverted lateral and the symmetrical lateral resistivity logs are presented and compared to each other. Corrections for the effects of borehole fluid, invasion zone and borehole diameter on the response characteristics of the resistivity logs have not been made to any of these data. The objective here is to compare the resistivity data in their raw form. The parameters investigated are coal seam recognition, bed-boundary resolution and the effect of finite bed thickness on the magnitude of the apparent resistivities.

SYMMETRICAL LATERAL VERSUS LATERAL ARRAY

Figure 2 shows the lateral, inverted lateral and symmetrical lateral apparent resistivity logs acquired in hole HV88-414. These logs were acquired at a logging speed of 1 m/minute with a measurement approximately every 2 cm. The asymmetrical response of the lateral and inverted lateral arrays is clearly indicated in Figure 2a and 2b. Maximum apparent resistivities are observed at the lower contacts of the coal

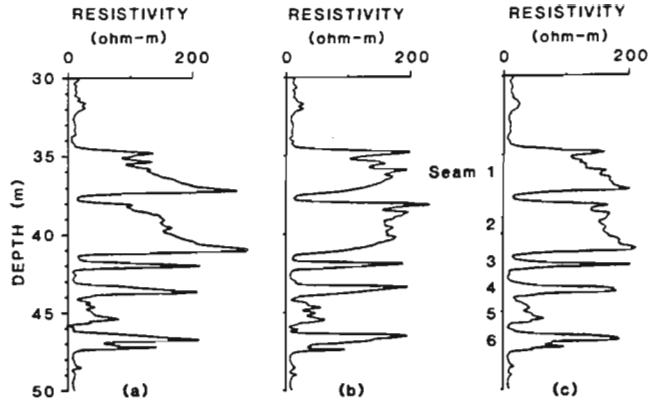

Figure 2. Conventional lateral (2a), inverted lateral (2b) and symmetrical lateral (2c) apparent resistivity logs acquired in hole HV88-414. The asymmetrical resistivity response of the lateral and inverted lateral is clearly shown across coal seam numbers 1 and 2. The conventional lateral array with a trailing current electrode indicates higher resistivities on the upper boundary of the coal seams whereas the inverted lateral with a leading current electrode downhole shows the reverse response. The symmetrical lateral array response is symmetrical across a bed of finite thickness and hence the variations in resistivities within the coal seams reflect true changes in resistivities.

seams for the conventional lateral array. The inverted lateral array resistivity log shows the opposite response; maximum resistivities on the upper contacts. Theoretical model results show that the lateral log resistivities are higher than the true resistivities near the contact of resistive beds (Dakhnov, 1959). Since the resistivities vary within the coal seams, the variations in apparent resistivities are difficult to interpret for these asymmetric arrays. The symmetrical lateral resistivity log in Figure 2c shows apparent resistivities within the coal seams, especially in seams 1 and 2, that should reflect true resistivity variations that may be interpreted to indicate changes in the quality of coal. The lower parts of the coal seams exhibit higher resistivities implying better coal at the bottom with decreasing resistivities towards the top indicating increasing ash content upwards. This interpretation is confirmed by the natural gamma ray and density logs which are discussed in a later section. Good bed-boundary definition is achieved by all of the three arrays, however, the resistivity variations within the coal seams are misleading for the lateral and inverted lateral logs and therefore quantitative interpretation based on the magnitude of the resistivities would be difficult with these data.

Figure 3 shows a more detailed response of the lateral, inverted lateral and symmetrical lateral logs across coal seam number 4 in the same hole. The asymmetrical resistivity responses of the lateral and inverted lateral are clearly indicated in these logs. The symmetrical lateral log shows a symmetrical resistivity response across the coal seam and bed-boundaries are more clearly defined. The resistivity response of the symmetrical lateral array is essentially the sum of the lateral and inverted lateral responses with the indicated resistivity being lower at the centre of the coal seam. This is a characteristic response for resistive beds whose thickness is less than the electrode spacing and it is also seen for example with the normal resistivity log (Dakhnov, 1959).

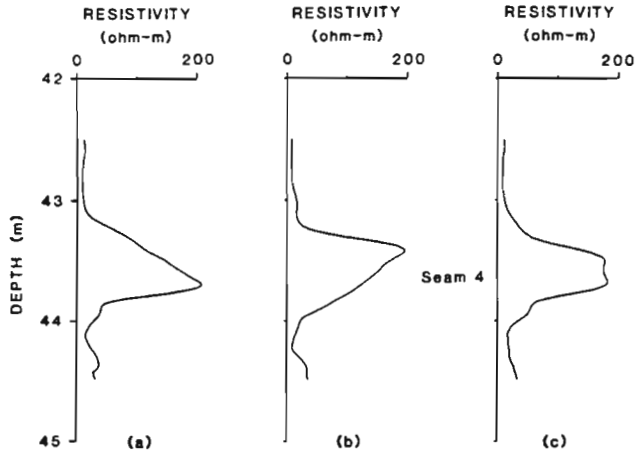

Figure 3. Expanded section of figure 2 showing a more detailed lateral (3a), inverted lateral (3b) and symmetrical lateral (3c) resistivity responses across coal seam number 4.

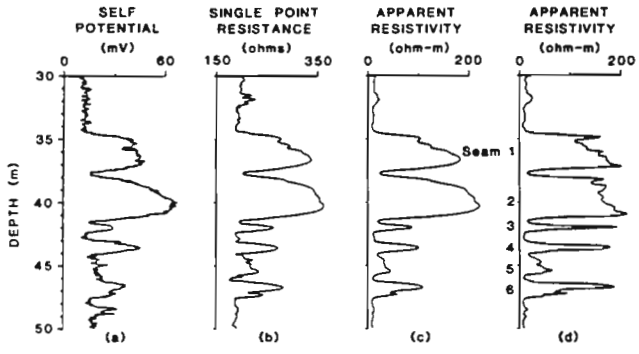

Figure 4. Symmetrical lateral resistivity log compared with the standard electrical logs; self potential (4a), single point resistance (4b) and 10-cm normal resistivity (4c) logs. Better boundary definition is clearly indicated on the symmetrical lateral resistivity log (4d). Apparent resistivities of the thin coal seams 3, 4 and 6 are comparable to those observed in thicker coal seams 1 and 2. Finite bed thickness effects are not as severe for the symmetrical lateral as for either the single point resistance or normal arrays.

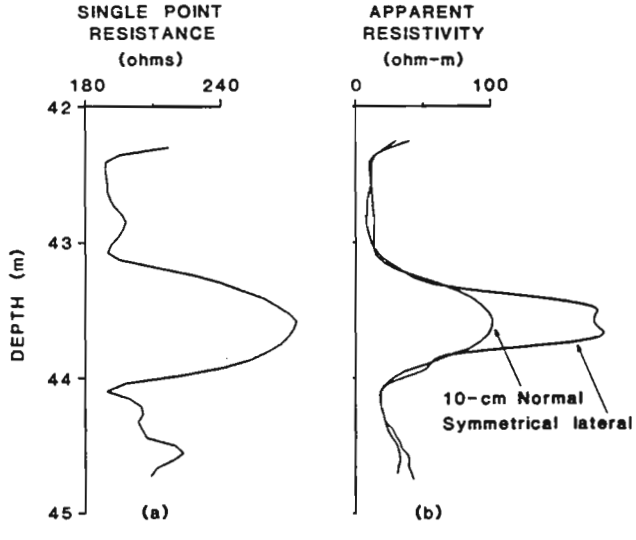

SINGLE POINT, NORMAL AND SYMMETRICAL LATERAL ARRAYS

Figure 4 compares the symmetrical lateral resistivity logs with the standard electrical logs; self potential, single point resistance and 10-cm normal resistivity logs. All logs clearly indicate the resistive coal seams and resolve the coal bed-boundaries fairly well. The single point resistance and normal resistivity logs show smooth variations in resistivities within the coal seams especially seams numbers 1 and 2 with increasing resistivities towards the lower contact. The resistivity response of the symmetrical lateral array is sharper at the contacts and hence provides better bed-boundaries definition. The fine details in the resistivity variations within the coal seams (seam numbers 1 and 2) are better defined with the symmetrical lateral logs than with the other electrical logs. These variations reflect changes in the quality of coal (ash content) within the seam. It is interesting to note that both the single point resistance and the normal resistivity logs show reduced amplitudes in seams 3, 4 and 6. This does not necessarily imply that the resistivities of these seams are lower than those of seam numbers 1 and 2 but rather this is a characteristic response of these logs to thin beds in these large diameter holes. The symmetrical lateral resistivity log, however, shows the magnitude of the resistivities of seams 3, 4 and 6 to be equivalent to those of the thicker seams 1 and 2.

Figure 5 shows an expanded section of Figure 4 showing the single point resistance, normal resistivity and symmetrical lateral log across seam number 4. It is clear that the symmetrical lateral log has better resolution and that the measured apparent resistivities are a better estimate of the true resistivities of these thin coal seams. The apparent resistivity values reach a maximum at the centre of a bed of finite thickness for both the normal and the symmetrical lateral logs. This value is usually less than the true resistivity of an infinitely thick bed. As the bed thickness decreases, the maximum apparent response decreases as well. The symmetrical lateral resistivity values of the thin coal seams are not severely affected by the finite bed thickness and therefore, can be used in quantitative assessment of the coal (relating coal quality to the resistivity values) thus obviating the need for special focused resistivity logging devices.

COMPARISON OF GAMMA RAY AND ELECTRICAL LOGS

Figure 6 compares the natural gamma ray log with the three electrical logs; single point resistance, 10-cm normal and symmetrical lateral resistivity logs. This data was obtained in hole HV88-428. All the electrical logs show an excellent negative correlation with the gamma ray log. Figure 7 is plot of the conductivities in Siemens/m (reciprocal of resistivity

Figure 5. Expanded section of Figure 4 illustrating the improved bed boundary resolution of the symmetrical lateral over the normal resistivity and single point resistance logs. Apparent resistivities observed with the symmetrical lateral array provide a better approximation to the true resistivities of the coal seams.

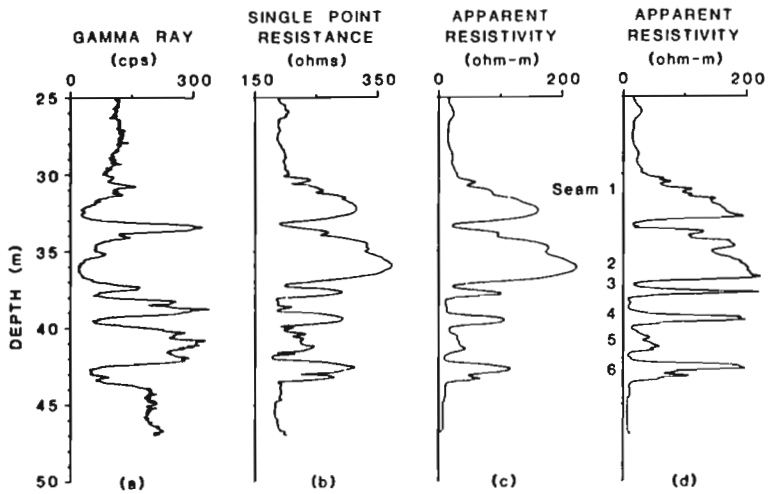

Figure 6. Natural gamma ray (6a), single point resistance (6b), 10-cm normal resistivity (6c) and the symmetrical lateral resistivity (6d) logs obtained in hole HV88-428. The electrical logs show a negative correlation with the gamma ray log.

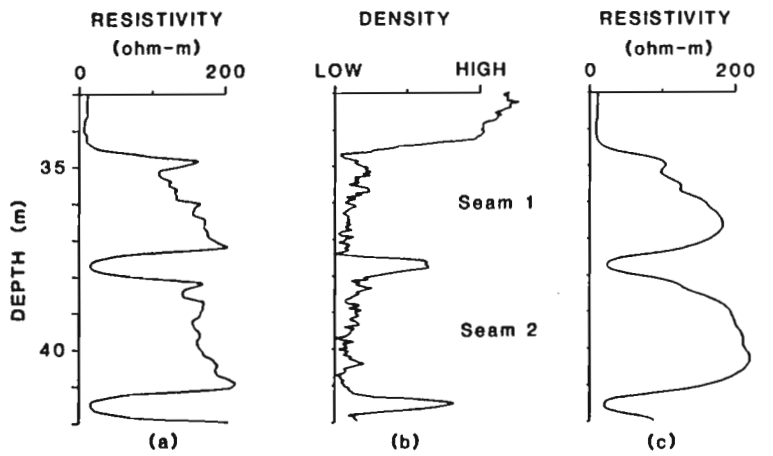

Figure 8. The symmetrical lateral resistivity log (8a) compared with the high resolution gamma gamma density log (8b) and the 10-cm normal resistivity log (8c). Data was acquired in hole HV88-414.

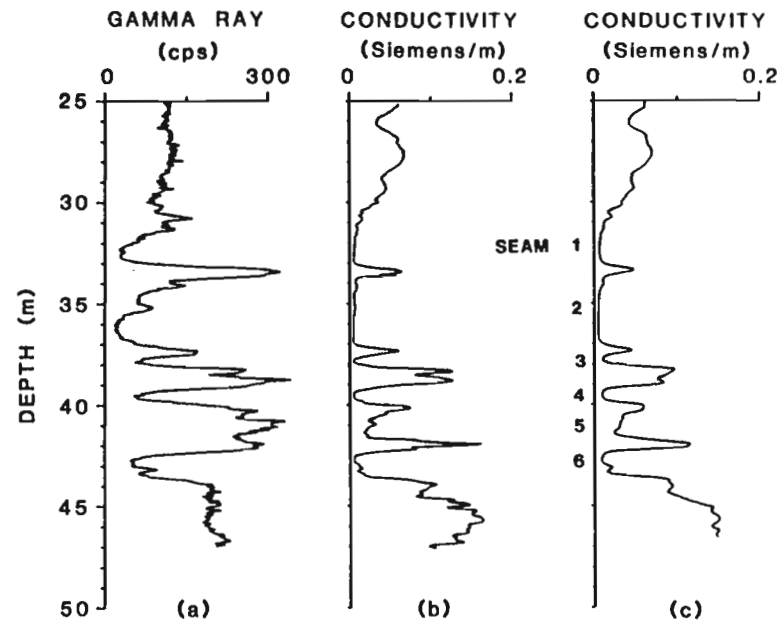

Figure 7. Conductivity logs derived from the symmetrical lateral (7b) and 10-cm normal resistivity (7c) logs of figure 6 are compared with the gamma ray log (7a). Both the conductivity logs show a good positive correlation with the gamma ray log. The symmetrical lateral conductivity log shows better fine detail correlation especially between 38 and 40 metres.

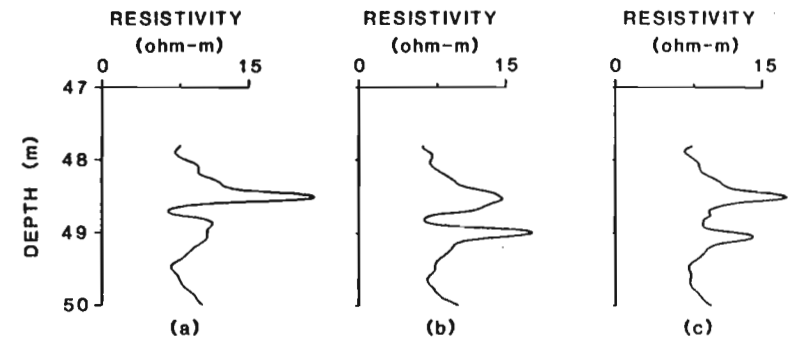

Figure 9. Expanded section of Figure 4 showing detailed characteristics of the lateral, inverted lateral and symmetrical lateral arrays across two narrow resistive calcareous sandstone layers. The symmetrical lateral resistivity log clearly resolves the two layers and establishes which one of the two is more resistive.

in ohm-m, presented in Figure 6) for the normal and symmetrical arrays compared with the total count gamma ray log. The presentation of the conductivities emphasizes the relationship between the in seam mudstone/bentonite layers and the natural gamma radiation. The positive correlation between the electrical conductivity and gamma radioactivity indicates that the major constituents of these in seam layers are conductive clays. The symmetrical lateral conductivity log defines these in seam layers better than the normal conductivity log especially the layer between seams number 3 and 4. The interesting thing to note in the amplitude relationship between the radioactivity and conductivity is that layers with the highest radioactivity are not necessarily the most conductive layers. The explanation is clear when one looks at the natural spectrometry data (not presented here). These data show that uranium is present in higher concentrations within these layers. Enrichment in uranium is not necessarily related to increases in conductive clays. The high gamma radioactivity layer between 40 and 42.5 m shows that the lower and upper zones are more conductive than the middle zone. The conductive zones consist of bentonitic mudstone whereas the resistive, high radioactivity, centre zone consists of carbonaceous mudstone with the poorly defined seam 5.

GAMMA GAMMA DENSITY VERSUS SYMMETRICAL LATERAL LOGS

Figure 8 compares the symmetrical lateral resistivity, gamma gamma density and the 10-cm micronormal resistivity logs. The high resolution gamma gamma density measurements (source-detector spacing of 15 cm) are frequently used for defining boundaries and coal bed thicknesses. The density measurements presented in Figure 8 were acquired with the GSC high resolution spectral density tool consisting of a source-detector spacing of 17 cm. The data are presented in arbitrary density units. It is clear that the coal bed-boundary definition provided by the symmetrical resistivity log is equivalent to that observed from the density data. There is an excellent negative correlation between these two logs. Subtle increases in density between 35 and 36 m within coal seam number 1 are clearly delineated as lower resistivity zones. Even the spike type, high resistivity anomaly at the top of the coal seam is indicated as having lower density implying better coal quality at this depth. The normal resistivity log does not provide good bed-boundary resolution.

RESOLUTION OF THIN MULTIPLE LAYERS

Figure 9 shows an expanded section of Figure 2 across two narrow, resistive calcareous sandstone layers between 48 and 50 metres. The conventional lateral resistivity log shows a pronounced resistivity high across the upper layer. The lower layer resistivity is suppressed to such an extent that it is virtually nonexistent. Both layers are clearly resolved on the inverted lateral resistivity log. However, the lower layer is indicated as a more resistive layer than the upper layer on the inverted lateral log whereas the upper layer is indicated as the more resistive one on the conventional lateral log. The symmetrical resistivity log clearly resolves the two layers and properly defines the relative amplitudes of the resistivities of the two layers.

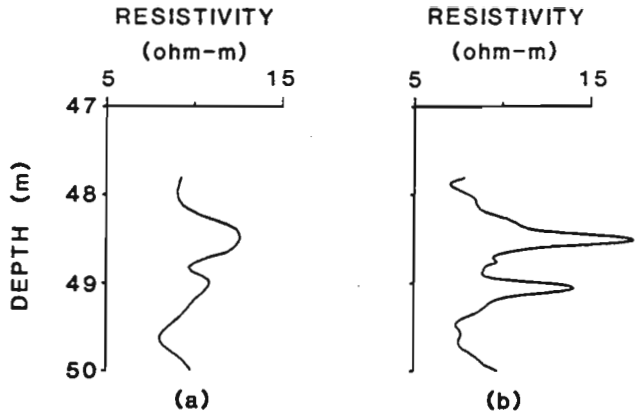

Figure10. Symmetrical lateral resistivity log across the two narrow resistive calcareous sandstone layer of figure 9, compared with the 10-cm normal resistivity log.

Figure 10 shows how the symmetrical lateral array compares with the normal resistivity log. Both the normal and symmetrical lateral resistivity logs clearly show the two layers and indicate that the upper layer is more resistive than the lower layer. The anomalies on the normal resistivity log are broader and the resistivities are lower than those observed on the symmetrical lateral log. These data demonstrate the superiority of the symmetrical lateral resistivity log over either the normal or the lateral resistivity logs. The asymmetrical resistivity response of the lateral array makes interpretation of the resistivity anomalies difficult. Multiple layers may be resolved but the significance of the amplitudes is ambiguous whether one uses the lateral or inverted lateral array. It is therefore recommended that the symmetrical lateral array be used instead of the lateral or inverted lateral array.

CONCLUSIONS

Even though the lateral resistivity logs are still being widely used to improve bed resolution, their resistivity response characteristics are asymmetrical and complicated to interpret. The symmetrical lateral resistivity log provides better bed-boundary definition than either the single point resistance, lateral or high resolution 10-cm micronormal resistivity logs. The departure of the measured apparent resistivities from the true resistivities of thin beds is not as drastic as for the other electrical resistivity logs. The apparent resistivities provide a better approximation to the true resistivities even in thin beds. The symmetrical lateral is non focusing and simple to implement. The bed-boundary resolution provided by the symmetrical array resistivity log is comparable to that from the high resolution density log.

ACKNOWLEDGMENTS

The author is indebted to TransAlta Utilities Corporation for the permission to carry out these experiments in their holes at the Highvale coal mine, Alberta. Thanks to Bill Hyatt and Steven Birk for the help in the data acquisition and Barbara Elliot for the help rendered in the processing of the data.

REFERENCES

Bristow, Q.
1986: A system for digital transmission and recording of induced polarization measurements in boreholes; in Borehole Geophysics for Mining and Geotechnical Applications, ed. P.G. Killeen, Geological Survey of Canada, Paper 85-27, p.127-143.

Dakhnov, V.N.
1959: The application of geophysical methods: electrical well logging, Moscow Petroleum Institute; translated by G.V. Keller (1962), Colorado School of Mines quarterly, v. 57, no. 2, 445 p.

Schlumberger Document 8.
1958: Introduction to Schlumberger Well Logging. Schlumberger, Houston.

MISE-À-LA-MASSE MAPPING OF GOLD-BEARING ALTERATION ZONES AT THE HOYLE POND GOLD DEPOSIT, TIMMINS, ONTARIO

Project 840031

C.J. Mwenifumbo
Resource Geophysics and Geochemistry Division

Mwenifumbo, C.J., Mise-à-la-masse mapping of gold-bearing alteration zones at the Hoyle Pond Gold deposit, Timmins, Ontario; in Current Research, Part A, Geological Survey of Canada, Paper 85-1A, p. 669-679, 1985.

Abstract

Drillhole mise-à-la-masse measurements were conducted between two holes at the Hoyle Pond Gold deposit, near Timmins, Ontario. Gold mineralization in this deposit occurs in carbonate alteration zones within magnesium-rich tholeiitic basalts. The alteration zones have relatively low resistivities compared to the unaltered basalts. The mise-à-la-masse method was successfully applied in correlating these zones between the holes. The limited mise-à-la-masse measurements between the two holes indicated that there are two possible orientations of the alteration zones, one nearly vertical which is concordant with the primary structures (foliation and in situ brecciation) within the basalts and another one which transects these primary structures.

Résumé

Au moyen de la méthode de la mise-à-la-masse, on a pris des mesures entre deux trous de forage localisés dans le gisement d'or de Hoyle Pond près de Timmins, en Ontario. L'or se presente dans des zones d'altération carbonatées contenues à l'intérieur de basaltes tholéiitiques riches en magnésium. Ces zones d'altération font preuve d'une faible résistivité par rapport aux basaltes non altérés. La méthode de la mise-à-la-masse a permis la corrélation de zones d'altération entre les trous. Les quelques mesures effectuées entre les trous de forage ont demontré que les zones d'altération se présentent selon deux orientations, soit (1) une première parallèle à la foliation et à la bréchification primaires dans les basaltes et, (2) une plus jeune qui recoupe ces structures primaires.

Introduction

Recent applications of borehole geophysics to gold exploration have indicated that significant geophysical anomalies may be observed in gold-bearing horizons. The single-hole geophysical logging methods that give promising results with respect to outlining gold-bearing alteration zones include gamma ray spectrometry, IP and resistivity (Mwenifumbo et al., 1983; Urbancic and Mwenifumbo, 1984). These single-hole geophysical logging techniques, however, provide information on the changes in the physical and chemical properties of the rock mass in the immediate vicinity of the drillhole. Geophysical anomalies observed in a number of holes are often difficult to correlate from hole to hole. This is mainly due to lack of characteristic signatures because of geological changes from one hole to the next. To provide information on the nature of the rock mass between holes and to determine whether anomalous features continue from hole-to-hole, techniques such as the mise-a-la-masse method are employed. The mise-à-la-masse method is a cross-hole or hole-to-surface electrical technique. With this technique, the potential field distribution is studied along a drillhole or on the surface while a current source is emplaced at an intersection of a conductive mineralization or structure. It is mainly used for mapping size and orientation of a conductor and for hole-to-hole correlation of the conductive structures.

The mise-à-la-masse method has been extensively and successfully applied during detailed mapping of massive sulphide ore bodies with high electrical conductivity (eg. McMurray and Hoagland, 1956; Parasnis, 1967; and Ketola, 1972). More recently the application of the mise-à-la-masse method has been extented to the mapping of fracture zones (relatively poor conductors compared to massive sulphide ores) in connection with the evaluation of areas for possible radioactive waste disposal sites (Jamtlid et al., 1982; Rouhianen and Poikonen, 1982). In this paper we present an example of the application of the mise-à-la-masse method for correlating gold-bearing alteration zones between holes. The study was carried out at the Hoyle Pond Gold deposit near Timmins, Ontario. The Hoyle Pond deposit is located just to the west of the Kidd Creek Metallurgical site, about 18 km northeast of the city of Timmins. Figure 78.1 shows the western part of the deposit and the location of the holes where the present study was carried out.

Geology and structure

The Hoyle Pond Gold deposit lies within the Abitibi Greenstone belt. Stratigraphically the area consists largely of ultramafic flows (komatiites) at the base, magnesium-rich tholeiitic basalts in the middle and sediments in the upper portion of the section.

Gold mineralization is found in carbonate alteration zones within a uniform sequence of magnesium-rich tholeiitic basalts. The zones are identified from the drill core by their distinctive steely blue-black colour and are characterized by the presence of free carbon (Downes et al., 1982). They have diffuse margins and become darker towards the centres that are black. The zones are structurally controlled and are characterized by in-situ brecciation and a strong schistosity in their centres. The foliation which strikes at 60 to 70 degrees and dips nearly vertical, increases in intensity from the margin to the core of the alteration zones. The alteration zones contain 1 to 3 per cent fine grained pyrite in the form of 1 to 5 mm 'snowflake'-like blotches occurring along fine cleavage fractures. Gold is present in quartz veins, 1 cm to 1 m wide, within the alteration zones and is also associated with the fine grained disseminated pyrite. The carbonate alteration zones in the Timmins area are believed to have been developed in a subseafloor volcanic environment by the passage of hydrothermal fluids up through joint or fracture sytems or along flow contacts (Fyon and Crocket, 1981).

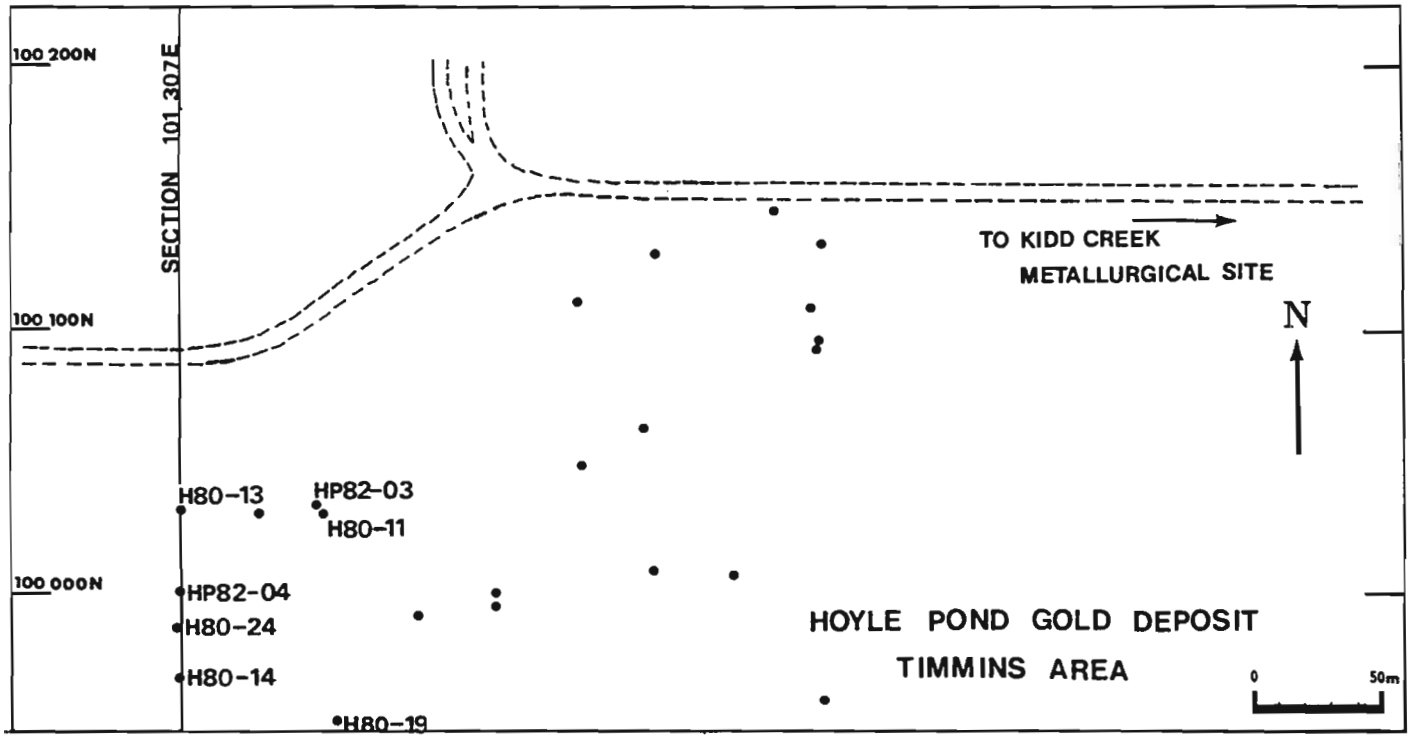

Figure 78.1. Map of the Hoyle Pond Gold Deposit showing the location of the drillholes where mise-à-la-masse data were obtained.

Figure 78.2 based on information provided by Kidd Creek Mines Ltd., shows the geology and structure of section 101,307E of the Hoyle Pond Gold deposit where the mise-à-la-masse measurements were carried out. Four holes were drilled along this section. They intersect about 20 m of glacial overburden and then the magnesium tholeiitic basalt flows. The holes were drilled with initial inclinations ranging from 55 to 65 degrees to intersect the steeply dipping alteration zones. A number of these alteration zones are intersected by drillholes. They vary in width from 5 to 30 m. The location of the zones that were identified in the drill core are displayed along the drillholes as shaded areas. Note the geological interpretation of the presence of alteration zones in areas where they were not identified on the drill core, especially along holes H80-24 and HP82-04. It is clear from the interpretation that even with this number of closely spaced drillholes on this section, the correlation of the alteration zones between the holes is a difficult task. It should be noted, however, that although core recovery was excellent the geological information from the drill core data represents only a small sample volume and the probability of not intersecting the target structure is quite high. The drillhole IP, resistivity and mise-à-la-masse measurements were carried out to outline the zones and to determine their continuity between holes. The measurements were conducted in drillhole H80-14 and HP82-04.

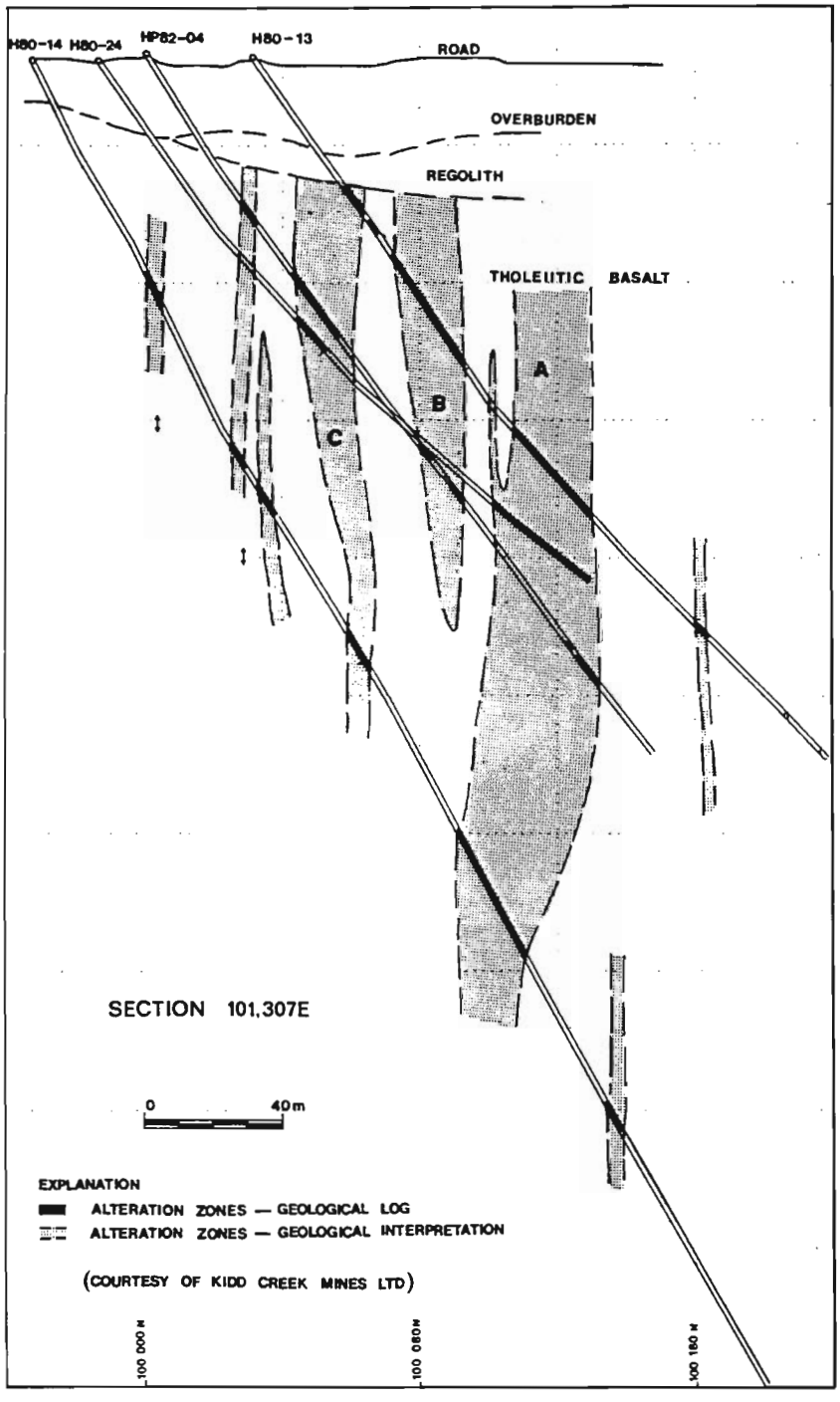

Drillhole IP and resistivity logging

Drillhole induced polarization (IP) and resistivity data were obtained with the lateral (pole-dipole) array. The potential dipole spacing (MN) was 0.4 m and the distance between the current electrode and the potential dipole centre was 2.8 m. The downhole current and potential electrodes consisted of gold-plated brass cylinders, 4 cm in diameter. The surface remote current electrode consisted of 3 steel rods about a metre in length, located approximately 500 m west of section 101,307E. The measurements were carried out with the GSC time domain IP/resistivity logging system (Bristow, 1984). The transmitter on this system is a constant current source, capable of supplying currents up to 250 mA. There are 4 selectable periods for the current waveform; 1, 2, 4 and 8 seconds. In cases where IP logging is done incrementally or continuously over short holes, long period waveforms (normally an 8 s period) are usually employed. However, for continuous logging in deep holes, it is expedient to log the holes with current waveforms of as short a period as possible in order to combine data resolution with reasonable speed. In the present study, IP and resistivity measurements were made using a period of 1 s (ie a current ON time of 0.25 s followed by an equal current OFF time with the polarity reversed during the second half cycle). Complete IP waveforms were recorded on 9 track magnetic tape. The apparent resistivities were computed from the primary voltages, that is, voltages observed during the current ON time, with the appropriate geometric factor. The IP chargeability data are determined from the decay voltages during the current OFF time. It is standard practice to integrate under a portion of the the decay curve and normalize it with the primary voltage.

Figure 78.2

Geological cross section along grid line 101,307E, Hoyle Pond deposit. (Unpublished data, courtesy Kidd Creek Mines Ltd.).

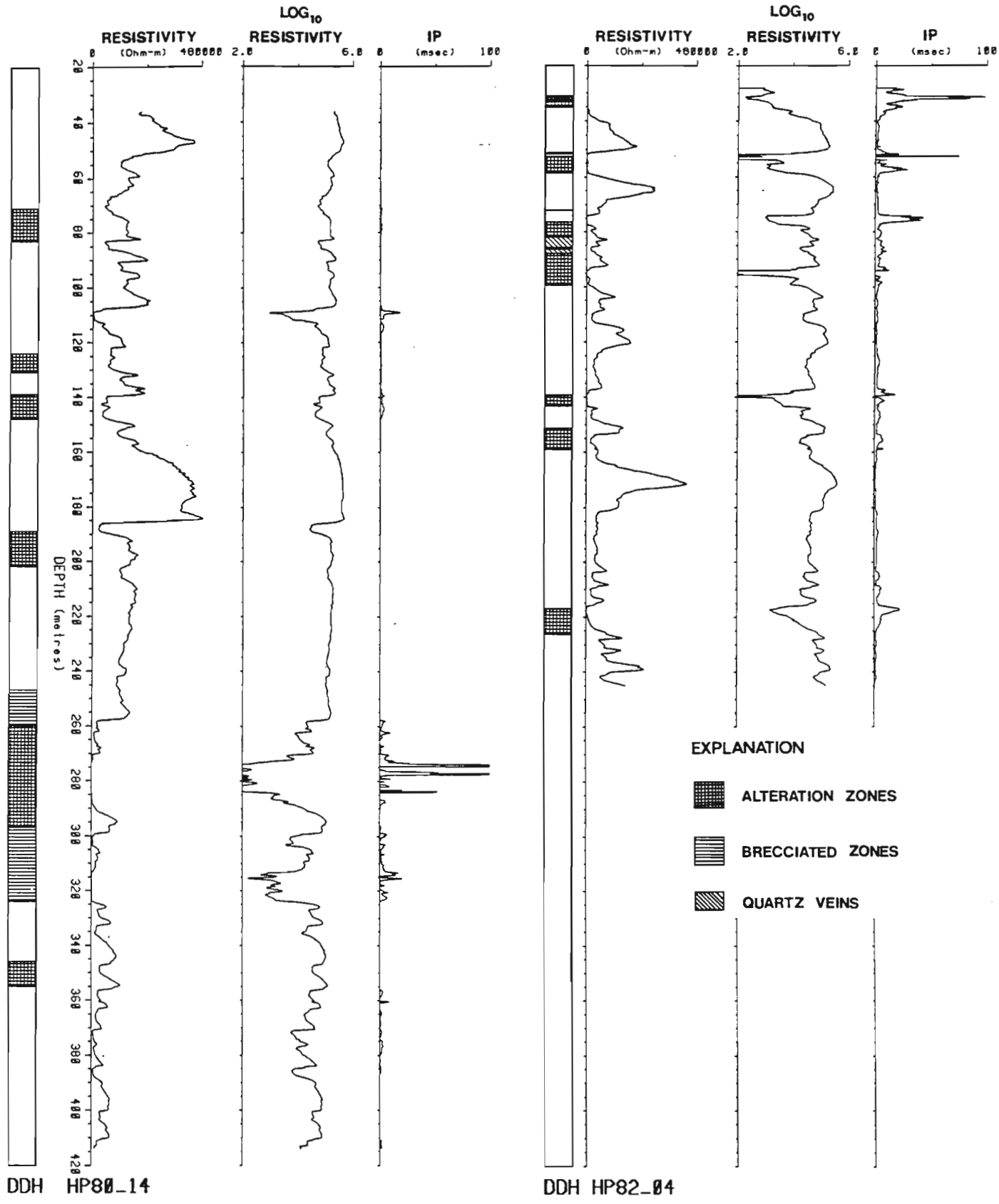

Figure 78.3. *Apparent resistivity and induced polarization logs obtained in holes HP82-04 and H80-14 with the lateral array.*

Since the integration is with respect to time the units of the apparent chargeability parameter are in milliseconds. In the present IP measurements, the chargeabilities were determined by integrating from 62 ms to 138 ms after the current is switched off. The logging speed was 3 m/min with measurements taken every second (equivalent to the hole sampling interval of 5 cm).

Figure 78.3 shows the IP and resistivity logs conducted along drill holes H80-14 and HP82-04. The locations of the alteration zones and in situ brecciated zones that were identified in the drill core are displayed in the columns next to the apparent resistivity log for each hole. The logarithm of the resistivity is also presented in the figure for each hole to enhance the low resistivity variations along the log. Chargeability highs and resistivity lows are observed across the majority of the alteration zones. This excellent correlation between the alteration zones and low resistivity high IP zones makes this type of log quite useful for detecting the alteration zones. There are a few low resistivity zones which do not correspond to any of the mapped alteration zones especially along drillhole H80-14. High chargeabilities and low resistivities are observed at about 110 m and between 370 and 390 m. These zones may correspond to alteration zones narrowly missed by the drill hole. The resistivities for most of the alteration zones vary between 10 000 and 1000 ohm-m except for the wide alteration zone between 260 and 330 m which has apparent resistivities lower than 100 ohm-m. The apparent resistivities of the unaltered basalts are around 100 000 ohm-m. The majority of the alteration zones along hole HP82-04 have apparent resistivities between 10 000 and 1000 ohm-m with some even lower than 1000 ohm-m. The resistivity contrast between the unaltered basalts and the alteration zones is, therefore, a factor of 10 or higher. This resistivity contrast is adequate for the mise-à-la-masse method.

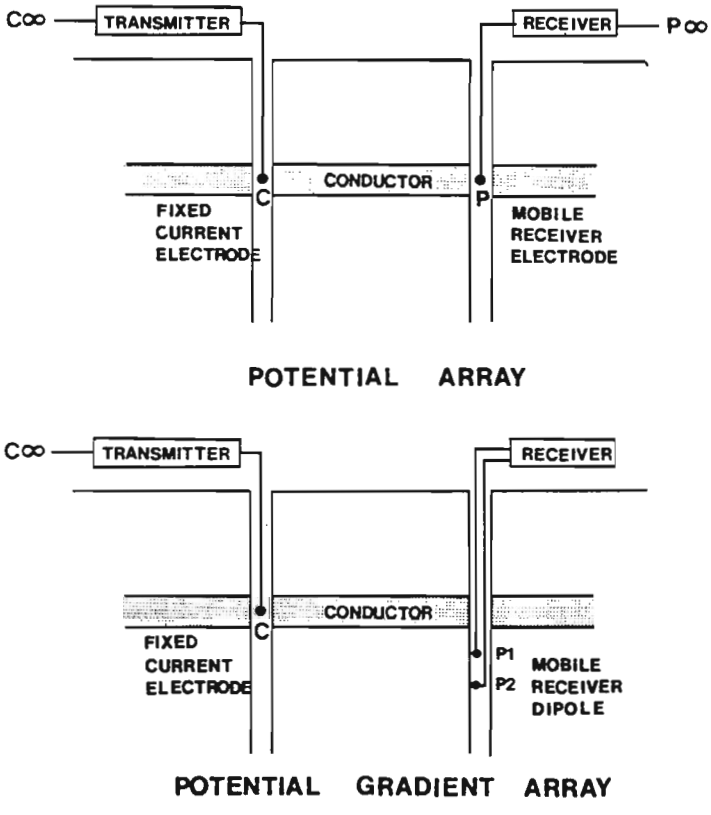

Figure 78.4. Electrode configurations in drill hole mise-à-la-masse measurements.

Drill hole mise-à-la-masse measurements

Field equipment and procedure

The mise-à-la-masse measurements were done with the same equipment used in the IP/resistivity logging. The measurements are accomplished by placing a current electrode in one borehole directly in a conductive zone to be studied and measuring the resulting potential field distribution in another borehole. The other return current electrode is located a large distance from the drillhole being studied (essentially at infinity). There are two possible arrays which can be used in drillhole mise-à-la-masse measurements; the potential array and the potential gradient array. Figure 78.4 shows the two electrode configurations. With the potential array one of the potential electrodes is fixed distant from the measurement hole (remote reference electrode placed effectively at infinity). The other potential electrode is moved along the measurement hole continuously or incrementally. In the potential gradient arrangement, the potential difference is measured by a mobile potential dipole, with the dipole spacing ranging from 2.5 to 10 m. The current electrode setup is the same for the two modes of operation. With the potential array, measurements of voltages do not require very sensitive receivers since the voltages are relatively large and directly referenced to a fixed potential electrode. The potential gradient array, however, involves measuring relatively small voltage drops across two closely spaced electrodes that are floating. A very sensitive receiver coupled with a powerful transmitter is required for accurate determination of the voltages. The choice of a particular array for the mise-à-la-masse surveys in typical field conditions is mainly dictated by the power of the transmitter and the sensitivity of the receiver used. The distance between holes and the conductivity contrast between the target structures and the surrounding rocks are also factors which must also be considered. The potential array has received more attention than the potential gradient array mainly because of the ease in interpreting the data. The potential gradient data, however, provide some characteristic features for quantifying the geometrical parameters of the conductive structure, for instance, estimation of the inclination and width of the conductors under study (Mwenifumbo, 1980). Potential gradients can be computed from the potential data if the measurements are taken at very small depth intervals. In the present study the potential array was used.

The downhole current electrode used in this study consisted of a 1 m long copper tube about 4 cm in diameter attached to an insulated copper wire to lower it into the selected drillhole. The lateral resistivity logs and the geological logs were used to locate the conductive zones where the current electrode was emplaced. In order to ensure that the current electrode was placed in zones with the highest conductivity (for maximum signal strength) contact resistances were monitored as the electrode was lowered into the conductive zone. The surface current electrode was placed approximately 500 m from section 101,307E (effectively at infinity). The in-hole potential measuring electrode was a gold-plated brass cylinder, 4 cm in length. The other potential electrode (remote reference electrode) was placed on the surface approximately 100 m away from the drillhole collar. Most of the logging was carried out at 3 m/min with one second data sample interval, giving a measurement every 5 cm. A few logs were obtained at 6 and 9 m/min with a one second data sample interval, giving measurements every 10 and 15 cm respectively. The current intensity was maintained constant during each run. Figure 78.5 shows a vertical section with the locations of the two holes logged and the positions of the energizing current electrodes. The apparent resistivity logs are also diplayed to show their proper depth perspective along the holes.

Presentation of the data

In the present study mise-à-la-masse potential gradients along the drillhole axis are also analyzed. The gradients are computed from the potential measurements using the Savitzky-Golay least squares derivative operator (Madden, 1978; Savitzky and Golay, 1964). The derived gradients are valid since the data sample interval in the hole was small. The mise-à-la-masse potential and the derived potential gradients are plotted for each source location. The potentials are designated as the P logs and the potential gradients as the G logs. In all the logs, the top scale and axis is for the potential data and the bottom scale and axis is for the gradient data. The zero for the gradient data is plotted as dotted lines. The dominant current flow path between the holes is indicated by a solid line between the drill hole geologic columns. This is determined from the maximum amplitudes in the potential logs and the zero-crossover point on the gradient logs. The depth scale on the logs does not represent the true vertical depths but lengths along the drillhole. All the values are normalized with respect to the current intensity in order to facilitate comparision of the amplitudes of the observed measurements for different source locations with different energizing current intensities. The potentials are expressed in volts/ampere and the potential gradients in millivolts/ampere-metre. The column of the holes with the source and the receiver are displayed with the location of the alteration zones identified from the drill core shown in hatched lines.

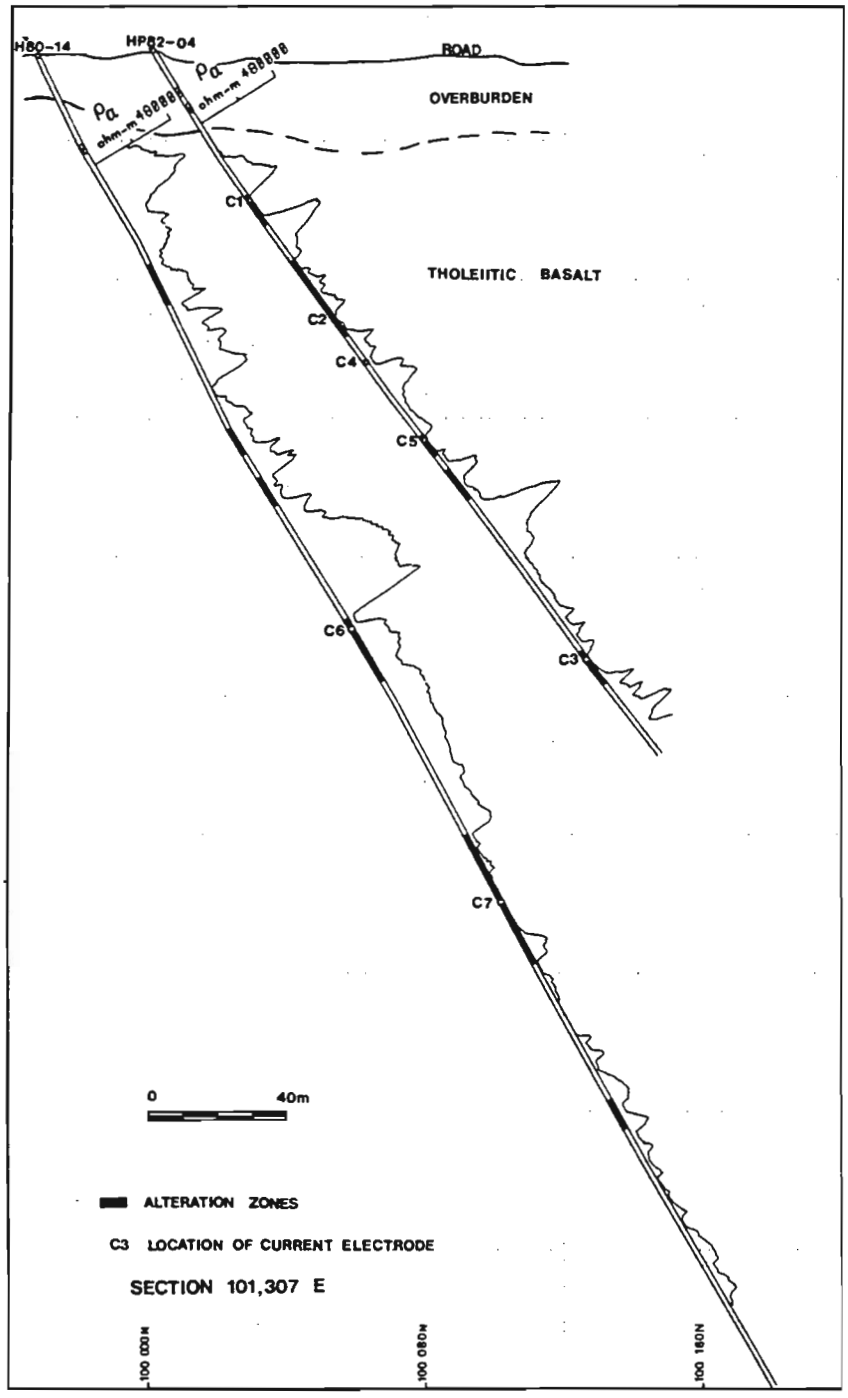

Figure 78.5. Vertical section showing the locations of the current electrodes used during measurements. Apparent resistivity logs are displayed along the drillholes.

For an electrically homogeneous and isotropic medium, the equipotential surfaces resulting from a buried current source are concentric about the source, governed by the equation, $V = \rho I/4 \pi R$ (V = volts, I = current, ρ = resistivity and R = distance from source to measurement point). In this situation, mise-à-la-masse data will indicate maximum potential amplitudes (zero-crossover points in the gradient data) at a point in the measurement hole which is closest to the source. When a current electrode is placed in a conductor, current tends to be channelled along the conductor and observations in a hole that intersects the energized conductor will show a flat potential maximum or zero gradients across the intersection. The intersection is not necessarily the shortest distance from the source. The peak-to-peak amplitude separation on the gradient data gives a rough estimate of the width of the conductor under investigation in the case of a simple, single conductor environment.

Results and discussion

Measurements in H80-14 - current electrodes in HP82-04

Figure 78.6 shows mise-à-la-masse measurements in drillhole H80-14 with the current electrodes implanted at three different low resistivity zones in drillhole HP82-04. C1-LOG, C2-LOG and C3-LOG represent mise-à-la-masse data obtained with the current electrode at C1, C2 and C3 respectively in hole HP82-04. The C1 electrode was placed at approximately 52 m and a current strength of 254 mA was injected into the medium. The C1-LOG shows maximum potential amplitudes and a zero-crossover point in the gradient at approximately 110 m in drillhole H80-14 indicating that electrical continuity exists between the alteration zone energized by C1 in HP82-04 and the location at 110 m in H80-14. No alteration zone has been mapped at this depth but the resistivity log

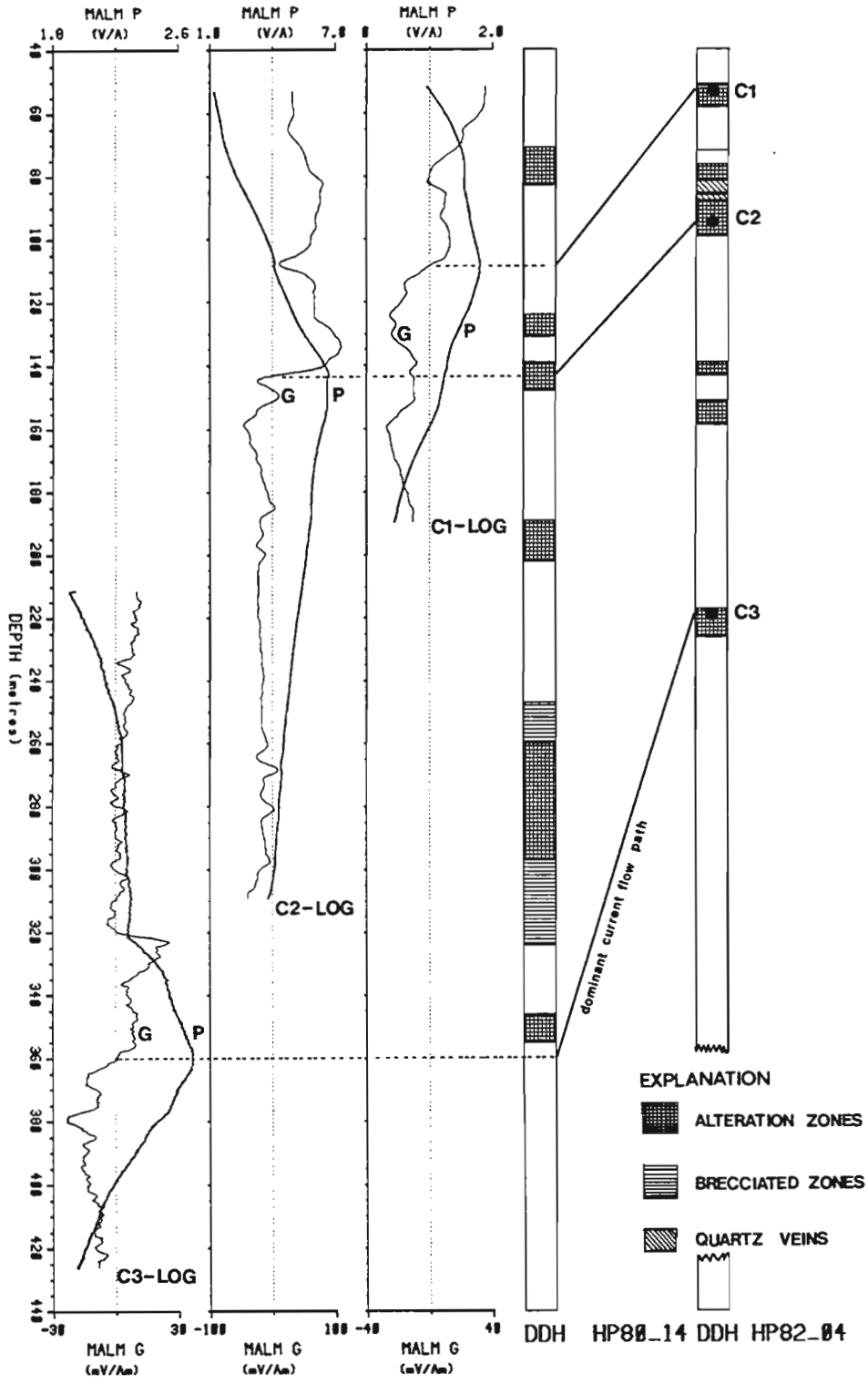

Figure 78.6. Mise-à-la-masse potential and gradient measurements obtained in drillhole H80-14 with the current electrodes in drillhole HP82-04. The C1-LOG, C2-LOG and C3-LOG represent measurements with the current electrodes located at C1, C2 and C3 respectively. P – potential log; G – gradient log. The solid lines between the geologic columns represent the dominant current flow path.

indicates a fairly conductive zone around this depth. The mise-a-la-masse potential flattens out and the gradients are fairly low and constant over the regions occurring at approximately 76-83 m and at about 140-150 m. These regions correlate with the low resistivity zones on the lateral resistivity log. This observation is characteristic of an electrically isolated conductor lying parallel to an energized one. It has been numerically modelled by Eloranta (1984) for drillhole mise-à-la-masse data and has been observed in a number of field cases.

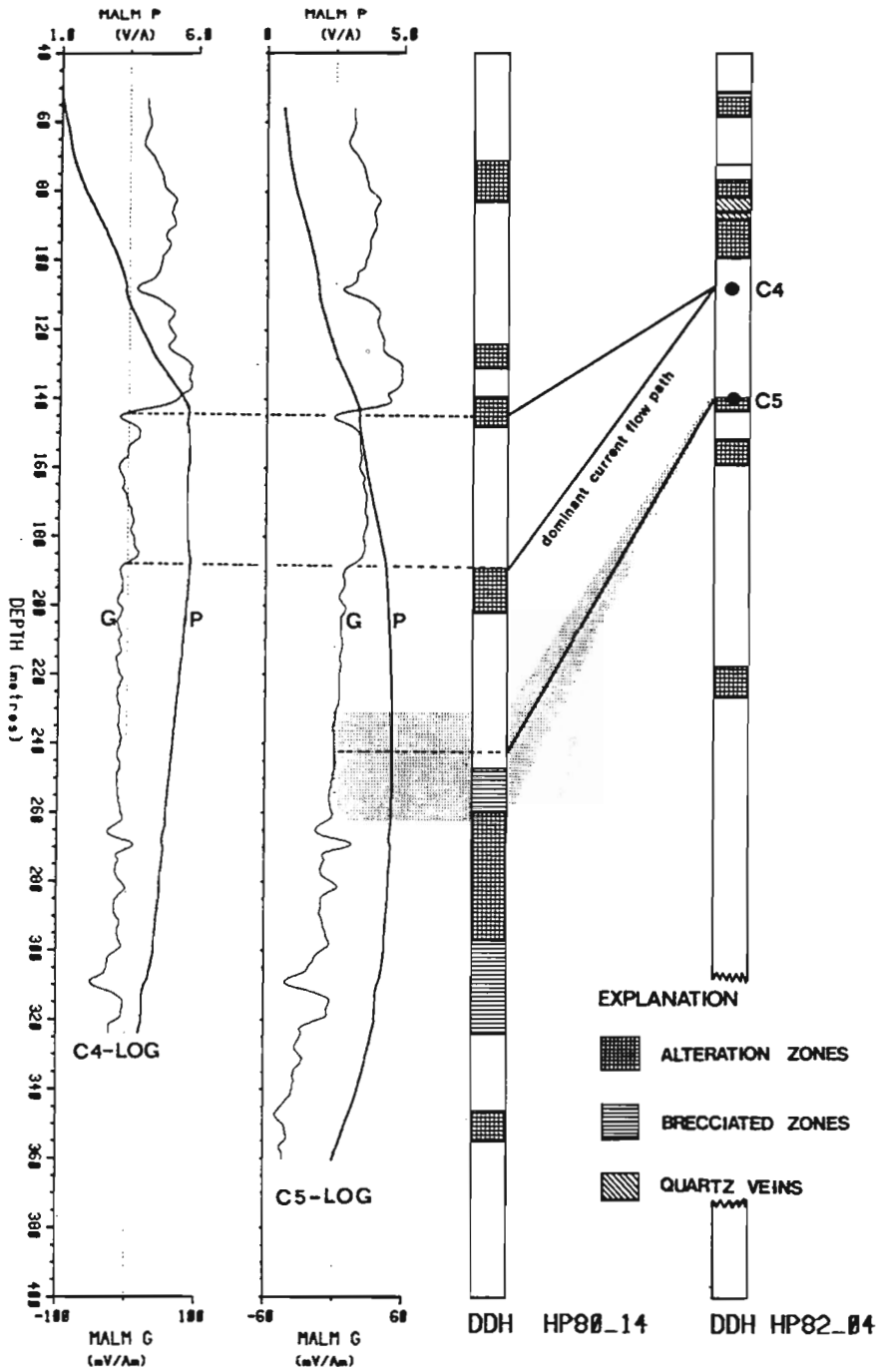

Figure 78.7. Mise-à-la-masse potential and gradient measurements obtained in drillhole H80-14 with the current electrodes in drillhole HP82-04. The C4-LOG and C5-LOG represent measurements with the current electrodes located at C4 and C5 respectively. The solid lines between the geologic columns represent the dominant current flow path.

The C2-LOGs were obtained with the current electrode placed at approximately 95 m in the lower part of the alteration zone between 75 and 105 m. A maximum current of 180 mA was supplied to the medium. The log exhibits high potentials between 140-150 m. This coincides with the location of an alteration zone. It is interesting to note that the rate of change of the potentials is gradual on the downhole side and rapid on the uphole side. This trend is more evident in the gradient data. This pattern suggests that the conductive structure from C2 intersects H80-14 at a fairly low angle on the downhole side. The main current axis is located at approximately 143 m (zero-crossover point in the gradient data with maximum peak-to-peak amplitude). The upper conductive zone that is electrically continuous with the C1 alteration zone is indicated on the C2-LOGs by the flattening of the potentials and a local minimum in gradients.

A current of 142 mA was injected through the C3 electrode at approximately 218 m down drillhole HP82-04. The C3-LOG indicates that the alteration zone at C3 intersects H80-14 at approximately 360 m. The separation between the peak-to-peak amplitudes around the zero-crossover point is about 10 m. This is approximately the width of the conductor at this location. It is interesting to note the abrupt step-like change in potential at approximately 320 m, above which the potentials are fairly low and flat (almost zero gradients). The conductive zone at 360 is well isolated from the conductive alteration zone above (between 260 and 320), contrary to the interpretation inferred from the drill core log (see Fig. 78.2).

Figure 78.7 shows mise-à-la-masse data along drillhole H80-14 with current electrodes placed at two locations in HP82-04. The C4-LOG represents mise-a-la- masse data with the C4 current electrode located just below the alteration zone with the C2 electrode at about 110 m. The apparent resistivities are not very low at this location (approximately 20 000 ohm-m) and hence a maximum current of about 60 mA could be put into the ground with the present lower-powered transmitter. The reason for putting a current electrode at this location will become clear later in discussion of the measurements in HP82-04 with the current electrodes in hole H80-14. The C4-LOGs indicate a fairly broad zone (from approximately 140 to 190 m) of high potentials. Maximum potentials of almost equal amplitudes are observed at 140 to 155 m and at about 187 m (zero-crossover points in the gradient data at 144 and at 187 m). The lateral resistivity log indicates a zone of high resistivity (greater than 100 000 ohm-m) between the conductive alteration zone at 145 m

and that at 187 m. The data indicate that the conductive zone intersected at C4 in HP82-04 splits into two zones; one intersecting H80-14 at approximately 145 m and the other one at approximately 187 m. The data also suggest that the lower conductive zone passes close to H80-14 but not close enough to be detected by the lateral resistivity log. As noted previously the resistivity log only provides information on the resistivity changes in the immediate vicinity of the drillhole.

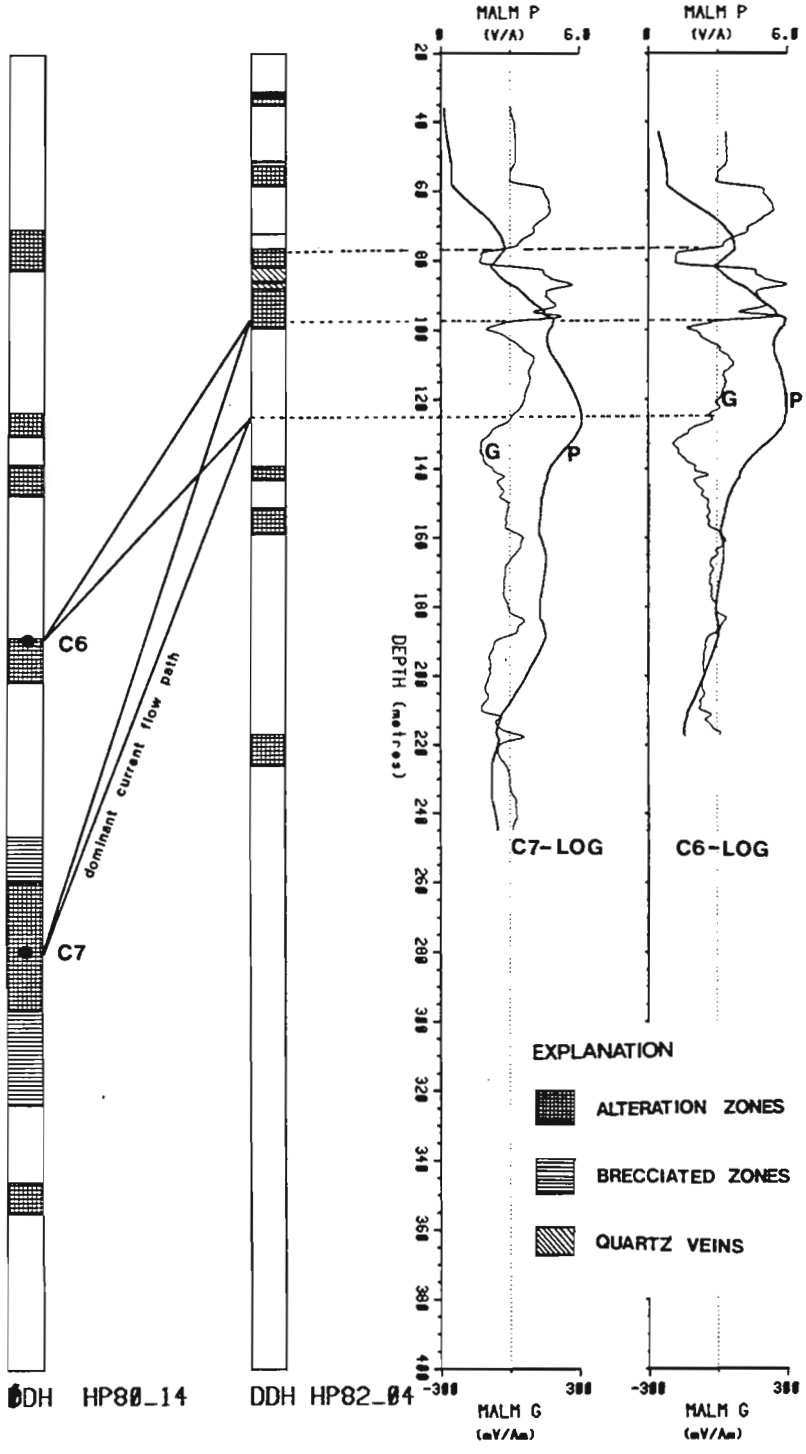

Figure 78.8. Mise-à-la-masse potential and gradient measurements obtained in drillhole HP82-04 with the current electrodes in drillhole H80-14. The C6-LOG and C7-LOG represent measurements with the current electrodes located at C6 and C7 respectively. The solid lines between the geologic columns represent the dominant current flow path.

The C5-LOG represents mise-à-la-masse data along H80-14 with the current electrode at about 139 m in HP82-04. Again we see a broad potential high from approximately 190 m to 270 m. The diffuse nature of the response indicates that the conductor at C5 is not in electrical continuity with any of the conductive zones along H80-14. The gradient data shows the location of maximum current flow at approximately 226-250 m which does not coincide with any of the low resistivity zones on the lateral resistivity log. The conductive zones at about 110 m and 145 m are indicated on the gradient logs as electrically isolated from the energized zone.

In all the above observations, the location of the potential maxima (or zero-crossover points on gradient data) showed considerable displacement from the location of the points along the observation hole with the minimum distance to the current sources. This indicates considerable current channelling along the more conductive paths. Conductive zones above and below the one in electrical continuity with the source are indicated by the flattening of the potentials (or local minima in potential gradients) confirming their electrical isolation from the energized one.

Measurements in HP82-04 - current electrodes in H80-14

Figure 78.8 shows mise-à-la-masse data obtained in drillhole HP82-04 with the C6 and C7 current electrodes emplaced at 190 m and 280 m, respectively, in H80-14. It is interesting to note the similarities in the observed potentials for the two current electrode positions. The gradients are almost identical. For both of the current electrode positions, the current flow axes are observed at 125 m and 97 m, suggesting that the two energized conductive zones at C6 and C7 converge and intersect hole HP82-04 at the same locations. There is a pronounced potential minimum on both the C6-LOG and C7-LOG at about 82 m followed by a pronounced local maximum at about 77 metres. This suggests that there is a fairly conductive path between the conductive zones at C6 and C7 in hole H80-14 and the location at 77 m in hole HP82-04. This location is the conductive upper part of the alteration zone identified between 75 and 100 m. It is separated by a fairly resistive section (about 100 000 ohm-m) from the lower conductive part at 100 metres and hence a pronounced minimum between the two parts. The observed high potentials between 110 to 130 m in HP82-04 do not coincide with any mapped alteration zones. The indicated current flow path from C7 and C6 to 120 m in HP82-04 is an excellent conductive path. The data suggest that there is strong current channelling along this conductor over a distance greater than 150 m between the holes. The measurements in hole H80-14, with the current electrode placed at about 110 m in hole HP82-04, were conducted to

determine where the zone near 110 m manifests itself in hole HP80-14. The data indicate that the zones at C6 and at C4 are in electrical continuity. There was little indication of electrical continuity between zones at C4 and C7 when the current electrode was at C4. This is probably because the current electrode at C4 was not located in zone with the optimum coupling to C7. This should have been at 125 m, the location of the current flow axis with the current electrode at C7.

The overall interpretation of the mise-à-la-masse observations and the lateral resistivity logs carried out between the drillholes HP82-04 and H80-14 are presented in Figure 78.9. This is a qualitative interpretation of the conductive structure between the two holes and is derived from dominant current flow paths determined by joining the location of the potential maxima (or zero-crossover points in the gradient data) with their respective energizing current sources. The widths of the conductive zones between the holes are speculative at the present time. Theoretical modelling of the structure may provide some realistic widths. As noted previously the observed alteration zones generally show high conductivity. Therefore it is interesting to compare the interpretation of the alteration zones based on the drill core data (Fig. 78.2) and that of the conductive zones based on the mise-à-la-masse data (Fig. 78.9). The most dramatic difference in the interpretation is the orientation of the alteration zones between 260 and 300 m in hole H80-14. This conductive zone intersects hole HP82-04 at about 125 m and dips steeply towards the north (conductive structure from C4 to C7 electrode locations) in contrast to the southerly or nearly vertical dips of the the rest of the conductors. It appears that there are two sets of conductive structures (alteration zones) which may represent two stages of fracturing and alteration. A more complete picture on the conductivity structure between the holes along this section could have been obtained by studying the alteration zones in other holes (holes H80-24 and H80-13). This was unfortunately not done because the holes in the area were not available for geophysical work at the time.

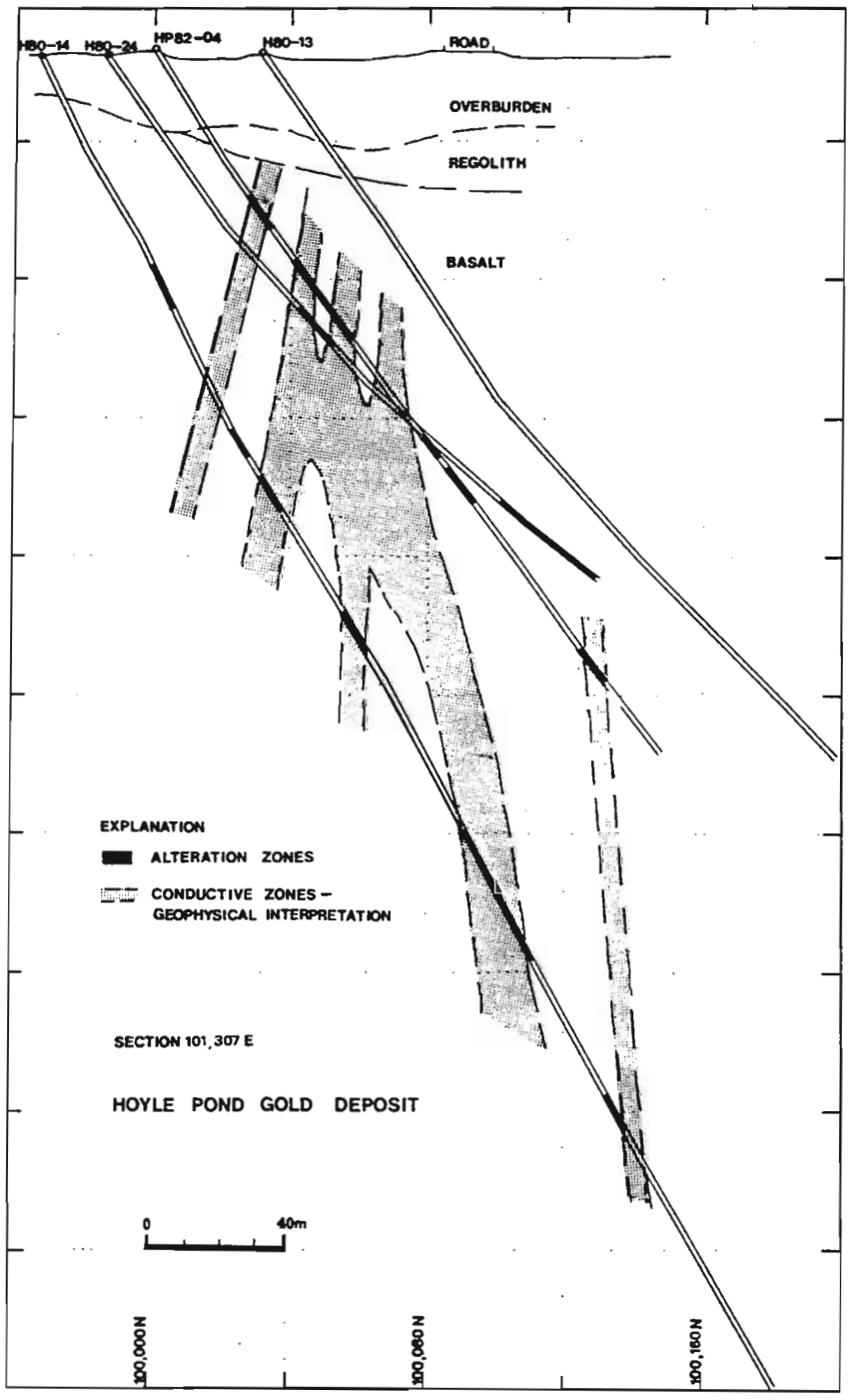

Figure 78.9. Conductivity structure between holes HP82-04 and H80-14 as inferred from the mise-à-la-masse and lateral resistivity logs.

Conclusion

The drill hole mise-à-la-masse measurements carried out between the two holes at the Hoyle Pond Gold deposit were successful in correlating the alteration zones between these holes. The alteration zones are relatively good conductors compared to the unaltered basalt flows and seem to be well suited for investigation by the mise-à-la-masse method.

Acknowledgments

I would like to thank Kidd Creek Mines Ltd. for permission to work on their property and to present these data. Special thanks are due to Dr. J.A. Slankis and D.J. Londry of Kidd Creek Mines who suggested this interesting study. I would also like to thank my colleagues at the GSC, especially, P.G. Killeen, for valuable discussions and comments, Q. Bristow who designed the IP/resistivity logging system and W.G. Hyatt for assistance in field data acquisition.

References

Bristow, Q.
1984: A system for the digital transmission and recording of Induced Polarization Measurements in Boreholes; in Proceedings of the International Symposium and Workshop on Borehole Geophysics: Mining and Geotechnical Applications.

Downes, M.J., Hodges, D., and Derweduwen, J.
1982: A Free Carbon and Carbonate Bearing Alteration Zone Associated with the Hoyle Pond Gold Deposit, Ontario, Canada; in Gold '82: The Geology, Geochemistry and Genesis of Gold Deposits, ed. R.P.Foster; Geological Society of Zimbabwe Special Publication No. 1. p.435-448.

Eloranta, E.
1984: A method for calculating mise-à-la-masse anomalies in the case of high conductivity contrasts by the integral equation technique; Geoexploration, v. 22, p. 77-88.

Fyon, J.A. and Crocket, J.H.
1981: Volcanic Environment of Carbonate Alteration and Stratiform Gold Mineralization, Timmins area; in Genesis of Archean, Volcanic Hosted Gold Deposits, Ontario Geological Survey, Miscellaneous Paper 97.

Jamtlid, A., Magnusson, K.A., and Olsson, O.
1982: Electrical borehole measurements for the mapping of fracture zones in crystalline rock; in Proceedings of a workshop on Geophysical Investigations in Connection with Geological Disposal of Radioactive Waste, Nuclear Energy Agency.

Ketola, M.
1972: Some points of view concerning mise-à-la-masse measurements; Geoexploration, v. 10, p. 1-23.

Madden, H.H.
1978: Comments on the Savatzky-Golay convolution method for least-squares fit smoothing and differentiation of digital data; Analytical Chemistry, v. 50, no. 9, p. 1383-1386.

McMurry, H.V. and Hoagland, A.D.
1956: Three dimensional applied potential studies at Austinville, Virginia; Bulletin Geological Society of America, v. 67, no. 6, p. 683-696.

Mwenifumbo, C.J.
1980: Interpretation of mise-à-la-masse data for vein type bodies; University of Western Ontario, London, Ontario, Ph.D. Dissertation.

Mwenifumbo, C.J., Urbancic, T.I., and Killeen, P.G.
1983: Preliminary Studies in Gamma Ray Spectral Logging in Exploration for Gold; in Current Research, Part A, Geological Survey of Canada, Paper 83-1A, p. 391-397.

Parasnis, D.S.
1967: Three dimensional mise-à-la-masse surveys of an irregular lead-zinc-copper deposit in central Sweden; Geophysical Prospecting, v. 15, no. 3, p. 407-437.

Rouhianen, P. and Poikonen, A.
1982: Geophysical studies in the power plant area of Loviisa in southern Finland; in Proceedings of a workshop on geophysical investigations in connection with geological disposal of radioactive waste, Nuclear Energy Agency.

Savitzky, A. and Golay, J.E.
1964: Smoothing and differentiating of data by simplified least squares procedures; Analytical Chemistry, v. 36, p. 1627-1638.

Urbancic, T.I. and Mwenifumbo, C.J.
1984: Multiparameter Logging Techniques Applied to Gold Exploration; in Proceedings of the International Symposium and Workshop on Borehole Geophysics: Mining and Geotechnical Applications.

60. FIELD EVALUATION OF A MAGNETIC SUSCEPTIBILITY LOGGING TOOL

Project 810008

Q. Bristow and G. Bernius
Resource Geophysics and Geochemistry Division

Bristow, Q. and Bernius, G., Field evaluation of a magnetic susceptibility logging tool; in Current Research, Part A, Geological Survey of Canada, Paper 84-1A, p. 453-462, 1984.

Abstract

A magnetic susceptibility borehole logging tool, only recently available in North America has been evaluated in field boreholes. Repeatability of logs from the same hole is excellent, as is the agreement with drill core magnetic susceptibility measurements from three different holes.

Résumé

Un outil de diagraphie de la susceptibilité magnétique, disponible depuis peu en Amérique du Nord, est évalué dans des sondages sur le terrain. La répétition des diagraphies dans le méme trou de sonde est excellente, de méme que la concordance avec les mesures de la susceptibilité magnétique des carottes provenant de trois trous différents.

INTRODUCTION

Borehole logging in the mining industry is gaining ever wider acceptance as a powerful and relatively inexpensive technique for gathering data to aid in geological interpretation, or in the recognition of mineralization intersected by a drill hole. Until fairly recently however, magnetic susceptibility tools have not been generally available and the few that were have been used mostly by researchers (George and Scott, 1982).

The magnetic susceptibility of a volume of matter is a function of the amount of ferrimagnetic material contained therein thus magnetic susceptibility measurements will readily indicate the presence of minerals which contain significant concentrations of ferrimagnetic material such as magnetite, ilmenite and pyrrhotite (see e.g. Telford et al., 1976, p. 121). Anomalously low values of magnetic susceptibility can also be significant in certain geological contexts. For example the uranium "roll front" deposits of the southwestern United States are precipitated from uranium bearing, oxidizing groundwaters moving through sandstone strata, and these waters cause magnetic minerals to be altered to nonmagnetic ones, e.g. magnetite to hematite, behind the advancing roll fronts (Ellis et al., 1968; Scott and Daniels, 1976), causing anomalously low magnetic susceptibility readings.

As with any measurement technique which is specific for some parameter, (in this case ferrimagnetic material), magnetic susceptibility measurements can be used to advantage in revealing trends in related parameters e.g. lithological correlation between boreholes.

Due to the time consuming and hence expensive nature of sample-by-sample magnetic susceptibility measurements, they are not normally made on drill core unless a special requirement exists for the data. Such requirements do arise, for example, in the geological and geophysical investigations connected with radioactive waste management projects. The availability of a logging tool can reduce the measurement time from several person-weeks to a few person-hours. Furthermore a borehole log provides a more representative bulk sample than drill core, which is typically less than 60 mm diameter.

This paper presents field data from three boreholes to show the comparison between magnetic susceptibility logs made with a recently available logging tool, and the corresponding logs made by closely spaced measurements on the drill cores from the same holes. Reproducibility is demonstrated with repeat logs of the same boreholes.

BACKGROUND

The Geological Survey of Canada has a program of research aimed at improving borehole geophysical methods. In support of this a logging truck has been equipped with a computer-based data acquisition system which records parameters such as natural gamma-ray spectral data, temperature, induced polarization, resistivity and self potential in digital form together with depth.

Geo Instruments of Finland recently introduced a magnetic susceptibility logging tool which is now available in Canada through Urtec Instruments Sales Ltd. of Toronto. The tool was interfaced to the GSC logging truck in September 1983 and logs were recorded from two test holes maintained by the GSC at Bells Corners in Ottawa and from three holes at a site in the Bancroft area of Ontario. Drill core magnetic susceptibility data were available for one of the holes at Bells Corners and for two at the Bancroft location.

THE MAGNETIC SUSCEPTIBILITY TOOL

The principle of operation of the Geo Instruments model TH-3C is based on the use of a coil in an electrical bridge circuit energized at a frequency of 1400 Hz. When the tool moves through magnetically susceptible material an apparent change of the coil inductance is sensed causing the bridge to become unbalanced. Circuitary contained in the tool drives the bridge to balance automatically by changing the energizing frequency as necessary. The frequency shift is thus a measure of the magnetic susceptibility of the material through which the tool is passing and is registered as such on a continuous basis by the recording equipment.

The Maxwell-bridge circuit which is used also allows resistivity of material close to the coil to be measured simultaneously with susceptibility. This is possible by resolving the change in complex impedance seen by the bridge into its inductive and resistive vector components. (Resistive material around the coil causes the coil to behave as a transformer with the resistive material acting as a combined and distributed "secondary winding" and "load"). Resistivity measurements using this technique are limited however to a range of 10^{-1} ohm-metres to 10^{3} ohm-metres. In practice only some sedimentary formations would normally have resistivities low enough to fall within this range, while in igneous rocks only graphitic conductors or mineralized zones would be included.

Table 60.1

TECHNICAL SPECIFICATIONS: TH-3C MAGNETIC SUSCEPTIBILITY LOGGING TOOL

Susceptibility measuring ranges:

Range switch	Display	Rear panel output	Susceptibility
1	0-2 000	0-10 Vdc	0-2 000 x 10^{-5} SI
2	0-2 000	0-10 Vdc	0-20 000 x 10^{-5} SI
3	0-1 000	0-5 Vdc	0-200 000 x 10^{-5} SI

Note: The output is linear within the calibration accuracy up to 5 000 x 10^{-5} SI. On higher values a calibration curve should be consulted or a correction formula applied to the results.

Resolution: 5 x 10^{-5} SI

Temperature Drift: less than 10 x 10^{-5} SI/°C
Note: this value may be temporarily exceeded after a sudden temperature change.

Pressure effect: less than 1 x 10^{-5} SI/bar

Drift from other sources: less than 1 x 10^{-5} SI/min

Calibration accuracy: 5%

RESISTIVITY:

Resistivity measuring range:

Display	Rear panel output	Resistivity
0-2 000	0-10 Vdc	$10^{-1}\Omega m$-$10^{3}\Omega m$

MECHANICAL DATA:

Length of the electronics section of the probe: 0.6 m

Length of the coil section: 0.5 m

Minimum diameter of the probe: 42 mm

Test pressure: 150 bar (1500 m depth)

Weights: Surface module: 1.2 kg
Probe: 3.8 kg
Shipping Weight: 13 kg

TH-3C:
POWER SUPPLY:

Surface module: 4 Ah, 5 V Ni-Cd batteries, current consumption 200 mA
Probe: 4 Ah, 5 V Ni-Cd batteries, current consumption 180 mA

MECHANICAL DATA:

Length of the electronics section of the probe: 1.0 m

Length of the coil section: 0.5 m

Minimum diameter of the probe: 42 mm

Test pressure: 150 bar (1500 m depth)

Weights: Surface module: 1.8 kg
Probe: 5.0 kg
Shipping Weight: 16 kg

The tool consists of a metal tube containing the necessary circuitry and recharageable batteries and a detachable sensing coil encapsulated in nonmetallic material. A variety of coils are available but the test runs under discussion were made with one which had the same diameter (42 mm) as the electronics portion of the tool. The metal tube is fitted with an electrical connector which is designed for use with a standard 4-pin Gearhart-Owens cable head. A surface module receives and decodes the combined magnetic susceptibility/resistivity signal which is transmitted as a frequency (susceptibility signal) superimposed on a D.C. level (resistivity). The surface module provides separate analogue outputs for the two parameters. The essential technical specifications for the TH-3C are shown in Table 60.1, taken from the manufacturers literature.

RECORDING OF MAGNETIC SUSCEPTIBILITY DATA BY THE GSC LOGGING SYSTEM

The GSC logging system has been described by Bristow (1979). One of the parameters routinely recorded with the GSC logging system is temperature. The interface for this tool is designed to measure the frequency of a monolithic voltage-to-frequency (V/F) converter housed in the temperature tool and the interface circuitry is contained on one of the circuit boards of the NOVA minicomputer, which controls the system. A very high measurement resolution is achieved by measuring the time for a fixed number of V/F converter pulses against a 10 MHz crystal controlled clock. By inserting an identical inexpensive integrated circuit V/F converter between the susceptibility output from the TH-3C surface module and the NOVA interface board, signal compatibility was readily achieved. Recording of the magnetic susceptibility logs then proceeded exactly as if temperature logs were being run, with the same software controlling the display and recording of depth and magnetic susceptibility data on standard nine-track tape.

RESULTS AND DISCUSSION

A total of five holes were logged with the TH-3C magnetic susceptibility tool. In each case the logging speed was 6.0 m/minute with a one second sampling time, giving a measurement at every 10 cm down the hole. Two logs were run in each of these holes, one down and one up. The hole diameters for Bancroft are "HQ" and for Bells Corners "NQ" (100 mm and 75 mm respectively), which are larger than the diameter for which the tool had been calibrated. A factor to correct for this was obtained from the manufacturer and applied to the data recorded. Absolute values so corrected agreed well with drill core values.

The probe incorporates compensation for quasi-static temperature changes, which is not effective when the unit is subjected to step changes in temperature. Accordingly the probe was allowed to come to thermal equilibrium by lowering it into the borehole fluid and leaving it there for 30 minutes before logging was started. The temperature variation over the total lengths of these holes is known to be of the order of 5°C or less, so that the rate of change was well within the "quasi-static" definition.

The Bells Corners test site consists of Precambrian gneiss overlain unconformably by approximately 65 m of sedimentary rocks (dolomite, sandy dolomite and sandstone). The Bancroft holes also penetrate gneiss but of a much higher degree of metamorphism and deformation than at Bells Corners, which is reflected in the greater range of susceptibility values.

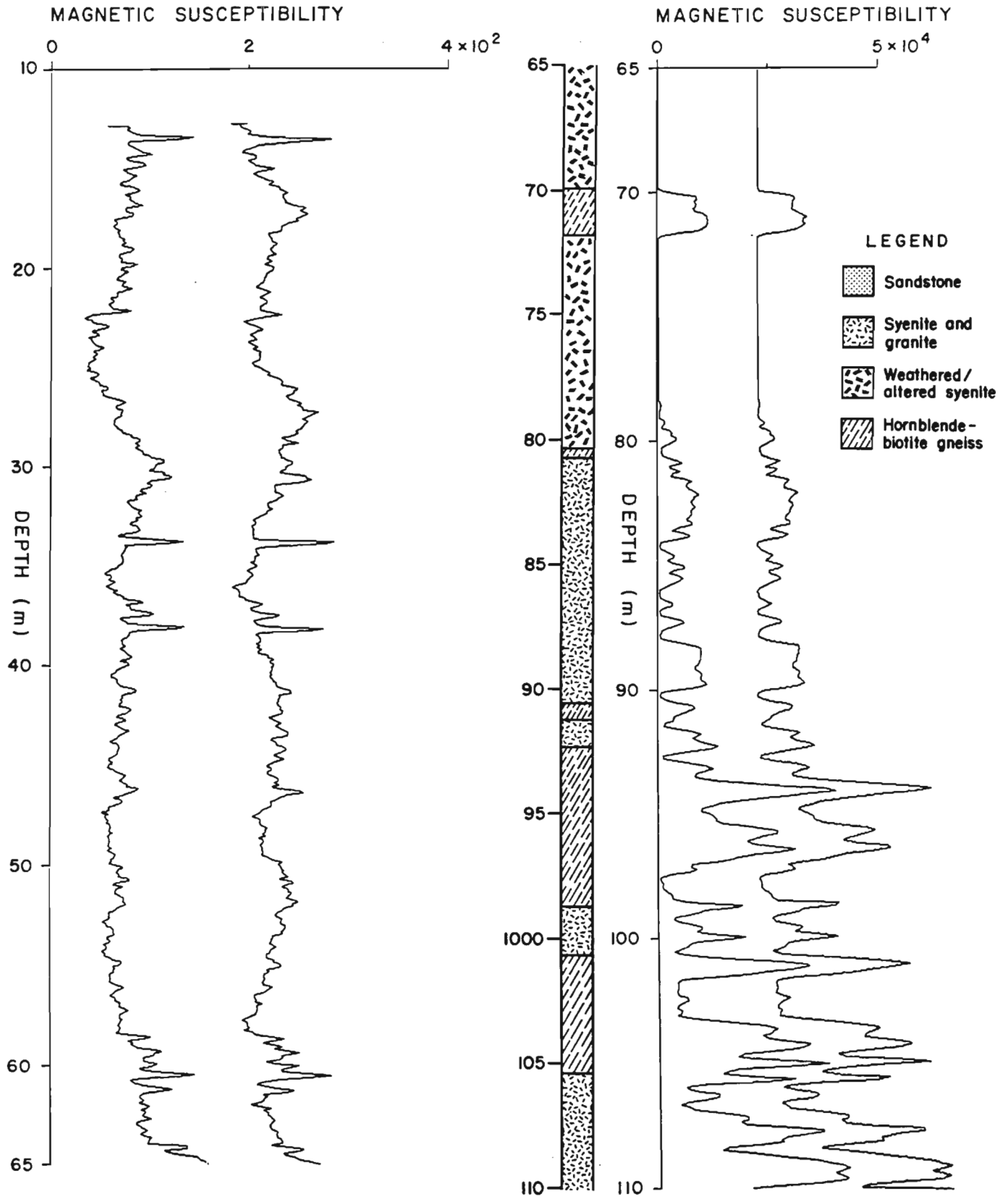

Figure 60.1. *A. Repeat logs 10-65 m in sedimentary strata of Bells Corners test hole BC-81-2. Expanded scale 0-400 x 10^{-5} SI units. B. Repeat logs 65-110 m in the Precambrian gneiss penetrated by Bells Corners test hole BC-81-2. Scale 0-50 000 x 10^{-5} SI units. (Logs offset for clarity).*

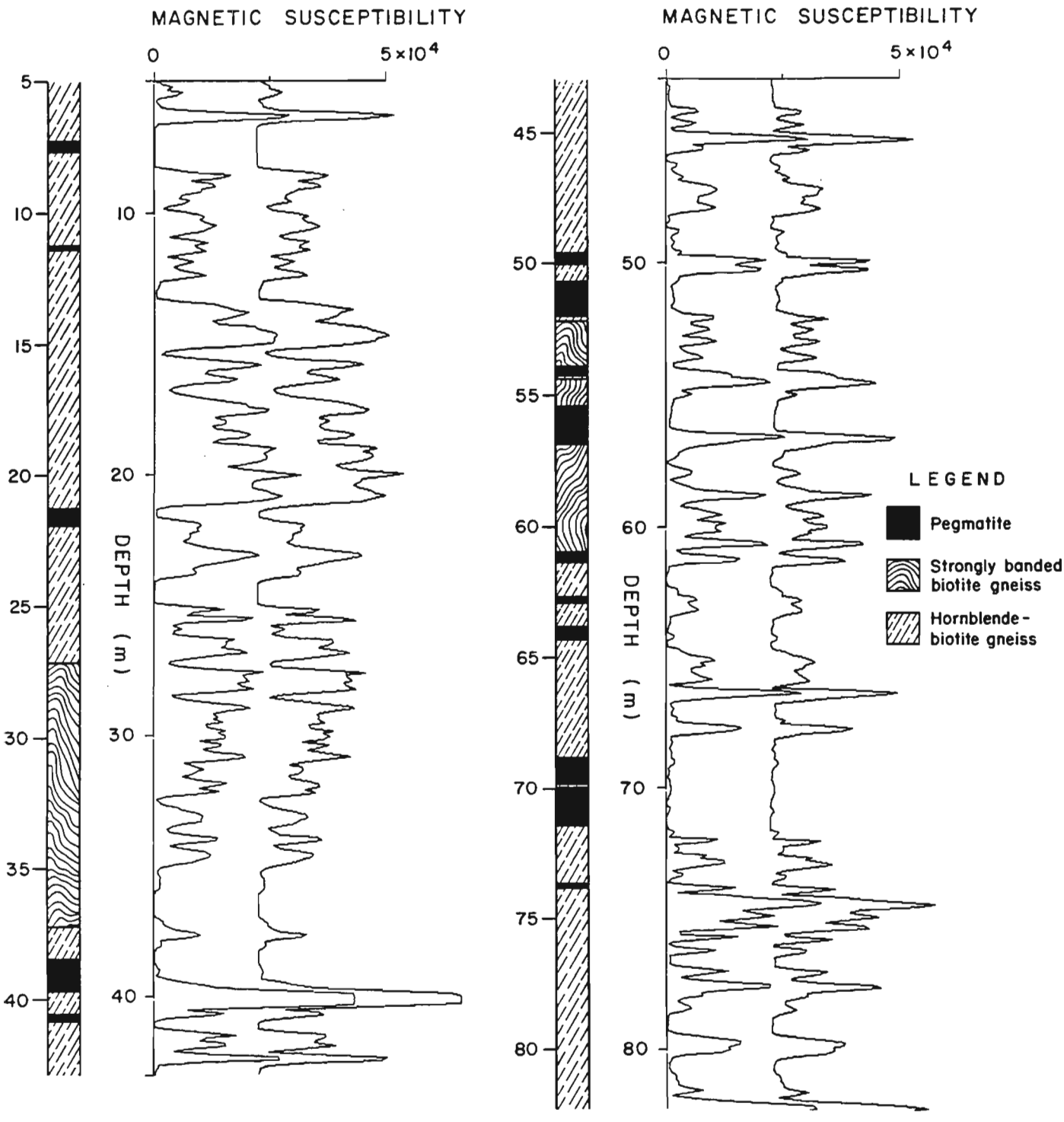

Figure 60.2. *Repeat logs in Bancroft hole No. BN-81-1. (Logs offset for clarity).*

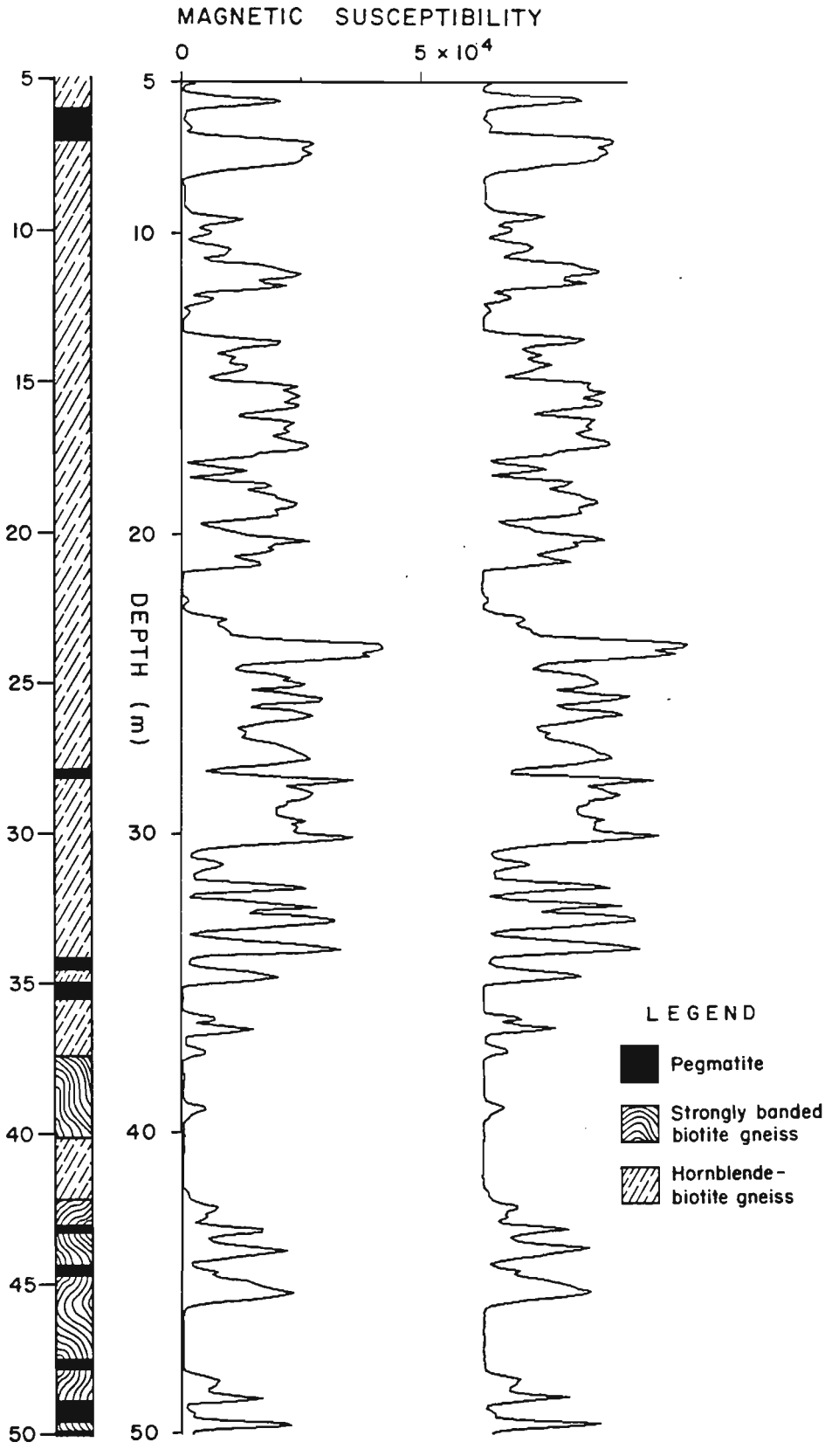

Figure 60.3. *Repeat logs in Bancroft hole No. BN-81-2. (Logs offset for clarity).*

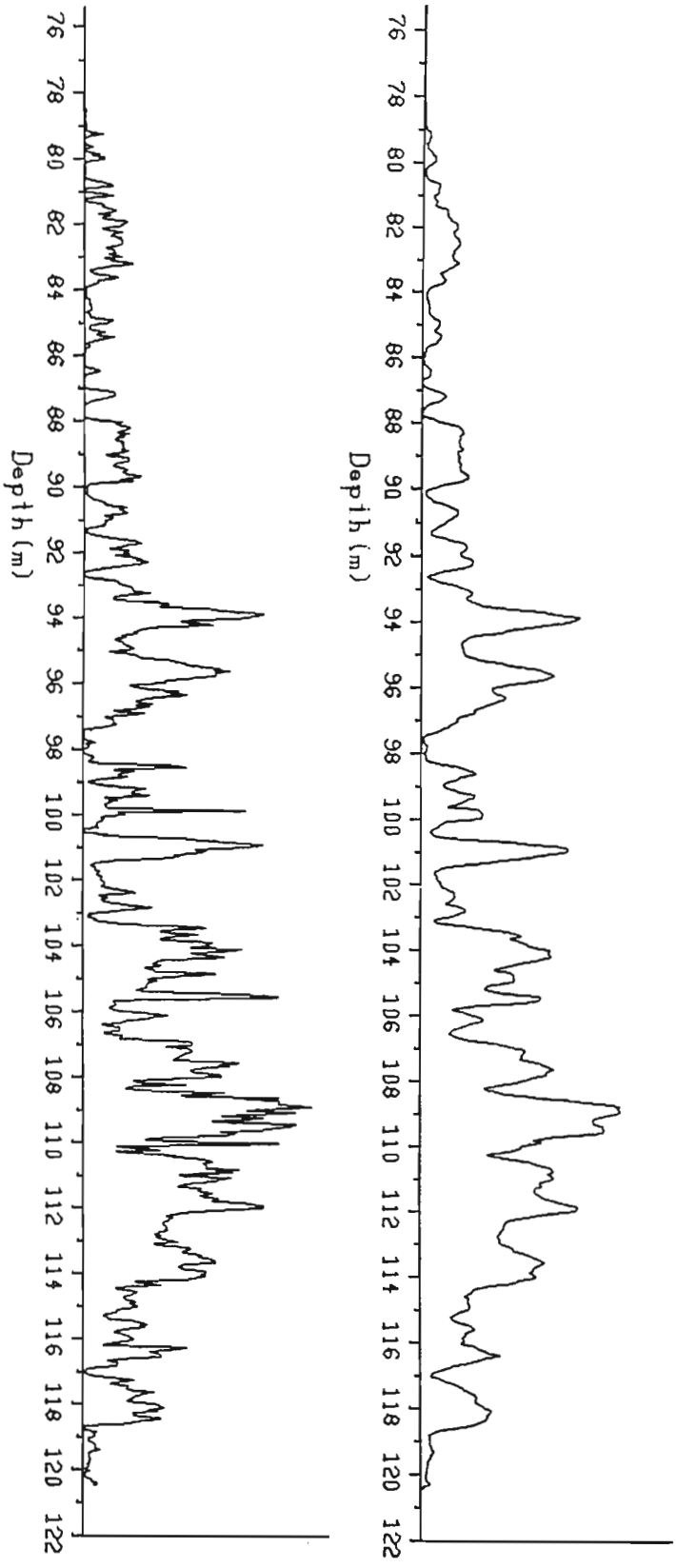

Figure 60.4. *A. Drill core magnetic susceptibility measurements on Precambrian segment of Bells Corners test hole as recorded. B. Measurements of Figure 60.4A after smoothing with 7 point running average filter.*

458

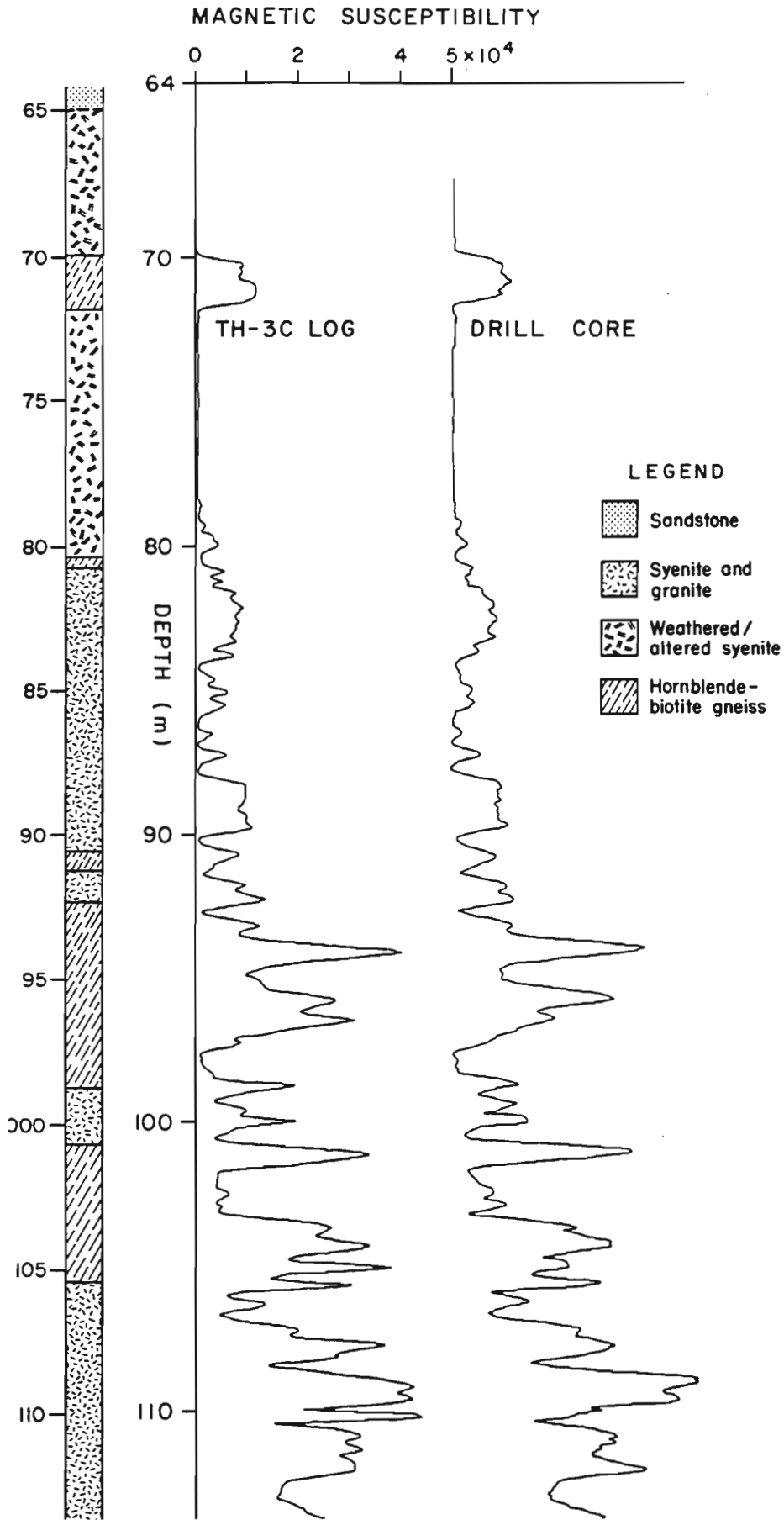

Figure 60.5. *Comparison of smoothed drill core log and TH-3C tool log for Precambrian segment of Bells Corners test hole BC-81-2 (logs offset for clarity).*

459

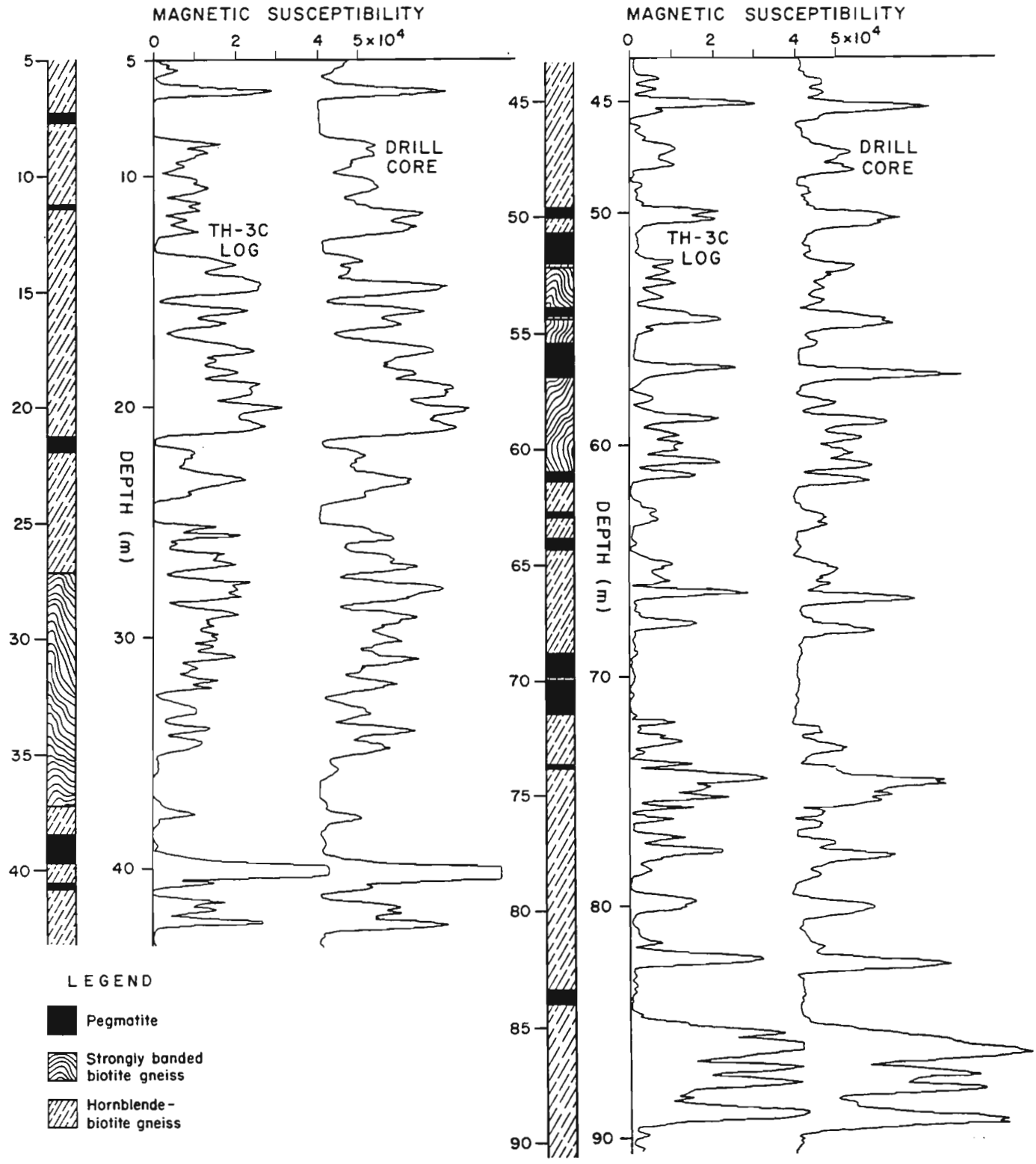

Figure 60.6. *Comparison of smoothed drill core log and TH-3C tool log for Bancroft hole No. BN-81-1.*

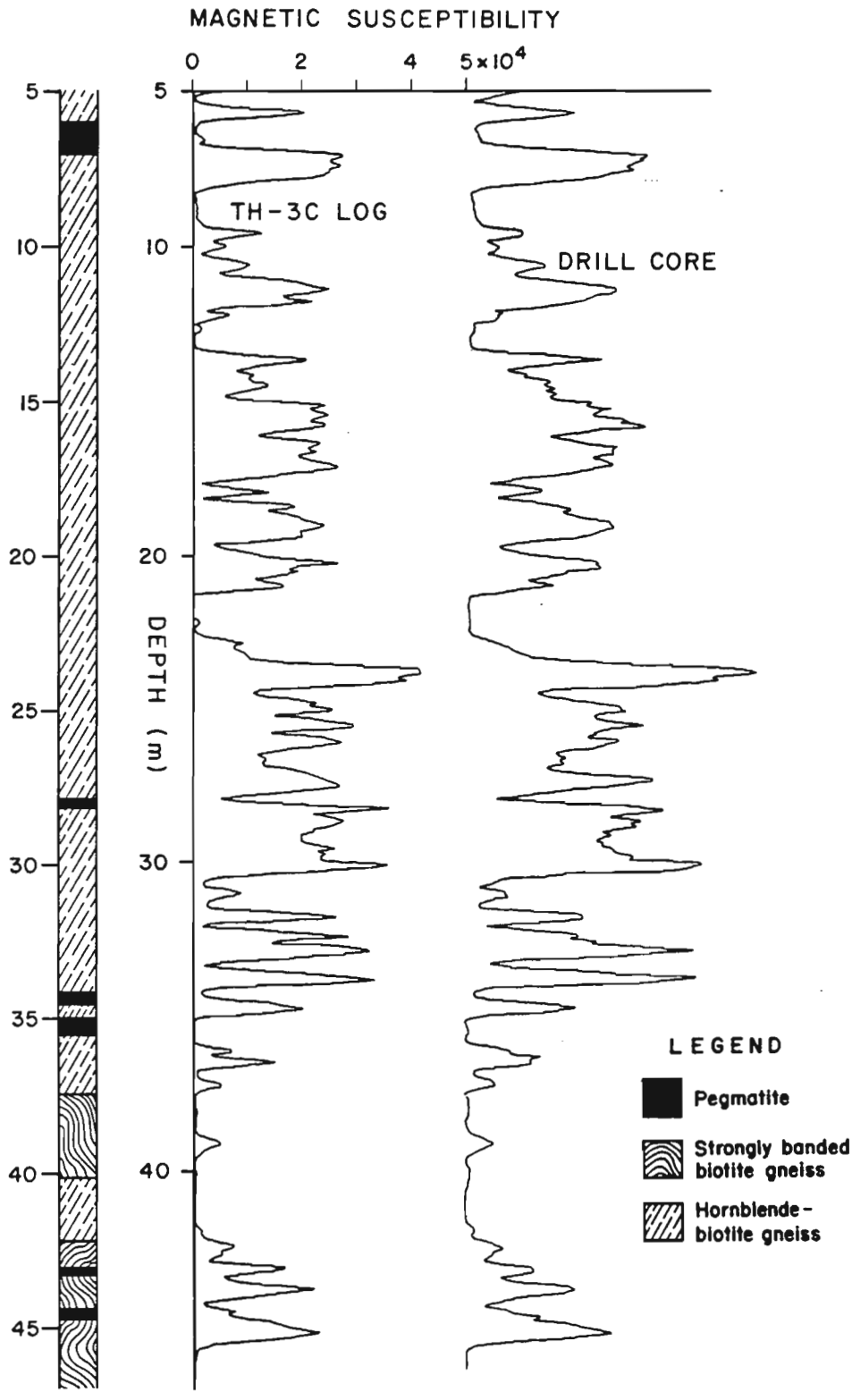

Figure 60.7. *Comparison of smoothed drill core log and TH-3C tool log for Bancroft hole No. BN-81-2.*

Figures 60.1 to 60.3 show the repeat logs obtained with the TH-3C tool in the three holes for which drill core measurements were available, (one at Bells Corners and two at Bancroft), together with the geological logs. The logs are plotted on a scale of 0-50 000 x10^{-5}SI units, with the repeat log offset by approximately 25 000 x 10^{-5}SI units for clarity in every case except Figure 60.1A. The pair of logs shown in Figure 60.1A are for the sedimentary sequence of the Bells Corners hole plotted on a scale of 0-400 x 10^{-5}SI units without offset. At the magnified scale which this represents it is evident that there is a displacement between the pair of approximately 100 x 10^{-5}SI units. This is almost certainly due to temperature dependent base-line drift, and is not considered problematical since the lithological detail is clearly reproducible at very low signal levels, confirming the 5 x 10^{-5}SI resolution capability given in the technical specifications. Excellent repeatability is apparent for all the other pairs of logs in Figures 60.1 to 60.3.

Magnetic susceptibility measurements on three drill cores had been made at 5 cm intervals. These measurements were made with a Scintrex model SM-5 magnetic susceptibility meter designed to measure on flat surfaces or drill core where geometry errors are small. Since the logging tool has a coil length of 50 cm compared with only 35 mm for the portable Scintrex instrument, it was felt that a better basis for comparison would be obtained if the core measurements were first smoothed using a seven-point running average filter, since this is in effect what the larger tool does to the real profile.

Figure 60.4 shows magnetic susceptibility measurements for the drill core from one of the holes as recorded compared with the same data after smoothing. Figures 60.5 to 60.7 show smoothed drill core measurements alongside the borehole logs for each of the three holes. The close agreement between the two in all cases provides convincing evidence that the logging tool accurately reflects the core measurements.

The relative amplitudes of the various peaks do not always correspond exactly between the pairs of logs. This is not surprising since the volume of material used for the drill core measurement represents only a small fraction of the volume sampled by the logging tool. Thus correlation of relative amplitudes at any point is an indication that the material is reasonably homogeneous in the vicinity of the borehole at that point.

CONCLUSION

The Geo Instruments TH-3C magnetic susceptibility logging tool showed excellent repeatability as evidenced by the data presented in Figures 60.1 to 60.3, and by similar data from two other holes. The validity of the measurements has been verified by the agreement between these logs and the independent measurements made on drill core from the holes.

The equipment as supplied is self contained and, interfacing to almost any logging system, either analogue or digital, is relatively simple. The principle of operation, using a Maxwell bridge circuit, calls for very close tolerances on the allowable inductance changes in the sensing coil due to changes in pressure and temperature which cause base-line drift in the signal level. These effects appear to have been minimized by careful mechanical and electrical design and allow excellent results to be achieved even in sedimentary strata where normal magnetic susceptibility levels are below the threshold of most hand held instruments. Even so, step changes in temperature of the tool should be avoided whenever possible. For example the initial step as the tool enters the borehole fluid should be avoided by allowing time for thermal equilibrium to be reached before logging is started.

Equipment of this type should find ready application in a number of fields of endeavour where borehole logging techniques are used to gather data.

ACKNOWLEDGMENTS

The authors wish to express their appreciation to Mikko Hamalainen of the Geo Instruments Company for his cooperation in making the tool available for these experiments, and to Bill Hyatt, Yves Blanchard and Jacques Parker for making modifications to the GSC logging system and conducting the logging operation.

REFERENCES

Bernius, G.R.
1981: Boreholes near Ottawa for the development and testing of borehole logging equipment – a preliminary report; in Current Research, Part C, Geological Survey of Canada, Paper 81-1C, p. 51-53.

Bristow, Q.
1979: NOVA-based airborne and vehicle mounted systems for real-time acquisition, display and recording of geophysical data; in Proceedings of Data General Corp. Users Group Conference, New Orleans, Dec. 1979.

Ellis, J.R., Austin, S.R., and Droullard, R.F.
1968: Magnetic susceptibility and geochemical relationships as uranium prospecting guides; USAEC, AEC-RI (1968) 21.

George, D.C. and Scott, J.H.
1982: Review of magnetic susceptibility logging and its application to uranium exploration; in Proceedings of Uranim Exploration Methods Symposium, OECD/IAEA, Paris, June 1982.

Scott, J.H. and Daniels, J.J.
1976: Non-radiometric borehole geophysical detection of geochemical haloes surrounding sedimentary uranium deposits; in Symposium on Exploration for Uranium Ore Deposits. IAEA/SM/208-16 Vienna 1976, p. 379-390.

Telford, W.M., Geldart, L.P., Sherriff, R.E., and Keys, D.A.
1976: Applied Geophysics; Cambridge University Press.

TEMPERATURE LOGGING IN MINERAL EXPLORATION

C.J. Mwenifumbo[1]

C.J. Mwenifumbo, Temperature Logging in Mineral Exploration; in Proceedings of the 4th International MGLS/KEGS Symposium on Borehole Geophysics for Minerals, Geotechnical and Groundwater Applications; Toronto, 18-22 August 1991

Abstract

Although a number of parameters affect the temperature-depth profile in a borehole, temperature measurements have been successfully used to detect and map fracture zones with moving water, massive sulphide mineralization and have been used to map lithology. In drill holes without water flow, the temperature gradient logs have been be used to map lithology where significant thermal conductivity contrasts exist between different materials. Because of the high thermal conductivity of massive sulphides, temperature measurements show significant anomalies near or within mineralized zones and were successfully used to locate sulphide occurrences. Although temperature measurements may not replace conventional electrical methods in exploration for most massive sulphide deposits, non-conducting and non-polarizable sulphides, such as sphalerite, may be explored for with temperature methods. Electrochemical reactions within massive sulphide deposits may generate sufficient heat to be detected on the temperature-depth profile. Their detection provides information to aid in interpreting self potentials within massive sulphide deposits. Field examples of four types of applications of temperature measurements in mineral exploration are presented; 1) lithological mapping, 2) fracture detection, 3) direct detection of massive sulphides, 4) use in correcting and interpreting other geophysical logs.

INTRODUCTION

Temperature logging is a useful method in mapping lithology, correlating stratigraphy (Beck, 1976; Conaway and Beck, 1977; Blackwell and Steele, 1987) and in mapping coal seams (Kayal, 1981; Kayal and Christoffel, 1982; Mwenifumbo, 1989). It has not been used to study problems in mineral exploration. Base metal sulphides should make excellent targets because of their high thermal conductivities compared to the host rocks (Figure 1). The lack of use of temperature logging in mineral exploration is due mainly to two reasons; 1) traditional electrical methods are quite effective, and 2) the effects of drilling fluid circulation and groundwater flow on the temperature-depth profile make interpretation difficult.

Although temperature measurements may not replace conventional electrical methods in exploration for most massive sulphide deposits, non-conducting and non-polarizable sulphides such as sphalerite may be explored with temperature methods. Sphalerite is thermally more conductive than any of the base metal sulphides (20-30 w/m/°C, average =26.6, Parasnis, 1974). The principle use of temperature logging would be to detect and map sphalerite-rich ore zones with a high thermal conductivity in the presence of poor thermal conductivity host rocks. Temperature measurements may also be used to map oxidation and reduction reactions occurring within massive sulphide deposits that often generate large self potential anomalies. Fractures and fault zones are the major conduits for groundwater flow and because most mineral deposits are highly fractured and associated with major fault zones, temperature logs may indirectly be used to map mineral deposits.

Temperature measurements are routinely carried out by the Borehole geophysics section of the Geological Survey of Canada (GSC). This paper documents temperature measurements made at a number of mineral deposits in Canada. The use of these logs as an aid in mineral exploration and development is examined.

[1]Geological Survey of Canada, 601 Booth Street, Ottawa, Ontario, K1A 0E8

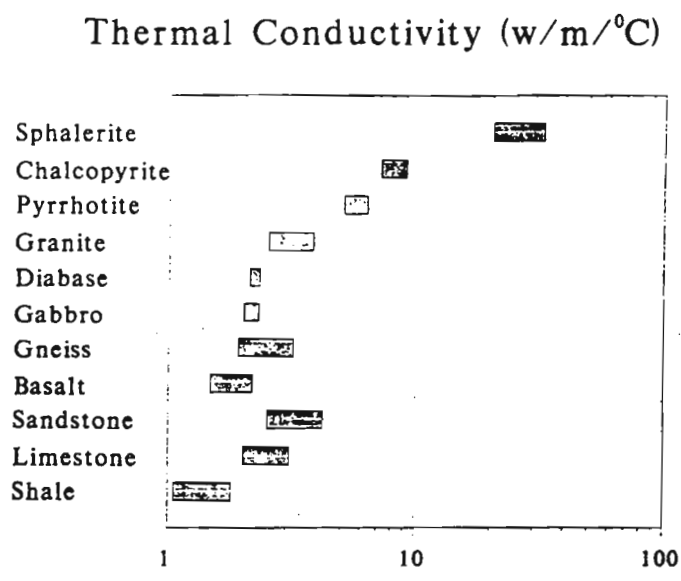

Figure 1: Thermal conductivities of some major rock types and sulphide minerals.

LOGGING EQUIPMENT

Details of the GSC high resolution temperature logging system are given in Bristow and Conaway (1984); the following is a brief description of the system. The temperature probe consists of a 10 cm long tip of thermistor beads with a 1 second time constant and a temperature sensitivity of 0.1 mK. This precision and short thermal time constant are required for continuous, high precision temperature measurements. The probe is connected to a 1 km cable and to a minicomputer-based data acquisition system in the logging truck. The thermistor signal is converted to frequency in the probe and data is transmitted digitally uphole. The digital transmission of the data eliminates problems inherent in signal transmission through long cables (conductor cable resistance, insulation leakage resistance and capacitive and/or inductive pickup in the logging cable (Beck, 1982; Bristow and Conaway, 1984)). Depths can be measured with an accuracy of 1 mm by an optical shaft encoder located on the wellhead pulley assembly. All temperature measurements are continuously recorded on a downhole run at logging speeds of 3 or 6 m/minute with data sampled approximately every 1.5 or 3 cm, respectively. This high spatial resolution of data is necessary for determining accurate gradients with the use of gradient operators. Changes in temperature are recorded as changes in thermistor resistance which are then converted into true temperatures. The deconvolution technique developed by Costain (1970) and Conaway (1977) is used to process and remove the effects of the probe time constant from the continuous measurements. The Savitzky-Golay derivative operator (Madden, 1978) is used to compute the gradients from the temperature data. Units of temperature gradient are given in SI as mK/m in all the following presentations. These units are numerically equal to the cgs system (°C/km).

FIELD PROCEDURE

Logging procedures for optimum, high-resolution borehole temperature measurements have been discussed in a number of papers (Conaway, 1987; Blackwell and Steele, 1987). Most of these procedures were followed during the acquisition of temperature logs presented in this paper. Temperature logs were always the first logs run on a given day and were acquired during a downhole run rather than an uphole run so that the thermal sensor was entering undisturbed water. In a number of cases, repeat runs were recorded after one or several days to allow the borehole water to stabilize from disturbances caused by logging.

In cases where repeat logging runs on following days may not be possible due to poor hole conditions, it is worthwhile recording another log after half an hour or later. An uphole log may also be made. These repeat logs may provide invaluable data for checking the repeatability of temperatures and increase confidence in interpreting any of the observed temperature anomalies. It is, however, not necessary to perform this type of logging if hole conditions are good and there are no time constraints such as those often imposed on logging when instruments are to be installed in the borehole. The following examples illustrate the type of data to be expected when repeat logging runs are made in large and small diameter holes soon after the first downhole run.

Figure 2 shows the reproducibility of temperature data recorded during downhole and uphole runs. Three logs are superimposed: one downhole log, an uphole log recorded immediately after completion of the downhole run and a downhole log recorded 30 minutes later. These logs were made

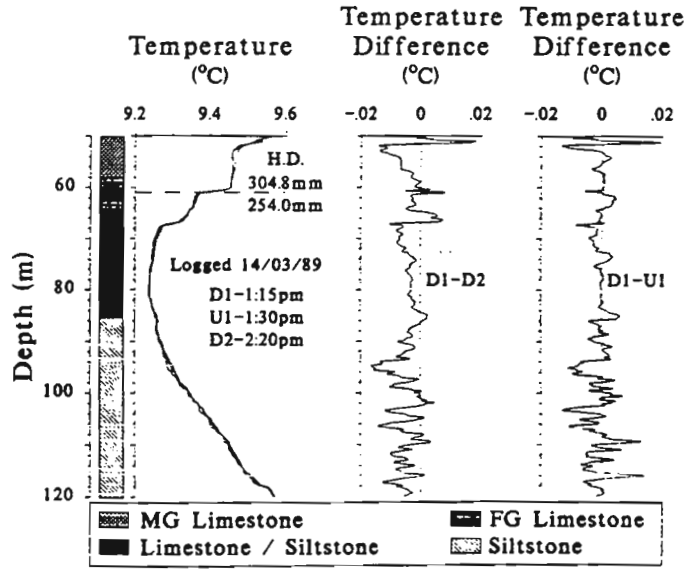

Figure 2: Comparison between temperature data recorded during downhole (D1 & D2) and uphole (U1) runs in a large diameter open hole (304.8 mm from 0-61 m and 254.0 mm from 61 to the bottom) at Carleton University, Ottawa. H.D.- hole diameter; MG - medium grained; FG - fine grained

in a large diameter open hole (304.8 mm hole diameter from surface to 61 m, and 254.0 mm in diameter to the bottom). The temperature-depth profiles indicate step-like changes in temperature at approximately 52, 61 and 66 m, suggesting the entry or exit of groundwater in the borehole. The change in temperature at 61 m coincides with a change in the borehole diameter. Some water may be exiting at this point but the temperature change is probably due to water flowing past a change in hole diameter. The nearly isothermal temperatures between 52 and 61 m suggests that the flow rate is fairly high. The temperature differences between the first downhole and uphole logs, and between the first downhole and last downhole log (Figure 2) indicate good agreement between the logs. Differences in temperatures are of the order of 0.02 °C, which are far less than those reported by Reiter et al., (1980). This is to be expected, since water is flowing in the borehole. Reiter et al., 1980, reported temperature differences of the order of 0.4 to 1 °C. These differences are in the range of the temperature variations observed within this depth interval of the hole and would not be acceptable. The large differences between downhole and uphole runs observed by Reiter et al., 1980, can be attributed to different logging speeds (7.6 m/minute for the downhole run and 30.5 m/minute for the uphole run) and may also be due to depth offsets between runs. Their temperature data were acquired at very coarse sample depth intervals of 1.52 m.

Figure 3 is another comparison between downhole and uphole temperature logs recorded in a smaller diameter open, NQ-hole (75.7 mm) at the Bells Corners Geophysical test site, Ottawa, Canada. The hole penetrates sandstone, weathered and then fresh bedrock which consists of gneiss and granite. The

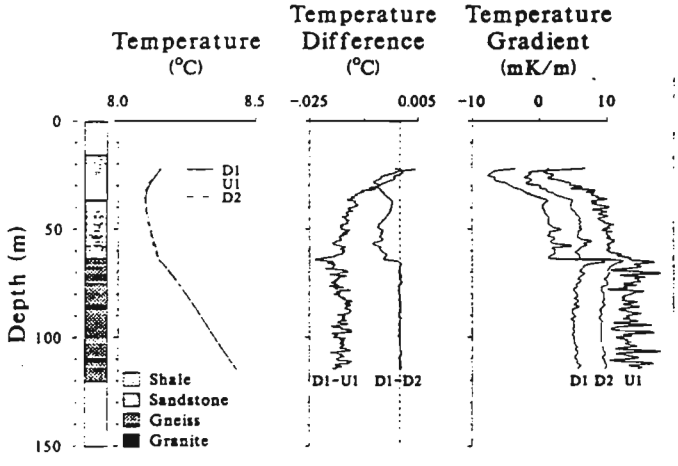

Figure 3: A comparison between downhole (D1 & D2) and uphole (U1) temperature logs recorded in an NQ-hole (75.7 mm) at the GSC Bells Corners Geophysical Test Site, Ottawa. The two downhole logs recorded on separate days (89.05.23 and 89.05.31) show temperature differences in the sandstone that are due to the influence of surface drainage. The temperature gradient logs are offset by 2.5 mK/m for clarity.

two downhole logs were recorded on different days (89.05.23 and 89.05.31). Temperatures recorded during the uphole run immediately after completing the first downhole run, show high frequency fluctuations which are higher than those recorded during downhole logging. Higher temperatures recorded during uphole logging are to be expected and are probably due to the warming effects of the logging cable and the probe assembly (Reiter et al., 1980). The average temperature differences between the downhole and uphole logs below the temperature minimum (zero-gradient point at approximately 35 m) is 0.016 °C. Despite these temperature differences, the uphole temperature log shows major changes in temperatures at the same depths as those recorded during the downhole log, thus providing a check on data reliability.

There is good agreement between the two downhole logs except for the section within the sandstone formation where significant differences are observed. The second temperature log was taken two days after heavy rainfall and the differences in temperature may reflect groundwater flow induced by surface drainage. The borehole fluid temperatures seem to be more stable with time in the granites and gneisses. The temperature gradient logs (Figure 3c) are plotted with an offset of 2.5 mK/m for clarity. A significant temperature gradient change at 65 m reflects a change in thermal conductivity between the sandstone and granite/gneiss. The basement rocks have higher temperature gradients (lower thermal conductivities) than the sandstone. Box-and-whiskers plots (Wilkinson, 1990; Velleman and Hoaglin, 1981) and summary statistics shown in Figure 4 compare the temperature gradient data in the sandstone and granite/gneiss precambrian rocks from the three logging runs. There is very little variability in the temperature gradients in the granite/gneiss for the two downhole runs. The uphole run, however, shows a spread in gradients three times greater than that of the downhole runs. This is mainly due to the fluid disturbances during the uphole logging run. It is interesting to note, however, that the mean temperature values are approximately the same for all the three runs.

TEMPERATURE LOGGING IMMEDIATELY AFTER DRILLING

Borehole logging is usually done immediately after drilling, especially in poorly consolidated sedimentary formations where boreholes are unstable. Temperature profiles recorded immediately after drilling are significantly affected by the drilling fluid circulation. The thermal effects of drilling fluid circulation have been dealt with in a number of papers (Jaeger, 1961: Lachenbruch and Brewer, 1959; Drury and Jessop, 1982; and Mwenifumbo, 1989). Although the use of temperature data acquired immediately after drilling is not recommended because the borehole fluid temperatures are not in thermal equilibrium with the formation temperatures, there have been a number of discussions on how to estimate the true formation temperatures from these data (Leblanc et al, 1982; Lee, 1982; Middleton, 1979; Luheshi, 1983). The temperature-depth profile in this case is dependent on a number of parameters

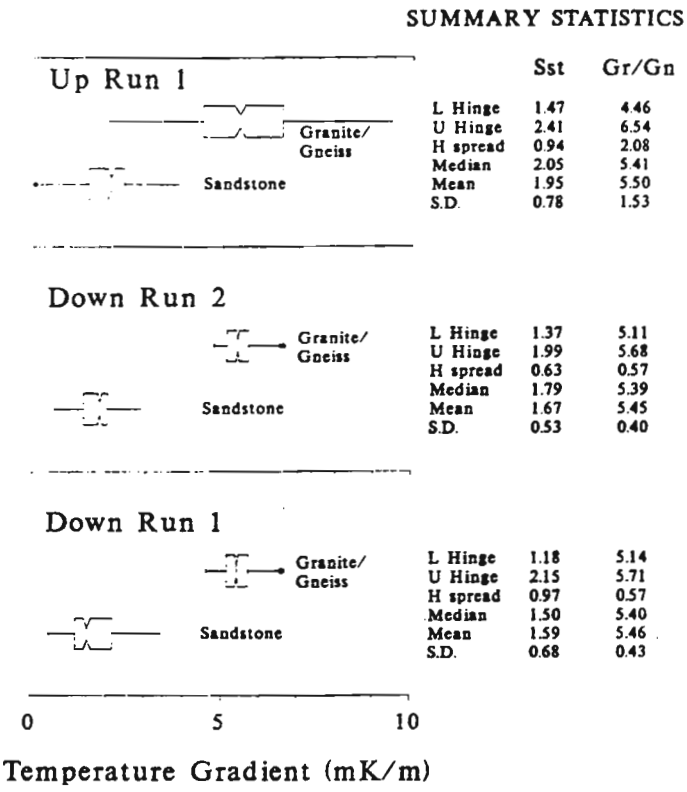

*Figure 4: Box-and-whiskers plots and summary statistics of the data presented in Figure 3 comparing the three sets of temperature gradient data within the sandstone and PreCambrian granite/gneiss rocks. The notched boxes are bounded by the 25th (lower hinge) and 75th (upper hinge) percentiles, i.e. 50 % of the data within each subset have values in the box. The notches locate the median (50th percentile) and its 95 % confidence bounds. The whiskers (lines drawn from the lower and upper hinges), are defined as:- (lower hinge - 1.5*H-spread) and (upper hinge + 1.5*H-spread), where H-spread is the hinge difference.*

including initial drilling fluid temperatures, drilling fluid circulation times, borehole diameter, type of drilling (diamond or rotary drilling) and thermal conductivity of the lithology intersected (Luheshi, 1983).

Disturbances in temperature due to drilling fluid circulation may provide valuable information on the location of fractures and permeable zones (Drury and Jessop, 1982) and variations in thermal resistivities of the formations (Mwenifumbo, 1989). Figure 5 shows temperature and temperature gradient logs recorded immediately after drilling in a 75.7 mm diameter hole at a massive sulphide deposit in British Columbia, Canada. The hole collapsed after this downhole logging run. High temperature anomalies between 120 and 160 m, and between 380 and 390 m are probably due to permeable fracture zones that accepted warmer drilling fluids. These anomalies should decay with time as the borehole fluid temperatures come to equilibrium with the formation temperatures (Killeen, 1986,

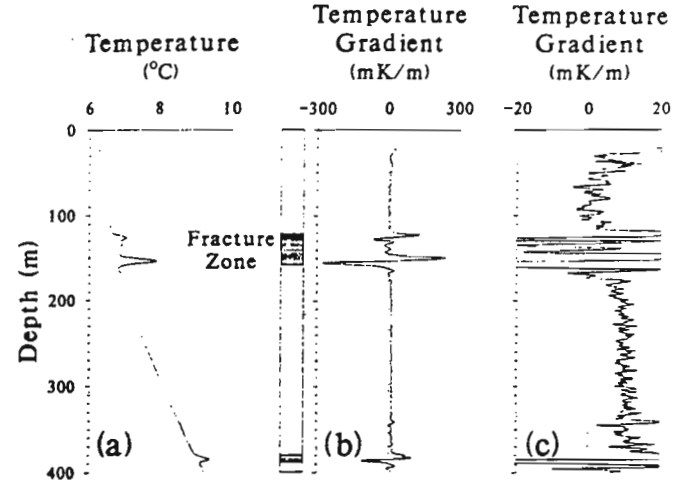

Figure 5: Temperature and temperature gradient logs recorded immediately after drilling in an NQ-hole (75.7 mm in diameter) at a massive sulphide deposit in British Columbia, Canada showing anomalous transient temperatures that are caused by warmer drilling fluids that infiltrated permeable fracture zones . These anomalies decay with time as the borehole fluid temperatures come to equilibrium with the formation temperatures.

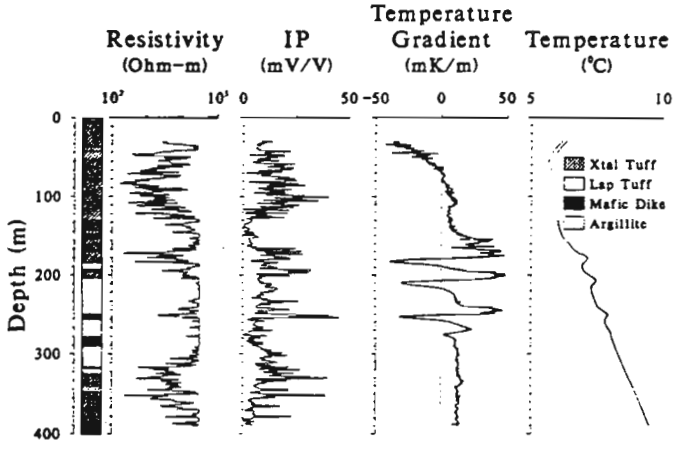

Figure 6: Resistivity, IP, temperature gradient and temperature logs recorded in an NQ-hole at the S5 massive sulphide deposit, New Brunswick. The hole was logged 17 days after drilling and the effects of drilling fluid circulation on the temperature-depth profile are clearly indicated. Two repeat temperature logs are shown. The resistivity and IP logs show zones with sulphide mineralization.

Drury and Jessop, 1982). There is an indication of a change in lithology at approximately 160 m. The temperature gradient above the anomaly is lower (approximately 2.0 mK/m) than that below (approximately 10.0 mK/m) suggesting that this wide anomaly between 120 and 160 m may be associated with fractures along a contact.

Figure 6 shows another example of the effects of drilling fluid circulation on the temperature-depth profile. This NQ-hole ST341 was drilled at the Stratmat massive sulphide deposit, New Brunswick. Drilling started on June 19, 1989 and was completed on July 5, 1989. The hole was temperature logged on July 22, 1989; 17 days after drilling completion. The hole intersects lapilli and felsic volcanic tuffs with disseminated sulphides. The three prominent temperature anomalies are caused by drilling fluid circulation and appear to be associated with fractured and permeable zones (see resistivity log). It is interesting to note that not all the low resistivity and high IP zones exhibit these elevated temperature anomalies. Only those zones that are permeable and able to accept drilling fluids during drilling produce these transient, heat-source-type anomalies. Logging in mineral exploration holes is often done months or more after drilling. Transient temperature anomalies due to drilling fluid circulation are at that time generally insignificant depending on the amount of heat initially transfered to the fracture system.

MAPPING LITHOLOGY

In a borehole without flowing water, temperature logs may be used in mapping lithology provided there is a significant contrast in thermal conductivity between the different lithological units. As illustrated in Figure 3, changes in thermal conductivity between the sandstone and granite/gneiss are clearly indicated on the temperature gradient logs. Figure 7 shows temperature and temperature gradient logs recorded in a coal hole in Alberta, Canada. The log shows subtle changes in slope resulting from changes in thermal conductivity between coal and mudstone. These features are barely visible but are enhanced in the temperature gradient log, making the individual coal seams clearly visible. Figure 8 shows box-and-whiskers plots and summary statistics of the temperature gradients in sedimentary rocks and coal seams. The H-spread for sedimentary rocks is quite large because these rocks are a mixture of siltstone, mudstone and bentonitic mudstone. Their distribution may well be multimodal. The boxes of the sedimentary rocks and coal are well separated indicating that these two types of lithology can be easily differentiated by using temperature gradients.

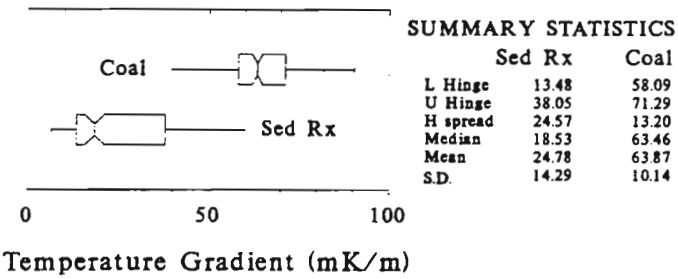

Figure 8: Box-and-whiskers plots and summary statistics of the temperature gradient data from Highvale coal mine presented in Figure 7 showing the distribution of temperature gradients in the sedimentary rocks and coal seams. The sedimentary rocks are mudstone, siltstone and bentonitic mudstone.

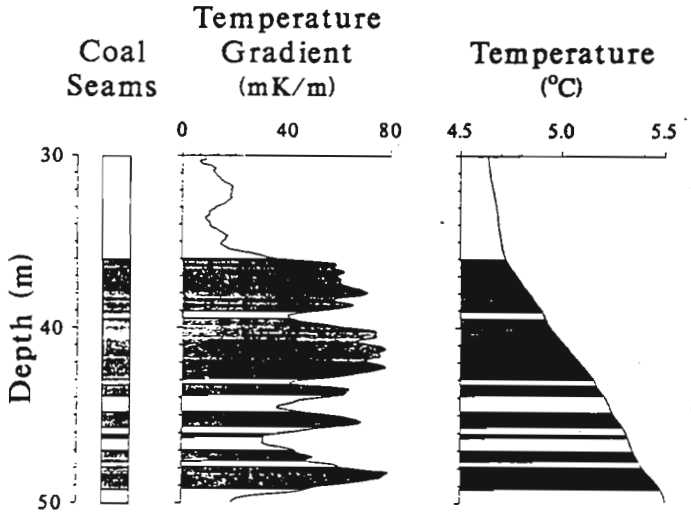

Figure 7: Temperature and temperature gradient logs recorded in a hole at the Highvale coal mine, Alberta, Canada. Coal seams are shaded on both of the logs. The temperature log shows subtle changes in slope resulting from changes in thermal conductivity between coal and mudstone. These barely visible features are greatly enhanced in the temperature gradient log.

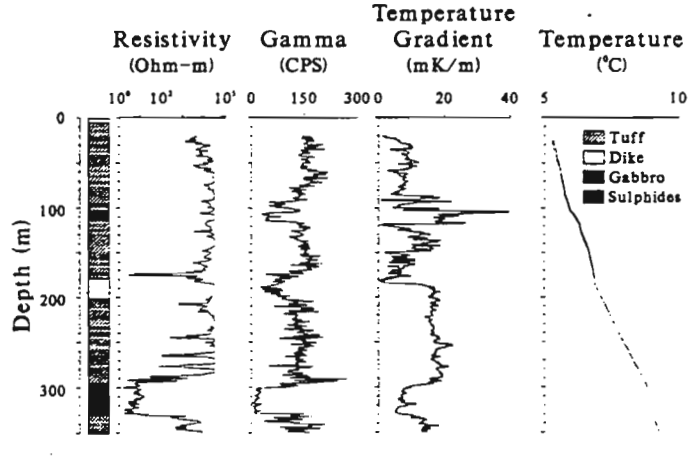

Figure 9: Resistivity, total count gamma ray, temperature gradient and temperature logs recorded in hole ST330 at the Stratmat Main Zone massive sulphide deposit, New Brunswick. Temperature logging was done 4 months after drilling when drilling induced temperature variations had almost completely disappeared. Two repeat temperature and temperature gradient logs are presented. The resistivity log locates massive sulphides but fails to distinguish between the different lithological units. There is, however, an excellent correlation between lithology, gamma ray and temperature logs.

Figure 9 shows resistivity, total count gamma ray, temperature gradient and temperature logs hole ST330 at the Stratmat massive sulphide deposit in New Brunswick, Canada. Drilling of this hole began on March 13 and was completed on March 22, 1989. Temperature logs were done on July 22, 1989; approximately 4 months drilling. Drilling induced temperature variations appear to be insignificant by this time. The hole intersects tuffs, mafic dikes, gabbro and massive sulphides. The resistivity log clearly locates massive sulphides but fails to discriminate between the different lithological units. There is, however, an excellent correlation between lithology, gamma ray and temperature data. Box-and-whiskers plots for the gamma ray and temperature gradient data are shown in Figure 10 to illustrate the distribution of these parameters for the four different rock types and sulphide occurrences. The summary statistics are given in Table 1.

Table 1: SUMMARY STATISTICS

	Lapilli Tuff	Sulphides	Felsic Tuff	Dike	Gabbro
Natural Gamma Ray (cps)					
Lower Hinge	137.80	8.65	122.05	66.01	40.52
Upper Hinge	163.33	19.00	151.33	87.60	50.31
Hinge Spread	25.53	10.35	29.28	21.59	9.79
Median	150.53	13.83	134.41	78.03	44.06
Mean	150.66	14.21	135.64	75.88	44.06
Standard Dev.	19.66	6.45	22.71	17.72	7.41
Temperature Gradient (mK/m)					
Lower Hinge	5.82	6.07	15.91	7.75	18.31
Upper Hinge	7.81	7.93	17.96	16.89	20.27
Hinge Spread	1.99	1.86	2.05	9.14	1.96
Median	9.69	7.18	16.76	15.47	18.76
Mean	7.79	7.12	16.82	12.79	19.41
Standard Dev.	3.11	1.25	1.62	5.42	1.76

The gamma ray data show overlapping boxes for the two different tuffs, which suggests that their population medians are not that different. However, in the temperature gradient data, the intervals between the Lapilli and Felsic tuffs are well separated indicating that the two population medians are significantly different and that the tuffs can be distinguished easily from each other based on the temperature gradient data. The gamma and temperature data are crossplotted in Figure 11 together with their probability density distribution. The data show clear clusters corresponding to all lithological units except dikes. The wide range of the temperature gradient data from the dike population is probably because fracturing. The dikes are also sometimes interbedded with argillite.

LOCATION OF GROUNDWATER FLOW

Water flow in boreholes is often considered a source of noise in temperature logging, obscuring features of interest such as thermal conductivity variations related to lithology or mineralization. Understanding groundwater flow near an ore deposit may, however, provide useful information to aid in mining operations. Most mineralized zones are highly altered and fractured and may provide pathways for groundwater flow. Knowing the precise location of water entry or exit zones is essential because most of these zones need to be plugged before the onset of mining operations. Otherwise there may be flooding and contamination of the groundwater system around the mine.

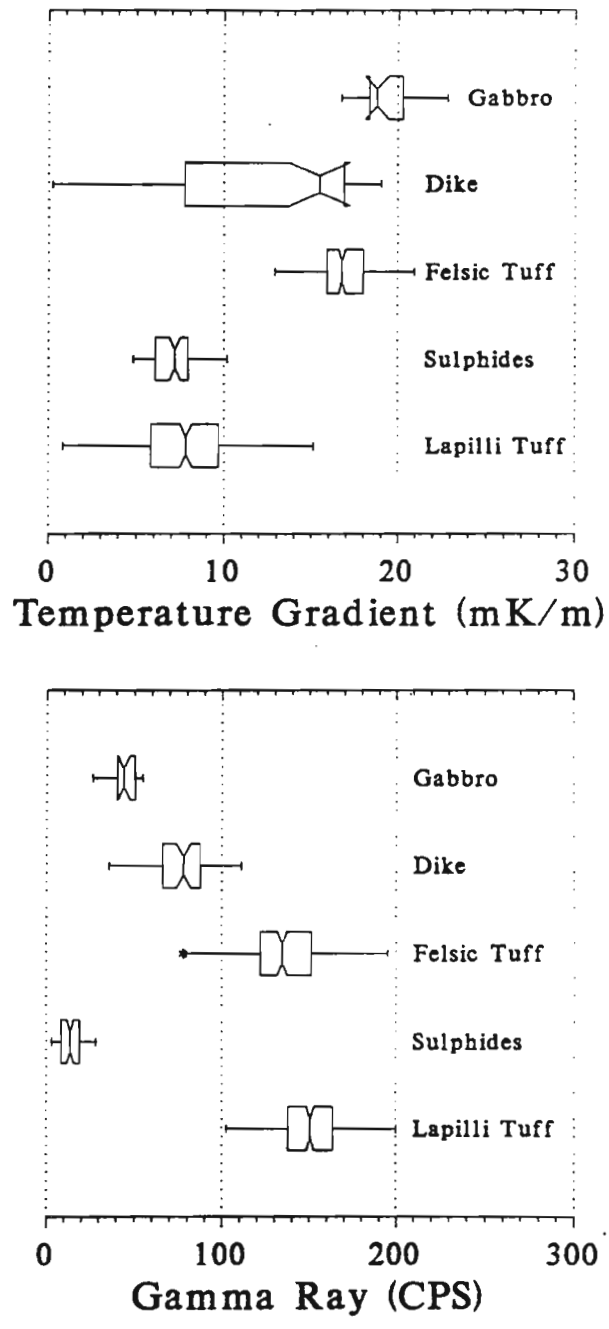

Figure 10: Box-and-whiskers plots for the gamma ray and temperature gradient data shown in Figure 9 illustrating the distribution of these parameters for the different rock types and sulphide mineralization. The boxes for the felsic and lapilli tuffs are were isolated in the temperature gradient data but overlap in the gamma ray data indicating that these two tuffs can be characterized by their temperature gradients and not by their gamma ray activity.

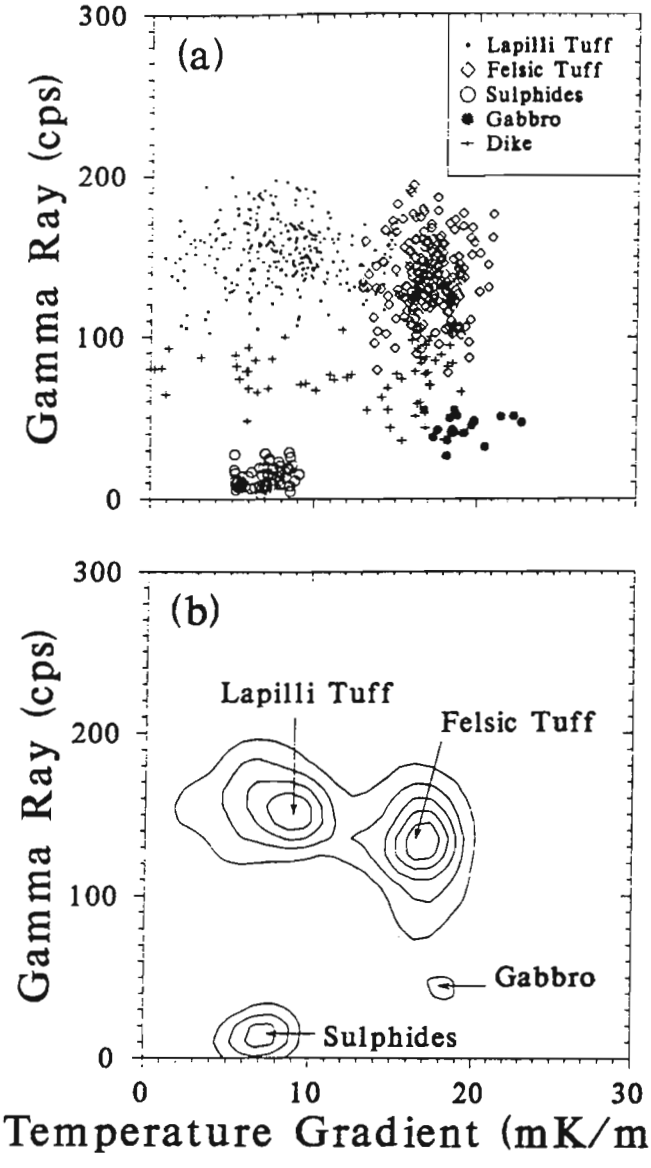

Figure 11: Crossplot of gamma ray versus temperature gradient data grouped into subsets according to lithology (Figure 11a) and a contour diagram of the kernel density estimate for the bivariate distribution of the data (Figure 11b). The data show clear clusters corresponding to all lithological units.

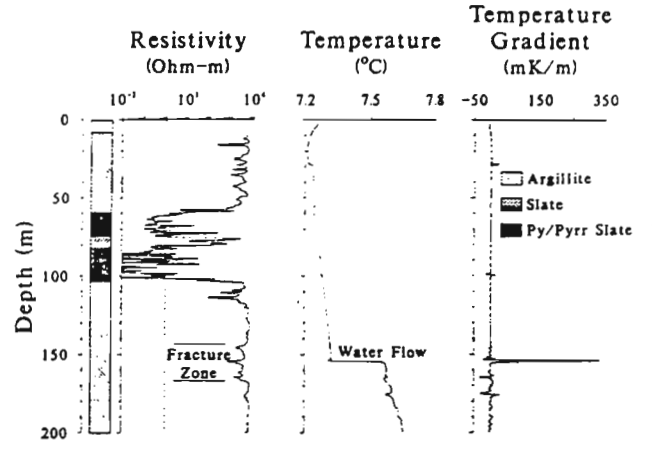

Figure 12: Resistivity, temperature and temperature gradient logs recorded at the Lake Charlotte Manganese prospect, Nova Scotia. The borehole intersects calcareous banded argillite, slate and mineralized (manganese, pyrite and pyrrhotite) carbonaceous slate. An abrupt change in temperature of about 0.26 °C at 150 m is characteristic of groundwater flow and coincides with fractured, low resistivity calcareous banded argillite between 140 and 170 m. Water is flowing uphole at fairly high rates obscuring the response from the highly conductive mineralized slates. Although this temperature data does not provide information on the mineralization, the location of the water entry and exit points are useful for hydrogeological studies.

Figure 12 shows resistivity, temperature and temperature gradient logs recorded in hole LC86-1 at the Lake Charlotte Manganese prospect, Nova Scotia, Canada. Hole LC86-1 intersects calcareous banded argillite, slate and carbonaceous slate with sulphide mineralization. Manganese mineralization occurs in the calcareous banded argillites above and below the Carbonaceous slates. Sulphides in the slates consist of pyrite and pyrrhotite and are indicated on the electrical resistivity log as very low resistivity zones. The temperature profile shows an abrupt change in temperature at about 154 m (from 7.31 to 7.57 °C, a change of 0.26 °C). This temperature anomaly is characteristic of groundwater flow and coincides with fractured, low resistivity calcareous banded argillite between 140 and 170 m. Cooler water is flowing downhole and exiting at approximately 154 m. The effects of the conductive mineralized slates on the temperature profile is obscured by water flow, although the slight change in temperature in the upper portion of the mineralized zone (between 55 and 65 m) may be related to the presence of the mineralization. Although this temperature data does not provide information on the mineralization, the location of these water entry and exit points provide useful hydrogeological information.

Fracture or permeable zones that provided pathways for the movement of mineralizing fluid may still provide pathways for groundwater flow if they are not completely cemented. Their detection may, therefore, provide useful information on the original structural constraints of the mineral deposit. Figure 13 shows groundwater flow zones indicated by abrupt changes in temperature and large temperature gradients that coincide with mineralized zones (see IP log). This suggests that the mineralized zones are more brittle and prone to fracturing and hence act as water conduits. These present water migration paths may also represent original mineralizing fluid flow paths. These temperature logs were recorded at the Yava sandstone-hosted lead deposit, Nova Scotia, Canada.

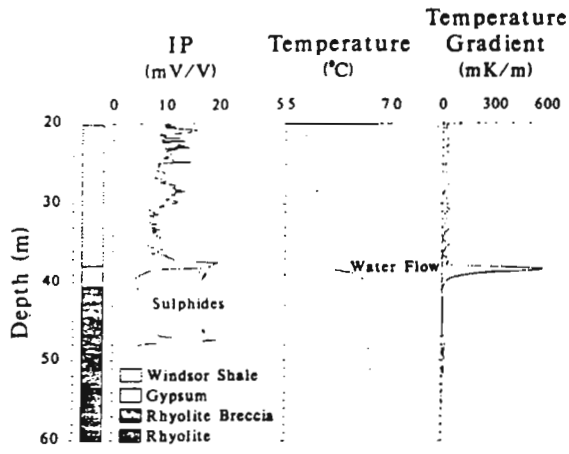

Figure 13: IP, temperature and temperature gradient logs for hole YA412 at the Yava sandstone lead deposit, Nova Scotia. The IP anomalies at approximately 38 and 47 m correlate fairly well with the water entry zones.

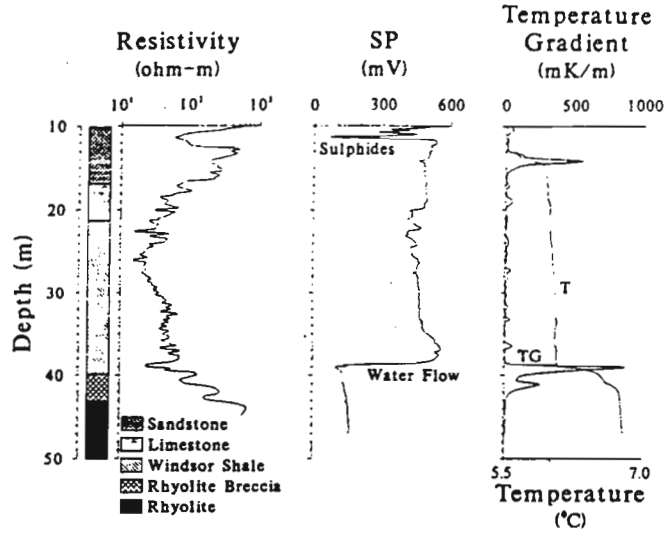

Figure 14: Resistivity, SP, and temperature logs from an NQ-hole YA405 at the Yava sandstone lead deposit, Nova Scotia. The SP log was acquired with a lead electrode. The step change in SP of approximately 500 mV at 39 m is associated with a 0.9°C step change in temperature that is due to groundwater flow. The SP anomaly is likely generated by both temperature change (thermal electric coupling) and water flow (electrokinetic or streaming potential).

EFFECTS OF TEMPERATURE AND GROUNDWATER FLOW ON SP MEASUREMENTS

Groundwater entry zones in boreholes produce abrupt changes in temperature. These changes may affect a number of borehole measurements such as SP. SP measurements in mineral exploration are usually recorded with lead or stainless steel electrodes. Large and abrupt changes in temperature may change the thermal, and electrical properties of the electrodes. These changes may generate voltage shifts that may be misinterpreted as spontaneous potentials related to lithology or mineralization. Figure 14 shows resistivity, SP, and temperature logs recorded in an NQ-hole 405 at the Yava lead deposit. The SP log was recorded with a lead electrode. The step change in SP of approximately 500 mV at 39 m is associated with a 0.9°C step change in temperature that is due to groundwater flow. There are no appreciable concentrations of sulphides at this depth which suggests that the SP anomaly is generated by either the temperature change (thermal coupling) or water flow (electrokinetic or streaming potential).

PERTURBATION OF LOCAL GEOTHERMAL GRADIENTS BY SULPHIDES

Massive sulphide zones are characterized by low electrical resistivity and high thermal conductivity. Since the high thermal conductivity affects the local geothermal gradient, temperature gradient measurements may be used to detect and map sulphide mineralization. Although temperature measurements may not replace conventional electrical methods in exploration for most massive sulphide deposits, non-conducting and non-polarizable sulphides such as sphalerite may be searched for using temperature methods. The following two field examples illustrate the temperature responses across massive and disseminated sulphides.

Massive sulphide deposit: Stratmat Main Zone, New Brunswick.

The Stratmat Main zone is a volcanogenic massive sulphide deposit. The sulphides consist of pyrite, galena, sphalerite and minor chalcopyrite. Temperature logs were recorded in five NQ-holes (75.7 mm diameter) ranging in depths from 150 to 180 m. The holes intersect thick sulphide zones (up to 10 m) with up to 85 percent sulphide. The rock type are mainly argillite, tuff and gabbro.

Figure 15 shows the lithology, temperature and temperature gradient data recorded in hole ST219. The temperature increases steadily from 50 to 85 m and flattens out in the massive sulphide zone. It then increases steadily past the sulphide zone at a rate that approaches the local geothermal gradient. The temperature gradient is very low in the sulphides. It is interesting to note that a thin argillite band in the sulphides is clearly indicated as a high temperature gradient zone. The temperature gradient in massive sulphides in other holes in the vicinity is very similar to that observed in this hole.

Disseminated Sulphides: Yava Lead Deposit, Nova Scotia.

The Yava deposit is a sandstone lead deposit with minor occurrences of sphalerite associated with the galena. The mineralization occurs at fairly shallow depths and the surface

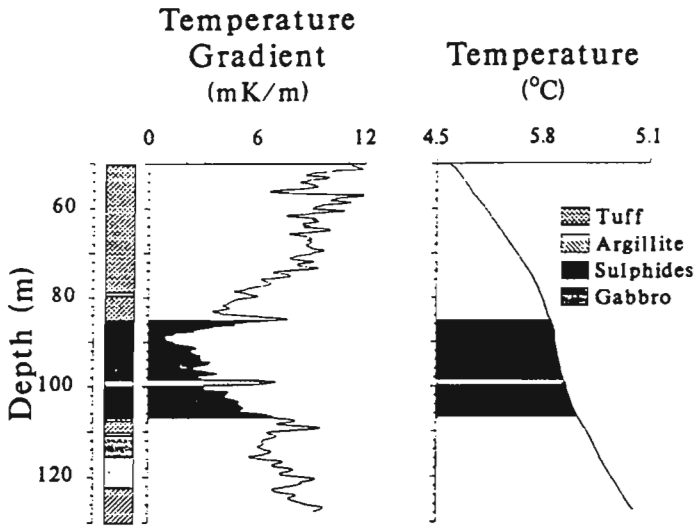

Figure 15: Temperature gradient and temperature-depth profiles recorded in hole ST219 at the Stratmat Main Zone massive sulphide deposit, New Brunswick. Very low temperature gradients are observed in the massive sulphide intersection (high thermal conductivity). Thin argillite bands in and at the upper and lower contacts correlate well with high temperature gradients.

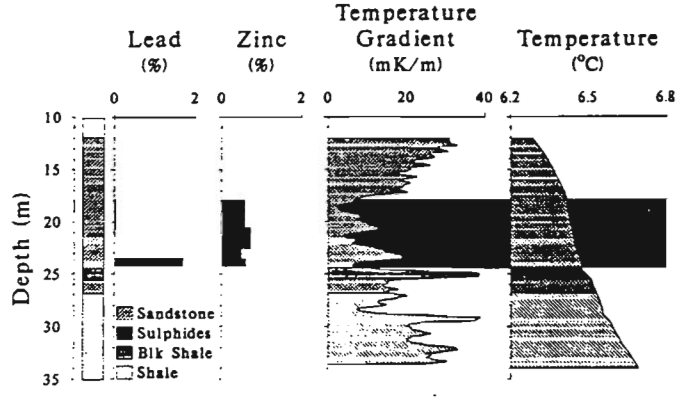

Figure 16: % lead, % zinc, temperature gradient and temperature-depth profiles for hole YA418 at the Yava sandstone lead deposit. The shaded area of disseminated mineralization correlates well with low temperature gradients and flattening in the temperature-depth profile. Low temperature gradients between 25 and 29 m are probably caused by mineralization in the vicinity that is not intersected by the drill hole.

temperature variations may affect the shallow local geothermal gradients. Temperature logs recorded in a number of holes without water flow show anomalously low gradients in mineralized zones. The disseminated galena and sphalerite in the sandstone deposit tend to increase the thermal conductivity of the sandstone which is usually fairly low (Figure 1). Figure 16 shows the lithology, lead and zinc assays, temperature

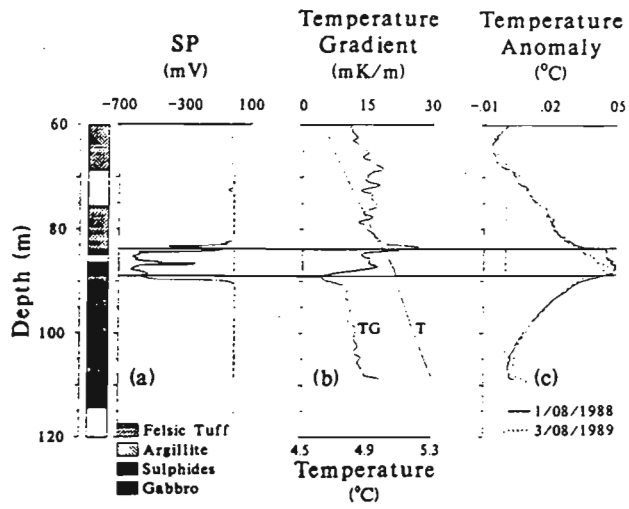

Figure 17: Lithology, SP and temperature logs recorded in hole S6119 in the vicinity of holes ST219 (Figures 15) at the Stratmat Main Zone massive sulphide deposit. The temperature data include a) recorded borehole temperatures; b) computed temperature gradients; and c) temperature anomaly (or residual temperatures after removing a geothermal gradient of 13.7 mK/m). Two temperature anomaly logs taken a year apart are shown. The shaded area across the logs represents the massive sulphide intersection. The temperatures within the sulphide zone are higher by about 0.05°C contrary to what was observed in hole ST219, and this correlates well with a high negative SP anomaly. Exothermic electrochemical reactions may be responsible for generating these large SP values.

gradient and temperature logs recorded in hole 418. The mineralized zones are indicated by low gradients and flattening temperatures even though zinc is less than 1 %. Low gradients between 25 and 29 m of hole 418 are not correlated with mineralization, but may be due to perturbation of the geothermal gradient from mineralization in the vicinity that it is not intersected by the drill hole. In spite of the effects of ground water flow and surface temperature changes on the temperature-depth profile, there are indications of the presence of mineralization.

EXOTHERMIC REACTIONS ASSOCIATED WITH ELECTROCHEMICAL PROCESSES.

Electrochemical oxidation and reduction processes that occur within massive sulphide deposits may generate heat which can be detected on the temperature logs. Locations of these exothermic reactions in mineralized zones may provide an understanding of the self potential generating mechanism in deposits. Figure 17 shows temperature and SP logs recorded in an old hole S6119 in the vicinity of hole ST219 (Figure 15) at the Stratmat massive sulphide deposit. The hole was drilled in 1961 and was first temperature-logged in 1988 and later revisited in 1989. Multiparameter logs, including SP, were recorded both times. The temperature data include a) recorded

borehole temperatures; b) computed temperature gradients; and c) temperature anomaly (or residual temperatures) which represent temperature data after removing a geothermal gradient of 13.7 mK/m. A large amplitude SP anomaly between 80 and 90 m is associated with the massive sulphides. The temperature log shows an increase in temperature at this location contrary to what was observed in hole ST219 and other nearby holes. The gradient and the residual temperatures highlight the temperature anomalies observed in the sulphides. The temperatures within the massive sulphides zone are elevated by about 0.05 °C compared to the host rock. The good correlation between SP and these higher temperatures suggests that electrochemical reactions that generate the SP are exothermic.

LOCATION OF UNDERGROUND OPENINGS AT EXISTING MINES

Figure 18 shows resistivity, percent sulphides (mainly sphalerite and minor galena and chalcopyrite), SP, temperature and temperature gradient logs recorded in a hole at the New Calumet mine, Quebec. The high temperature at 130 m suggests a local heat source in the vicinity. Although this high temperature anomaly appears to be associated with the sulphide mineralized zone, there are numerous old underground mine workings at this deposit that may be responsible for generating these high temperatures. The sulphides may just act as a path for conducting heat from the mine openings.

Figure 19 shows another example of the use of temperature measurements in detecting underground mine openings. These temperature measurements were recently recorded at the Selbaie mine, Quebec. The high temperature anomalies do not correlate with the mineralization. These anomalies are due to underground mine openings in the vicinity of the hole. There are openings approximately 4 and 7 m away, corresponding to the upper anomaly at approximately 270 m and the lower anomaly at approximately 340 m, respectively.

CONCLUSION

In a number of temperature measurements made over mineral deposits, the perturbation of the local geothermal gradients due to the presence of sulphides is often obscured by groundwater flow. Temperature logs may, therefore, be used to yield information on the groundwater flow system within a site. Information on the location of water flow in a borehole is vital during mine development. Boreholes are usually plugged to alleviate flooding problems or groundwater contamination.

Temperature logs may provide complementary information to the electrical resistivity measurements. Massive sulphide zones are characterized by low temperature gradients because of their high thermal conductivities. Some of the groundwater flow zones correlate with mineralized zones. This suggests that the mineralization represent a zone of 'weak' rock and is susceptible to fracturing and hence carries water. The electrochemical processes that generate the large SP anomalies associated with massive sulphides are often exothermic, generating heat that is observable on temperature logs.

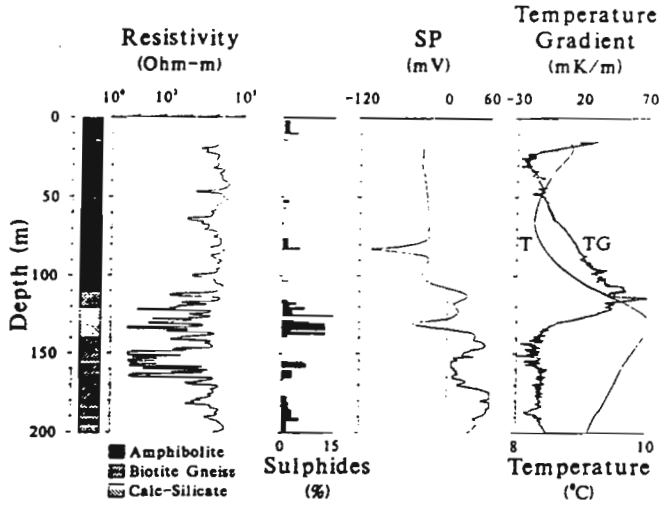

Figure 18: Resistivity, percent sulphide (mainly sphalerite and minor galena and chalcopyrite), SP, temperature and temperature gradient logs recorded in a hole at the New Calumet lead-zinc mine, Quebec, Canada. The high temperature anomaly near 130 m suggests a local heat source. Although this high temperature anomaly appears to be correlated with the sulphide mineralization, there are numerous old underground mine workings at this deposit that may be responsible for generating these high temperatures. The sulphides conduct heat from the mine openings.

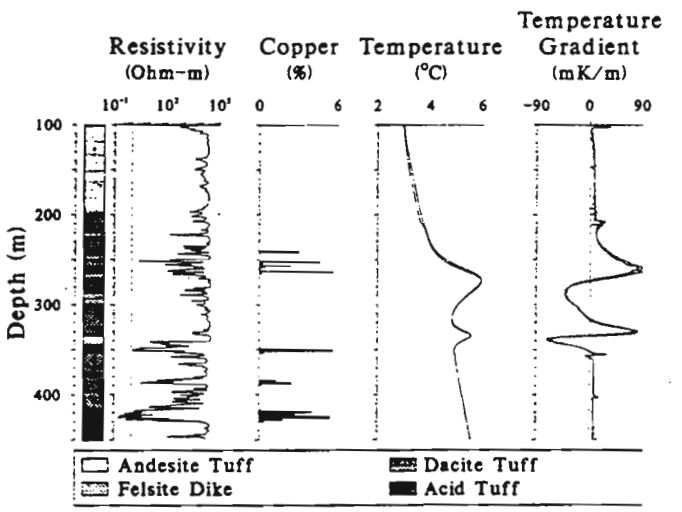

Figure 19: Resistivity, percent copper, temperature and temperature gradient logs from a hole at the Selbaie mine, Quebec, Canada. The temperature data show two anomalies representing local heat sources caused by underground openings approximately 4 m away (upper anomaly) and 7 m away (lower anomaly). The lower anomaly seems to correlate with low resistivity and copper sulphides.

Although temperature profiles in a borehole are affected by a number of parameters, all the information extracted from the logs may be useful during exploration and development of a mineral prospect. While looking for specific information, the interpreter should be aware of all possible information that may be derived from these logs (groundwater flow, thermal conductivity variations due to the presence of sulphides or lithological difference, exothermic or endothermic processes). Heat pumps utilizing groundwater are often installed in underground mines and the knowledge of the temperature distribution around the mine site and groundwater flow system would, therefore, be very useful.

REFERENCES

Beck, A.E., 1976, The use of thermal resistivity logs in stratigraphic correlation: *Geophysics*, 41:300-309.

Beck, A.E., 1982, Precision logging of temperature gradients and the extraction of past climate: *Tectonophysics*, 83:1-11.

Blackwell, D.D. and Steele, J.L, 1987, Thermal conductivity of sedimentary rock - measurement and significance: *in* Thermal History of Sedimentary Basins - Methods and Case Histories, eds. N.Naeser and T. McCulloh. Springer-Verlag, New York.

Bristow, Q., and Conaway, J.G., 1984, Temperature gradient measurements in boreholes using low noise high resolution digital techniques: *in* Current Research, Part B, *Geological Survey of Canada Paper* 84-1B, p.101-108.

Conaway, J.G., 1977, Deconvolution of temperature gradient logs: *Geophysics*, 42:823-837.

Conaway, J.G., and Beck, A.E., 1977, Fine-scale correlation between temperature gradient logs and lithology: *Geophysics*, 42:1401-1410.

Conaway, J.G., 1987, Temperature logging as an aid to understanding groundwater flow in boreholes: *in* 2nd International Symposium on Borehole Geophysics for Minerals, Geotechnical, and Groundwater Applications Proceedings, *Minerals and Geotechnical Logging Society.*

Costain, J.K., 1970, Probe response and continuous temperature measurements: *Journal Geophysical Research*, 75:3968-3975.

Drury, M.J., and Jessop, A.M., 1982, The effect of a fluid-filled fracture on the temperature profile in a borehole: *Geothermics*, 11:145-152.

Jaeger, J.C., 1961, The effect of the drilling fluid on temperature measured in bore hole: *Journal of Geophysical Research*, 66:563-569.

Kayal, J.R., 1981, Correlation of T-log with E-log in coal-bearing formations: *Pure and Applied Geophysics*, 119:349-35.

Kayal, J.R. and Christoffel, D.A., 1982, Relationship between electrical and thermal resistivities for differing grades of coal: *Geophysics*, 47:127-129.

Killeen, P.G., 1986, A system of deep test holes and calibration facilities for developing and testing new borehole geophysical techniques, ed. P.G. Killeen, *Geological Survey of Canada, Paper* 85-27, p.29-46.

Lachenbruch, A.H., and Brewer, M.C., 1959. Dissipation of the temperature effect of drilling a well in Arctic Alaska: *US Geological Survey, Bulletin* 1083-C, p.73-109.

Leblanc, Y., Lam, H-L., Pascoe, L.J. and Jones, F.W., 1982, A comparison of two methods of estimating static formation temperature from well logs: *Geophysical Prospecting*, 30:348-357.

Lee, Tein-Chang, 1982, Estimation of formation temperature and thermal property from dissipation of heat generated by drilling: *Geophysics*, 47:1577-1584.

Luheshi, M.N, 1983, Estimation of formation temperature from borehole measurements: *Geophysical Journal of the Royal Astronomical Society*, 74:747-776.

Madden, H.H., 1978, Comments on the Savitzky-Golay convolution method for least-squares fit smoothing and differentiation of digital data: *Analytical Chemistry*, 50:1383-1386.

Middleton, M.F., 1979, A model for bottom hole temperature stabilization: *Geophysics*, 44:1458-1462.

Mwenifumbo, C.J., 1989, Application of temperature logging in mapping coal seams: in press.

Parasnis, D.S., 1974, Some present-day problems and possibilities in mining geophysics: *Geoexploration*, 12:97-120.

Peacock, D.R., 1965, Temperature logging, paper F, *in* 6th Annual Logging Symposium Transactions, Society of Professional Well Log Analysts, p.F1-18.

Reiter, M., Mansure, A.J., and Peterson, B.K., 1980, Precision continuous temperature logging and comparison with other types of logs: *Geophysics*, 45:1857-1868.

Velleman, P.F. and Hoaglin, D.C., 1981, *Applications, Basics and Computing of Exploratory Data Analysis*: Duxbury Press, Boston, 354p.

Wilkinson, L., 1990, SYSTAT: *The system for Statistics*: Evanston, IL: SYSTAT, Inc.

Wilkinson, L., 1990, SYGRAPH: *The system for Graphics*: Evanston, IL: SYSTAT, Inc.

Application of temperature logging to mapping coal seams

C.J. Mwenifumbo
Mineral Resources Division

Mwenifumbo, C.J., 1994: Application of temperature logging to mapping coal seams; in Current Research 1994-E; Geological Survey of Canada, p. 291-298.

Abstract: High precision, high resolution continuous temperature measurements were recorded in shallow holes at the Highvale open pit coal mine, Alberta. The temperature data acquired shortly after drilling provided useful information on the location of permeable zones within sandstones and also detected the coal seams. Higher temperatures were observed within coal seams compared to sedimentary rock formations. Temperature logging done ten to fifteen days after drilling indicated that borehole fluid temperatures were close to equilibrium formation temperatures. Temperature gradient data derived from these quasi-equilibrium borehole temperature measurements accurately defined the depths and thicknesses of coal seams and were successfully used in hole-to-hole correlation of coal seams between several holes separated by up to 2.5 km.

Résumé : Des mesures continues haute précision et haute résolution de la température ont été enregistrées dans des trous peu profonds forés dans la mine de charbon à ciel ouvert Highvale en Alberta. Les données sur la température acquises peu de temps après le forage ont fourni des informations utiles sur l'emplacement des zones perméables au sein des grès et ont permis en outre de détecter les filons de charbon. Les températures étaient plus élevées dans les filons de charbon que dans les formations de roche sédimentaire. Les diagraphies de la température effectuées de dix à quinze jours après le forage ont indiqué que les températures des fluides dans les trous étaient proches des températures de formation d'équilibre. Les données sur les gradients de température établies à partir des mesures des températures des trous en situation de quasi-équilibre ont permis de définir avec exactitude les profondeurs et les épaisseurs des filons de charbon et de corréler avec succès les filons de charbon entre plusieurs trous séparés par une distance allant jusqu'à 2,5 km.

INTRODUCTION

In the oil industry, temperature logs are frequently used to determine the location of cement tops after a recent cementing operation, to delineate zones of lost circulation in a well while drilling is in progress, and to locate fluid entry and exit points in production and injection wells (Peacock, 1965; Bateman, 1985). Other uses of borehole temperature measurements include determining the equilibrium geothermal gradients in terrestrial heat flow studies or studying the transient temperature changes when heat is added to or extracted from the formation. However, temperature gradient logging has been shown to be a potentially useful method in lithostratigraphic correlation (Beck, 1976; Conaway and Beck, 1977; Blackwell and Steele, 1989) and in the identification and evaluation of coal seams (Beck, 1976; Kayal, 1981; Kayal and Christoffel, 1982). Temperature gradient logs were successfully used, in conjunction with electrical resistivity logs, to discriminate between coal seams with high electrical resistivity and high temperature gradients, and resistive sandstones having low temperature gradients. Although temperature gradient measurements reported by Beck (1976) and Kayal (1981) indicated the usefulness of the technique in coal seam mapping, the measurements lacked detail and could not be used to determine accurately the depth and thicknesses of coal seams. The logging was also conducted in fairly deep, cased holes. Deep holes ensure that surface temperature variation effects are minimal. Data obtained in uncased sections of the holes were previously found to be not accurately reproducible (Beck, 1982; Conaway and Beck, 1977).

This paper presents high precision, high resolution temperature measurements acquired at the Highvale open pit coal mine, Alberta. The boreholes were drilled with fresh water as the drilling fluid. These holes were 15 cm in diameter, uncased, and drilled to fairly shallow depths ranging from 60 to 80 m. At these depths, climatic changes can be a major cause of perturbation in the geothermal gradient, especially in high latitude areas. Beck (1982) observed that surface temperature variations may disturb the equilibrium temperatures in boreholes to depths of more than 100 m and it was feared that they would have adverse effects on the use of these measurements in mapping lithology and coal seams. The objective of the temperature logging was to assess the usefulness of these measurements in mapping coal seams.

LOGGING EQUIPMENT AND FIELD PROCEDURE

The temperature logging equipment developed at the Geological Survey of Canada (Bristow and Conaway, 1984) was used in the acquisition of the data. The temperature probe sensor consists of a 10-cm long tip of thermistor beads and has a thermal time constant of less than 2 seconds in stirred water. The thermistor signal is converted in the probe to a square wave, the frequency of which is a function of temperature. The square wave signal is transmitted uphole via a 1 km cable to a mini-computer-based data acquisition system in the logging truck where very accurate period measurements give temperatures with a resolution of better than 0.1 mK. Probe depths are measured with a resolution of 1 mm by an optical shaft encoder on a well head pulley assembly. Details of the logging system are given in Bristow and Conaway (1984).

All temperature data were acquired during a downhole run at a logging speed of 6 m/minute with data sampled every 200 milliseconds giving a measurement approximately every 2 cm. This high spatial resolution is necessary for the determination of accurate temperature gradients with the use of derivative operators (Conaway and Beck, 1977). The deconvolution technique developed by Costain (1970) and Conaway (1977) was used to process and remove the effects of the probe time constant from the temperature measurements. The Savitzky-Golay operator (Madden, 1978) was used to compute the gradients from the temperature data.

The electrical resistivity data presented in this paper were acquired with a 10-cm normal array at a logging speed of 3 m/minute with a sample depth interval of 5 cm. The total count natural gamma-ray log (energy window from 0.1 to 3 MeV) was acquired with a 3.2 cm by 12.7 cm sodium iodide detector. The logging speed for this data set was 3 m/minute with a one second sample time interval (equivalent to a sample depth interval of 5 cm).

GEOLOGY

The lithology above the coal seams consists largely of mudstones, siltstones, and sandstones (Fig. 1). A few of the sandstones are occasionally cemented by calcite. The layer just above the first coal seam is usually mudstone, 3 to 4 m thick with its base frequently consisting of bentonitic clays. The depth to the top of the first of six coal seams ranges from approximately 30 to 60 m. The first and second coal seams are approximately 3 m thick. The other four coal seams range in thickness from 15 cm to 2 m. The coals are sub-bituminous and are characterized by high electrical resistivity, low thermal conductivity, extremely low natural gamma radioactivity, and low density.

TRANSIENT TEMPERATURE LOGGING

Experiments were carried out to investigate the usefulness of transient temperature measurements recorded shortly after drilling in lithological mapping, and in the detection of porous and permeable zones, and also to address the question of how long a hole must be allowed to stand after drilling in order to carry out "quasi-equilibrium" temperature measurements for lithological and coal-seam mapping. Logging was carried out in 15-cm diameter holes which were diamond drilled with fresh water as the drilling fluid.

Short-period transient temperatures disturbances within a borehole may be caused by the addition or extraction of heat from the formation during the circulation of fluids as the borehole is being drilled (Hoang and Somerton, 1981). The process of drilling also causes a disturbance of formation temperatures by the frictional heat generated at the bit

(Lachenbruch and Brewer, 1959; Jaeger, 1961). The heat exchange between the fluid and the formation penetrated either warms or cools the formation depending on the relative temperatures of the drilling fluid and the formation.

Formation temperatures are changed by different amounts in rocks of differing thermal conductivities and permeabilities during the circulation of drilling fluids (Hoang and Somerton, 1981). It has been suggested that transient temperature logging can be used to map sedimentary rock formations such as sandstone, shale, and limestone (Dakhnov, 1959). The borehole fluid around the sandstone formation returns to equilibrium temperatures faster than the shales that have lower thermal conductivities. Within a formation with fairly uniform thermal conductivity but variable permeability, the more permeable zones will be most affected and are often the zones where transitory heat sources or sinks are observed (Drury and Jessop, 1982).

Lithology and coal seam mapping

Figure 1 shows gamma-ray and electrical resistivity logs for hole HV88-427 compared with the temperature log recorded one day after drilling. The coal seams exhibit characteristic high electrical resistivities and extremely low radioactivity. The overall temperatures within the low thermal conductivity coal seams are high compared to the rest of the formations. The individual coal seams are poorly resolved but can be detected from these temperature data. There is a positive correlation between temperature and electrical resistivity data. The inseam mudstone and shale layers exhibit lower temperatures, low electrical resistivities, and high radioactivity. In the upper section of the hole above the coal seams between 25 and 35 m, there is a positive correlation between natural gamma radioactivity and temperature. The sandstone layers with high thermal conductivity are characterized by low gamma radioactivity and low temperatures whereas the bentonitic silty mudstones with lower thermal conductivities exhibit high gamma radioactivity and high temperatures. The electrical resistivity is, however, negatively correlated with both temperature and natural gamma radioactivity. The negative correlation of transient temperature and electrical resistivity within the sandstone layers is a useful characteristic that may aid in distinguishing resistive coal seams from resistive sandstone layers.

Detection of porous and permeable zones

Figure 2 shows the electrical resistivity, self potential, and transient temperature logs acquired in borehole HV88-422. The resistivity log indicates a more resistive zone between 29 and 36 m. Variations in resistivity within this sandstone unit may reflect changes in porosity, higher porosity suggesting

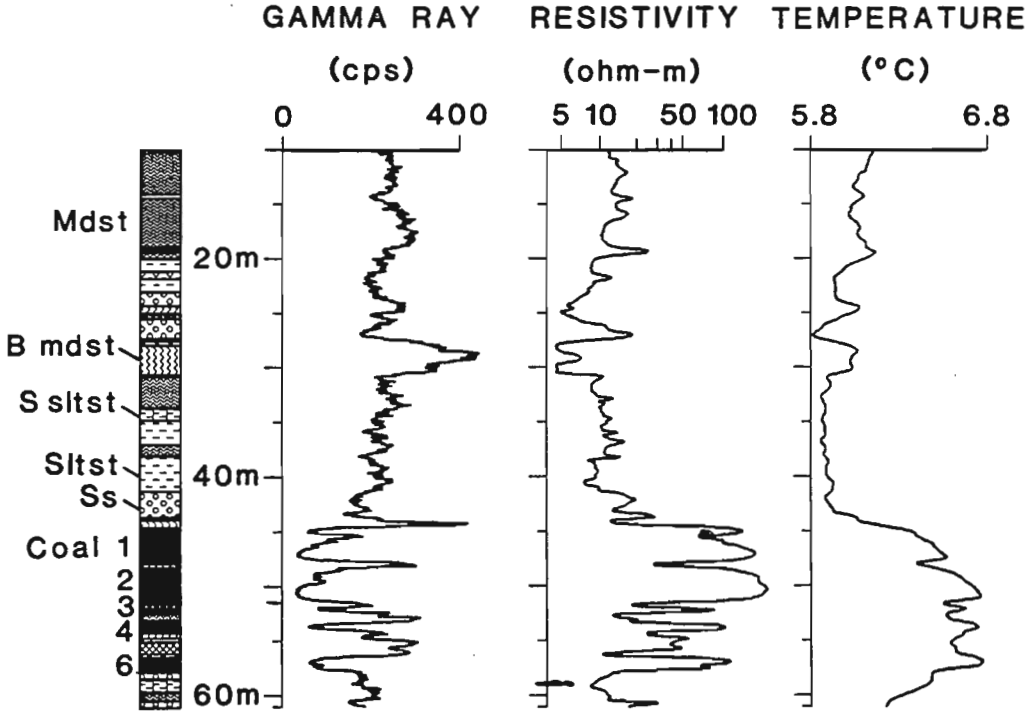

Figure 1. Temperature logs recorded in hole HV88-427 one day after drilling compared with gamma-ray and electrical resistivity logs. The coal seams exhibit characteristic high electrical resistivities and extremely low radioactivity. Temperature and electrical resistivity logs are positively correlated in the coal seams. In the upper section of the hole above the coal seams (between 20 and 35 m), electrical resistivity is negatively correlated with temperature. B mdst - bentonitic mudstone, Mdst - mudstone, S sltst - sandy siltstone, Sltst - siltstone, Ss - sandstone.

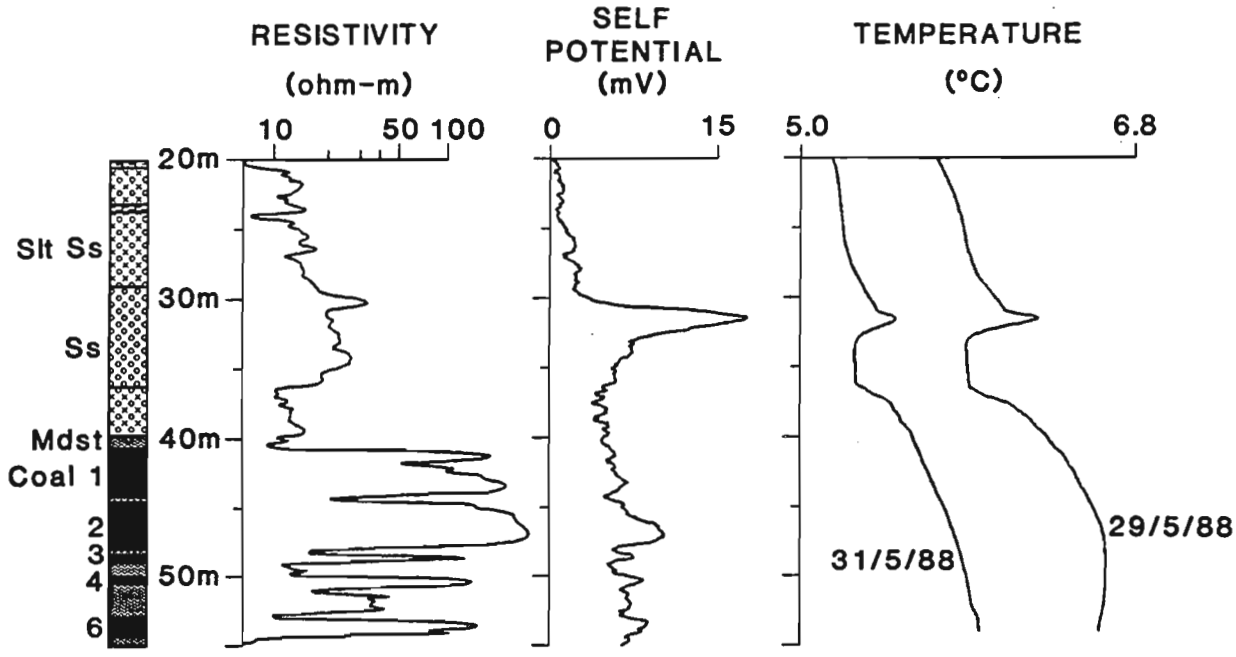

Figure 2. Electrical resistivity, self potential, and transient temperature logs acquired in borehole HV88-422. The prominent peak on the temperature profiles indicates a permeable zone within the sandstone, which is confirmed by a corresponding high SP anomaly and lower resistivity. Temperature measurements were recorded one and three days after drilling. Mdst - mudstone, Slt Ss - silty sandstone, Ss - sandstone.

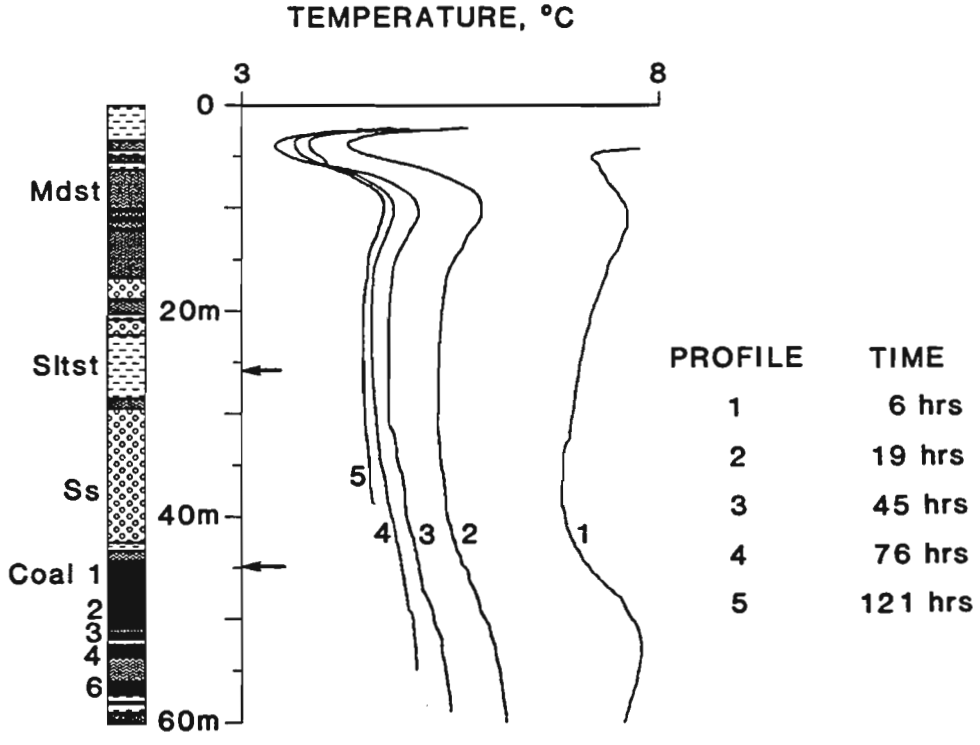

Figure 3. Five temperature logs recorded in hole HV88-424 at approximately the following times after drilling had stopped: 6, 19, 45.5, 76.5, and 121.5 hours. The influence of the drilling fluid, which was warmer than the ambient formation temperatures, is fairly obvious. Mdst - mudstone, Sltst - siltstone, Ss - sandstone.

less cementation. Calcareous cementation is prevalent in a number of sections within the sandstone units in this region. A transient high temperature anomaly is observed around 31.5 m. This anomaly correlates with a self potential anomaly and coincides with a slightly lower resistivity zone within the sandstone. It is interpreted as resulting from the warmer drilling fluids infiltrating a more permeable zone within this sandstone unit creating a transient heat source that decays with time. This may explain the self potential anomaly, which is probably due to filtration of water from the pores into the borehole. SP data have at times been used in detecting porous and permeable zones of the formation surrounding the borehole (Dakhnov, 1959). These measurements indicate that temperature logging shortly after drilling can be used to delineate coal seams, distinguish between mudstone and sandstone, and possibly detect high porosity and high permeability zones.

Return to equilibrium temperatures after drilling

The time required for a borehole to return to equilibrium formation temperatures after drilling will vary depending on the temperature difference between the drilling fluid and formation temperatures, the thermal conductivity of the formation, and the fluid circulation time. Kayal and Christoffel (1982) recorded their temperature measurements three days after drilling and considered this time adequate for equilibrium temperature gradient measurements. The negative gradients observed in their data, however, suggest that the borehole fluid temperatures may not have reached equilibrium with the formation temperatures.

Figure 3 shows five temperature logs carried out in hole HV88-424 to determine the time required after drilling for the borehole to attain quasi-equilibrium temperatures. These logs were recorded at approximately 6, 19, 45.5, 76.5, and 121.5 hours after drilling stopped. The hole collapsed approximately 39 m during the fifth run and measurements were discontinued. The influence of the drilling fluid on the temperature-depth profile is fairly obvious. Unfortunately, the temperature of the drilling fluid was not measured and no detailed evaluation of the data was carried out. The temperatures were raised by more than 4°C from the ambient temperatures. The first log shows increased temperatures between 45 and 60 m due to the low thermal conductivity of the coal seams. Figure 4 shows the approach of the borehole fluid temperatures to equilibrium with time after the circulation of drilling fluid had ceased in borehole HV88-424. The temperatures are plotted for two different locations in the borehole: one within the coal seam at 50 m and the other within the siltstone at approximately 25 m (indicated by arrows in Figure 3). The approach to equilibrium temperatures is roughly exponential. If we assume that the dominant heat transfer process is conduction, then the formation with the highest thermal conductivity will dissipate heat away from the borehole faster than the lower thermal conductivity formations. The rate of return of the borehole fluid temperatures to equilibrium is faster within the mudstone with higher thermal conductivities. After five days the borehole fluid temperatures appear to be approaching equilibrium formation temperatures. Temperature logging in most of holes was done ten to fifteen days after drilling. After this period, reproducible temperature gradients were obtained and no negative gradients were observed.

EQUILIBRIUM TEMPERATURE LOGGING: FIELD RESULTS

In environments where there are no heat sources or sinks, the highest geothermal gradients will be observed in rocks with the lowest thermal conductivity and vice versa. Figure 5 shows the natural gamma-ray and electrical resistivity logs compared with the equilibrium temperature logs for borehole HV88-414. The temperature log was recorded fifteen days after drilling. The water table in this hole was at approximately 6 m and the zero gradient zone or temperature inversion point was fairly shallow, approximately 13 m. Above this point large temperature gradient anomalies exist that are due to surface temperature variations. Below this point, the temperatures are mainly affected by variations in the thermal conductivity of the formation, assuming little or no heat transport by groundwater flow. Temperatures range from 4.5 to 5.5°C. Gross correlations of the temperature log and lithology are apparent. The temperature increases slowly with depth within the siltstone/sandstone/mudstone section from 10 to 35 m. There is an abrupt temperature change at 35 m, and the temperature increases rapidly up to 48 m and flattens thereafter. The region between 35 and 48 m consists of coal seams. The subtle changes in temperature within this section indicate the location of individual coals seams.

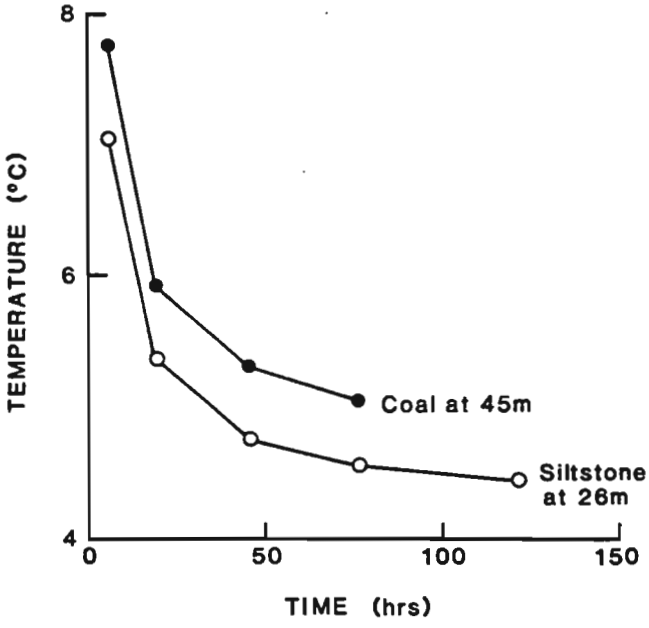

Figure 4. Temperature-time curves showing the approach of borehole fluid temperatures to equilibrium after circulation of fluid had ceased. The two curves are obtained within siltstone at approximately 25 m and within coal seam no. 1 at 50 m in borehole HV88-424.

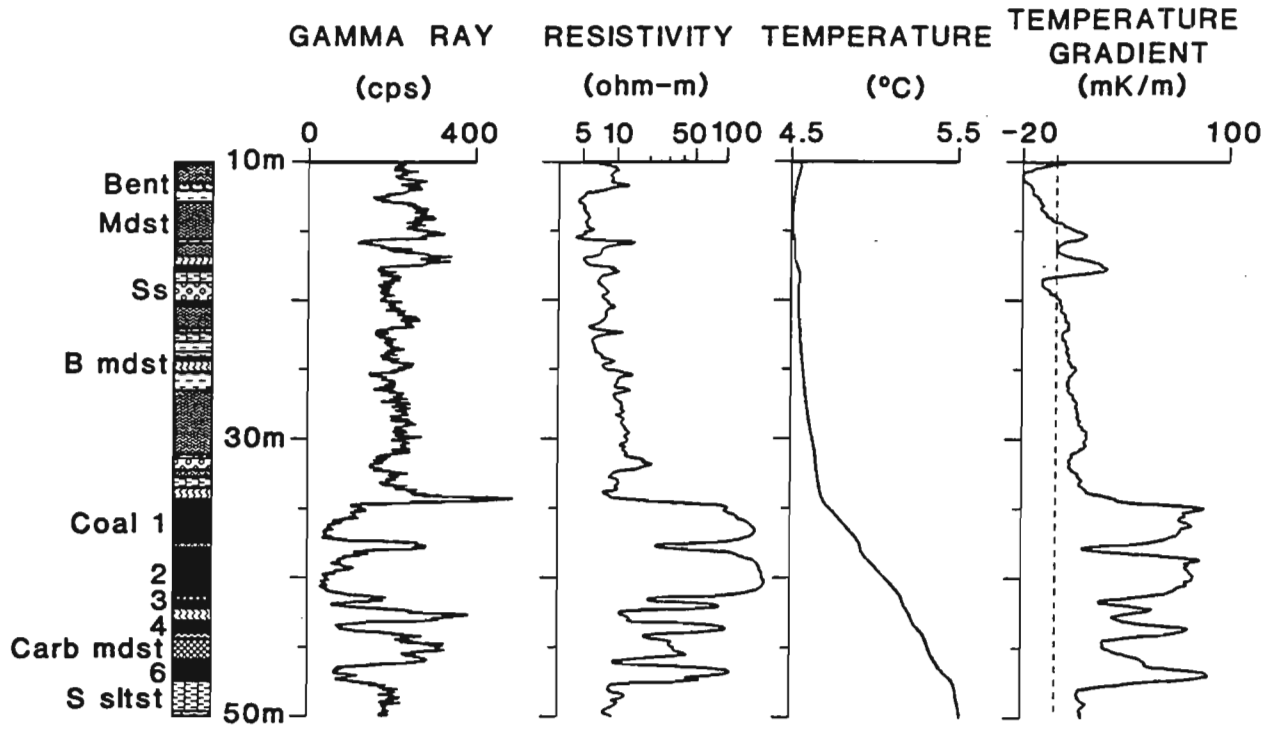

Figure 5. Gamma-ray and electrical resistivity logs compared with equilibrium temperature logs recorded 15 days after drilling in borehole HV88-414. The subtle variations in the smooth temperature profile are transformed into peaks in the temperature gradient profile that correlate well with the location of the coal seams. Bent - bentonite, B mdst - bentonitic mudstone, Mdst - mudstone, Carb mdst - carbonaceous mudstone, S sltst - sandy siltstone, Ss - sandstone.

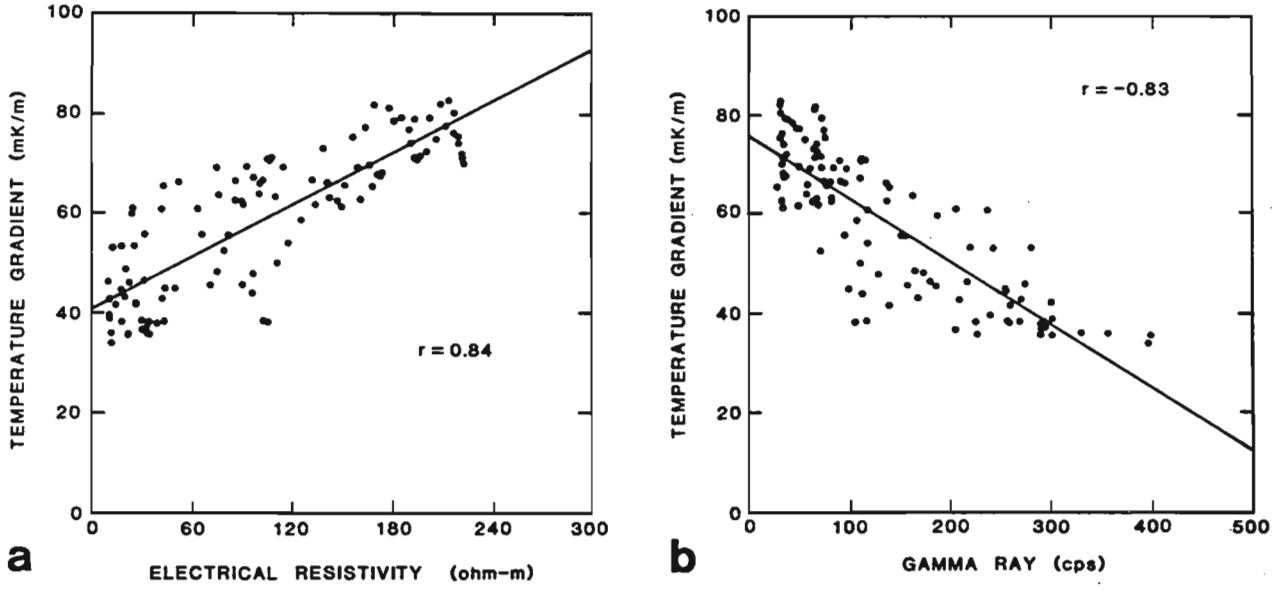

Figure 6. Crossplots of electrical resistivity versus temperature gradient, (a), and gamma-ray versus temperature gradient, (b), for hole HV88-412 within coal seams between 36 and 47 m.

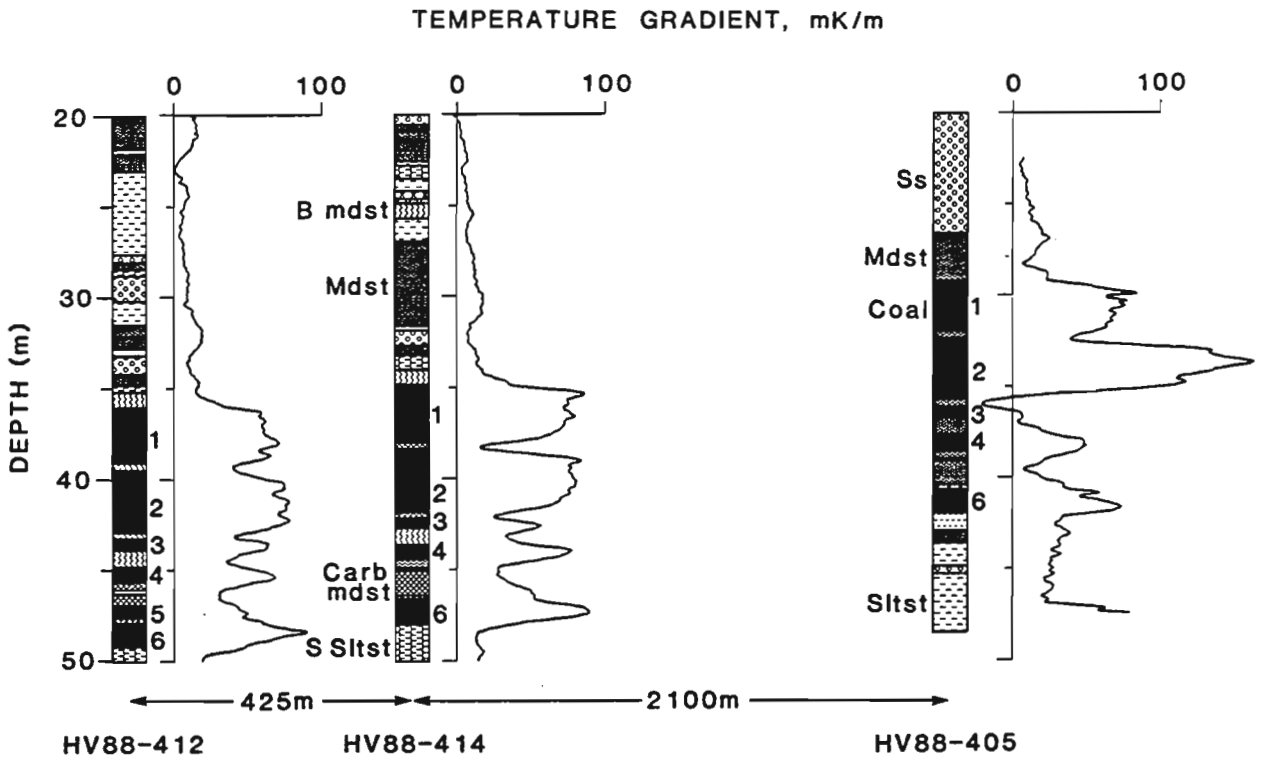

Figure 7. Temperature gradient logs in hole-to-hole correlation of coal seams. Hole HV88-405 is more than 2 km from the other two holes and exhibits similar correlation between coal seams and temperature gradient. This makes temperature gradient logging an effective tool for mapping the extent of coal seams. B mdst - bentonitic mudstone, Carb mdst - carbonaceous mudstone, Mdst - mudstone, S Sltst - sandy siltstone, Sltst - siltstone, Ss - sandstone.

The temperature gradient log shows good correlation with the electrical resistivity log, the gamma-ray log, and the coal seams. All the coal seams are clearly delineated on the temperature gradient log except for coal seam number 5, which is very thin and also poorly defined on the resistivity and gamma-ray logs. The inseam layers of mudstone, siltstone, and carbonaceous shales are clearly identified as high radioactivity, low resistivity, and low temperature gradient zones. Coal seam temperature gradients are approximately 80 mK/m and mudstone gradients are less than 25 mK/m. Variations in the resistivity and natural gamma radioactivity within the coal probably reflect changes in the ash content. Coal seams number 1 and 2 show relatively higher radioactivity and lower resistivities at the top of the seams suggesting an increase in clay content. Therefore, better quality coal is inferred at the bottom of the coal seams (higher resistivities and extremely low radioactivity).

Figures 6a and 6b are crossplots of the electrical resistivity versus temperature gradient and gamma-ray versus temperature gradient for hole HV88-412 within the coal seams. The correlation between these parameters is excellent ($r>0.8$). The temperature gradients decrease with increasing radioactivity.

Figure 7 illustrates the application of temperature gradient logs in hole-to-hole correlation of coal seams. Hole HV88-414 is 425 m from HV88-412 and hole HV88-405 is 2.1 km from HV88-412. Holes HV88-412 and HV88-414 are at approximately the same elevation, and the collar of hole HV88-405 is approximately 12 m higher than the other two. An adjustment has been made to the depths of logs from HV88-405 to reflect this elevation difference. It is clear that temperature gradient logs are an excellent tool for hole-to-hole correlation of coal seams over fairly large distances.

CONCLUSION

It has been shown that both temperature and temperature gradient logs can be successfully used in coal seam and lithological mapping. Coal seams are clearly delineated on the temperature gradient logs and exhibit high gradients, high electrical resistivities, and extremely low natural gamma radioactivity. Accurate depths and thicknesses of the coal seams can be determined from these high spatial resolution temperature data and compare remarkably well with the resistivity logs. There is a negative correlation between temperature gradient and electrical resistivity in sandstone and mudstone. High-resolution temperature measurements in conjunction with electrical resistivity and gamma-ray logs can distinguish between mudstone and sandstone. Temperature logs acquired immediately after drilling may be used to locate more permeable zones within sandstone layers. Since most of the holes drilled in coal environments are not stable,

they often collapse a few days after drilling due to the nature of incompetent rock. Casing the holes would be the most logical way of ensuring that they remain open if logging is contemplated at a later date. Galvanic electrical logs cannot be run in either steel- or plastic-cased holes. Temperature gradient logs in a cased hole offer an alternative parameter to electrical logs as well as providing their own unique response characteristics. The environment at the Highvale coal mine indicates that for fine scale lithological correlation, equilibrium temperature logs should not be recorded until at least ten days after drilling fluid circulation has ceased.

ACKNOWLEDGMENTS

I am indebted to TransAlta Utilities Corporation for permission to carry out these logging measurements in their holes at the Highvale coal mine, Alberta. I am also grateful to Professor A.E. Beck and Dr. J.G. Conaway for reading the manuscript and offering many valuable suggestions. Thanks are due to P.G. Killeen and Q. Bristow for their valuable discussions, to Bill Hyatt and Steven Birk for help in data acquisition, and to Barbara Elliott for help rendered in data processing.

REFERENCES

Bateman, R.M.
1985: Cased-hole log analysis and reservoir performance monitoring; International Human Resources Development Corporation.
1976: The use of thermal resistivity logs in stratigraphic correlation; Geophysics, v. 41, p. 300-309.

Beck, A.E.
1982: Precision logging of temperature gradients and the extraction of past climate; Tectonophysics, v. 83, p. 1-11.

Blackwell, D.D. and Steele, J.
1989: Thermal conductivity of sedimentary rocks: measurement and significance; in Thermal History of Sedimentary Basins: methods and case histories, (ed.) Nancy D. Naeser and Thane H. McCulloh; Springer-Verlag.

Bristow, Q. and Conaway, J.G.
1984: Temperature gradient measurements in boreholes using low noise high resolution digital techniques; in Current Research, Part B; Geological Survey of Canada, Paper 84-1B, p. 101-108.

Conaway, J.G.
1977: Deconvolution of temperature gradient logs; Geophysics, v. 42, p. 823-837.

Conaway, J.G. and Beck, A.E.
1977: Fine-scale correlation between temperature gradient logs and lithology; Geophysics, v. 42, p. 1401-1410.

Costain, J.K.
1970: Probe response and continuous temperature measurements; Journal of Geophysical Research, v. 75, p. 3968-3975.

Dakhnov, V.N.
1959: Geophysical well logging; Quarterly of the Colorado School of Mines, v. 57, no. 2, 1962; translated by G.V. Keller.

Drury, M.J. and Jessop, A.M.
1982: The effect of a fluid-filled fracture on the temperature profile in a borehole; Geothermic, v. 11, p.145-152.

Hoang, V.T. and Somerton, W.H.
1981: Effect of variable thermal conductivity of the formations on the fluid temperature distribution in the wellbore; Transactions, Twenty-Second Annual Logging Symposium, Society of Professional Well Log Analysts, p. L1-L24.

Jaeger, J.C.
1961: The effect of the drilling fluid on temperatures measured in bore holes; Journal of Geophysical Research, v. 66, p. 563-569.

Kayal, J.R.
1981: Correlation of T-log with E-log in coal-bearing formations; Pure and Applied Geophysics, v. 119, p. 349-355.

Kayal, J.R. and Christoffel, D.A.
1982: Relationship between electrical and thermal resistivities for differing grades of coal; Geophysics, v. 47, p. 127-129.

Lachenbruch, A.H. and Brewer, M.C.
1959: Dissipation of the temperature effect of drilling a well in Arctic Alaska; U.S Geological Survey Bulletin 1083-C, p. 73-109.

Madden, H.H.
1978: Comments on the Savitzky-Golay convolution method for least-squares fit smoothing and differentiation of digital data; Analytical Chemistry, v. 50, p. 1383-1386.

Peacock, D.R.
1965: Temperature logging; Transactions, Sixth Annual Logging Symposium, Society of Professional Well Log Analysts, p. F1-F18.

Geological Survey of Canada Project 880030

Acoustic velocity logging at the McConnell nickel deposit, Sudbury area, Ontario: preliminary in situ measurements[1]

K.A. Pflug, P.G. Killeen, and C.J. Mwenifumbo
Mineral Resources Division

Pflug, K.A., Killeen, P.G., and Mwenifumbo, C.J., 1994: Acoustic velocity logging at the McConnell nickel deposit, Sudbury area, Ontario: preliminary in situ measurements; in Current Research 1994-C; Geological Survey of Canada, p. 279-286.

Abstract: An acoustic velocity logging probe has been used to acquire data on the seismic characteristics of the McConnell nickel deposit in the Sudbury area. Preliminary results indicate good velocity contrasts in the stratigraphic sequence associated with the massive sulphides. These velocity contrasts are related to the density and elastic properties of the rocks; density was measured in the same borehole with a density logging probe. One interesting observation is that the high density massive sulphides have low P-wave velocities relative to the host rocks. This is not a universally applicable condition because some massive sulphides in other areas being investigated have higher velocities. Full sonic waveforms were recorded and these will be further studied to extract S-wave velocities. The P- and S-wave velocity and amplitude logs will then be used to derive valuable geotechnical information.

Résumé : On a utilisé une sonde diagraphique de vitesse acoustique pour obtenir des données sur les caractéristiques sismiques du gisement nickélifère de McConnell dans la région de Sudbury. Les résultats préliminaires indiquent que la séquence stratigraphique associée aux sulfures massifs présente des vitesses d'ondes nettement différentes. Ces différences sont liées à la densité et aux propriétés élastiques des roches; la densité a été mesurée dans le même trou à l'aide d'une sonde diagraphique de densité. On a relevé une observation intéressante, soit que la vitesse des ondes P est faible dans les sulfures massifs à densité élevée, comparativement à la vitesse dans les roches encaissantes. Cette caractéristique n'est pas universelle, car certains sulfures massifs à l'étude ailleurs présentent des vitesses plus élevées. Des trains d'ondes acoustiques complets ont été enregistrés et feront l'objet d'études plus détaillées visant à déterminer la vitesse des ondes S. Les diagraphies de la vitesse et de l'amplitude des ondes P et S serviront à dériver des renseignements géotechniques utiles.

[1] Contribution to Canada-Ontario Subsidiary Agreement on Northern Ontario Development (1991-1995), under the Canada-Ontario Economic and Regional Development Agreement.

INTRODUCTION

An accurate knowledge of the acoustic velocity of P waves in the various lithologies encountered will aid the application of seismic methods (such as surface seismic reflection and hole to hole tomography) to base metal exploration.

Although acoustic velocities can be determined in the laboratory on rock samples or drill core, greater accuracy is possible with in-situ borehole measurements using an acoustic velocity logging tool. The Borehole Geophysics Section of the GSC has begun acoustic velocity logging using a tool with a piezoelectric transducer for an energy source, and two piezoelectric transducer receivers separated by 30 cm. The difference in arrival times of the transmitted pulses (P waves) at the two fixed receivers is converted to a velocity measurement. In addition, the amplitude of the first arrival is recorded as an amplitude log, which can be used to give a qualitative measurement of the attenuation factor (Q). The equipment, manufactured by Mount Sopris Instrument Co. of Colorado, records the full sonic waveform, making it possible to reprocess the field data to improve the precision of the first arrival picks, or in some cases, to pick the arrival time of the slower S waves which will provide additional information on the mechanical properties of the rocks.

By pulsing the energy source every half second and recording alternately with the 2 receivers, an average velocity is obtained every second, which, at a logging speed of 3 m/min, represents a sample every 5 cm in the borehole.

The physical characteristics of the acoustic velocity probe are shown in Figure 1. The 45 mm diameter probe consists of 2 sections: the transmitter section, and the receiver section, separated by a flexible acoustic isolator 0.5 m long. The manufacturer recommends a logging speed of less than 40 ft/min (12 m/min).

Tests were run at the GSC's Bells Corners Borehole Geophysics Test Site near Ottawa (Killeen, 1986; Schock et al., 1991) to gain experience with recording at different logging speeds from 0.5 to 10 m/min. Two of the four preset gains in the probe were also tested. The probe should be centralized in the hole with suitable flexible rubber spacers (centralizers). This is a relatively simple matter in the NQ test holes (75 mm diameter) with the 45 mm diameter probe. However in inclined holes typical of Canadian shield mineral exploration, centralizing the probe is more difficult. In a BQ (60 mm diameter) borehole, there is little space for a centralizer around the probe. The logging data from the McConnell deposit discussed below were acquired without a centralizer.

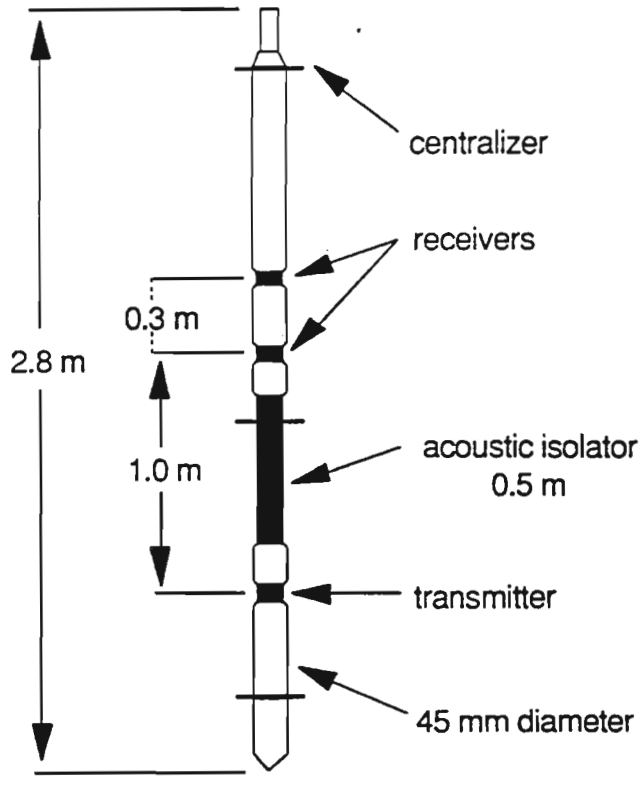

Figure 1. Acoustic velocity probe; not to scale (model CLP-4681, Mount Sopris Instrument Co.).

DATA PROCESSING METHODS

During data acquisition, the arrival time of the transmitted pulse at each receiver is determined when the signal crosses a threshold level selected by the operator. The thresholds of the two receivers can be set independently. As different rock types are traversed, the received signal amplitude may vary and sometimes not cross the threshold until the second (or later) cycle in the waveform. When this occurs at the far receiver but not the near receiver the travel time between receivers appears anomalously long. This "cycle skipping" results in apparent low velocity spikes in the velocity logs. Spikes may also be generated in the logs if the system triggers early on noise at the front of the waveform; this can be a problem in inclined holes where the probe is subjected to vibrations as it moves along the borehole wall.

Reprocessing the data to remove these spikes generally requires locating the spikes in the log, examining individual waveform pairs and adjusting the thresholds such that the first arrivals are correctly picked. This can be tedious if the data are particularly noisy. Preliminary tests suggest that reprocessing the data by cross-correlating the near and far waveforms against each other (Scott and Sena, 1974) to determine the travel time of the first arrival removes most of the spikes in the velocity log. The method is simple to automate and may be useful in determining the velocities of later arrivals.

THE McCONNELL NICKEL DEPOSIT

As part of a project within the Northern Ontario Development Agreement (NODA), the GSC is working to establish borehole geophysics test sites at major deposit-types in Ontario. The McConnell deposit (Garson Offset) represents the nickel (pentlandite, pyrrhotite, chalcopyrite) deposits of the Sudbury area. First described in a 1992-93 NODA summary report (Mwenifumbo et al, 1993), a fence of five holes intersecting

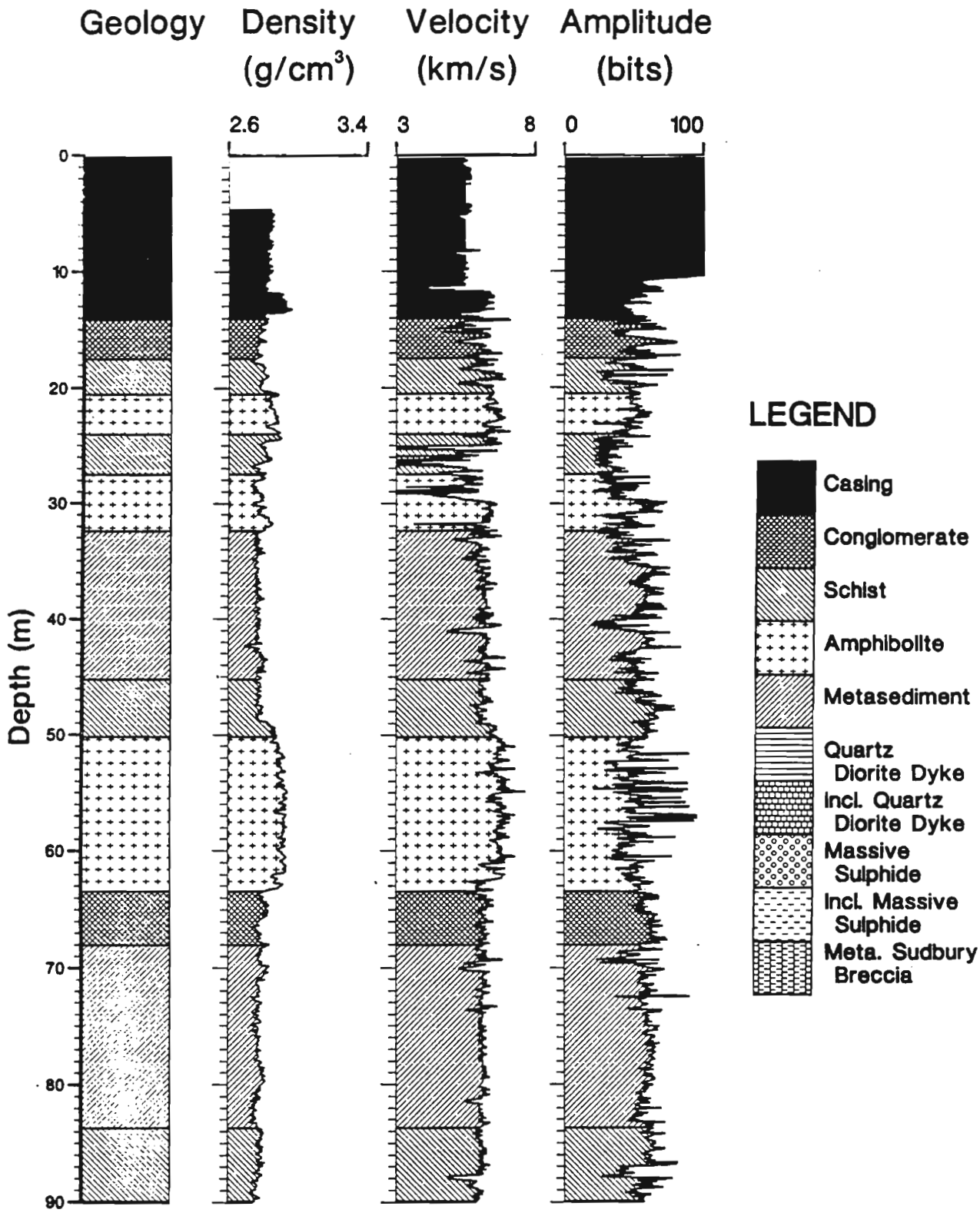

Figure 2. Density, acoustic velocity and amplitude (P wave) logs for the top half of hole 78930, McConnell deposit (Garson Offset), Sudbury, Ontario.

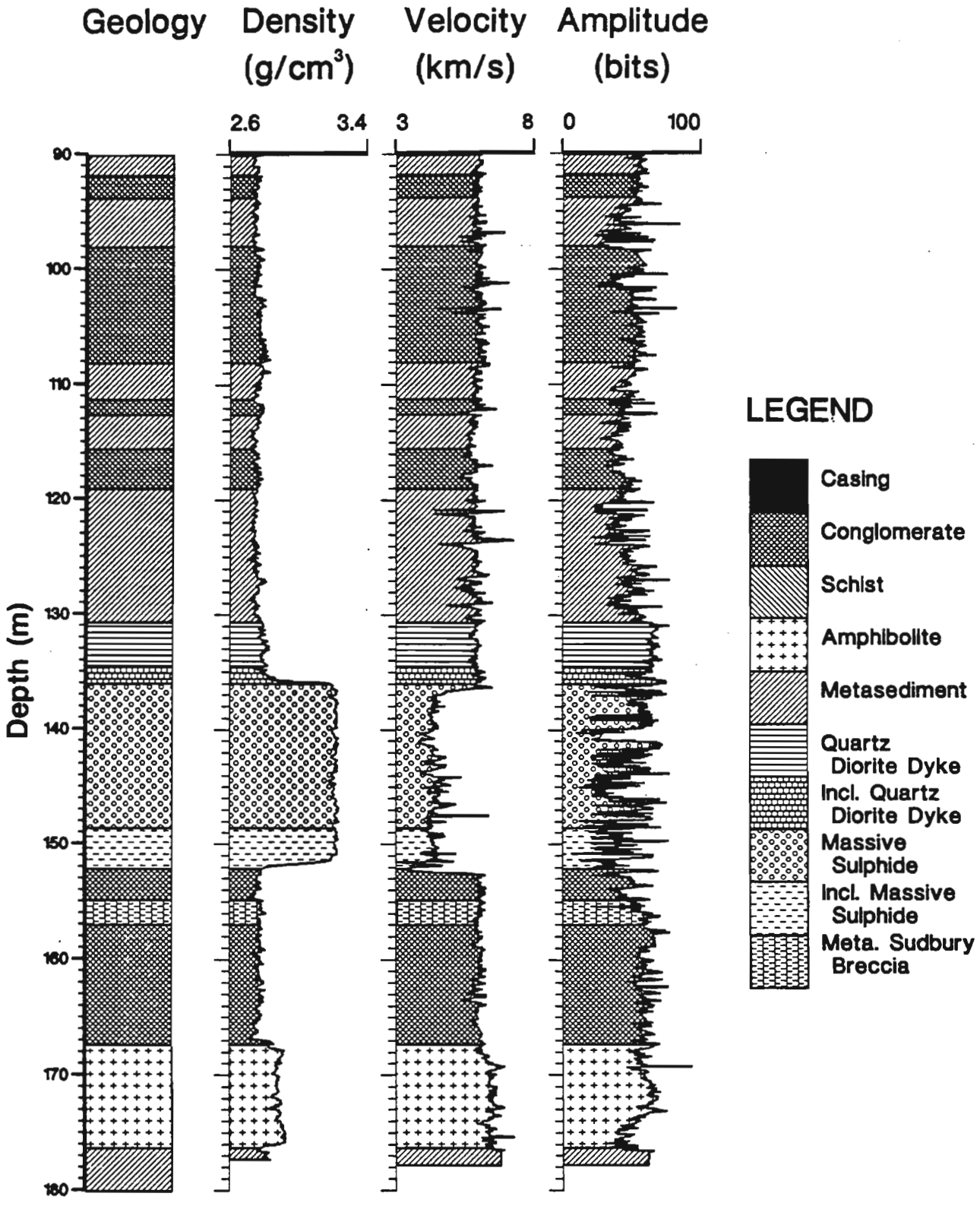

Figure 3. Density, acoustic velocity and amplitude (P wave) logs for the bottom half of hole 78930, McConnell Deposit (Garson Offset), Sudbury, Ontario.

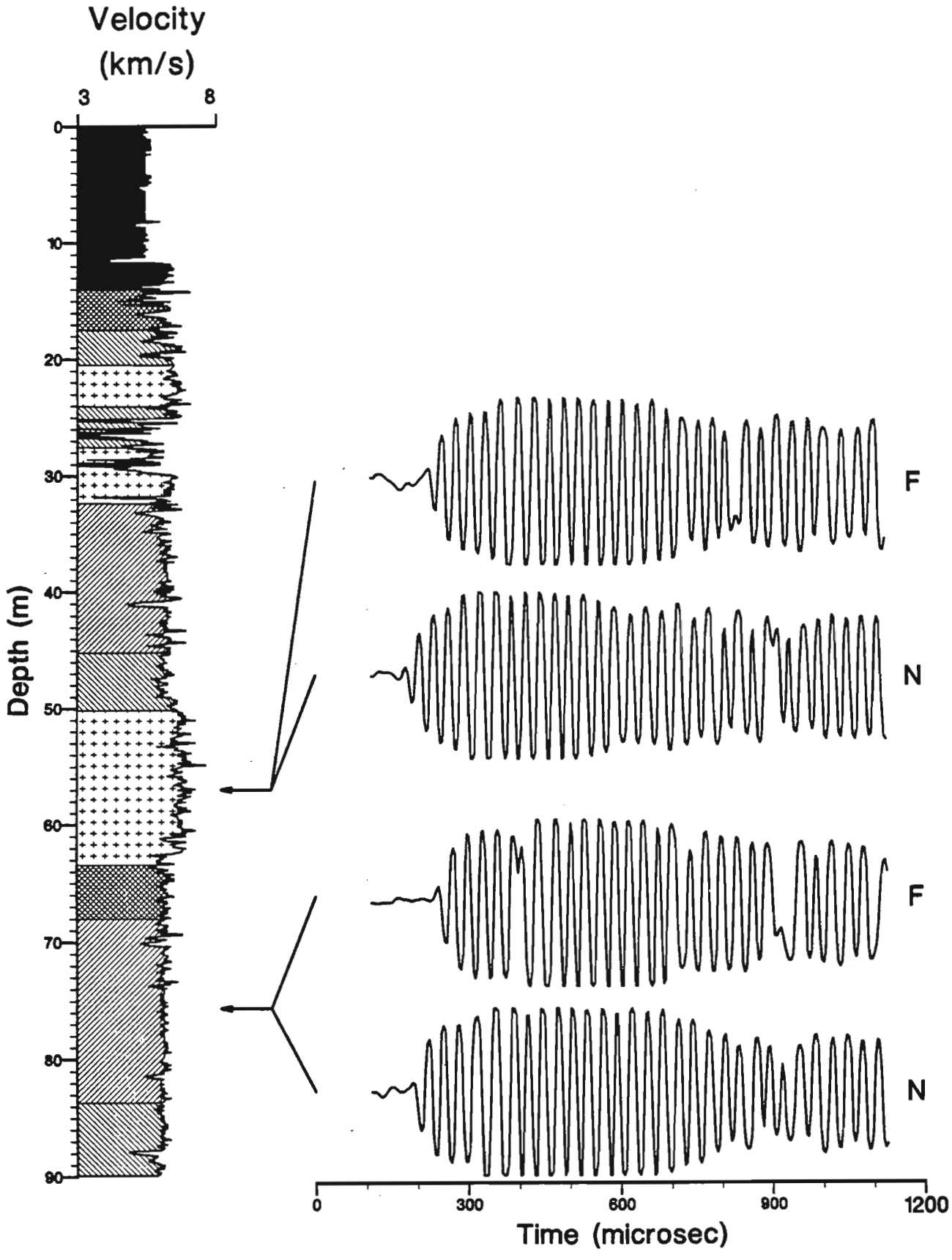

Figure 4. Typical waveforms recorded at the near (N) and far (F) receivers in the amphibolite (50-63 m) and metasediment (68-83 m) for the top half of hole 78930.

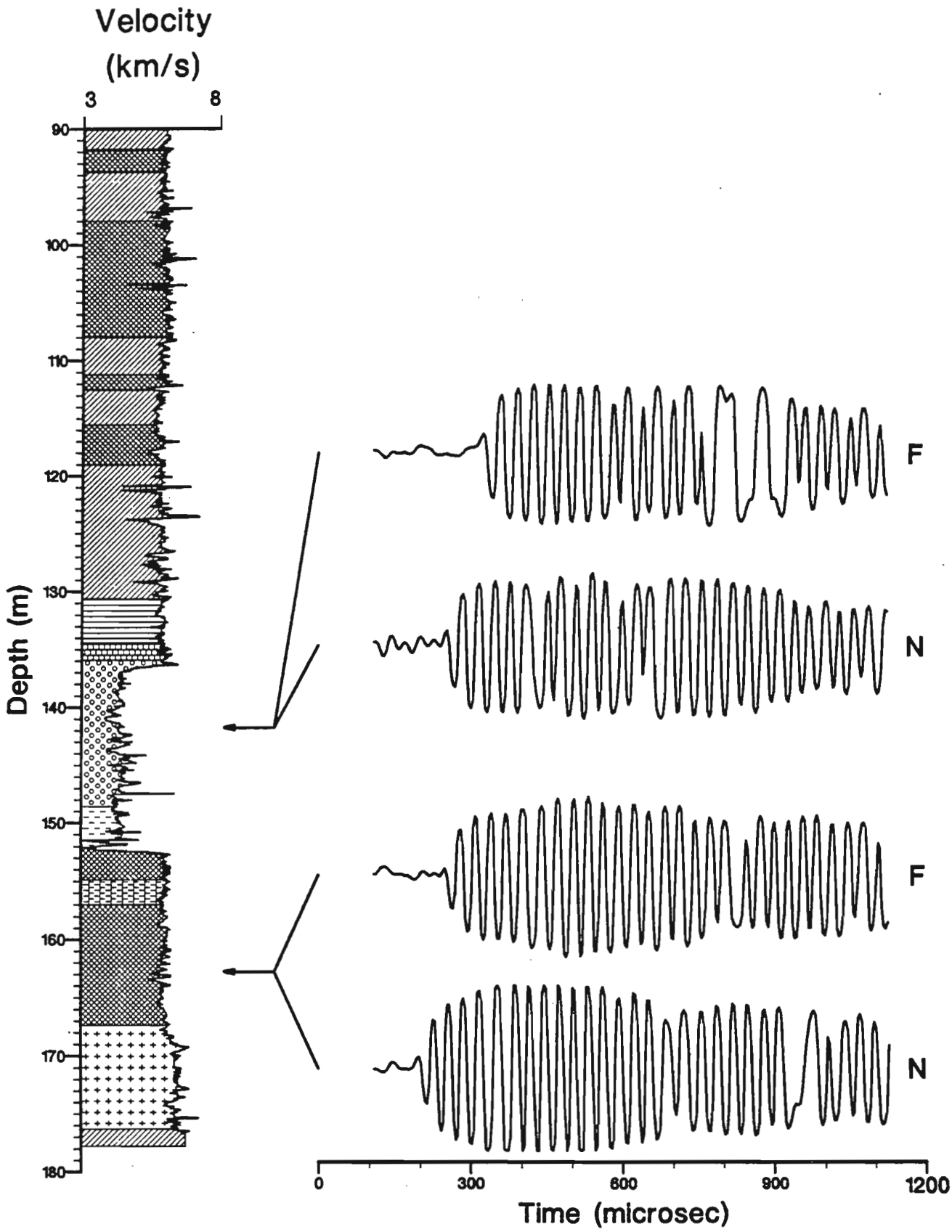

Figure 5. Typical waveforms recorded at the near (N) and far (F) receivers in the massive sulphides (136-148 m) and conglomerate (157-167 m) for the bottom half of hole 78930.

the ore body has now been logged with numerous geophysical parameters. The stratigraphic sequence which contains the massive sulphides consists of schists, amphibolites, conglomerates, metasediments, Sudbury breccia and quartz diorite dykes. The massive sulphides form a steeply dipping ore body which extends from the surface to a depth of about 350 m. The body is intersected at depths of 50 m in the shallowest hole, and about 300 m in the deepest hole.

The acoustic velocity probe was run in the middle hole in the fence, which intersected the massive sulphides at about 150 m. Figures 2 and 3 show the acoustic velocity and amplitude logs recorded in the borehole at 3 m/min, plotted with the density log. The density and acoustic velocity are related as follows:

$$Vp = \sqrt{(\lambda + 2\mu)/\rho} \qquad (1)$$

where Vp is the P-wave velocity, ρ is the density, λ is Lamé's constant and μ is the shear modulus. The velocity log has been edited to remove spikes due primarily to triggering on noise at the front of the waveform. The amplitude log has not been filtered in this way so it appears noisier.

A few selected recorded waveforms are shown with the acoustic velocity log in Figures 4 and 5. The amplitude variations in these waveforms (and in the P-wave amplitude logs) are suppressed because the acoustic signal is passed through a logarithmic amplifier in the probe. In the waveform displays, the signal that first crosses the preset threshold is the down-going motion evident at the front of the packet of seismic energy. This down-going pulse has a small amplitude relative to later arrivals in the wave train. The velocity logs and the amplitude logs refer to this signal as the first arrival (P wave).

The density log in Figure 2 shows that the density of the amphibolite from 50 to 63 m depth is relatively homogeneous and higher than the adjacent schist and conglomerate. The acoustic velocity is also higher (~6.7 km/s) than the schist (~6.0 km/s) or conglomerate (~6.1 km/s). Typical waveforms for the amphibolite zone for both the near and far receivers are shown in Figure 4. The velocity measured in the metasediment from 68 to 83 m is relatively constant at about 6.0 km/s. The first arrival amplitudes (Fig. 2) as exemplified by waveforms for near and far receivers (Fig. 4) are slightly higher on average (and less noisy) for the metasediment than for the amphibolite, suggesting the P waves are attenuated more by the amphibolite than the metasediment.

Figures 3 and 5 show the lower half of the hole from 90 to 180 m and include the massive sulphides between 136 and 148 m depth. Note the very high (and relatively constant) density within the sulphides. The acoustic velocity log indicates a velocity of less than 5.0 km/s in the ore and a sharp contrast between the velocity in the ore and in the host rocks. The ore is a low velocity zone. The amplitude log also shows a relatively low average value but this is mostly due to triggering on noise in front of the transmitted pulse. The correct value for the average amplitude lies between the values in the amphibolite and metasediment. Typical waveforms in the massive sulphides are shown in Figure 5. These were selected from a zone in which the amplitude of the first arrival was quite high. Below the ore zone, from 157 to 167 m, is a relatively homogeneous conglomerate zone with density about equal to the metasediments (Fig. 2), but a slightly lower velocity (5.9 km/s). The amplitude log in the conglomerate is about the same level as in the metasediment but more variable, implying the P-wave attenuation in the conglomerate is similar to but more variable than that in the metasediment. (See also the recorded waveforms for the near and far receivers, Fig. 5.)

CONCLUSIONS

Acoustic logging can provide detailed measurements of compressional wave velocity as well as measurements of the attenuation of seismic energy in the immediate vicinity of a borehole. As well as being lithological indicators, these measurements provide valuable information for seismic reflection or tomographic surveys or modelling. Additionally, they can be used to determine physical properties of the rocks encountered. This will be the subject of more detailed investigation in the future. It is also possible to pick the arrival time of the slower S waves, which are hidden in the recorded waveform. The P wave is the first arrival in the wave train, and hence is reasonably easy to pick. Poisson's ratio which relates to the mechanical properties of the rocks, can be determined from the ratio of the velocities of the P and S waves. S-wave analysis will be investigated as further experience is obtained with acoustic logging in different ore environments. Methods of enhancing the data and improving the speed and ease of extracting information from the raw data are presently being tested.

We see this as a significant development leading to reliable determination of velocities in a wide diversity of rocks associated with base metal (and gold) deposits. These data will be extremely useful for practitioners of surface reflection seismic surveys, and for surface to borehole, or hole to hole seismic tomography. In addition, geotechnical engineering parameters of importance in mining operations may be determined more accurately (in situ) over larger and more representative volumes of rock (than laboratory samples), using acoustic logging techniques.

ACKNOWLEDGMENTS

The authors wish to thank Barry Krause and Alan King of INCO Exploration and Technical Services Inc. for their help in establishing the McConnell deposit as a test site for borehole geophysics. We are grateful to Yves Blanchard for modifying the equipment to operate with our logging system. We thank Susan Pullan for critically reviewing the manuscript.

REFERENCES

Killeen, P.G.
1986: A system of deep test holes and calibration facilities for developing and testing new borehole geophysical techniques; in Borehole Geophysics for Mining and Geotechnical Applications, (ed.) P.G. Killeen; Geological Survey of Canada, Paper 85-27, p. 29-46.

Mwenifumbo, C.J., Killeen, P.G., and Bernius, G.R.
1993: Ore deposit signatures by borehole geophysics; in Summary Report, 1992-93, Northern Ontario Development Agreement, minerals, (ed.) N. Wood, R. Shannon, L. Owsiacki, and M. Walters; co-published by Energy, Mines and Resources Canada, p. 123-125.

Schock, L.D., Killeen, P.G., Elliott, B.E., and Bernius, G.R.
1991: A review of Canadian calibration facilities for borehole geophysical measurements; in Proceedings of the 4th International MGLS/KEGS Symposium on Borehole Geophysics for Minerals, Geotechnical and Groundwater Applications, Toronto 18-22 August, 1991, p. 191-202.

Scott, J.H. and Sena, J.
1974: Acoustic logging for mining applications; in Transactions of the Fifteenth Annual Logging Symposium; Society of Professional Well Log Analysts, Paper P, June 2-5, p. 1-11.

Geological Survey of Canada Project 880030

SURVEYING THE PATH OF BOREHOLES: A REVIEW OF ORIENTATION METHODS AND EXPERIENCE

P.G.Killeen, G.R.Bernius and C.J.Mwenifumbo
Geological Survey of Canada, 601 Booth St., Ottawa, K1A 0E8

P.G.Killeen, G.R.Bernius and C.J.Mwenifumbo, Surveying the Path of Boreholes: A Review of Orientation Methods and Experiences; in *Proceedings of the 6th International MGLS Symposium on Borehole Geophysics for Minerals, Geotechnical and Groundwater Applications; Santa Fe, New Mexico, October 22-25, 1995.*

ABSTRACT

Boreholes are designed to obtain information in the third dimension, ie. at depth, below the two-dimensions of the earth's surface. Today it is relatively easy to determine position on the surface, but not so at depth. Unfortunately, all too often, the path of the hole is erroneously assumed to follow the original dip (or inclination) and azimuth (or direction) established at the collar, at the top of the hole. Numerous borehole surveying devices have been developed, none of which are perfect, however quite accurate results are possible by using the right tool in the right hole.

Surveying a borehole is usually accomplished by moving a probe along the hole and sensing the movement of the probe relative to one or more frames of reference which may include the earth's gravitational field, magnetic field or other inertial reference, and/or by sensing the distortion or bending of the housing of the probe itself. The different methods each have their own advantages and limitations such as ability/inability to operate inside steel casing, speed and complexity of operation, accuracy, cost, distance between measurements, ruggedness and reliability.

The Borehole Geophysics Section of the Geological Survey of Canada has reviewed and compared many of the available methods, and has experience surveying a borehole with five different commercially available systems. There is no 'winner', but a review of the above-mentioned is useful in selecting the appropriate borehole surveying methodology.

INTRODUCTION

Only under ideal conditions will the path of a drilled hole follow the original dip (or inclination) and azimuth (or direction) established at the top of the hole. It is more usual that the borehole will deflect away from the original direction as a result of layering in the rock, the variation in the hardness of the layers, and the angle of the drill bit relative to these layers as illustrated in **Figure 1.** The drill bit will be able to penetrate the softer layers easier than the harder layers, resulting in a preferential direction of drill bit deviation. In some areas experienced drillers have been able to predict the deviation somewhat, and adjust the dip and azimuth of the collar of the hole such that when the drill reaches the desired depth, it will be travelling in the desired azimuth and dip. Deviation of the borehole is encountered in both 'soft-rock' and 'hard-rock' drilling. In base metal exploration for example, the strata being drilled are usually geologic units in a volcanic pile, often dipping very steeply. Drilling perpendicular to a steep dip is almost impossible and the drill bit will definitely penetrate the layers at a more shallow angle than 90 degrees.

Because the purpose of a borehole is to obtain information in the third dimension, i.e. at depth, the location is just as important as the information itself. Most often the information consists of the geology of the drill core, or assays of the core at selected depths. If the hole has deviated significantly, then that information can not be properly assigned to a location in 3-dimensional space beneath the earth's surface. Conclusions about geological structure or models of the size, shape, tonnage and average grade of ore-bodies based on the 'mis-placed' information may be erroneous.

Numerous borehole surveying devices have been developed, none of which are perfect. However, quite accurate results are possible by properly using the right tool in the right hole. Surveying the path of a borehole is referred to as a borehole 'orientation' survey or a 'deviation' survey, and 'dip' at any point refers to the angle between the horizontal and the path of the hole. 'Inclination' is used by some workers to refer to the angle between the vertical and the hole, although in some literature inclination is used (incorrectly) as a synonym for dip. Another confusion is created by the logging tool called the 'dipmeter' which does not survey the path of a hole but measures the dip of strata relative to the hole. This is usually acomplished with an array of multiple electrodes which touch the wall of the hole and sense the dip of the beds intersected by the hole.

Surveying a borehole is usually accomplished by moving a probe along the hole and sensing the movement of the probe relative to one or more frames of reference which may include the earth's gravitational field, magnetic field or other inertial reference, and/or by sensing the distortion or bending of the housing of the probe itself. Different methods have their own advantages and limitations. Some have the ability to operate inside steel casing, and others cannot. Some methods are time consuming and others are fast. Some are relatively simple to use and others are complex to operate.

Other considerations are accuracy, cost, distance between measurements, ruggedness and reliability.

The Borehole Geophysics Section of the Geological Survey of Canada has reviewed and compared many of the available methods, and has experience surveying boreholes with several different systems. A review of methods for surveying a borehole follows, based roughly on the chronological evolution of the technology. Experience with five different commercially available systems is illustrated with a comparison of survey results from a single borehole in the Val d'Or area of Quebec. A review of the above-mentioned experience is useful in selecting the appropriate borehole surveying methodology.

SURVEYING A BOREHOLE

A survey of a borehole should provide an accurate plot of the path of the hole in 3-dimensional space, i.e. the (x,y,z) coordinates (northing, easting, true depth) of every point along the path is known. In practice, the coordinates of a finite number of points are determined, and the path between these points is calculated by extrapolation. From this, it should be obvious that: the greater the number of known data points, the less extrapolation required, and the more accurate the survey. The coordinates of points are not measured directly, but are computed from measurements of the dip, azimuth and length-along-the-hole (usually called 'depth'), as shown in **Figure 2**. These are the three components of the 'hole vector', The first data set are the dip, azimuth, and depth (which is zero) at the collar of the hole. The (x,y,z) coordinates of the top of the hole are based on the surface survey grid being used in the area, and of course do not have to be computed from the dip and azimuth data. However, along the length of the hole the dip and azimuth will change from that at the collar.

Measuring length along the hole is relatively easy, although not a trivial problem. The calibration of the pulley or sheave wheel and the depth encoder attached to it is subject to error, since it relies on an accurate determination of the number of pulses from the encoder for each metre of cable that passes over the pulley. In addition, the cable used for the depth measurement may stretch, or it may effectively increase in diameter due to icing conditions in winter, or the pulley may effectively increase in diameter for the same reason, or decrease diameter due to wear. A one percent error in depth measurement, for example, may mean a 5 metre depth error at a depth of 500 metres, and this could be larger than the error caused by precision dip and azimuth measurements. This review, however, is primarily concerned with dip and azimuth measurements.

The Acid Etch Clinometer: One of the earliest and simplest surveying devices is based on a measurement inside the drill rod with an acid bottle **(Figure 3)**. A 4% hydrofluoric acid solution etches the wall of the glass etch tube leaving a permanent record of the dip of the hole, which can be read upon retrieval of the probe (Urban and Diment, 1989). Etching time is a minimum of 20 minutes, but as soon as the etching time

has elapsed, the drilling can begin again. Further etching is slight and does not erase the etch line made while stationary. In a deep hole, etching time (stationary) must be increased to equal the time required to lower the device to the measurement depth, which may be up to 2 hours. In about 4 hours the acid will have neutralized. The acid etch device will fit inside the smallest diameter drill rods (size E). The method is still in use today usually for a single measurement at the bottom of a hole when drilling has stopped. This gives a 'quick and dirty' indication of hole deviation, but it provides dip information only.

The path of the hole could be in any direction on a cone of equal dip as shown in **Figure 4**, until the azimuth with respect to North is also measured. Even if the dip of the hole were known at numerous points along the hole, the true path could be virtually anywhere as illustrated in **Figure 5**. Here, three dip measurements are made along the path of a borehole, and the three cones of equal dip angle are shown. The azimuth of the hole is also included on each cone to illustrate three straight-line segments of the hole. It is easy to see that without the azimuth information, there is an infinite number of possibilities for the true path of the hole based on dip measurements alone.

The Tropari (and its successor the Pajari): In this instrument, a compass and clockwork mechanism are mounted on gimbals with the bottom side weighted to maintain the gravitational vertical reference (i.e. as an inclinometer) as it moves freely in its housing **(Figure 6a, 6b, and 6c)**. It is lowered in the hole to the measurement depth, and at a preset time the clock locks all the moving parts and the tropari is retrieved from the hole to read the dip and magnetic azimuth value at that measurement depth. The dip is measured to within 1 degree and the azimuth is read to the nearest half degree. Two versions are available with a maximum time period of 90 or 150 minutes. The clockwork locking takes place in the last 10 minutes of the set time period, during which time the instrument should be stationary in the hole. Measurements are usually made at 50 or 100 m intervals in the hole, depending on the depth of the hole and the desired accuracy. The device will fit inside an EX (46 mm) hole. It is available with pressure rating to 1675 metres depth and with thermal housing for temperatures over 100 degrees celsius. It can be run in an open hole on a wireline, or at the end of a drill string by raising the drill-rod string 6 or 7 metres and allowing the tropari to pass through the drill bit to a position about 5 m away from it. The tropari, a Canadian invention, is still widely used in mineral exploration in Canada and throughout the world.

The Magnetic Single Shot: Using basically the same principle as the tropari, the magnetic single-shot replaces the clockwork locking mechanism with a camera that takes a photo (shot) of the dip and compass needle at the measurement depth. The probe is then retrieved to read the film disc. Probably the most widely used version is that developed by Sperry-Sun Drilling Services, Inc. (see **Figure 7a, 7b, 7c and 7d)** which is available in two diameters: the standard "A" size of 1.75" (44 mm) diameter and the "B" size of 1.38" (35 mm) diameter, and thermal shielding is available for hot holes. The

'shot' is taken at a time based on several possible mechanisms, including a timer, a motion sensor that senses when the probe has stopped moving, or a magnetic sensor that senses when the probe has reached a special nonmagnetic section of the drill rod near the drill bit. The insertion and removal of the film disc is done quickly through a slot in the housing. Development of the film disc takes about five minutes. The disk is placed in a magnifying reader to determine the dip and azimuth measurement.

The Magnetic Multi-shot: Sperry-Sun made a significant advance by installing in the probe, an 8mm film camera **(Figure 8)** that takes photos of the dip and azimuth readings at several measurement depths in one trip in the hole. Krebs (1964) described such a multiple exposure system as early as 1964. The multishot timer advances the film and turns on the battery-powered lights at each measurement. Normal operation consists of synchronizing a stopwatch with the camera and taking note of the time at each measurement-depth where the probe is stopped for about 45 seconds. Since the standard time interval between shots is 20 seconds, one or two good (stationary) readings will fall within the 45 second stopover. The "A" size tool holds 6 hours (1000 readings) of film at 20 second times and the "B" size tool holds 3 to 14 hours of film depending on a variable clock setting which may be set from 15 seconds to 1 minute. The film is developed on-site in a dark-bag and read in a projector fitted with a time counter/frame counter. The film is advanced to the times (frames) that correspond with the recorded measurement-depth/time data, and the dip and azimuth values are read.

Solid State Devices: Although it has been possible to measure magnetic field directions electronically for about 50 years, the physical size of the components was more suitable to installation inside an aircraft than a borehole probe. However as miniturization of electronic devices evolved, this changed. Holm (1964) utilized a compass and pendulum mechanism which could be recorded electrically and remotely at the surface. In recent years, new hardware was adapted from satellite and guided missile technology for use in logging tools. The magnetic compass was replaced by a ring-core fluxgate magnetometer (**Figure 9**) and the dip measurement was made by solid state tilt-meters or accelerometers with no moving parts.

The solid state tiltmeters are oriented orthogonal to each other in the probe to measure dip, and at the same time compensate for roll of the probe as it moves in the hole. The tiltmeters consist of an electrolyte which half fills the space between two conductors on opposite sides of a disc-shaped glass container. As the container rotates (tilts), the electrolyte moves, changing the resistance between the conductors on opposite sides, which is calibrated in terms of the degree of tilt (Balch and Blohm, 1991). The accelerometers use the principle of sensing the position and movement of a 'pendulous mass', as it tries to move when the probe tilts, and driving it back to a 'zero' position with a servo-motor. The current required to drive the motor is proportional to the degree of tilt.

Dip and azimuth data are transmitted to the surface in real time for recording and display as exemplified by probes developed by OWL Technical Associates Inc., USA and IFG Corp., Canada or stored in solid state memories in the probe (e.g. Boretrak, UK).

These three typical examples of the technology use 38 mm (1.5") diameter probes.

OWL (**Figure 10**) quotes a sensitivity of 0.1 degrees (maximum RMS error of +/- 0.2 degrees) over a range of dip from 90 degrees (vertical) to 10 degrees. The azimuth has a sensitivity of 1 degree (maximum RMS error +/- 2 degrees) over a range from 0 to 359 degrees. A special version is available which extends the range of dip measurements to include a full sphere (i.e. 360 degrees).

IFG (**Figure 11**) quotes a sensitivity (resolution) of 0.1 degrees (overall accuracy better than 0.5 degrees) over the entire range of dip from 89 degrees (nearly vertical) to 10 degrees, and an uncertainty of +/- 0.3 degrees for the azimuth over a range from 0 to 359 degrees (Balch and Blohm, 1991; Killeen et al, 1996).

The Boretrak (**Figure 12**) claims a resolution of 0.01 degrees over a range of +/- 30 degrees of dip, and a maximum depth of 300 metres. The azimuth data are not measured and recorded but rather kept constant by means of fixed lightweight rods used to lower the probe in the hole. Early development of systems such as this were described by Roxstrom (1959) and Holz (1961).

Geographic North vs Geomagnetic North: Although the progression of the technology as described above was impressive, the magnetic azimuth must still be converted to geographic azimuth (**Figure 13**). The desired final computed coordinate positions of the borehole are with respect to the geographical coordinate system in which every point along the path of the hole has a northing, easting and vertical depth. However, the measurements described thus far, are made with respect to the geomagnetic field. The computed azimuth is a magnetic azimuth until it has been converted into a geographic azimuth. Using the declination of the local field, the magnetic coordinates of the borehole can be rotated into the geographical coordinate system. It is usual to obtain the value for the geomagnetic declination from regional geomagnetic declination and inclination maps.

Although these magnetic-based methods are adequate for most holes, surveys based on magnetic azimuth cannot be done inside steel casing, or where there are anomalous magnetic fields (discussed later). All of these considerations led to the development of non-magnetic systems.

Azimuth measurement based on gyroscopic platforms: The inertia of a spinning mass can be used as a stable reference for a series of directional measurements in a borehole. The gyroscope mechanism (**Figure 14**) replaces the magnetic compass, and its orientation with respect to geographic north must be determined at the collar of the hole. The inertia of the gyro and its stability (freedom from drift) are related to both the mass and its rate of spin. A spin of 40,000 rpm is common, and the jewelled bearings can wear out quickly, adding to the cost. However, surveys can be carried out inside metal pipe and in the presence of magnetic anomalies. Early versions were combined with a camera as in the 'Single-shot' device (see for example the Sperry-Sun gyro-based probe in **Figures 15, 16 and 17**). Recent versions called 'surface recording gyros' transmit the data to the surface digitally in real time. New optical gyros with virtually no moving parts, such as the ring-laser gyros described by Anderson (1986), may eventually replace the

mechanical gyroscopes.

Optical instruments; Light Beam Methods: A completely different borehole surveying technique is based on a light source in one end of a long rigid tube, with the lightbeam focused on a target in the other end of the tube. Bending of the tube as it moves in the borehole causes deflections of the light on the target, and this information is converted into borehole orientation survey data. The technique is not affected by magnetic fields and can be used inside metal pipe or drill rod. For best results, the probe should have only about 1 mm clearance between it and the wall of the hole for maximum sensitivity to the bending effect. This means that surveying inside the drill rod is actually preferable since it is safer than logging in an open hole where the chance of getting the probe stuck is greater.

In the first version, designed in Sweden (the 'Fotobor' (Hood, 1975), by Reflex Instruments AB; **Figure 18**), the illuminated target was a set of concentric rings and a level bubble, used as the vertical reference (**Figure 19**). A camera recorded the data on film (**Figure 20**) for processing and correlation with the time and depth data recorded at the surface. Another optical system made by Gyro-log Ltd., Canada; (**Figure 21**) uses the position of the lightbeam 'spot' on a target (**Figure 22**) (instead of rings) for measuring the bending of their 'Light-Log' instrument, and calculating the path of the hole. The most recent Swedish version (the 'Maxibor', **Figure 23**) detects the position of the rings with optical sensors and the data are recorded in a solid state memory in the probe for later processing and display at the surface.

RAW SURVEY DATA

Raw data consists of a series of dip and azimuth values measured at numerous depth points ranging from 100 m apart to less than 0.1 m apart depending on the method. The examples shown in **Figure 24** are the data from five surveys of a 950m deep borehole in the Val d'Or mining area of Quebec. Remember that the figures do not show the path of the hole, but rather the variation in the measured azimuth and dip plotted versus 'depth' which for raw data is actually 'length along the borehole'. The results include data from Tropari, Sperry multi-shot, OWL, IFG, and Maxibor surveys. All, except the Maxibor, rely on the earth's magnetic field for the azimuth determination. In figure **24a**, the measured azimuth values are plotted versus depth. The azimuth varies from 150 degrees (i.e.south-southeast) at the top of the hole, to an azimuth at the bottom of the hole of 170 degrees (almost due south), according to the magnetic-based methods, and 135 degrees for the optical method (Maxibor).

In summary, the magnetic methods indicate that the hole direction swung southward by about 20 degrees as it deepened but the optical method indicated the hole swung northward by 15 degrees. The magnetic methods produce absolute measurements at each depth and results of the survey are not dependent on previous measurements. Thus, even though the casing obviously affected the results of the OWL, IFG and Tropari tools near the surface, the survey data for the rest of the hole is unaffected. Note also the OWL and IFG tools 'saw' the two steel wedges in the hole at 350 and 450 metres, but make a 'recovery' as they leave the anomalous areas. It is interesting that the Maxibor

also 'saw' the two wedges as indicated by slight jogs in the azimuth log shown in **Figure 24a**. This is consistent with the fact that the wedges are placed in the hole to produce a correction factor (change the dip and/or azimuth) of a deviating borehole during drilling. The Sperry Multi-shot data points are about 30 or 40 m apart, and the Tropari data are 100 m apart and they did not detect the wedges. The dip data from all five tools plotted in **Figure 24b** seem to be in agreement. One Multi-shot data point at about 750 m appears to be anomalous and would not influence the survey results. However if we look at the results closely, the dip at the bottom of the hole is measured as 22 degrees by OWL and IFG, 26 degrees by Sperry and Maxibor, and 21 degrees by Tropari.

DESURVEYING

The raw dip and azimuth data must be converted into a plot of the path of the hole in 3 dimensional space by interpolating between measurement points as shown in **Figure 25**. Called 'desurveying' (Howson and Sides, 1986), a number of different algorithms can be used for the interpolation. After desurveying, the visual output is a display of the path of the hole projected on planes in an east-west or north-south direction, or in plan view one scheme of which is illustrated by **Figure 26**.

The selection of the desurveying algorithm is especially important if the data points are sparse and can be a large source of error if the wrong method is used. This is the case when only a few points in the hole have been measured with some of the slow borehole surveying devices. For example, a straight-line interpolation between measured points would be one desurveying method which could be used. However the true path of the hole doesn't usually follow straight line segments. Various computation methods involving curve-fitting between points have also been proposed. Reviews of the various methods of computing borehole position, and their possible errors have been presented by several authors including Walstrom et al., (1969), Walstrom et al., (1972), Harvey et al., (1971), Truex (1971) and Wolff and deWardt (1981). These methods include the Angle Averaging Method, Balanced Tangential Method, Radius of Curvature Method, and Minimum Curvature Method, details of which are beyond the scope of this paper.

Most modern orientation probes make measurements continuously, and these are sampled as often as every half-second. Measurements of dip and azimuth can be made every 5 cm along the path of the hole at a logging speed of 6 metres per minute for example. This data interval is much smaller than the length of the orientation probe itself. Because the interval between readings is so small, the borehole desurveying method used to compute the position coordinates of the hole will have very little effect on the results. Therefore, in that case, the simplest method which assumes a straight path between measurements may be chosen.

SOME SOURCES OF POSSIBLE ERROR IN GEOMETRY OF THE BOREHOLE

The effect of increasing the interval between measurements was investigated by Balch and Blohm (1991). They presented an example of a survey of a 600 m deep borehole using the IFG orientation probe. By using only part of the measured data, thus

simulating measurements at larger intervals, they recomputed the position of the bottom of the hole. In their worst case example with an average sample interval of up to 10 metres, the position of the bottom of the hole varied by about +/- 4 metres. They also compared logging continuously at 9m/minute with logging in an incremental mode, stopping every 5 metres in the hole. They found the error in computing the position of the bottom of the hole was within +/- 2 metres, between the continuous and incremental mode.

Balch and Blohm (1991) also considered possible errors in converting measured magnetic azimuths into geographic azimuths. They repeated the computations using the wrong geomagnetic declination, for the 600 m depth borehole used in their other field tests. By varying the declination up to one degree west (from 346° to 345°), the position of the bottom of the hole varied up to +/- 5 metres. They concluded that the error in the position of the bottom of the hole is more sensitive to errors in the value of the geomagnetic declination used in the computations, than the errors that might arise from the orientation probe measurements in the borehole. Killeen et al, (1996) summarized the other sources of possible error in a magnetic-based orientation probe, including errors due to:

1) Zero offset, 2) Gain adjustment, 3) Orthogonality, 4) Linearity, and 5) Temperature drift, all of which can be corrected by post-processing.

Another possible external source of error is the presence of anomalous magnetic fields caused by magnetite or other magnetic minerals nearby or intersected by the hole. Good results may be obtained when using the new magnetic orientation probes in boreholes where strongly magnetic (but relatively thin) units are present. This success is primarily a result of the high sample rate which provides closely spaced measurements making it possible to eliminate the erroneous measurements. In the case where the magnetic anomalies are large and broad in extent, they will effectively swing the apparent azimuth of the hole around in the direction of the source of the anomaly. The possibilities for using this to detect the location of off-hole magnetic bodies was also briefly discussed by Killeen et al (1996).

RESULTS OF FIVE DIFFERENT SURVEYS IN A SINGLE BOREHOLE

The five raw data sets were desurveyed using straight-line interpolation as mentioned above, and the resulting five paths of the hole are displayed together for comparison. The geographical path of the Val d'Or borehole is displayed in four different ways: in **Figure 27a** as the projection of the path of the hole in a North-South vertical section, in **Figure 27b** as an East-West vertical section, in **Figure 27c** as a plan view, and in **Figure 27d** as a combination of all of the above views in a wire grid box showing the path in "3-D".

It is instructive to observe the differences in the computed paths of the hole as shown in their different projections. The North-South section (**Figure 27a**) shows the true vertical depth to be about 750 m. The Tropari and Maxibor paths are almost identical, but they show the hole bottom to be located about 100m north of the position indicated by the OWL, IFG and Sperry paths. In the East-West section (**Figure 27b**), the Tropari

and Sperry paths agree, the OWL and IFG paths agree but show the hole bottom to be about 40 m further east, and the Maxibor indicates the hole bottom is an additional 150 m further east. The plan view (**Figure 27c**) shows how the magnetic methods roughly group together. The optical method (Maxibor) indicates a significantly different hole path. The path of the hole shown as a dashed line in the '3-D' view (**Figure 27d**) is based on the IFG tool alone, since plotting all five paths and their projections (the solid lines) would be too confusing.

DISCUSSION AND CONCLUSIONS

It must be remembered that there is no 'right answer' in this case. For example, there may be a magnetic anomaly affecting the results of four of the surveying probes, but not the Maxibor. Even among the magnetic-based methods, there are significant differences in the computed path of the hole. These data should give the reader some qualitative appreciation at least, of the possible errors in surveying boreholes with today's technology. It is unfortunate that a gyro-based method was not included here, but the hole had to be cemented due to mining constraints before a gyro tool became available. It is hoped to be able to find a hole which breaks through into a mine drift, at a future date. In that case, the exact position of the bottom of the hole could be determined with traditional engineering survey methods and this could be used as a basis for a more definitive comparison of the results.

ACKNOWLEDGEMENTS

The authors would like to acknowledge the contributions to this study by Aur Resources, Val d'Or, who provided the hole and the Multi-shot data, and in particular we thank Yves Rougerie and Louis Martin. We also acknowledge the material used in the illustrations of the borehole surveying equipment, much of which originated in company brochures. In particular we thank Steve Balch of IFG Corp. for his constructive comments, Cris Lovett of OWL Technical Associates for probe details, Measurement Devices Limited for the Boretrak information, Reflex Instruments AB, for the Fotobor and Maxibor information and BHP Minerals Canada Ltd., for the loan of their Maxibor, Gyro-Log Ltd. for the Light-Log data, J.K.Smit & Sons International Ltd. for the Acid Etch Clinometer data, Pajari Instruments Ltd. for the Tropari data, Sperry-Sun Drilling Services of Canada for the Single-shot, Multi-Shot and Gyro data, and Steve Birk and Doug Robinson of the GSC, for their contributions to the field tests. We also thank Sue Davis for production of all of the line drawings and Rob Kelly and Gilles Lemieux for the photographs.

REFERENCES

Anderson D.Z., 1986. Optical Gyroscopes; Scientific American, Vol. 254, No. 4, p 94-99.

Balch S.J. and Blohm D., 1991. Development of a new borehole orientation probe; in Proceedings of the 4th International MGLS/KEGS Symposium on Borehole Geophysics for Minerals, Geotechnical and Groundwater Applications; Toronto, 18-22 August, p. 9-20.

Harvey, R.P., Walstrom, J.E. and Eddy, H.D., 1971. A mathematical analysis of errors in directional survey calculations; Journal of Petroleum Technology, Nov. 1971, p. 1368-1374.

Holm, A., 1964. An instrument for the determination of drill hole geometry; Geoexploration, Vol. 2, No. 1, p 20-27.

Holz, P., 1961. New electronic instrument to survey boreholes; Canadian Mining Journal, Vol. 82, No. 1, p 45-46.

Hood, P.J., 1975. Mineral Exploration: Trends and developments in 1974; Canadian Mining Journal, Vol. 96, No. 2.

Howson, M. and Sides, E.J., 1986. Borehole desurvey calculations; in Computers and Geosciences, Vol. 12, No. 1, p. 97-104.

Killeen, P.G., Mwenifumbo, C.J. and Bernius, G.R., 1996. Development of a borehole surveying probe using 3-component fluxgate magnetometers; in EXTECH I: A Multidisciplinary Approach to Massive Sulphide Research in the Rusty Lake-Snow Lake Greenstone Belts, Manitoba, (ed.) G.F. Bonham-Carter, A.G. Galley and G.E.M. Hall; Geological Survey of Canada Bulletin 426. (in press).

Krebs, E., 1964. Modern borehole surveying; Mining Magazine, Vol. 3, No. 4, p. 220-233.

Roxstrom, E., 1959. Craelius EM bore-hole dip indicator; Canadian Mining Journal, Vol. 80, No. 11, p. 78-84.

Truex, J.N., 1971. Directional survey problems, east Wilmington Oil Field, California; Bulletin, AAPG, April 1971, Vol. 55, No. 4, p. 621-628.

Urban, T.C., and Diment W.H., 1989. Capillary corrections for acid-etch inclinometry in boreholes for glass tubes ranging in diameter from 6-25 mm and over a temperature range of 4-80 degrees C; in Proceedings of the 3rd International MGLS Symposium on Borehole Geophysics for Minerals, Geotechnical and Groundwater Applications; Las Vegas, 2-5 October, p. 233-260.

Walstrom, J.E., Brown, A.A. and Harvey, R.P., 1969. An analysis of uncertainty in directional surveying; Journal of Petroleum Technology, April 1969, Vol. 21, p. 515-523.

Walstrom, J.E., Harvey, R.P. and Eddy, H.D., 1972. A comparison of various directional survey models and an approach to model error analysis; Journal of Petroleum Technology, August 1972, p. 935-943.

Wolff, C.J.M., deWardt, J.P., 1981. Borehole position uncertainty - analysis of measuring methods and derivation of systematic error model; in Journal of Petroleum Technology, December 1981, p. 2339-2350.

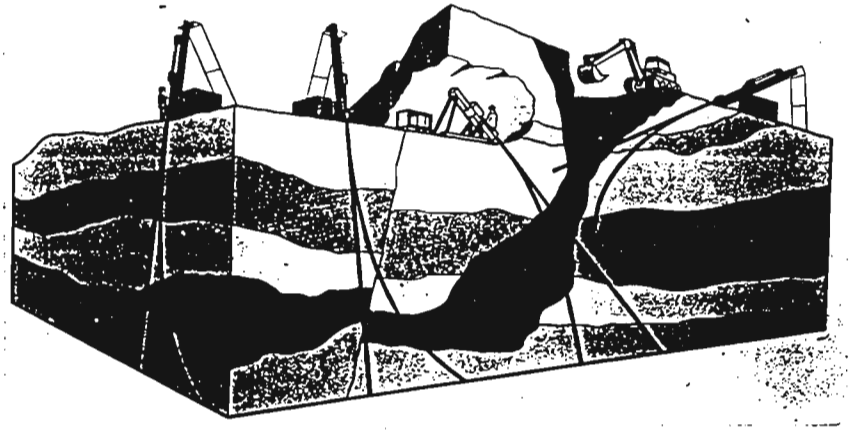

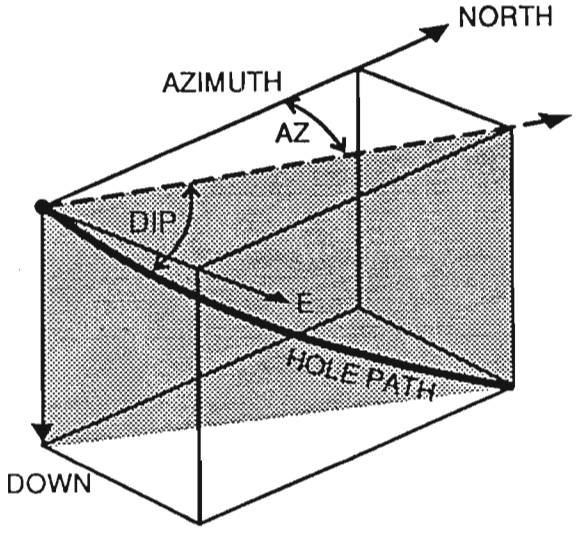

Figure 1. (above) Typical deviated boreholes in exploration and mining: Straight lines show the planned path of the holes and curved lines show the surveyed actual path. (diagram courtesy Reflex Instruments AB)

Figure 2. (left) The three components of the 'hole vector'; the dip, azimuth and depth.

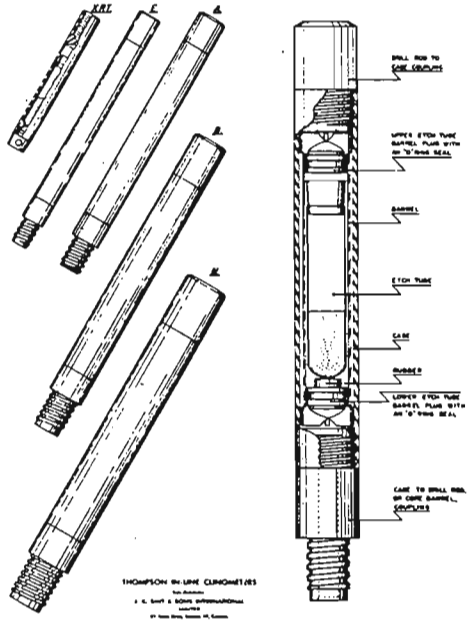

Figure 3. The acid etch clinometer showing the etch tube with hydrofluoric acid, and various housings for use in different size holes.

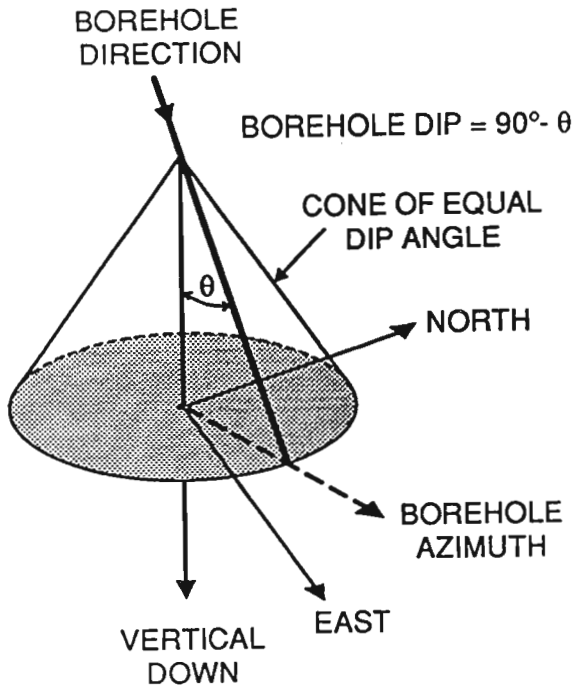

Figure 4. The Cone of Equal Dip: Even if the dip of the hole were known, its path could be in any direction on a cone of equal dip as shown, until the azimuth with respect to North is also measured.

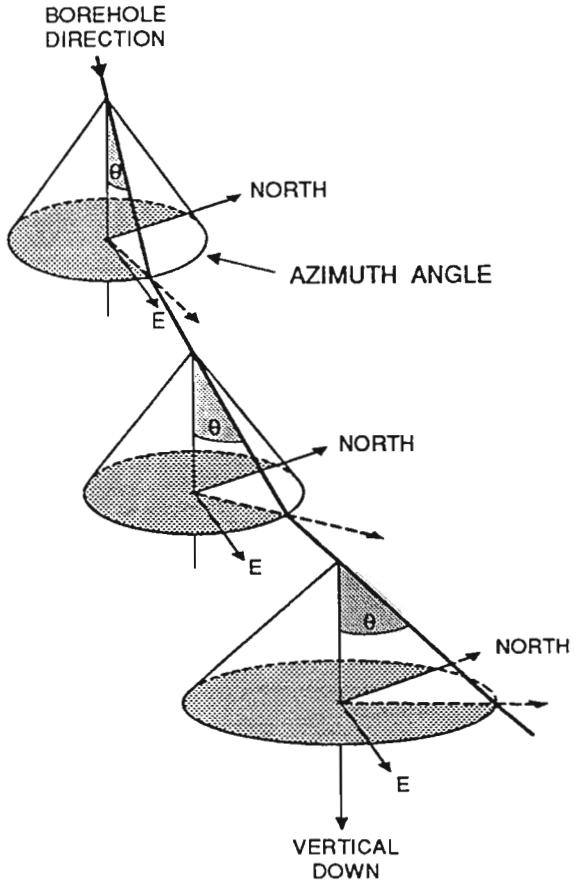

Figure 5. Three dip measurements along the path of a borehole showing the cone of equal dip at each point. The azimuth of the hole between each point must be assumed, as shown by the straight-line segments of the hole. This leads to an infinite number of possibilities for the path. The azimuth must be measured to obtain the true path.

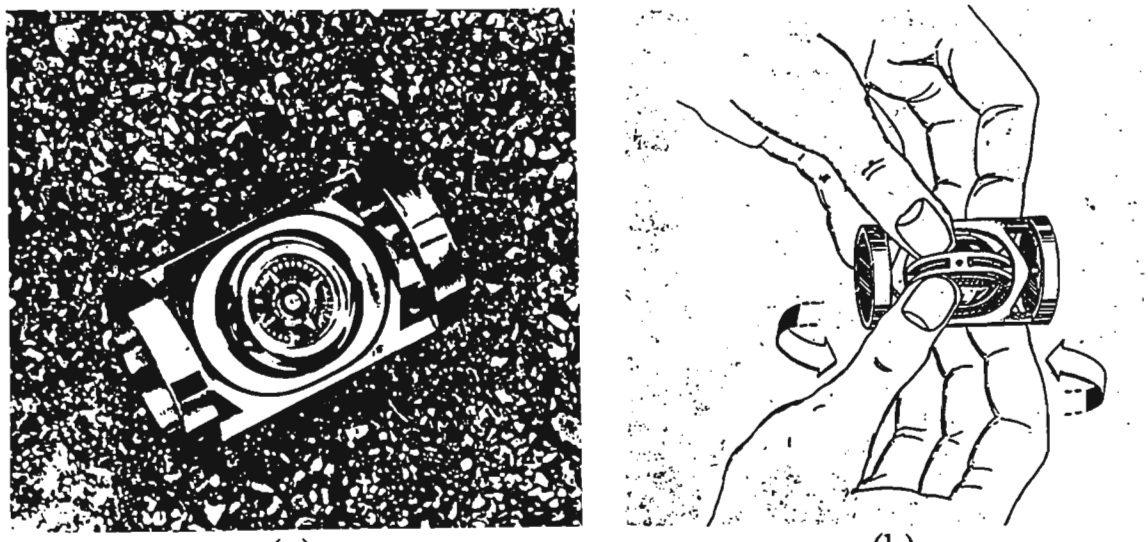

(a) (b)

Figure 6a,6b and 6c. The Tropari: A compass and clockwork mechanism (6a, top left) are mounted on gimbals with the bottom side weighted to maintain the gravitational vertical reference as it moves freely in its housing. It is lowered in the hole to the measurement depth, and at a preset time, the clock (6b, top right) locks all the moving parts. The tropari is retrieved from the hole to read the dip and magnetic azimuth value (6c, below). The tropari is still widely used throughout the world in mineral exploration.

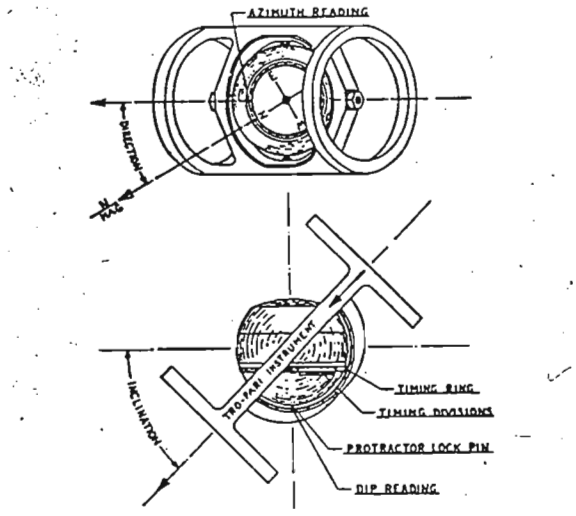

(c)

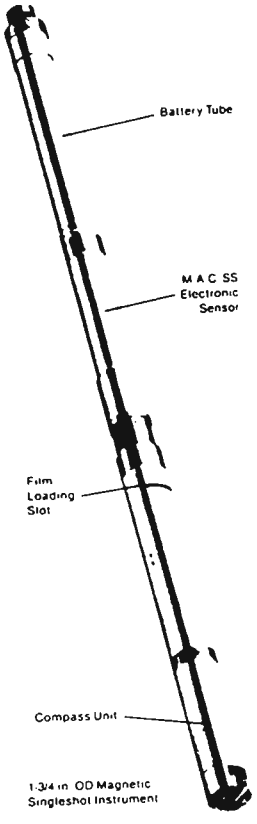

(a)

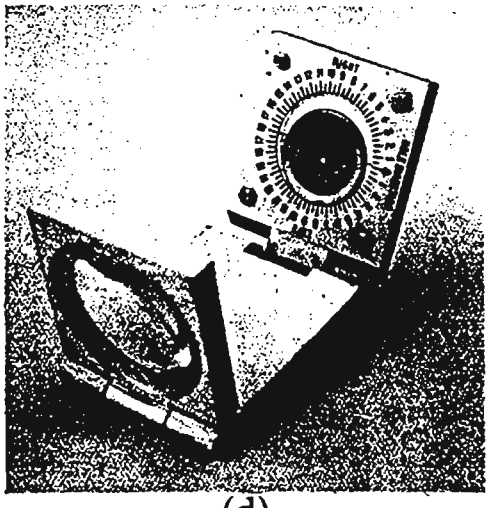

(d)

Figure 7a, 7b, 7c and 7d. The Magnetic single-shot: Using the same principle as the tropari, it replaces the clockwork locking mechanism with a camera which takes a photo of the dip and compass needle at the measurement depth. The probe is then retrieved. In the Sperry-Sun Single Shot (7a, top left), the insertion (7b, lower left) and removal (7c, lower right) of the film is done through a slot in the housing, saving the disassembly time. The film disk reader is shown in 7d (upper right).

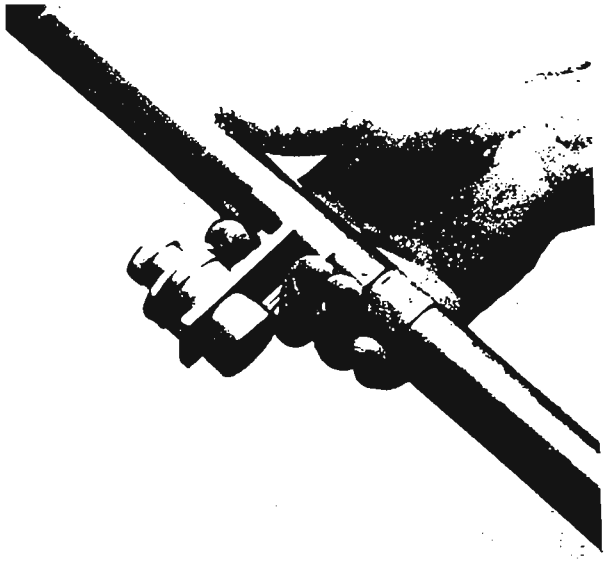

(b)

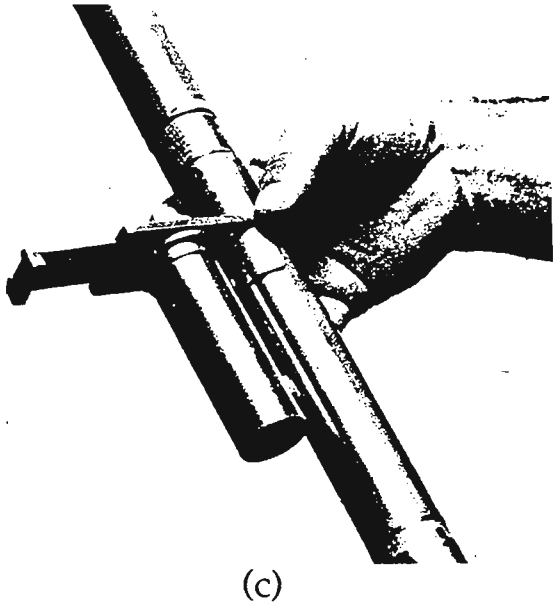

(c)

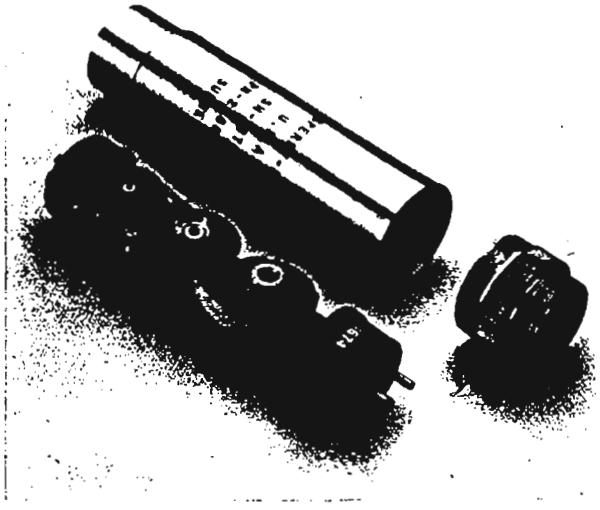

Figure 8. The Magnetic Multi-shot: An 8mm film camera installed in the probe, takes photos of the dip and azimuth readings at several measurement depths, in one trip in the hole. The Sperry-Sun version is shown here.

Figure 9. With the advancement of electronic technology, the magnetic compass was replaced by three component ring-core fluxgate magnetometers similar to that shown here. The dip measurement was made by solid state tilt-meters or accelerometers with virtually no moving parts.

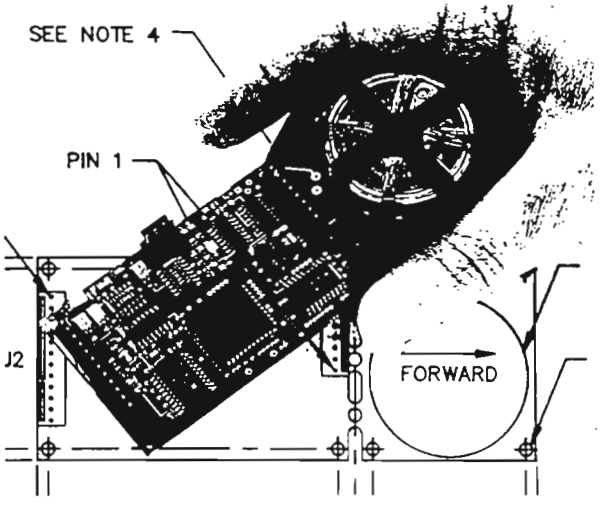

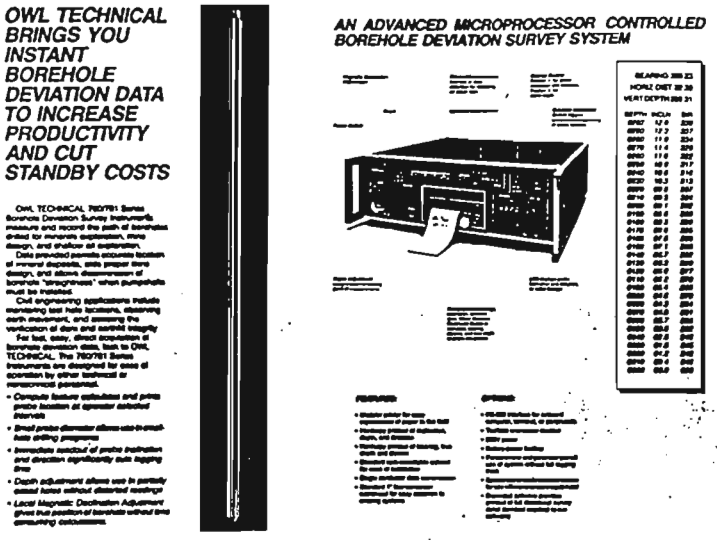

Figure 10. The OWL Technical Associates borehole deviation survey system is a typical magnetic-based system using fluxgate magnetometers and accelerometers as the sensors for surveying a borehole.

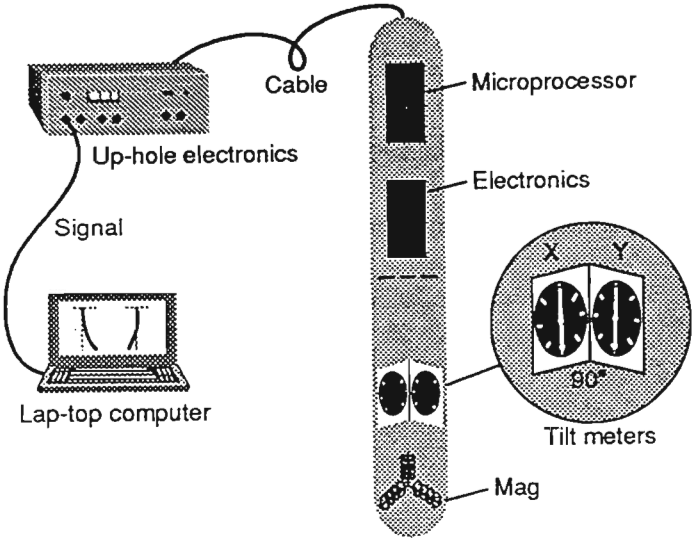

Figure 11. The IFG Corp. borehole orientation system is a magnetic-based system which uses fluxgate magnetometers and solid state tilt-meters to survey a borehole. Data are transmitted to the surface during logging.

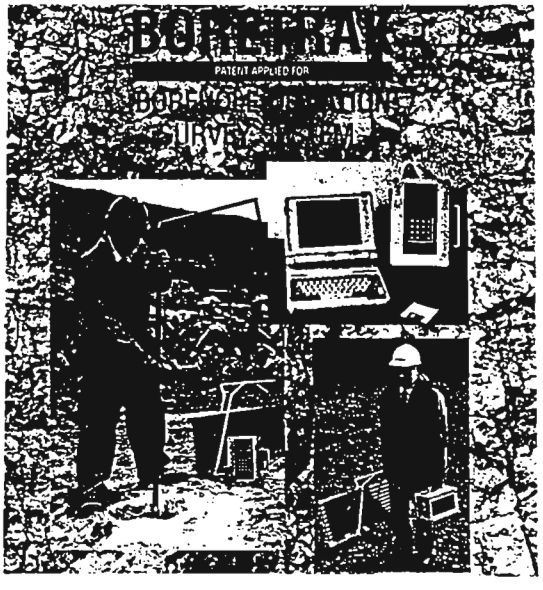

Figure 12. Measurement Devices Limited, of the U.K., produces the Boretrak system which uses an electronic inclinometer for dip measurement and maintains constant azimuth with lightweight rods attached to the probe. Data are recorded in the probe memory.

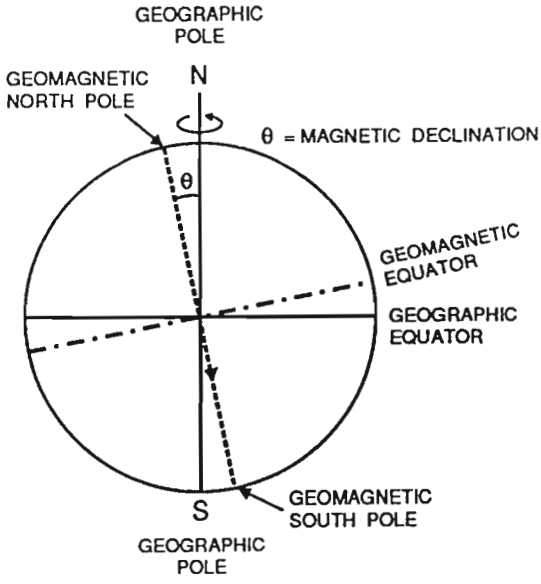

Figure 13. The magnetic azimuth must be converted to geographic azimuth by applying the magnetic declination for the survey area.

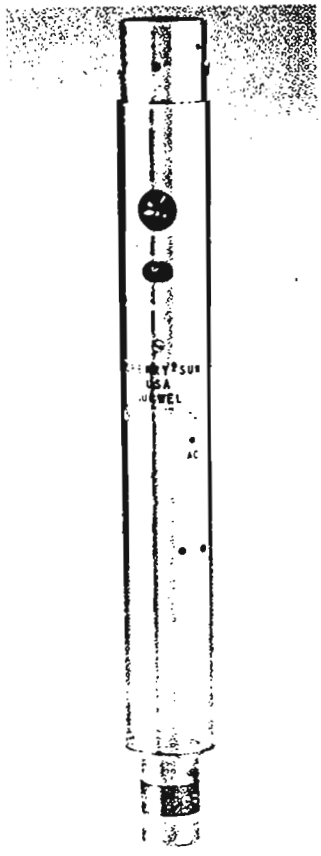

Figure 14. (below) Azimuth measurement can be based on a gyroscopic platform; the inertia of a spinning mass is a stable reference for a series of directional measurements in a borehole. The gyroscope mechanism replaces the magnetic compass.

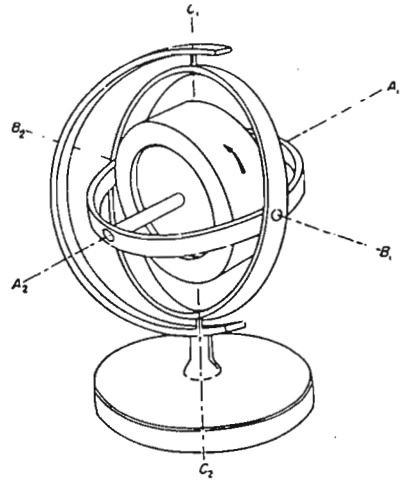

Figure 15. The Sperry-Sun Level Rotor Gyro shown at left is 43 mm in diameter.

Figure 16. Azimuth measurement is read from a gyroscopic compass card in a Sperry-Sun probe. Earlier versions were combined with a camera similar to the 'Single-shot' device. Recent versions called 'surface recording gyros' send the data to the surface in real time.

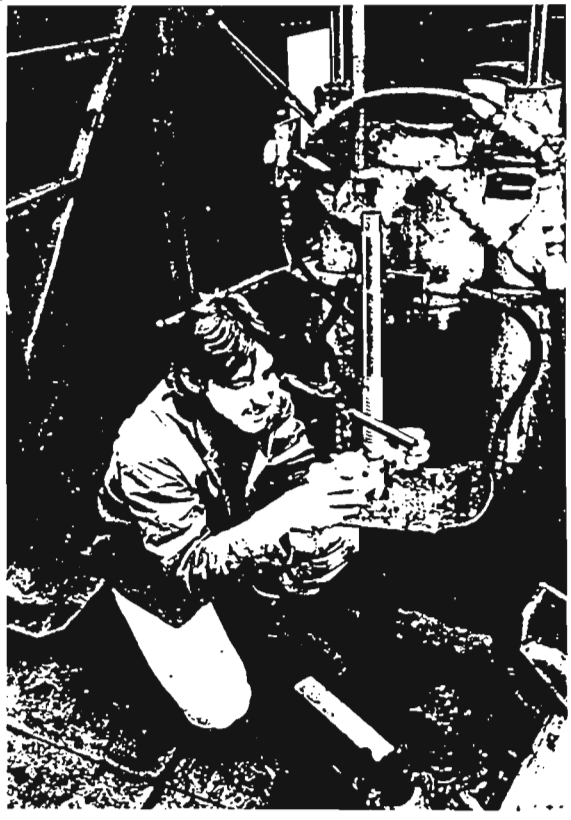

Figure 17. Although the gyroscope mechanism replaces the magnetic compass, the orientation of the gyroscope must be determined at the collar of the hole with respect to geographic north by sighting on known points.

ABEM Reflex-Fotobor
Dip & Direction Indicator

Atlas Copco

a multi-shot optical instrument for finding out, simply and accurately, where the drill hole went.

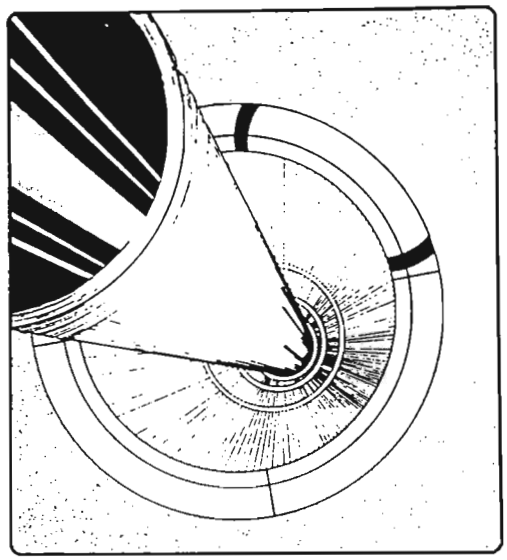

Figure 18. The Fotobor by Reflex Instruments of Sweden was one of the first optical instruments. The technique is based on a light in one end of a long rigid tube with the lightbeam focused on a target in the other end. The tube bends as it moves in the borehole causing deflections of the light on the target. This information is converted into borehole orientation survey data.

Figure 19. The illuminated target (top right) in the Fotobor is a set of concentric rings. A level bubble is used as the vertical reference.

Figure 20. (Below) A camera recorded the 'lightbeam-target' data on film for processing. Correlation with the time and depth data recorded at the surface, was done later.

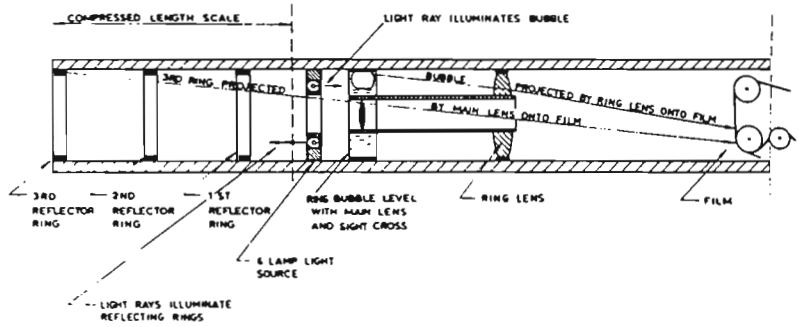

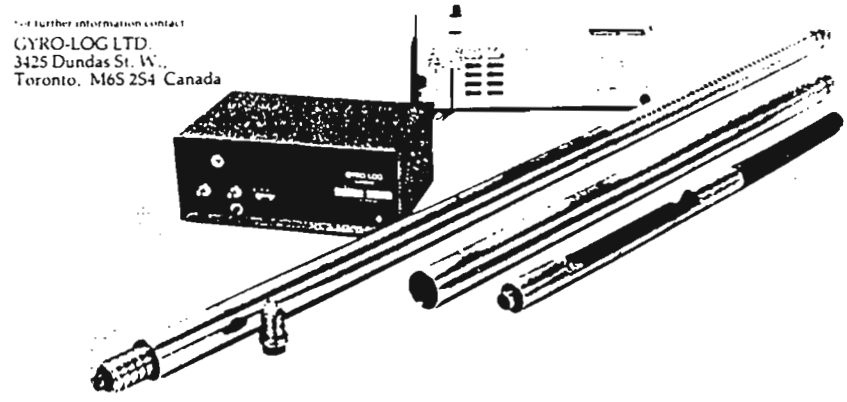

Figure 21. The Light-Log; an optical system made by Gyro-log Ltd..

Figure 22. (Below, left) The Light-Log instrument photographs the position of the lightbeam 'spot' on a target instead of concentric rings, for measuring the bending of their 'Light-Log' instrument. The position is used for calculating the path of the hole.

Figure 23. (Below, right) The most recent Swedish version (the 'Maxibor'), detects the position of the rings with optical sensors. The data are recorded in a solid state memory in the probe for later processing at the surface.

"LIGHT-LOG"
Instrument

(U.S. Patent 4047306, 4142193 others pending)

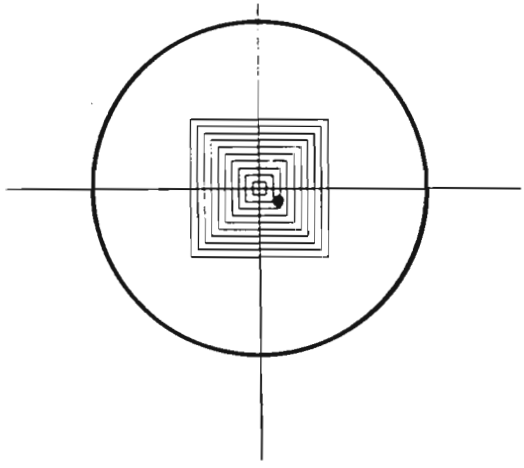

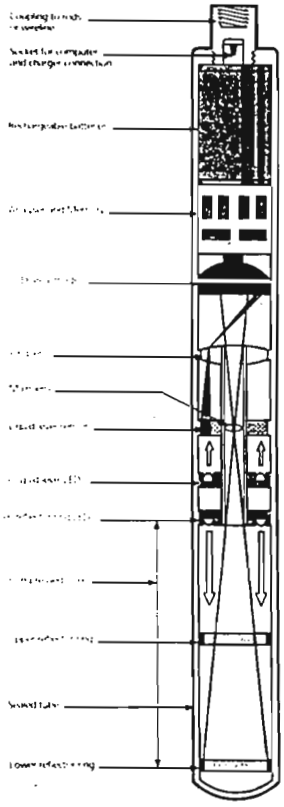

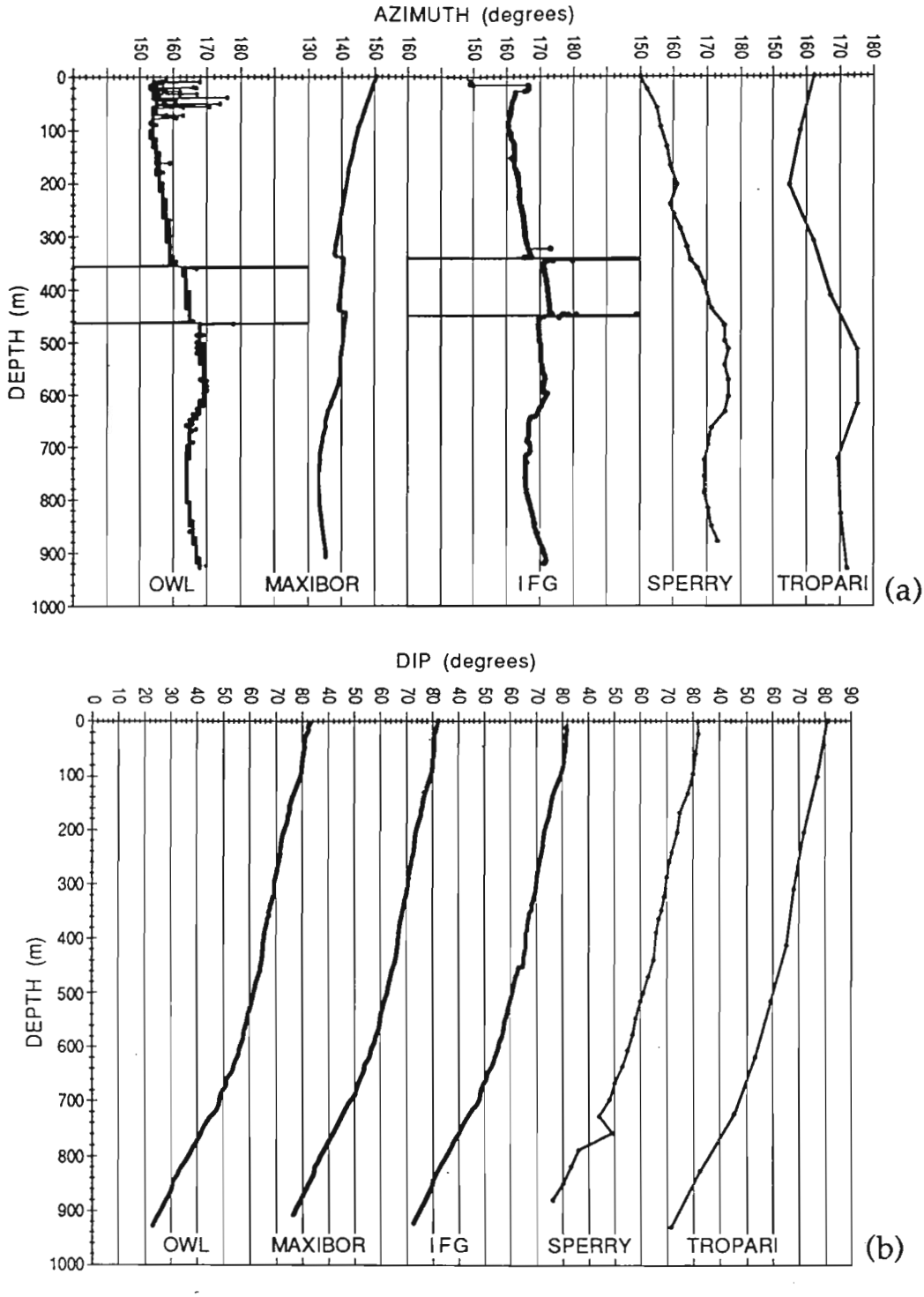

Figure 24. Raw survey data consisting of azimuth (a, top) and dip (b, bottom) values measured at numerous depth points ranging from 100m apart for the Tropari, to about 10cm apart for the IFG survey of a 950 m deep hole.

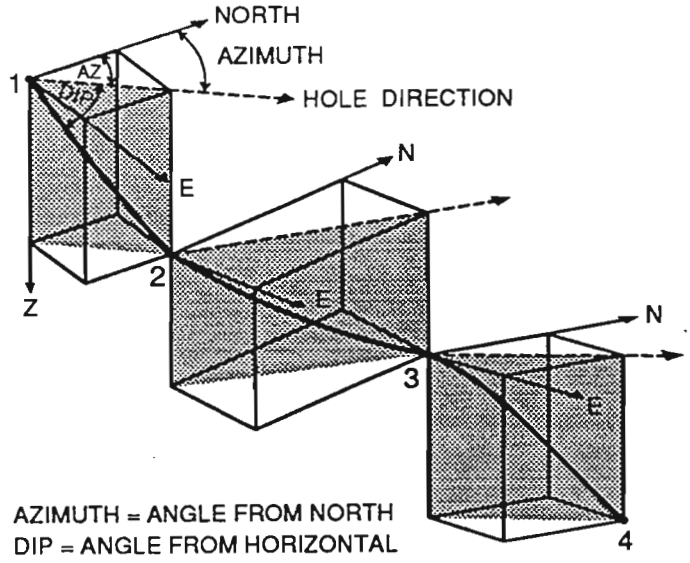

Figure 25. The raw data must be converted into a plot of the path of the hole by interpolating between measurement points in a process called desurveying. Here, three measured data points indicating depth, dip and azimuth are shown. In 'desurveying', a number of different algorithms can be used for the interpolation.

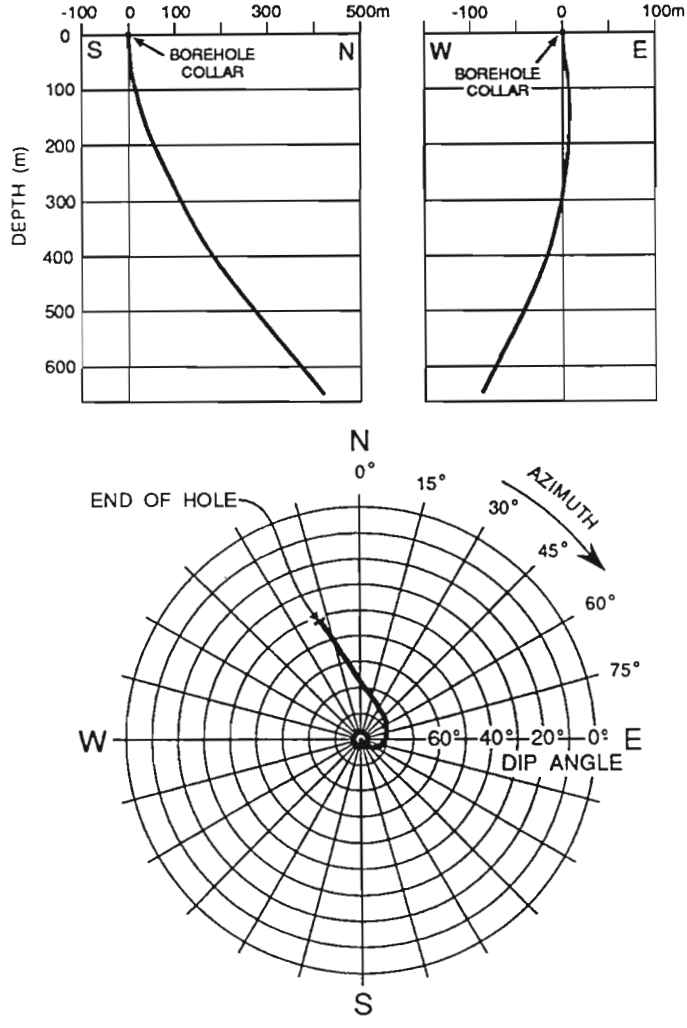

Figure 26. The visual output after surveying a borehole is a display of the path of the hole projected on planes in an east-west or north-south direction, or in plan view.

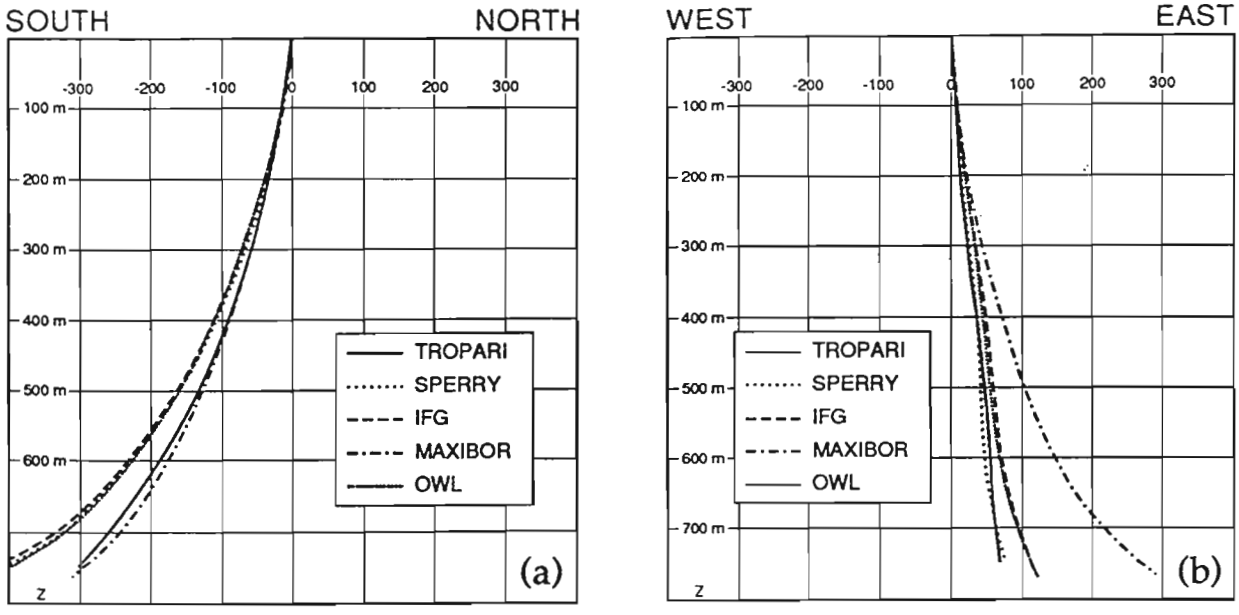

Figure 27a, 27b, 27c and 27d. The five raw data sets were desurveyed and the resulting five paths of the hole are displayed together for comparison. The geographical path of the Val d'Or borehole is displayed in four ways:
Figure 27a (top left) Projection of the path of the hole in a North-South vertical section
Figure 27b (top right) East-West vertical section
Figure 27c (lower left) plan view, and
Figure 27d (lower right) combination of all of the above views in a wire grid box showing the path in "3-D".

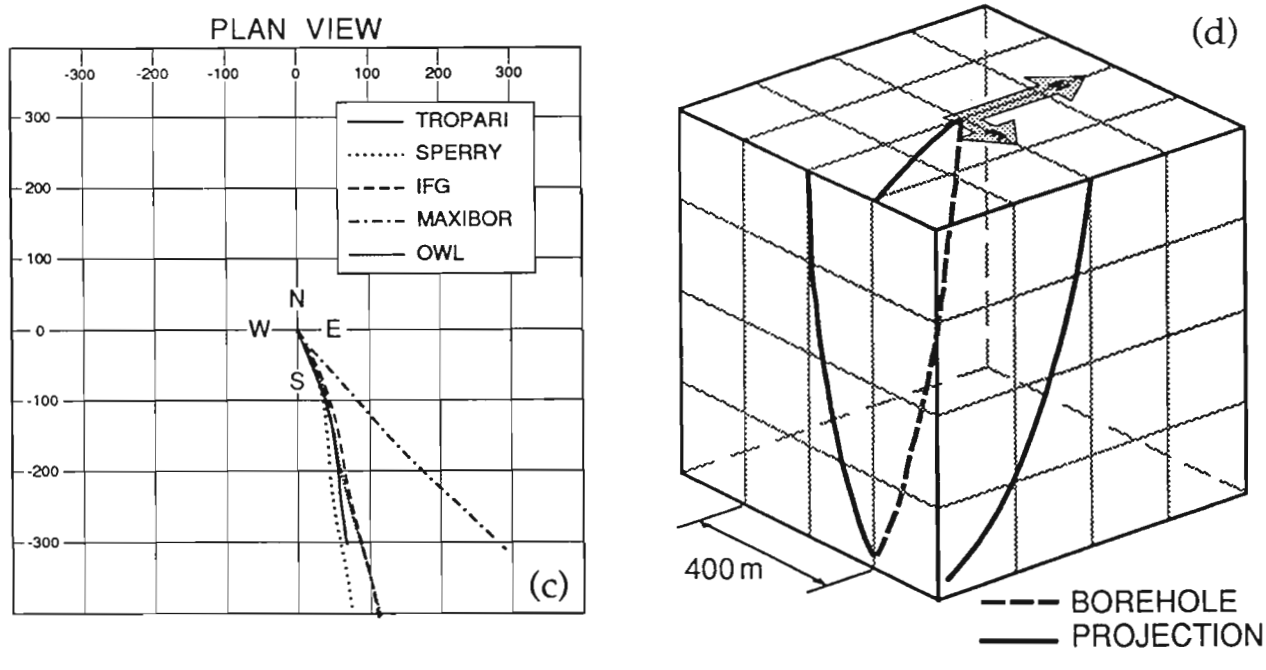

AN OVERVIEW OF PROCESSING, DISPLAY AND ENHANCEMENT METHODS USED ON BOREHOLE GEOPHYSICAL LOGGING DATA AT THE GEOLOGICAL SURVEY OF CANADA

B.E. Elliott[1]

B.E. Elliott, An overview of processing, display and enhancement methods used on borehole geophysical logging data at the Geological Survey of Canada; in Proceedings of the 4th International MGLS/KEGS Symposium on Borehole Geophysics for Minerals, Geotechnical and Groundwater Applications; Toronto, 18-22 August 1991

Abstract

The Borehole Geophysics Section, of the Geological Survey of Canada (GSC) presently acquires borehole geophysical data on 9-track magnetic tapes, using a truck-mounted digital data acquisition system based on a Data General minicomputer. Up to twelve geophysical parameters are recorded from runs with five different logging tools. Some insight into the data handling methods used at the GSC may be obtained from this brief overview.

Each parameter recorded requires the application of appropriate calibration and correction factors as well as enhancement (filtering, etc.). Efficient and effective methods for the compilation, amalgamation and display of these multiparameter logs and related data are required to present the data in a form that can be easily interpreted in relation to mineral exploration and geotechnical problems.

Data from magnetic susceptibility and spectral gamma probes are used to illustrate the various stages of processing necessary to produce archival data and final plots ready for interpretation and publication. Examples of multiparameter logs compiled from data obtained with Temperature, IP, and Spectral Gamma-gamma tools are also presented. Some of the compilation, display and enhancement techniques used within the Borehole Geophysics Section are described.

INTRODUCTION

The Borehole Geophysics Section, Mineral Resources Division of the Geological Survey of Canada (GSC) carries out research projects directed at the advancement of applications of borehole geophysical methods to mineral exploration and geotechnical problems.

Consistent methods of processing and applying correction factors and innovative display and enhancement techniques allow optimum use of the data collected as part of this research.

Using example data logged in GSC test hole BC81-2 at Bells Corners, near Ottawa, (Schock, Killeen, Elliott and Bernius, 1991) this paper briefly describes natural gamma ray spectrometry and magnetic susceptibility logging and gives details on the multi-step processing used to produce presentation material from field data. The resultant logs from these two tools are plotted alongside logs from a suite of other tools.

Techniques for correction of drift in data and for determining depth correlation on related logs are described. Examples of data displayed in a variety of formats are presented.

This paper was originally presented in poster format, taking full advantage of colour illustrations. Although the content will be similar to that presented in the poster, some of the impact of the diagrams is lost in black and white.

[1]Geological Survey of Canada, 601 Booth Street, Ottawa, Ontario, K1A 0E8

THE GSC LOGGING SYSTEM

The GSC R and D logging system, mounted in a four-wheel drive truck has five logging tools that measure twelve different physical parameters. Data acquisition, as illustrated in Figure 1, is based on a 16-bit Data General Corporation Nova computer. All digital measurements are acquired in a continuous mode and recorded on 9-track magnetic tape. Some field processing can be done in 'replay' mode, but most post-processing of the tapes is carried out using a 32-bit Data General MV4000 in Ottawa. A PC-based logging system that will record data on 20 Mb Bernoulli disks is currently under development.

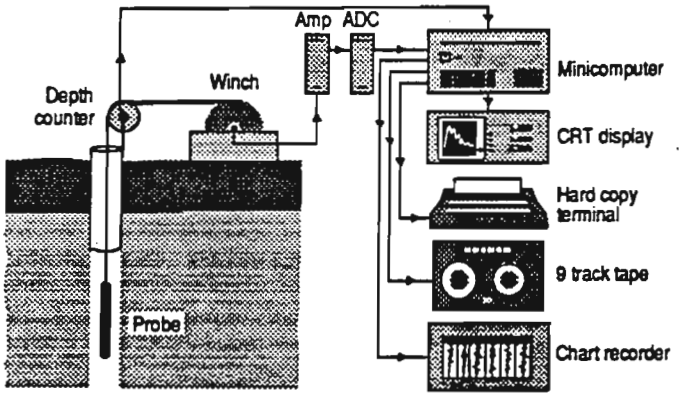

Figure 1 GSC Borehole Logging System.

SPECTRAL GAMMA RAY LOGGING

Recording of Spectral Gamma Ray Data

Borehole gamma ray measurements are used to detect variations in natural radioactivity due to changes in concentrations of the elements potassium (K), uranium (U) and thorium (Th) in the rocks through which the probe is travelling. The probe's sensor is either a cesium or sodium iodide scintillation detector and the counting time is normally one second. The energy of each detected gamma ray is measured, and the gamma-ray energies are sorted into an energy spectrum by the computer. For each counting period, a record consisting of depth and the gamma-ray count recorded in each of 256 channels (representing energies of 0 to 3.0 MeV), is recorded on magnetic tape.

Initial Processing of Spectral Gamma Ray Data

The first processing steps involve retrieving the recorded channel data and summing channel counts in pre-selected energy windows centered on the K, U and Th peaks, as well as in two total count (TC1 and TC2) windows.
The energy windows used are as follows:

TC1:	0.10 to 3.00 MeV
TC2:	0.40 to 3.00 MeV
K:	1.36 to 1.56 MeV
U:	1.61 to 2.30 MeV
Th:	2.40 to 3.00 MeV

Several logging runs in a borehole can be recorded on one tape. Calibration spectra are recorded before and after each series of runs in a hole, using a set of radioactive sources with known energy peaks. By locating these peaks and the channels in which they occur, calibration for gain (keV/channel) and energy intercept can be computed. These factors are then used to convert channel data to energy window data for logging runs on that tape.

The count rate in each channel must also be corrected for deadtime; the time taken for the equipment to analyze a single gamma ray and during which the equipment is busy and cannot analyze other gamma rays.

The probe is zeroed for depth at the top of the hole casing, but a depth correction must be made for the position of the sensor along the length of the tool as well as for the height of the casing above ground level.

The logs illustrated in Figure 2 have been corrected as follows:

1) depth has been corrected for casing height and probe length;
2) TC1, TC2, K, U and Th logs have been generated using the correct gain and intercept, corrected for deadtime and normalized to counts per second.

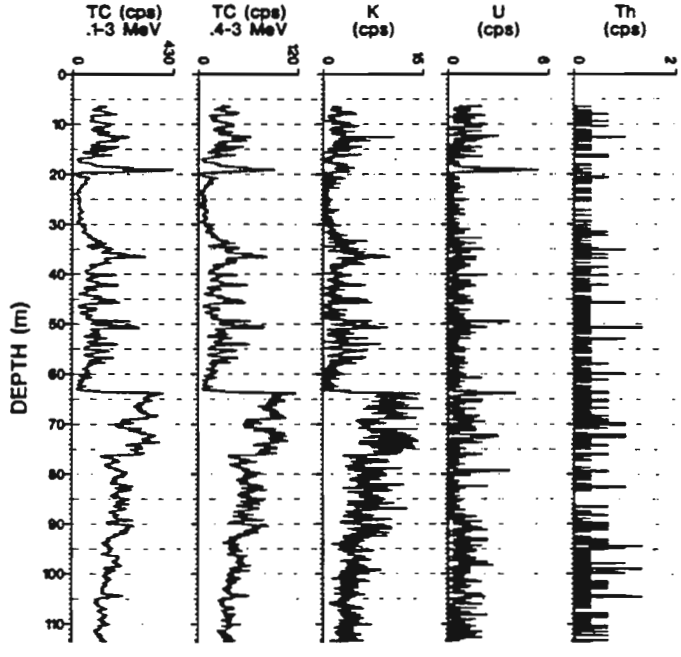

Figure 2 Bells Corners Hole BC81-2: Total count and raw potassium, uranium and thorium logs.

The depth and channel data are archived at this stage for possible use later if there is a need to generate logs based on different energy windows.

Further Processing of Spectral Gamma Ray Data

To convert data values in the K, U and Th files from counts per second into concentrations in % and ppm, calibration factors for each probe are computed at the beginning of the field season.

Radiation from thorium is detected in both the uranium and potassium windows and that from uranium in the potassium window. The necessary corrections can be computed by acquiring spectra in special model holes which have well defined zones containing known (but different) concentrations of the three radioelements. These corrections are known as "stripping ratios", and must be determined for a given tool by an individual calibration. The same calibration procedure also allows the absolute sensitivities in terms of counts/second per unit concentration to be determined for each of the radioelements. The data can then be stripped in order to assign the counts detected in the K, U and Th windows to their proper source element. The logs of corrected counts can be deconvolved and converted to % K and ppm U and ppm Th by using the correct sensitivity for each element. Killeen (1983) describes fully the method of calibrating spectral gamma ray logging systems.

Any editing, averaging or filtering of logs can also be done at this time.

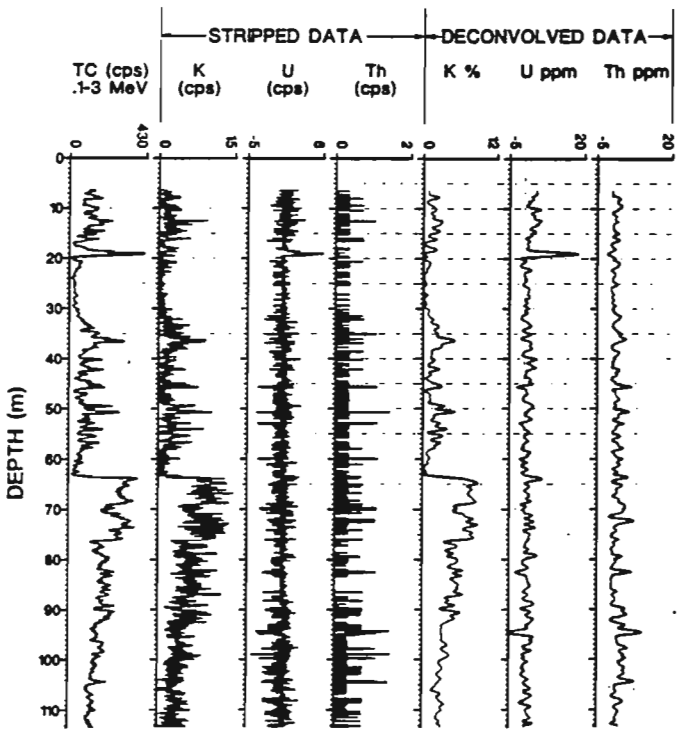

Figure 3 Bells Corners Hole BC81-2: Stripped and deconvolved potassium, uranium and thorium logs plotted along with the total count log.

Figure 3 shows an example of stripped and deconvolved K, U and Th logs plotted with the TC1 log. The deconvolved logs were computed using an inverse filter and simultaneously smoothed with a 21 point Savitzky-Golay filter (Savitzky and Golay,1964).

MAGNETIC SUSCEPTIBILITY LOGGING

Recording of Magnetic Susceptibility Data

The Geo Instruments model TH-3C, makes use of a coil in an electrical bridge circuit energized at a frequency of 1400 Hz (Bristow and Bernius, 1984). As the tool moves through magnetically susceptible material, an apparent change in coil inductance is sensed, causing the bridge to become unbalanced. Tool circuitry changes the energizing frequency to balance the bridge. This frequency shift is related to the magnetic susceptibility of the material through which the tool is travelling, and is recorded with depth on a continuous basis. Calibration is carried out periodically by noting the frequency shift as the tool passes a specific isolated anomaly in a test hole, the drill core from which has been measured using a laboratory magnetic susceptibility apparatus.

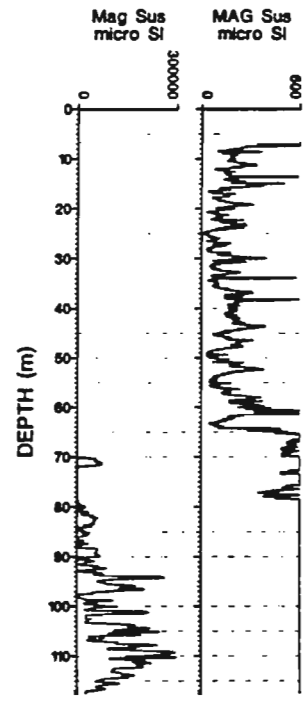

Figure 4 Bells Corners Hole BC81-2: Magnetic Susceptibility log plotted at two different scales.

Initial Processing of Magnetic Susceptibility Data

The initial processing of magnetic susceptibility data consists of converting recorded frequency to magnetic susceptibility units using a calibration factor. Recorded values differ with hole diameter, so a hole size correction factor is also applied at this time.

As in spectral gamma logging, the recorded depth must be corrected for casing height and probe length. The example log in Figure 4 is plotted at two different scales, since the hole logged contains zones with both low amplitude and high amplitude magnetic susceptibility variations. Note, for example, the zone from 65 to 80 metres has different magnetic susceptibility than that from 0 to 65 metres. This would not have been noticed if only the log on the left were plotted.

The log has been corrected as follows:

1) depth has been corrected for casing height and probe length;
2) magnetic susceptibility values have been generated by converting frequency to magnetic susceptibility units, and correcting for hole diameter.

Further Processing of Magnetic Susceptibility Data

If laboratory magnetic susceptibility measurements on core are available, these values may be correlated with averaged values along the log to check the validity of the calibration .

At this stage, any editing, averaging or filtering of logs can be done.

Figure 5 compares the logged magnetic susceptibility data to laboratory measurements on the core using a Sapphire Instruments "Sapphire II" magnetic susceptibility meter.

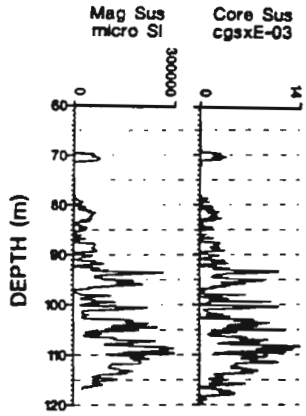

Figure 5 Bells Corners Hole BC81-2: Magnetic susceptibility log plotted with magnetic susceptibility data obtained on core using a SAPPHIRE II magnetic susceptibility meter.

COMBINING LOGS FROM SEVERAL LOGGING TOOLS

The usual practice is to log holes with several different tools to maximize available information. Data from runs with each tool are processed separately to provide the logs detailed in Table I. The next step produces a plot that combines the geophysical logs from different tools with other information available for the hole, such as geological and assay data. Fine depth adjustments between the geology and the logs, and between logs from different tools are made at this time. One method for determining necessary depth adjustments is described in a later section of this paper. In figure 6, multiparameter logs from a suite of tools are presented. For the purposes of this paper, a black and white diagram is used; normally the logs would be plotted with a coloured geology overlay to make interpretation easier.

TOOL	LOGS GENERATED
Spectral Gamma Ray	Total Count Potassium(%) Uranium(ppm) Thorium(ppm)
Magnetic Susceptibility	Magnetic Susceptibility
Spectral Gamma-Gamma(SGG)	Density SGG Ratio
Induced Polarization	Resistivity Induced Polarization Self Potential
Temperature	Temperature Temperature Gradient

Table I : Logs Generated from Borehole Logging Tools

The hole in which these logs were acquired transverses 60 metres of sandstone before entering crystalline rock. There is known to be groundwater movement at the contact between the formations. This contact is highlighted by a sharp increase in the potassium natural gamma log and the magnetic susceptibility log and also by a self potential and a temperature gradient anomaly. The resistivity (RHO) log also indicates an abrupt change at this level.

ARCHIVING OF BOREHOLE LOGGING DATA

Data are archived on optical disk cartridges on the Data General MV4000. The following data sets are stored:

1) log data (depth and parameter values) at various stages of processing;
2) files that have been created to generate all plots.

EXAMPLES OF CORRECTION TECHNIQUES

Drift Correction of Magnetic Susceptibility Data

Since most instruments are temperature sensitive, proper temperature stabilization procedures to avoid drift are followed, but occasionally data drift still occurs, especially when logging deep holes. The magnetic susceptibility log in Figure 7

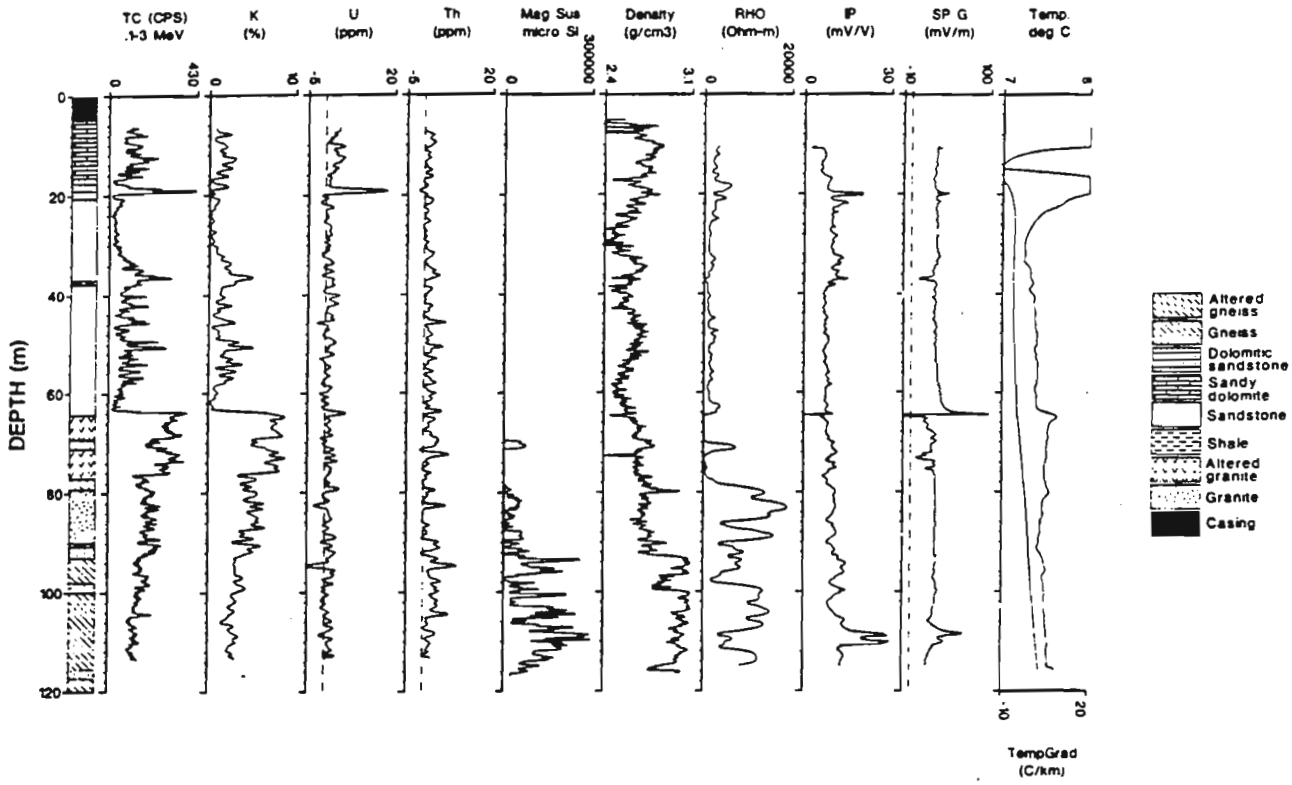

Figure 6 Bells Corners Hole BC81-2: Geophysical logs from spectral gamma ray, magnetic susceptibility, spectral gamma-gamma, induced polarization and temperature tools with geological log.

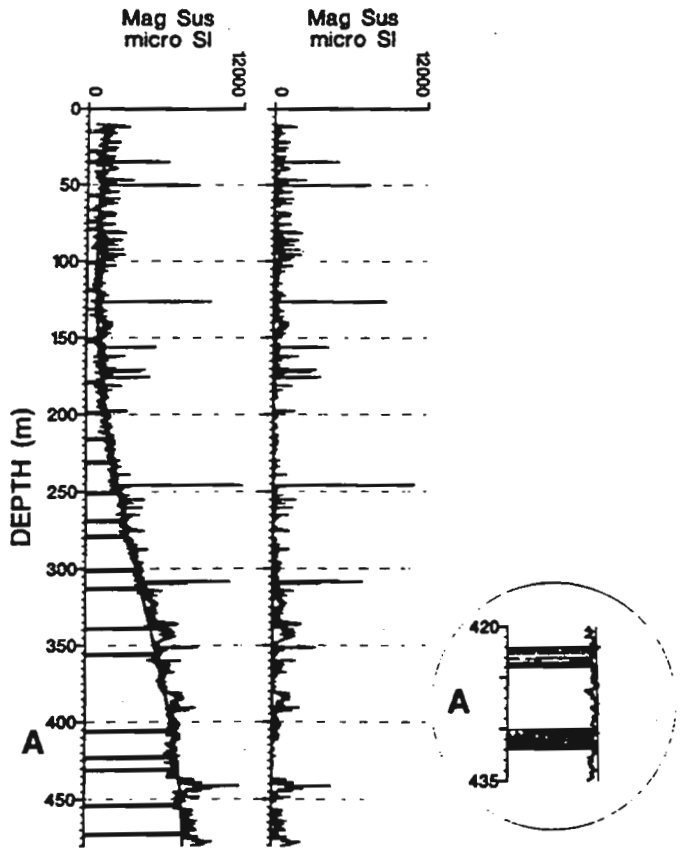

Figure 7 Illustration of correction of drift on magnetic susceptibility data.

illustrates a technique to correct such drift. Several relatively flat sections along the log are selected, and the data values in those sections averaged. A polynomial is fitted to these average values and the resultant polynomial is used to correct the original data. On the left in Figure 7, the original log is shown with the averaged sections shaded and the best fit polynomial overlaid. The drift- corrected log is shown on the right.

Cross-Correlation of Logs for Depth Shifting

Because logging a hole with a suite of different tools may result in minor discrepancies in recorded depth, a final processing step of depth adjustment between logs is made.

The usual procedure is to adjust one log from a particular tool to match the geological log, and then to adjust the other geophysical logs to match the chosen log. The depth shift between two logs can be computed using the following method:

1) The logs are plotted, side by side.
2) The logs are interpolated to the same depth interval.
3) Sections of the logs where there is an apparent visual correlation (either positive or negative), are chosen. A short section of one log is chosen for correlation with a longer section from the other log.
4) The shorter section of data points is moved, point by point, along the longer section of data points, with the correlation coefficient being calculated at each point.

The depths in each section, associated with the values that produce the best absolute correlation, positive or negative, can then be used to compute the required depth shift.

5) The processes in 3) and 4) can be repeated using several sections of the logs to confirm the correlation.

In Figure 8, two examples of use of this correlation technique are illustrated. The total count log is used to correlate first the density log and then the resistivity log. In the left two logs in both examples the sections picked for correlation are shaded. The right two logs in each example compare the logs after depth shifting. The density log has been shifted up 5.14 metres and the resistivity log shifted down 3.12 metres. Normally depth shifts of less than a metre occur; in these examples, the necessary depth shifts between logs have been exaggerated to better demonstrate the technique.

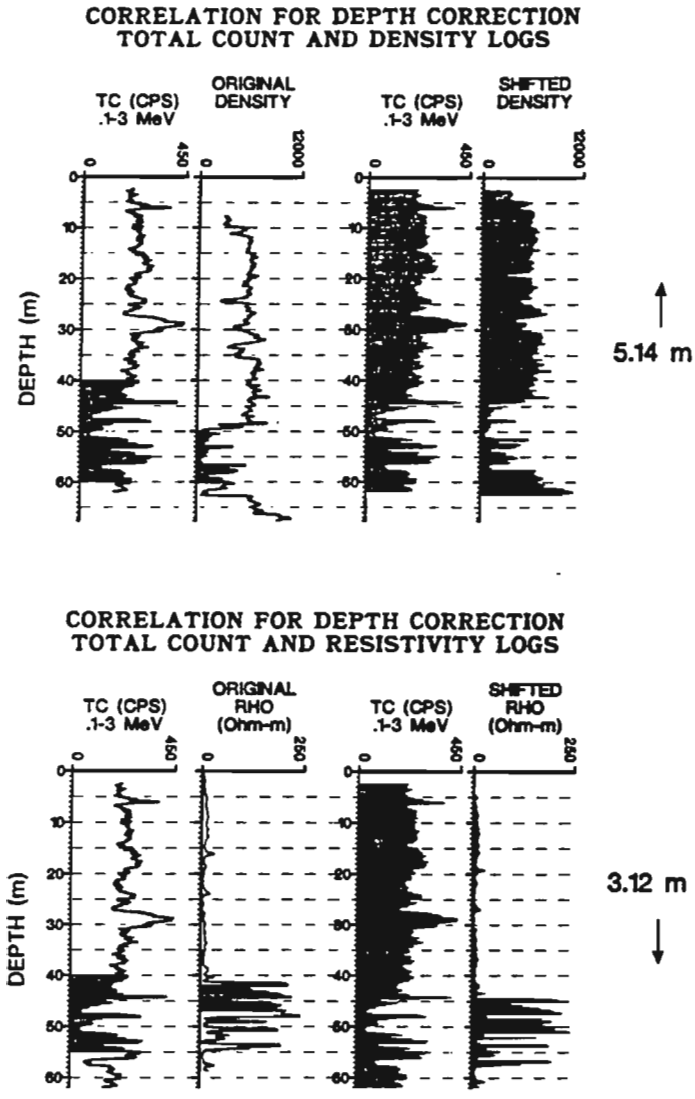

Figure 8 Illustration of correlation for depth correction between total count and density logs and total count and resistivity logs. (Explained in text)

EXAMPLES OF ENHANCEMENT TECHNIQUES

Assays Plotted with Geophysical Logs

By plotting geophysical logs alongside assays obtained from the drill core, as shown in Figure 9, relationships between the two types of data can be more readily seen. This helps in choosing the best geophysical parameters for predicting element content.

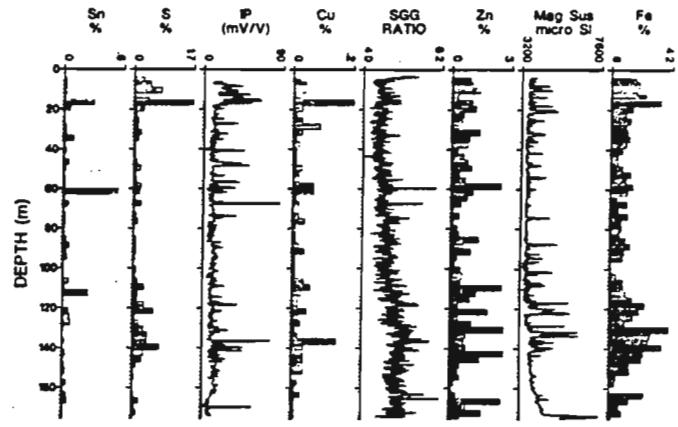

Figure 9 Geophysical logs of spectral gamma-gamma ratio, induced polarization and magnetic susceptibility plotted with assay data.

Log Data and Histograms

Figure 10 illustrates the use of a histogram to show how different lithologies are represented by variations in the gamma-ray total count rate. The log of total count is plotted versus depth (Fig.10a), but interpretation is further aided by also plotting a histogram of the frequency of occurrence of specific count rates (Fig.10b). Count rate ranges can then be associated with different rock types.

Crossplotting Examples

Cross plotting techniques provide additional ways of analyzing data.

Figure 11 shows logs of lead assays on drill core and the spectral gamma-gamma (SGG) ratio (Fig.11a), and the lead versus SGG ratio crossplotted (Fig.11b). The crossplot shows a good correlation between the assay results and the geophysical log and the resultant least squares equation for the best fit line can be used to predict lead content from the SGG ratio. (For more detail on the use of the SGG ratio as an assaying tool see Killeen, Schock and Elliott, 1989)

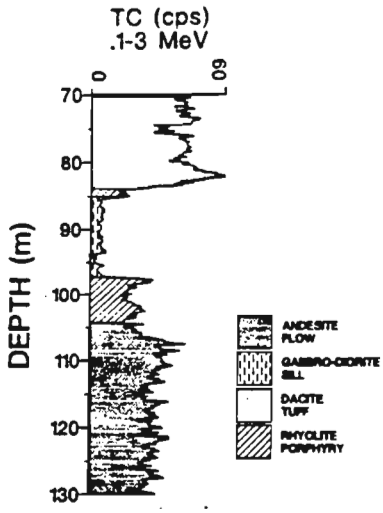

(a)

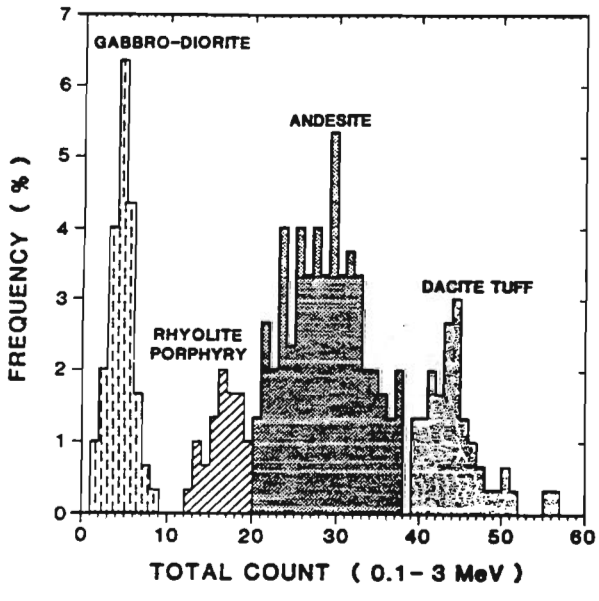

(b)

Figure 10 Total count data represented both as a borehole log (10a) and as a histogram illustrating the variation in frequency of count rate (10b).

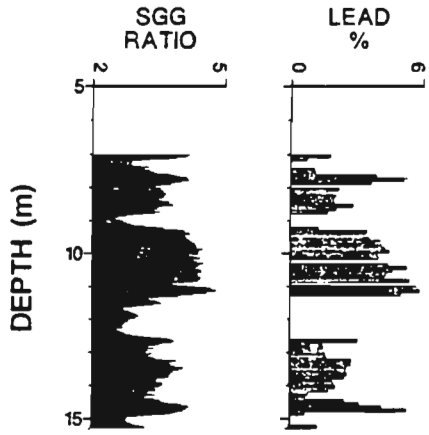

(a)

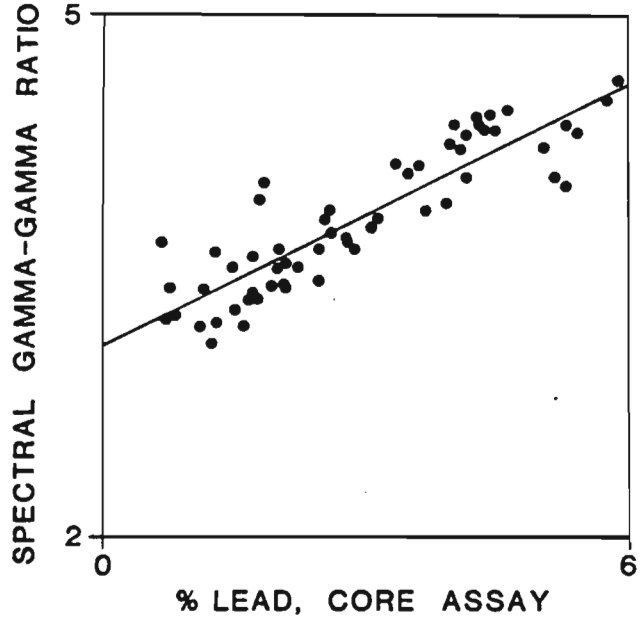

(b)

Figure 11 Lead assay log based on drill core and spectral gamma-gamma ratio log (11a) and also crossplotted versus each other (11b).

The Total Count and Magnetic Susceptibility logs shown in Figure 12a were acquired from a hole which intersected clays and sands in the Fraser Delta of British Columbia. Figure 12b shows a crossplot of the two data sets. The clustering of the data at high values relates to clays and at low values to sands. (Mwenifumbo, Killeen and Elliott, 1991).

Figure 13 shows total count, K, U and Th logs (Fig.13a) and a ternary plot of K, U and Th (Fig.13b). The clustering distinguishes the data logged through bentonites from that logged through siltstones in a coal mining area of Alberta. Mwenifumbo and Pawlowicz (1990) describe the use of spectral gamma ray logging for clay mineralogy.

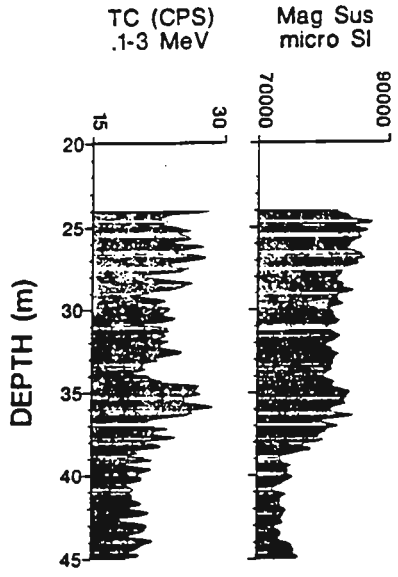

(a)

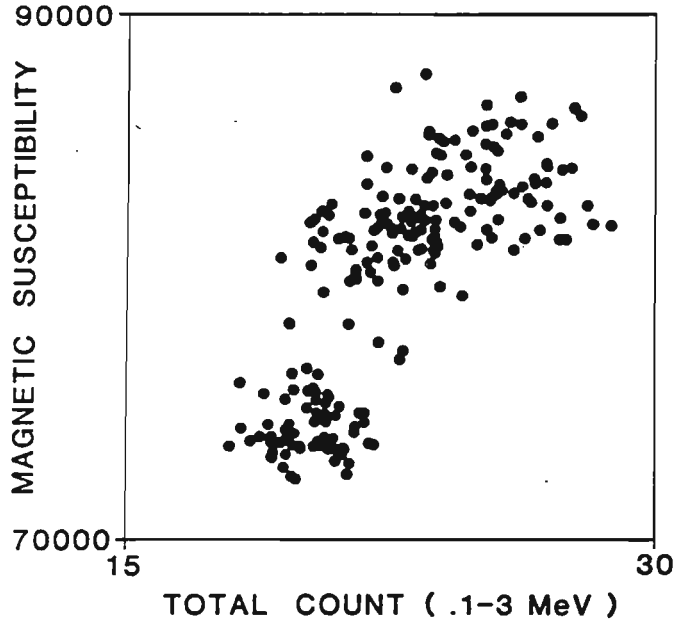

(b)

Figure 12 Geophysical logs of total count and magnetic susceptibility plotted with depth (12a) and also cross plotted (12b).

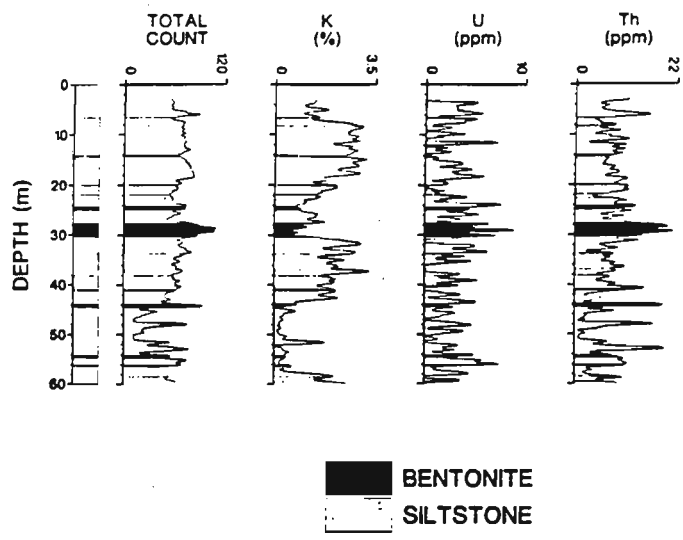

(a)

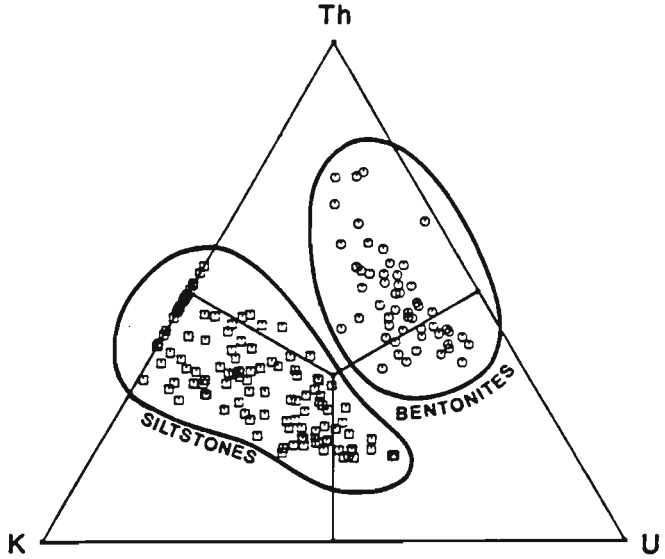

(b)

Figure 13 Potassium, uranium and thorium logs plotted versus depth beside the total count log (13a) and then cross plotted in a ternary format (13b).

CONCLUSIONS

It has been shown by the use of spectral gamma and magnetic susceptibility data as examples, that the procedure for conversion of borehole geophysical logging data from field tapes to a finalized format can often be quite complex. Data gathered using other logging tools requires application of similar processing methods. Techniques for data display have been demonstrated with examples from a variety of methods that can be used as an aid to interpretation. These methods will undoubtedly see rapid advances with the advent of relatively inexpensive colour plotting reproductions and the availability of even more powerful PC processors and related software.

ACKNOWLEDGEMENTS

The author wishes to thank P.G. Killeen, C.J. Mwenifumbo, J.M. Carson and Q. Bristow for their critical reading of this manuscript, G.R. Bernius for his contribution to the data from Bells Corners Test Hole BC81-2 and S.J. Davis for her contribution to the diagrams in this paper.

REFERENCES

Bristow, Q. and Bernius, G. (1984) Field evaluation of a magnetic susceptibility logging tool; in Current Research, Part A, Geological Survey of Canada, Paper 84-1A, p.453-462.

Killeen, P.G. (1983) Borehole logging for uranium by measurement of natural gamma radiation; in International Journal of Applied Radiation and Isotopes Vol.34,No.1, p.231-260.

Killeen, P.G., Schock, L.D. and Elliott, B.E. (1989) A slim hole assaying technique for base metals and heavy elements; in Proceedings of the Third International Symposium on Borehole Geophysics for Minerals, Geotechnical and Ground Water Applications; held in Las Vegas, 2-5 Oct., 1989.

Mwenifumbo, C.J., Killeen, P.G. and Elliott, B. (1991) Downhole logging measurements in the Fraser Delta, British Columbia; GSC paper in press.

Mwenifumbo, C.J. and Pawlowicz, J.G. (1990) Use of spectral gamma for clay mineralogy; report available for public release March 1,1992, Alberta Research Council Information Series No. 110, section 6.

Savitzky, A. and Golay, M.J.E. (1964) Smoothing and differentiation of data by simplified least square procedures; Analytical Chemistry, 36, p.1627-1639.

Schock, L.D., Killeen, P.G., Elliott, B.E., Bernius, G.R. (1992) A review of Canadian calibration facilities; in Proceedings of the Fourth International Symposium on Borehole Geophysics for Minerals, Geotechnical and Groundwater Applications; held in Toronto, 18-22 Aug.,1991.

LOGVIEW: BOREHOLE GEOPHYSICAL SOFTWARE FOR PRESENTATION QUALITY OUTPUT

B.E. Elliott, P.G. Killeen, K.A. Pflug and C.J. Mwenifumbo,
Geological Survey of Canada, 601 Booth St., Ottawa, K1A0E8,

LogView: Borehole Geophysical Software for Presentation Quality Output; in Proceedings of the 6th International MGLS Symposium on Borehole Geophysics for Minerals, Geotechnical and Groundwater Applications; Santa Fe, October 22-25, 1995 (in press).

Abstract

The Borehole Geophysics Section of the Geological Survey of Canada (GSC) has developed LogView, a Microsoft Windows 3.1 application, to provide presentation quality screen and hardcopy output in both colour and black and white to display combinations of logs generated from a series of GSC logging probes. LogView has been released as GSC Open File 3055, and is available through the GSC bookstore.

LogView can be used to view, print and zoom/pan borehole logs and associated lithology. The data file formats and software allow logging parameters recorded with different depth intervals to be plotted beside one another. Logs of data can be stretched, compressed, depth shifted and smoothed for display and a limited amount of annotation can be added to enhance the presentation.

LogView creates 'log display list' files, that allow attributes for a specific layout of logs to be saved for future use and revision.

Windows on-line help is provided, both from a HELP menu and from individual screens.

Details about the menus, file formats and features of LogView are presented, including examples of plots utilizing different features.

INTRODUCTION AND BACKGROUND

The Borehole Geophysics Section, Mineral Resources Division, of the Geological Survey of Canada (GSC), carries out research projects directed at advancing the use of borehole geophysical methods as applied to mineral exploration, geotechnical and environmental problems.

Applying ideas resulting from many years use of earlier GSC in-house software plotting packages and using Microsoft Windows 3.1, LogView was developed to facilitate the layout, viewing and printing of combinations of logs generated from a series of GSC logging probes used in this research.

OVERVIEW OF LOGVIEW

Borehole geophysical logs, associated geology, and other related data such as assays can be viewed on screen (with zoom/pan mode available) and printed on any Windows 3.1 supported printer.

Logging parameters recorded with different probes and different sampling rates do not have to be interpolated to the same depth intervals. This allows the maximum detail in each data set to be retained.

Displayed logs of data can be stretched, compressed, depth shifted and smoothed. Attributes ranging from lithology log area fills, colours, line styles, titles and font sizes can be edited and annotation objects can be added to enhance the presentation. While manipulating screen displays, the cursor position can be displayed in terms of log units (depth and parameter) or as X-Y paper position in mm.
A lithology legend, with identifying labels for the lithology colours and patterns, can be placed anywhere on the layout. A depth axis reference grid at regular depth intervals or at specific depths can also be added to the display.

In the design of a single layout, LogView allows for three different colour tables to be used. This would, for example, let you design a layout in colour in one colour table, and in black and white in a second colour table, without having to specify size and other attributes twice.

The attributes for a specific layout can be saved for future use and revision.

HELP FEATURE

The on-line help can be accessed from either the HELP MENU for a general look at contents and to search for keywords, or from individual menus and screens when specific help is required.
If hardcopies of some help items are desired, any section can be printed from the HELP menu.

MACHINE REQUIREMENTS

LogView is a Microsoft Windows 3.1 application which requires an 80386 PC or better. Four MB of RAM are needed to run smoothly, and a math co-processor is recommended, since LogView relies heavily on floating-point calculations. The installed LogView files require less than half a MB of hard disk space. Hardcopy output quality will depend on the printer.

DATA FILE FORMATS

GSC Acquisition of Borehole Geophysical data

GSC borehole logs are acquired with several probes at different logging speeds and sampling rates. The depth ranges and the data sampling intervals recorded for each logging run will therefore vary. It is standard procedure to plot logs from several probes beside one another, so the data for each run in a borehole for each parameter are stored as separate data files. The file detailing the geology for the borehole is also stored as a separate lithology file. LogView was designed to plot any combination of these data files, and to allow the lithology file to be plotted as coloured or patterned infill underlying the log traces.

Filename Extensions:

GSC borehole logging data are archived in several different formats and internal structures. Filename extensions are used by our software to determine the internal structure and format of the file. The first character of the extension determines the format of the data. (A for ASCII and B for binary). The second character of the extension determines the internal data structure of the file. (Z for depth-value data pairs, Y for data over equal depth intervals, H for histogram and L for lithology). The third character is left to the user. (For example: 1,2,3.. for version number, or P for permanent, T for temporary, O for original.)

Data Formats:

Data files (Z, Y and H) can be either ASCII or binary format. Lithology is stored as an ASCII file. Logview has a built in utility to convert ASCII files to binary, which may be used to save disk space.

Internal Structure of Data Files:

All files have two 8 character titles at the beginning of the file. For GSC data, we have used these titles as log-title and units. Logview allows you to change the 'titles' that will be plotted. Depth and data values are single precision floating point numbers.

Z data files have data values at non-regular depth intervals, and consist of two 8 character titles, followed by records of pairs of depth and measured value.
For example:

```
TC
(CPS)
40.01     79.41
40.06     72.76
40.11     86.47
40.16     79.42
...
```

Y data files have data values at regular depth intervals, and consist of two 8 character titles, then a record with depth-start and depth-increment, followed by records of measured values.
For example:

```
TC
(CPS)
1.0 .2
79.41
72.76
86.47
...
```

H data files, or histogram files can be used for data such as assays which may be taken at irregular depth intervals. H data files have triplets of data values, and consist of two 8 character titles, followed by records of two depth values; a start and stop depth for each sample, and the measured value.
For example:

```
K
(%)
40.2      41.0      1.05
41.0      42.5      3.57
42.5      43.2      1.66
43.2      44.8      2.47
...
```

L data files, or lithology files contain the geological units, and consist of two 8 character titles, followed by records of lithology unit label, (enclosed in double quotes if it has embedded blanks), and depth start and depth end for the lithology unit.
For example:
GEOLOGY

```
-------
MTSD        40.00  45.20178
"GRN SCH"   45.20  50.13953
AMPHIB      50.13  63.39832
CONGLOM     63.39  67.97031
MTSD        67.97  83.66749
"GRN SCH"   83.66  89.91588
...
```

OTHER FILES USED BY LOGVIEW

'Log display List' Files

LogView creates ASCII 'log display list' (LDL) files to save the attributes of a specific layout. The LDL file can be opened to reproduce the layout as originally designed, or to copy and edit it to produce a similar layout.

The specifications stored in the LDL file include a list of the logs to be plotted, along with an associated set of attributes such as line styles, titles, font sizes, filters, transforms, and clipping options for each displayed log. Also stored in the LDL file are the attributes for the layout as a whole. These includes details such as page titles, reference grid and depth axis options and paper size. Before a new layout is created, a printer and paper size must be selected. Paper sizes available will depend on the chosen printer, and portrait or landscape orientation may be used. If the paper size is changed while designing the layout, LogView will give you the option to resize the logs to fit the new paper size.

Depth axes, which can be placed anywhere alongside the other logs, and annotation files which contain objects (eg. a box with text) that are drawn on the layout, are also included in the LDL list of files.

There are a few items that can not be changed in any LogView menu, but may be edited in the LDL file. These include setting the depth axis label on the right instead of on the default left, matching the log title colour to the axis colour, setting colours for the reference grid and page titles, and setting a font for the entire layout.

Annotation Files

'Annotation' (LAN) files can be added to the list of files to be plotted for a particular layout. Size specifications in annotation files are based on sizes in mm on paper, so the type of printer and the paper size to be used must be known. By turning on 'smart cursor' in the options menu and choosing 'show paper position', it can be determined where to place the annotation. The following annotations can be added:

LINES, BOXES, ROUNDED BOXES, POLYLINES, POLYGONS AND TEXT BLOCKS.

The annotations can use different fonts, line styles and colours/patterns.

This feature is particularly useful if there will be several pages of log output with the same surrounding annotation on each. One LAN file could be created and added to each LDL file.

The specific formats of each annotation feature are detailed in the LogView on-line HELP.

Support Files

LogView utilizes two types of support files.

The first support file is referred to as the 'LITHOLOGY LOOKUP' file (LLL). This file relates the names assigned to geological units to colours and patterns to be displayed for these units, for the three colour tables used in LogView. One master file can be created with all geological units to be used or individual files can be created for each project area. LogView allows you to choose the LLL file you wish to currently use.

The second support file is a 'CUSTOM PATTERN FILE' (PAT). This file allows you to create your own custom patterns to add to those provided by Windows.

Windows INI File

LogView creates and updates a LOGVIEW.INI file in your Windows directory. This file keeps track of your current choices in LogView for features such as background colour, cursor mode, memory option and auto-redraw. It also records the path of your last used lithology lookup table file and custom pattern file. This is an ASCII file which can be edited.

MENUS

LogView menus are typical Windows 3.1 menus, and are listed below, with details about some of the functions:

FILE MENU

CREATE NEW LAYOUT
OPEN LAYOUT
CLOSE LAYOUT
SAVE LAYOUT
SAVE LAYOUT AS
CHANGE PAPER
- choose printer and paper size

PRINT
- to Windows 3.1 supported printer

GO TO DOS
- open a DOS window

EXIT

EDIT MENU

DISPLAY LIST
- edit the list of files to be displayed
- look at the depth and value range for each file

DEPTH VIEWING RANGE
- pick the depth viewing range of each log displayed

LAYOUT & COLOURS
- choose colours/patterns and line styles and 'in-fill' colours
- choose lithology 'in-fill' files
- choose the axis sizes and spacing between logs

LOG DETAILS
- for each log, choose titles and fonts, choose if depth axis is to be displayed or not and choose to have the filename printed below the log

Y-AXIS
- for each log, choose min and max display values, choose whether log is to be clipped, choose the value for a Y axis baseline, and choose the number of decimals and multiplier for axis labels

Y-AXIS DETAILS
- for each log, choose to have the baseline and it's value labelled, or just the line, or just the label
- for each log, choose to have the value axis at the top, bottom or both and the axis and axis labels displayed or not

Z & Y TRANSFORMS
- for each log, choose to transform (linear only) the depth and/or data values
- for each log, apply a smoothing filter or take the logarithm

LITHOLOGY LEGEND
- create a 'Lithology Legend', specifying labels, sizes and position of legend

PAGE TITLES
- set up page titles text and font sizes

REFERENCE GRID
- on the depth axis, choose no grid, regular grid intervals or grid lines at specific depths

Z AXIS APPEARANCE
- choose the tick mark/labelling interval for the depth axes

Z AXIS MARGINS
- choose top/bottom page margins or set a specific depth scale

COPY TO CLIPBOARD

VIEW MENU

REDRAW

ZOOM
- with mouse

ZOOM BY RANGE
- to a specific depth range

UNZOOM

OPTIONS MENU

CONSERVE MEMORY
- runs a little slower, but requires less memory, since data files are not kept in memory

CROSSHAIRS
- turn on the crosshairs cursor instead of the arrow cursor

SMART CURSOR
- depth and value of logs OR the X-Y position in mm on 'paper' will be displayed when this feature is on. This allows you to compare depth positions for similar features on several logs, and also allows you to determine where to put annotation.

COLOUR TABLE
- choose the current colour table

SUPPORT FILES
- choose 'support files' for lithology lookup and for custom patterns

TOOLS MENU

CONVERT ASCII LOGS TO BINARY

HELP MENU

CONTENTS
SEARCH FOR
ABOUT LOGVIEW

EXAMPLES

This paper was originally presented in poster format, taking full advantage of colour illustrations. Although the content will be similar to that presented in the poster, some of the impact is lost in black and white.

Figure 1 is an example of multiparameter logs plotted for a single hole. Other features to be noted in this example are the TempGrad axis plotted at the bottom of the log, Low and High used for relative Density values, and a legend created in LogView with legend notes created in an annotation file.

Figure 2 is an example of the Gamma Ray logs for several holes plotted with the geology beside as well as underlying each log. The legend and other text features were created in an annotation file.

Figure 3 is an example of assays plotted beside logged parameters. Text has been added for description. (SGG Ratio is the ratio of the counts in a high energy window to those in a low energy window for a spectral gamma-gamma probe measuring a full energy spectrum. It can be used as a 'heavy element indicator'.)

Figure 4 demonstrates some of the transforms available for both depth and value data. The Gamma Ray log appears as unsmoothed data and then with two smoothing filters. The Resistivity log is presented on a linear scale, and then as a logarithm to base e and as a logarithm to base 10. The Density log is shown untransformed and then with a depth shift, and with a value transformation (multiplied by 2). Note also, in this example, that grid lines at standard depth intervals have been added. (Grid lines at specific depths could have been added instead.) Y-axis baselines (with lines, labels and both) are also shown.

Figure 5 displays the use of clipping, at the minimum for IP and at the maximum for Resistivity, A lithology fill under the log is also shown.

Figure 6 shows portrait plot orientation. Note also that the geology is labelled beside the lithology file, instead of a legend.

Figure 7 presents some of the many types of annotation which can be added to a LogView layout.

CONCLUSION

Within the Borehole Geophysics Section of the GSC, LogView has become a standard viewing and plotting package. Since it was felt that others could use this type of software, LogView, version 1.0, was released as GSC Open File 3055 in April,1995 and is available through the GSC bookstore.

GSC Open File 3055 includes the following, on one diskette:

1) an ASCII 'read me' file, with general information and details on LogView installation procedures.
2) a self extracting file with: the LogView executable and HELP file, a sample lithology lookup file, a sample patterns file, a directory of sample data which includes examples of data, lithology, display list and annotation files and a directory with a Windows 3.1 dynamic link library file, CTL3DV2.DLL, which creates 3D effects and which must be installed on your computer.

The GSC is continuing to upgrade LogView, and when a significant number of new features have been added, the next version of LogView will be released.

ACKNOWLEDGEMENTS

The authors wish to thank D. Markarian for writing LogView under the guidance of J.A. Grant, J.A. Grant for initial and continuing recommendations on LogView and J.M. Carson for the critical reading of this manuscript.

REFERENCES

Geological Survey of Canada Open File 3055
LogView - A Microsoft Windows 3.1 application to view borehole log (geophysical and geological) data; D. Markarian, J.A. Grant and B.E. Elliott
Distributed through the Geological Survey of Canada Bookstore,
601 Booth St., Ottawa, Ontario, K1A 0E8.
Tel: (613) 995-4342 Fax: (613) 943-0646 e-mail: gsc_bookstore@gsc.emr.ca

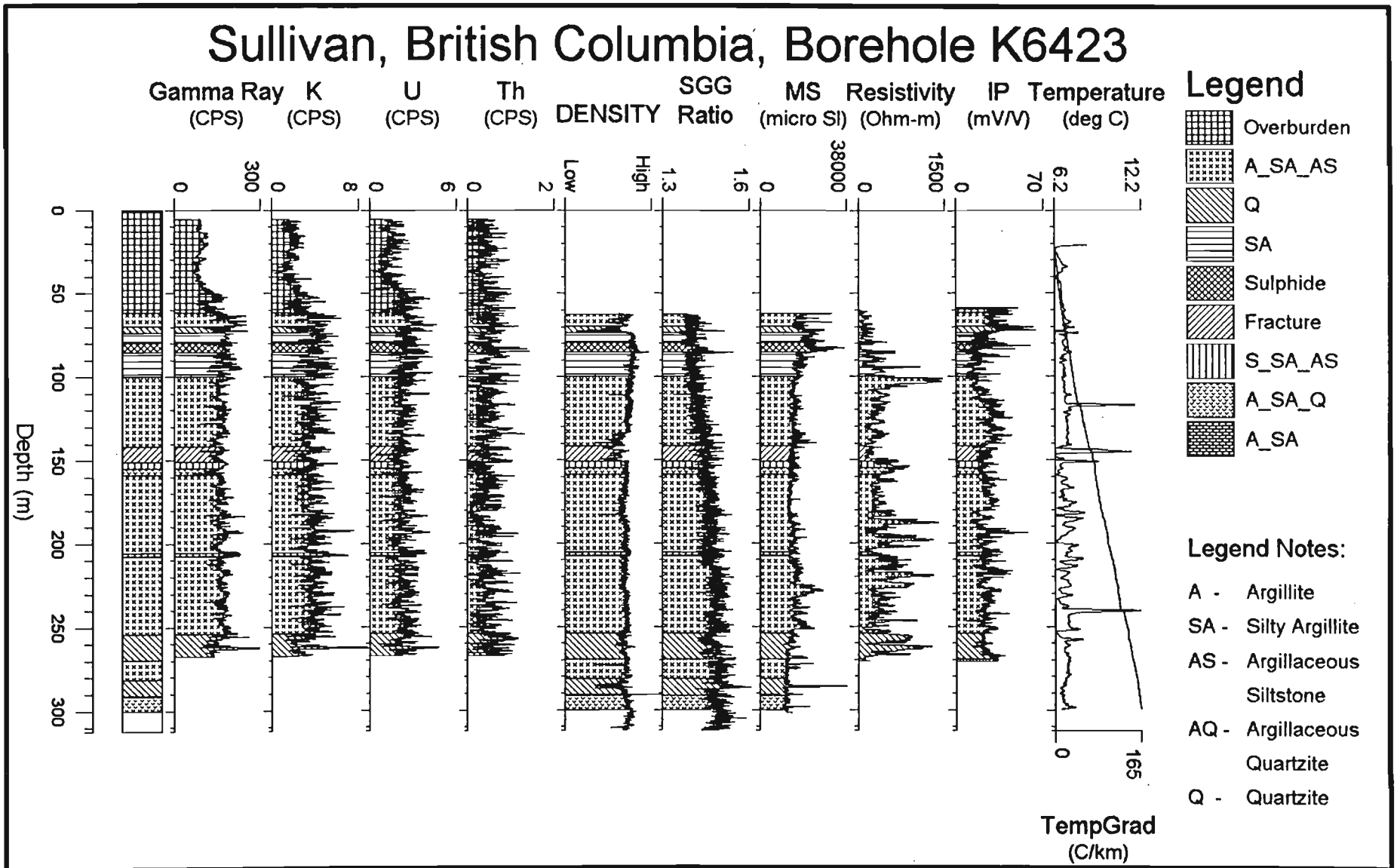

Figure 1: Multiparameter logs plotted for a single hole.

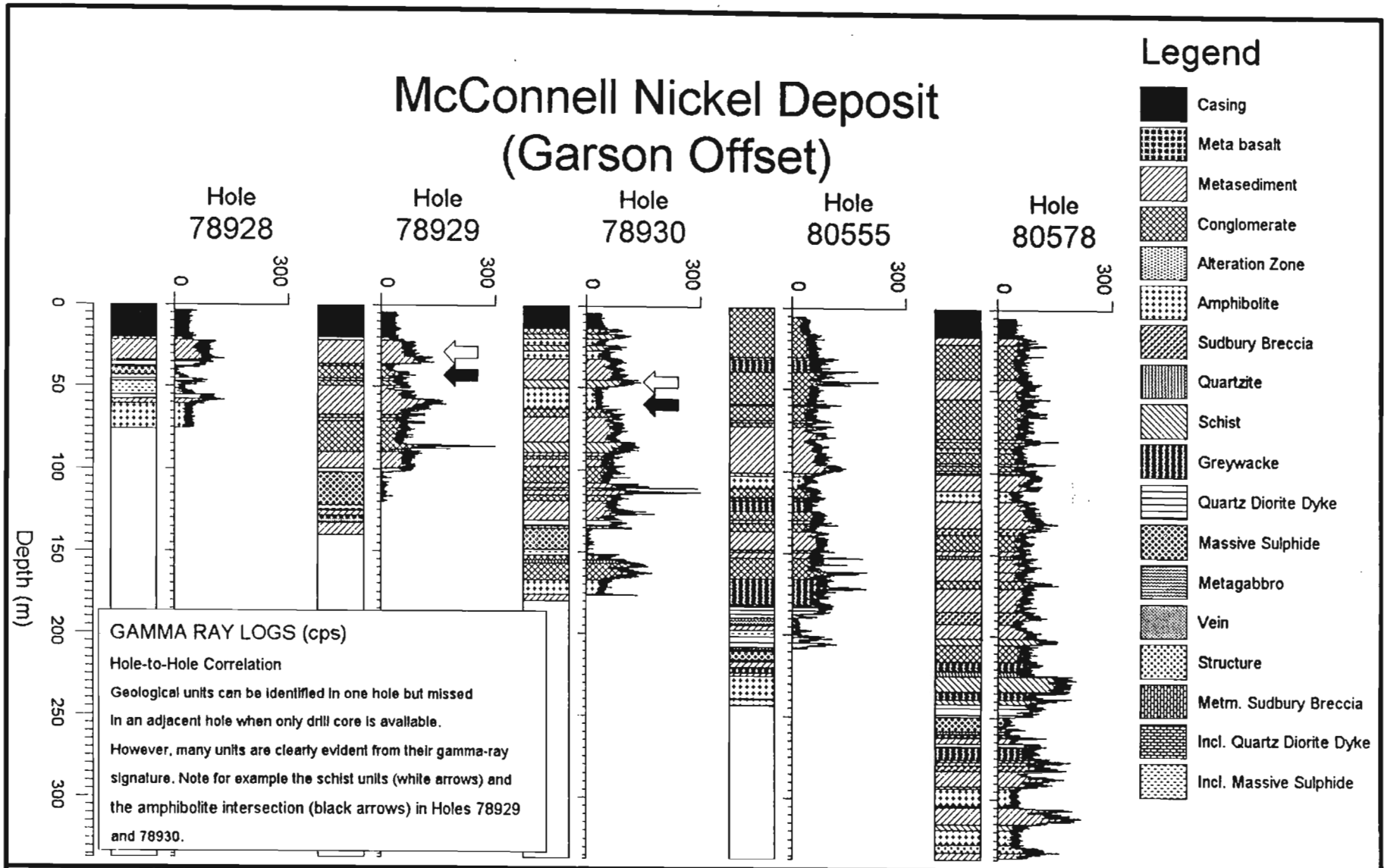

Figure 2: Gamma Ray logs for a fence of holes.

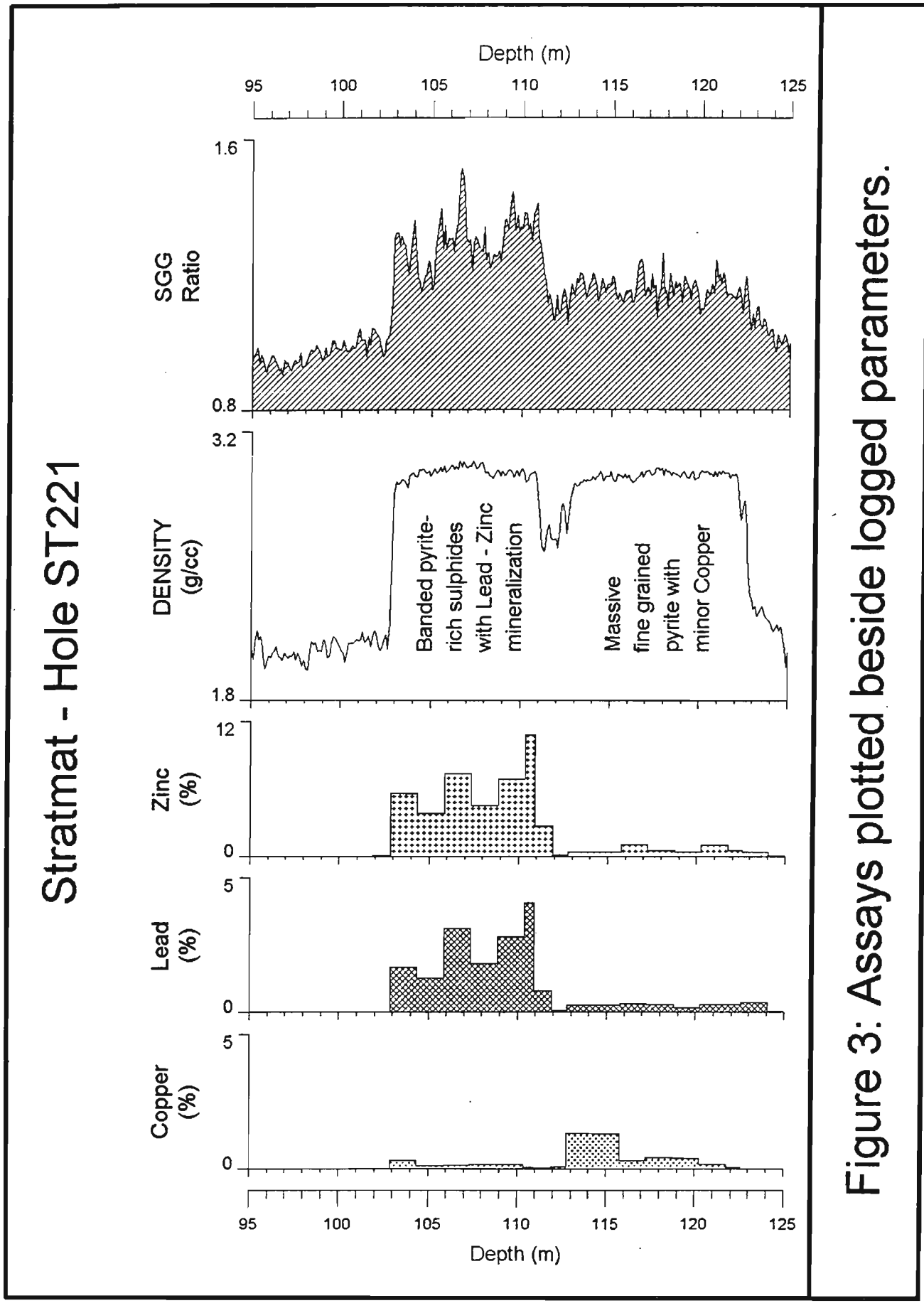

Figure 3: Assays plotted beside logged parameters.

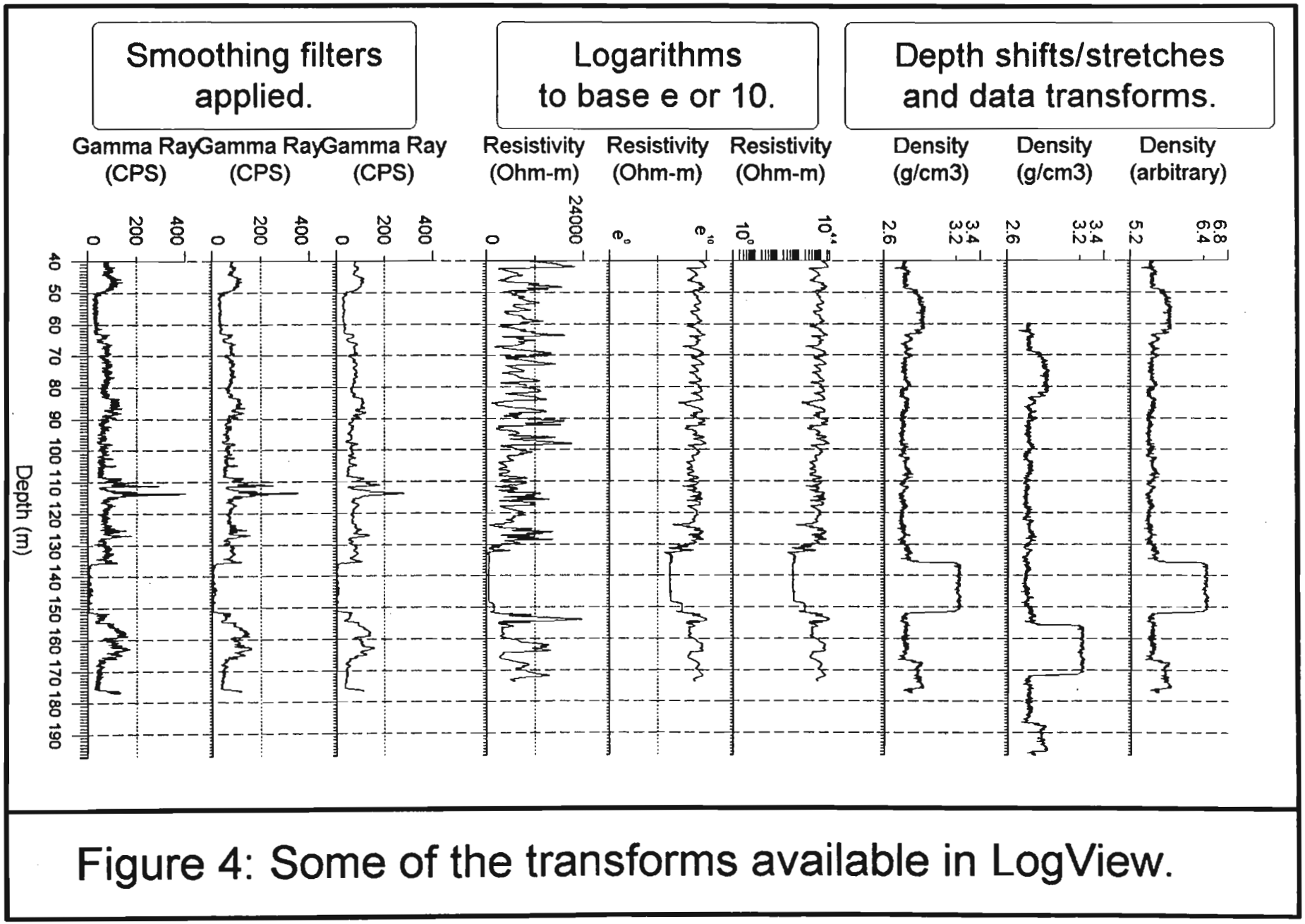

Figure 4: Some of the transforms available in LogView.

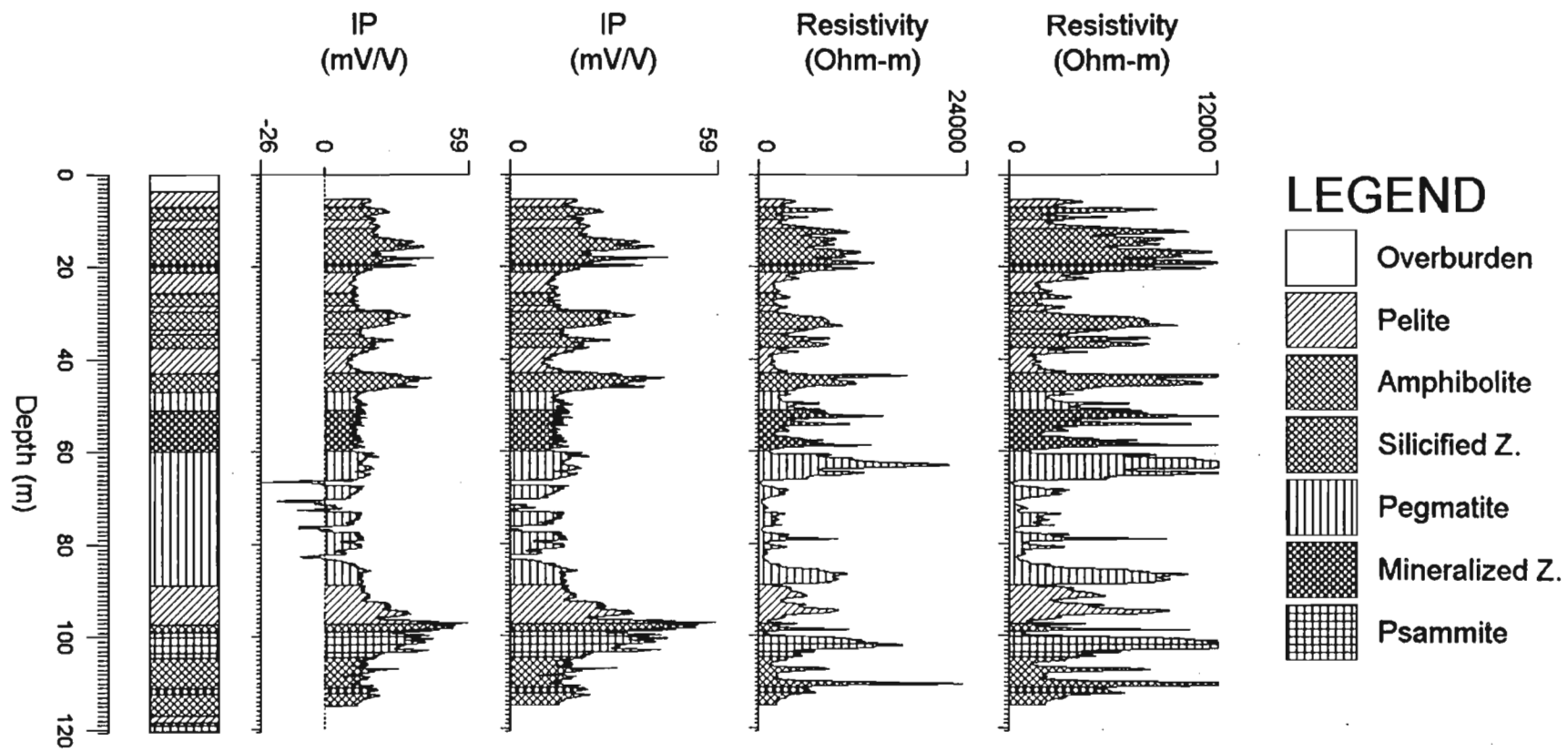

Figure 5: IP and Resistivity logs plotted to show clipping.

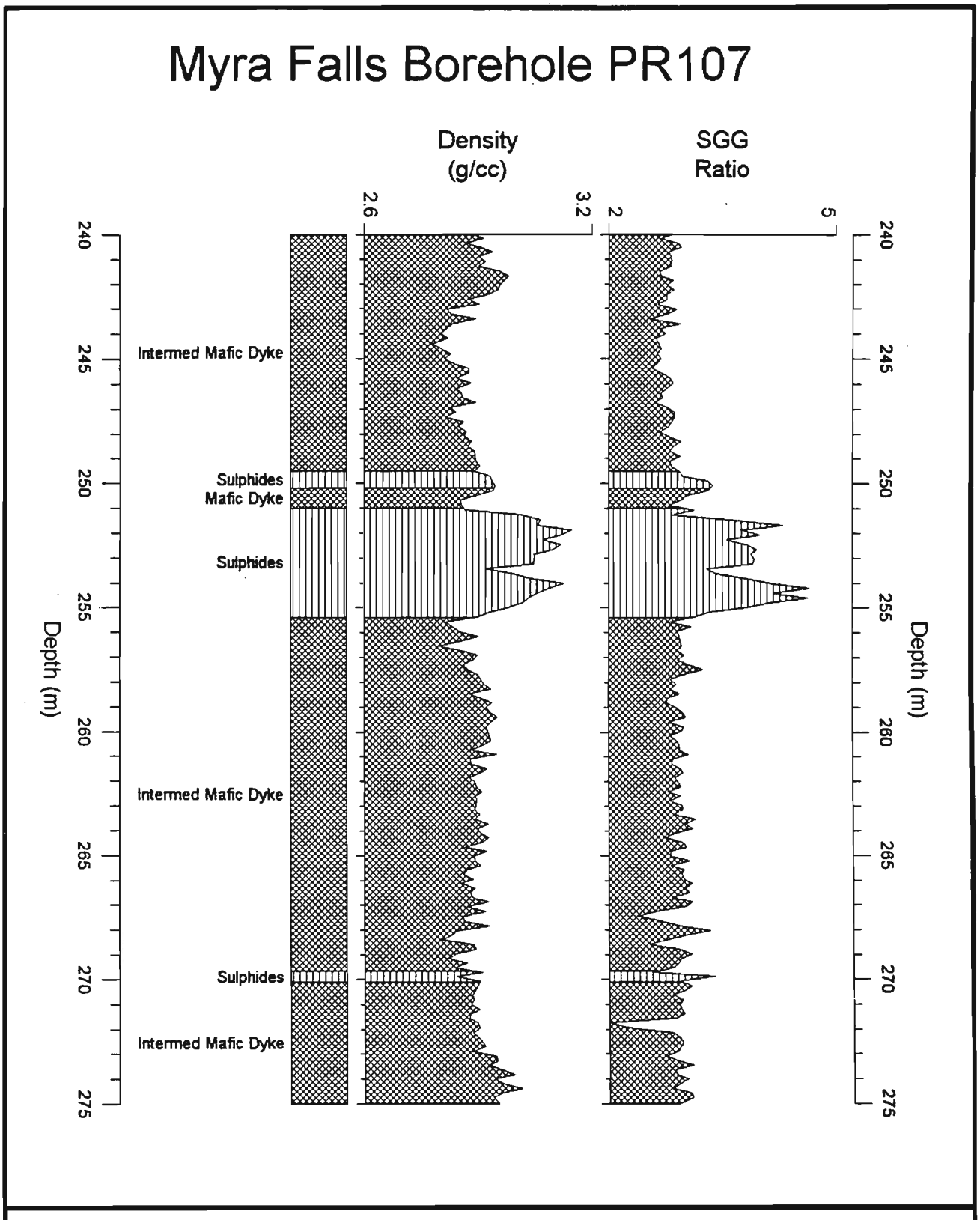

Figure 6: Plot can be portrait orientation.

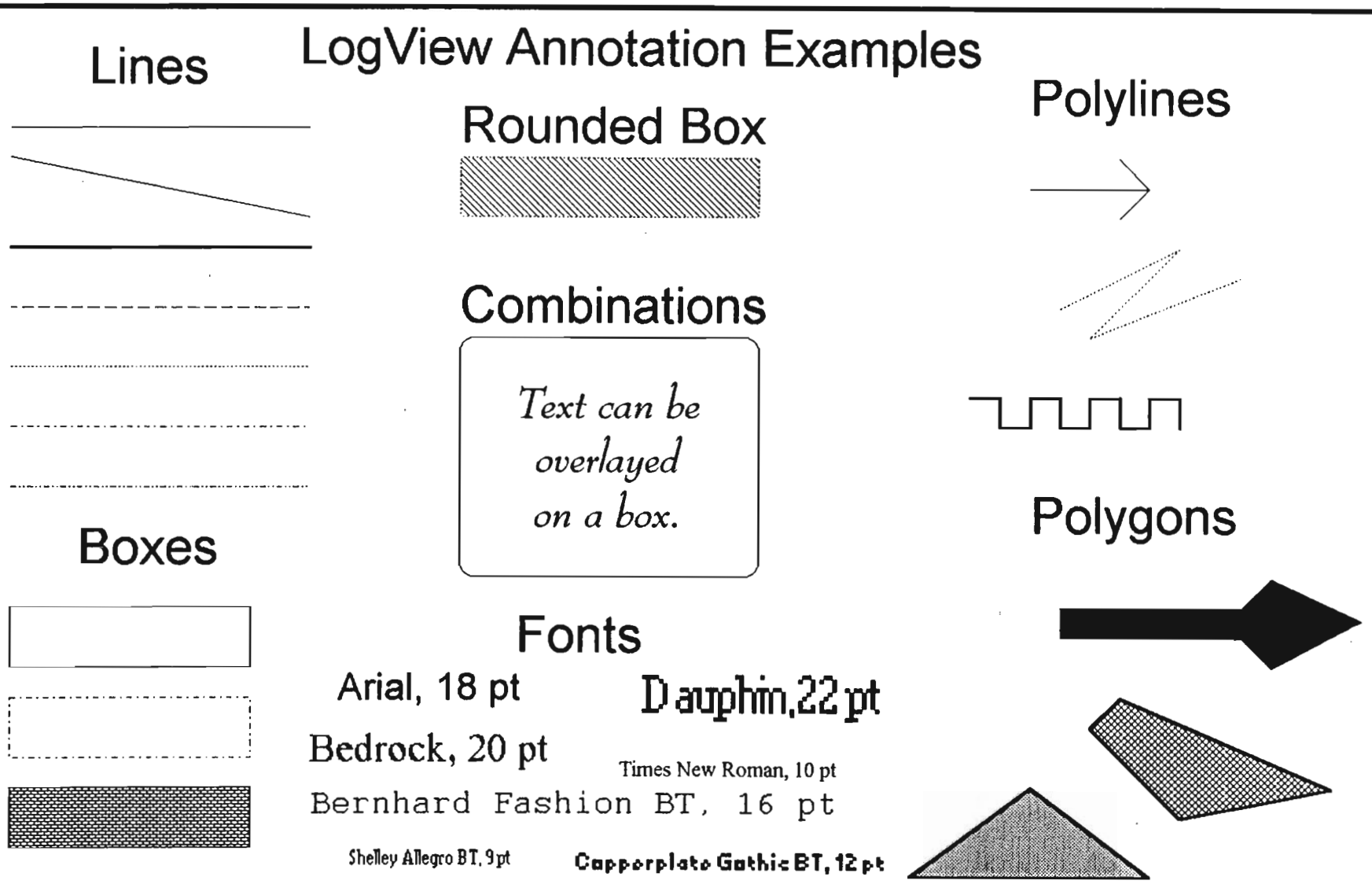

Figure 7: Samples of annotation available in LogView.

CLASSIC EXAMPLES FROM THE GEOLOGICAL SURVEY OF CANADA DATA FILES ILLUSTRATING THE UTILITY OF BOREHOLE GEOPHYSICS

C.J. Mwenifumbo, P.G. Killeen and B.E. Elliott
Geological Survey of Canada, 601 Booth St., Ottawa, Ontario K1A 0E8

C.J. Mwenifumbo, P.G. Killeen and B.E. Elliott, Classic examples from the Geological Survey of Canada data files illustrating the utility of borehole geophysics: in Proceedings of the 5th International Symposium of the Minerals and Geotechnical Logging Society, Tulsa, 24-28 October, 1993.

ABSTRACT

Over fifteen years of experience in the application of borehole geophysical measurements to geoscience problems has provided the Geological Survey of Canada with numerous examples which clearly illustrate the benefits of borehole logging. Several 'classic' examples have been assembled for use in explaining applications of borehole geophysics to various problems. These 'typical examples' include the following parameters; 1) natural-γ radioactivity, 2) γ-γ density, 3) heavy element content, 4) resistivity, 5) induced polarization, 6) self potential, 7) magnetic susceptibility, and 8) temperature. Several of these examples are presented with a brief description of what these parameters measure.

INTRODUCTION

The Borehole Geophysics Section of the Geological Survey of Canada (GSC) operates an R&D borehole logging system that has been used to acquire borehole geophysical data at a number of sites across Canada and for various types of applications. The main objective of carrying out these borehole geophysical surveys has been to demonstrate the utility of borehole geophysics in a variety of geoscience problems including mineral exploration, stratigraphic mapping, and geotechnical and hydrogeological problems in various geological environments. The applications have included the delineation of mineralized zones, mapping of alteration zones associated with mineralization, lithologic interpretation and hole-to-hole stratigraphic correlation, in situ assaying of base metals, in situ physical rock properties, mapping fracture zones and detecting groundwater flow patterns. The borehole geophysical parameters that have been measured include resistivity (with various electrode array geometries), induced polarization (IP), self potential (SP), natural γ-ray spectrometry (total count, K, U and Th), spectral γ-γ (density, and heavy element assay), magnetic susceptibility, temperature and temperature gradient. In this paper we present some 'classic' examples of the geophysical responses of most of these parameters that have been acquired with the GSC R&D logging system. A brief discussion of the response characteristics of each of the geophysical logging parameters precedes the examples.

NATURAL γ-RAY

γ-ray measurements detect variations in the natural radioactivity originating from uranium (U), thorium (Th) and potassium (K) in rocks. In igneous and metamorphic rocks these sources of natural radiation may contribute almost equally to the total γ-rays detected by a gamma probe. In sedimentary rocks, ^{40}K is in general the principal source of natural γ-radiation, primarily originating from clay minerals such as illite and montimorillonite. Since the concentrations of these naturally occurring radioelements vary between different rock types, natural γ-ray logging provides an important tool for lithologic mapping and stratigraphic correlation. Also some of the alteration processes associated with mineralization are characterized by the development of sericite (sericitization) that results in an increase in potassium and hence a corresponding increase in the ^{40}K isotope. This makes sericitized zones excellent targets for γ-ray logging.

Although natural γ-ray logging is standard practice in uranium exploration, oil exploration and coal evaluation, there has been a limited application of the technique to geologic mapping in igneous and metamorphic terrains. The following two examples illustrate some typical responses of the total count γ-ray logs in volcanic rocks. Figure 1 is a total count γ-ray log recorded in a hole that intersects mainly volcanic rocks at a massive sulfide deposit in Newfoundland (Mwenifumbo and Killeen, 1987). The volcanic rocks intersected include andesites, rhyolites and diabase dikes. These major volcanic units can be readily distinguished on the γ-ray log. Rhyolites have the highest γ-ray activity, followed by andesite. The diabase intrusions are characterized by extremely low γ-ray activity. All of these units have fairly uniform

distribution of the radioelements indicating probable chemical homogeneity within the individual units. Most of the γ-ray activity within these volcanic units is derived from ^{40}K, the more felsic the volcanic rock, the higher the γ-ray activity. It is interesting to note that the upper rhyolite flow has lower γ-ray activity than the feldspathic rhyolite. The higher γ-ray activity of the feldspathic rhyolite is due to higher concentrations of potassic minerals. Another interesting feature in the γ-ray log is the higher γ-ray activity between 190 and 210 m within the andesite. The geologic log does not indicate any change in lithology., however, the γ-ray data suggest that it is a rhyolite.

Figure 2 is an example of a γ-ray log from an ultramafic volcanic rock environment. This log was recorded at a nickel deposit in the Timmins area of Ontario. The major lithologic units intersected by this hole are ultramafic, mafic and felsic volcanics. These units are readily distinguished from each other. The γ-ray response within the ultramafic is virtually zero implying that the ultramafic is almost devoid of all the natural occurring radioelements. The highest activity is within felsic rocks. Since geological logging in volcanic rocks is often difficult due to similarities in the appearances of the rocks, logging of the drill core would be much easier and less subjective with the aid of geophysical logs such as γ-ray logs. Further distinction between different rock units can be enhanced by the use of spectral γ-ray logs.

DENSITY

The γ-γ density probe response is primarily a function of the rock bulk density. The probe consists of a γ-ray source and a γ-ray detector. γ-rays emitted by the source are scattered by the enclosing rock wall and absorbed as a direct function of the electron density of the rock. The compton-scattered γ-radiation that is measured at the γ-ray detector on the probe is inversely related to the electron density of the rock that is proportional to the rock bulk density. The density of the rock is also affected by secondary physical properties which include porosity, water content and chemical composition of the rock as it affects the ratio of average atomic number to the average atomic weight, Z/A. Most of the density variations within igneous and metamorphic rocks are due to variations in mineralogical composition. Rocks with higher percentages of mafic minerals (Fe, Mg, Al silicates) have higher densities than those with higher percentages of felsic minerals (Ca, Na, K, Al silicates). The presence of minerals containing heavy elements such as base metals tend to increase the overall density of the host rock.

Density logs are routinely acquired in oil and coal exploration (mostly sedimentary environments) but fairly seldom acquired in igneous and metamorphic environments for geologic mapping. Figure 3 illustrates the use of density logs in geologic mapping in a metamorphic environment. This log was acquired at the Calumet Pb-Zn-Cu massive sulfide deposit, Quebec. The amphibolites have the highest densities followed by the amphibolitic biotite and then siliceous biotite gneiss. Pegmatite is characterized by low density due to the preponderance of light minerals in its composition. Figure 4 shows a density log acquired at the McConnell nickel deposit in Sudbury, Ontario. The hole intersects massive sulfides which are clearly distinguished by their high density. Again we see that the amphibolite has higher densities than the metasediments/conglomerate/schists. The density log gives an excellent response to massive sulfide zones and can be effectively used in geologic mapping.

HEAVY ELEMENT CONTENT

The heavy element assay log is derived from the spectral γ-γ probe that also provides the density (Killeen and Mwenifumbo, 1988). Complete backscattered γ-ray spectra are recorded in 1024 channels over an energy range of approximately 0.03 to 1.0 MeV. Density information is determined from the count rate in an energy window above 200 keV while information about the elemental composition or heavy element content is derived from the ratio of the count rates in two energy windows (spectral γ-γ ratio, SGG); one at high energy (above 200 keV) and one at low energy (below 200 keV). When there is a change in the density of the rock being measured, the count rates recorded in both windows will increase or decrease due to the associated change in compton-scattered γ-rays reaching the detector. However, if there is an increase in the content of high Z (atomic number) elements in the rock, the associated increase in photoelectric absorption will cause a significant decrease in count rate in the low energy window with little change in the high energy window. Since the low energy window is affected by both density and Z effect while the high energy window is mainly affected by density, the ratio of counts in the high-energy window to the counts in the low-energy window can be used to obtain information on changes in Z. This ratio increases when the probe passes through zones containing high Z materials. Thus the log can be considered as a heavy

element indicator, and can be calibrated to produce an assay tool for quantitative determination of the heavy element concentration in situ along the borehole, without resorting to chemical assaying of the core (Killeen and Mwenifumbo, 1988).

Figure 5 shows the chemical lead assay and the SGG ratio recorded at the Yava Pb deposit, Nova Scotia. . The host rock for the lead mineralization is sandstone with occasional interbedded black shales. This deposit is essentially a monomineralic deposit. Chemical assays of Pb, Zn and Fe were determined from the drill core every 10 cm over the interval shown in Figure 5. There is an excellent correlation between the Pb mineralization and the SGG ratio (figure 6) with a correlation coefficient, r=0.897. The linear relationship established from the crossplot of Pb versus SGG ratio (Figure 6) was used as a calibration to determine the in situ assay log in other holes that did not have any detailed chemical assay.

INDUCED POLARIZATION (IP)

In time domain IP measurements, the rate of decay of the measured voltages during the current off-time is related to the electrical polarizability of the rock and is called chargeability. A high chargeability response is an indication of the presence of metallic sulfides and oxides or cation-rich clays such as illite and montmorillonite (Mwenifumbo, 1989). One of the major alteration processes within a number of base metal and gold mining camps is pyritization and this is a target for most IP logging. Continuous time domain IP logs are presented from three different geological environments; (i) a carbonate-hosted zinc deposit, (ii) a disseminated sandstone lead deposit, and (iii) a massive sulphide deposit.

Figure 7 shows the resistivity, standard-, and multiple-window, continuous time-domain IP data from a carbonate-hosted Zn deposit in Newfoundland. Zn assays from the drill core are also shown with values ranging up to 8 %. Although sphalerite is a poor conductor and does not generally give an IP response, the Zn mineralization is easily detected on the IP logs. The IP response may be due to the presence of polarizable minerals such as pyrite associated with Zn mineralization.

Figure 8 shows resistivity and IP logs from the Yava sandstone Pb deposit in Nova Scotia. These data were obtained with a 10-cm normal array. The borehole intersects three major lithologic units; 1) the sandstone which is the host for lead mineralization, 2) the underlying Windsor shale, and 3) rhyolite breccia. The IP data clearly indicate the zones with disseminated galena in the sandstone by high IP values. The occurrence of Pb mineralization is also apparent at the base of the Windsor shale and within the rhyolite breccia where there are anomalous IP responses. The Pb mineralization at these locations was confirmed from the drill core data.

Figure 9 shows resistivity, inductive conductivity and IP logs from a massive sulphide deposit in British Columbia. The borehole intersects phyllite and graphitic phyllite which contain disseminated and massive sulfide mineralization. IP measurements in highly conductive massive sulfides or graphitic phyllite are unreliable because of poor signal-to-noise ratio. However, at this deposit, the IP log may be used to distinguish the phyllite containing disseminated sulfides from those that are devoid of sulfide mineralization. Sulfides seen visually in core are indicated on the figure. It is clear from the IP log that a number of zones with disseminated sulfide mineralization (e.g.from 85 - 90 m) were not noted in the core log. Most of the phyllite/quartz unit between 100 and 130 m contains disseminated sulfides, mainly pyrite.

RESISTIVITY

The electrical resistivity of rocks depends on several factors including the presence of conductive minerals such as base metal sulfides or oxides and graphite in the rock. Most rocks without these minerals are usually poor conductors and their resistivities are governed primarily by their porosity and salinity of the pore water and to a lesser extent by the intrinsic minerals that constitute the rock. Some alteration processes such as silicification and carbonatization tend to reduce the porosity of the rock and hence increase the resistivities of the rocks. Thus in rocks where no significant amounts of conductive minerals occur, the most important factors affecting the resistivities are fracturing, porosity, the degree of saturation of pore spaces and the nature of the electrolytes in the pore fluids. The resistivity log is, therefore, useful mainly in mapping conductive minerals and fracture zones. In sedimentary rocks, the resistivity log is frequently used in lithologic mapping. The following two examples illustrate the use of resistivity logs in lithology and fracture mapping, and delineating conductive minerals such graphite and sulfides.

Figure 10 shows 40-cm normal resistivity logs from three drill holes at the Bells Corners borehole geophysical test site near Ottawa. The holes penetrate up to 65 m of Upper Cambrian Nepean sandstone which unconformably overlies Precambrian granites and

gneisses. Just below the sandstone is a zone of severely weathered Precambrian granite with abundant chlorite and clay minerals. Within the PreCambrian granites and gneisses are several fracture zones varying in width from 2 to 10 m. The apparent resistivities of the Nepean sandstone are around 1000 ohm-m and those of the Precambrian granite/gneiss are around 10000 ohm-m. The majority of the fracture zones within the Precambrian basement rocks have apparent resistivities less than 10000 ohm-m. The lower resistivities in these fracture zones is due to increased porosity of the granite and gneiss. The wide low-resistivity anomaly at the contact between the sandstone and the Precambrian granite/gneiss (between 64 and 80 m) is the weathered basement whose low resistivity can be attributed to both porosity increase and the presence of conductive clay minerals. These logs are a good example of the use of resistivity logs for lithologic and fracture mapping.

Figure 11 shows the resistivity log response through graphite at the Victoria graphite deposit, Ontario. The conductive graphite is clearly distinguished as low values on the resistivity log. At this deposit there was an excellent inverse correlation between the percentage graphite and the resistivity. Another example of the use of the resistivity log in mapping conductive minerals can be seen in Figure 9. Graphitic phyllite with a high percentage of sulfide minerals is characterized by very low resistivity.

SELF POTENTIAL (SP)

SP anomalies are mainly an indication of the presence of graphite and/or high concentrations of base metal sulfides including pyrite. Large self potentials observed within and around sulfide and graphite bodies are mainly caused by electrochemical processes (Sato and Mooney, 1960, Hovdan and Bolviken, 1984). Low resistivity anomalies correlating with SP and IP anomalies are, therefore, good indications of the presence of conductive minerals. Also SP anomalies can be generated by fluid flow in porous media (electrokinetic or streaming potentials - Bogoslovsky and Ogil'vy, 1970, 1972) and heat flow (thermal electric coupling - Corwin and Hoover, 1979). The following two examples illustrate the SP anomalies generated by electrochemical reactions and fluid flow.

Figure 12 shows an SP log acquired at the Stratmat volcanogenic massive sulfide deposit, New Brunswick. Continuous SP measurements were made between a stationary reference nonpolarizable $Cu/CuSO_4$ electrode placed at the surface near the drill hole collar and a lead electrode in the hole. Large negative potentials are observed across the massive sulfide zone. The sulfides consist mainly of pyrite, galena, sphalerite and minor chalcopyrite and the host rock comprises of argillite, tuff and gabbros. This is a typical SP anomaly developed due to electrochemical reactions within the metallic sulfide body (Sato and Mooney, 1960).

Figure 13 illustrates an SP anomaly generated by fluid flow. The SP log was acquired at the Yava sandstone Pb deposit. The normal SP anomaly associated with sulfide occurrences is observed within the mineralized sandstone around 10 m. The step change in SP of approximately 75 mV at 39 m is associated a 0.9 °C change in temperature caused by groundwater flow as indicated by the temperature and temperature gradient logs. This SP anomaly is likely generated by both temperature change (thermal electric coupling) and water flow (streaming potential). This hole has been re-logged 3 times over a period of 3 years and repeatedly showed the same amplitude SP anomaly.

MAGNETIC SUSCEPTIBILITY

The magnetic susceptibility (MS) of a volume of rock is a function of the amount of ferrimagnetic minerals - magnetite, ilmenite and pyrrhotite - contained within the rock. MS measurements can provide a rapid estimate of the magnetic minerals in the rock. These measurements can be interpreted to reflect lithological changes, degree of homogeneity and the presence of alteration zones in the rock mass. Basic flows and diabase dikes containing higher concentrations of magnetic minerals are easily delineated with magnetic susceptibility measurements when they occur within a sedimentary sequence which normally contains little or no magnetic minerals. During the process of hydrothermal alteration, primary magnetic minerals in the host rock (e.g. magnetite and ilmenite) may be altered (or oxidized) to weakly- or non- magnetic minerals (e.g. hematite and limonite). Anomalously low susceptibilities within an otherwise homogeneous high susceptibility rock unit may be an indication of altered zones.

Figure 14 shows a borehole magnetic susceptibility log acquired at the Redstone Nickel deposit, Ontario. This is a typical example of susceptibility responses within ultramafic, mafic and felsic volcanic rocks. Ultramafic rocks have fairly high magnetite content and hence are characterized by high susceptibility values. The felsic rocks with little or no magnetic minerals are clearly indicated as low susceptibility zones. In Figure 14, the upper ultramafic/mafic volcanic rock sequence between 50 and 180 m consists of ultramafic, mafic and felsic rocks. The felsic rocks are indicated by very low

susceptibilities. The upper part of the sequence is mainly mafic while the lower portion with extremely high susceptibilities is mainly ultramafic.

TEMPERATURE

Temperature measurements with the GSC R&D logging system are made with a probe consisting of a 10-cm long tip of thermistor beads with an equivalent temperature sensitivity of 0.0001 degrees Celsius (Bristow and Conaway, 1984). Changes in temperature are recorded as changes in the thermistor resistance that are converted into true temperatures by means of an inverse operator with the appropriate probe time constant. The temperature gradient data are derived from the temperatures by means of a combined gradient and smoothing operator. Parameters that affect the temperature-depth profile in a borehole include drilling fluid circulation, variations in the thermal conductivities of the rock intersected, and ground water flow (Mwenifumbo, 1993). Four examples are presented showing some of the typical responses of the temperature to changes in lithology, presence of highly-thermally conductive sulfides, and ground water flow within a borehole.

Figure 15 shows temperature logs acquired at the Bells Corners geophysical test site over a 16 day period starting immediately after drilling. Temperature profiles recorded immediately after drilling are significantly affected by the drilling fluid circulation and these disturbances in temperature due to drilling fluid circulation provide useful information on the location of fractures and permeable zones. In this example fracture zones between 240 and 250 m, and between 270 and 275 m show elevated temperatures that decay with time. The permeable fracture zones accepts warmer drilling fluids that eventually comes into thermal equilibrium with the formation waters.

Groundwater entry zones in boreholes produce abrupt changes in temperature. Figure 16 illustrates the temperature-depth profile recorded in an artesian borehole. Groundwater enters at 115 m and flows upward at extremely high rates as indicated by the constant temperatures and zero gradients above the entry zone.

Figure 17 shows an example on the use of temperature logs in mapping coal seams. Coal has fairly low thermal conductivity relative to the sedimentary host rocks. The temperature and temperature gradient-depth profiles in Figure 17 were recorded at the Highvale mine in Alberta. The temperature log shows subtle changes in slope resulting from changes in thermal conductivity between the coal and mudstone. These features are barely visible but are enhanced in the temperature gradient log making the individual coal seams clearly visible.

Massive sulfides are characterized by high thermal conductivity and Figure 18 is an example of the thermal response across massive sulfides. The temperature and temperature gradient-depth profiles were recorded at the Stratmat Cu-Pb-Zn massive sulfide deposit, New Brunswick. Very low temperature gradients are observed within the sulfide intersection with high thermal conductivity. Such anomalous temperature profiles may also be observed in a 'near-miss' borehole. The argillite bands with low thermal conductivity are clearly indicated as high gradients within the massive sulfide zone.

ACKNOWLEDGMENTS

The data presented in this paper were acquired over a period of several years at a number of deposits across Canada. The authors would like to thank various mining companies and Government agencies for logistical support and funding provided during the acquisition of these data. Thanks are also extended to colleagues in the Exploration Geophysics Subdivision for many helpful discussions and critical reading of the manuscript. W.G. Hyatt assisted in field data acquisition.

REFERENCES

Bogoslovsky, V.A. and Ogil'vy, A.A.
1970: Natural potential anomalies as a quantitative index of the rate of seepage from water reservoirs. Geophysical Prospecting, 18:261-268.

Bogoslovsky, V.A. and Ogil'vy, A.A.
1972: The study of streaming potentials on fissured media models (faults). Geophysical Prospecting, 20:109-117.

Bristow, Q. and Conaway,J.G.
1984: Temperature gradient measurements in boreholes using low noise high resolution digital techniques; *in*: Current Research, Part B. geological Survey of Canada Paper, 84-1B, pp.101-108.

Corwin, R.F. and Hoover, D.B.,
1979: The self-potential method in geothermal exploration. Geophysics, 44:226-245.

Hovdan, H. and Bolviken, B.,
1984: Sulphide self potentials in relation to oxygen content in drill-hole water. Geoexploration, 23:387-394.

Killeen, P.G. and Mwenifumbo, C.J.
1988: Downhole assaying in Canadian mineral deposits with the spectral gamma-gamma method; *in*: Current trends in nuclear borehole logging techniques for elemental analysis, IAEA-TECDOC-464, p.23-29

Mwenifumbo, C.J.
1989: Optimization of logging parameters in continuous, time-domain induced polarization measurements. Proceeding of the 2nd International Symposium on Borehole Geophysics for Mineral, Geotechnical, and Groundwater Applications, MGLS, Las Vegas, Nevada,1,201-232.

Mwenifumbo, C.J.
1993: Temperature logging in mineral exploration. Journal of Applied Geophysics, 30:297-313.

Mwenifumbo, C.J. and Killeen, P.G
1987: Natural gamma ray logging in volcanic rocks: the Mudhole and Clementine base metal prospects; *in*: Buchans Geology, Newfoundland, ed. R.V. Kirkham; Geological Survey of Canada, Paper 86-24, pp.263-272, Report 16, 1987.

Sato, M. and Mooney, H.M.
1960: The electrochemical mechanism of sulphide self potentials. Geophysics, 25:226-249.

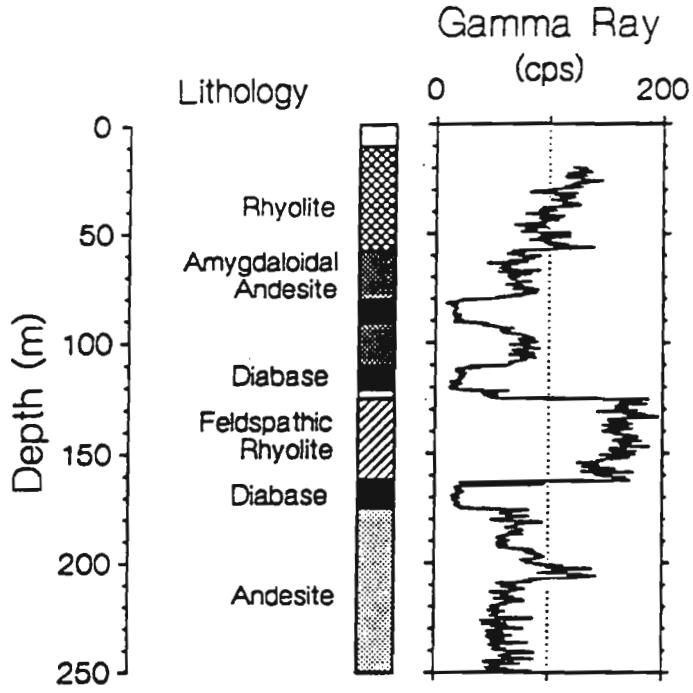

Figure 1. Total count γ-ray log recorded at the Buchans mine, Newfoundland, illustrating its use in mapping volcanic rocks.

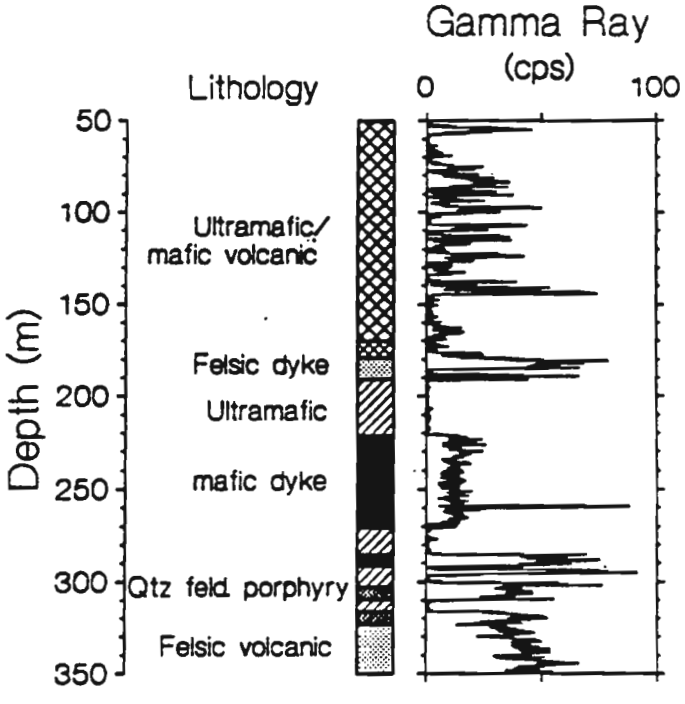

Figure 2. Total count γ-ray log in ultramafic, mafic and felsic volcanics, Redstone nickel deposit, Timmins, Ontario.

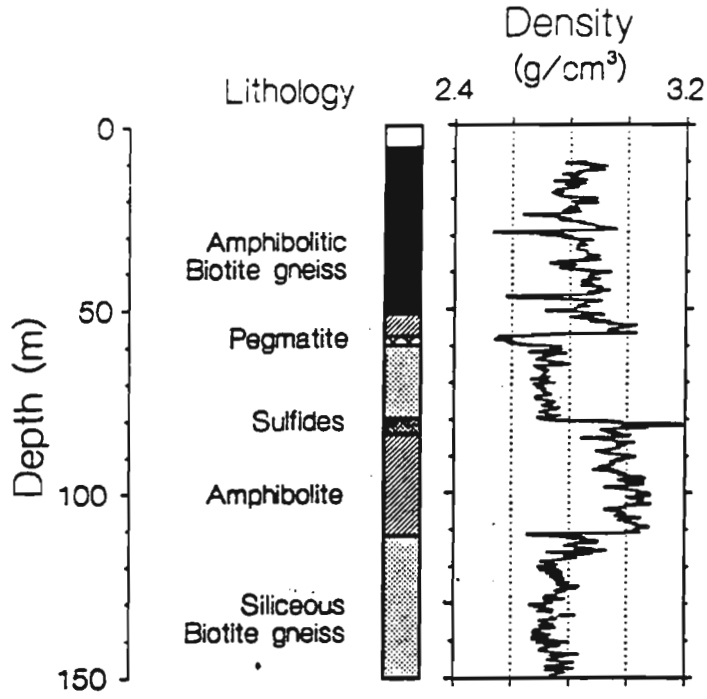

Figure 3. Density log in metamorphic rocks, Calumet Pb-Zn mine, Quebec.

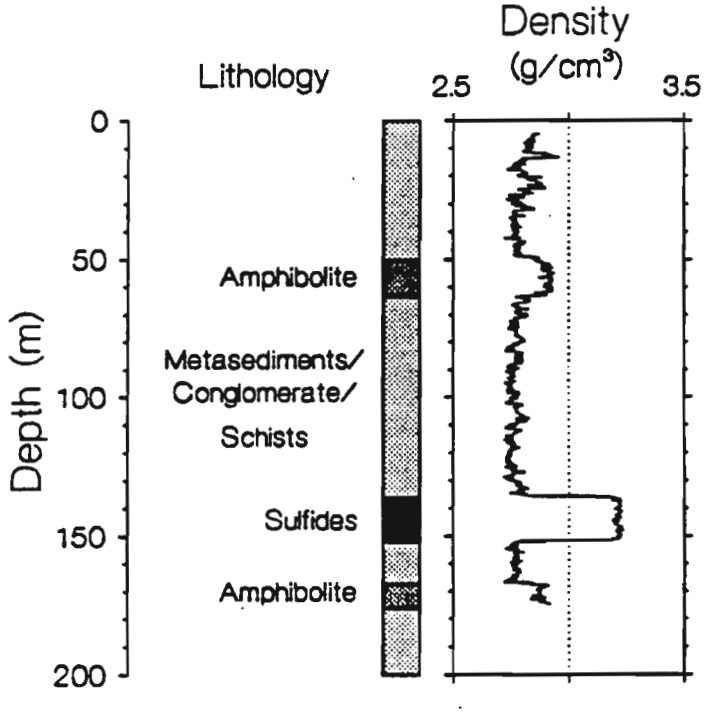

Figure 4. Lithologic mapping and sulfide delineation using density log, McConnell nickel deposit, Sudbury, Ontario.

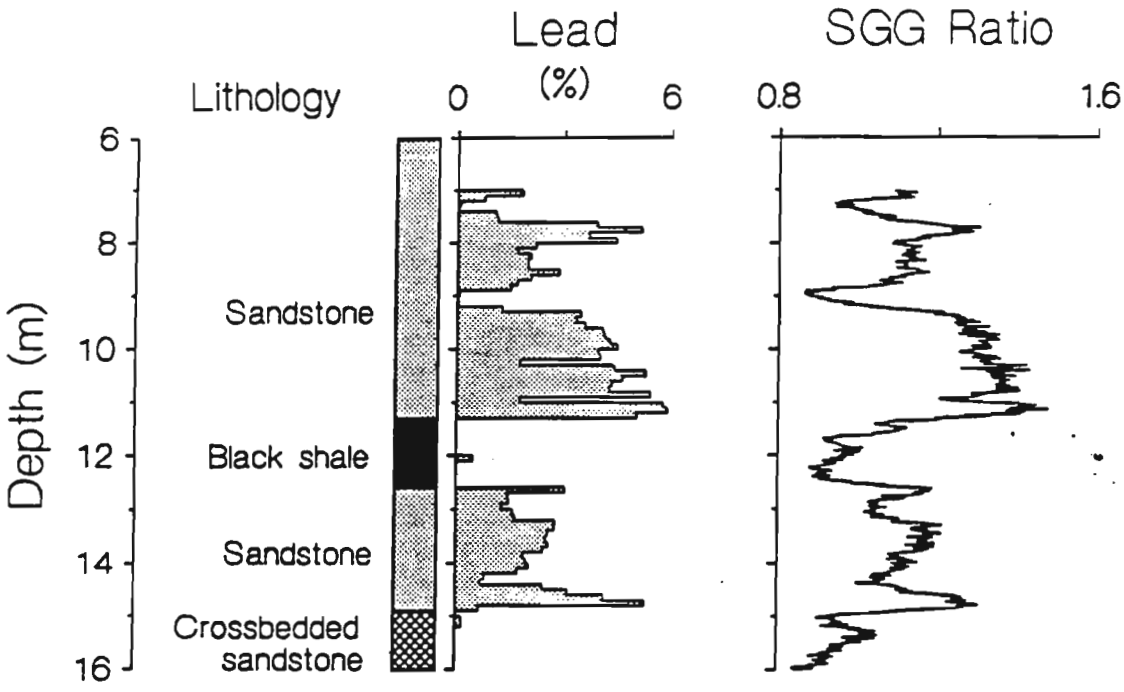

Figure 5. Detailed assays of drill core over 10 cm lengths and the SGG ratio log at the Yava sandstone Pb deposit. These data were used to accurately calibrate the SGG log for in situ Pb assaying.

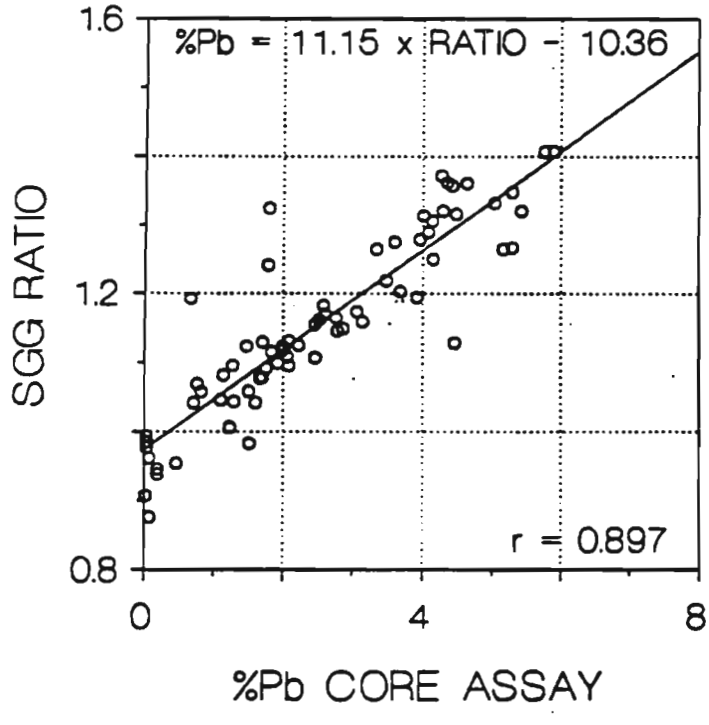

Figure 6. Crossplot of the SGG ratio versus drill core assays to determine the calibration equation for the SGG probe for in situ Pb assaying.

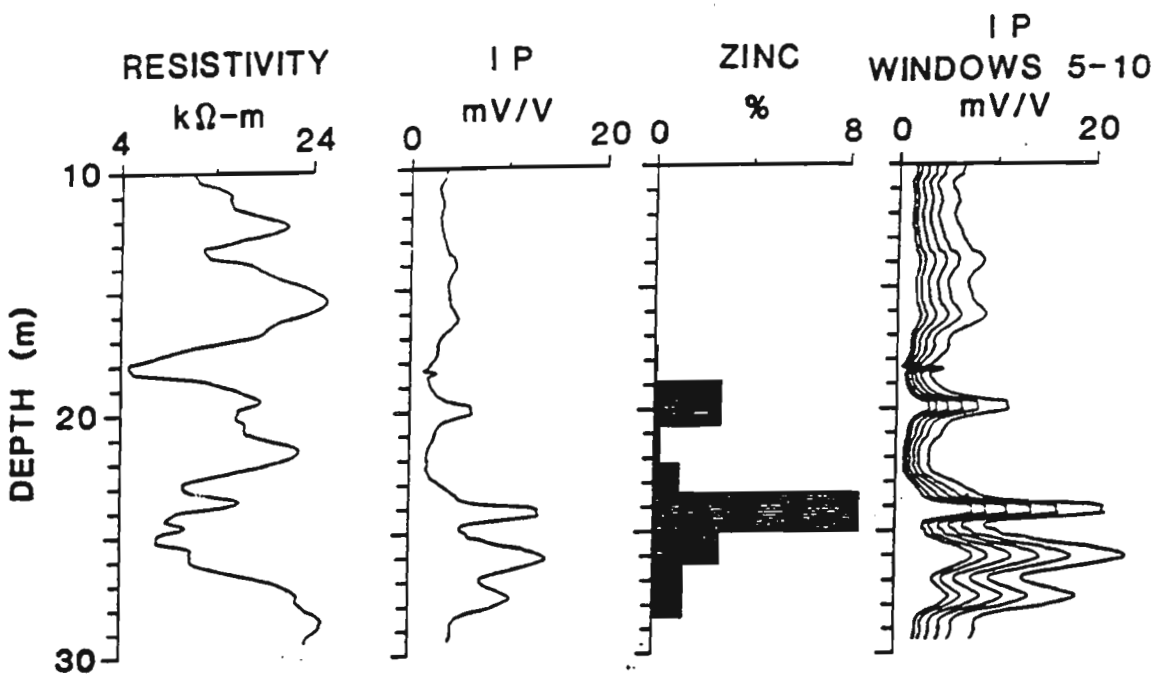

Figure 7. Continuous time-domain IP data through carbonate-hosted zinc deposit, Newfoundland. Detection of Zn mineralization is probably due to associated disseminated pyrite.

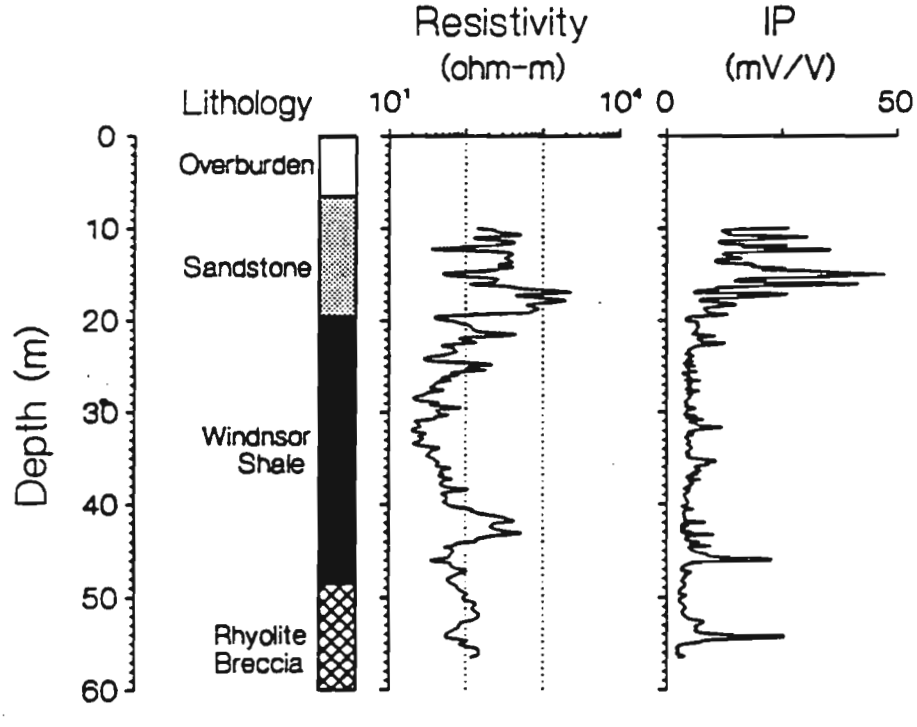

Figure 8. Resistivity and time-domain IP data through disseminated Pb mineralization within sandstone, Yava Lead Deposit, Nova Scotia.

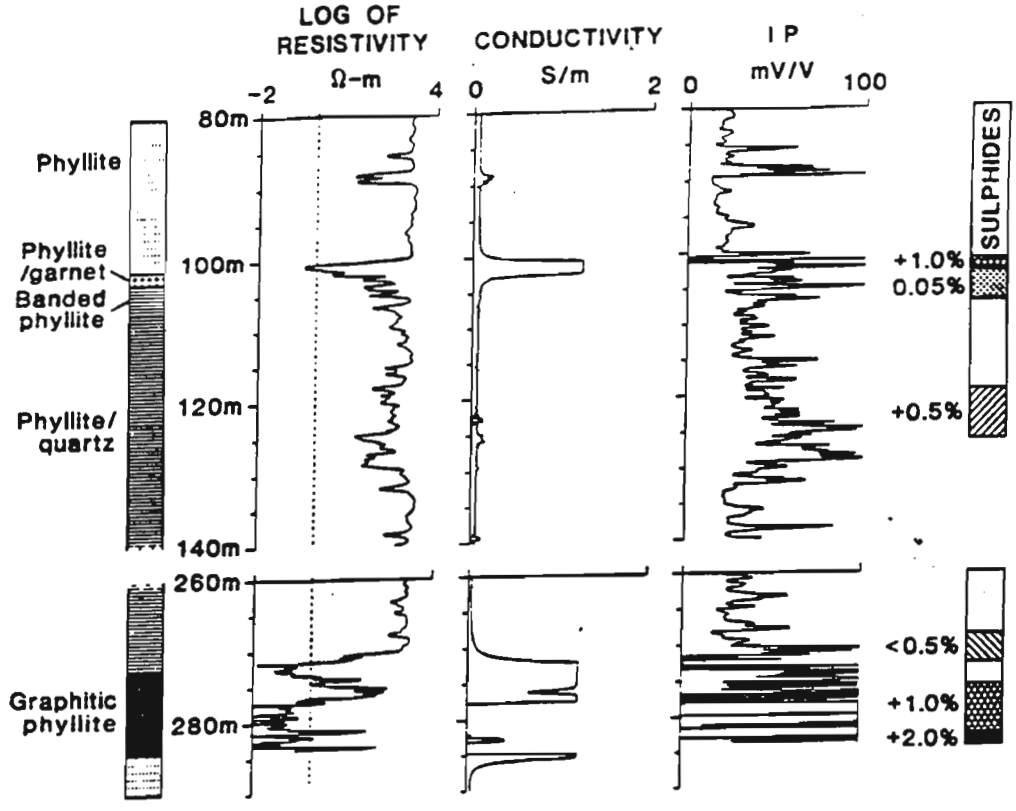

Figure 9. Continuous time-domain IP data through a volcanogenic massive sulfide deposit, British Columbia. The borehole intersects phyllite and graphitic phyllite with disseminated and massive sulfides.

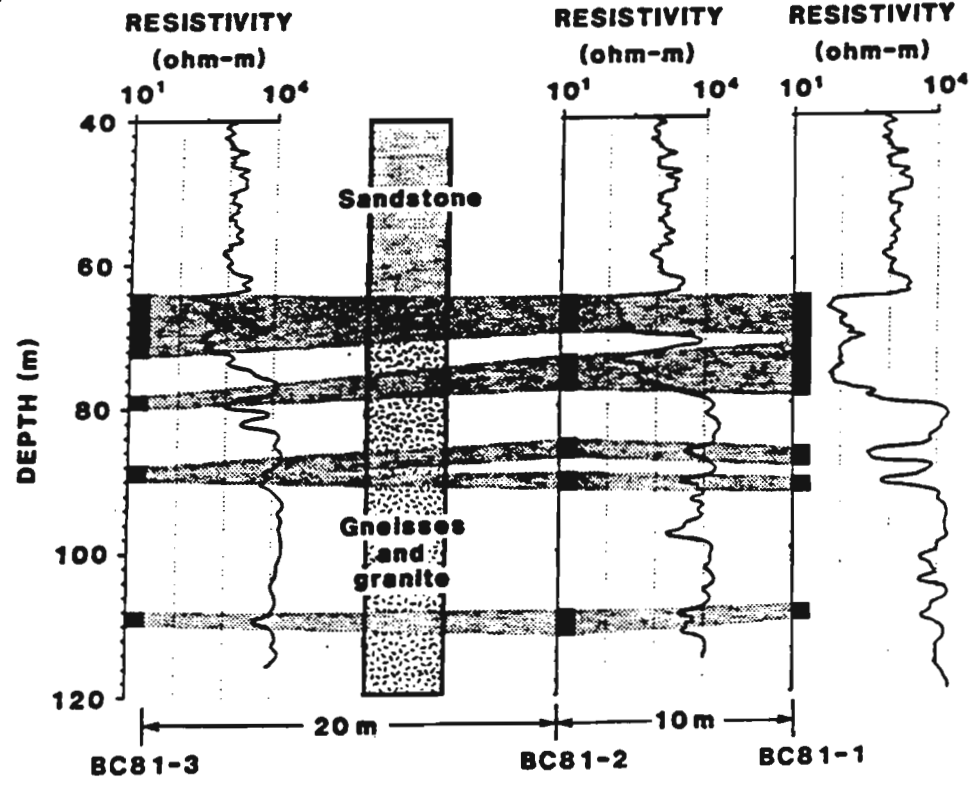

Figure 10. Normal array resistivity logs at the Bells Corners borehole geophysical test site near Ottawa, Ontario.

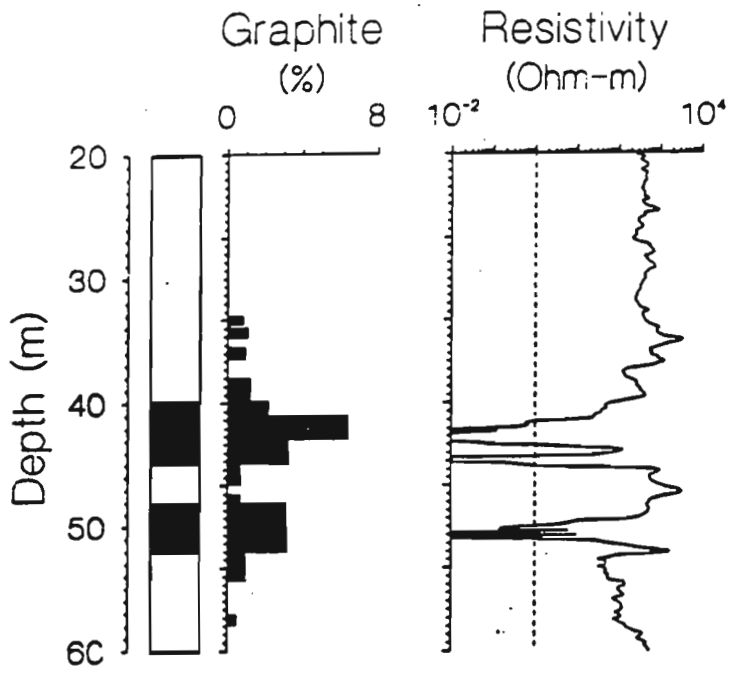

Figure 11. Resistivity log in mapping high-grade graphite ore zones, Victoria Graphite deposit, Ontario.

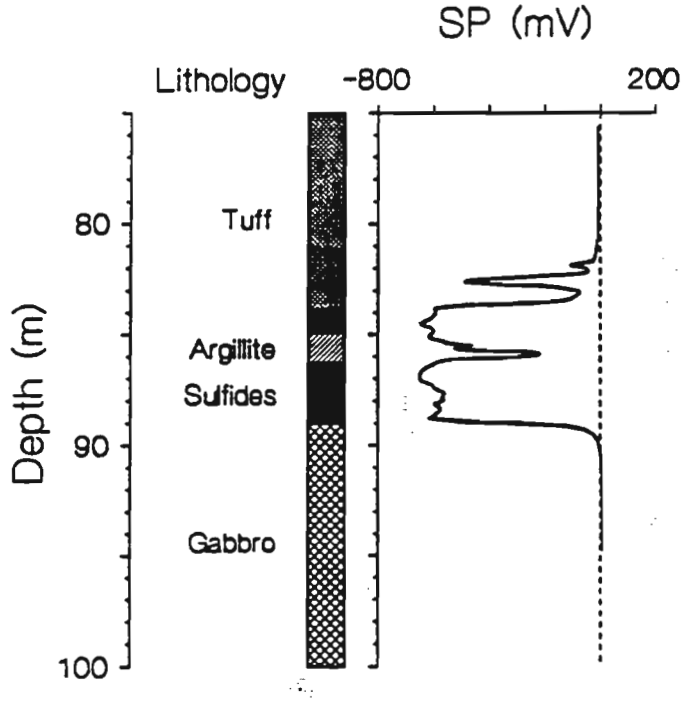

Figure 12. Self potential log through a volcanogenic massive sulfide deposit, New Brunswick.

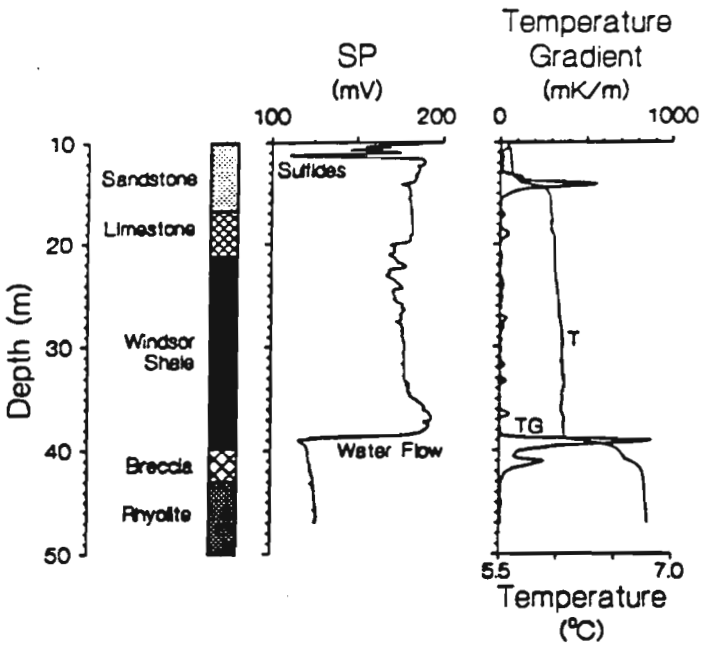

Figure 13. SP and temperature logs from the Yava sandstone lead deposit, Nova Scotia. The SP anomaly between 10 and 12 m represents the normal SP anomaly due to the presence of Pb sulfides. The anomaly at 39 m is likely generated by both temperature change and fluid flow.

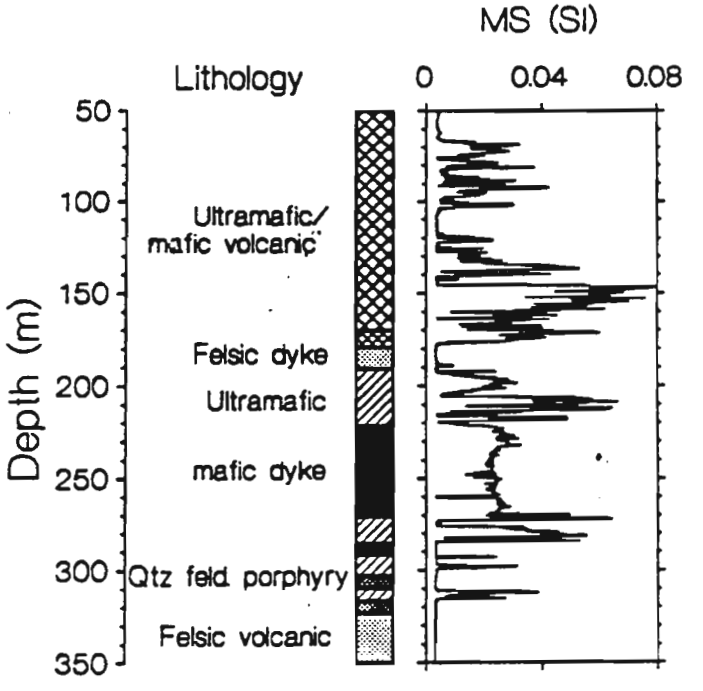

Figure 14. Borehole magnetic susceptibility log acquired at the Redstone nickel deposit, Timmins, Ontario. The borehole intersects ultramafics, mafics and felsic volcanics within susceptibilities ranging from extremely high within ultramafics to very low in felsics.

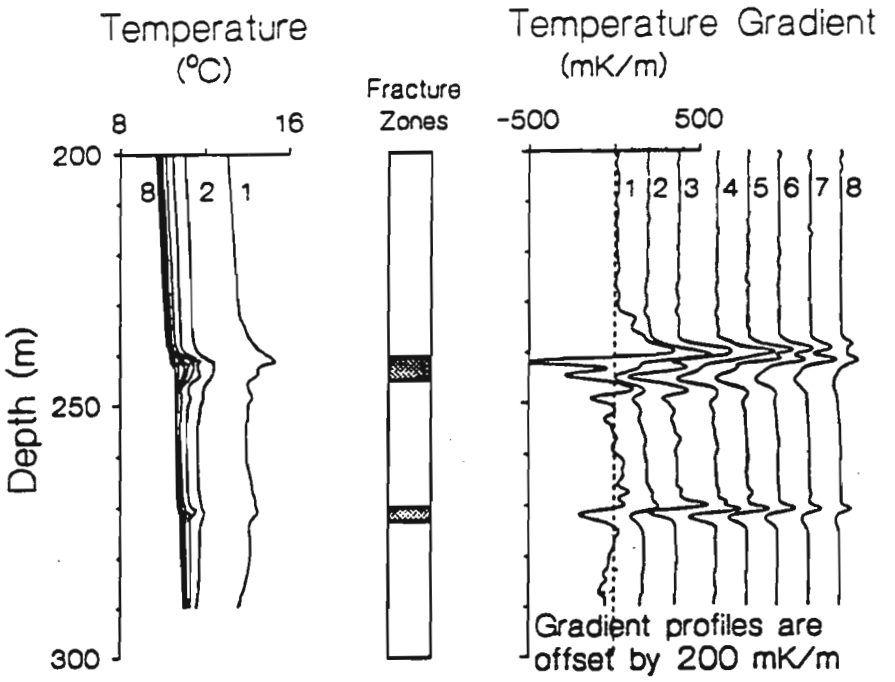

Figure 15. *Temperature logs recorded at various times after drilling showing thermal effects of the drilling process and the return to equilibrium borehole temperatures. Permeable fracture zones appear as transient heat sources on the temperature profiles. Profiles 1 to 8 represent time lapse after drilling of 4, 28, 52, 100 hrs, and 6, 8, 12, 16 days, respectively.*

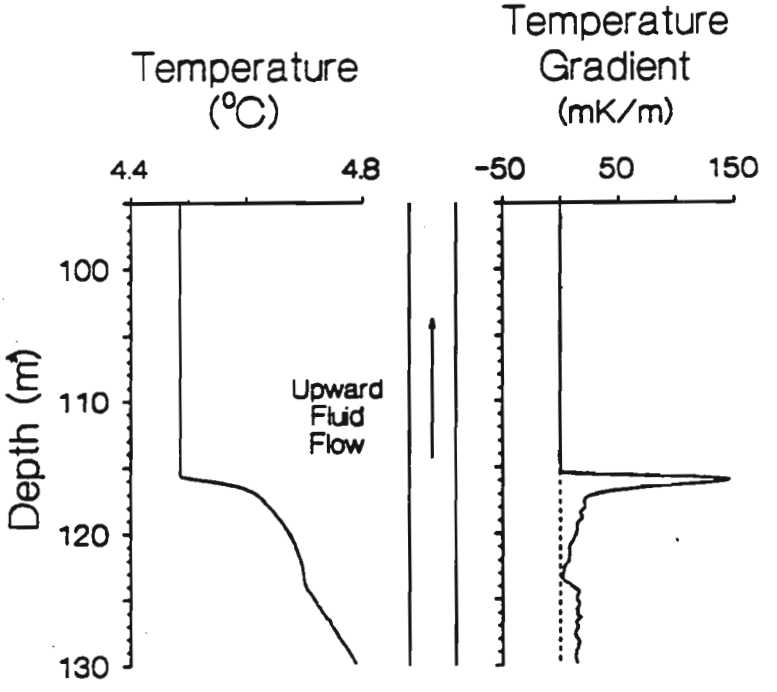

Figure 16. *Temperature- and temperature gradient-depth profiles recorded in an artesian borehole showing constant temperatures (zero gradients) above the zone of water entry.*

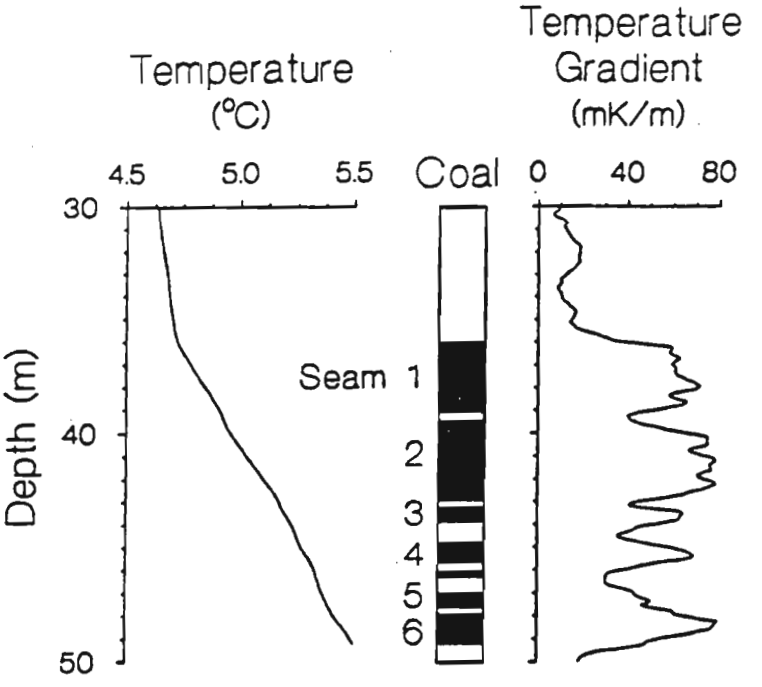

Figure 17. Temperature and temperature gradient-depth profiles recorded at the Highvale coal mine in Alberta. The subtle variations in the smooth temperature-depth profile are transformed into peaks in the temperature gradient-depth profile that correlate well with the location of the coal seams.

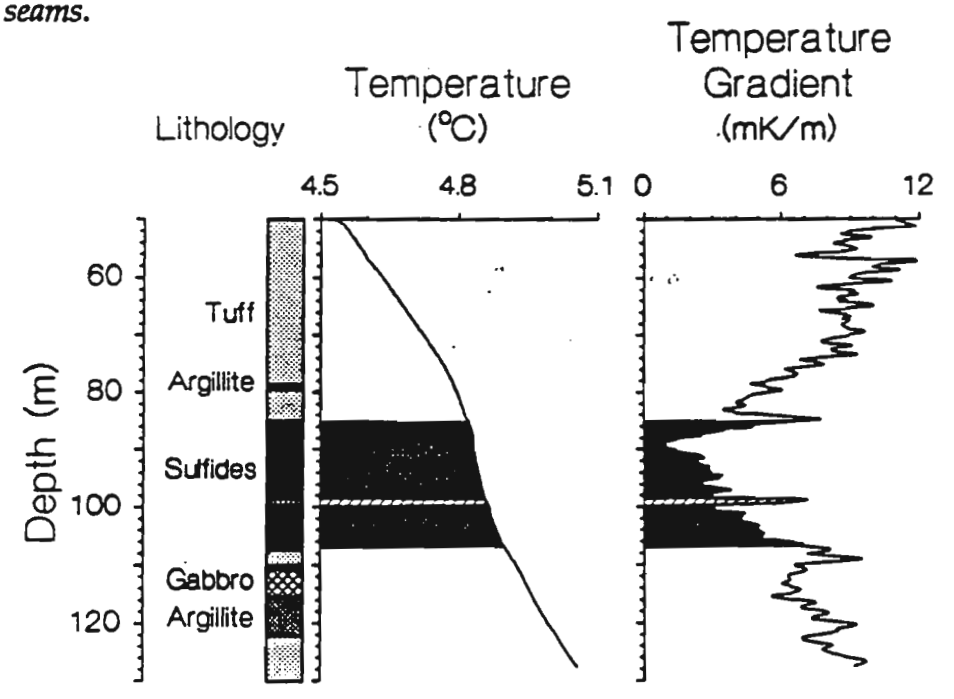

Figure 18. Temperature and temperature gradient-depth profiles recorded at a massive sulfide deposit, New Brunswick.

The pseudo-geological log: using geophysical logs as an aid to geological logging in volcanogenic massive sulphides

P.G. Killeen, C.J. Mwenifumbo, and B.E. Elliott
Mineral Resources Division

Killeen, P.G., Mwenifumbo, C.J., and Elliott, B.E., 1995: The pseudo-geological log: using geophysical logs as an aid to geological logging in volcanogenic massive sulphides; in Current Research 1995-E; Geological Survey of Canada, p. 321-330.

Abstract: Geophysical borehole logs, which measure the physical properties of the rocks surrounding the hole, can be used as an aid to geological core logging, because they are continuous with no missing sections, and because they show changes that are not detectable with the naked eye. Three examples of the application of borehole geophysical logs to the problem of core logging in areas of volcanogenic massive sulphide deposits, are discussed. The Mudhole prospect in Newfoundland is a simple case of the obvious relation between geophysical logs and geological logs. In the Buttle Lake area of British Columbia, the experience gained from the Mudhole prospect was used to derive a pseudo-geological log based on the gamma-ray log. The pseudo-geological log was improved further in the Kam-kotia mine area in Ontario by using three geophysical parameters. In all three cases, the geological interpretation from the geophysical logs was subjective. An objective, computer-based method of deriving the pseudo-geological log, as a tool for the geologist, is being investigated.

Résumé : Les diagraphies de sondage géophysiques qui mesurent les propriétés physiques des roches autour du trou peuvent servir à compléter les données fournies par les carottes (diagraphie géologique) étant donné qu'elles sont continues sans section manquante et qu'elles montrent des changements non décelables à l'oeil nu. L'application des diagraphies géophysiques pour résoudre les problèmes de carottage dans les zones renfermant des gisements de sulfures massifs volcanogènes est traitée à l'aide de trois exemples. Le prospect Mudhole à Terre-Neuve est un cas simple de la relation évidente qui existe entre les diagraphies géophysiques et les carottages. Dans la région de lac Buttle en Colombie-Britannique, l'expérience acquise au prospect Mudhole a servi à dériver une diagraphie pseudo-géologique basée sur la diagraphie par rayons gamma. La diagraphie pseudo-géologique a pu être améliorée dans la région de la mine Kam-kotia en Ontario en utilisant trois paramètres géophysiques. Dans les trois cas, l'interprétation géologique établie à partir de diagraphies géophysiques s'est révélée subjective. La mise au point d'une méthode informatisée objective pour établir une diagraphie pseudo-géologique comme outil géologique est à l'étude.

INTRODUCTION

For more than ten years, the Borehole Geophysics section of the Geological Survey of Canada (GSC) has conducted multiparameter geophysical logging in boreholes associated with volcanogenic massive sulphide deposits, at locations from Newfoundland to British Columbia (Killeen and Mwenifumbo, 1988; Killeen, 1991). Excellent correlation of geophysical logs with geological logs has been observed, as well as cases indicating incorrect depth assignments of some geological units or features, due to core loss or other errors.

Geological logging of the drill core in greenstone belts can be difficult because different volcanic and volcaniclastic rocks are often visually similar. Geophysical logging tools measure physical and chemical properties that are not visible and therefore complement observations made in geological logs. The geophysical data provide a more complete and reassuring geological interpretation of the lithology intersected by the drillholes.

Three examples will be discussed here: the Mudhole base metal prospect near Buchans, Newfoundland; the Buttle Lake (Myra Falls) area on Vancouver Island, British Columbia; and the Kam-kotia mine area near Timmins, Ontario. The examples demonstrate the benefits of using geophysical logs as an aid to core logging, and point out the possibilities for development of a semi-automated interactive 'pre-picking' of the geology by computer, based on the geophysical logs. Before discussing the examples, some background on the relation between geology and geophysical parameters measured will be reviewed.

RELATIONSHIP BETWEEN GEOPHYSICAL LOGS AND GEOLOGY

In general, different rock types have different physical and chemical properties. An understanding of the physical rock properties to which each of the geophysical parameters respond is critical to interpreting correctly the relation between the logging data and the geology. Some of the geophysical logs respond to specific physical properties while others respond to a variety of physical properties (Killeen et al., 1994; Mwenifumbo et al., 1993a, b; Pflug et al., 1994). The following is a brief discussion of the response characteristics of each of the geophysical logs recorded in the areas mentioned in this paper.

1. Magnetic susceptibility

The magnetic susceptibility (MS) of a volume of rock is a function of the amount of ferromagnetic minerals – magnetite and pyrrhotite – contained within the rock. Magnetic susceptibility measurements can provide a rapid estimate of the magnetic minerals in the rock. These measurements are interpreted to reflect lithological changes, degree of homogeneity and the presence of alteration zones. Basic flows and diabase dykes containing higher concentrations of magnetic minerals are easily detected with magnetic susceptibility measurements. During hydrothermal alteration, magnetic minerals such as magnetite in the host rock tend to be altered to weakly magnetic minerals (e.g. hematite) or to non-magnetic minerals. Therefore, within a given lithological unit, anomalously low magnetic susceptibilities will generally indicate altered zones.

2. Induced polarization

In time domain induced polarization (IP) measurements a current is passed through the earth in a series of off-on pulses and the rate of decay of the voltage is measured during the current off-time. The measured voltage is related to the electrical polarizability of the rock and is called chargeability. A high chargeability response is an indication of the presence of metallic sulphides and oxides or cation-rich clays such as illite and montmorillonite (Mwenifumbo, 1989). One of the major alteration processes within a number of base metal and gold mining camps is pyritization and this is a target for most IP logging.

3. Resistivity

The electrical resistivity of rocks depends on several factors. Conductive minerals such as base metal sulphides, oxides, and graphite in the rock have a strong influence on the resistivity. Most rocks are usually poor conductors and their resistivities are governed primarily by their porosity and salinity of the pore fluids and to a lesser extent by the intrinsic minerals that constitute the rock. Some alteration processes such as silicification and carbonatization tend to reduce the rock porosity and hence increase the formation resistivities. Thus in rocks where no significant amounts of conductive minerals occur, the most important factors affecting the resistivities are fracturing, porosity, the degree of saturation of pore spaces, and the nature of the electrolytes in the pore fluids. Since resistivities depend on a number of factors, geological interpretation from resistivity measurements is fairly difficult without complementary information from other geophysical measurements or geological logs. Massive sulphide deposits however, often consist of conductive ore zones and therefore delineation of the ore horizons by electrical resistivity logging is usually straightforward.

4. Self potential

Large self potentials observed within and around sulphides are mainly caused by electrochemical reactions (oxidation-reduction reactions). Electrofiltration processes may also be responsible for generating some relatively small amplitude anomalies where there is groundwater flow in the presence of ionic concentration gradients. Low resistivity anomalies correlating with SP anomalies are, therefore, good indications of the presence of conductive base metal sulphides. At Buttle Lake, SP anomalies generally indicate the presence of base metal sulphides including pyrite.

5. Temperature

Although a number of variables affect the temperature-depth profile in a borehole, temperature measurements have been successfully used to map lithology where significant thermal

conductivity contrasts exist. They can also be used to detect and map fracture zones, and to delineate massive sulphide mineralization.

Large concentrations of metallic sulphides and oxides perturb the local isothermal regime since metallic minerals have high thermal conductivities. The perturbation of the local geothermal gradient, however, would be observed only in a thermally quiet environment. In areas where there are numerous fracture zones with ground water movements, thermal anomalies due to ground water flow are much larger than those that would be caused by changes in the thermal conductivity (e.g. the presence of metallic minerals).

6. Natural gamma-ray spectrometry

The gamma ray probe measures the natural gamma radiation emitted by potassium-40 (K), and uranium (U) and thorium (Th) series nuclides in the rocks. Four logs are produced: the Total Count (TC), K, U and Th logs. The main minerals contributing to an increase in potassium-40 are the K-feldspars and micas. Uranium and thorium are usually contained in minerals such as allanite, apatite, monazite, sphene, and zircon. Differences in the percentages of these minerals in various rocks make it possible to identify and characterize different units by their levels of radioactivity.

At the Buttle Lake area, for example, the different volcanic units have different amounts of potassium minerals (potassium-40 being the principal source of the natural gamma radiation). Feldspar porphyry sills with higher concentrations of K-feldspar minerals should be easily identified as anomalously high radioactivity zones on the gamma ray logs. Often during hydrothermal alteration processes associated with mineralization, the radioactive elements potassium, uranium, and thorium may be preferentially concentrated in certain lithological units. Alteration in the Buttle Lake area is mainly characterized by the development of sericite (a potassium mineral), epidote, and chlorite. Sericite enriched zones are excellent targets for gamma ray logging.

7. Spectral gamma-gamma (density and heavy element indicator)

The spectral gamma-gamma probe measures the density of the rock around the borehole and provides information on the effective atomic number (Zeq) of the rock. The spectral gamma-gamma ratio (SGGR) is the measured quantity that is related to the presence of heavy elements.

In most mining environments, minerals forming the country rock consist mainly of low-atomic number (Z) elements (e.g. silicates and carbonates with the major elemental constituents being Al, Fe, Mg, Ca, K, Na, C and O) while the base metal sulphide ores consist of high Z elements (e.g. Pb, Cu, Zn, Fe sulphides and/or oxides). The high Z elements within the ore raise the Z_{eq} of the rocks as well as their density. Thus on SGGR and density logs, base metal ore zones are evident as zones of anomalously high values. Since the SGGR correlates so well with the ore grade, a simple regression can be used to establish a predictor of ore grade based on the SGGR log.

The density response is not only affected by variations in the whole rock chemistry of the formation but also by secondary physical properties that include porosity and water content. Porosity can be estimated from the density log by simple empirical linear transformations. Decreases in densities generally indicate increases in porosities.

THE MUDHOLE BASE METAL PROSPECT, NEWFOUNDLAND

This example is a 'text-book' case of the correlation between geology and geophysical logs in volcanic rocks.

Natural gamma ray logging was carried out in two holes at the Mudhole prospect near Buchans, Newfoundland. The gamma ray logs recorded with the GSC R&D logging system in hole MH2572 were published by Mwenifumbo and Killeen (1987). The 280 m hole was logged at 3 m/min using a 25 x 76 mm BGO detector and a 4 second sample time. The holes intersected volcanic, volcaniclastic, and sedimentary rocks which included andesite, rhyolite, dacite, diabase intrusions, tuff, agglomerate, arkose, siltstone, and greywacke. These rock units were easily characterized by their natural gamma ray activity. The Total Count gamma ray logs showed rhyolite and trachyte as producing the highest gamma ray count rate while the diabase intrusions were characterized by their extremely low gamma ray activity. A frequency distribution plot (histogram) of the Total Count gamma log was clearly multi-modal, with five peaks which could be related to diabase, andesite, amygdaloidal andesite, rhyolite, and trachyte, in increasing order of gamma ray count.

That study indicated that the total count gamma ray logs could be applied in the Buchans area with a high degree of confidence for the identification of the different volcanic rock types. Because contacts between major volcanic units were well defined on the gamma ray logs, the thicknesses of individual units could also be easily determined. Mwenifumbo and Killeen (1987) concluded: "Gamma ray logs, in conjunction with the geological logs can be used to provide a more complete and reassuring geological interpretation of the lithology intersected in diamond-drill holes".

The use of gamma ray spectral logs in the area might provide additional information on the relative concentrations of the naturally occurring radioelements, U, Th, and K, permitting further subdivision of the geological units not possible on the basis of the total count logs alone.

In most cases it is not as simple to relate the geology directly to a single geophysical parameter. Usually two or more physical rock property measurements are necessary to yield a unique signature for any given rock unit.

THE BUTTLE LAKE AREA, BRITISH COLUMBIA

Borehole geophysical measurements were made in several boreholes in the Buttle Lake area on Vancouver Island, British Columbia. The geophysical logging objectives were to

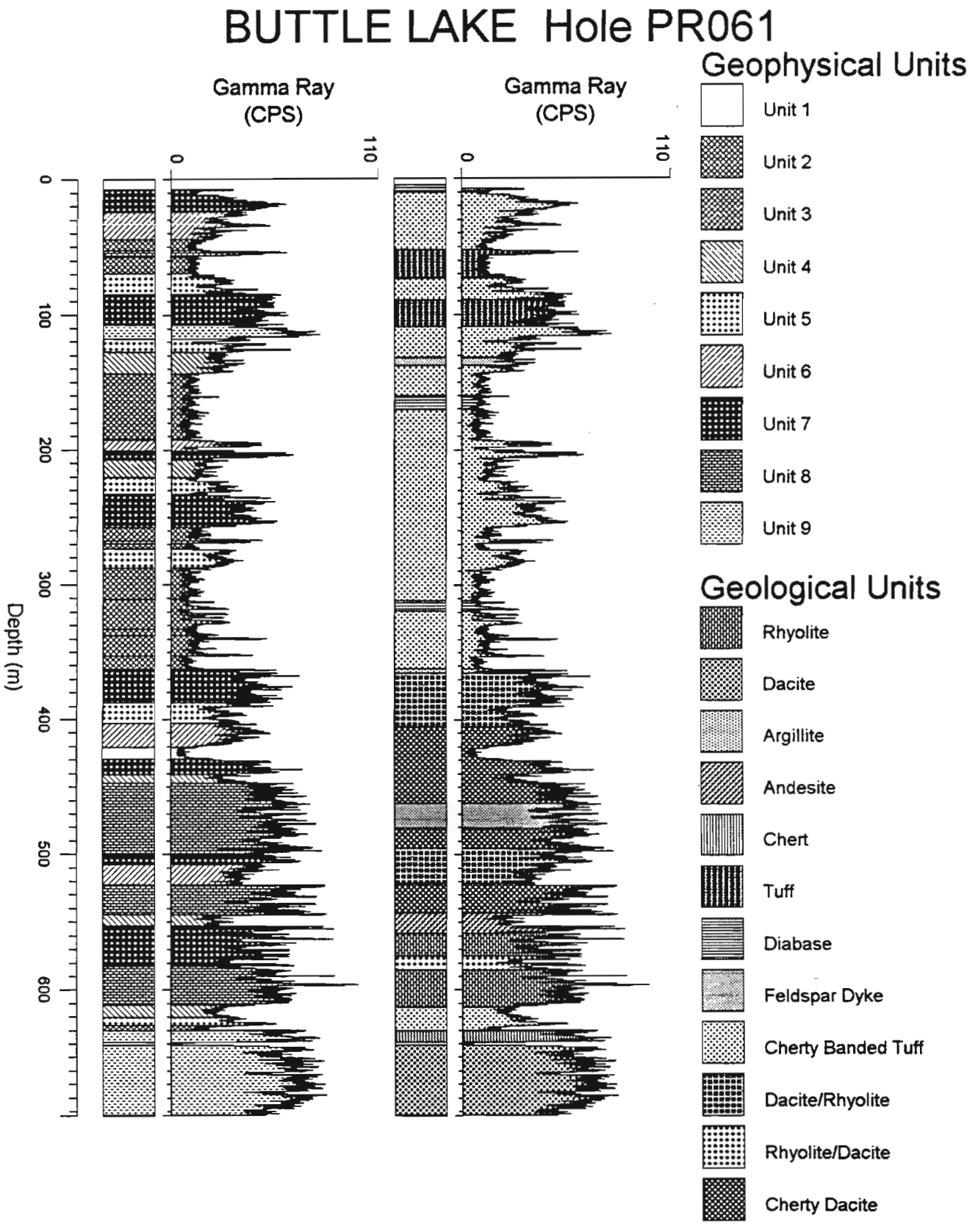

Figure 1. *Gamma-ray log from Buttle Lake hole PR061 plotted twice for comparison of pseudo-geological log (left) and core log (right).*

determine the geophysical signature of the deposit and host rocks, and to establish an in situ physical rock property database that would facilitate the development of geophysical methods for discovering new ore bodies (Killeen et al., 1989). The holes were drilled in 1979 at the Myra Falls mining operations by Wesmin Resources in one of several polymetallic (Cu-Zn-Pb) volcanogenic massive sulphide orebodies comprising pyrite, chalcopyrite, and sphalerite with minor galena. The mineralization is hosted by felsic volcanic rocks that are intruded by quartz-feldspar porphyritic bodies. The volcanic stratigraphy and structure of the deposit are fairly complex.

Geophysical logs were acquired with the GSC R&D logging system in 1987, as part of a multi-year, multi-deposit project, using five different probes. Variables measured included: three electrical logs (IP, Self Potential and Resistivity), Magnetic Susceptibility, Natural Gamma ray Spectrometry (Total Count, K, U, Th), Spectral Gamma Gamma (density and SGGR), Temperature and Temperature Gradient. The results of the multiparameter logging are presented in a GSC Open File Report covering work at several deposits in British Columbia (B.E. Elliott et al., in prep.).

In general, the geophysical logs provided information regarding the lithology, alteration, sulphide distribution, and fracturing. Of the logs recorded, several gave distinct signatures in different volcanic rocks whereas other logs were able to accurately delineate sulphide mineralization. Only the gamma ray logs digitally recorded in one 700 m hole (PR061) with a 25 x 76 mm sodium iodide detector, at 3 m/min, will be discussed here because they best reflected the geology.

Development of the 'pseudo-geological' log

The most significant indicators of geological variations were the nuclear logs; the natural gamma and the SGG/density logs. These respond to the geochemical changes in the rock; the natural gamma ray responding to lithology due to variations in the concentrations of potassium, uranium, and thorium. The density log is often a good indicator of changes in lithology, however, the density response to alteration and the degree of fracturing sometimes obscures the lithological variations.

Using the experience with the observations at the Mudhole prospect as a guide, an attempt was made to produce a 'pseudo-geological' log from the Buttle Lake geophysical logs. As a first step it was decided to use the gamma ray log as a means of defining different 'geophysical units' which had different count rates or degree of variability (homogeneity). The result is shown in Figure 1, where for comparison purposes, the gamma ray log from hole PR061 is plotted twice, with cross-hatched fill under the log trace representing the 'real' and the 'pseudo' geological logs. On the left is the log composed of 9 different 'geophysical units', and on the right is the traditional geological core log composed of 12 different geological units. The similarities are obvious but there are a number of significant differences. It is apparent that the geophysical log has more boundaries or contacts (44 zones in total) than the core log (27 zones), even though the gamma log indicated there were only nine different units and the core log had twelve different units. This shows that geological features such as sericite alteration for example, can change a physical property (such as the natural gamma radiation), but not represent a change in rock type. Therefore a pseudo-geological log based on a single geophysical log will be inadequate for determining the geological log, although it will be of some help to the geologist doing core logging, in directing his attention to changes in the core, some of which may be subtle and difficult to discern with the naked eye. For example, at depth 190 to 290 m, the pseudo-log is divided into variable thin zones of geophysical units 6, 7, 4, 5, 7, and 3, from top to bottom, whereas the core log describes the entire depth range as 'cherty banded tuff'. However, the detailed core log contains an entire page of notes regarding changes in the core observed in this section, such as 'minor carbonate stringers; variations in the percentage of chert; laminations; siliceous zones; minor mafic clasts; weakly sheared zones; colour changes, and other variations'. Some of these changes are likely distinguishable on the geophysical logs because they represent changes in physical properties which are measureable. However, 'these changes do not a different rock type make'.

Similarily, the 'cherty dacite' from 400 to 460 m was divided into five different geophysical units. It is fair to say that more bed boundaries are in agreement than in disagreement between the core and pseudo logs. However the geophysicist is perhaps overly optimistic in selecting geological contacts solely on the basis of gamma ray logs. The next example from the Kam-kotia mine area in Ontario is an attempt to improve the pseudo-geological log by using the 'best' three logs selected from a multiparameter suite of logs recorded with the GSC R&D logging system.

THE KAM-KOTIA MINE AREA, ONTARIO

In November 1993 a suite of more than ten logs was recorded in a 600 m deep hole, immediately after it was drilled, in the Kam-kotia mine area, west of Timmins. Strictly on the basis of variations in physical properties, a pseudo-geological log was produced, before the geologist had logged the core from the hole. Based on the use of multiple logs, the results were much more accurate than for the previous examples, with about 90% of the geological units being 'picked' correctly by the pseudo-log. It was determined that the geophysical parameters that most closely reflected the changes in the geology were the gamma ray, density and magnetic susceptibility logs.

Figure 2 shows the three logs plotted with the area under the log-trace filled with the different geophysical unit symbols. The three logs illustrate how one parameter may change within a single unit, while the others are relatively constant. For example in unit 1 between 130 and 220 m the gamma ray log and density log are fairly homogeneous, but the MS log shows large variations indicating this unit has 'magnetic' sections (increased magnetite content). Based on what was learned in the two previous examples, new geophysical units were not defined on the basis of variations in the MS alone. It was also tempting to subdivide the log between 400 and 500 m into more and thinner geophysical units based on the observed changes in the logs. The derivation of the pseudo-geological log was subjective, but the experience gained would be invaluable in formulating an algorithm for objective production of the pseudo-log by a computer.

Figure 3 shows the geological log which was produced from observation of the core. The rocks consist of massive flows, felsic volcanics, tuffs and diabase sills, with varying degrees of alteration. The zone between 130 and 220 m mentioned above is identified as 'massive flow/intrusive', and the MS log variations were not the result of an identity change. Between 400 and 500 m, the geologist did assign an additional unit (chloritic intermediate tuff), not defined as a geophysical unit. A good method of comparing the core and pseudo-logs is to display them in the same form as was done for the Buttle Lake logs in Figure 1.

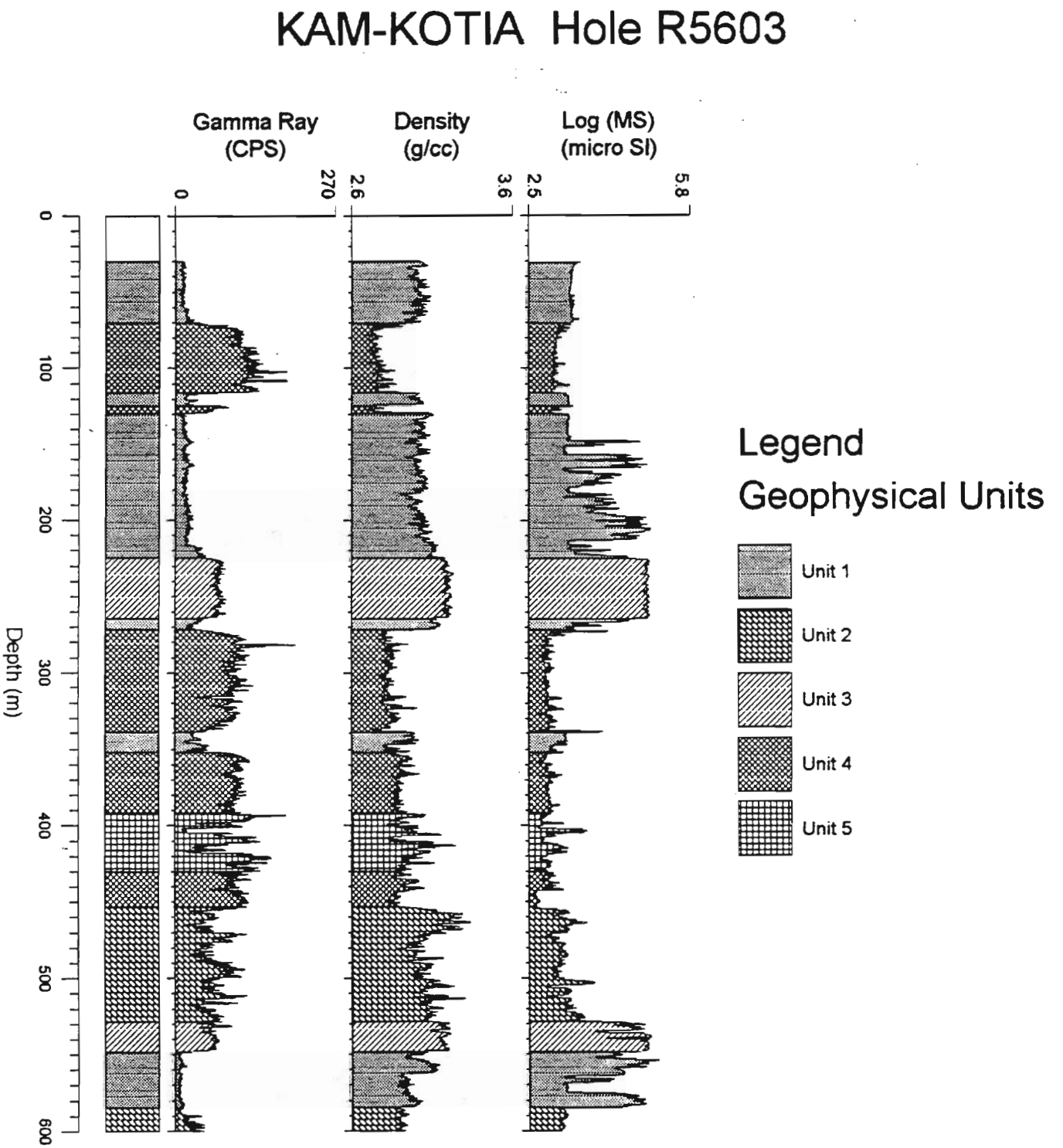

Figure 2. Gamma-ray, density and magnetic susceptibility (MS) logs for Kam-kotia hole R5603 showing the pseudo-geological log as cross-hatched fill.

The gamma-ray logs from the Kam-kotia hole R5603 are plotted twice in Figure 4, with the geophysical unit log (pseudo-geological log) on the left, and the geological log (core-log) on the right. Most of the geophysical contacts agree with the geological contacts. Some geological units relate to specific geophysical units such as:

unit 1 = massive flow/intrusive;
unit 2 = intermediate mafic tuffite and chloritic intermediate tuff;
unit 3 = diabase;
unit 4 = felsic volcanic, felsic intrusive volcanic, and felsic quartz eye tuff;
unit 5 = chloritic/sericitic felsic tuff.

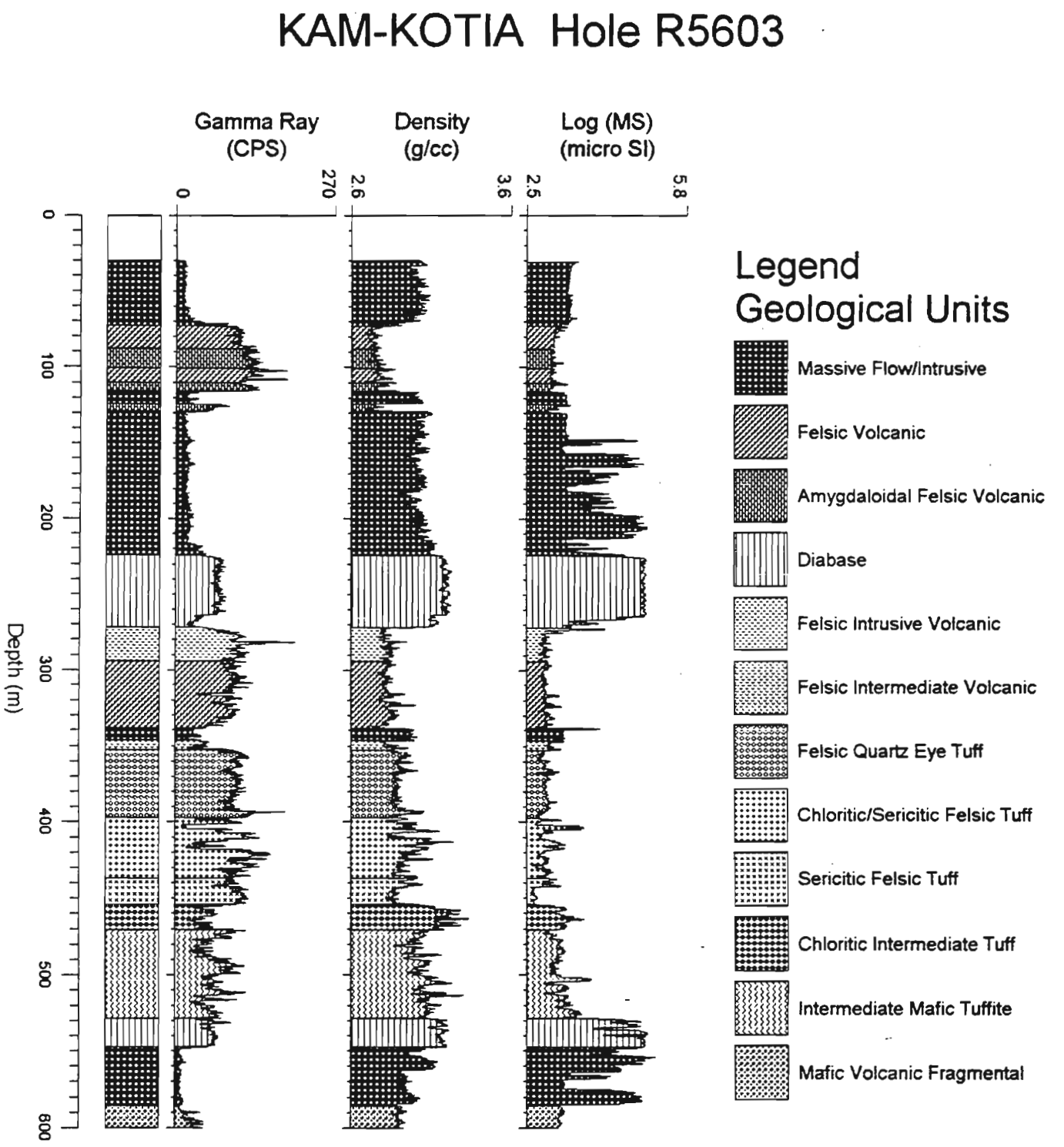

Figure 3. *Gamma-ray, density and magnetic susceptibility (MS) logs for Kam-kotia hole R5603 showing the core log as cross-hatched fill.*

It is clear that both geological contacts and geological units bear a distinct relationship to the geophysical logs in the Kam-kotia example shown in Figures 2, 3 and 4.

CONCLUSIONS

The experience in determining the relation between geology and geophysics via in situ logging of physical rock property measurements leads to the conclusion that considerable time could be saved and accuracy in depth positioning of geological contacts could be improved through the aid of geophysical logs. In a given area, such as local exploration in the vicinity of a mine, it may be possible to rely on pseudo-geological logs for rapid information during a drilling program. This would permit the explorationist to use the knowledge to direct the drill during the program. It is entirely feasible to develop computer software to produce the pseudo-geological log objectively, in real-time in the field. Its accuracy would be dependant on the number of parameters it had to work with, as well as previous 'training' from other holes in the area.

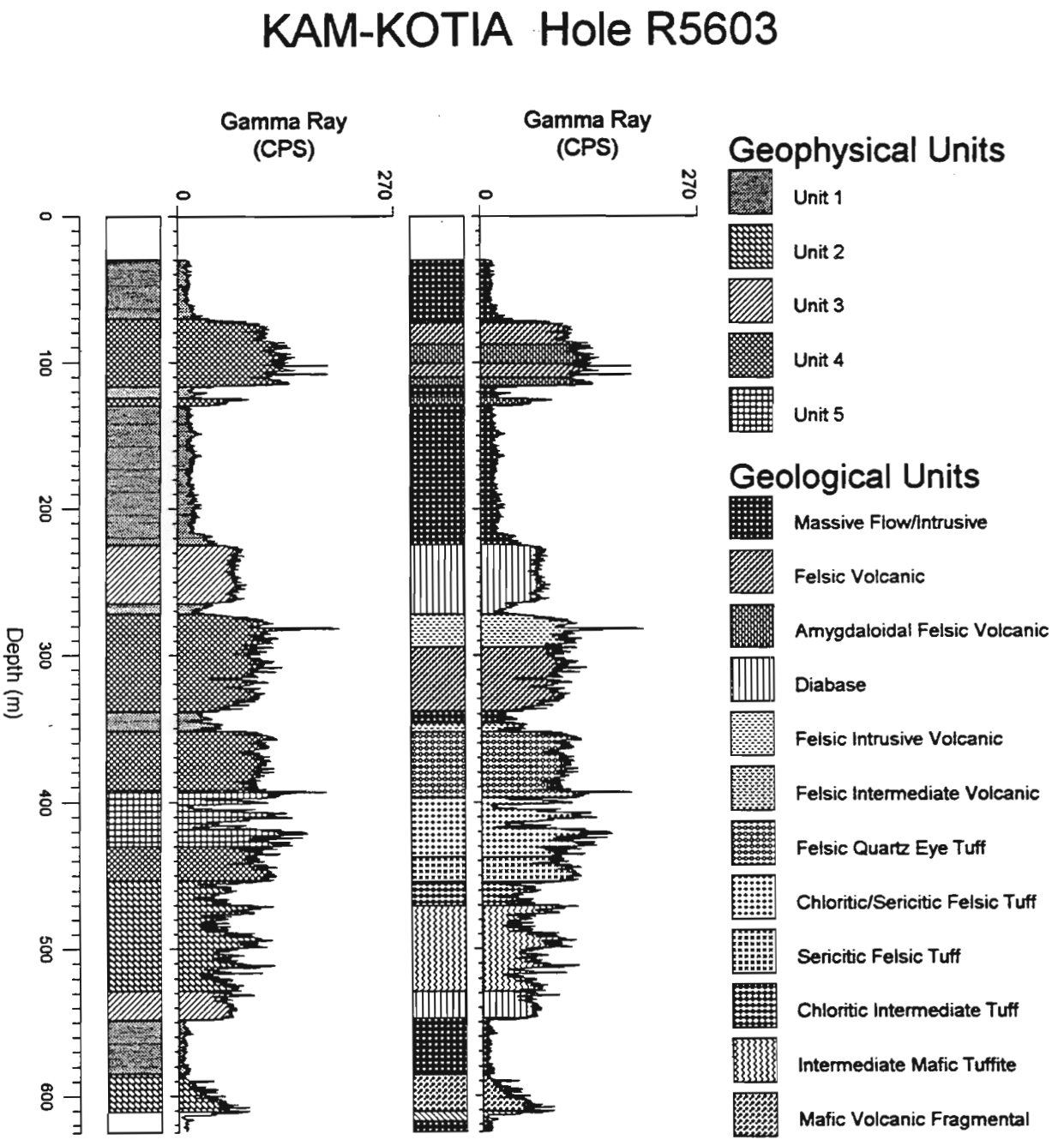

Figure 4. *Gamma-ray log from Kam-kotia hole R5603 plotted twice for comparison of pseudo-geological log (left) and core log (right).*

The GSC has commenced work towards development of such an 'artificial intelligence' system.

ACKNOWLEDGMENTS

We wish to thank Bill Hyatt and Andrew Wray for their contribution to the data acquisition and processing. We also thank Cliff Pearson of Wesmin Resources, Ray Band and John Pattison of Falconbridge, and ASARCO Inc. and Abitibi-Price Inc. for their collaborative support of this work, as well as permission to publish the results.

REFERENCES

Killeen, P.G.
1991: Borehole geophysics: taking geophysics into the third dimension; GEOS, v. 20, no. 2, p. 1-10.

Killeen, P.G. and Mwenifumbo, C.J.
1988: Interpretation of new generation geophysical logs in Canadian mineral exploration; in 2nd International Symposium on Borehole Geophysics for Minerals, Geotechnical and Groundwater Applications, Oct. 6-8, 1987, Golden, Colorado, p. 167-178.

Killeen, P.G., Elliott, B.E., and Mwenifumbo, C.J.
1989: Borehole geophysics applied to massive sulphide deposits in the Cordillera: a report on the 'B.C. Mineral Logging Group' Study, Preliminary Report, May, 2, 1989, submitted to the B.C. Mineral logging Group, 44 p.

Killeen, P.G., Mwenifumbo, C.J., Pflug, K.A., and Elliott, B.E.
1994: Borehole geophysical signatures and test sites at major deposits in Ontario: New developments in 1993; in Summary Report, 1993-1994, Northern Ontario Development Agreement, (ed.) N. Wood, R. Shannon, L. Owsiacki, and M. Walters, co-published by Natural Resources Canada, and the Ontario Ministry of Northern Development and Mines, p. 122-125.

Mwenifumbo, C.J.
1989: Optimization of logging parameters in continuous, time-domain induced polarization measurements; in Proceedings of the third International Symposium on Borehole Geophysics for Mineral, Geotechnical, and Groundwater Applications, Oct. 2-5, 1989, Las Vegas, Nevada, v. 1, p. 201-232.

Mwenifumbo, C.J. and Killeen, P.G.
1987: Natural gamma ray logging in volcanic rocks: the Mudhole and Clementine base metal prospects; in Buchans Geology, Newfoundland: 1982-1984, ed. R.V. Kirkham, Geological Survey of Canada, Paper 86-24, p. 263-272, Report 16.

Mwenifumbo, C.J., Killeen, P.G., and Bernius, G.R.
1993a: Ore deposit signatures by borehole geophysics; in Summary Report, 1992-1993, Northern Ontario Development Agreement, (ed.) N. Wood, R. Shannon, L. Owsiacki and M. Walters, co-published by Energy, Mines and Resources Canada and Ontario Ministry of Northern Development and Mines, p. 123-125.

Mwenifumbo, C.J., Killeen, P.G., Elliott, B.E., and Pflug, K.A.
1993b: The borehole geophysical signature of the McConnell Nickel Deposit, Sudbury area; in Proceedings of the 5th International Symposium of the Minerals and Geotechnical Logging Society, Tulsa, 24-28 October 1993.

Pflug, K.A., Killeen, P.G., and Mwenifumbo, C.J.
1994: Acoustic velocity logging at the McConnell nickel deposit, Sudbury area, Ontario: preliminary in situ measurements; in Current Research 1994-C; Geological Survey of Canada, p. 279-286.

Geological Survey of Canada Project 880030

APPENDIX 1

GEOPHYSICAL LOGGING PROCEDURES

The following brief notes provide information on some of the relevant logging procedures related to depth determination accuracy, sampling density, and other correlation considerations.

The depths are measured with an accuracy of 1 mm by the optical depth encoder located on the wellhead pulley assembly. All logs were obtained continuously at a speed of 3 to 6 m/minute while sampling at a depth interval of 5 to 20 cm (based on a 1 or 2 second sample time interval). Data were acquired while logging both downwards (downrun) and upwards (uprun) providing redundancy of data for most of the parameters recorded.

Correlation problems: matching the logs to the geology

There are sometimes problems in making correlations between the geophysical responses and the geological information. The greatest difficulty arises with discrepancies in depths between the two data sets. Errors exist in core data depths due to possible missing or lost core during drilling. Depth errors can also exist in geophysical logs that are mainly due to slippage and/or cable stretching. These errors must be corrected for all the logging data. The zero depth reference for the logging data is at the top of the casing which may not be the zero reference level for the geological log. (All depths on the geophysical logs are lengths along the drillholes and not true vertical depths, which is also true for the core log.) Another problem arises from the fact that geological contacts are not always well defined. They are quite often gradational and hence are somewhat subjective. The interpreted geological contacts may not coincide with the changes in the bulk physical or chemical properties of the formation.

THE BOREHOLE GEOPHYSICAL SIGNATURE OF THE MCCONNELL NICKEL DEPOSIT, SUDBURY AREA

C.J. Mwenifumbo, P.G. Killeen, B.E. Elliott and K.A. Pflug
Geological Survey of Canada, 601 Booth Street, Ottawa, Ontario K1A 0E8

C.J. Mwenifumbo, P.G. Killeen, B.E. Elliott and K.A. Pflug, The borehole geophysical signature of the McConnell nickel deposit, Sudbury area: in Proceedings of the 5th International Symposium of the Minerals and Geotechnical Logging Society, Tulsa, 24-28 October 1993.

ABSTRACT

The McConnell nickel deposit, located in the Sudbury Breccia between norites to the north and metavolcanics to the south, is a small tabular body approximately 20 m wide, 152 m in strike length and 610 m in depth extent. This massive sulfide deposit, comprised of pyrrhotite and pentlandite, is highly magnetic and very conductive. It has been extensively drilled and numerous drillholes remain open. Preliminary multiparameter borehole geophysical measurements were made in some of these holes with the GSC's R&D logging system for an initial compilation of the geophysical signatures of the deposit and its host rock. This deposit is targeted as one of several potential borehole geophysical test sites to be established in Ontario under the Northern Ontario Development Agreement. Such sites will be used to test new technological developments in borehole geophysics by geophysical instrument manufacturers, mining industry and research organizations.

The borehole geophysical measurements made at the McConnell deposit include natural gamma ray spectrometry (total count, K, U, Th), self potential, single point resistance, electrical resistivity, induced polarization, spectral gamma gamma (density, heavy element assay), temperature, magnetic susceptibility, acoustic velocity, borehole orientation and 3-component magnetometer. Most of the geophysical parameters give excellent responses that are characteristic of the deposit and its host rocks. The density, magnetic susceptibility and electrical resistivity accurately delineate the distribution of the mineralized zones along the drillholes and provide some basic physical property data to help in the interpretation and modelling of surface and airborne geophysical data. The natural gamma ray data provide useful information for mapping alteration and stratigraphy.

INTRODUCTION

As part of a 5-year federal-provincial government agreement (1991-95 Ontario-Canada Mineral Development Agreement), the Geological Survey of Canada (GSC) will make an inventory of ore deposit signatures, using borehole geophysics, for a variety of ore deposit types that are representative of major deposits in Ontario (Killeen and Mwenifumbo, 1992, Mwenifumbo et al., 1993). The project will also establish test sites that will support the development of new borehole geophysical technology, and foster the development of a geophysical logging service industry. Additional details regarding this project and the establishment of test sites are given by Killeen et al., (this volume).

Borehole geophysical logging is one of the best methods of defining the physical properties of a deposit, its host rocks and any associated alteration. The *in situ* measurements, compared to laboratory measurements, are more representative of the rocks since the sample volume is much larger than for a laboratory sample. Furthermore, the measurements are made under field conditions of temperature, pressure, pore fluids, etc., representing relatively undisturbed samples (except for the borehole). Initial measurements of deposit signatures have been made at the McConnell nickel deposit with the GSC's R&D logging system and several commercially available logging systems.

THE MCCONNELL DEPOSIT (GARSON OFFSET)

The McConnell nickel deposit (Garson Offset) which is owned by INCO, is located near the town of Garson in the Sudbury basin of Ontario. It is situated in the Sudbury Breccia between norites to the north and metavolcanics to the south. It is a small tabular body approximately 20 m, wide, 152 m in strike length and 610 m in depth extent. This massive sulfide deposit is fairly representative of the Sudbury type nickel deposits comprising pyrrhotite and pentlandite that are highly magnetic and very conductive. The ore body has been extensively drilled and is easily accessible. A number of BQ-size drillholes were 'dummy probed' and fifteen were found to be open.

In the summer of 1992 preliminary multiparameter borehole geophysical measurements were made in some of these holes with the GSC's R&D logging system for

an initial compilation of the geophysical signatures of the deposit and its host rock. In the summer of 1993 a fence of five drillholes intersecting the massive sulfide ore zone were logged with the GSC R&D logging system and several commercially available logging systems. The geophysical measurements made included induced polarization, electrical resistivity, single point resistance, self potential, magnetic susceptibility, natural gamma ray spectroscopy (total count, K, U, Th), spectral gamma gamma (density, heavy element assay), temperature, acoustic p-wave velocity, borehole orientation, borehole 3-component magnetics and borehole 3-component VLF-EM.

The results of all the borehole geophysical measurements at the McConnell Nickel deposit will be compiled and presented in the form of GSC Open Files.

THE GEOPHYSICAL SIGNATURE OF THE MCCONNELL DEPOSIT

Five examples which exemplify the geophysical characteristic of the McConnell deposit are presented. Most of the geophysical parameters give excellent responses characteristic of the deposit and its host rocks. The density, magnetic susceptibility and electrical resistivity accurately delineate the distribution of the mineralized zones along the drillholes and provide some basic physical property data to help in the interpretation and modelling of surface and airborne geophysical data. The natural gamma ray data provide useful information for mapping alteration and stratigraphy.

Figure 1 shows the total count gamma ray logs recorded in five boreholes intersecting the massive sulfides. Characteristic levels of natural gamma ray activity within the different rock types are extremely useful for hole-to-hole lithologic correlation. For example, the amphibolites are defined by a low response and the schists by a high response in the gamma ray logs. It is apparent from the logs that numerous details are missing from the geological logs since they are difficult to discern in the drill core. The gamma ray logs provide the geologist with a means of interpreting the geology other than visual examination. It is clear from these five logs that a simple gamma log run in these boreholes would be of significant benefit in preparation of detailed geological logs.

The gamma ray spectral logs recorded in hole 78929 are shown in Figure 2. Spectral logs provide information on the distribution of K, U and Th in addition to the total radioactivity data provided by a total count gamma ray log. Note, for example, that the schists contain potassium and thorium but virtually no uranium. This distribution of radioelements may be characteristic of the schists at this deposit and could provide additional data for more accurate hole-to-hole lithologic correlation. The thin high gamma ray count zone indicated at about 87 m in the total count log appears to be primarily a uranium enrichment with some thorium, but no increase in potassium. This example shows the possibility of obtaining a detailed radioelement 'fingerprint' using gamma ray spectral logs.

Figure 3 shows the acoustic p-wave velocity logs measured with a Mt. Sopris probe (Pflug et al., 1994) in hole 78930. The logs include the density, p-wave velocity, acoustic amplitude and acoustic impedance (velocity x density). The velocity log shows some significant variations associated with different rock types. The amphibolite (50-65 m) appears to have relatively high velocity and density while the massive sulfides (135 to 152 m) have low velocity and high density. Further work is being done to extract the shear wave velocity from the full waveform data which were recorded. This will make it possible to compute several geotechnical parameters of interest in planning a mining operation. The acoustic velocity data, besides being used for mapping lithology and defining massive sulfide zones, provide fundamental information for planning possible seismic surveys and hole-to-hole seismic tomographic investigations.

A set of eight geophysical logs acquired in hole 78930 is shown in Figure 4 along with the geological log. The magnetic susceptibility data (MS) are shown at two different scales; the first log emphasizes details in the host rock with low susceptibility values, and the second log shows variations within the sulfides that are off scale in the first log. The exceptionally high susceptibility values within the massive sulfide zone are caused by pyrrhotite that is associated with pentlandite in this nickel ore. The negative susceptibility values within the massive sulfide zone are due to cross-coupling between the conductivity and susceptibility channels. The susceptibility measurements have to be corrected for the extremely high conductivity within the sulfide zone (not done in the present data set).

In addition to the density log, the spectral gamma gamma (SGG) ratio log is presented in Figure 4. This log is the ratio of a high energy-to-low energy window count rate in the backscattered gamma ray spectrum of the density tool's source. It is considered a 'heavy element indicator' because it is a function of the effective atomic number of the scattering medium. The very high values in the massive sulfides are consistent with their high average atomic number caused by the iron and nickel content. Smaller variations are evident in other rock types such as the schists, metasediments

and amphibolite, reflecting changes in their average atomic number due to variations in their content of iron, magnesium, aluminum, silicon and other elements. This SGG ratio adds a new parameter to the deposit signature which could provide valuable qualitative information on the elemental composition of the different rock types. This relatively new method is currently being applied to mineral exploration environments (Killeen et al., 1992). Also shown in Figure 4 are the resistivity and IP (induced polarization) logs. The IP log reflects the 'polarizability' of the rocks which is primarily associated with distribution of disseminated sulfides.

The temperature and temperature gradient logs (Figure 4) show the characteristic temperature minimum (100 m) observed in areas with past glaciation periods. Although these logs do not show anomalous behaviour within the massive sulfide zone, it has been shown by Mwenifumbo (1993) that the high thermal conductivity of some massive sulfides (especially sphalerite) can produce anomalous T and T-gradient values. Temperature measurements can also be used to detect water flows in and out of fractures and joints which make them ideal for predicting water flow in a mining operation.

The results of logging with a 3-component magnetometer and borehole orientation tool are shown in Figure 5. These logs were recorded in hole 78930 and include the X, Y and Z components of the magnetic field, the computed total field, the computed dip and azimuth of the hole (based on solid state tilt meters as well as the magnetic data), the magnetic susceptibility, resistivity, single point resistance and temperature. These are recorded with a single probe; the BMP-04 of IFG Corp. Interpretation of the magnetic logs in terms of the magnetic signature of the deposit is in progress.

SUMMARY

The geophysical data described here are to be compiled for all of the holes logged and published as a GSC Open File report. It is intended that updates to this Open File will be published periodically as further information becomes available. The McConnell deposit may become a borehole geophysical test site representing the Sudbury type nickel deposits.

ACKNOWLEDGEMENTS

The authors wish to acknowledge financial support for this project from the Canada-Ontario Subsidiary Agreement on Nothern Ontario Development (1991-1995), under the Canada-Ontario Economic and Regional Development Agreement. The authors would also like to thank Barry Krause and Alan King of INCO Exploration and Technical Services Inc. for their help in establishing the McConnell deposit as a test site for borehole geophysics.

REFERENCES

Killeen, P.G. and Mwenifumbo, C.J.
1992: A NODA project to develop geophysical test sites at major deposits in Ontario, with emphasis on borehole geophysics. Oral Presentation, Ontario Mines and Minerals Symposium, December 9-11, 1992. Abstract (p.9).

Killeen, P.G., Elliott, B.E. and Mwenifumbo, C.J.,
1993: Ore deposit signatures and borehole geophysics test sites in Ontario; in: Proceedings of the 5th International Symposium of the Minerals and Geotechnical Logging Society. Tulsa, 24-28 October 1993.

Mwenifumbo, C.J., Killeen, P.G. and Bernius, G.R.,
1993: Ore deposit signatures by borehole geophysics: in Summary Report, 1992-1993, Northern Ontario Development Agreement, (ed.) N. Wood, R. Shannon, L. Owsiacki and M. Walters, co-published by Energy, Mines and Resources Canada, p.123-125.

Mwenifumbo, C.J.
1993: Temperature logging in mineral exploration. Journal of Applied Geophysics, 30:297-313.

Pflug, K.A., Killeen, P.G. and Mwenifumbo, C.J.
1994: Acoustic velocity logging at the McConnell Nickel Deposit, Sudbury area: Preliminary *in situ* measurements; *in* Geological Survey of Canada Current Research, 1994-C, in press.

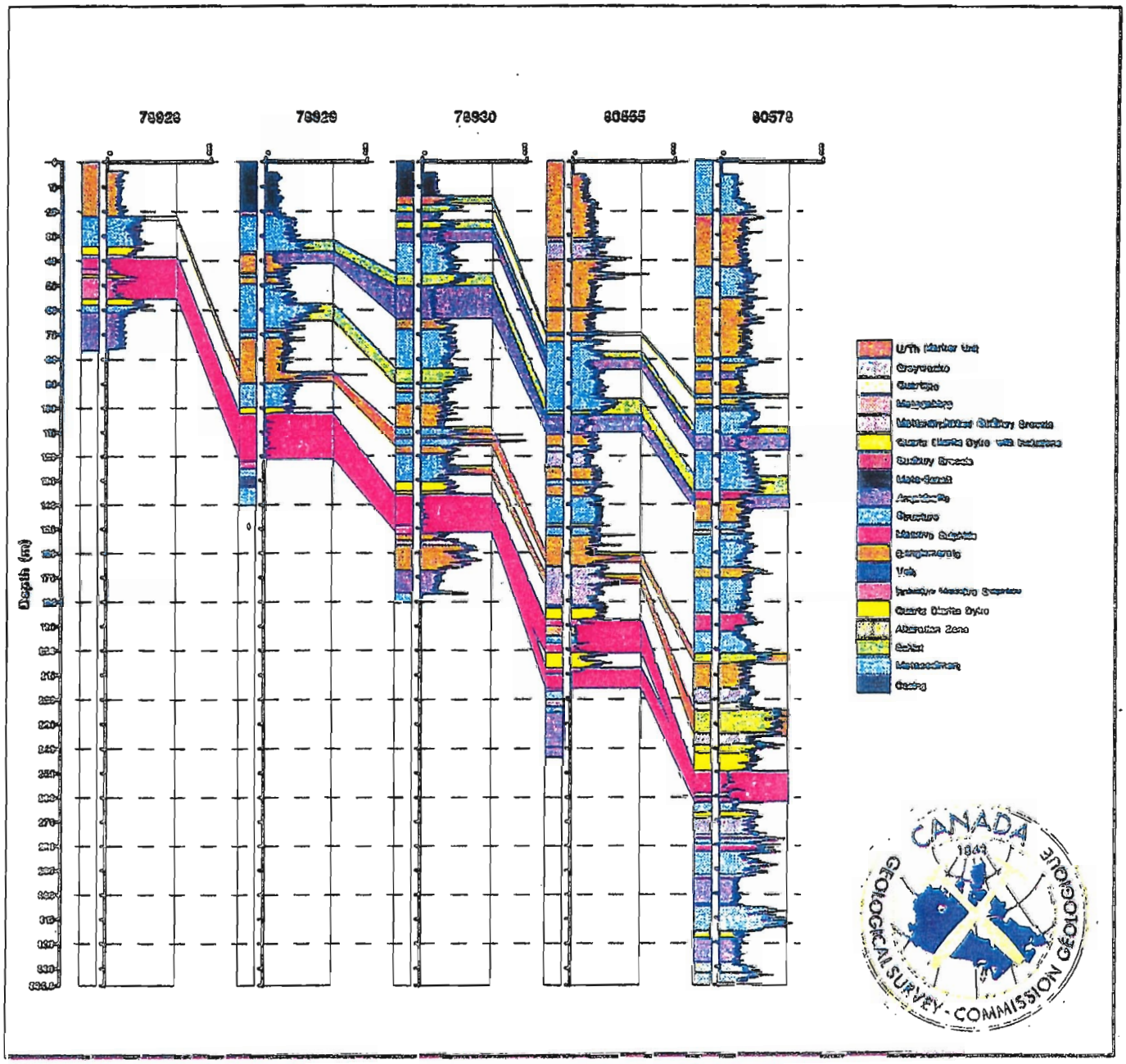

Figure 1. Total count gamma ray logs (in cps) illustrating their use in hole-to-hole lithologic correlation at the McConnell nickel deposit.

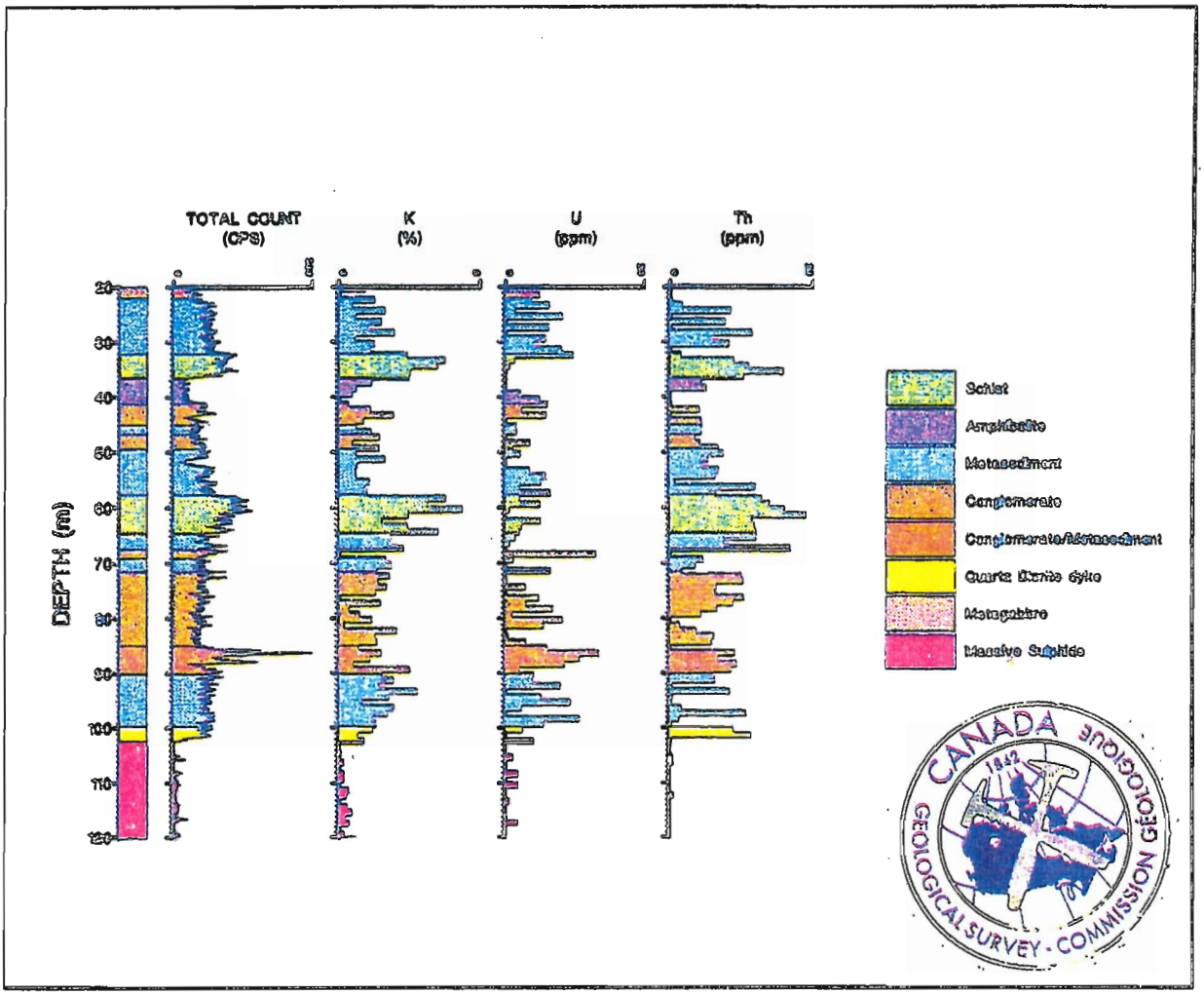

Figure 2. Gamma ray spectral logs (total count, K, U, Th) recorded in hole 78929 showing the distribution of radioelements within various rock types at the McConnell nickel deposit.

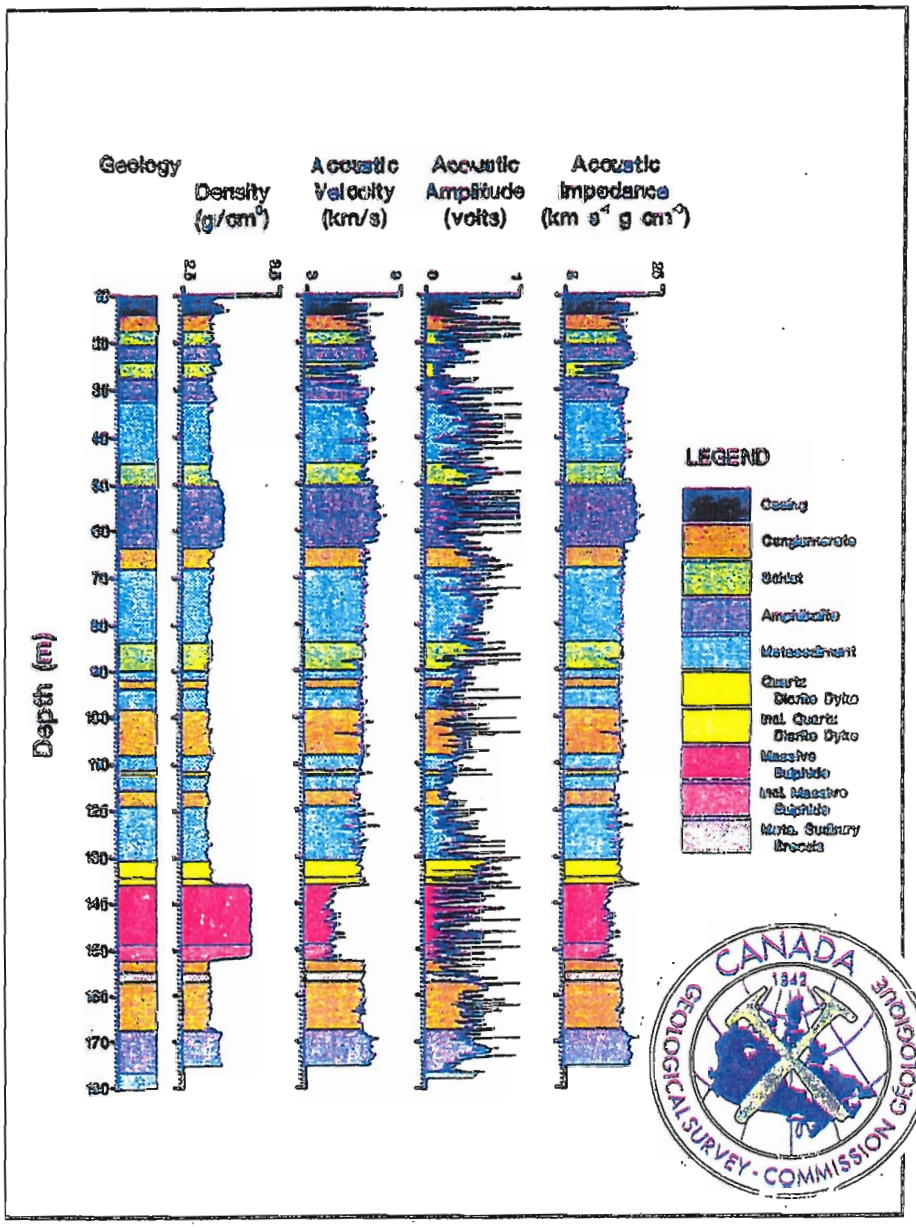

Figure 3. Density, acoustic velocity, amplitude and impedance logs recorded in hole 78930.

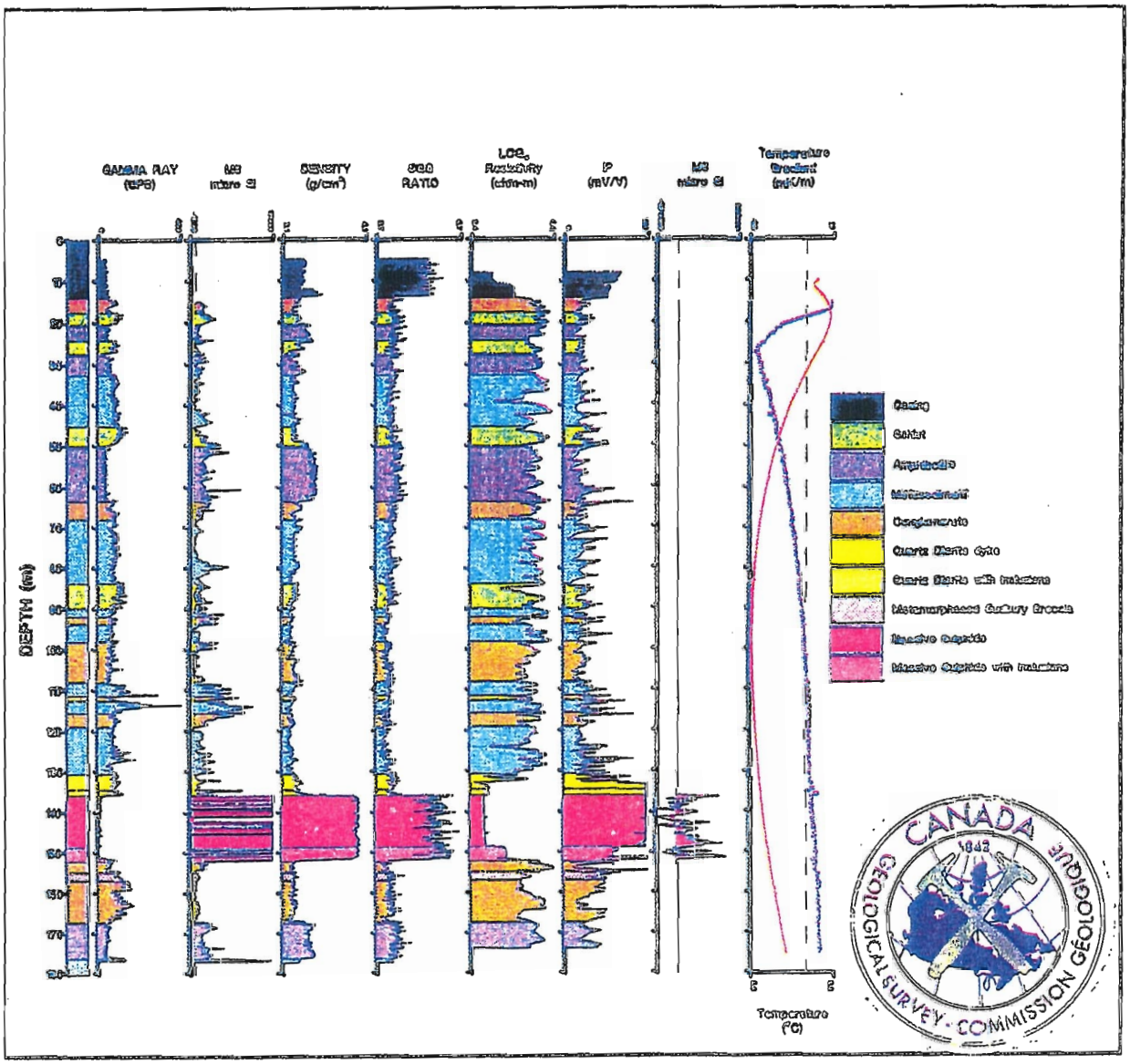

Figure 4. Multiparameter geophysical logs recorded in hole 78930 with the GSC R&D logging system.

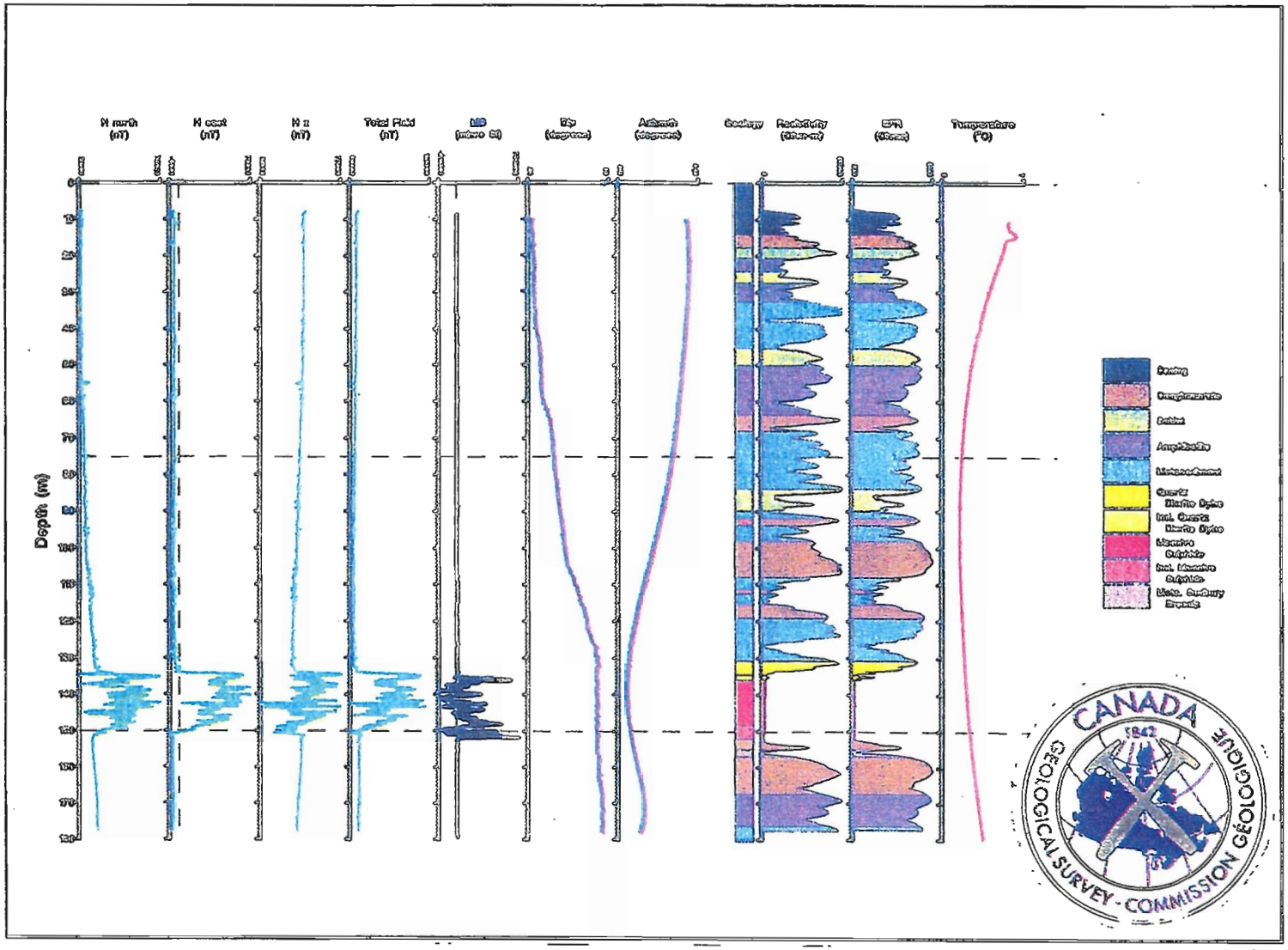

Figure 5. Borehole 3-component magnetometer/orientation data recorded in hole 78930 with the IFG Corp. BMP-04 multiparameter probe.

Borehole geophysics applied to mapping Paleozoic stratigraphy, Grand Rapids area, Manitoba

C.J. Mwenifumbo
Mineral Resources Division

Mwenifumbo, C.J., 1994: Borehole geophysics applied to mapping Paleozoic stratigraphy, Grand Rapids area, Manitoba; in Current Research 1994-E; Geological Survey of Canada, p. 141-149.

Abstract: Multiparameter geophysical measurements, including natural gamma-ray spectrometry, gamma-gamma density, resistivity, induced polarization (IP), magnetic susceptibility, temperature, and temperature gradient, were made in borehole M-6-91 in the Grand Rapids area of Manitoba. The stratigraphy intersected by M-6-91 consists of Silurian and Ordovician carbonate formations. The different Paleozoic carbonate formations are accurately mapped by their distinctive geophysical signatures. Argillaceous horizons that define some formation boundaries are characterized by relatively high radioactivity and can be easily detected on the total count gamma-ray log. The different formations, consisting mainly of dolomite, have distinctive densities and resistivities that proved useful in defining lithostratigraphic boundaries in zones without a prominent argillaceous marker horizon. There are slight variations in the natural gamma-ray count rate and IP response within the dolomites, and these variations are probably due to the presence of clay in the dolomites. Temperature logs show changes that indicate groundwater flow zones.

Résumé : Des mesures de plusieurs paramètres géophysiques, dont la spectrométrie à rayons gamma naturels, la densité gamma-gamma, la résistivité, la polarisation induite, la susceptibilité magnétique, la température et le gradient de température, ont été prises dans le trou de sondage M-6-91 foré dans la région de Grand Rapids au Manitoba. La stratigraphie traversée par le trou M-6-91 comporte des formations carbonatées d'âge ordovicien et silurien. Les différentes formations carbonatées paléozoïques sont cartographiées avec précision en utilisant leurs signatures géophysiques caractéristiques. Les horizons argileux qui définissent certaines limites de formation sont caractérisés par une radioactivité relativement élevée et ils peuvent être facilement détectées sur la diagraphie de rayons gamma à comptage total. Les différentes formations, composées surtout de dolomie, présentent des densités et résistivités distinctes qui se sont avérées utiles pour définir les limites lithostratigraphiques dans les zones sans horizon repère argileux marqué. Il existe de légères variations dans le taux de comptage des rayons gamma et la réponse de la polarisation induite au sein des dolomies, variations qui sont probablement dues à la présence d'argile dans les dolomies. Les diagraphies de la température indiquent des changements révélant des zones d'écoulement d'eau souterraine.

INTRODUCTION

The Manitoba Geological Services Branch drilled several holes in the Grand Rapids area (NTS 63F, 63K) to study the Paleozoic and Precambrian stratigraphy (Bezys, 1991, 1992, 1993). Some of these holes were kept open for hydrogeological and borehole geophysical measurements. Geological core logging in carbonate formations is sometimes difficult because the entire core appears to be quite similar. If the strata are without distinct horizons, such as structural or textural features, differences in the units can be difficult to see. In 1991, the Geological Survey of Canada (GSC) made multiparameter borehole geophysical measurements in stratigraphic hole M-6-91 at Cooks Cave Southeast, Grand Rapids, in order to define the Paleozoic stratigraphy. M-6-91 is a BQ-size hole (60 mm diameter), drilled to a total depth of 163.7 m and intersecting Precambrian granodiorite at 161.8 m.

STRATIGRAPHY AND LITHOLOGY

Hole M-6-91 intersected a Paleozoic carbonate sequence ranging in age from Ordovician to Silurian and comprised of dolomite, dolomitic mudstone, and argillaceous dolomitic mudstone. These dolomitic units overlies the Winnipeg Formation (shale and sandstone), which is underlain by Precambrian granodiorite. A description of the drill core geology (Bezys, 1993) is given in Figure 1, along with ages, formations, and members.

Silurian strata consist of the Interlake Group (East Arm, Atikameg, Moose Lake, Fisher Branch, and Upper Stonewall Formations). These various formations are defined by prominent argillaceous dolomitic mudstone units. The East Arm Formation is a crystalline brown to buff dolomite overlying the Atikameg Formation, which is a buff to yellow, vuggy dolomite. Porosity in the Atikameg Formation, estimated to be ~10%, may be due to fossil solutioning (Bezys, 1991). The Moose Lake Formation, an irregular laminated to mottled dolomite, is bounded above and below by argillaceous dolomitic mudstone beds. The lower argillaceous dolomitic mudstone, the U1-marker, forms the contact between the Moose Lake and Fisher Branch Formations. The Fisher Branch Formation is a fossiliferous, vuggy dolomite with porosity estimated to be 5-8%.

Ordovician carbonate beds include the Stonewall, Stony Mountain, and Red River Formations. The Stonewall Formation is subdivided into nine units (Figure 1), and is bounded by the Stonewall marker bed above and the Williams Member, an argillaceous dolomite unit, below. The argillaceous T-marker (unit 7) in the middle of the Stonewall Formation marks the Ordovician/Silurian boundary. The Stony Mountain Formation underlying the Williams Member consists of two major subdivisions: the Gunton Member, is a cherty, mottled, buff and grey nodular dolomite, and the Penitentiary Member, an argillaceous and slightly nodular dolomite. At the bottom of the Stony Mountain Formation is a transition bed consisting of mottled, crystalline dolomite with enhanced porosity due to fossil solutioning. The Red River Formation consists of the Upper Red River (Fort Garry Member), which is subdivided into five units, and the Lower Red River Formations. The Fort Garry Member is composed of interbedded argillaceous dolomite, calcitic dolomite, and massive dolomite. The Lower Red River Formation is a finely crystalline, massive, fossiliferous, slightly granular cherty dolomite.

Some of these formations are sources of industrial minerals. The Gunton Member of the Stony Mountain Formation and the Stonewall Formation are major sources of building stone (Bamburak, 1992). Geophysical measurements provide information on lithology and stratigraphy and may also yield information on the quality of the carbonate as a source of building stone.

GEOPHYSICAL MEASUREMENTS

Borehole geophysical measurements may detect changes in physical and chemical properties of rocks that are invisible to the geologist. These data complement observations made by examining cores. The GSC R&D logging system was used to acquire multiparameter borehole geophysical measurements in hole M-6-91. Measurements included self potential (SP), single point resistance (SPR), normal array resistivity, induced polarization, natural gamma-ray spectrometry, spectral gamma-gamma density, magnetic susceptibility, temperature, and temperature gradient. A brief description of the parameters measured follows.

Electrical resistivity of rocks depends on several factors. The most important factors affecting resistivity in carbonate rocks are fracturing, porosity, degree of saturation of pore spaces, and salinity of pore fluid. The presence of clay minerals may also have an affect. Argillaceous sediments containing conductive clay minerals may be detected on the resistivity and single point resistance log. Induced polarization measurements primarily respond to the presence of polarizable and conductive minerals such as base metal sulphides/oxides and graphite. There are no such minerals in the strata intersected by hole M-6-91. Variations in IP response in this hole are probably due to the presence of polarizable cation-rich clays such as illite and montmorillonite (Mwenifumbo, 1989).

Gamma-ray measurements detect variations in natural radioactivity originating from uranium (U), thorium (Th), and potassium (^{40}K) in rocks. Estimates of the equivalent concentrations of these three radioelements can be made from gamma-ray spectrometry measurements. Gamma-ray spectrometry measurements were taken in hole M-6-91. The low count rates recorded in the carbonates yield poor counting statistics that make it impossible to separate the different contributions from K, U, and Th in the spectra. Therefore, the gamma-ray log presented in this paper is the total count log (energy window, 0.3-3.0 MeV). In M-6-91, which intersects carbonates and argillaceous sediments, ^{40}K originating from clay minerals such as illite and montmorillonite is likely the principal source of natural gamma radiation. Variations in the concentrations of these minerals in carbonate rock make gamma-ray logs an important tool for lithological mapping and stratigraphic correlation.

Density response is primarily a function of rock bulk density, which depends on the mineralogical composition of the rock and on porosity and water saturation. In carbonate rocks, variations in porosity and possibly variations in magnesium content of dolomite are the primary causes of density variations.

Parameters affecting the temperature-depth profile in a borehole include drilling fluid circulation, variations in thermal conductivities of the rocks intersected, and ground water flow (Mwenifumbo, 1993). Dolomites and mudstones have distinctive thermal conductivities and can be distinguished on the temperature gradient profile, provided water is not moving in the borehole. Groundwater flow in the borehole from fractures and other porous zones produces easily detectable temperature anomalies that mask variations in the thermal conductivities of the formations.

Magnetic susceptibility measurements did not show any response.

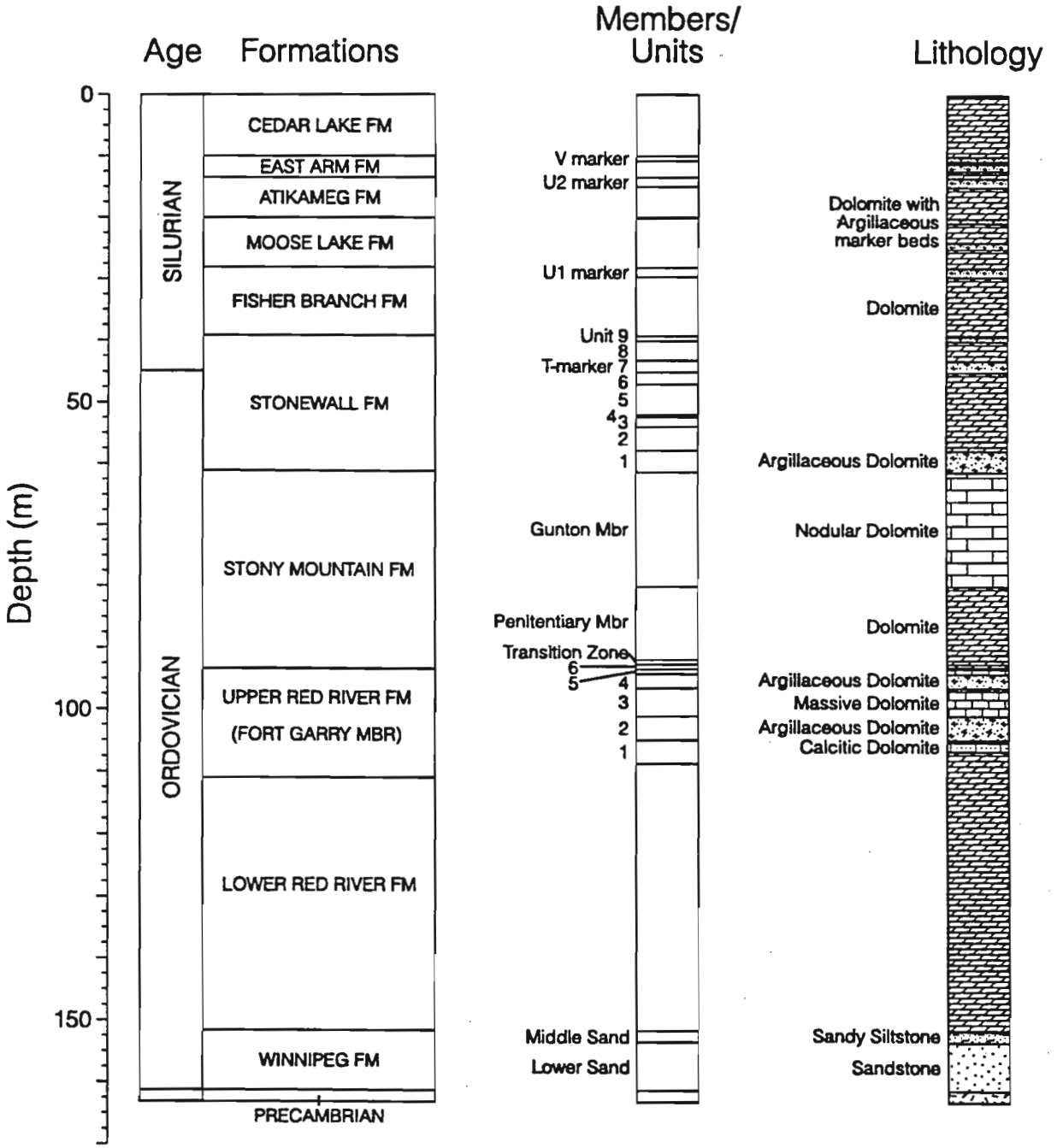

Figure 1. Summary of the stratigraphy and lithology intersected by hole M-6-91.

DISCUSSION OF RESULTS

Multiparameter borehole geophysical measurements acquired in hole M-6-91 are presented in Figures 2 and 3. Figure 2 shows lithology, gamma-ray, IP, resistivity, and density logs, and Figure 3, lithology, SPR, temperature gradient, and temperature logs (lithology is defined in Figure 1).

A distinctive, high gamma-ray response is associated with argillaceous dolomitic beds. These beds act as marker horizons and are used to determine the boundaries of the formation and/or member. They can be located on the gamma-ray log. A low gamma-ray response is observed from the carbonate formations. Three Silurian carbonate formations, the lower Moose Lake, Fisher Branch, and Stonewall Formations, are somewhat lower in gamma-ray activity than the underlying Ordovician carbonate formations. This suggests that these formations contain less clay minerals, and evidence of this is also seen in the lower IP response. The Stony Mountain and Lower Red River Formations have a slightly higher gamma-ray activity. Following this interpretation based on the gamma-ray log and other geophysical parameters, the drill core was re-examined and a more accurate stratigraphic sequence was constructed.

The IP log shows responses similar to gamma-ray activity in the dolomites, i.e. extremely low IP values in the Fisher Branch and Stonewall Formations correspond to extremely low gamma-ray activity. There is good positive correlation between IP and gamma-ray activity in the argillaceous dolomitic mudstones, with a notable exception, however, in unit 2 (101.2-105.1 m) of the Fort Garry Member where high gamma-ray activity is associated with a low IP effect. This suggests clay mineralogy different from that in the other argillaceous beds.

Resistivity and density logs show distinct responses in the various formations. Variations in these geophysical parameters in dolomites are mainly a function of variations in porosity. Resistivity and density show good positive correlation in the various formations except in the Penitentiary Member of the Stony Mountain Formation and the Fort Garry Member. Mean resistivities in these formations (Table 1) are lower than those of the overlying and underlying formations, and mean densities are higher.

Box-and-whiskers plots (Figures 4, 5, and 6) compare the distributions of density, resistivity, and IP parameters for the various formations intersected in hole M-6-91. They show how these geophysical parameters vary within the different formations. Both resistivity and density data indicate that the Moose Lake, Fisher Branch, and Stonewall Formations and the Gunton Member are significantly different. Resistivities and densities are quite variable within the Fort Garry Member as indicated by box spreads and whisker extensions. While box-and-whiskers plots are designed to compare median levels, they do not provide an accurate picture of the distribution of the parameters. The modality of the distributions is not apparent. Histograms provide a better graphical representation of how the parameters are distributed in the prescribed values. They provide information on whether the distributions consist of unimodal or multimodal populations. Figures 7 and 8 show histograms of the density and resistivity for six formations and members. The density distribution in the Fort Garry Member is bimodal while the resistivity is multimodal and shows a wide range of values.

From the geophysical measurements (refer to Figures 2 and 3), the Stonewall Formation can be subdivided into three major units, the upper unit consisting of geological units 6-9, the middle unit consisting of units 2-5, and the lower geophysical unit consisting of the Williams Member, an argillaceous dolomite. These units may correspond to the Upper Member, Middle Member, and Williams Member subdivisions (Bamburak, 1992). The Williams Member, an argillaceous and arenaceous dolomite, is characterized by higher density, higher resistivity, high IP effect, and higher gamma-ray activity. The Middle Member has the lowest gamma-ray activity and lowest resistivity of the three subdivisions. The Upper Member (39.5 to 46 m) consists of three argillaceous units that exhibit higher densities and lower resistivities than the Middle Member, except for the T-marker horizon.

The argillaceous T-marker bed that defines the Ordovician/Silurian contact is unique among the argillaceous marker beds; it has high natural gamma-ray activity, an anomalously low resistivity, and a corresponding high IP effect, but is higher in density. All other argillaceous marker beds show high radioactivity and high density, but the resistivity does not show a pronounced change relative to the dolomitic beds. In some areas of northern Manitoba the T-marker bed is rarely seen or absent (Bezys, 1991). Since the Silurian Stonewall beds have distinctly higher resistivities and densities than those observed within the Devonian Stonewall strata, it is possible to define the Ordovician/Silurian boundary using these geophysical parameters. The Silurian Stonewall geophysical response is similar to that of the Fisher Branch Formation.

The Gunton/Penitentiary Member contact within the Stony Mountain Formation was established from the drill core logs at 75.75 m. However, the geophysical logs indicate that this contact should be near 80 m, where there is a change

Table 1. Mean values of density, resistivity, and IP.

Formation/Member	Depth (m)	Density (g/cm³)	Resistivity (ohm-m)	IP (mV/m)
Moose Lake Fm	20-27	2.77	11148.00	4.33
Fisher Branch Fm	29-40	2.62	1246.00	2.42
Stonewall Fm	46-57	2.54	735.00	2.18
Stony Mountain Fm				
Gunton Mbr	62-80	2.74	3701.00	4.13
Penitentiary Mbr	80-92	2.78	1990.00	4.80
Red River Fm				
Forty Garry Mbr	92-108	2.74	1269.00	3.70
Lower Red River Fm	112-150	2.72	3213.00	5.06

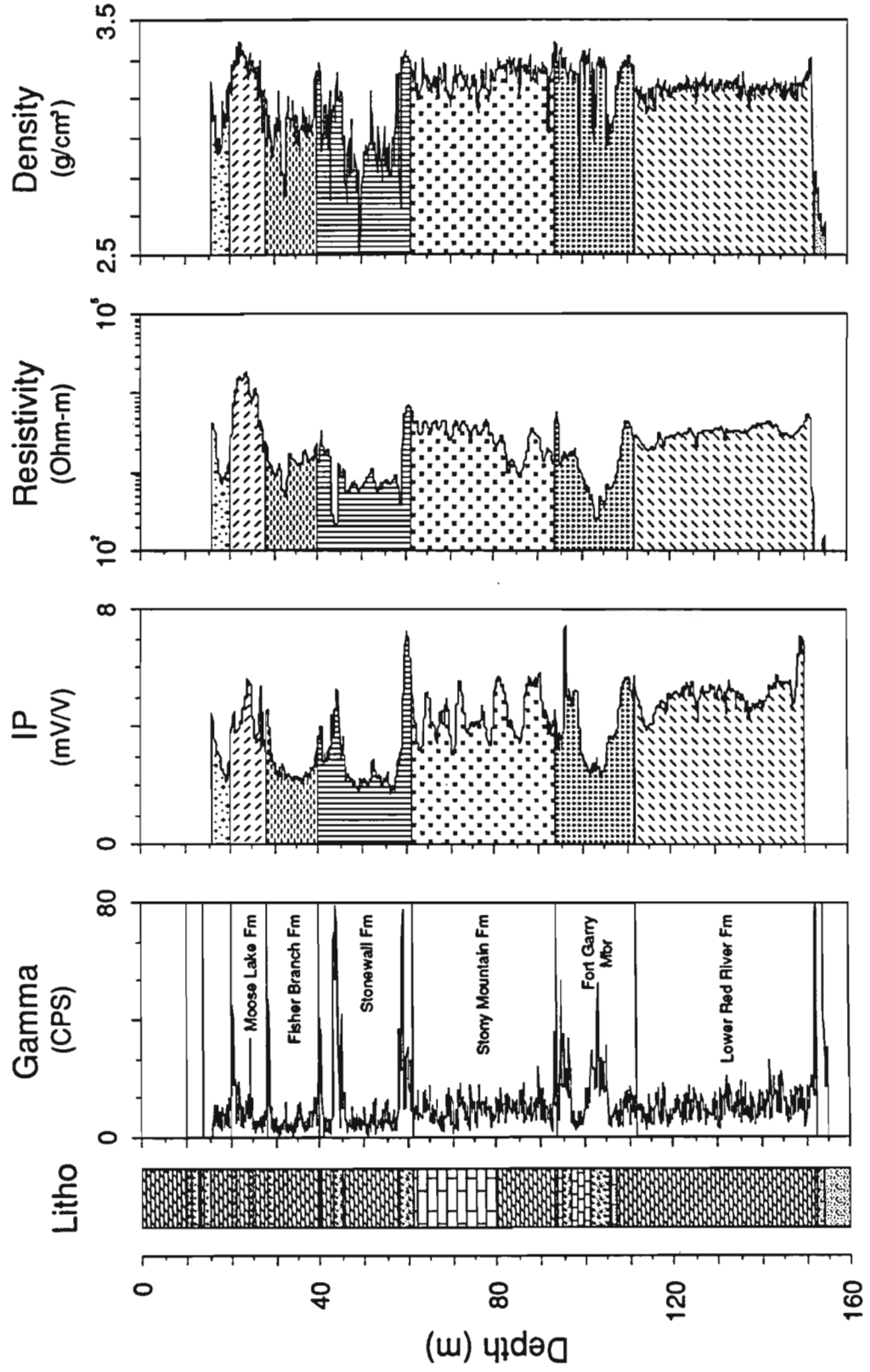

Figure 2. *Lithology, total count gamma-ray, IP, 40-cm normal array resistivity, and gamma-gamma density logs recorded in hole M-6-91. The shadings on each of the geophysical logs indicate the different formations. The lithology column is as indicated in Figure 1.*

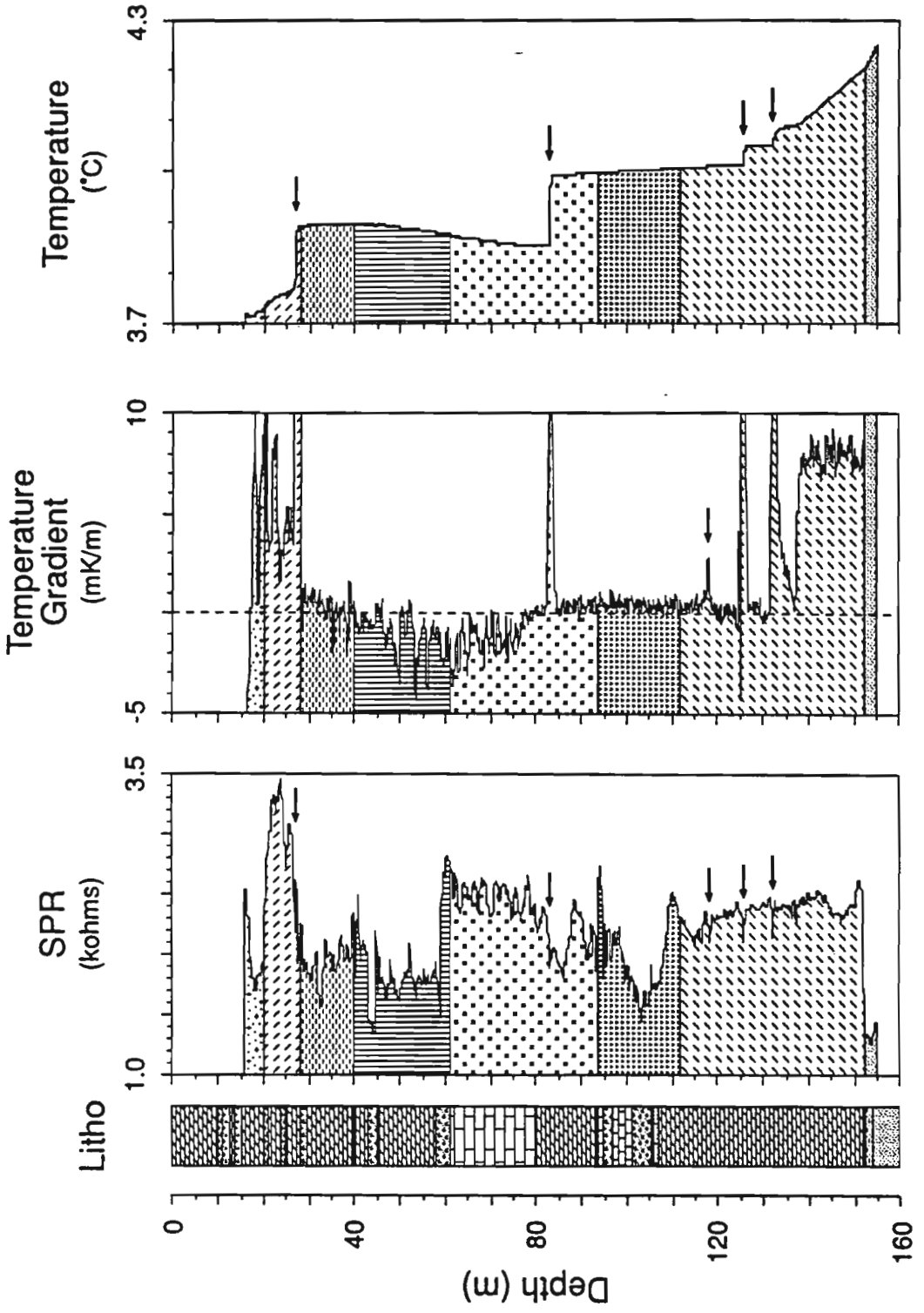

Figure 3. *Lithology, single point resistance (SPR), temperature, and temperature gradient logs recorded in M-6-91. Temperature gradient data are truncated at 10 mK/m (°C/km). The arrows on the temperature logs indicate the location of water entry/exit zones in the borehole. These correspond to low-resistance anomalies on the SPR log interpreted as fracture zones. The lithology column is as indicated in Figure 1.*

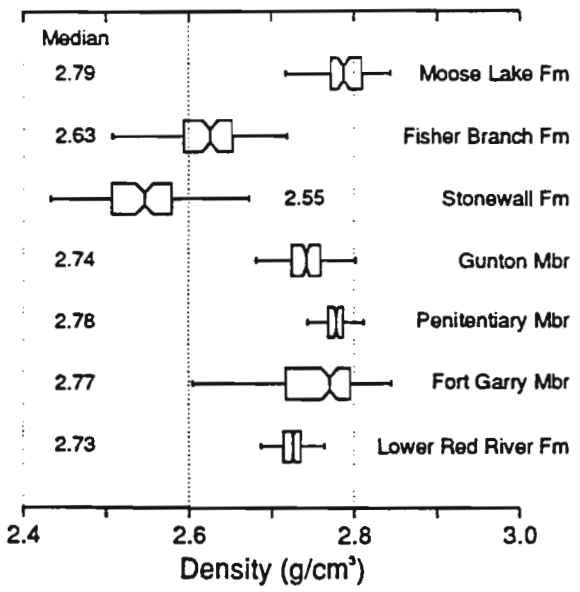

Figure 4. Box-and-whiskers plots showing density distribution for the different formations intersected in M-6-91. The boxes are bounded by the 25th and 75th percentiles while the whiskers represent the extension of data to the 10th and 90th percentiles. The notches represent the 95 percent confidence interval for the medians. The boxes for the Gunton and Penitentiary Members indicate that density distributions within these two Stony Mountain Formation Members are distinct.

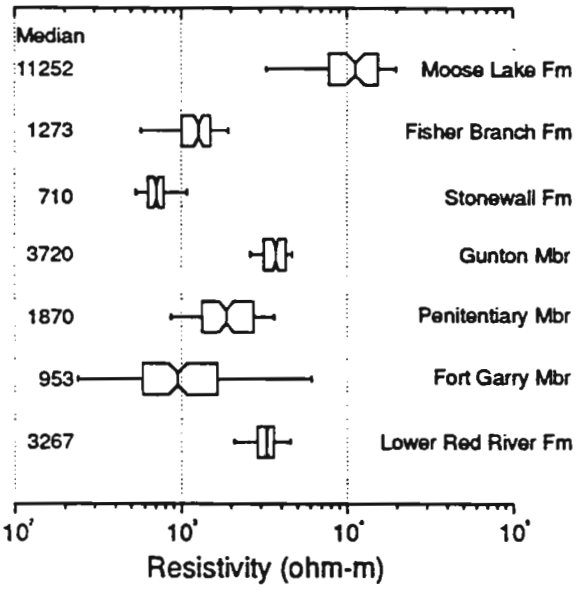

Figure 5. Box-and-whiskers plots showing resistivity distribution for the different formations intersected in M-6-91. Resistivities are lowest in the Stonewall Formation and highest in the Moose Lake Formation. The Fort Garry Member shows a wide range of resistivities because of the variability in lithology: dolomite, argillaceous dolomitic mudstone, and calcitic dolomite.

in resistivity and density. The overlying Gunton Member is noticeably lower in density and higher in resistivity than the Penitentiary Member. There is also a slight change in the character of the borehole gamma-ray signature at this location. The resistivity, IP, and density logs show periodicity in the Gunton Member, with high IP correlating with high density and high resistivity. This periodic signature reflects alternating lithological changes in the dolomite that may represent depositional cyclicity. The density and gamma-ray data show the Penitentiary Member to be homogeneous. The resistivity, however, is highly variable (Figures 5 and 8). There are subtle indications of fracture zones at approximately 83 and 86 m as seen on the resistivity, SPR, and density logs. Two zones portraying characteristic low density and low resistivity responses due to porosity changes occur within the Fisher Branch Formation (32-33 m, vuggy, very light yellow buff dolomite) and near the lower contact of the Fort Garry Member (105-107 m, vuggy, calcitic dolomite).

The temperature and temperature gradient logs (Figure 3) show distinct, abrupt temperature changes and high temperature gradients at several locations along the borehole. These temperature anomalies are characteristic of groundwater flow. Ground water enters or exits the borehole at these locations. The water flow zone at approximately 26.5 m occurs at the contact between the Moose Lake (a highly resistive and dense dolomite) and Fisher Branch Formations. This zone apparently rests directly upon a significant aquiclude, the U1-marker, a persistent dolomitic shale-mudstone horizon (Bezys, 1993). Temperature logging was carried out in another hole located 25 m away, where the temperature-depth profile was similar to that observed in M-6-91, suggesting laterally extensive groundwater flow zones. Another major water inflow/outflow zone is at approximately 83 m in the Stonewall Formation. Three other zones in the Lower Red

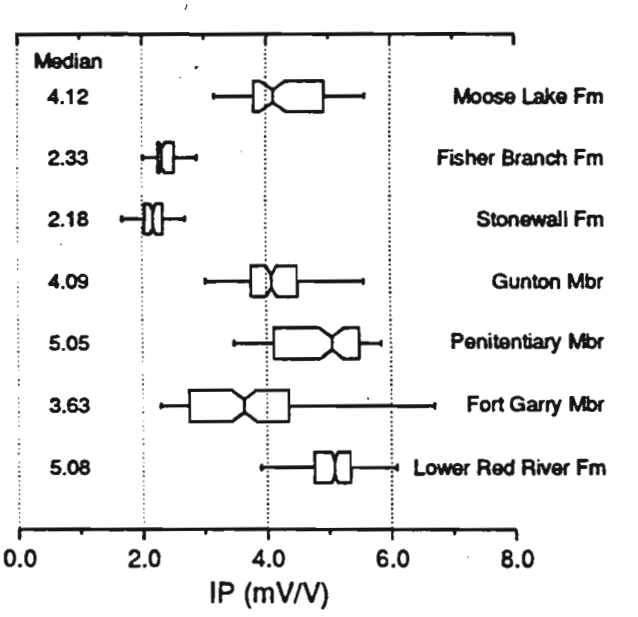

Figure 6. Box-and-whiskers plots showing induced polarization distribution (IP effect) for the different formations intersected in M-6-91.

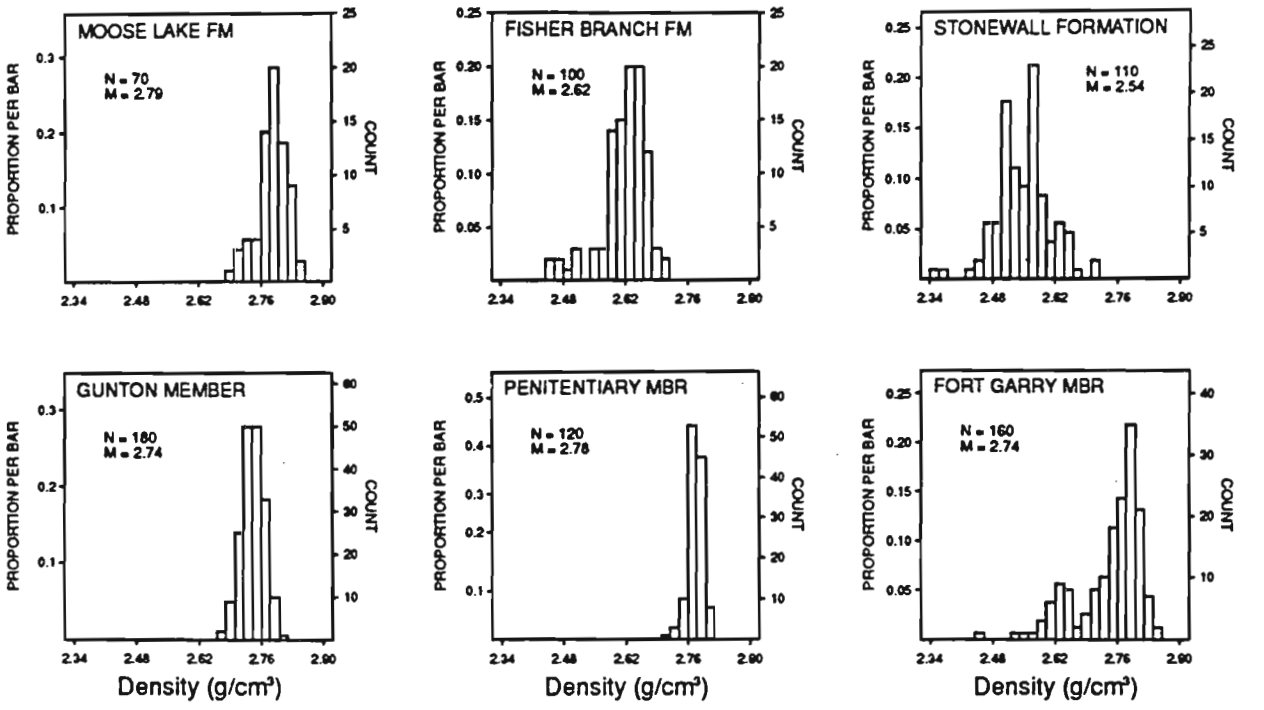

Figure 7. Histograms showing density distribution within six formations. Note that the Fort Garry Member shows a wide range of density values as portrayed on the box-and-whiskers plots. The histogram, however, shows that the distribution is bimodal. M – mean value.

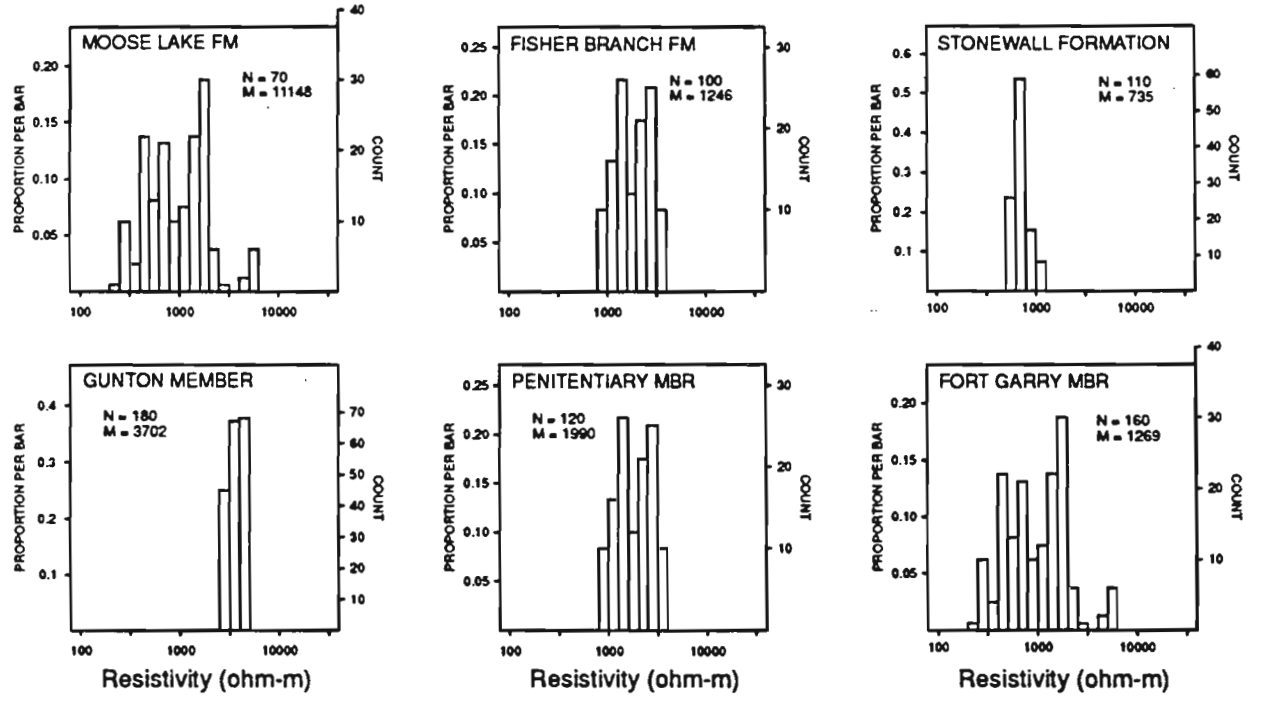

Figure 8. Histograms showing resistivity distribution (in logarithmic scale) within six formations. M – mean value.

River Formation are located at 125 m, 132 m, and 137.5 m. The electrical logs show distinct low-resistivity, v-type anomalies (possibly due to washouts) at these water inflow/outflow zones in the Red River Formation. Variations in the thermal conductivities of dolomite and argillaceous dolomitic mudstone could not be distinguished on the temperature gradient profile because of water movements in the borehole. For the same reason, the normal geothermal gradients could not be established. The bottom of the hole (140-150 m), however, shows temperature gradients that may be close to the normal geothermal gradients (mean=7.9 mK/m).

CONCLUSION

The geology and stratigraphy of Paleozoic carbonate formations intersected in hole M-6-91 were more clearly understood with the use of multiparameter geophysical logs. The gamma-ray log helped to identify and determine the positions of marker beds. Although some dolomitic beds in the various formations appear to be similar, they can be distinguished by their characteristic geophysical signatures. There are differences in electrical resistivity and density in different formations, and these differences are due to variations in porosity. Measurements from more than one hole are necessary to determine if these geophysical signatures (e.g., resistivity and density) are diagnostic of the different Paleozoic formations across a wider area. This information would help to correlate stratigraphy, especially where there are a few recognizable (marker) horizons. For this purpose, a proposal has been submitted to NATMAP to drill and log five stratigraphic coreholes in north-central Manitoba. Information from the geophysical logs will provide a more definitive stratigraphic signature for the Paleozoic formations and will enhance hole-to-hole correlations. Temperature logs may provide useful information on the hydrogeology of the area.

ACKNOWLEDGMENTS

Hole M-6-91 was funded and drilled by the Manitoba Department of Energy and Mines. Borehole logging was done with the GSC R&D system with A-base funding. Thanks are due to Bill Hyatt for the field data collection, and to Barbara Elliott for assistance in data processing.

REFERENCES

Bamburak, J.D.
1992: Industrial minerals investigations in the Selkirk Area (NTS 621); in Report of Activities, 1992, Manitoba Energy and Mines, Minerals Divisions, p. 145-148.

Bezys, R.K.
1991: Stratigraphic mapping (NTS 63F, 63K) and core hole program; in Report of Activities, 1991, Manitoba Energy and Mines, Minerals Division, p. 61-73.
1992: Stratigraphic mapping and core hole program; in Report of Activities, 1992, Manitoba Energy and Mines, Minerals Division, p. 123-131.
1993: Stratigraphic mapping and core hole program; in Report of Activities, 1993, Manitoba Energy and Mines, Minerals Division, p. 127-133.

Mwenifumbo, C.J.
1989: Optimization of logging parameters in continuous, time-domain induced polarization measurements; in Proceedings of the 2nd International Symposium on Borehole Geophysics for Mineral, Geotechnical, and Groundwater Applications, MGLS, Las Vegas, Nevada, v. I, paper N, p. 201-232.

Mwenifumbo, C.J.
1993: Temperature logging in mineral exploration; Journal of Applied Geophysics, v. 30, p. 297-313.

Geological Survey of Canada Project 880030

INTERPRETATION OF NEW GENERATION GEOPHYSICAL LOGS IN CANADIAN MINERAL EXPLORATION

P.G Killeen and C.J. Mwenifumbo
Geological Survey of Canada
601 Booth Street
Ottawa, Ontario
K1A 0E8 Canada

ABSTRACT

Technological advances in the past few years have led to the development of a new generation of slimhole logging tools for mineral exploration. While some are completely new developments, others are adaptations of technology from surface geophysical surveying or from petroleum logging. The application of these new geophysical methods requires considerable testing and development of new interpretation techniques for the different geological environments encountered in mineral exploration. At the Geological Survey of Canada (GSC) one objective of research in borehole geophysics has been to investigate the application of these methods to mineral exploration in various mining areas across Canada. The GSC R&D logging system has five 'new generation' logging probes which measure thirteen different parameters:

1. Temperature probe: temperature, temperature gradient;
2. I.P. probe: I.P., resistivity, S.P.;
3. M.S. probe: magnetic susceptibility, conductivity;
4. Gamma Spectral probe: total count, K, U, and Th;
5. Spectral Gamma Gamma: density, heavy element assay.

Examples will be described showing interpretations of the logs from various mining areas in Canada which include lead, copper, zinc, and uranium deposits.

INTRODUCTION

Probably the three most commonly used logs in borehole geophysics for mineral exploration are the gamma ray log, resistivity log and gamma-gamma density log. Technological developments have made it possible for these three logging techniques to evolve into a new generation of techniques (spectral gamma ray, induced polarization, and spectral gamma-gamma, respectively) which provide much more information than the 'state-of-the-use' logs as indicated in Table 1. The temperature log has also existed for a long time but has not been widely used. A new generation of high sensitivity temperature logging equipment makes temperature logs more attractive because they can be used to compute detailed temperature gradient logs for interpretation of water flow in fractures. Finally, magnetic susceptibility logging equipment has greatly improved since it first came into use about ten years ago. New generation magnetic susceptibility logs which have high sensitivity and thermal stability open up numerous possibilities for obtaining information about alteration processes which change the magnetic properties of rocks.

These five 'new generation' logging techniques have been applied in a number of mining areas, using the R&D logging system of the Geological Survey of Canada (GSC). Some examples of these logs will be given to illustrate the additional information which can be obtained through their interpretation, and to point out some of the possibilities for further developments in interpretation of the new generation logs. First however, the GSC logging system and the principles of operation of the five logging techniques will be briefly reviewed.

THE GSC LOGGING SYSTEM

The GSC logging system is typical of modern digital data acquisition systems, being built around a minicomputer as shown in Figure 1. As an R&D system, specialized software has been written to acquire data in greater detail than might be required for a 'production' logging system (see Bristow, 1979). Data are recorded on 9-track magnetic tape. A digital CRT displays data, spectra or waveforms as required for the operator to run the system. Data input is via modules specific to the parameters being measured. Communication with the system is by standard keyboard terminal. A software-controlled, 'smart', electrostatic, chart recorder provides customized logs with alphanumerics for field quality control. Some field processing is done in 'replay' mode but detailed interpretations are based on post-processing of the tapes on a 32 bit Data General Corp. MV4000 at headquarters.

This is a preprint: to be published in: Proceedings of the 2nd International Symposium on Borehole Geophysics for Minerals, Geotechnical and Groundwater Applications, October 1987, Golden, Colorado.

'STATE-OF-THE-USE' LOGS		'NEW GENERATION' LOGS	
Log	Parameter Measured	Log	Parameter Measured
① Gamma Ray	Total Count	Spectral Gamma Ray	Total Count, K, U, Th
② Resistivity	R, SP	Induced Polarization	IP, R, SP
③ Temperature	T	High Sensitivity Temp.	T, T gradient
④ Gamma Gamma	Density	Spectral Gamma Gamma	Density, Heavy Elements
⑤ -----	-----	Magnetic Susceptibility	MS, Conductivity (Inductive)

Table 1

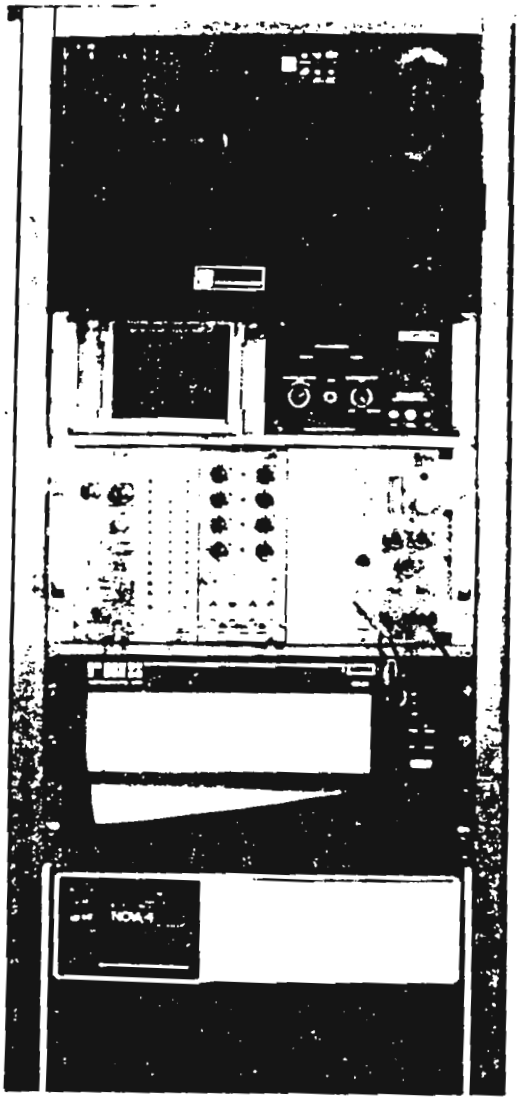

Figure 1: *Instrumentation in the R&D logging system developed at the Geological Survey of Canada (GSC).*

The characteristics of the logging tools and the measurements which they make are described below.

1. Spectral Gamma Ray Logging Tool: (Outside Diameter (O.D.) = 32, 38 or 50 mm)

Gamma ray measurements are used to detect variations in natural radioactivity due to changes in concentrations of the trace elements, uranium and thorium, as well as changes in concentration of the major element potassium, which may indicate alteration zones as well as rock types. Full gamma ray spectra are recorded in 256 channels covering an energy range from approximately 0.1 MeV to 3.0 MeV. Gamma ray counts in 10 selected energy windows can be accumulated and recorded during the data acquisition. Four windows provide information on total count (0.4 to 3.0 MeV), potassium, uranium, and thorium. Several sizes of scintillation detectors (sodium iodide and cesium iodide) are available for use in each probe size. A number of factors determine the logging speeds, size of detector and sample times during the acquisition of gamma ray data, the critical one being the anticipated levels of radioactivity. Usually the largest detector compatible with the borehole diameter is used to give maximum sensitivity and logging is done at 3 m/minute . More detailed information on gamma ray spectral logging can be found in Killeen (1979).

2. Induced Polarization (IP/R/SP) Logging Tool: (O.D. = 38 mm)

The IP/R/SP components include a time domain transmitter, probe electronics and the electrode arrays. The system has been described in detail by Bristow (1986). The transmitter is a constant current source capable of supplying up to 250 mA. There are 4 selectable pulse times for the current waveforms; 0.25s, 0.5s, 1s and 2s (i.e., full waveform of 1 second to 8 seconds duration). The long pulse times would mean logging at very low speeds in order to avoid errors that may be introduced in sampling over large depth intervals. Experiments however, indicate the IP response from data acquired with short pulse times are virtually identical to those acquired with long pulse times. With short pulse times (0.25s) we can log at 6m/minute with a sample depth interval of 10 cm or

at 9 m/minute with a sample depth interval of 15 cm. The choice of the logging speed depends on the required depth (spatial) resolution. Data from a receiver in in the downhole probe are transmitted digitally uphole. This eliminates coupling problems that are inherent in systems with uphole receivers. A complete waveform (digitized at 4 ms intervals) is recorded on the 9 track tape. This provides the option to select any appropriate decay time windows at the time of processing. There are from 256 to 2048 data points on each complete waveform depending on the period of the full waveform (1 to 8 seconds). This high density of data points would make it relatively easy to determine spectral IP parameters from the data. Currently 10 semi-logarithmically spaced time windows are determined from the decay waveform.

Induced Polarization (IP)

The standard IP parameter is the chargeability determined during the early part of the 'off' time of the decaying waveform, from the Newmont window (0.45 to 1.1s) or equivalent for pulse times other than 2s. The apparent chargeabilities can be measured with 3 types of electrode arrays: 40 cm normal array, lateral array (pole-dipole array) and the 10 cm Dakhnov micronormal. The downhole current and potential electrodes are gold-plated brass cylinders, 40 mm in diameter.

Self Potential (SP)

The self potential is determined during the late 'off' time of the IP decay waveform. SP measurements are carried out either in the gradient mode with the same arrays as are used in the IP/Resistivity measurements, or in the Potential mode with a single Pb or $Cu/CuSO_4$ electrode downhole and a reference electrode on the surface. SP can be measured simultaneously with the IP/Resistivity measurements or in a separate logging run with current off. The latter is the preferred approach. In the potential mode an analogue SP signal is transmitted uphole.

Resistivity (R)

The resistivity measurements are derived from the waveforms received during the constant current 'on' time of the square IP waveform, after the initial IP charging effects are over.

3. Temperature Logging Tool: (O.D. = 25 mm)

The temperature probe consists of a 10 cm long tip of thermistor beads with sensitivity of 0.0001 degrees Celsius. Changes in temperature are recorded as changes in the thermistor resistance and then converted into true temperature with the use of an inverse operator and appropriate probe time constants. The temperature gradients are derived from the temperature data by means of a combined gradient and smoothing operator. All temperature logging is carried out during a downhole run and the usual logging speed is 6m/minute with data sampled every 1/5 of a second giving a measurement approximately every 2 cm. This high spatial resolution of data is necessary if accurate temperature gradients are to be determined with the use of gradient operators. Detailed information on this high sensitivity temperature logging tool has been given by Bristow and Conaway (1984). Temperature measurements are used to detect changes in thermal conductivity of the rocks along the borehole or water flow through cracks or fractures.

4. Spectral Gamma Gamma (SGG) Logging Tool: (O.D. = 32, 38 or 50 mm)

This is our newest logging tool. The tool is essentially the spectral gamma ray logging tool in a gamma gamma density configuration. The probe consists of a 10 millicurie gamma ray source (^{60}Co, ^{137}Cs or ^{192}Ir) and a scintillation detector (sodium iodide or cesium iodide) as shown in Figure 2(a). The data acquisition system is the same as that used in natural gamma spectral logging. Full backscattered gamma ray sepctra are recorded on a 9 track magnetic tape in 1024 channels covering an energy range from approximately 0.1 to 3.0 MeV. Ten selected energy windows are also accumulated and recorded on tape. Logging speed is usually 6 m/minute.

Density information is determined from the count rate in an energy window from about 100 keV to an energy less than that of the source. In some situations information about naturally occurring potassium, uranium and thorium can be determined from count rates in the energy region above that of the source as in the spectral gamma ray probe mentioned earlier. Information about the elemental composition of the rock can be obtained from the ratio of the count rates in two energy windows, one at high energy, one at low energy as follows.

The principle of the SGG log can best be understood by referring to the two spectra shown in figure 2(b). The positions of a low energy window (W10) and a high energy window (W3) are indicated in the figure. When there is a change in the density of the rock being measured, the count rates recorded in both windows will increase or decrease due to the associated change in compton scattered gamma rays reaching the detector. However, if there is an increase in the content of high Z (atomic number) elements in the rock, the associated increase in photoelectric absorption will cause a significant decrease in count rate in the low energy window W10 but little change in W3. W10 is affected by both density and Z effect while W3 is only affected by density. Therefore a ratio of counts in W3 to the counts in W10 can be used to obtain information on changes in Z.

The spectral ratio log is a ratio of counts in W3 to counts in W10 (i.e. W3/W10). This ratio increases when the probe passes through zones containing high Z materials. Thus the log can be considered as a heavy element indicator, and could be calibrated to produce an assay tool for quantitative determination of the heavy element concentration in situ along the borehole, without resorting to chemical assaying of the core. Additional information regarding experimentation with the SGG log was presented by Killeen & Mwenifumbo (1988).

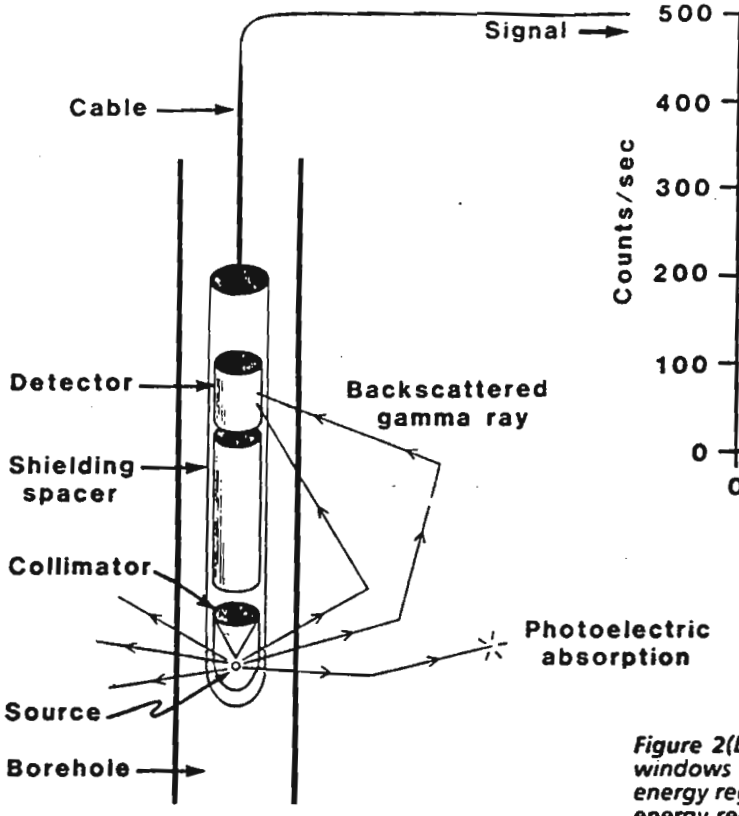

Figure 2(a): (left) The principle of the gamma-gamma density log extended to produce the Spectral Gamma-Gamma (SGG) log. By looking at the energy spectrum of the back scattered gamma rays information, about the elemental composition of the rock can be obtained in addition to density information.

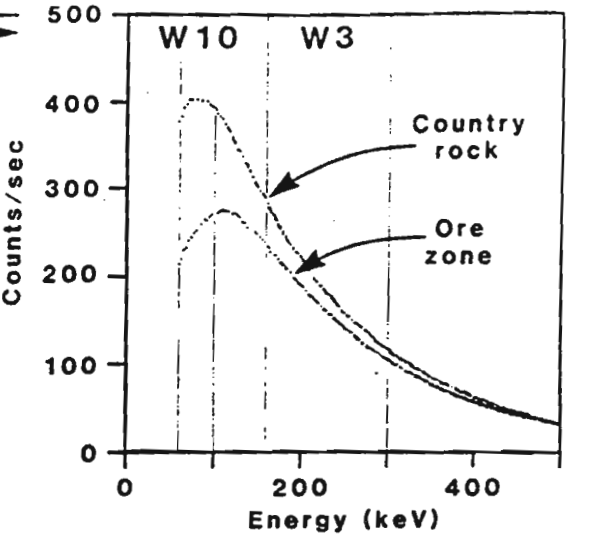

Figure 2(b): (right) In the SGG log, two energy windows are set to count gamma rays in the low energy region of the spectrum (W10) and the high energy region (W3). Two spectra are shown here, one in country rock, the other in a mineralized 'ore' zone containing heavy elements. In the ore zone the number of low energy gamma rays recorded in window 10 is reduced relative to the number recorded in window 3. The SGG log is a plot of the spectral ratio W3/W10. The presence of heavy elements causes the ratio to increase.

5. Magnetic Susceptibility Logging Tool: (O.D. = 42 mm)

Magnetic susceptibility measurements indicate changes in content of magnetite or other magnetic minerals and these changes may be correlated with lithology. The tool measures magnetic susceptibility and electrical conductivity. Since the measurements are made inductively, the tool can be used inside plastic casing. The electrical conductivity values are limited to a high conductivity range, (virtually massive sulphides or equivalent conductors) as a result of optimizing the tool parameters for the magnetic susceptibility measurements. The data are acquired with a Geo-instruments Ky of Finland Model TH-3C probe. The coil dimensions are 42 mm in diameter by 0.5 m in length. The coil is in an electrical bridge circuit energized at a frequency of 1400 Hz. A digital signal processing unit developed by the GSC is used with the Geo-instrument probe (Bristow & Bernius, 1984; Bristow, 1985). There are 4 sensitivity ranges on this system: 20, 80, 320 and 1280 x 10^{-3} S.I. units, with the highest setting giving a measurement resolution of approximately 0.005 x 10^{-3} S.I. units. Susceptibility data are acquired continuously and five readings are taken every second. Usual logging speed is 6 m/minute which provides samples every 2 cm along the hole.

INTERPRETATION

The following ten examples illustrate some of the advantages which can be obtained by using the new generation logs compared to the previous generation or 'state-of-the-use' logs.

Buchans, Newfoundland and Bancroft, Ontario

The first two examples relate to gamma ray and spectral gamma ray logs. The gamma ray log in figure 3 illustrates the variations in natural radioactivity in the volcanic rocks of the Buchans area, Newfoundland. These represent the host rocks for massive sulphide deposits. Four levels of

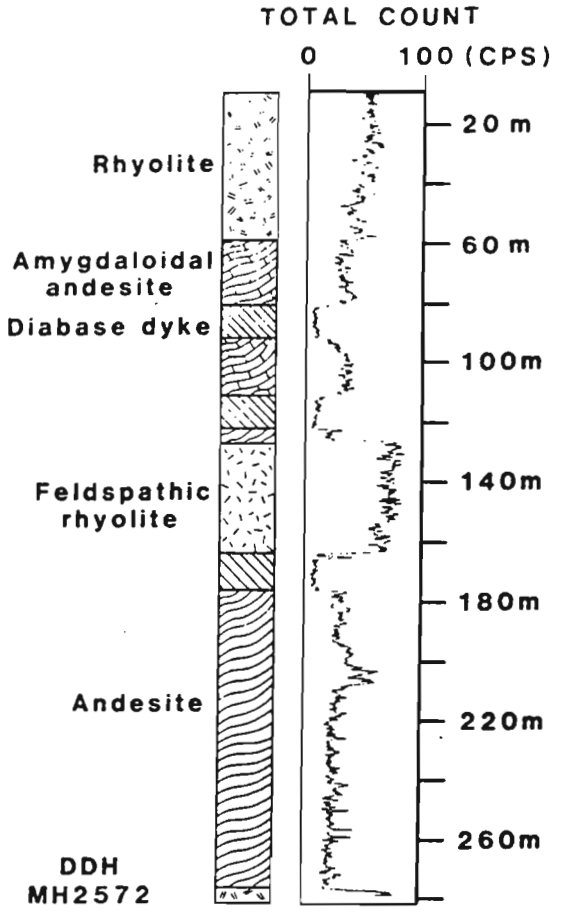

Figure 3: Gamma Ray log recorded in volcanic rocks of the Buchans area, Newfoundland. The characteristic levels of radioactivity for the different rock types can help the geologist with the interpretation, but the source of radioactivity (potassium (K), uranium (U), or thorium (Th)) remains unknown.

radioactivity can be seen in the log. From lowest to highest count rate these levels are characteristic of the diabase dykes, andesite, rhyolite, and feldspathic rhyolite. It can be easily appreciated how this log could be an aid to a geologist preparing a geological log, or trying to do hole-to-hole lithologic correlations. In this example the gamma ray log indicates that there is a zone between 190 and 210 metres not noted in the geological log. This zone is interpreted as ryholite based on its similarity to the log between 20 and 40 metres (Mwenifumbo & Killeen, 1987).

No information about the relative contributions to the gamma ray log by potassium, uranium or thorium, can be determined because only the total count is recorded.

The spectral gamma ray logs shown in figure 4 provide information which cannot be obtained from the total count gamma ray log alone. This set of logs was recorded in the gneisses and cataclastic rocks of the Bancroft area, Ontario. These are the host rocks for uranium deposits. The total count log shows three significant anomalies at approximately 35, 45, and 50 metres. The potassium (K), uranium (U) and thorium (Th) logs show the relative contributions of these three radioelements to the total count gamma ray log. All three anomalies are associated with pegmatites.

The radioactivity associated with the pegmatite at 35 m is primarily due to uranium minerals such as uraninite. There is no significant gamma ray response in the Th log. The pegmatite near 45 m has a mixture of uranium and thorium minerals, perhaps some uranothorite, as indicated by the U log and Th log. The third pegmatite near 50 m also contains a mixture of uranium and thorium minerals, but the U and Th logs indicate that thorium minerals predominate. It should also be noted that spectral gamma ray logs, when properly calibrated can be converted from count rate logs to radioelement concentration logs yielding the potassium values in percentages and the Th and U values in ppm (parts per million). See Killeen & Conaway (1978) or Conaway & Killeen (1979) for more details.

The Yava Deposit, Nova Scotia

A good example of the use of the SGG log in mineral exploration is shown in figure 5. Here both a qualitative density log and a spectral ratio log are shown alongside a log of the lead concentrations from drill core assays. The lead in the form of galena is primarily concentrated in the sandstone overlying the Windsor Shale in the Yava lead deposit of Nova Scotia. The density log shows a slight increase in the region where the lead is concentrated but the spectral ratio clearly indicates the increase in heavy elements in the mineralized zones. Some additional thin mineralized zones below the main ore body which were not assayed, are also evident in the log. Note that lead values considerably less than 4% are easily detectable. It is apparent that the spectral ratio log could be calibrated to produce a lead-assay log in this environment.

The Newfoundland Zinc Deposit, Newfoundland

The logs in figure 6 illustrate the response of the IP/R logs and the SGG log to an ore zone in a zinc deposit in limestone. The zinc assays from drill core are also shown in histogram form, with values ranging up to 8% zinc. Note that the assays are averaged over about 1.5 m of drill core. The spectral ratio log, which indicates the concentrations of heavy elements, in this case zinc, shows the mineralized zones are actually about 0.5 m thick. In addition the amplitude of the spectral ratios is proportional to the assay values. The zinc mineral is sphalerite which is known to be a poor conductor. As expected the resistivity log does not show any direct relationship to the mineralized zones. However the IP log shows 6 windows in the IP decay which indicate that there are polarizable particles associated with the ore, and this is believed to be the sphalerite itself, contrary to expectation. No other polarizable mineral in the ore has been reported.

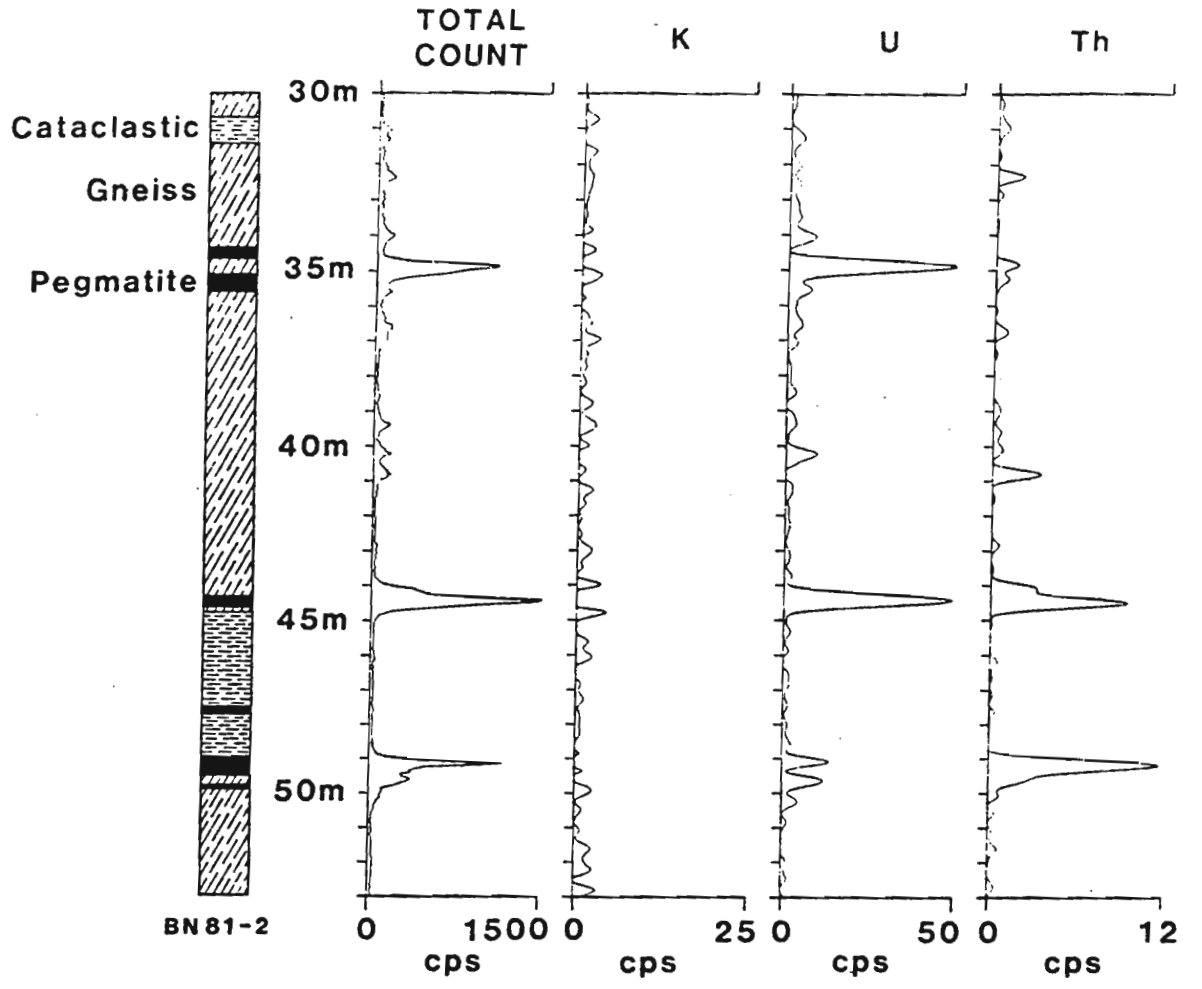

Figure 4: Spectral Gamma Ray log recorded in gneissic rocks and pegmatites of the Bancroft area, Ontario. The three major anomalies in the Total Count (TC) log caused by pegmatites at about 35 m, 44 m and 49 m are explained by the spectral gamma logs of K, U, and Th (see text).

Water Flow/Fracture Detection at the Yava Deposit

An excellent example of the use of high sensitivity temperature and temperature gradient logs for fracture detection is shown in figure 7. The figure shows temperature and temperature gradient logs for three holes in the Yava deposit. The temperature logs show the expected slow increase with increasing depth and in addition a few abrupt changes indicating water flow into or out of fractures. These changes are emphasized by the T-gradient logs which show peaks at these locations where the rate-of-change of temperature is high. There appears to be a continuous aquifer indicated in all three boreholes just above the rhyolite breccia, at the base of the sedimentary column. Hole 405 in the middle of the figure shows a water flow in the sandstone near 16 m, and hole 404 shows water flow at about 33 m near a gypsum/Windsor Shale contact. The T-gradient logs in hole 404 appear at first sight to be noisy but in fact are not. The character of the log is a result of the T-gradient being plotted at an expanded scale. This shows the water flow must be considerably less than in the other two boreholes.

Gold Deposits, Larder Lake Area, Ontario

Gold occurs in such low concentrations that no geophysical log can detect it directly. In gold exploration the logs must be used to detect associated mineralization, alteration, or other related geologic features in order to locate the gold indirectly.

Figure 8 shows the geology, gold assays, and logs of magnetic susceptibility, resistivity, I.P. and the K log in %K derived from a spectral gamma ray log. The gold which occurs in volcanic rocks is associated with pyrite as indicated by low values in the

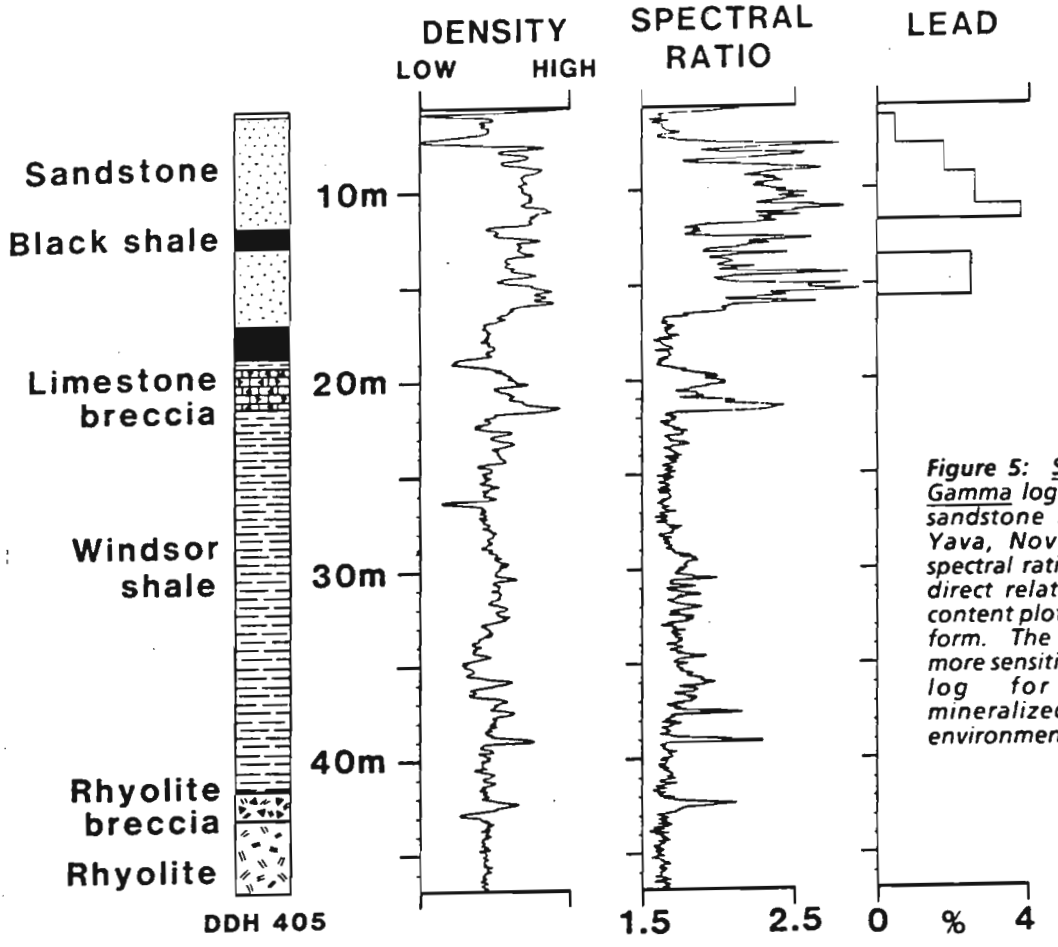

Figure 5: Spectral Gamma-Gamma log recorded in the sandstone lead deposit at Yava, Nova Scotia. The spectral ratio clearly bears a direct relation to the lead content plotted in histogram form. The spectral ratio is more sensitive than a density log for delineating mineralized zones in this environment.

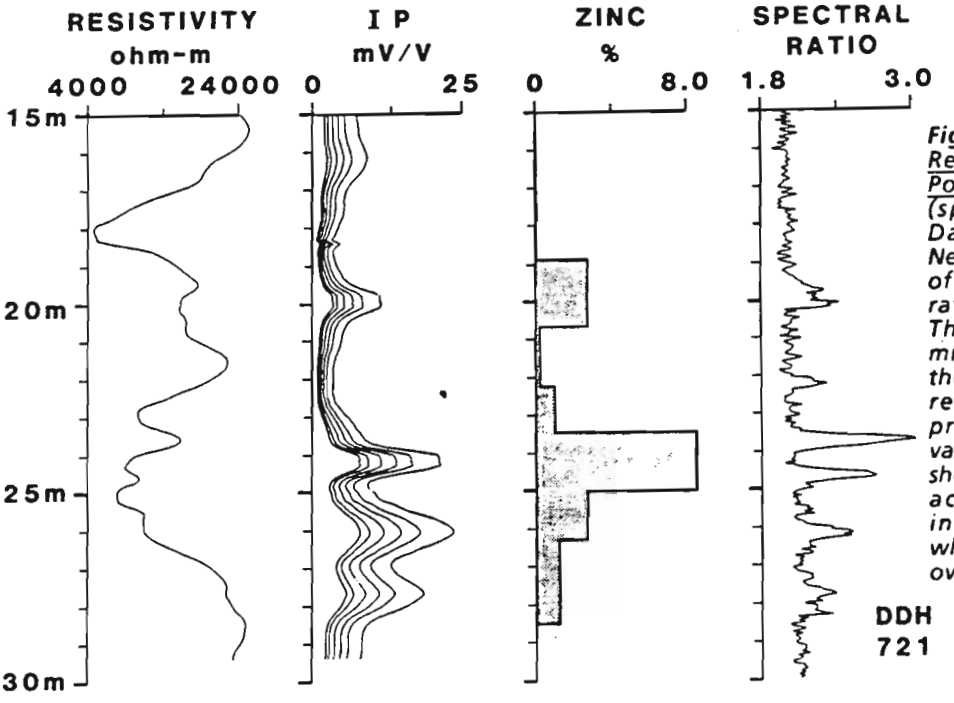

Figure 6: Comparison of Resistivity log to Induced Polarization log in a zinc (sphalerite) deposit at Daniels Harbour, Newfoundland. Zinc assays of drill core and the spectral ratio log are also shown. The IP log indicates the mineralized zones (unlike the resistivity log), but the response is not directly proportional to the assay values. The spectral ratio log shows the zinc-rich zones are actually narrower than indicated by the assays which have been averaged over 1.5 to 2 m of drill core.

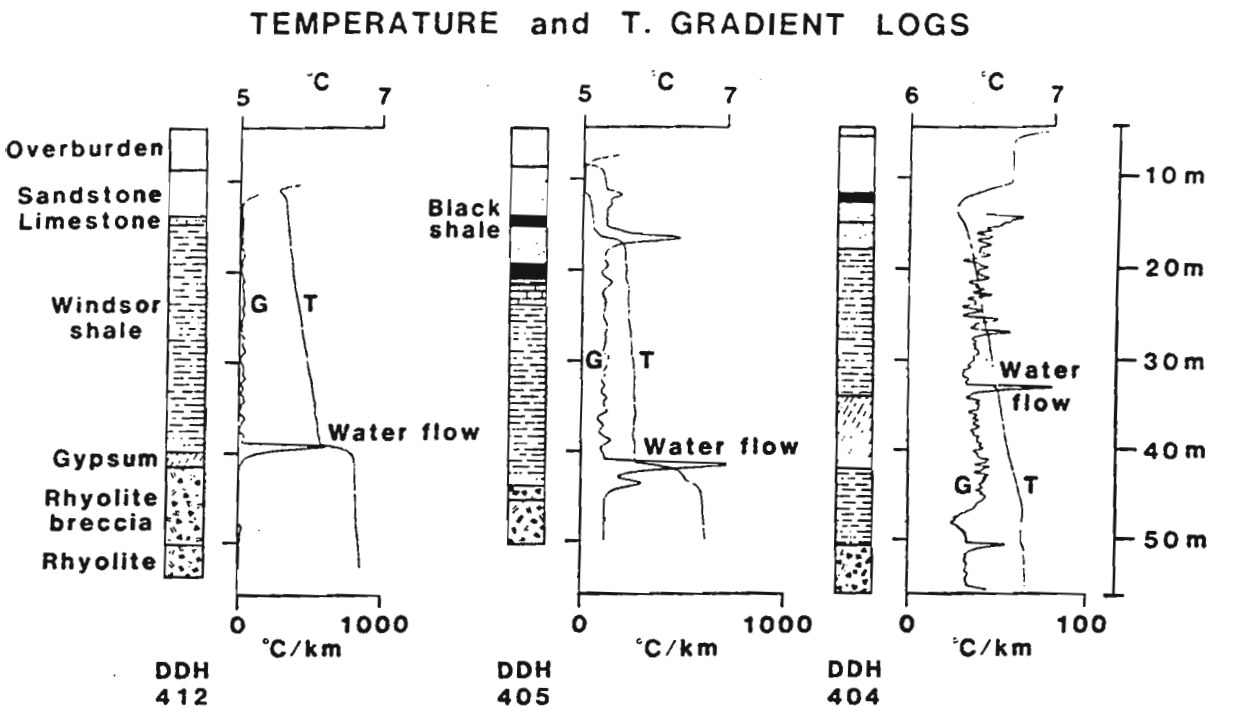

Figure 7: High Sensitivity Temperature logs (T) and the computed Temperature Gradient logs (G) for three boreholes in the Yava lead deposit. Inflections in the T-logs represent changes in temperature caused by water flowing into or out of the borehole in fractures. The T-gradient log emphasizes these water flow zones, making it possible to pick out very small temperature changes. (Note the change in scale on hole 404.)

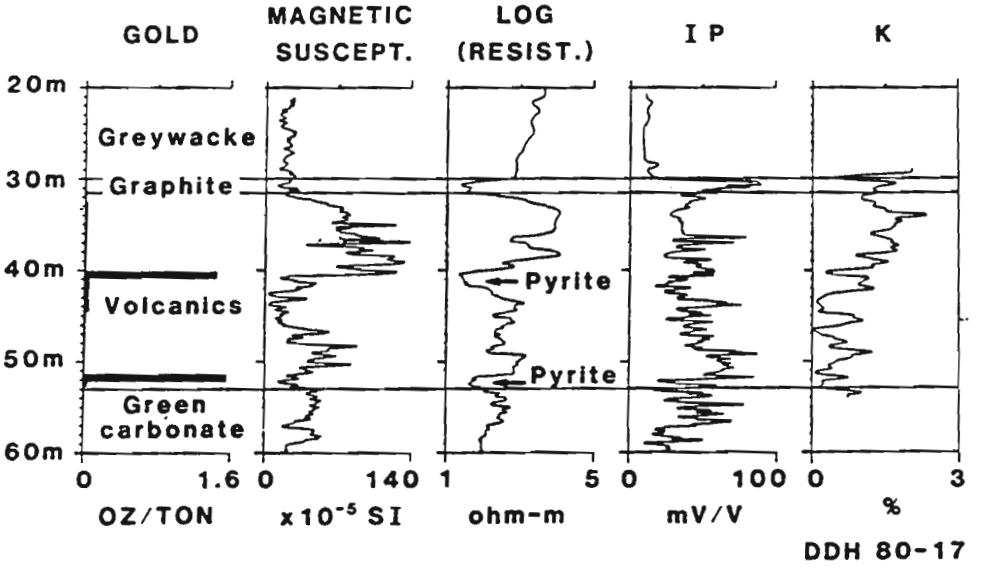

Figure 8: Geophysical logs and gold assays recorded in hole 80-17 at the Larder Lake gold deposit (Ontario).

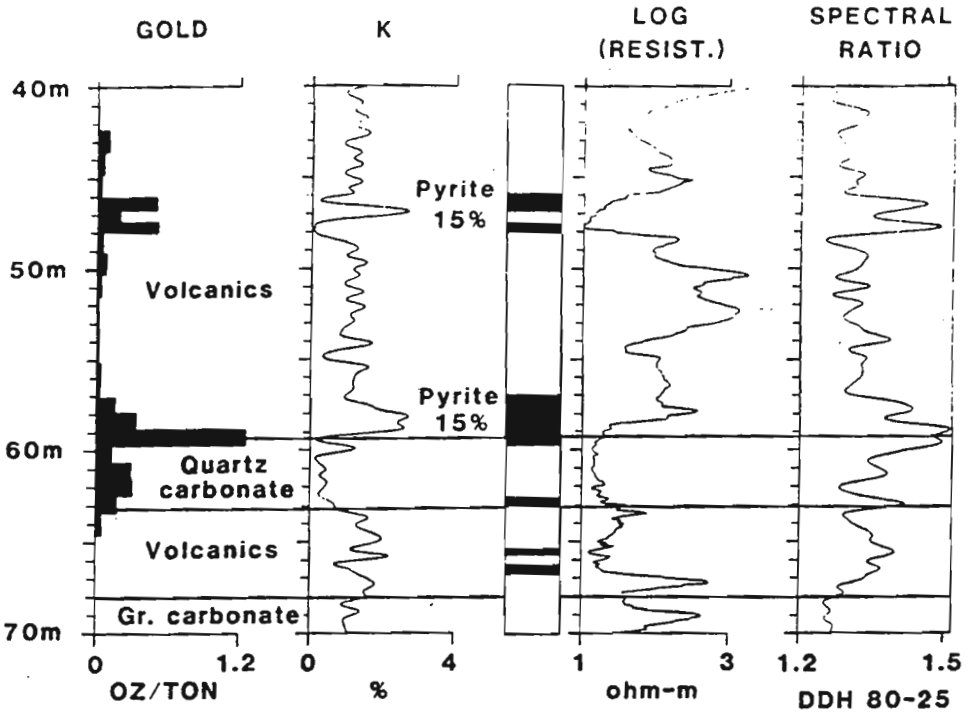

Figure 9: Gold assays and pyrite estimates, the K log, Resistivity (log scale) and spectral ratio logs recorded in the Larder Lake gold deposit (hole 80-25).

resistivity log (plotted on a logarithmic scale). The high IP log response in the volcanics compared to the values in the greywacke is due to pyrite disseminated throughout the entire volcanic sequence. Near the gold, the pyrite is sufficiently massive to decrease the resistivity values to as low as those in the graphite zone just below 30 m. The lower half of the volcanic zone is strongly altered as shown by the decrease in values on the magnetic susceptibility log (magnetite converted to hematite) and the decrease on the K values on the spectral gamma-ray log (potassium alteration). The gold is located at the top and bottom of the altered zone.

A second example related to gold in the Larder Lake area is shown in figure 9. The geology and gold assays are shown on the left side of the figure. The spectral ratio log on the right appears to be directly related to the gold assay log. In fact it is showing the distribution of pyrite (the heavy element being iron) associated with the gold. The pyrite estimates taken from the geological log of the drill core are shown in the middle of figure 9. It is believed that the spectral ratio log is a more accurate portrayal of the pyrite distribution than the geologist's visual estimates. The low resistivity zones also coincide with the high pyrite content associated with the gold mineralization. Low potassium values in the K-log also delineate the pyrite. There are indications that the potassium displaced by the pyrite remains adjacent to the pyrite as at 47 m depth.

The Hemlo Gold Deposits, Ontario

In the Hemlo area the gold is located in a complex sequence of metamorphic rocks. The companies working in the area have had to attempt to subdivide the complex sequence by describing the same rock with different adjectives such as "garnetiferous" etc. The geological log in Figure 10, showing units 3A, 7E and 7D, represents one such attempt and the details are not important here. The gold is associated with high barite content in strongly pyritized zones. These ore zones are indicated by low magnetic susceptibility values, high densities and high spectral ratios. The barite and pyrite cannot be separated by the spectral ratio log or by the density log but the distribution of these combined heavy minerals is clearly evident in greater detail in the logs than indicated by the assay estimates. In this case the pyrite and barite content is sufficiently high that the density log also clearly indicates these zones. The low magnetic susceptibility values in the ore zone are indicative of the alteration of magnetite to hematite.

Massive Sulphide Deposit, British Columbia

Geophysical logs recorded in a non-economic massive sulphide zone about 5 metres thick are shown in figure 11. They include resistivity, conductivity, magnetic susceptibility and the spectral ratio. The resistivity log was measured galvanically and the conductivity log was measured

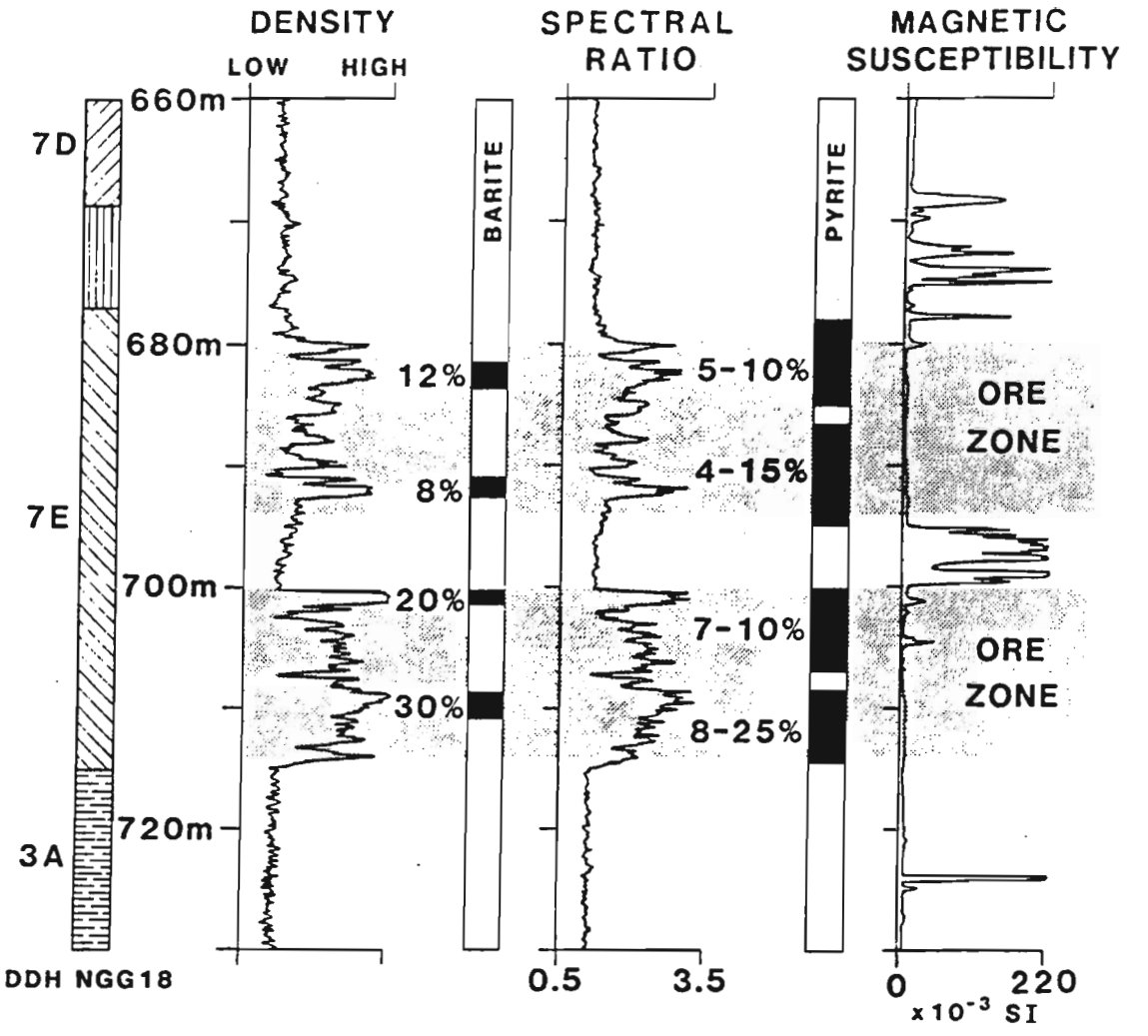

Figure 10: Density, spectral ratio and magnetic susceptibility (MS) logs recorded in the area of the Hemlo gold deposits (Ontario).

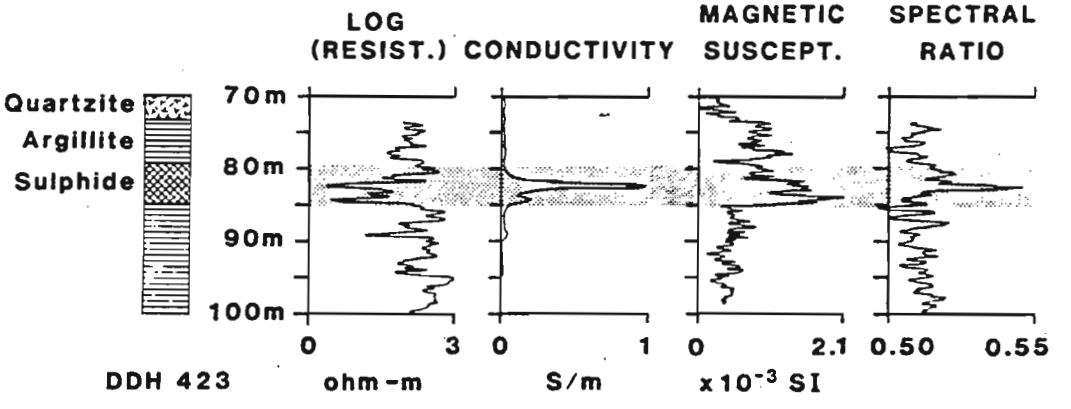

Figure 11: Geophysical logs recorded in a massive sulphide deposit in British Columbia including Resistivity, Conductivity, Magnetic Susceptibility, and Spectral Ratio.

inductively. The sulphide zone is indicated by low resistivity values at a depth of about 85 m. The logarithmic plot of the resistivity logs shows two distinct lows which were only evident as a single low in the original linear plot (not shown here). The conductivity log also shows that within the sulphide zone there are two narrow very high conductivity bands, the upper one being the most conductive. The relative conductivity information could not be observed on the galvanic resistivity log. The spectral ratio log also indicates that the upper band contains the highest concentration of heavy elements (sulphides). The magnetic susceptibility log indicates that both zones contain magnetic minerals, likely pyrrhotite (or possibly magnetite). The local geologist confirmed that the massive sulphide zone was pyrrhotite. It is interesting to note that the highest magnetic susceptibility values coincide with the lower band and not with the upper pyrrhotite band, which has the highest conductivity and spectral ratio value.

Magnetic Susceptibility Logs Versus Measurements on Drill Core

In recent years many geologists have become convinced of the usefulness of magnetic susceptibility measurements in their work. However, these measurements are most often made in a lab on drill core or in the field with a hand held susceptibility meter scanning drill core. Figure 12 is a comparison between magnetic susceptibility logs obtained by core scanning and by logging the hole (Bristow & Bernius, 1984). The results are essentially the same but the advantage of obtaining magnetic susceptibility logs from borehole geophysics instead of from measurements on drill core, is the tremendous saving in time. In this example about 40 m of core was measured at 5 cm intervals in about 7 hours, while the borehole log at 6m/minute was completed in about 7 minutes. Other advantages of logging include the increase in sample volume (relative to core), as well as the ability to make measurements where core is missing.

SUMMARY

A new generation of borehole logging tools has evolved making it possible to derive information previously unobtainable by borehole geophysical methods. As additional experience in their use and interpretation becomes available they should become state-of-the-use methods. In summary some of their primary applications are for: (1) interpretation of lithology, (2) mineral identification, (3) alteration identification, (4) water flow detection, (5) in situ physical properties, (6) stratigraphic correlation, and (7) in situ assaying.

ACKNOWLEDGMENTS

The authors would like to thank the mining companies who collaborated in this logging R&D work especially the B.C. Mineral Logging Group for permission to publish the logs from British Columbia and the Nova Scotia Mineral Development Agreement for funding the logging at the Yava deposit. Field data acquisition by Bill Hyatt and computer data processing by Barbara Elliott are gratefully acknowledged as are the constructive criticisms by K.A. Richardson all of the GSC.

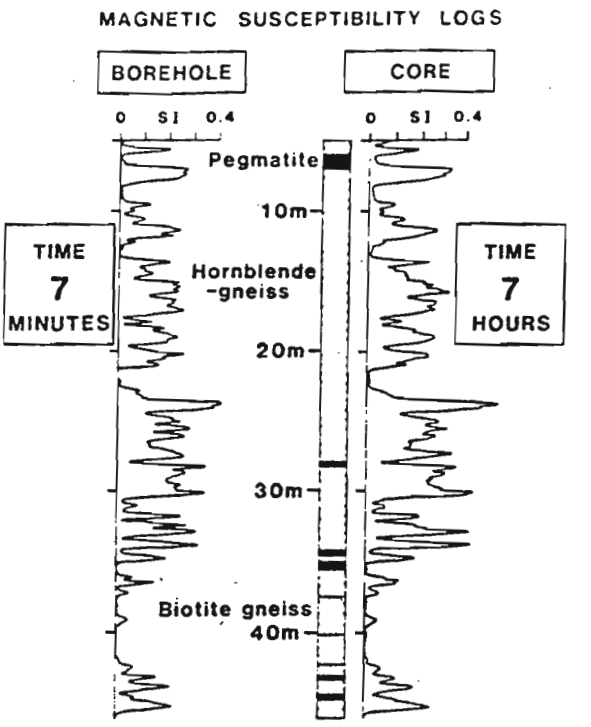

Figure 12: Comparison of Magnetic Susceptibility logs from borehole geophysics and from measurements on drill core showing the time to acquire the data in each case.

REFERENCES

Bristow, Q. (1979) NOVA-based airborne and vehicle mounted systems for real-time acquisition display and recording of geophysical data; Proceedings of the 1979 Annual Meeting of the Data General Users Group.

Bristow, Q. (1985) A digital processing unit for the GeoInstruments magnetic susceptibility sensors, with analogue and RS-232C outputs; in Current Research, Part B, Geol. Surv. Can., Paper 85-1B, p. 463-466.

Bristow, Q. (1986) A system for the digital transmission and recording of induced polarization measurements in boreholes; in Borehole Geophysics for Mining and Geotechnical Applications, ed. P.G. Killeen, Geol. Surv. Can., Paper 85-27, p. 127-143.

Bristow, Q. & Bernius, G.R. (1984): Field evaluation of a magnetic susceptibility logging tool; in Current Research, Part A, Geol. Surv. Can., Paper 84-1A, p. 453-462.

Bristow, Q. & Conaway, J.G. (1984) Temperature gradient measurements in boreholes using low noise high resolution digital techniques; in Current Research, Part B, Geol. Surv. Can., Paper 84-1B, p. 101-108.

Conaway, J.G. & Killeen, P.G. (1979) Gamma-ray spectral logging for uranium; CIM Bull., Vol. 73, No. 813, p. 115-123.

Killeen, P.G. (1979) Gamma ray spectrometric methods in uranium exploration - application and interpretation; in Geophysics and Geochemistry in the Search for Metallic Ores; Peter J. Hood, editor, Geol. Surv. Can., Economic Geology Report 31, p. 163-229.

Killeen, P.G. & Conaway, J.G. (1978) New facilities for calibrating gamma-ray spectrometric logging and surface exploration equipment; CIM Bull. Vol. 71, No. 793, p. 84-87

Killeen, P.G. & Mwenifumbo, C.J. (1988) Downhole assaying in Canadian mineral deposits with the spectral gamma-gamma method; in Proceedings of meeting of IAEA coordinated research program on 'Nuclear Borehole Logging Techniques for the Determination of Rock Characteristics', Ottawa, Dec. 2-6, 1987 (in press).

Mwenifumbo, C.J. & Killeen, P.G. (1987) Natural gamma ray logging in volcanic rocks: the Mudhole and Clementine base metal prospects; in Buchans Geology, Newfoundland: 1982-1984, ed. R.V. Kirkham, Geol. Surv. Can., Paper 86-24, Report 16.

Borehole geophysics in environmental applications

C.J. Mwenifumbo, Geological Survey of Canada, Ottawa, Ontario

ABSTRACT

Preservation of groundwater quality is a major environmental concern. The disposal of hazardous material from urban waste dumps, milling wastes in tailings ponds, and industrial wastes in injection wells may contaminate potential sources of potable groundwater. The containment or migration of contaminants in the subsurface depends on bedrock characteristics and type of overlying sediments. Fractured bedrock and permeable sediments that may provide pathways for the transport of potentially harmful contaminants should be avoided when selecting a disposal site. The role of borehole geophysics in hazardous waste-site investigations is reviewed in three categories: (1) site selection; (2) determination of the extent of contamination at existing sites; and (3) long-term monitoring of migration of contaminants. In the first category, borehole geophysical techniques developed for lithology and fracture identification, and for porosity determination, provide some of the necessary information for understanding the subsurface hydrogeology. Lithological information can be obtained from gamma-ray, electrical resistivity, induction, magnetic susceptibility, and sometimes induced polarization logs; fracture detection and characterization can be accomplished with the use of caliper, density, resistivity, temperature, and acoustic televiewer logs. Estimates of porosity are derived primarily from neutron-neutron, resistivity, density, and sonic logs. Borehole geophysical techniques used in water-quality determinations include self-potential, fluid resistivity, Eh (redox potentials) and pH measurements, and these can be used to map the extent of contamination at an existing waste site. Cross-borehole and borehole-to-surface electrical methods can also be used in this application. Long-term monitoring of contaminant migration in boreholes can be accomplished with techniques that respond to changes in electrical conductivity, temperature and fluid chemistry caused by the presence of contaminants.

Keywords: Environmental geology, Geophysics, Borehole geophysics.

Paper reviewed and approved for publication by the Geological Society of CIM.

Campbell Jonathan Mwenifumbo received a B.Sc. honours degree in 1972 in geology from The University of British Columbia, an M.Sc. in applied geophysics in 1974 from the University of Birmingham, and a Ph.D. in geophysics in 1980 from the University of Western Ontario.

From 1972 to 1973, Dr. Mwenifumbo worked with the Geological Survey of Malawi conducting geophysical surveys in exploration for minerals and groundwater. He has worked with Phoenix Geophysics where he participated in the field evaluation of the spectral IP system in Canada, the United States and Australia. Since 1980, Dr. Mwenifumbo has been with the Geological Survey of Canada as a research scientist. His research activities are in the application of borehole geophysics to geotechnical and enviromental problems, and to mineral, uranium, coal and groundwater exploration. He has been closely involved in the development and evaluation of a number of borehole logging techniques at the GSC. Dr. Mwenifumbo has also been involved in borehole geophysical logging in the Ocean Drilling Program and LITHOPROBE.

He is a member of the SEG, EAEG and Minerals and Geotechnical Logging Society.

Introduction

The disposal of hazardous material from urban waste in garbage dumps, milling wastes in tailings ponds, and industrial wastes in injection wells poses a considerable threat to the environment. If the geological and hydrogeological conditions at the disposal sites permit the migration of these wastes, potential sources of potable surface and groundwater may be contaminated. Because the migration of contaminants is mainly by seepage through groundwater, an ideal disposal site should have no fracture zones and should have confining lithology that is impermeable to the migration of fluids. Borehole geophysics can play an important role in the selection and assessment of such a disposal site.

The subsurface conditions at a number of landfills that pose a threat to the environment have not been properly delineated. The extent of contamination from injection wells used for the disposal of industrial waste needs to be properly mapped. Borehole geophysics can be used to map landfills and contamination plumes from industrial waste disposal. Borehole geophysics can also play an important role in monitoring the migration of contaminants because such contaminants create significant changes in the physical and chemical properties of the site.

Borehole Geophysical Methods

Most of the borehole geophysical techniques that have been developed for hydrogeological investigation (Keys and MacCary, 1971), mineral (Glenn and Nelson, 1979; Hearst and Nelson, 1985), petroleum (Serra, 1984, 1986) and geotechnical (Reeves, 1989) applications can be used for investigating hazardous-waste sites (Daniels and Keys, 1990; Howard, 1990). Conventional borehole logging techniques currently used at such sites include caliper, fluid conductivity, galvanic resistivity, inductive conductivity, self potential, temperature, natural gamma-ray, gamma-gamma density, neutron-neutron, sonic compressional wave (P-wave) velocity, and acoustic televiewer. Although other borehole logging techniques such as induced polarization, Eh, pH, magnetic susceptibility, and magnetometer measurements could also be used in the investigation of hazardous-waste disposal sites, at present these techniques are not routinely applied.

Not all of the techniques mentioned above may be successfully applied at any given site. The choice of techniques is dependent on the geological environment and the borehole-logging environment (e.g. sedimentary vs igneous and metamorphic environments). The borehole-logging environment creates one of the major constraints on what measurements can be made. Boreholes may be air- or fluid-filled, or they maybe cased with either plastic or steel. Table 1 lists the methods that are best suited to the different borehole

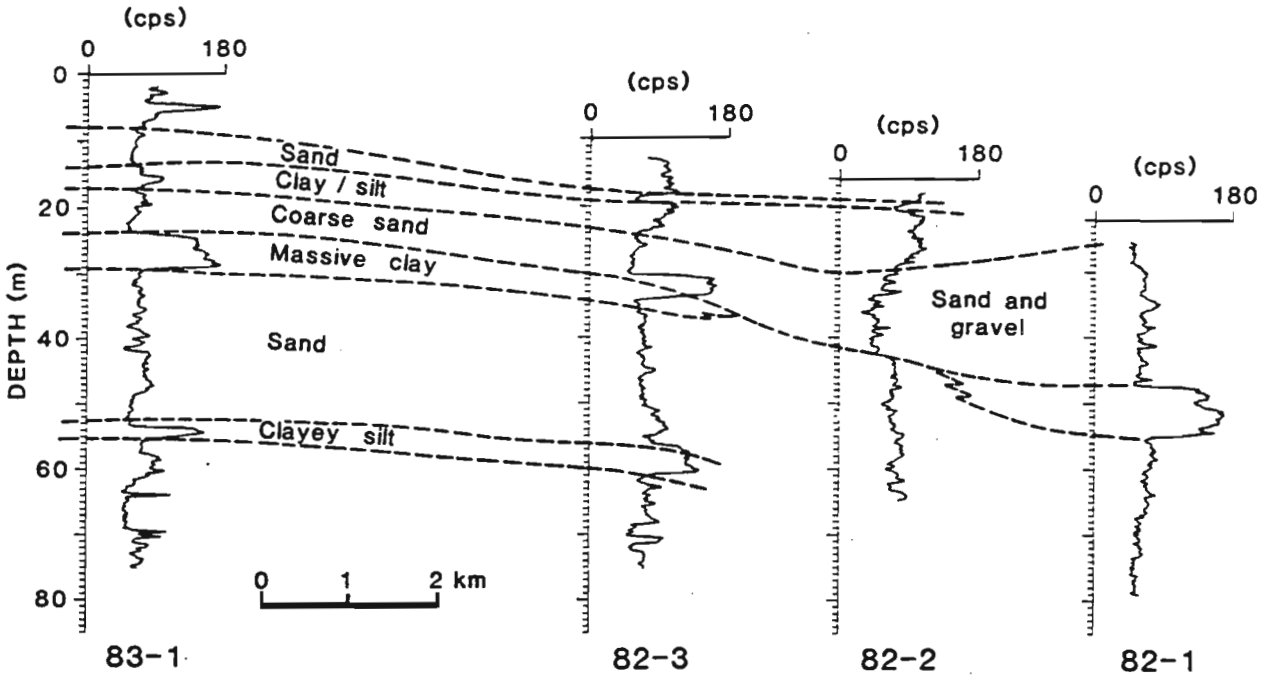

FIGURE 1. Stratigraphic correlation using natural gamma-ray logs. Numbers at the bottom (e.g. 83-1) are borehole numbers.

environments, and these are briefly discussed in the following sections.

Natural Gamma-Ray

Natural gamma-ray measurements detect variations in natural radioactivity due to changes in concentration of the radioelements uranium (U) and thorium (Th), and potassium (^{40}K). The principal source of natural gamma radiation in sedimentary rock formations is ^{40}K contained in clay minerals such as illite and potassium feldspars. In igneous and metamorphic environments, K, U, and Th may contribute equally to the total gamma radiation. As different rock types contain variable amounts of these radioactive minerals, the gamma-ray log has commonly been used for lithological mapping. The gamma-ray log is also used in the petroleum industry to determine the clay content of formations, which in turn is used to correct porosities determined from electrical logs.

TABLE 1. Logging parameters in different borehole environments

	Uncased		Cased	
	Air-filled	Fluid-filled	Plastic	Steel
Nuclear				
Gamma-ray	X	X	X	X
Gamma-gamma density	X	X	X	X
Neutron-neutron	X	X	X	
Electrical				
Self potential (SP)		X		
Resistivity		X		
Induced polarization (IP)		X		
Inductive conductivity	X	X	X	
Sonic velocity		X		
Acoustic televiewer		X		
Temperature		X	X	X
Magnetic susceptibility	X	X	X	
Borehole magnetometer	X	X	X	
Geochemical methods		X		
Caliper	X	X		

Gamma-Gamma Density

The gamma-gamma density tool measures the backscattered gamma rays emitted by an artificial gamma-ray source. Gamma rays with energies less than 1 MeV interact with atoms in the rock formations mainly by Compton scattering and through photoelectric effects. Gamma rays with energies of 150 keV and higher are used in density computation because they are affected mainly by the Compton scattering process. The bulk density of the rock formation is determined from Compton-scattered gamma rays, which are a function of the electron density. Because the low-energy gamma rays are subject to photoelectric absorption, a low-energy window is used to monitor photoelectric effects. Spectral gamma-gamma logging systems or litho-density tools use the ratio of the low- to high-energy windows to compute the photoelectric index. Because the photoelectric index is mainly a function of atomic number, the index can be used as a lithology indicator to provide information about the elemental composition of the rock.

The density-log response is highly variable and dependent on the geological environment. In sedimentary environments, the density log is used to identify lithology or to determine porosity. In igneous and metamorphic rocks, however, density logs may be difficult to interpret because the density is altered by the presence of graphite, base metal sulphides, and oxides.

Neutron-Neutron Porosity

The neutron-neutron well-logging probe consists of a low-energy neutron source and a neutron detector. Neutrons emitted by the source are scattered and absorbed within a rock formation. Neutrons measured by the detector indicate the amount of neutron absorber in the rock. As the primary moderator of neutrons in the earth is hydrogen, the neutron-neutron log response is primarily an indicator of water content. It is, therefore, an indirect indicator of the porosity of the rock. In a sedimentary environment, this is the standard log for porosity determinations. In igneous and metamorphic rocks, however, changes in apparent neutron porosity may not reflect the porosity of the rock mass because the response is increased by the presence of minerals containing crystallographically-bound hydrogen.

Spontaneous Polarization or Self Potential (SP)

The SP method involves the determination of natural potentials that arise from electrochemical differences in the subsurface. In mineral prospecting, borehole SP measurements are widely used for delineating sulphide and graphitic conductors. The self potentials are developed within these conductors by electrochemical reactions. In sedimentary environments, SP anomalies may be generated by fluid flow (electrofiltration), temperature changes (thermoelectric), changes in the chemical composition and concentration of electrolyte of the formation fluids, and shaliness of a porous formation. These measurements have, therefore, been used primarily for geological correlation, estimating groundwater quality (Radhakrishna and Gangadhara Rao, 1990), detecting porous and permeable zones in a formation (Keys and MacCary, 1971), and for investigating fluid flow (Corwin, 1990).

Resistivity

The resistivities of rocks are primarily a function of porosity, salinity, and temperature of the pore fluid because the conducting medium is mainly water. Because resistivities primarily reflect porosity changes in a formation, apparent porosities can be determined from the resistivity logs using Archie's Law (1942). Conductive minerals such as graphite, sulphides, and metallic oxides, however, strongly influence resistivity. In non-sedimentary rocks, low resistivity is due either to significant concentrations of sulphides and metallic oxides, or to an increase in porosity because of fracturing. Clay minerals also decrease the resistivity of a formation.

Electrical resistivity measurements can be made in either a single-hole (electrical resistivity log) or cross-hole mode. The electrical resistivity log is the arrangement most commonly used. In cross-borehole electrical measurements, there are a number of variants in electrode configurations. Generally, at least two holes are used, one as a transmitting hole and the other as a receiving hole.

Galvanic electrical measurements can be made only in fluid-filled uncased holes. This restriction considerably limits applications in monitoring contaminant migration because most of the monitoring wells drilled in poorly unconsolidated sediments are cased.

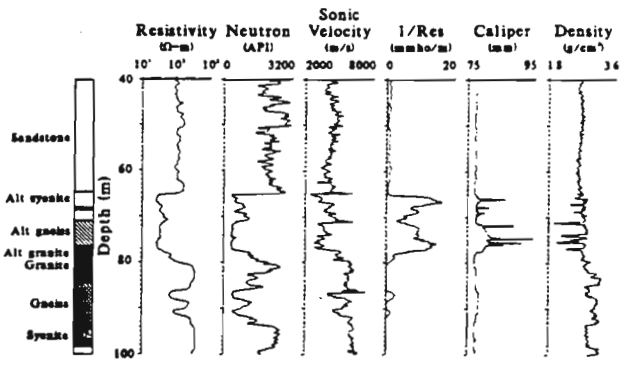

FIGURE 2. Resistivity, neutron, sonic velocity, reciprocal of resistivity, caliper, and density logs recorded in Bells Corners hole BC-81-1. The wide fractured/altered zone between 64 m and 78 m is clearly delineated by all logs except the density log which indicates only narrow open fractures within this wide zone.

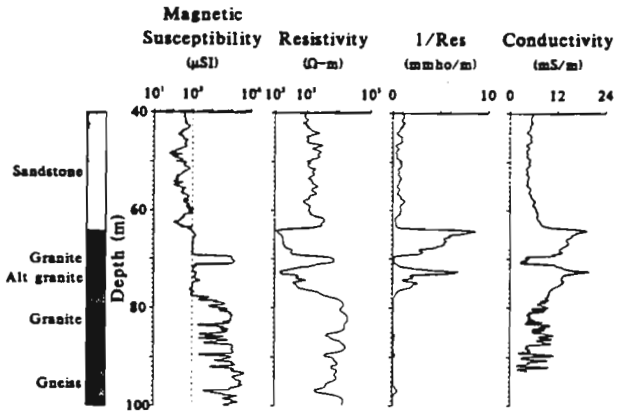

FIGURE 3. Magnetic susceptibility, normal resistivity, reciprocal of resistivity, and inductive conductivity logs recorded in Bells Corners hole BC-81-2. Low-susceptibility zones that indicate fractured and altered rock correlate well with electrical logs.

Induced Polarization

Induced polarization (IP) measurements primarily indicate the presence of polarizable and conductive minerals. Although the borehole IP method has been used primarily in exploration for sulphides (Glenn and Nelson, 1979), this method has been shown to be potentially useful in formation evaluation for the petroleum logging industry (Snyder *et al.*, 1977; Vinegar *et al.*, 1986). In sedimentary rocks that are free from graphite or sulphide minerals, polarization arises wherever the pore paths are lined with clay minerals that have a cation-exchange capacity (membrane polarization). The porosity and permeability of these rocks are largely controlled by clay within the pore spaces. Clean, porous sedimentary rocks have virtually no IP response. IP can, therefore, be used to estimate the clay content of dirty sands. These data are useful in correcting the resistivity for the effects of clay (Snyder *et al.*, 1977; Vinegar *et al.*, 1986). The corrected resistivity is then used to determine the apparent porosity of the rock formation. The IP response within sedimentary rocks may also reflect changes in lithology and can be used as a mapping tool.

Electromagnetic Methods

Electromagnetic (EM) methods can be used in single-hole logging measurements (the inductive conductivity log) or in cross-hole measurements. The inductive conductivity (resistivity) log is extensively used in the petroleum logging industry, but has only recently been adapted for use in hydrogeological, geotechnical, or environmental applications. One of the reasons is that the range of resistivity variations is wide. The electromagnetic systems used in mineral exploration typically are designed to detect highly conductive massive sulphides and can not be used in environmental applications.

Most of the applications in hydrogeological, geotechnical, and environmental fields are in relatively resistive rocks. Geonics (Toronto) has recently developed an inductive tool (the EM-39) that can be used in these applications. One of the major incentives for this development is that logging can be done in air-filled and plastic-cased holes. Electrical resistivity (conductivity) is a very important physical parameter for monitoring contamination when a change in the dissolved ionic solids alters the electrical conductivity of the formations.

Cross-borehole electromagnetic methods have been used recently to map the conductivity variations between holes in enhanced oil recovery monitoring (LaBrecque, 1990), and to map structures such as solution cavities in karst topography. This technique seems promising for mapping and evaluating existing landfills and associated contaminant plumes.

Sonic P-Wave Velocity

The sonic or acoustic tool provides measurements of interval travel time of P-waves through a formation. As the interval travel time of the P-wave through the formation is the sum total of the time spent in the solid matrix and the time spent in the pore fluids, the response of the sonic log is related to the interstitial pore water content which, in saturated rocks, is equivalent to rock porosity. P-wave velocities are also computed from interval travel times.

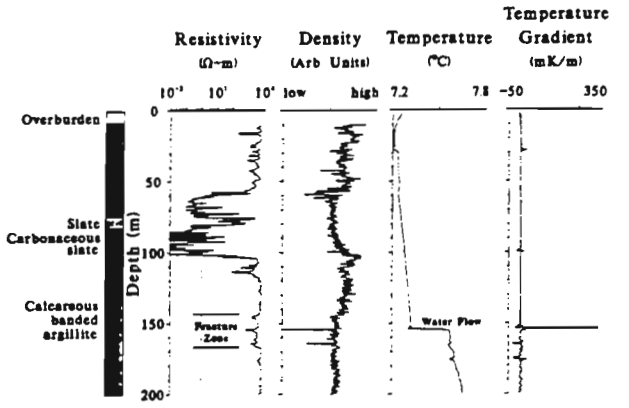

FIGURE 4. Normal resistivity, density, temperature, and temperature-gradient logs recorded in shales and slates. The steep change in temperature at 155 m, with a corresponding resistivity low and density anomaly, is caused by water inflow through a fracture zone.

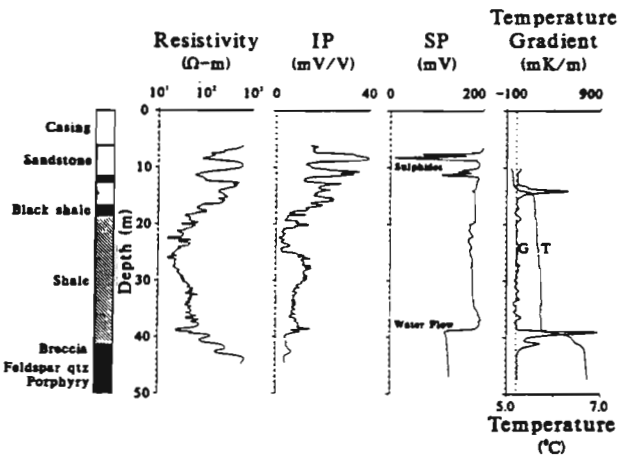

FIGURE 5. Resistivity, IP, SP, temperature, and temperature-gradient logs recorded in hole YA405 at the Yava lead deposit, Nova Scotia. A temperature and SP anomaly caused by groundwater flow is indicated at approximately 40 m. The IP log distinguishes SP anomalies due to sulphides (7 m to 12 m) from those caused by water flow and temperature change.

Acoustic Televiewer

The borehole acoustic televiewer is a high-frequency logging device that provides an ultrasonic picture of the borehole wall. A high-frequency acoustic signal is transmitted from the televiewer, and the amplitude of the reflected signal from the borehole wall is a function of the acoustic properties of the rocks. The acoustic televiewer is an excellent tool for fracture detection and characterization, and yields the most detailed information about the borehole wall. It is, however, a very expensive tool to run or purchase.

Temperature Logging

The temperature profile in a borehole is variably affected by several factors, including (a) drilling fluid circulation; (b) changes in lithology with different thermal properties; (c) groundwater flow; (d) presence of massive conductive sulphides; and (e) seasonal and climatic temperature variations. The most prominent temperature anomalies are those caused by groundwater flow: water has a heat capacity 3 to 5 times that of the rock. Fractures or shear zones that provide groundwater pathways can be located easily if hydrological gradients exist within the rock mass or if logging is done immediately after drilling (Drury and Jessop, 1982).

Magnetic Susceptibility

The magnetic susceptibility of a volume of rock is primarily dependent on the amount of ferromagnetic minerals present, especially magnetite, ilmenite, and pyrrhotite. Magnetic susceptibility is an important physical property that can be used to identify lithology in igneous and metamorphic rocks. During hydrothermal or other types of alteration, primary magnetic minerals in the rock may be replaced by weakly to non-magnetic minerals. Thus, anomalously low magnetic susceptibilities in an otherwise homogeneously high-susceptibility rock unit may be an indication of altered zones. These zones may be porous and permeable, thus enabling transportation of contaminants through the groundwater system. Magnetic minerals within sedimentary formations tend to concentrate in the finer sediments, and susceptibility measurements, therefore, may be used to distinguish siltstone/mudstone from clean sands. Some fine beach sands, however, may show higher susceptibility because of the presence of magnetite and ilmenite.

Because magnetic susceptibility measurements are made inductively, the tool can be used in fluid-filled or air-filled plastic-cased holes. These measurements can also be made on drill core, but the advantage of borehole measurements is that they can be done where core is missing or in holes that have not been cored. Zones where core is missing are commonly of great interest because they are generally associated with fracture zones. Borehole magnetic susceptibility measurements are virtually unknown in hydrogeological, geotechnical, or environmental applications.

Borehole Magnetometer

The other magnetic method that can be used to study environmental problems is the borehole three-component magnetometer. This logging tool is currently readily available for trial in this type of application, an example of which may be landfills that contain drums and metallic objects. This method may be used in uncased air- and fluid-filled holes, as well as in plastic-cased holes.

Geochemical Methods

Geochemical logging methods are the most promising borehole tools for monitoring contaminant migration because several contaminants substantially affect the chemistry of groundwater. The geochemical methods currently developed for logging include fluid conductivity, Eh, and pH measurements. Fluid conductivity logs are the most widely used logs for water-quality assessment. Eh and pH logging are not usually done, even though these measurements are routinely carried out on water samples collected for environmental purposes.

Caliper

The hole diameter is measured by a caliper. Caliper measurements are primarily used for correcting log responses that are sensitive to hole size. Because a hole is commonly enlarged within fractured zones, the caliper log is often used in fracture detection.

Applications

The following are examples of how some of the geophysical logging techniques may be used in investigating waste-disposal sites. Most of the examples are taken from logging done by the Geological Survey of Canada (GSC). Some are tests conducted by the mining and petroleum logging industry at the GSC's Borehole Geophysical Test Site in Ottawa.

Site Selection

In selecting a hazardous waste-disposal site, among the requirements is that the wastes be contained within the site of deposition

and not migrate to contaminate any nearby surface or groundwater supply. Therefore, site evaluation involves identifying unfractured rocks and relatively impermeable sediments. Within a sedimentary environment, waste should be confined by stratigraphy of extremely low permeability. The permeabilities of most igneous and metamorphic rocks are very low, but most of these rocks are also highly altered or fractured. Fractured rocks are more porous and permeable, and may therefore provide pathways for the transport of potentially harmful subsurface contaminants. It is also necessary that the water quality be determined prior to disposal of waste at any new site to provide background data for future assessment of the degree of contamination. Borehole geophysics may be used in site evaluation to map lithology and stratigraphy, to determine porosity of the rock formations, to detect fractures and alteration zones, and to detect fluid flow.

Lithology and Stratigraphic Mapping

Natural gamma-ray logs are widely used to identify lithology and to map stratigraphy. Stratigraphic correlation permits lateral extrapolation of hydrogeological data. This is done by matching log character and amplitude between holes. The log-based interpretations are often confirmed with lithologic data where such data are available. Figure 1 shows a cross section of gamma-ray logs from four wells drilled by the University of Waterloo (Karrow *et al.*, 1990) for hydrogeological investigations. The sand and gravel layer between 30 m and 50 m is a potential aquifer, and the massive clay layer between 25 m and 30 m is a good upper confining bed. As this clay layer is not intersected in borehole 82-2, this location has an open groundwater communication system with the surface recharge area. This indicates a potential danger for groundwater contamination from the surface or near surface waters. Disposal of waste near this site should be avoided.

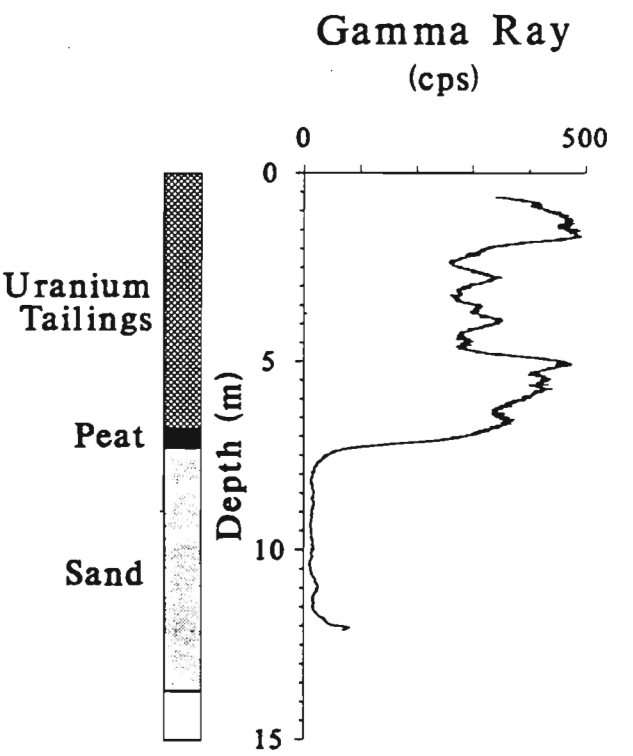

FIGURE 6. Total-count natural gamma-ray log recorded in a hole drilled through a uranium tailings pond. The radioactive wastes have not migrated far into the underlying sand aquifer. Logging at regular intervals would reveal the progress of the contaminants through the aquifer.

Porosity Determination

Quantitative porosity determinations are made mainly from four geophysical logs: neutron-neutron porosity, resistivity, density, and sonic velocity. The neutron-neutron porosity log is the standard porosity tool.

The relationship between resistivity and porosity is obtained using Archie's Law (1942) which applies mainly to sedimentary rocks such as clean sands. This relationship is not readily applicable to igneous and metamorphic rocks, where increases in conductivity may be related to the presence of sulphides and graphite rather than to porosity changes; the distinction, however, can be made by examining IP logs. Low resistivity without a corresponding high IP response is an indication of fractured porous zones which do not contain conductive minerals, whereas low resistivity with a high IP response will indicate zones containing conductive minerals which, therefore, may be unrelated to porosity changes.

The relationship between sonic velocity and porosity is commonly called the time-average equation (Hearst and Nelson, 1985). This relationship requires knowledge of the matrix and pore-fluid sonic velocities, which may not be easily obtainable. The density log may be related to porosity if the matrix and pore-fluid densities are known.

Detection of Fracture and Alteration Zones

Borehole geophysical techniques that can be used to detect and characterize fracture and alteration zones include resistivity, density, sonic velocity, neutron-neutron porosity, acoustic televiewer, caliper, and temperature logs. Figure 2 shows some of these logs acquired through fractured and altered granite and gneiss at the GSC's Ottawa test site. The neutron log is in API units, where low values correspond to high porosity; low values on the interval sonic-velocity log correspond to high porosity. All logs except density seem to map the fractured/altered zone fairly accurately. An increase in hole diameter within the fractured rock is indicated by the caliper log. The density log response does not show a wide, high-porosity zone in the fractured bedrock, but indicates a number of open fractures. These are also clearly seen on the caliper log. The resistivity log is presented in two modes: logarithm to the base 10 of resistivity, and as its reciprocal (1/resistivity = conductivity).

Figure 3 is an example of how magnetic susceptibility measurements, in conjunction with electrical measurements, may be used to detect fracture and alteration zones. The electrical logs include the normal resistivity log and its reciprocal, and the inductive conductivity log. Low susceptibilities indicate fractured and altered basement rocks and are well-correlated with increased conductivity. A notable correlation between the inductive conductivity and susceptibility log occurs at approximately 90 m.

Figure 4 shows resistivity, density, temperature, and temperature-gradient logs acquired in a hole drilled through argillite and shale. The low-resistivity zones between 55 m and 100 m are due to sulphide mineralization. A wide fracture zone between 145 m and 165 m is indicated by low resistivity. Once again, the density log does not show a corresponding wide, low-density zone. However, two narrow, fairly low-density zones are indicated at approximately 155 m and 164 m within this broader resistivity low. These two zones are probably due to an increase in hole diameter caused by open fractures. The temperature and temperature-gradient logs indicate water production at 155 m, and in fact the hole is flowing artesian.

Single-hole geophysical logging provides information on the rock characteristics in the immediate vicinity of a borehole. The integrity of the rock mass between holes can be investigated by cross-borehole logging techniques. Such a study would reduce the chance of overlooking the presence of solution channels (especially in a karst environment) or fault zones that were not intersected by the boreholes. The cross-borehole geophysical techniques that can be used to evaluate waste-disposal sites include electrical, electromagnetic, and seismic

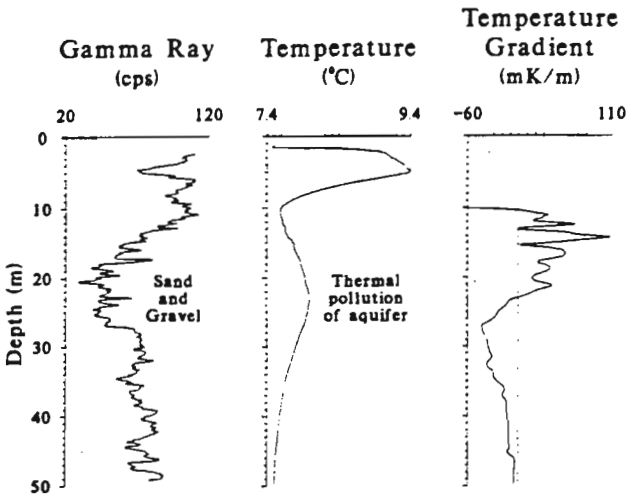

FIGURE 7. Temperature and temperature-gradient logs showing thermal pollution within the gravel aquifer.

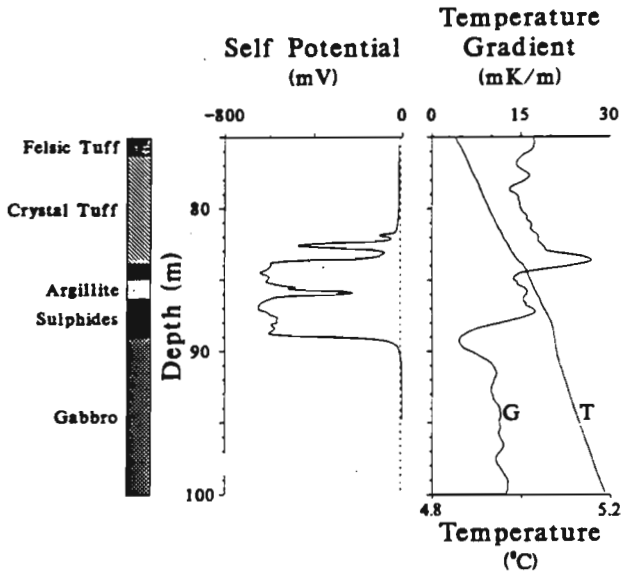

FIGURE 8. Self-potential, temperature, and temperature-gradient logs through a massive sulphide zone. The increase in temperature within the massive sulphide zone suggests oxidation-reduction reactions that are exothermic.

methods. However, these are relatively new applications that are fairly expensive to run.

Detection of Fluid-flow

Fluid-flow detection within a borehole can generally be achieved with SP and temperature measurements. The detection of fracture zones with fluid movement in boreholes is important if the holes need to be cemented to avoid mixing of groundwater between different aquifers. An excellent example of the use of SP, temperature, and temperature-gradient logs for fluid-flow detection is shown in Figure 5. Also included in Figure 5 are resistivity and IP logs. This hole was drilled through mineralized sandstone, shales, and quartz-feldspar porphyry. SP anomalies observed within the sandstone are due to the presence of lead mineralization (see corresponding high IP anomalies). A major water-producing zone at approximately 39 m is indicated by a significant change in the SP response, and the temperature and temperature gradient. This SP anomaly apparently is generated by fluid flow and a temperature change. Another zone of water flow occurs at approximately 14 m, within the sandstone. There is a proposal to carry out solution mining at this deposit. A necessary precaution would be to ensure that the aquifer at the base of the shale sequence is not contaminated by the leach solution.

Mapping Existing Disposal Sites

A number of landfill sites that pose a threat to the environment have not been properly studied. The extent of contamination from injection wells used for the disposal of industrial waste needs to be properly mapped. Borehole geophysical techniques that can be used to map landfills and contamination plumes from the disposal of industrial waste include cross-borehole electrical and electromagnetic methods, cross-borehole seismic methods, and magnetometer methods. Cross-borehole measurements require that the holes be located outside the suspected site. Landfills would be expected to be low in resistivity, and metal drums, chemicals, and related aqueous plumes should be detectable by electrical and borehole three-component magnetometer measurements.

Monitoring of Contaminant Migration

Currently, only hydrological instrumentation is installed in most wells constructed to monitor waste and tailings facilities. Borehole geophysical logging (to monitor the migration of contaminants) is possible because contaminants change the physical and chemical characteristics of the formation fluids. These characteristics include electrical conductivity (detectable by electrical and EM methods), changes in Eh and pH, and development of spontaneous polarization potentials related to oxidation and reduction in tailings containing sulphides, and in dump sites with metallic objects. Oxidation and reduction reactions may also cause significant changes in temperature distribution, which can be monitored by borehole temperature measurements. It should be noted that Eh, pH, and self-potential measurements can only be run in uncased fluid-filled or perforated plastic-cased holes.

Monitoring organic contaminants, such as petroleum products or solvents in shallow aquifers, poses a difficult problem (Greenhouse, 1991). There is generally no significant change in the physical properties of the formation that can be detected by present borehole geophysical methods. Geothermal methods offer some possibility of detecting these contaminants if the initial fluids are discharged at temperatures considerably different from those of pore fluids.

Monitoring Contaminant Migration from a Uranium Tailings Pond

Figure 6 shows a gamma-ray log through a plastic-cased hole in a uranium tailings pond at Elliot Lake in northern Ontario. The uranium ore at this mine comes from a quartz-pebble conglomerate containing 5% to 15% pyrite. Ore processing is by a sulphuric acid-leach process and the tailings are neutralized by lime and hydroxide to a pH of 8 to 10 before being discharged into the tailings ponds. The tailings consist of a mixture of sand- and silt-size particles in a porous, moderately permeable mass consisting of quartz, feldspar, and approximately 5% pyrite. The tailings are deposited in a valley formerly occupied by a spruce bog, which has formed into peat, underlain by a very permeable glacio-fluvial sand and gravel aquifer. The gamma-ray log shows that the radioactive wastes from the tailings had not migrated through the peat layer into the aquifer.

Monitoring Changes in Fluid Temperatures

In a number of industrial plants, groundwater or water from the supply mains is continuously pumped for cooling, or for use in the production processes. Waste water at some sites is disposed of in injection wells. These waste waters may be chemically polluted and at higher temperatures than the groundwater. Seepage

of the waste water into shallow aquifers can be monitored by temperature measurements. Figure 7 shows a monitoring well drilled through a permeable aquifer close to an automobile plant in the Kitchener-Waterloo area, Ontario. An increase in groundwater temperatures within the aquifer may be caused by leakage of warm water from heating systems, or by conduction of thermal energy into the aquifers from the heating pipes of the nearby plant. It is not known whether injection wells exist around the plant. Other holes logged within a few kilometres of this hole (Fig. 1) do not show this type of temperature distribution. Although thermal pollution of groundwater is not as serious as chemical pollution, closely monitoring temperature anomalies may prove to be useful where thermal pollution is accompanied by chemical pollution.

In mill-tailings ponds, sulphide oxidation-reduction reactions may generate sufficient heat which could be monitored by using temperature logs. Figure 8 shows a temperature log through a massive sulphide zone that is accompanied by large self potentials. The self potentials are generated by electrochemical reactions among the sulphides, and the increase in temperature suggests that heat is generated by these reactions.

Monitoring Changes in Fluid Chemistry

In tailings piles, the oxidation of sulphide minerals in unsaturated zones produces acidic water that lowers the pH and may generate spontaneous potentials. Lowering of the pH may cause otherwise insoluble substances to dissolve, thus changing the fluid conductivity. The Eh (redox potential) values in the borehole fluids also change. Currently, borehole fluid-conductivity measurements are routinely done. Eh and pH logging tools have been developed for use in the mineral-logging industry, but have not been widely applied to environmental studies. Fluid-resistivity, and Eh and pH measurements are, however, routinely made on surface and borehole water samples collected for environmental assessment and monitoring. The GSC is developing a geochemical probe that will measure fluid resistivity, Eh and pH, as well as pressure. This probe should prove to be very useful in monitoring contaminant migration from chemical waste-disposal sites and tailings ponds.

Conclusions

Borehole geophysics can provide valuable information necessary for the selection of suitable waste-disposal sites. Not all of the borehole geophysical techniques may be successful at any given site: the choice of techniques is dependent on the geological environment (sedimentary vs igneous/metamorphic) as well as on the borehole environment (air-filled vs fluid-filled, cased vs uncased holes).

The physical-property determinations from density, sonic, and resistivity logs can be used in interpreting and modelling surface geophysical data acquired from techniques such as seismic, resistivity, and electromagnetic methods. Caliper, fluid-resistivity, and temperature logs may also be used in correcting other logs, such as resistivity and density logs, so that accurate hydrogeological parameters are determined.

The most promising borehole geophysical methods for monitoring and mapping the migration of contaminants include fluid resistivity, temperature, Eh, pH, self-potential, and cross-borehole methods such as electrical and seismic tomography. Temperature logs can be used to detect fluid-flow, monitor thermal pollution, and detect redox reactions.

Acknowledgments

The author acknowledges the help received from members of the Exploration Geophysics subdivision during the preparation of this manuscript. Sue Davis drafted the illustrations.

REFERENCES

ARCHIE, G.E., The electrical resistivity log as an aid in determining some reservoir characteristics; American Institute of Mining and Metallurgy, Petroleum Engineering Technical Publication 1422, *pp. 1-8*, 1942.

CORWIN, R.F., The self-potential method for environmental and engineering applications; Geotechnical and Environmental Geophysics, Volume II: Environmental and Groundwater; Stanley H. Ward, ed., *pp.127-145*, 1990.

DANIELS, J.J., and KEYS, W.S., Geophysical well logging for evaluating hazardous waste sites; Geotechnical and Environmental Geophysics, Volume 1: Review and Tutorial; Stanley H. Ward, ed., *pp. 263-285*, 1990.

DRURY, M.J., and JESSOP, A.M., The effect of a fluid-filled fracture on the temperature profile in a borehole; *Geothermics, Vol. 11, pp. 145-152, 1982.*

GLENN, W.E., and NELSON, P. H., Borehole logging techniques applied to base metal ore deposits; *In* Geophysics and Geochemistry in Search for Metallic Ores; Peter J. Hood, ed., Geological Survey of Canada, Economic Geology Report 31, *pp. 273-294*, 1979.

GREENHOUSE, J.P., Environmental geophysics: It's about time; Geophysics: The Leading Edge of Exploration, *pp. 32-34*, 1991.

HEARST, J.R., and NELSON, P.H., Well Logging for Physical Properties; McGraw-Hill Book Company, New York, 571 p., 1985.

HOWARD, K.W.F., The role of well logging in contaminant transport studies; Geotechnical and Environmental Geophysics, Volume 1: Review and Tutorial; Stanley H. Ward, ed., *pp. 287-307*, 1990.

KARROW, P.F., GREENHOUSE, J.P., and DUSSEAULT, M.B., Subsurface Quaternary stratigraphy using borehole geophysics; Ontario Geological Survey Open File Report 5734, 249 p., 1990.

KEYS, W.S., and MACCARY, L.M., Applications of borehole geophysics to water resources investigation; U.S. Geological Survey, TW12-E1, Book 2, Chapter E1, 1971.

LABRECQUE, D.J., Cross-borehole TEM for enhanced oil recovery — a model study; Borehole geophysics: Petroleum, Hydrology, Mining and Engineering Applications; Extended Abstracts, 1990.

RADHAKRISHNA, I., and GANGADHARA RAO, T., Evaluation of hydrogeochemical parameters with spontaneous potential logs; *Journal of Hydrology, Vol. 114, pp. 245-257, 1990.*

REEVES, G.M., Borehole geophysical logging techniques for geotechnical investigations — A TransAtlantic review; *In* Proceedings of the Third International Symposium on Borehole Geophysics for Minerals, Geotechnical, and Groundwater Applications, Oct. 25, Las Vegas, Nevada, *pp. 271-295*, 1989.

SERRA, O., Fundamentals of well-log interpretation, 1. The acquisition of logging data; Elsevier Science Publishers B.V., 1984.

SERRA, O., Fundamentals of well-log interpretation, 1. The interpretation of logging data; Elsevier Science Publishers B.V., 1986.

SNYDER, D.D., MERKEL, R.H., and WILLIAMS, J.T., Complex formation resistivity — The forgotten half of the resistivity log; Transactions, 8th International Well Logging Symposium, Society of Professional Well Log Analysts, pp. Z1-Z39, June 5-8, 1977.

VINEGAR, H.J., WAXMAN, M.H., BEST, M.H., and REDDY, I.K., Induced polarization logging: Borehole modelling, tool design and field tests; *The Log Analyst, pp. 25-61, Mar.-Apr. 1986.*

PART C BIBLIOGRAPHIES, REFERENCES, STANDARD SPECTRA, PROBE DIMENSIONS AND TABLES OF DRILL INFORMATION AND CONVERSION FACTORS

C1. BIBLIOGRAPHY OF GSC PUBLICATIONS ON BOREHOLE GEOPHYSICS

C1.1 Selected publications of the borehole geophysics section

Killeen, P.G.
1975: Nuclear techniques for borehole logging in mineral exploration; in Borehole Geophysics applied to Metallic Mineral Prospecting - a review. Ed. by A.V. Dyck, Geol. Surv. Can., Paper 75-3l, p. 39-52.

Killeen, P.G.
1976: Portable borehole gamma-ray spectrometer tests; Geol. Surv. Can., Paper 76-1A, p. 487-489.

Killeen, P.G. and Bristow, Q.
1976: Uranium exploration by borehole gamma-ray spectrometry using off- the-shelf instrumentation; Exploration for Uranium Ore Deposits (Proc. Symp. Vienna, 1976) IAEA Vienna, STI/PUB/434 p. 393-414.

Killeen, P.G. and Dyck, A.V.
1977: Geophysical logging of MacDougall Core Hole 1A, Prince Edward Island; Appendix 3, p. 23 in R.D. Howie, Geological Studies and Evaluation of MacDougall Core Hole 1A, Western Prince Edward Island, Geol. Surv. Can., Paper 77-20.

Conaway, J.G. and Killeen, P.G.
1978: Quantitative uranium determinations from gamma-ray logs by application of digital time series analysis; Geophysics, Vol. 43, No. 6, p. 1204-1221.

Conaway, J.G. and Killeen, P.G.
1978: Computer processing of gamma-ray logs: iteration and inverse filtering; in Geol. Surv. Can., Paper 78-1B, p. 83-88.

Killeen, P.G., Conaway, J.G. and Bristow, Q.
1978: A gamma-ray spectral logging system including digital playback with recommendations for a new generation system; in Geol. Surv. Can., Paper 78-1A, p. 235-241.

Killeen, P.G.
1978: Gamma-ray spectrometric calibration facilities - a preliminary report; in Geol. Surv. Can., Paper 78-1A, p. 243-247.

Killeen, P.G. and Conaway, J.G.
1978: New facilities for calibrating gamma-ray spectrometric logging and surface exploration equipment; CIM Bull., Vol. 71, No. 793, p. 84-87.

Conaway, J.G. and Killeen, P.G.
1979: Gamma-ray spectral logging for uranium; CIM Bull., Vol. 73, No. 813, p. 115-123.

Conaway, J.G., Allen, K.V., Blanchard, Y.B., Bristow, Q., Hyatt, W.G. and Killeen, P.G.
1979: The effects of borehole diameter, borehole fluid, and steel casing thickness on gamma-ray logs in large diameter boreholes; in Current Research, Part C, Geol. Surv. Can., Paper 79-1C, p. 37-40.

Killeen, P.G.
1979: Gamma ray spectrometric methods in uranium exploration - application and interpretation; in Geophysics and Geochemistry in the Search for Metallic Ores; Peter J. Hood, editor, Geol. Surv. Can., Economic Geology Report 31, p. 163-229.

Richardson, K.A. and Killeen, P.G.
1979: Calibration facilities for gamma-ray spectrometers made available by Geological Survey of Canada; The Northern Miner, March 8, p. C2, C9.

Conaway, J.G., Killeen, P.G. and Hyatt, W.G.
1980: A comparison of bismuth germanate, cesium iodide, and sodium iodide scintillation detectors for gamma ray spectral logging in small diameter boreholes; in Current Research, Part B, Geol. Surv. Can., Paper 80-1B, p. 173-177.

Conaway, J.G., Killeen, P.G. and Bristow, Q.
1980: Variable formation parameters and nonlinear errors in quantitative gamma-ray log interpretation; in Technical Papers - Annual International Meeting and Exposition, Society of Exploration Geophysicists 50, p. 2523-2534.

Conaway, J.G., Bristow, Q. and Killeen, P.G.
1980: Optimization of gamma-ray logging techniques for uranium; Geophysics, Vol. 45, No. 2, p. 292-311.

Bernius, G.R.
1981: Boreholes near Ottawa for the development and testing of borehole logging equipment - a preliminary report; in Current Research, Part C, Geol. Surv. Can., Paper 81-1C, p. 51-53.

Mwenifumbo, C.J.
1981: Interpretation of Mise-a-la-masse data. Paper presented at the Fifty- first Annual International Meeting and Exposition, Society of Exploration Geophysicists, Los Angeles, October 11-15, 1981. SEG, Technical Papers, p. 701-739.

Bristow, Q., Killeen, P.G. and Mwenifumbo, J.C.
1982: Comparison of standardized gamma-ray log calibration measurements: Ottawa, Adelaide and Grand Junction; Proceedings of the Symposium on Uranium Exploration Methods, Review of the NEA/IAEA R&D Programme, Paris, 1st-4th June 1982, p. 715-728.

Bristow, Q. and Killeen, P.G.
1982: Natural gamma-ray spectral logging using scintillation detectors; Proceedings of the Symposium on Uranium Exploration Methods, Review of the NEA/IAEA R&D Programme, Paris, 1st-4th June 1982, p. 777-792.

Killeen, P.G.
1982: Borehole logging for uranium by measurement of natural gamma radiation - a review; International Journal of Applied Radiation and Isotopes, Vol. 34, No. 1, p. 231-260.

Killeen, P.G.
1982: Gamma-ray logging and interpretation; Chapter 4 in "Developments in Geophysical Exploration Methods", Vol. 3, Applied Science Publishers Ltd. (Elsevier), p. 95-150.

Killeen, P.G. (with Hallenburg, J.K., Furlong, V.L.R. and Duray, J.)
1982: Borehole logging for uranium exploration - a manual; IAEA Technical Report Series No. 212, 279 p.

Killeen, P.G.
1982: New scintillation detectors: a review of comparisons of bismuth germanate, cesium iodide and sodium iodide; Proceedings of the Symposium on Uranium Exploration Methods, Review of the NEA/IAEA R&D Programme, Paris, 1st-4th June 1982, p. 639-652.

Killeen, P.G., Bristow, Q. and Mwenifumbo, C.J.
1983: Gamma-ray logging for uranium: status of international efforts to resolve discrepancies in calibration models; in Transactions of the SPWLA (Society of Professional Well Log Analysts) 24th Annual Logging Symposium, Calgary. Paper AA, p. 1-16.

Killeen, P.G.
1983: Getting the most from borehole geophysics; Northern Miner, Volume 69, No. 11, p. B1, B2.

Killeen, P.G.
1983: Borehole logging for uranium by measurement of natural gamma radiation; in Nuclear Geophysics, edited by C.G. Clayton, Pergamon Press, p. 231-260.

Mwenifumbo, C.J., Urbancic, T.I. and Killeen, P.G.
1983: Preliminary studies on gamma-ray spectral logging in exploration for gold; in Current Research, Part A, Geological Survey of Canada, Paper 83-1A, p. 391-397.

Bristow, Q. and Bernius, G.R.
1984: Field evaluation of a magnetic susceptibility logging tool; in Current Research, Part A, Geol. Surv. Can., Paper 84-1A, p. 453-462.

Bristow, Q., Conaway, J.G. and Killeen, P.G.
1984: Application of inverse filtering to gamma-ray logs: a case study; Geophysics, Vol. 49, No. 8, p. 1369-1373.

Killeen, P.G., Bernius, G.R., Schock, L.D. and Mwenifumbo, C.J.
1984: New developments in the GSC borehole geophysics test area and calibration facilities; in Current Research, Part B, Geological Survey of Canada, Paper 84-1B, p. 373-374.

Mwenifumbo, C.J.
1984: An application of the Mise-à-la-masse method to the mapping of gold-bearing alteration zones. CIM Geophysics for Gold Symposium, Nov. 12-13, Val D'Or, Quebec. Extended Abstract, p. 133-148.

Mwenifumbo, C.J.
1985: Application of borehole geophysics in exploration for gold. SPWLA Twenty-sixth Annual Logging Symposium, Dallas, Tx., paper VV p.1-24.

Mwenifumbo, C.J.
1985: Mise-à-la-masse mapping of gold-bearing alteration zones at the Hoyle Pond gold deposit, Timmins, Ontario; in Current Research, Part A, Geol. Surv. Can., Paper 85-1A, p. 669-679.

Schock, L.D. and Killeen, P.G.
1985: Establishment of coal logging field calibration facilities: a progress report; in Current Research, Part B, Geol. Surv. Can., Paper 85-1B, p. 459-462.

Killeen, P.G.
1986: A system of deep test holes and calibration facilities for developing and testing new borehole geophysical techniques; in Borehole Geophysics for Mining and Geotechnical Applications, ed. P.G. Killeen, Geol. Surv. Can., Paper 85-27, 1986, p. 29-46.

Killeen, P.G. and Mwenifumbo, C.J.
1986: Current developments in nuclear techniques for coal logging in Canada; Proceedings of an Advisory Group Meeting on Gamma, X-Ray and Neutron Techniques for the Coal Industry; International Atomic Energy Agency, Vienna, 4-7 December 1984, p. 67-79.

Killeen, P.G. (with V.L.R. Furlong and D.C. George)
1986: Practical borehole logging procedures for mineral exploration, with emphasis on uranium; IAEA Technical Report Series No. 259, 44p.

Killeen, P.G.
1986: Borehole Geophysics for Mining and Geotechnical Applications, editor, P.G. Killeen, Geol. Surv. Can., Paper 85-27, 400 p.

Mwenifumbo, C.J.
1986: Drill hole Mise-à-la-masse IP and Potential measurements in a Zn-Pb- Cu sulphide deposit; in Borehole Geophysics for Mining and Geotechnical Applications, ed. P.G. Killeen, Geol. Surv. Can., Paper 85-27, p. 145-158.

Mwenifumbo, C.J. and Killeen, P.G.
1986: Natural gamma ray logging in volcanic rocks: the Mudhole and Clementine base metal prospects; in Buchans Geology, Newfoundland, ed. R.V. Kirkham; Geological Survey of Canada, Paper 86-24, p. 263-272.

Mwenifumbo C.J.
1986: Mise-à-la-masse experiments in the Maclean Extension orebody, Buchans Mine, Newfoundland; in Buchans Geology, Newfoundland, ed. R.V. Kirkham; Geological Survey of Canada, Paper 86-24, p. 251-261.

Mwenifumbo, C.J. and Killeen, P.G.
1986: Multiparameter borehole geophysical measurements at the Yava lead deposit: a progress report in Program and Summaries, 10th Annual Open House and Review of Activities Nov. 1986, Information Series No. 12, Nova Scotia Department of Mines and Energy, p. 199-200.

Urbancic, T.I. and Mwenifumbo, C.J.
1986: Multiparameter logging techiques applied to gold exploration; in Borehole Geophysics for Mining and Geotechnical Applications, ed. P.G.Killeen, Geol. Surv. Can., Paper 85-27, p. 13-28.

Mwenifumbo, C.J., Killeen, P.G. and Cinq-Mars, A.
1987: Downhole geophysics at the Yava lead deposit, 1987 field season; in Report 87-5, Nova Scotia Dept. of Mines & Energy, Mines and Minerals Branch Annual Report of Activities, 1987, Part A, p. 231-234.

Killeen, P.G. and Mwenifumbo, C.J.
1988: Interpretation of new generation geophysical logs in Canadian mineral exploration; in: 2nd International Symposium on Borehole Geophysics for Minerals, Geotechnical and Groundwater Applications, Oct. 6-8, 1987, Golden, Colorado, p. 167-178.

Killeen, P.G. and Mwenifumbo, C.J.
1988: Downhole assaying in Canadian mineral deposits with the spectral gamma-gamma method; in Current Trends in Nuclear Borehole Logging Techniques for Elemental Analysis. International Atomic Energy Agency Technical Document IAEA-TECDOC-464, p. 23-29.

Mwenifumbo, C.J.
1988: Cross-borehole Mise-à-la-masse mapping of fracture zones at the Bells Corners Borehole Geophysics Test Area, Ottawa, Canada; Proceedings of the 2nd International Symposium on Borehole Geophysics for Minerals, Geotechnical and Groundwater Applications, Oct. 6-8, 1987, Golden, Colorado, p. 151-165.

Killeen, P.G. and Mwenifumbo, C.J.
1989: Gamma-ray Spectral Borehole logging at Chalk River; in Geophysical and related geoscientific research at Chalk River, Ontario, ed. by M.D. Thomas and D.F. Dixon; AECL-9085, p. 349-356.

Mwenifumbo, C.J.and Killeen, P.G.
1989: Borehole geophysics applied to heat pump technology at Carleton University; in Proceedings of ASHRAE Conference on Earth Energy, Carleton Univ., 9 May 1989, p. 11-14.

Mwenifumbo, C.J.
1989: The symmetrical lateral resistivity log in coal seam mapping, Highvale Mine, Alberta; in Current Research, Part D, Geol. Surv. Can., Paper 89-1D, p. 1-8.

Mwenifumbo, C.J., Thorleifson, L.H., Killeen, P.G. and Elliott, B.E.
1989: Preliminary results on the use of borehole geophysics in overburden stratigraphic mapping near Geraldton, northern Ontario; in Current Research, Part C, Geol. Surv. Can., Paper 89-1C, p. 305-311.

Desbarats, A.J. and Killeen, P.G.
1990: A least-squares inversion approach to stripping in gamma-ray spectral logging; in Nuclear Geophysics, Vol. 4, No. 3, p. 343-352.

Killeen, P.G., Schock, L.D. and Elliott, B.E.
1990: A slim hole assaying technique for base metals and heavy elements based on spectral gamma-gamma logging; in Proceedings of the 3rd International Symposium on Borehole Geophysics for Minerals and Geotechnical Logging, 2-5 Oct., 1989, Las Vegas, Nevada, paper Y p. 435-454.

Killeen, P.G. and Elliott, B.E.
1990: Model boreholes for gamma ray logging: Intercalibration of North American and European Calibration Facilities; in Transactions of the 13th SPWLA European Formation Evaluation Symposium, Budapest, Oct. 22-26, 1990, paper GG, 14 pages.

Mwenifumbo, C.J.
1990: Optimization of logging parameters in continuous time domain induced polarization measurements; in Proceedings of the 3rd International Symposium on Borehole Geophysics for Minerals, Geotechnical and Groundwater Applications, 2-5 Oct. 1989, Las Vegas, Nevada, paper N, p. 201-232.

Mwenifumbo, C.J., Killeen, P.G. and Graves, M.C.
1990: Borehole geophysical logging at the Lake Charlotte Manganese Prospect, Meguma Group, Nova Scotia; in Mineral Deposit Studies in Nova Scotia, Volume 1, edited by A.L. Sangster, Geol. Surv. Can., Paper 90-8, p. 195-202.

Mwenifumbo, C.J., Killeen, P.G. Cinq-Mars, A.
1990: Borehole geophysical logging in the Sudbury Basin; in Lithoprobe Sudbury Transect Newsletter, No. 1, 1990, p. 6-7.

Wilson, H.C., Michel, F.A., Mwenifumbo, C.J. and Killeen, P.G.
1990: Application of borehole geophysics to groundwater energy resources; in Proceedings of the 3rd International Symposium on Borehole Geophysics for Minerals and Geotechnical Logging, 2-5 Oct., 1989, Las Vegas, Nevada, Paper T, p. 317-336.

Elliott,B.E.
1991: An Overview of Processing, Display and Enhancement Methods used on Borehole Geophysical Logging Data at the Geological Survey of Canada. Proceedings; in Proceedings of the 4th International Symposium on Borehole Geophysics for Mineral and Geotechnical Logging, August 18-22, Toronto, Ontario, p. 227-235.

Killeen,P.G., Schock,L.D., Elliott,B.E., Cinq-Mars,A., Mwenifumbo,C.J., Bernius,G., Hyatt,W., Birk,S.
1991: An Overview of Borehole Geophysical Research at the Geological Survey of Canada. in Proceedings of the 4th International Symposium on Borehole Geophysics for Mineral and Geotechnical Logging, August 18-22, Toronto, Ontario, p. 203-209.

Killeen, P.G. and Schock, L.D.
1991: Borehole assaying with the spectral gamma-gamma method: some parameters affecting the SGG ratio: in Proceedings of the 4th International Symposium on Borehole Geophysics for Mineral and Geotechnical Logging, August 18-22, Toronto, Ontario, p.399-406.

Killeen, P.G.
1991: Borehole geophysics: Taking geophysics into the third dimension; in GEOS, Vol. 20, No. 2, 1991, p. 1-10.

Mwenifumbo,C.J.
1991: Field Evaluation of Electrodes for Drillhole Self Potential Measurements. in Proceedings of the 4th International Symposium on Borehole Geophysics for Mineral and Geotechnical Logging, August 18-22, Toronto, Ontario, p. 179-189.

Mwenifumbo,C.J.
1991: Temperature Logging in Mineral exploration. in Proceedings of the 4th International Symposium on Borehole Geophysics for Mineral and Geotechnical Logging, August 18-22, Toronto, Ontario, p. 237-247.

Mwenifumbo, C.J. and Blangy, J.P.
1991: Short-term spectral analysis of downhole logging measurements from Site 704, ODP Leg 114; in Ciesielski, P.F. and Kristofferson, Y. et al., Proc. ODP, Sci, Results, 114, College Station, TX (Ocean Drilling Program), p. 577-585.

Mwenifumbo, C.J. and Blangy, J.P.
1991: Depositional environment and diagenesis of sediments at Site 700 inferred from downhole measurements; in Ciesielski, P.F. and Kristofferson, Y. et al., Proc. ODP, Sci, Results, 114, College Station, TX (Ocean Drilling Program), p. 649-656.

Mwenifumbo, C.J.
1991: On the possibility of discriminating between economic and non-economic sulphides; Cover photo: *The Log Analyst*, v.32, no.6.

Nobes, D.C., Mienert, J., Mwenifumbo, C.J. and Blangy, J.P.
1991: An estimate of heat flow on the Meteor Rise, Site 704; in Ciesielski, P.F. and Kristofferson, Y., et al., Proc. ODP, Sci. Results, 114: College Station, TX (Ocean Drilling Program), p. 39-45.

Nobes, D.C., Mwenifumbo, C.J., Mienert, J. and Blangy, J.P.
1991: The problem of porosity rebound in deep sea sediment cores: A comparison of laboratory and in situ physical property measurements; in Ciesielski, P.F. and Kristofferson, Y., et al., Proc. ODP, Sci. Results, 114: College Station, TX (Ocean Drilling Program), p. 711-716.

Nobes, D.C., Mienert, J. and Mwenifumbo, C.J.
1991: An estimate of the heat flow on the Meteor Rise, Subantarctic South Atlantic: *Journal of Geophysical Research*, 96(B4):5947-5953.

Schock,L.D., Killeen,P.G., Elliott,B.E. and Bernius,G.R.
1991: A Review of Canadian Calibration Facilities for Borehole Geophysical Measurement. in Proceedings of the 4th International Symposium on Borehole Geophysics for Mineral and Geotechnical Logging, August 18-22, Toronto, Ontario, p. 191-202.

Cinq-Mars, A. Mwenifumbo, C.J., Killeen, P.G. and Chouteau, M.
1992: Multiparameter geophysical logging at the Yava lead deposit: A statistical approach; in Geophysical Prospecting, Volume 40, p.829-848.

Killeen, P.G., Pflug, K., Mwenifumbo, C.J., Zelmer, R.L. and McCallum, B.A.
1992: Preliminary results of spectral gamma-ray logging applied to low-level radioactive waste management studies at Port Hope, Ontario, Canada; in Application of Nuclear Techniques for Environmental Preservation in Resource Extraction and Processing, IAEA, December 1992, 14 p.

Killeen, P.G. Mwenifumbo, C.J. and Pflug, K.
1993: Evaluation by GSC of borehole logging and analysis protocols at a Port Hope landfill site. Report prepared for the Low-Level Radioactive Waste Management Office, Atomic Energy of Canada Ltd., Feb. 1993, 200 pages.

Killeen, P.G., Pflug, K.A., Mwenifumbo, C.J., Zelmer, R.L. and McCallum, B.A.
1993: Application of spectral gamma-ray logging to low-level radioactive waste management studies at Port Hope, Ontario, Canada; Nuclear Geophysics, 7(4), p. 501-514.

Killeen, P.G. and Pflug, K.A.
1993: Detection of ^{234}Pa in low-level radioactive waste by gamma-ray spectral logging; in Current Research, Part E, Geol. Surv. of Can., Paper 93-1E, p. 307-312.

Killeen, P.G., Elliott, B.E. and Mwenifumbo, C.J.
1993: Ore deposit signatures and borehole geophysics test sites in Ontario; in Proceedings of the 5th International Symposium of the Minerals & Geotechnical Logging Society, Tulsa, 24-28 October 1993, Paper G (5 pages).

Mwenifumbo, C.J.
1993: Kernel Density Estimation in the Analysis and presentation of Borehole Geophysical Data. *The Log Analyst*, Vol. 34, No. 5, pp. 34-45.

Mwenifumbo, C.J.
1993: Borehole Geophysics in Environmental Applications. CIM Bulletin, January, 1993, p. 43-49.

Mwenifumbo, C.J.
1993: Temperature Logging in Mineral Exploration. *Journal of Applied Geophysics*, 30(1993) 297-313.

Mwenifumbo, C.J.
1993: On the possibility of discriminating between economic and non-economic sulfides by the spectral gamma-gamma method; in Proceedings of the 5th International Symposium of the Minerals & Geotechnical Logging Society, Tulsa, 24-28 October 1993, Paper J/L (15 pages).

Mwenifumbo, C.J.,
1993: On the Cover; Colour contour plot of the Kernel Density estimate. The Log Analyst, September-October, 1993.

Mwenifumbo, C.J., Killeen, P.G., Elliott, B.E. and Pflug, K.A.
1993: The borehole geophysical signature of the McConnell Nickel Deposit, Sudbury area; in Proceedings of the 5th International Symposium of the Minerals & Geotechnical Logging Society, Tulsa, 24-28 October 1993, Paper I (8 pages).

Mwenifumbo, C.J., Killeen, P.G. and Elliott, B.E.
1993: Classic examples from the Geological Survey of Canada data files illustrating the utility of borehole geophysics; in Proceedings of the 5th International Symposium of the Minerals & Geotechnical Logging Society, Tulsa, 24-28 October 1993, Paper K (15 pages).

Mwenifumbo, C.J., Killeen, P.G. and Bernius, G.R.
1993: Ore deposit signatures by borehole geophysics; in Summary Report, 1992-1993, Northern Ontario Development Agreement, (ed.) N. Wood, R. Shannon, L. Owsiacki and M. Walters, co-published by Energy, Mines & Resources Canada, p. 123-125.

Pflug, K.A., Killeen, P.G. and Mwenifumbo, C.J.
1993: Application of spectral gamma-ray logging to low-level radioactive waste management studies; in Proceedings of the 5th International Symposium of the Minerals & Geotechnical Logging Society, Tulsa, 24-28 October 1993, Paper V (18 pages).

Killeen, P.G.
1994: Canadian Trends and Developments in Borehole Geophysics; in Proceedings of the AMIRA Symposium on the Application of Borehole Logging to Mineral Exploration and Mining, 20 February, 1994, Perth, WA.

Killeen, P.G., Pflug, K.A., Zelmer, R.L. and McCallum, B.A.
1994: Advantages and disadvantages of gamma-ray spectral logging for site characterization of low-level radioactive waste; in Proceedings of the 20th Annual Nuclear & Hazardous Waste Symposium, "WM94", Tucson, Arizona, Feb. 27-March 3, 1994, p.909-914.

Killeen, P.G., Mwenifumbo, C.J., Pflug, K.A. and Elliott, B.E.
1994: Borehole geophysical signatures and test sites at major deposits in Ontario: New developments in 1993; in Summary Report, 1993-1994, Northern Ontario Development Agreement, (ed.) N. Wood, R. Shannon, L. Owsiacki and M. Walters, co-published by Natural Resources Canada and the MNDM (Ont.) p. 122-125.

Mwenifumbo, C.J.
1994: Borehole geophysics applied to mapping Paleozoic stratigraphy, Grand Rapids area, Manitoba; in Geological Survey of Canada, Current Research 1994-E, pages 141-149.

Mwenifumbo, C.J.
1994: Application of temperature logging to mapping coal seams; in Geological Survey of Canada, Current Research 1994-E, pages 291-298.

Mwenifumbo, C.J., Killeen, P.G. and Elliott, B.E.
1994: Downhole logging measurements in the Fraser Delta, British Columbia; in Geological Survey of Canada, Current Research 1994-E, pages 77-84.

Pflug, K.A., Killeen, P.G. and Mwenifumbo, C.J.
1994: Acoustic velocity logging at the McConnell nickel deposit, Sudbury area, Ontario: preliminary in situ measurements; in Current Research 1994-C, Geological Survey of Canada, p. 279-286.

Cinq-Mars, A., Mwenifumbo, C.J. and Killeen, P.G.
1995: Borehole geophysics logs from lithoprobe project boreholes at Les Mines Selbaie and Lac Matagami, Quebec; GSC Open File 2813

Killeen, P.G.
1995: Borehole geophysics poised for mining applications; in Canadian Mining and Innovations Magazine, January 1995, p. 24-27.

Killeen,P.G., Mwenifumbo,C.J. and Elliott,B.E.
1995: The pseudo-geological log: using geophysical logs as an aid to geological logging in volcanogenic massive sulphides; in Geological Survey of Canada, Current Research 1995-E, pages 321-330.

Killeen,P.G., Mwenifumbo,C.J. and Elliott,B.E.
1995: Borehole geophysical logs and physical property tables for massive sulphide deposits in the Cordillera, British Columbia: Buttle Lake, Chu Chua, Equity Silver, Goldstream, Highland Valley, Lara and Sullivan Deposits; GSC Open file 2610.

Killeen,P.G., Mwenifumbo,C.J. and Elliott,B.E.
1995: Mineral deposit signatures by borehole geophysics:
Data from the borehole geophysical test site at the McConnell nickel deposit (Garson Offset), Ontario; GSC Open File 2811.

Mwenifumbo, C.J., Killeen, P.G. and Thorleifson, L.H.
1995: Borehole geophysical logs: Overburden Holes, Southeastern Manitoba; GSC Open File 2775.

Mwenifumbo, C.J., Bezys, R., Betcher, R. and Killeen, P.G.
1995: Borehole geophysical logs Manitoba (1992) (including logs from Grand Rapids and Winnipeg); GSC Open File 2734.

Mwenifumbo, C.J. and Killeen, P.G.
1995: Preliminary results of geophysical logging in exploration holes at the Halfmile Lake massive sulphide deposit, New Brunswick; in New Brunswick Current Research 1995 Volume.

Pflug, K.A., Killeen, P.G. and Mwenifumbo, C.J.
1995: Multiparameter logging in the Kirkland Lake gold camp in 1994: preliminary borehole geophysical signatures; in Summary Report, 1994-95, Northern Ontario Development Agreement, Minerals, (ed.) N. Wood, R. Shannon, L. Owsiacki and M. Walters, co-published by Natural Resources Canada and the Ministry of Northern Development and Mines (Ontario), p. 117-119.

Richardson, K.A., Katsube, T.J., Mwenifumbo, C.J., Killeen, P.G.,Hunter, J.A.M., Gendzwill, D.J. and Matieshin, S.D.

1995: Geophysical studies of kimberlite in Saskatchewan; in Investigations Completed by the Saskatchewan Geological Survey and the Geological Survey of Canada Under the Geoscience Program of the Canada-Saskatchewan Partnership Agreement on Mineral Development (1990-1995), Geological Survey of Canada Open file 3119, (ed. D.G. Richardson), p. 197-205.

Killeen, P.G., Mwenifumbo, C.J. and Bernius, G.R.

1996: Development of a borehole surveying probe using 3-component fluxgate magnetometers; in EXTECH I: A Multidisciplinary Approach to Massive Sulphide Research in the Rusty Lake-Snow Lake Greenstone Belts, Manitoba, (ed.) G.F. Bonham-Carter, A.G. Galley and G.E.M. Hall; Geological Survey of Canada Bulletin 426. (in press).

Mwenifumbo, C.J., Hunter, J.A.M. and Killeen, P.G.

1996: Geophysical Characteristics of Canadian Kimberlites; in Searching for Diamonds in Canada; Geological Survey of Canada Open file 3228, (eds. A.N. Lecheminant, R.N.W. DiLabio and K.A. Richardson), (in press).

C1.2 GSC Open File descriptions and ordering information

The following open files are available from:

Geological Survey of Canada Bookstore,
601 Booth St., Ottawa, Ontario, K1A 0E8.
Tel: (613) 995-4342 Fax: (613) 943-0646.
e-mail: gsc_bookstore@gsc.emr.ca

GSC OPEN FILE 2610
Borehole geophysical logs and physical property tables for massive sulphide deposits in the Cordillera, British Columbia: Buttle Lake, Chu Chua, Equity Silver, Goldstream, Highland Valley, Lara and Sullivan Deposits
P.G.Killeen, C.J.Mwenifumbo, B.E.Elliott

Results of multiparameter (Total Count gamma ray, density, spectral gamma-gamma ratio, self potential, resistivity, induced polarization, magnetic susceptibility, conductivity and temperature) geophysical logging of thirteen boreholes in seven deposits are presented in a bound portfolio including nineteen 11" x 17" colour plots and accompanying 58-page text. Tables of in situ measurements of physical properties derived from the logs, for rock units intersected by the holes, are included.

Viewing: Crown Publications, Victoria
Sales: GSC (Ottawa)
Price: $75 ($97.50 outside Canada)

GSC OPEN FILE 2734
Borehole Geophysical Logs Manitoba (1992)
(Including logs from Grand Rapids and Winnipeg)
C.J. Mwenifumbo, R. Bezys, R. Betcher, P.G. Killeen

Results of multiparameter (gamma ray, density, spectral gamma-gamma, self potential, resistivity, induced polarization, magnetic susceptibility, and temperature) geophysical logging of a 160 m Palaeozoic stratigraphic hole near Grand Rapids and two 125 m water wells in Winnipeg are presented in a bound portfolio including four 11" x 17" colour plots and accompanying text.

Viewing: Manitoba Department of Energy and Mines, Winnipeg
Sales: GSC (Ottawa)
Price: $25 ($32.50 outside Canada)

GSC OPEN FILE 2775

Borehole Geophysical Logs: Overburden Holes, Southeastern Manitoba

C.J. Mwenifumbo, P.G. Killeen, L.H. Thorleifson

Results of multiparameter (gamma ray, conductivity, magnetic susceptibility) geophysical logging of seventeen holes and density, spectral gamma-gamma, and temperature logs which were also recorded in five of the holes, are presented in a bound portfolio including fifteen 11" x 17" colour plots and accompanying text.

Contribution to the Southern Prairies NATMAP Project.

Viewing: Manitoba Department of Energy and Mines, Winnipeg
Sales: GSC (Ottawa)
Price: $60 ($78 outside Canada)

GSC OPEN FILE 2811

Mineral deposit signatures by borehole geophysics:
Data from the borehole geophysical test site at the McConnell nickel deposit (Garson Offset), Ontario

P.G.Killeen, C.J.Mwenifumbo, B.E.Elliott

Results of multiparameter (Total Count gamma ray, K%, Uppm, Thppm, density, spectral gamma-gamma ratio, self potential, resistivity, induced polarization, magnetic susceptibility, and temperature) geophysical logging of five boreholes and acoustic velocity and 3-component magnetometer logs which were also recorded in one of the holes at the McConnell deposit are presented in a bound portfolio including twenty 11" x 17" colour plots and accompanying text.

Contribution to Canada-Ontario Subsidiary Agreement on Northern Ontario Development (1991-1995), under the Canada-Ontario Economic and Regional Development Agreement.

Viewing: Ontario Geological Survey, Toronto, Sudbury
Sales: GSC (Ottawa)
Price: $75 ($97.50 outside Canada)

GSC OPEN FILE 2813
Borehole geophysical logs from LITHOPROBE project boreholes at Les Mines Selbaie and Lac Matagami, Quebec;
A. Cinq-Mars, C.J. Mwenifumbo, P.G. Killeen

Results of multiparameter (total count gamma ray, density, spectral gamma-gamma ratio, self potential, resistivity, single point resistance, induced polarization, magnetic susceptibility, and temperature) geophysical logging in Quebec, in two boreholes (450 and 650 m depth) at Les Mines Selbaie, and a deep hole (1450 m) in the Matagami Lake area are presented in a bound portfolio including ten 11" x 17" colour plots and accompanying text.

Viewing: GSC (Quebec)
Sales: GSC (Ottawa)
Price: $45 ($58.50 outside Canada)

GSC OPEN FILE 3055
LogView - A MICROSOFT WINDOWS 3.1 APPLICATION TO VIEW BOREHOLE LOG (GEOPHYSICAL AND GEOLOGICAL) DATA
D. Markarian, J.A. Grant and B.E. Elliott
1 diskette

LogView can be used to view, print and zoom/pan borehole logs and associated lithology. The software was originally created to provide presentation quality colour and black and white screen and hardcopy output for combinations of logs generated from a series of GSC logging probes. The data file formats and software allow logging parameters with different depth intervals to be plotted beside one another. Logs of data can be stretched, compressed, depth shifted and smoothed for display and a limited amount of annotation can be added to enhance the presentation. LogView creates 'log display list' files, that allow attributes for a specific layout of logs to be saved for future use and revision. On-line help is provided.

Sales: GSC (Ottawa)
Price: $75 ($97.50 outside Canada)

C2. RECOMMENDED TEXTBOOKS ON BOREHOLE GEOPHYSICS

Bateman, Richard M., **Cased-Hole Log Analysis and Reservoir Performance Monitoring**, International Human Resources Development Corporation, Boston, 1985; pp. 319

_____, **Log Quality Control**, International Human Resources Development Corporation, Boston, 1985; pp. 398

Crain, E.R., **The Log Analysis Handbook: Quantitative Log Analysis Methods**, Vol. 1, Pennwell Books, Tulsa, 1986; pp. 684

Doveton, John H., **Log Analysis of Subsurface Geology: Concepts and Computer Methods**, John Wiley and Sons, New York, 1986; pp. 273

Ellis, Darwin V., **Well Logging for Earth Scientists**, Elsevier, New York, 1987; pp. 532

Hallenburg, James K., **Geophysical Logging for Mineral and Engineering Applications**, Pennwell Books, Tulsa, 1984; pp. 254

Hilchie, Douglas W., **Applied Openhole Log Interpretation for Geologists and Petroleum Engineers**, Douglas W. Hilchie Inc., Golden Colorado, 1978.

Hoffman, G.L., G.R. Jordan, and G.R. Wallis, **Geophysical Borehole Logging Handbook for Coal Exploration**, The Coal Mining Research Centre, Edmonton, 1982; pp. 270

International Atomic Energy Agency, **Borehole Logging for Uranium Exploration: A Manual**, Technical Reports Series No. 212, International Atomic Energy Agency, Vienna, 1982; pp. 279

International Atomic Energy Agency, **Practical Borehole Logging Procedures for Mineral Exploration with Emphasis on Uranium**, Technical Reports Series No. 259, International Atomic Energy Agency, Vienna, 1986; pp. 44

Labo, J., **A Practical Introduction to Borehole Geophysics: An Overview of Wireline Well Logging Principles for Geophysicists**, Geophysical References, Vol. 2, Society of Exploration Geophysicists, Tulsa, 1986; pp. 330

Pirson, Sylvain J., **Geologic Well Log Analysis**, 2nd ed., Gulf Publishing Company, Houston, 1977; pp. 377

The Working Group on Nuclear Techniques in Hydrology of the International Hydrological Decade, **Nuclear Well Logging in Hydrology**, Technical Reports Series No. 126, International Atomic Energy Agency, Vienna, 1971; pp. 90

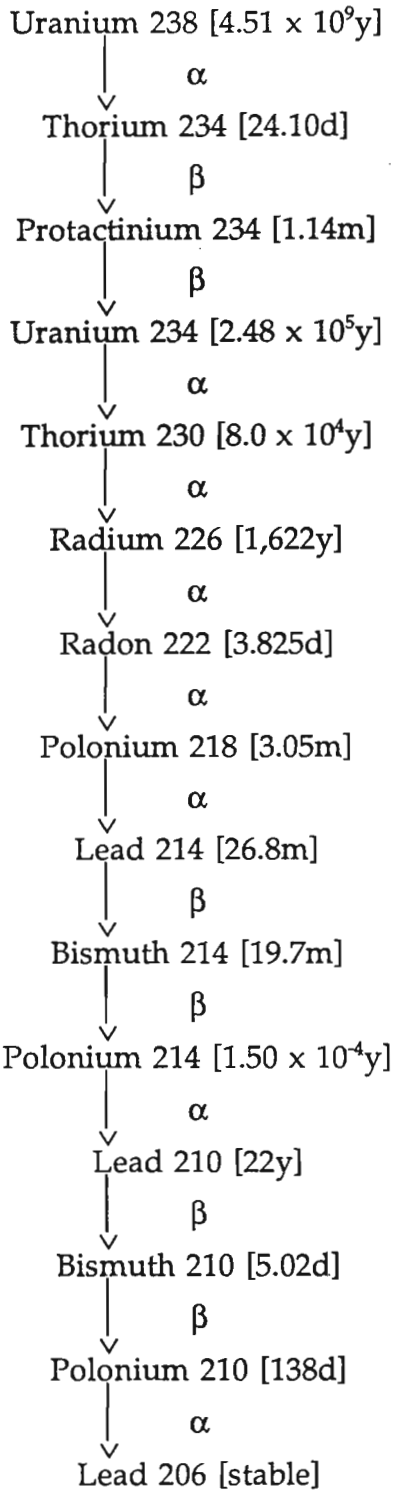

C3.1 **Disintegration series of uranium-238**

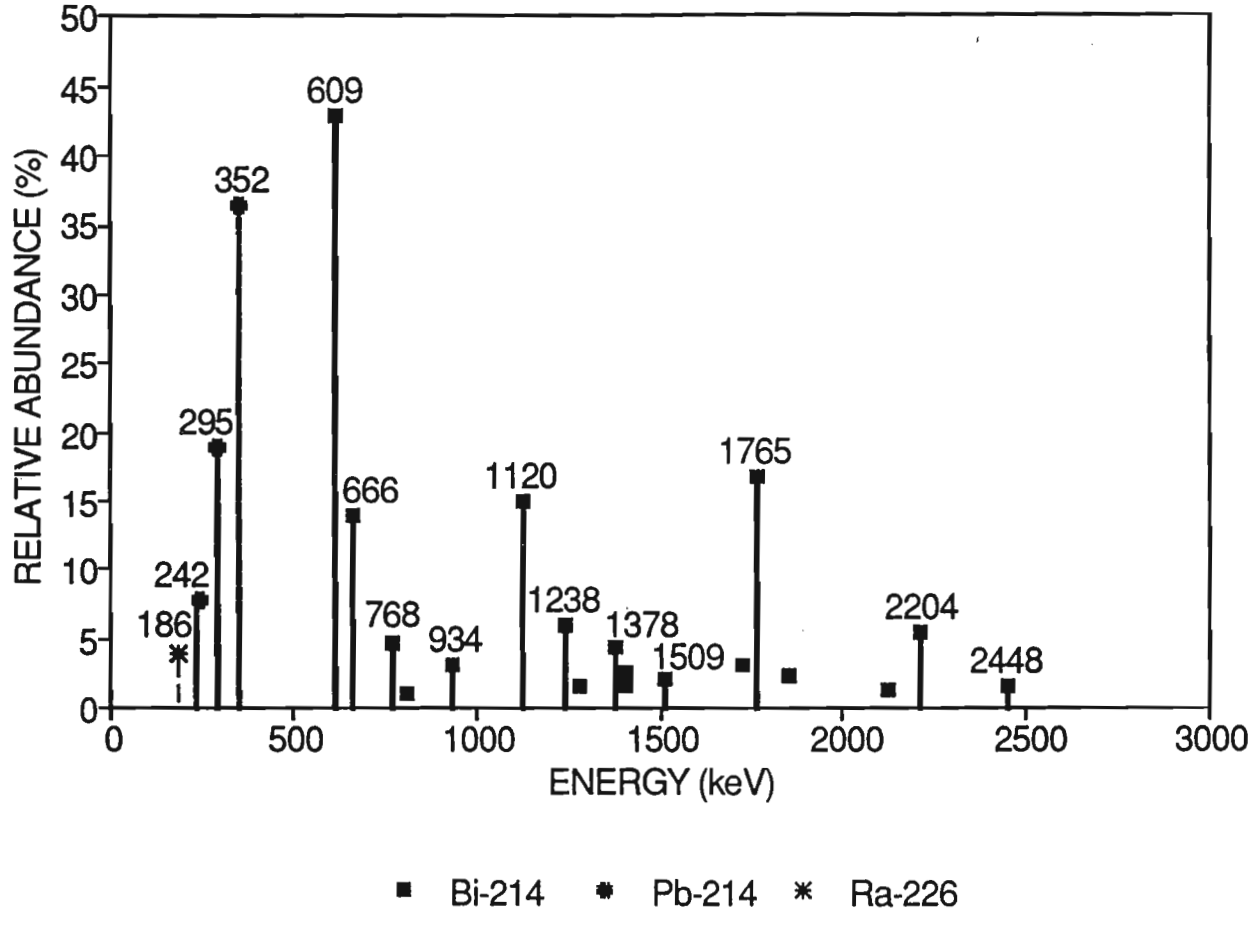

Characteristic decay energies of the uranium series in equilibrium. Gamma rays with relative abundance of 1% or greater are shown.

C3.2 Characteristic decay energies of the uranium series

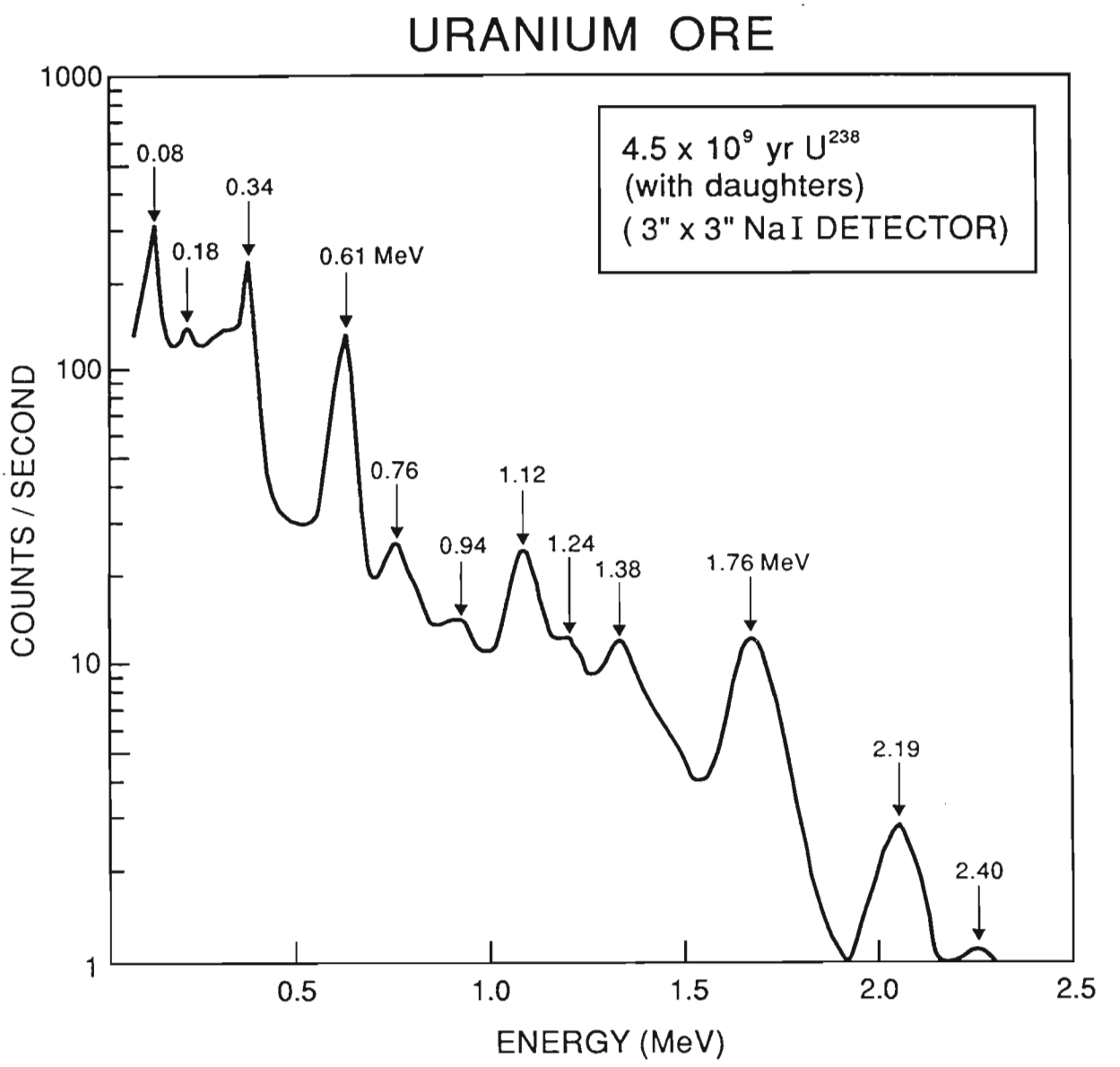

C3.3 Laboratory gamma ray spectrum from uranium ore

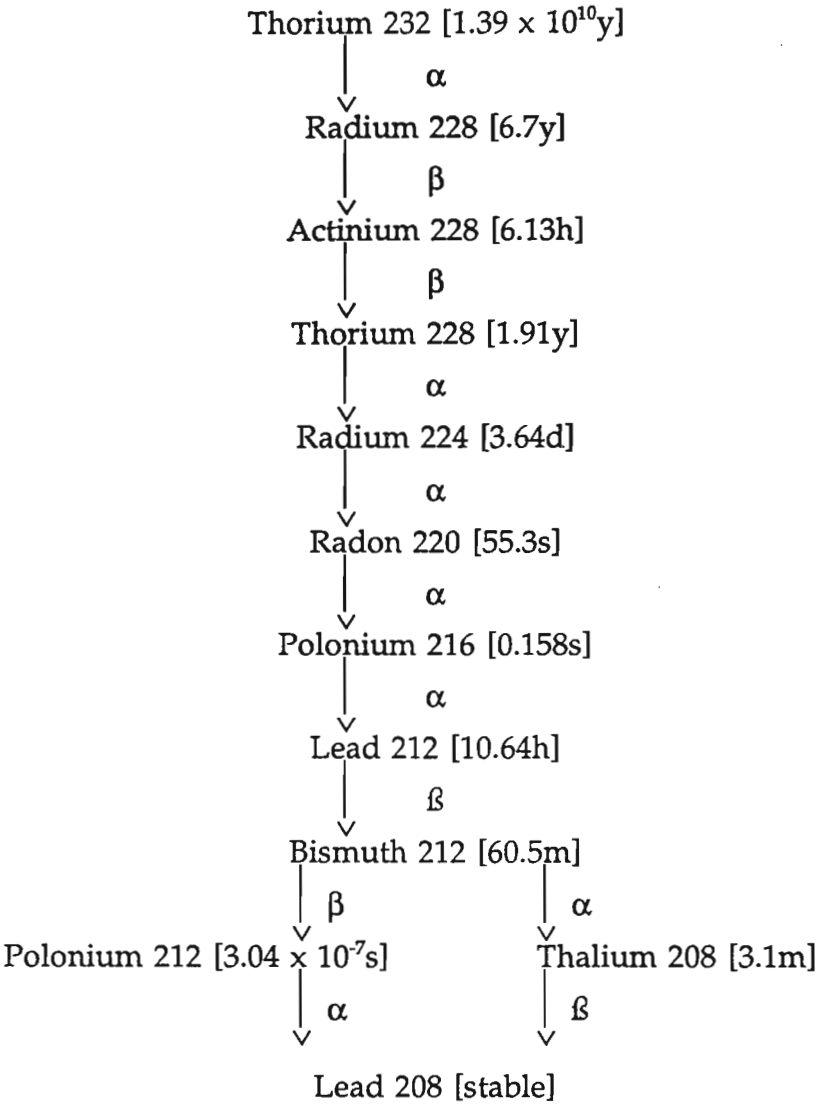

C4.1 Disintegration series of thorium-232

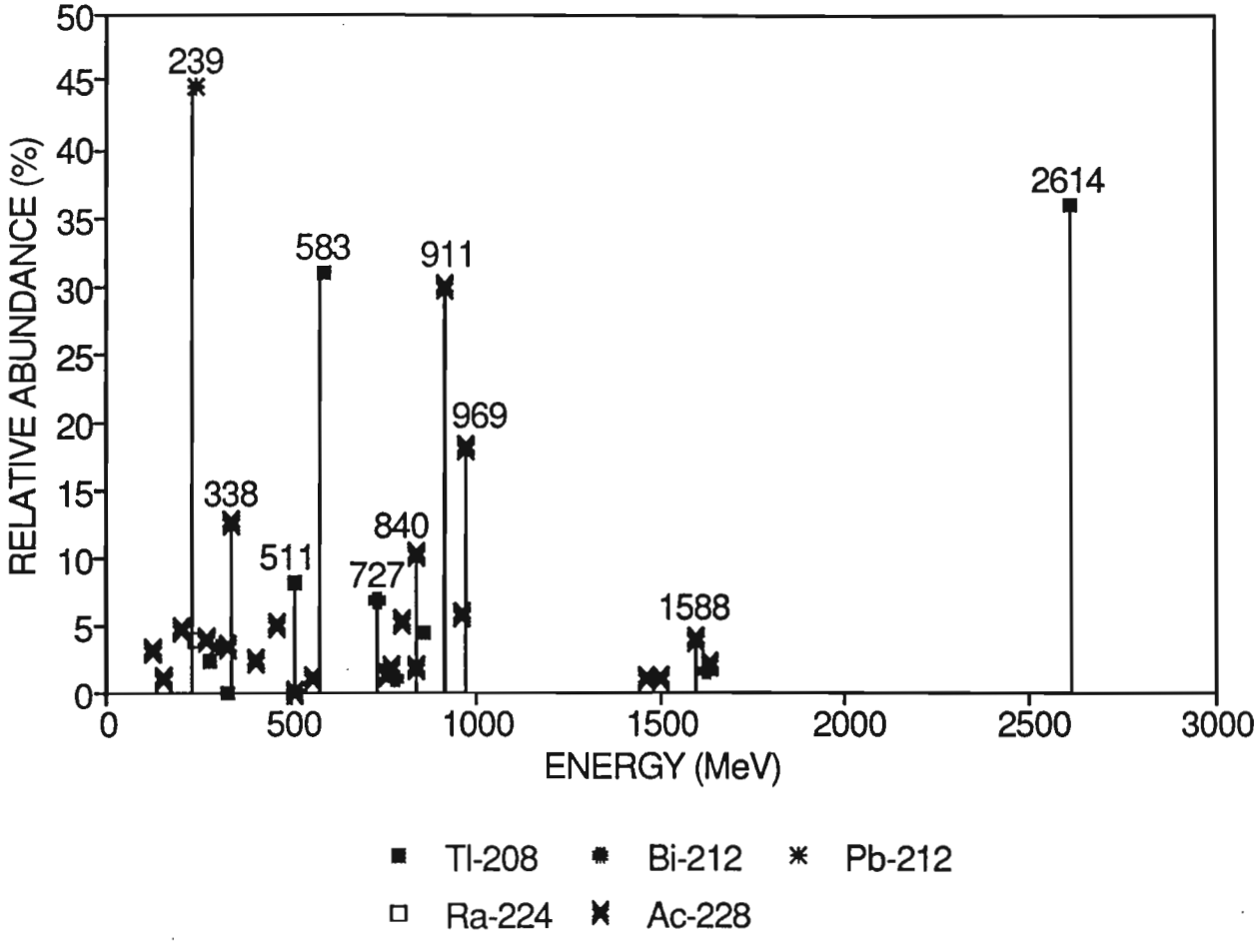

Characteristic decay energies of the thorium series in equilibrium. Gamma rays with relative abundance of 1% or greater are shown.

C4.2 Characteristic decay energies of the thorium series

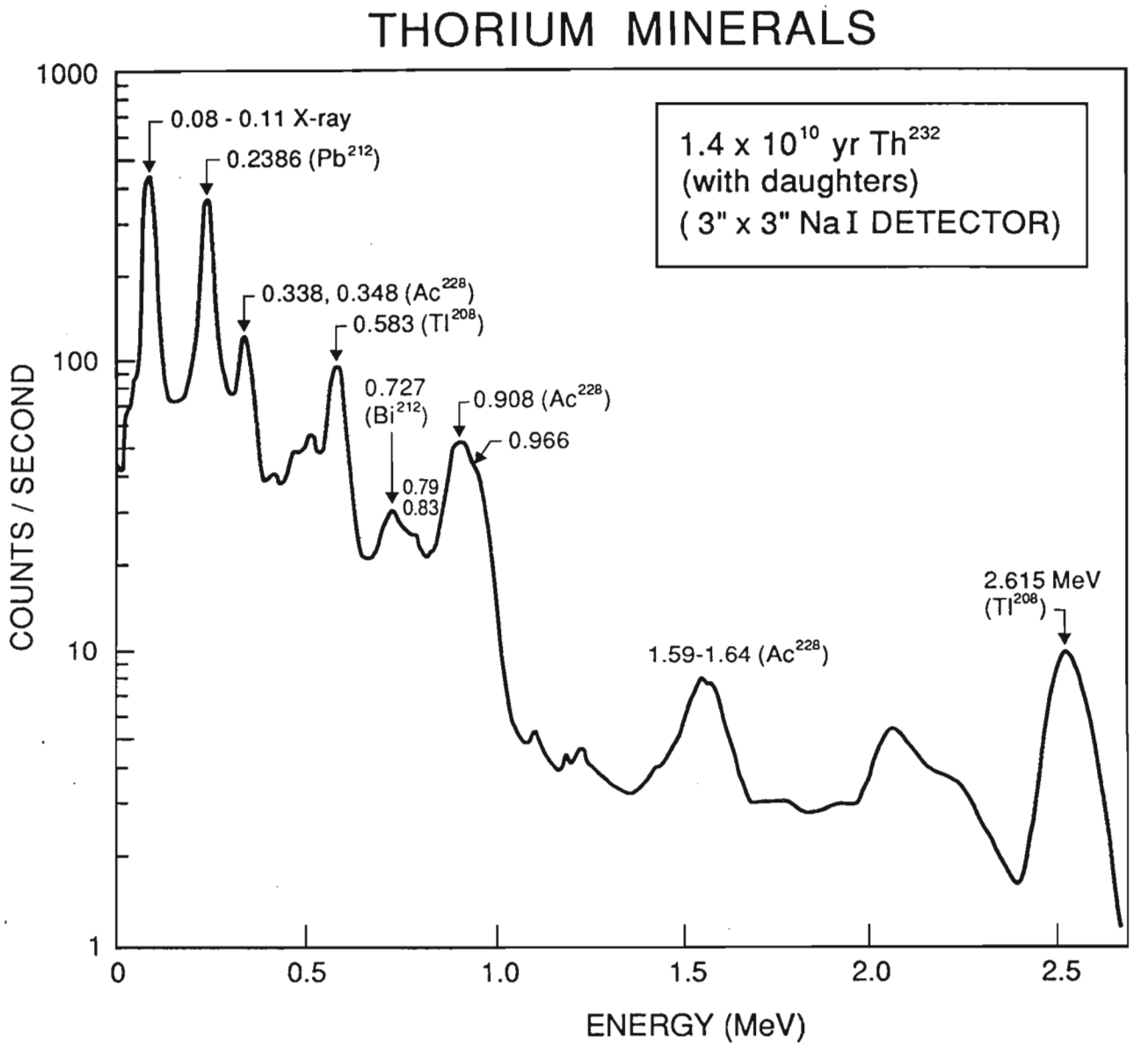

C4.3 Laboratory gamma ray spectrum from thorium ore

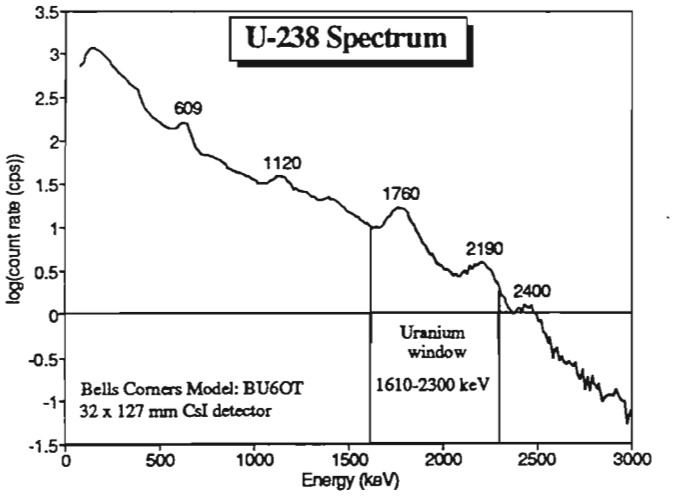

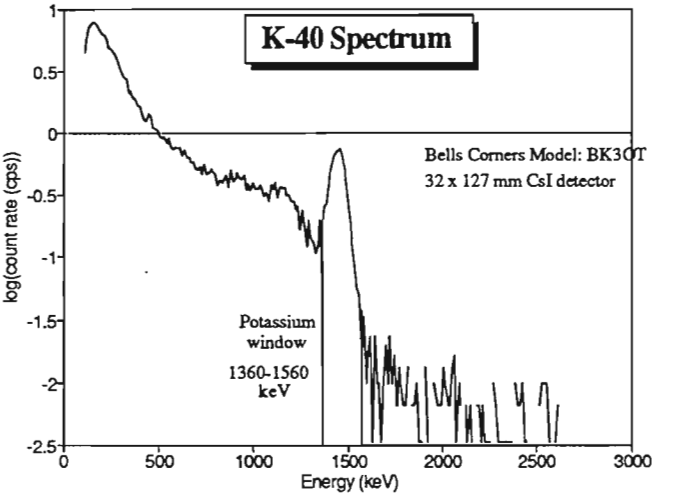

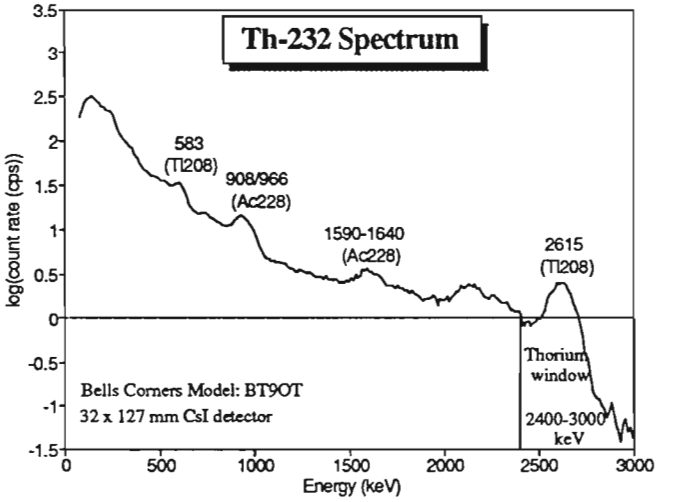

C5.1 Borehole K-40, U-238 and Th-232 spectra

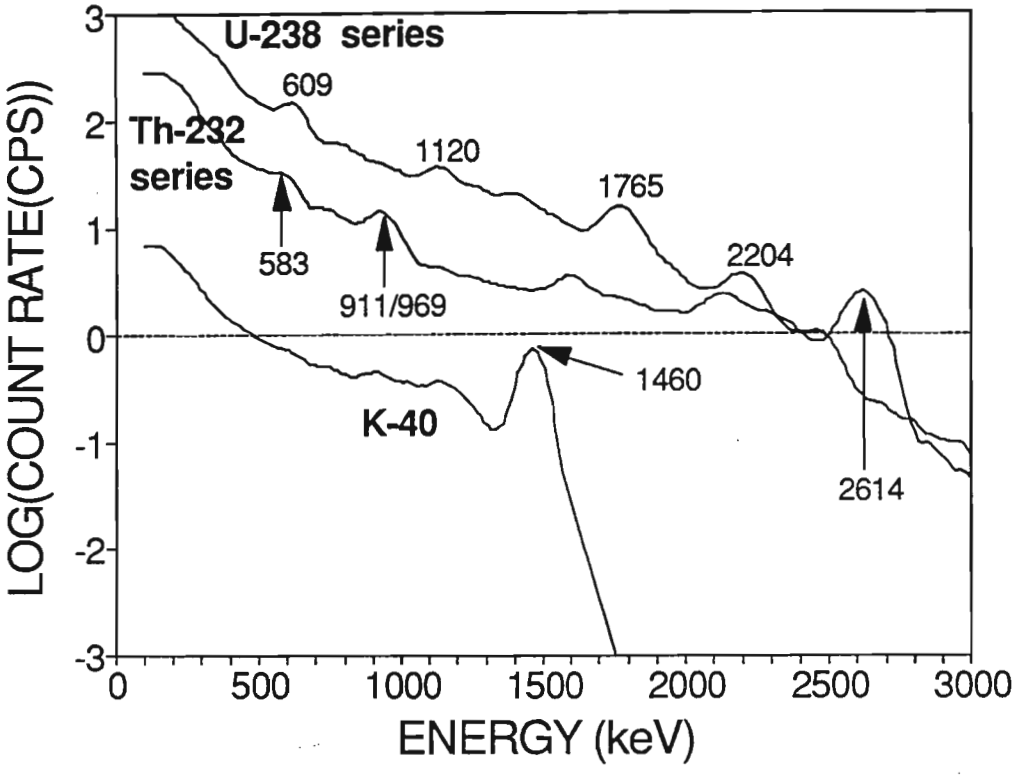

5 minute spectra in the 'ore' zones of the GSC's 997.9 ppm uranium model (U-238 series), 503.5 ppm thorium model (Th-232 series) and 3.28 % potassium model (K-40). 76 mm diameter air-filled holes. 32 x 127 mm cesium iodide detector.

C5.2 Combined borehole K-40, U-238, and Th-232 spectra

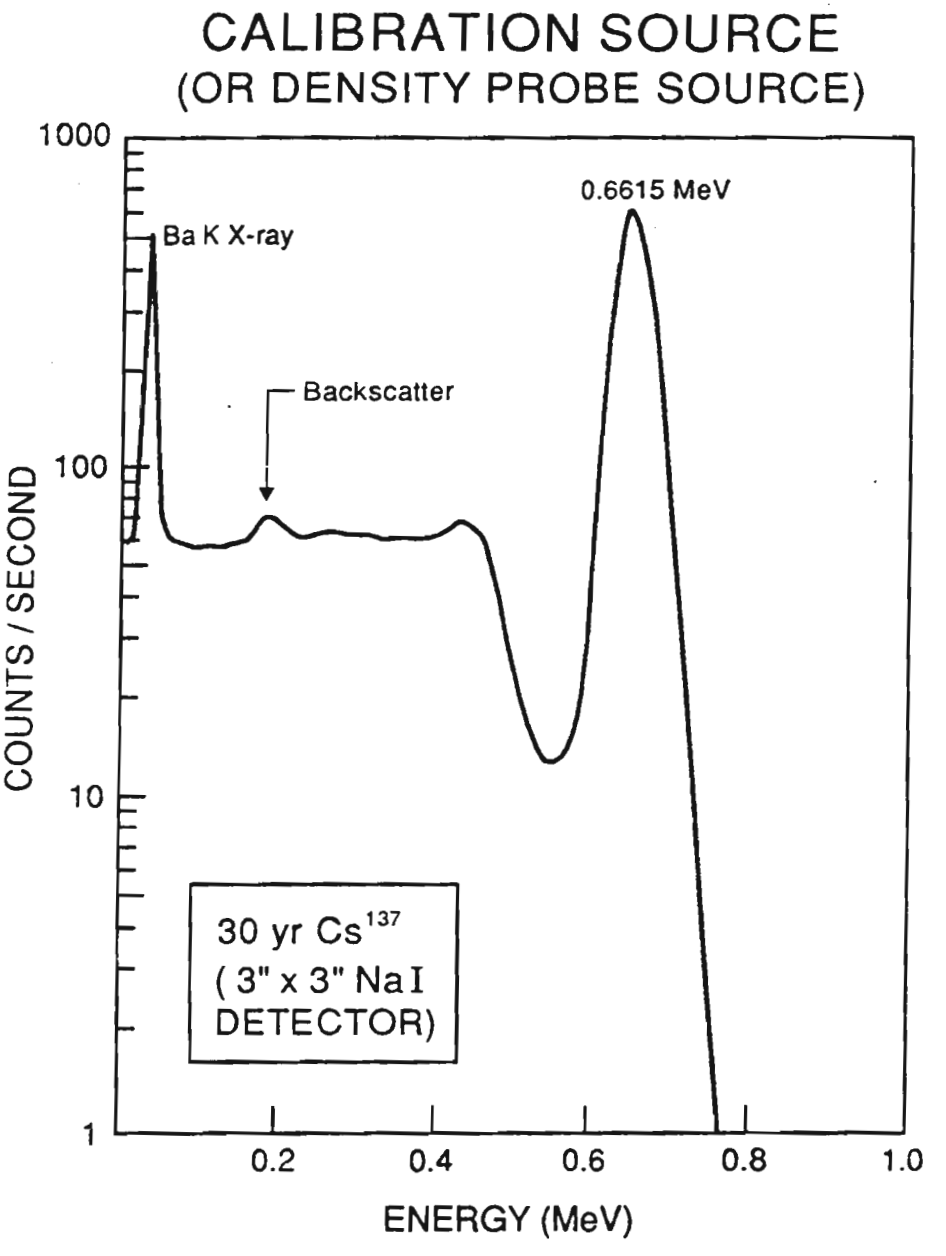

C6.1 Spectrum from Cs-137 calibration (or density probe) source

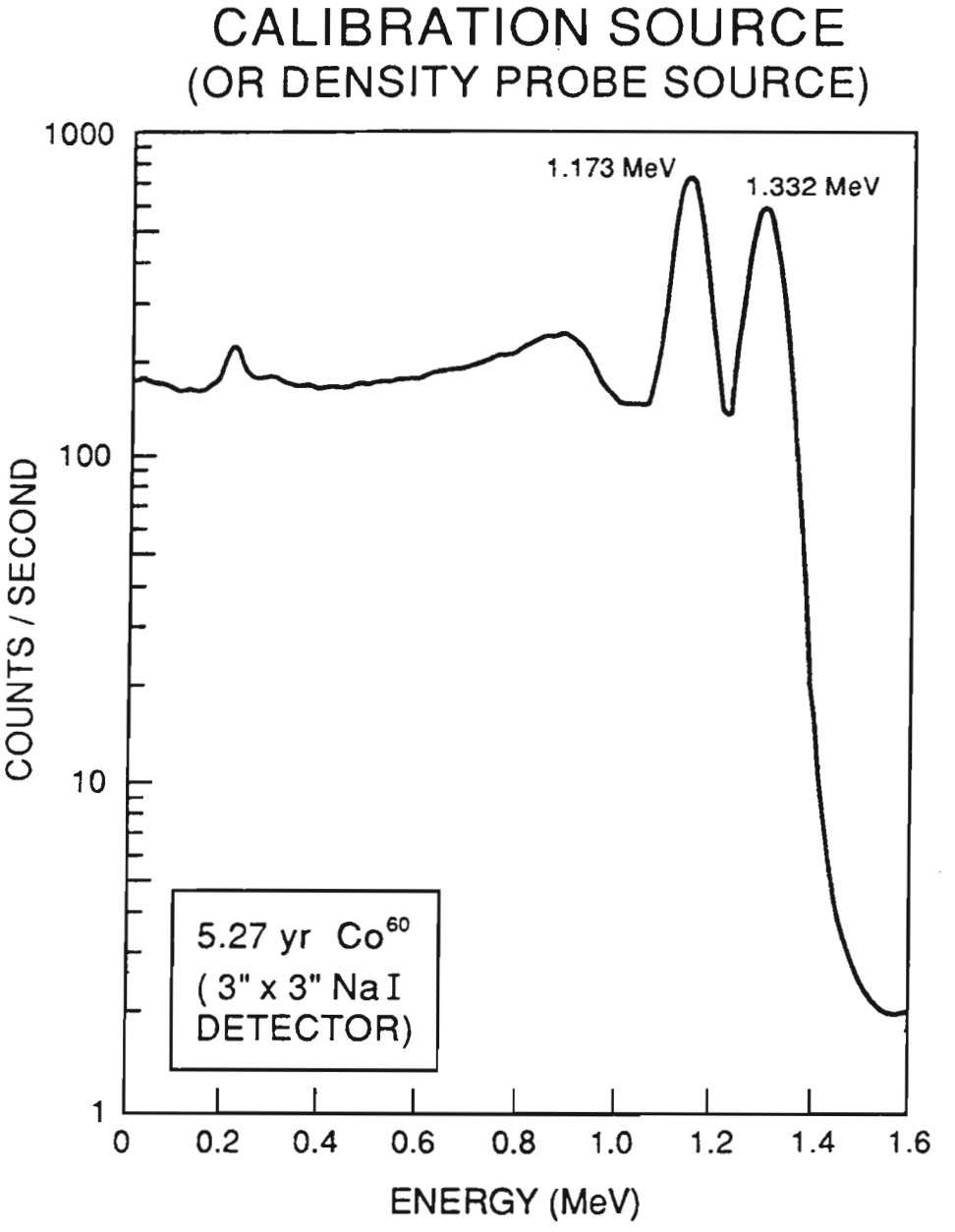

C6.2 Spectrum from Co-60 calibration (or density probe) source

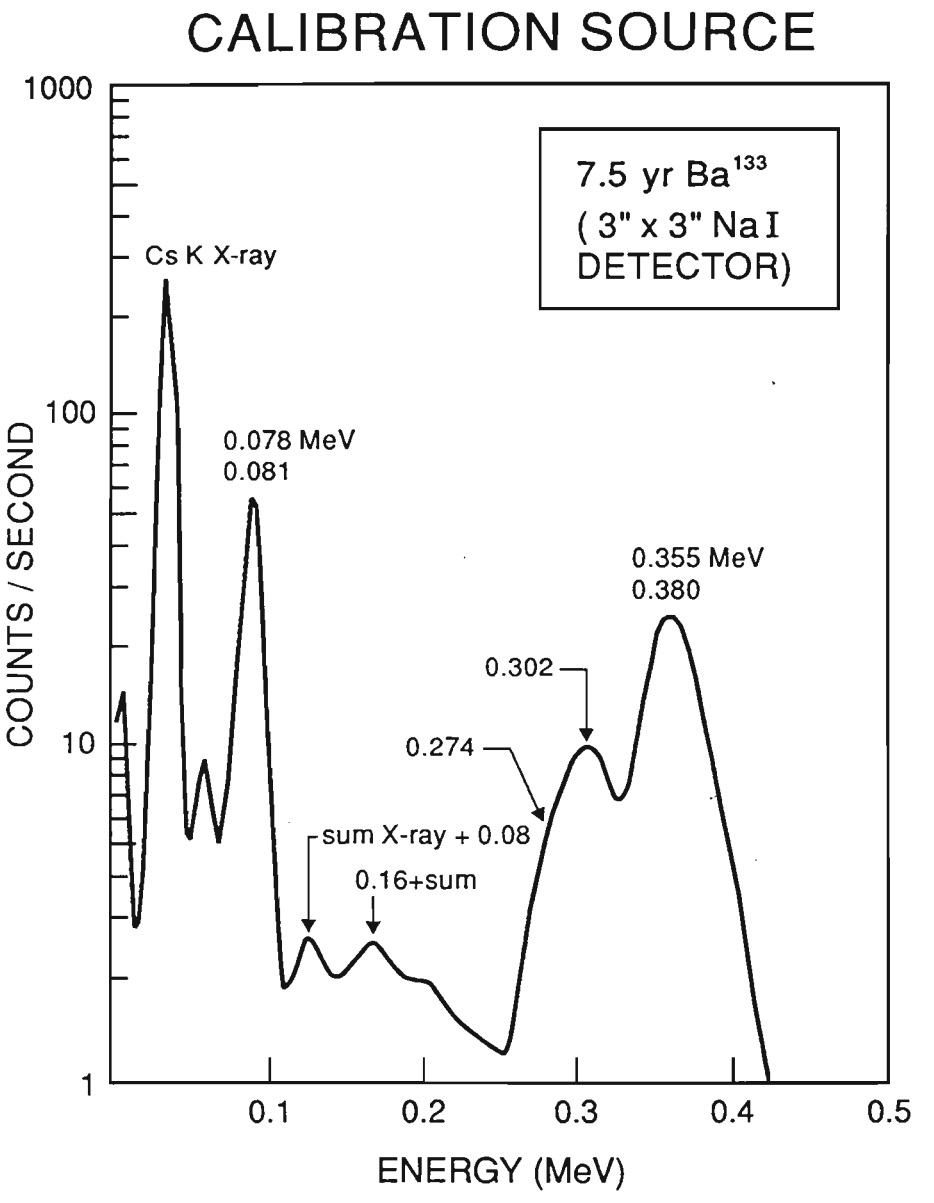

C6.3 Spectrum from Ba-133 calibration source

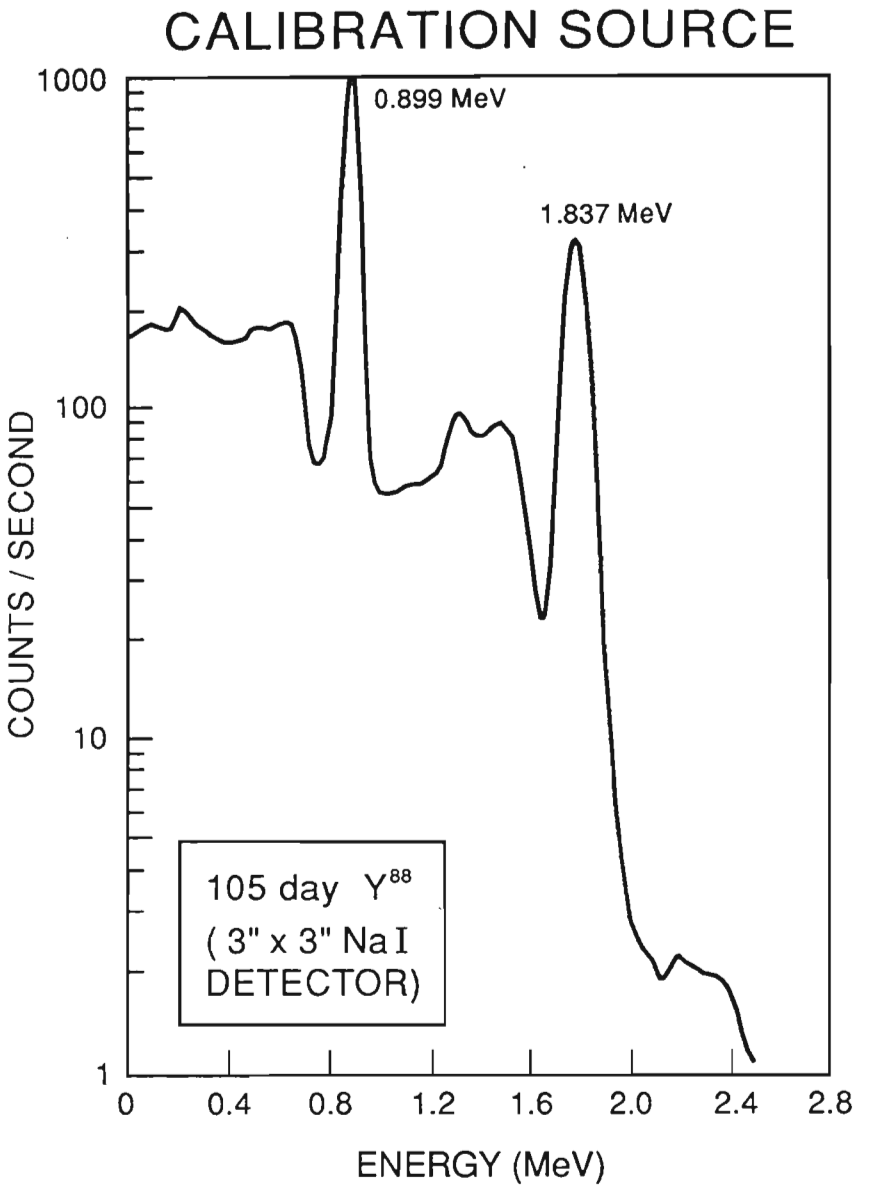

C6.4 Spectrum from Y-88 calibration source

NATURAL GAMMA RAY SPECTRAL PROBE

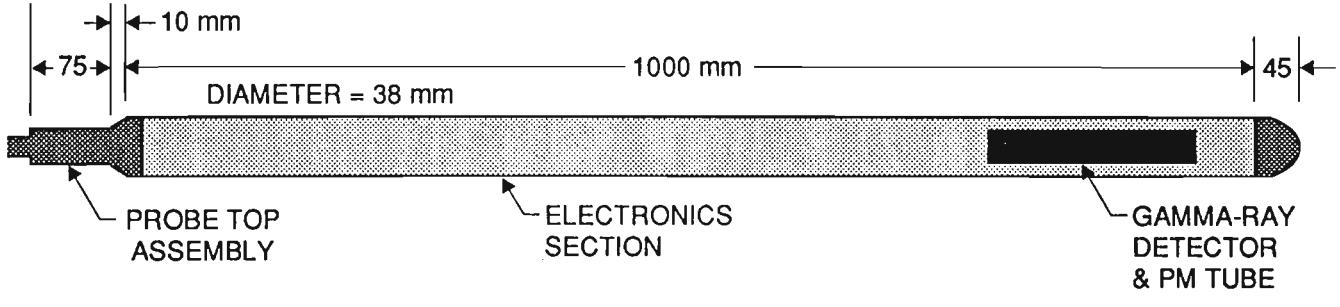

TOTAL LENGTH = 1130 mm

C 7.1 Dimensions of Natural Gamma Ray Spectral probe

SPECTRAL GAMMA GAMMA / DENSITY PROBE

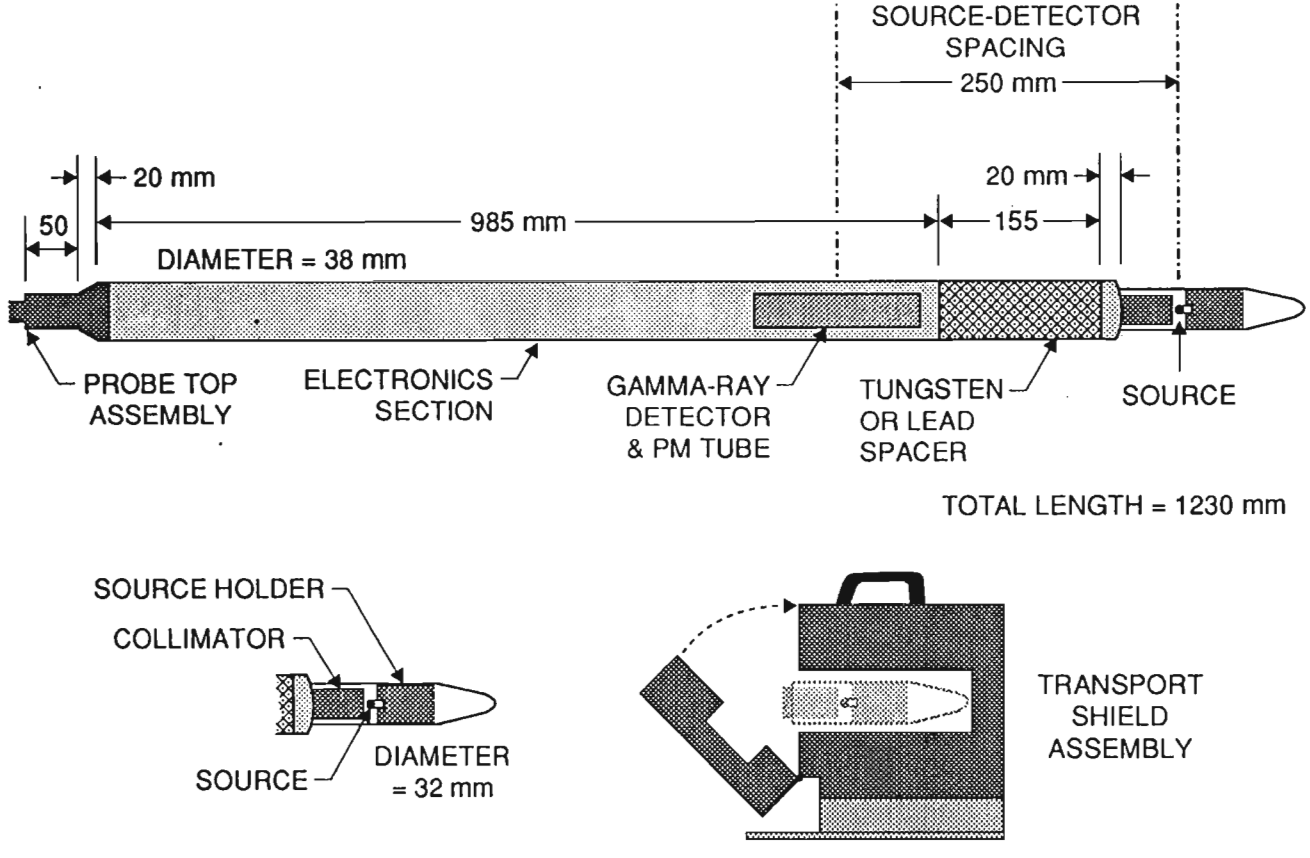

C 7.2 Dimensions of Spectral Gamma Gamma / Density probe

IP / R / SP PROBE

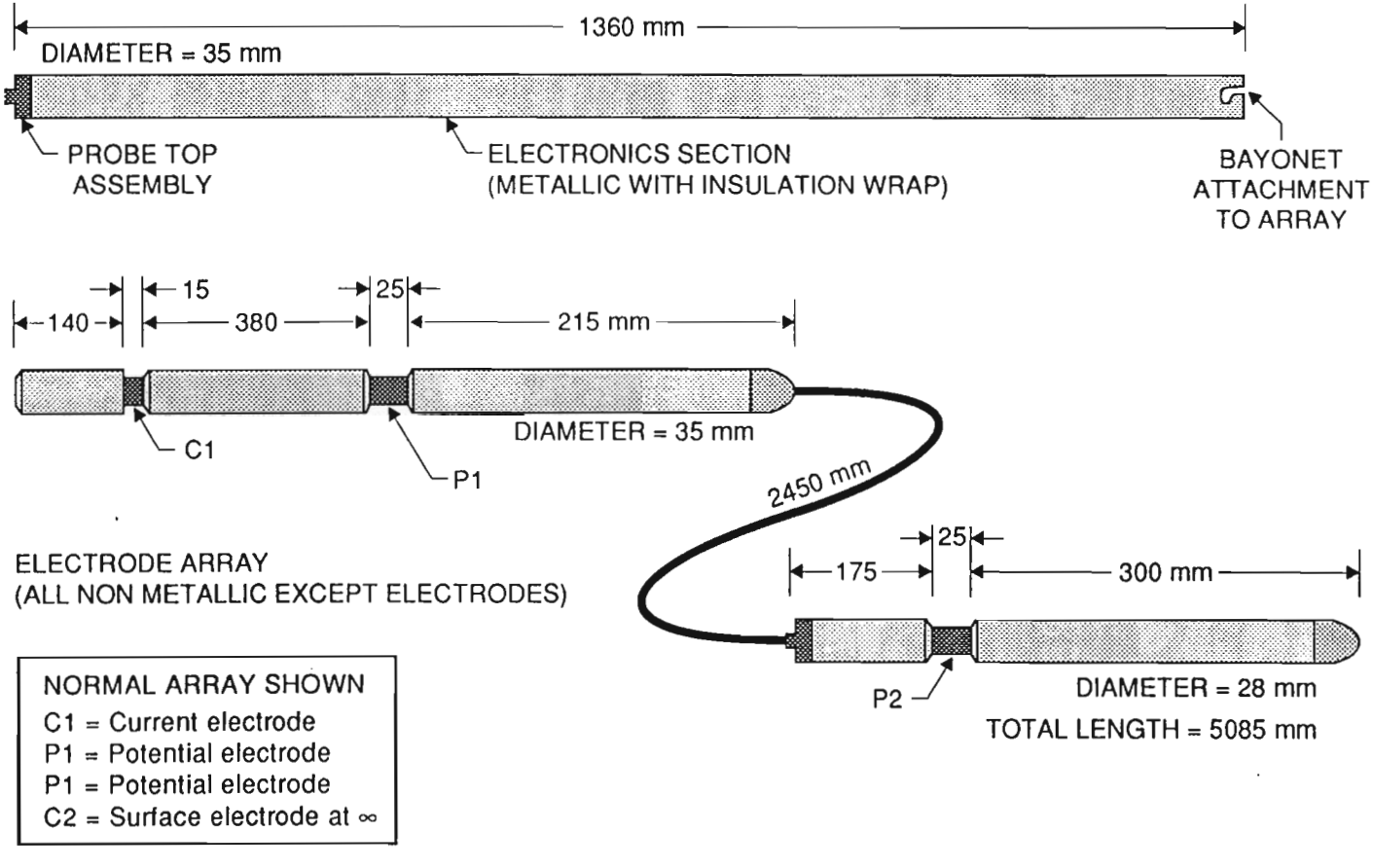

C 7.3.1 Dimensions of IP/R/SP probe

SELF POTENTIAL / SINGLE POINT RESISTANCE PROBE

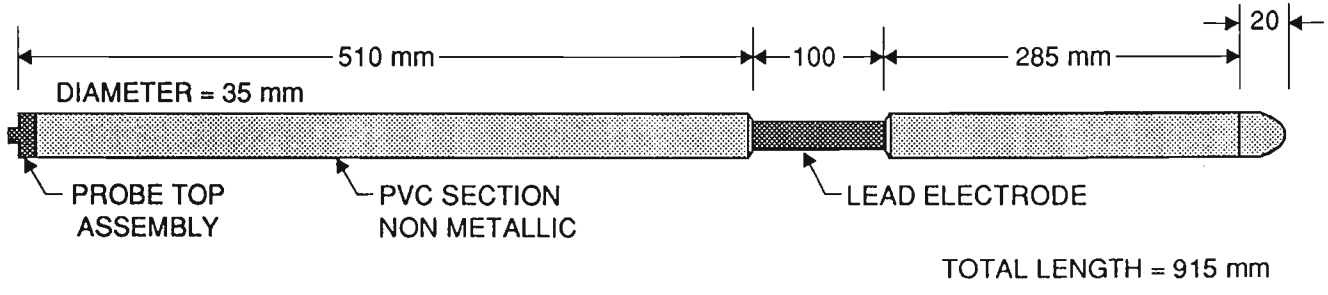

C 7.3.2 Dimensions of Self Potential probe

MAGNETIC SUSCEPTIBILITY PROBE

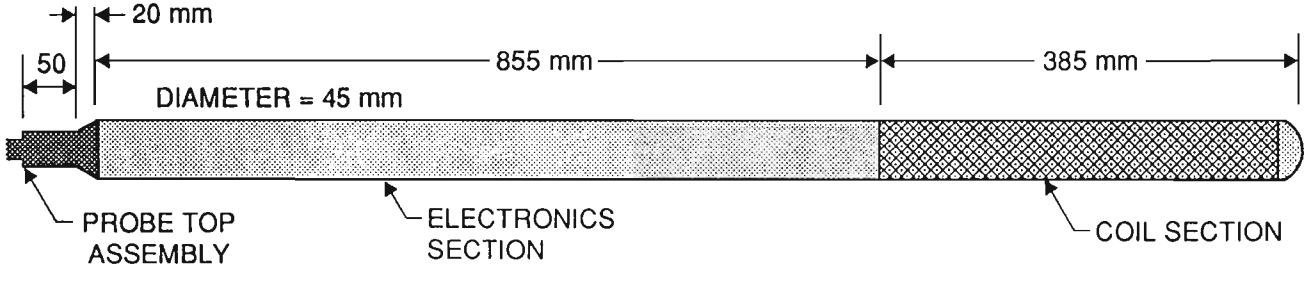

C 7.4 Dimensions of Magnetic Susceptibility probe

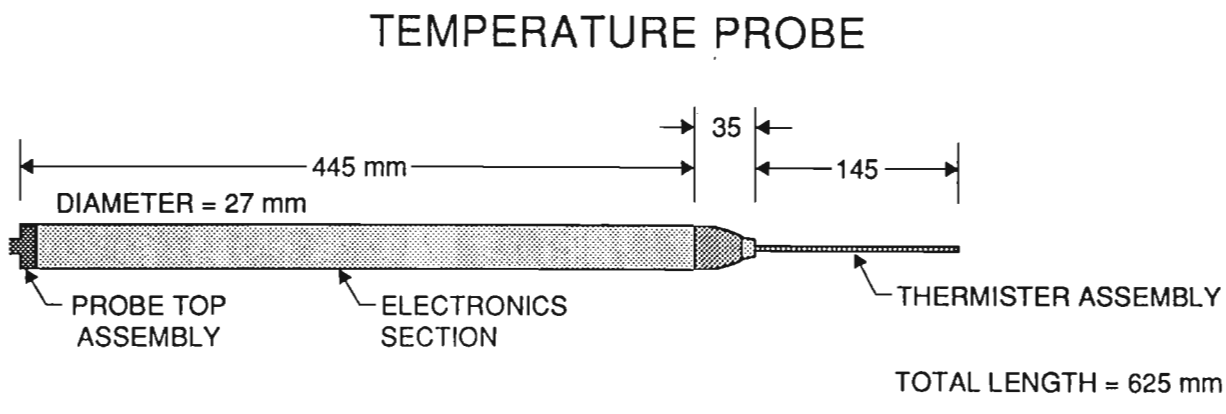

C 7.5 Dimensions of Temperature probe

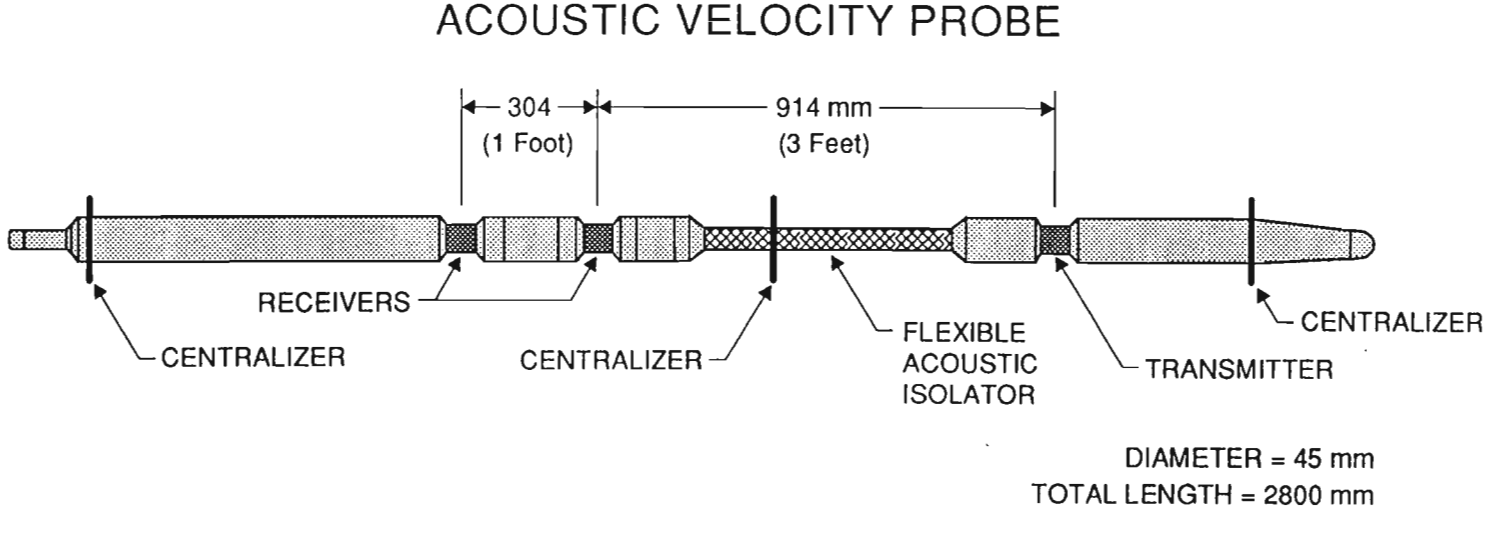

C 7.6 Dimensions of Acoustic Velocity probe

3-COMPONENT MAGNETIC / ORIENTATION PROBE

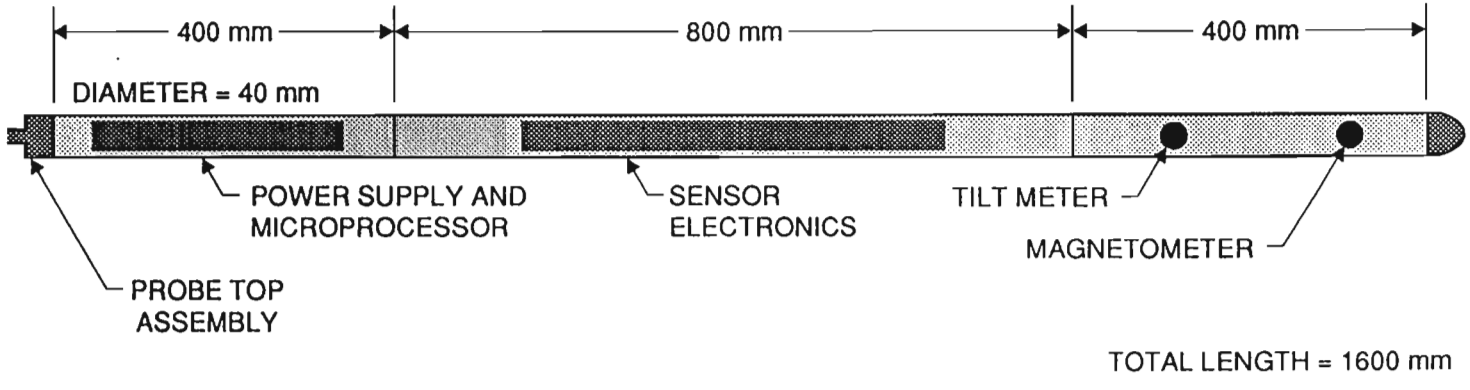

C7.7 Dimensions of 3-Component Magnetic / Orientation probe

C8.1 Drill Rod and Casing Diameters

Drill Rod					Casing (flush joint)				Casing (flush coupled)			
Size	I.D.		O.D.		I.D.		O.D.		I.D.		O.D.	
	inches	mm	inches	mm	inches	mm	inches	mm	inches	mm	inches	mm
AW	1.22	30.9	1.75	44.4	1.91	48.4	2.25	57.1	2.00	50.8	2.25	57.1
BW	1.75	44.5	2.12	54.0	2.38	60.3	2.88	73.0	2.56	65.1	2.87	73.0
NW	2.25	57.2	2.63	66.7	3.00	76.2	3.50	88.9	3.19	80.9	3.50	88.9
HW	3.06	77.8	3.50	88.9	4.00	101.6	4.50	114.3	4.13	104.8	4.50	114.3

C8.2 Drill Rod and Casing Diameters

Drill Rod						
Size	O.D.		I.D.		Weight	
	inches	mm	inches	mm	lb per 10 ft	kg/m
A	1 5/16	33	27/32	21	28	4.2
E	1 5/8	41	1 1/8	29	38	5.6
B	1 29/32	57	1 13/32	36	46	6.8
N	2 3/8	60	2	51	49	7.3
Flush-coupled casing						
RX	1 7/16	36	1 13/16	30	18	2.7
EX	1 13/16	46	1 5/8	41	18	2.7
AX	2 1/4	57	2	51	29	4.3
BX	2 7/8	73	2 9/16	65	47	7.0
NX	3 1/2	89	3 3/16	81	60	8.9
HX	4 1/2	114	4 1/8	105	90	13.4

C8.3 Wireline Drill rod and drill Bits

	Drill rod (wireline)				Drill bit			
Size	I.D.		O.D.		Core diameter		Hole diameter	
	inches	mm	inches	mm	inches	mm	inches	mm
AQ	1.38	34.9	1.75	44.5	1.06	27.0	1.89	48.0
BQ	1.81	46.0	2.19	55.6	1.43	36.5	2.36	60.0
NQ	2.38	60.3	2.75	69.9	1.88	47.6	2.98	75.7
HQ	3.06	77.8	3.50	88.9	2.50	63.5	3.78	96.0
PQ	4.06	103.2	4.63*	117.5*	3.35	85.0	4.83	122.6

C8.4 Some Useful Conversion Factors

becquerel	1 Bq	= 2.7027×10^{-11} Ci (= 1 dis/s)
disintegrations per second	1 dis/s	= 1.00×10^{0} Bq
curie (=3.7×10^{10} dis/s)	1 Ci	= 3.70×10^{10} Bq
ton (long) (= 2240 lbm)	1 ton	= 1.016×10^{3} kg
ton (short) (= 2000 lbm)	1 short ton	= 9.072×10^{2} kg
ton (short) of U_3O_8		= 0.769 t U
tonne (= metric ton)	1 t	= 1.00×10^{3} kg
foot	1 ft	= 3.048×10^{-1} m
inch	1 in	= 2.54×10^{-2} m
pound mass/inch^3	1 lbm/in^3	= 2.768×10^{-5} kg/m^3
pound mass/foot^3	1 lbm/ft^3	= 1.602×10^{1} kg/m^3